THE INTEGRATIVE PHYSIOLOGY OF METABOLIC DOWNSTATES

EDITED BY: Alessandro Silvani
PUBLISHED IN: Frontiers in Physiology

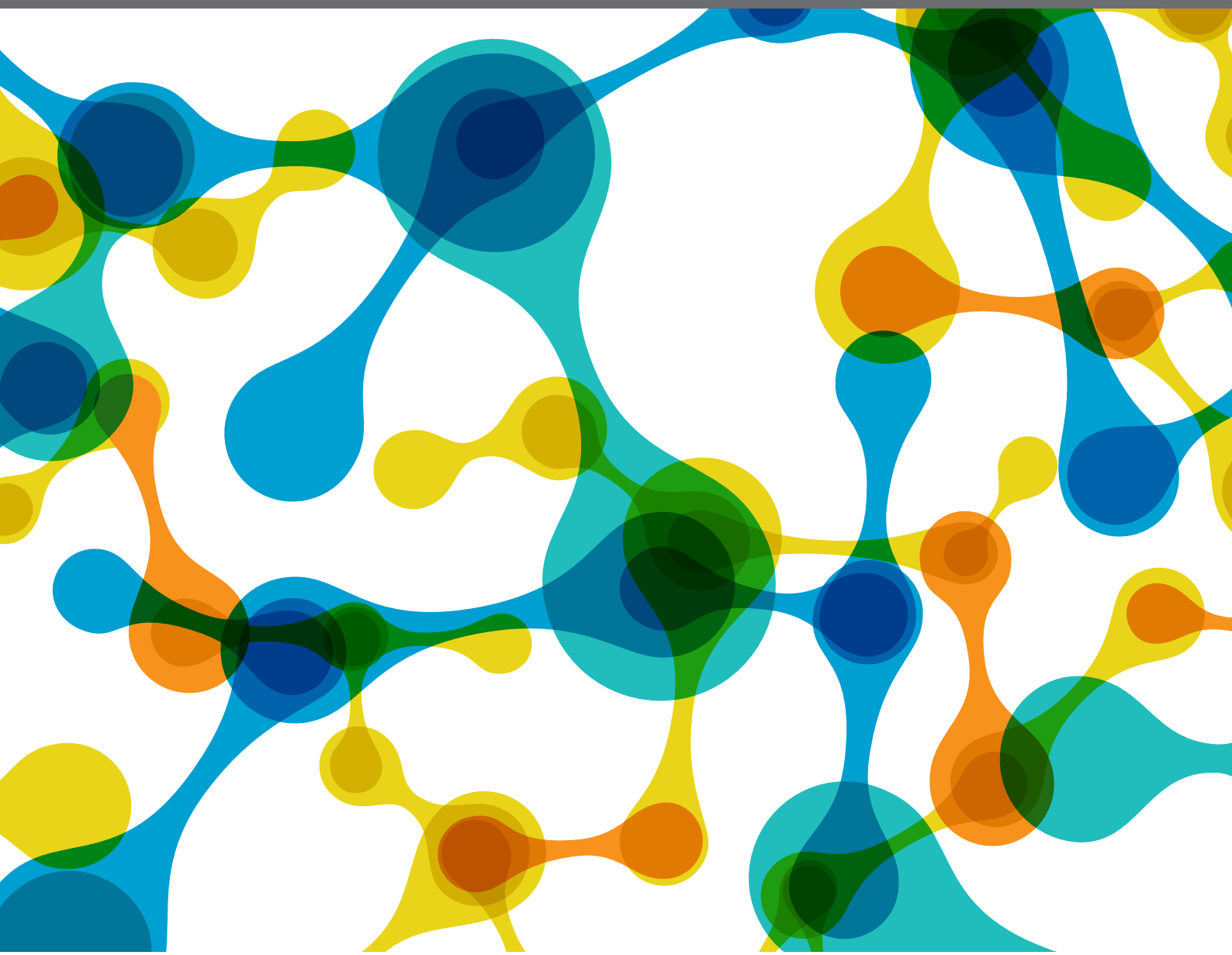

frontiers Research Topics

frontiers

ISSN 1664-8714
ISBN 978-2-88971-580-0
DOI 10.3389/978-2-88971-580-0

About Frontiers

Frontiers is more than just an open-access publisher of scholarly articles: it is a pioneering approach to the world of academia, radically improving the way scholarly research is managed. The grand vision of Frontiers is a world where all people have an equal opportunity to seek, share and generate knowledge. Frontiers provides immediate and permanent online open access to all its publications, but this alone is not enough to realize our grand goals.

Frontiers Journal Series

The Frontiers Journal Series is a multi-tier and interdisciplinary set of open-access, online journals, promising a paradigm shift from the current review, selection and dissemination processes in academic publishing. All Frontiers journals are driven by researchers for researchers; therefore, they constitute a service to the scholarly community. At the same time, the Frontiers Journal Series operates on a revolutionary invention, the tiered publishing system, initially addressing specific communities of scholars, and gradually climbing up to broader public understanding, thus serving the interests of the lay society, too.

Dedication to Quality

Each Frontiers article is a landmark of the highest quality, thanks to genuinely collaborative interactions between authors and review editors, who include some of the world's best academicians. Research must be certified by peers before entering a stream of knowledge that may eventually reach the public - and shape society; therefore, Frontiers only applies the most rigorous and unbiased reviews.
Frontiers revolutionizes research publishing by freely delivering the most outstanding research, evaluated with no bias from both the academic and social point of view. By applying the most advanced information technologies, Frontiers is catapulting scholarly publishing into a new generation.

What are Frontiers Research Topics?

Frontiers Research Topics are very popular trademarks of the Frontiers Journals Series: they are collections of at least ten articles, all centered on a particular subject. With their unique mix of varied contributions from Original Research to Review Articles, Frontiers Research Topics unify the most influential researchers, the latest key findings and historical advances in a hot research area! Find out more on how to host your own Frontiers Research Topic or contribute to one as an author by contacting the Frontiers Editorial Office: frontiersin.org/about/contact

THE INTEGRATIVE PHYSIOLOGY OF METABOLIC DOWNSTATES

Topic Editor:
Alessandro Silvani, University of Bologna, Italy

Citation: Silvani, A., ed. (2021). The Integrative Physiology of Metabolic Downstates. Lausanne: Frontiers Media SA. doi: 10.3389/978-2-88971-580-0

Table of Contents

04 ***Editorial: The Integrative Physiology of Metabolic Downstates***
Alessandro Silvani

06 ***A Temporal Examination of Cytoplasmic Ca^{2+} Levels, Sarcoplasmic Reticulum Ca^{2+} Levels, and Ca^{2+}-Handling-Related Proteins in Different Skeletal Muscles of Hibernating Daurian Ground Squirrels***
Zhe Wang, Jie Zhang, Xiu-Feng Ma, Hui Chang, Xin Peng, Shen-Hui Xu, Hui-Ping Wang and Yun-Fang Gao

21 ***Regulation of Peroxisome Proliferator-Activated Receptor Pathway During Torpor in the Garden Dormouse,* Eliomys quercinus**
Alexander J. Watts, Samantha M. Logan, Anna Kübber-Heiss, Annika Posautz, Gabrielle Stalder, Johanna Painer, Kristina Gasch, Sylvain Giroud and Kenneth B. Storey

35 ***Dynamic RNA Regulation in the Brain Underlies Physiological Plasticity in a Hibernating Mammal***
Rui Fu, Austin E. Gillen, Katharine R. Grabek, Kent A. Riemondy, L. Elaine Epperson, Carlos D. Bustamante, Jay R. Hesselberth and Sandra L. Martin

53 ***The Torpid State: Recent Advances in Metabolic Adaptations and Protective Mechanisms***
Sylvain Giroud, Caroline Habold, Roberto F. Nespolo, Carlos Mejías, Jérémy Terrien, Samantha M. Logan, Robert H. Henning and Kenneth B. Storey

77 ***Body Protein Sparing in Hibernators: A Source for Biomedical Innovation***
Fabrice Bertile, Caroline Habold, Yvon Le Maho and Sylvain Giroud

102 ***Dynamic Function and Composition Shift in Circulating Innate Immune Cells in Hibernating Garden Dormice***
Nikolaus Huber, Sebastian Vetter, Gabrielle Stalder, Hanno Gerritsmann and Sylvain Giroud

114 ***Discrepancies in the Time Course of Sleep Stage Dynamics, Electroencephalographic Activity and Heart Rate Variability Over Sleep Cycles in the Adaptation Night in Healthy Young Adults***
Ai Shirota, Mayo Kamimura, Akifumi Kishi, Hiroyoshi Adachi, Masako Taniike and Takafumi Kato

125 ***Unraveling the Big Sleep: Molecular Aspects of Stem Cell Dormancy and Hibernation***
Itamar B. Dias, Hjalmar R. Bouma and Robert H. Henning

144 ***Body Temperature and Activity Adaptation of Short Photoperiod-Exposed Djungarian Hamsters (*Phodopus sungorus*): Timing, Traits, and Torpor***
Elena Haugg, Annika Herwig and Victoria Diedrich

frontiers in Physiology

EDITORIAL
published: 13 September 2021
doi: 10.3389/fphys.2021.758972

Editorial: The Integrative Physiology of Metabolic Downstates

*Alessandro Silvani**

Department of Biomedical and Neuromotor Sciences, Alma Mater Studiorum Università di Bologna, Bologna, Italy

Keywords: hibernation, sleep, torpor, metabolism, physiology

Editorial on the Research Topic

The Integrative Physiology of Metabolic Downstates

Homeostasis relies upon the exquisite integration of diverse physiological functions, such as neuromuscular and cardiorespiratory functions and energy and thermal balance, in the face of external and internal challenges. The latter include physical exercise, which represents a short-term "metabolic upstate" of increased energy expenditure. To the other end of the spectrum, diverse physiological behaviors including sleep, daily torpor, and hibernation represent "metabolic downstates" of decreased energy expenditure. The study of physical exercise has been key for our current understanding of integrative physiology, for instance highlighting the role of feedforward control by central commands in complementing negative feedback regulation of physiological variables. In contrast, the integrative physiology of "metabolic downstates" remains insufficiently understood.

This Research Topic aimed to contribute to bridge this knowledge gap by bringing together cutting-edge updates on the integrative physiology of "metabolic downstates." Remarkably, the Research Topic attracted important contributions on the molecular, cellular, and metabolic aspects of the integrative physiology of hibernation. Focusing on molecular mechanisms, Fu et al. reported exciting new evidence on dynamic RNA regulation in the brain of 13-lined ground squirrels (*Ictidomys tridecemlineatus*) in physiologically distinct phases of hibernation, providing evidence for regulated transcription and RNA turnover during hibernation. Wang et al. uncovered hitherto unrecognized dynamics of calcium ions and calcium-handling proteins in the skeletal muscles of hibernating Daurian ground squirrels (*Spermophilus dauricus*), in the face of significantly decreased metabolic activity. Relevant to the cellular aspects of the integrative physiology of metabolic downstates, Huber et al. reported novel evidence of a temperature-compensated reduction of neutrophil oxidative burst capacity in hibernating garden dormice (*Eliomys quercinus*), while Dias et al. reviewed the evidence comparing the molecular aspects of cellular quiescence of hematopoietic stem cells with hibernation at the cellular level, revealing several key shared factors. The general aspects of metabolic adaptation associated with hibernation were reviewed by Giroud et al., who emphasized the mechanisms enabling heterotherms to protect their key organs against potential threats, such as reactive oxygen species. The evidence on protein metabolism in hibernation was reviewed by Bertile et al., focusing on the mechanisms that spare muscle proteins in the face of the inactivity that accompanies hibernation. Lipid metabolism was addressed by Watts et al. who demonstrated that metabolic rate and body mass loss in hibernating garden dormice do not differ with the dietary levels of essential polyunsaturated fatty acids in the fall season preceding hibernation, highlighting a preserved regulation of peroxisome proliferator-activated receptor pathway. Lastly, system-level adaptations to short photoperiod exposure in terms of body mass, fur insulation, locomotor activity, and core body temperature were investigated by Haugg et al. in Djungarian hamsters (*Phodopus sungorus*), providing insights into preconditions and proximate

OPEN ACCESS

Edited and reviewed by:
Geoffrey A. Head,
Baker Heart and Diabetes Institute, Australia

***Correspondence:**
Alessandro Silvani
alessandro.silvani3@unibo.it

Specialty section:
This article was submitted to Integrative Physiology, a section of the journal Frontiers in Physiology

Received: *15 August 2021*
Accepted: *23 August 2021*
Published: *13 September 2021*

Citation:
Silvani A (2021) Editorial: The Integrative Physiology of Metabolic Downstates. Front. Physiol. 12:758972. doi: 10.3389/fphys.2021.758972

stimuli of hibernation. On an apparently different note, Shirota et al. contributed a detailed report of discrepancies in the time course of sleep stage dynamics, electroencephalographic activity and heart rate variability over sleep cycles in the night of adaptation to the sleep laboratory in healthy young adults. Their study is of interest for the design and interpretation of human sleep studies and is appropriate to this Research Topic because sleep is also a "metabolic downstate" (Silvani et al., 2018).

Taken together, the research and review papers in this Research Topic drafted a remarkable picture of the complexity of the integrative physiology of hibernation, which is the metabolic downstate that was addressed by most contributions. This complexity stems not only from the multiplicity of the levels of physiological integration, but also from the temporal dynamics of hibernation, which is typically interrupted by short inter-bout arousals, and by differences among hibernator species. This complexity also brings about the potential to uncover basic mechanisms that may be conserved in evolution and harnessed to improve healthcare. For instance, understanding the mechanisms that preserve protein mass during hibernation could conceivably help limit muscle protein loss in conditions of inactivity or weight loss therapy. Knowledge of the mechanisms that limit circulating innate immune cell activity in hibernation could have clinical relevance in the context of therapeutic hypothermia and reperfusion injury. In perspective, it is tempting to speculate that greater knowledge of the integrative physiology of hibernation may allow its artificial reproduction in human subjects, with potential implications for healthcare as well as for long-range space exploration (Cerri et al., 2021).

By subtraction, the topics that were less covered in this article collection indicate important areas for future research. One such topic concerns whether and to what extent findings in multi-day hibernating species may be replicated during shallower daily torpor bouts in the house mouse (*Mus musculus*). This replication would allow researchers to leverage the power of genetic manipulations and analyses in Mus musculus, although, as shown by Fu et al. in this article collection, tools for genetic analysis in hibernating mammals are catching up. The other underrepresented topic is integrative sleep physiology, particularly as related to decreases in metabolic rate during sleep. The technical difficulty of measuring multiple physiological variables simultaneously without altering sleep physiology cannot be underestimated, as shown by the distinct physiological effects of habituation to the recording setup reported in this article collection by Shirota et al. even with non-invasive recordings in large animals such as human subjects. Nevertheless, increased knowledge of the integrative physiology of the sleep "metabolic downstate" could also have relevant translational implications, considering the high combined prevalence of sleep disorders and their association with cardiometabolic risk (Silvani, 2019).

AUTHOR CONTRIBUTIONS

AS drafted and reviewed the submission.

ACKNOWLEDGMENTS

The author wishes to thank prof. Jean-Pierre Montani and, particularly, prof. Steven J. Swoap for their outstanding editorial contribution to this Research Topic, as well as all the expert Reviewers who contributed time and effort to evaluate and improve the papers in this article collection.

REFERENCES

Cerri, M., Hitrec, T., Luppi, M., and Amici, R. (2021). Be cool to be far: exploiting hibernation for space exploration. *Neurosci. Biobehav. Rev*. 128, 218–232. doi: 10.1016/j.neubiorev.2021.03.037

Silvani, A. (2019). Sleep disorders, nocturnal blood pressure, and cardiovascular risk: a translational perspective. *Auton. Neurosci.* 218, 31–42. doi: 10.1016/j.autneu.2019.02.006

Silvani, A., Cerri, M., Zoccoli, G., and Swoap, S.J. (2018). Is adenosine action common ground for NREM sleep, torpor, and other hypometabolic states? *Physiology* 33, 182–196. doi: 10.1152/physiol.00007.2018

Conflict of Interest: The author declares that the research was conducted in the absence of any commercial or financial relationships that could be construed as a potential conflict of interest.

frontiers in Physiology

ORIGINAL RESEARCH
published: 21 October 2020
doi: 10.3389/fphys.2020.562080

A Temporal Examination of Cytoplasmic Ca^{2+} Levels, Sarcoplasmic Reticulum Ca^{2+} Levels, and Ca^{2+}-Handling-Related Proteins in Different Skeletal Muscles of Hibernating Daurian Ground Squirrels

Zhe Wang[1,2,3†], Jie Zhang[1,2†], Xiu-Feng Ma[1,2], Hui Chang[1,2], Xin Peng[1,2], Shen-Hui Xu[1,2], Hui-Ping Wang[1,2] and Yun-Fang Gao[1,2*]*

[1] Shaanxi Key Laboratory for Animal Conservation, College of Life Sciences, Northwest University, Xi'an, China, [2] Key Laboratory of Resource Biology and Biotechnology in Western China, Northwest University, Ministry of Education, Xi'an, China, [3] College of Life Sciences, Qufu Normal University, Qufu, China

To explore the possible mechanism of the sarcoplasmic reticulum (SR) in the maintenance of cytoplasmic calcium (Ca^{2+}) homeostasis, we studied changes in cytoplasmic Ca^{2+}, SR Ca^{2+}, and Ca^{2+}-handling proteins of slow-twitch muscle (soleus, SOL), fast-twitch muscle (extensor digitorum longus, EDL), and mixed muscle (gastrocnemius, GAS) in different stages in hibernating Daurian ground squirrels (*Spermophilus dauricus*). Results showed that the level of cytoplasmic Ca^{2+} increased and SR Ca^{2+} decreased in skeletal muscle fiber during late torpor (LT) and inter-bout arousal (IBA), but both returned to summer active levels when the animals aroused from and re-entered into torpor (early torpor, ET), suggesting that intracellular Ca^{2+} is dynamic during hibernation. The protein expression of ryanodine receptor1 (RyR1) increased in the LT, IBA, and ET groups, whereas the co-localization of calsequestrin1 (CSQ1) and RyR1 in GAS muscle decreased in the LT and ET groups, which may increase the possibility of RyR1 channel-mediated Ca^{2+} release. Furthermore, calcium pump (SR Ca^{2+}-ATPase 1, SERCA1) protein expression increased in the LT, IBA, and ET groups, and the signaling pathway-related factors of SERCA activity [i.e., β-adrenergic receptor2 protein expression (in GAS), phosphorylation levels of phospholamban (in GAS), and calmodulin kinase2 (in SOL)] all increased, suggesting that these factors may be involved in the up-regulation of SERCA1 activity in different groups. The increased protein expression of Ca^{2+}-binding proteins CSQ1 and calmodulin (CaM) indicated that intracellular free Ca^{2+}-binding ability also increased in the LT, IBA, ET, and POST

OPEN ACCESS

Edited by:
Steven Swoap,
Williams College, United States

Reviewed by:
Val Andrew Fajardo,
Brock University, Canada
Sandra L. Martin,
University of Colorado Anschutz Medical Campus, United States

***Correspondence:**
Hui-Ping Wang
wanghp@nwu.edu.cn
Yun-Fang Gao
gaoyunf@nwu.edu.cn

† These authors have contributed equally to this work

Specialty section:
This article was submitted to Integrative Physiology, a section of the journal Frontiers in Physiology

Received: *14 May 2020*
Accepted: *30 September 2020*
Published: *21 October 2020*

Citation:
Wang Z, Zhang J, Ma X-F, Chang H, Peng X, Xu S-H, Wang H-P and Gao Y-F (2020) A Temporal Examination of Cytoplasmic Ca^{2+} Levels, Sarcoplasmic Reticulum Ca^{2+} Levels, and Ca^{2+}-Handling-Related Proteins in Different Skeletal Muscles of Hibernating Daurian Ground Squirrels. Front. Physiol. 11:562080. doi: 10.3389/fphys.2020.562080

groups. In brief, changes in cytoplasmic and SR Ca^{2+} concentrations, SR RyR1 and SERCA1 protein expression levels, and major RyR1 and SERCA1 signaling pathway-related factors were unexpectedly active in the torpor stage when metabolic functions were highly inhibited.

Keywords: hibernation, calcium homeostasis, skeletal muscle, calcium pump, ryanodine receptor

INTRODUCTION

Calcium (Ca^{2+}) is homeostatically controlled in mammals (Thomas et al., 1996). Prolonged skeletal muscle disuse (e.g., during spaceflight, hindlimb unloading, and bed rest) can lead to disturbance of intracellular Ca^{2+} homeostasis, mainly exhibited by cytoplasmic Ca^{2+} overload (Ingalls et al., 2001; Wu et al., 2012; Hu et al., 2017). Cytoplasmic Ca^{2+} overload can activate the calpain protein degradation system and promote skeletal muscle protein degradation, which is an important mechanism leading to skeletal muscle atrophy (Goll et al., 2003; Gao et al., 2018).

Hibernation is an important strategy for survival under low environmental temperatures and food scarcity during the winter months (Martin and Yoder, 2014; van Breukelen and Martin, 2015; Nordeen and Martin, 2019). Numerous hibernators, including Daurian ground squirrels (*Spermophilus dauricus*), avoid loss of muscle mass and force during prolonged fasting and torpor inactivity, thus providing a natural model to study the mechanisms involved in the prevention of and resistance to disuse-induced skeletal muscle atrophy (Gao et al., 2012; Hindle et al., 2015). Our previous study showed that cytoplasmic Ca^{2+} is markedly elevated in the skeletal muscle fibers of ground squirrels during inter-bout arousal, but also shows partial recovery after inter-bout arousal, thus suggesting that intracellular Ca^{2+} is dynamic during different stages in hibernating ground squirrels (Fu et al., 2016). Periodic torpor-arousal cycles may be involved in the antagonism of skeletal muscle atrophy by alleviating excessive Ca^{2+} in the cytoplasm of muscle fibers and mitigating increased protein degradation. Therefore, studies on the potential mechanisms involved in Ca^{2+} homeostasis in the skeletal muscle fibers of hibernators are of great significance for revealing the mechanism controlling disuse-induced skeletal muscle atrophy.

A dynamic balance between intracellular pools and cytoplasmic Ca^{2+} is the main factor affecting intracellular Ca^{2+} homeostasis. The measurement of Ca^{2+} levels can thus reflect the maintenance or loss of intracellular Ca^{2+} homeostasis. In skeletal muscle, the endoplasmic reticulum is specialized into the sarcoplasmic reticulum (SR), an important organelle in the maintenance of intracellular Ca^{2+} homeostasis (MacIntosh et al., 2012). Research on Ca^{2+} homeostasis in skeletal muscles under disuse conditions has mainly focused on the SR, with changes in key Ca^{2+} handling proteins in the SR found to be closely related to cytoplasmic Ca^{2+} overload (Kraner et al., 2011).

Earlier studies have demonstrated that the increase in protein expression of the SR Ca^{2+} release channel ryanodine receptor1 (RyR1) and decrease in protein expression or activity of the calcium pump (sarco/endoplasmic reticulum Ca^{2+} ATPase isoform 1, SERCA1) are important mechanisms leading to Ca^{2+} overload and skeletal muscle atrophy in non-hibernating animals (Hunter et al., 2001; Donoghue et al., 2004; Kraner et al., 2011). Compared with non-hibernators (Silvani et al., 2018), only a few studies have been conducted on key SR Ca^{2+}-handling proteins in hibernators, and results have been relatively inconsistent. For example, the protein expression levels of SERCA1, RyR1, and calsequestrin1 (CSQ1) are reported to decrease in the hindlimb skeletal muscles in Siberian ground squirrels (*Spermophilus undulatus*) during torpor (Malysheva et al., 2001). Conversely, our previous study showed that SERCA activity increases in the soleus (SOL) and extensor digitorum longus (EDL) muscles of ground squirrels during inter-bout arousal and torpor compared with that during pre-hibernation (Guo et al., 2017). Furthermore, calmodulin (CaM) protein expression is reported to increase in the mixed hindlimb skeletal muscles of thirteen-lined ground squirrels (*Ictidomys tridecemlineatus*) during torpor (Zhang and Storey, 2016b). Importantly, however, the underlying mechanisms related to the above changes, especially the specific regulation of RyR1 and SERCA activity, are still not clear.

We also previously found that distinct skeletal muscles respond to cytoplasmic Ca^{2+} overload after arousal from and re-entry into torpor in different ways (Fu et al., 2016). We hypothesize that maintaining the dynamic balance between SR and cytoplasmic Ca^{2+} through regulating SR Ca^{2+} uptake and excretion channels is an important mechanism used to avoid or reduce cytoplasmic Ca^{2+} overload in hibernators, and may be related to skeletal muscle type. To test this hypothesis, we used the SOL, EDL, and gastrocnemius (GAS) muscles of Daurian ground squirrels to study cytoplasmic and SR Ca^{2+} concentrations in skeletal muscle fibers, as well as changes in the expression levels of RyR1, SERCA1, Ca^{2+} binding proteins, and signaling pathway-related proteins to investigate the relationship between changes in SR Ca^{2+} and cytoplasmic Ca^{2+} levels and the expression of key Ca^{2+} handling proteins in skeletal muscles during different stages in hibernating ground squirrels.

Abbreviations: CaM, calmodulin; CaMK2, calmodulin kinase 2; Ca^{2+}, calcium; CSQ1, calsequestrin1; DAPI, 4′-6′-diamidino-2-phenylindole; DHPR, dihydropyridine receptor; EDL, extensor digitorum longus; ET, early torpor; FKBP12, 12-kDa FK506 binding protein; Fluo-3/AM, fluo-3-acetoxymethylester; IBA, inter-bout arousal; GAS, gastrocnemius; LT, late torpor; mag-Fluo-4/AM, magnesium-Fluo-4-acetoxymethylester; MWW, skeletal muscle wet weight; MWW/BW, ratio of skeletal muscle wet weight to body weight; PLB, phospholamban; POST, post-hibernation; PRE, pre-hibernation; RT-PCR, real-time PCR; RyR1, ryanodine receptor1; SA, summer active; SERCA1, sarco/endoplasmic reticulum Ca^{2+} ATPase isoform 1; SLN, sarcolipin; SOL, Soleus; SR, sarcoplasmic reticulum; β-AR2, β-adrenergic receptor2.

MATERIALS AND METHODS

Animals and Groups

All animal procedures and care and handling protocols were approved by the Committee on the Ethics of Animal Experiments of Northwest University (Permit Number: SYXK 2010-004). Daurian ground squirrels were caught within the Weinan region in Shaanxi Province, China. After transfer to our laboratory, the ground squirrels were individually housed in 50 cm × 50 cm × 20 cm cages. Animals were weight-matched and divided into six groups (male to female ratio of ∼1:2): (1) summer active (SA): samples were collected in mid-June from ground squirrels with a body surface temperature (Tb) range of 36–38°C; (2) pre-hibernation (PRE): samples were collected in mid-September from ground squirrels with a Tb range of 36–38°C; (3) late torpor (LT): samples were collected 2 months after first entering torpor from ground squirrels with a Tb range of 5–8°C for more than 5 days (d); (4) inter-bout arousal (IBA): samples were collected 2 months after first entering torpor from ground squirrels with a Tb range of 34–37°C for less than 12 h (h); (5) early torpor (ET): samples were collected 2 months after first entering torpor and after animals entered a new torpor bout with a Tb range of 5–8°C for less than 24 h; (6) post-hibernation (POST): samples were collected in March of the following year from ground squirrels aroused from torpor with a Tb range of 36–38°C for more than 2-day. The body surface and environmental temperatures are shown in **Figure 1**. As described in previous study, after the animals were anaesthetized with sodium pentobarbital (90 mg/kg), the skeletal muscles (slow-twitch SOL, fast-twitch EDL, and mixed GAS) were separately used for all experiments (Fu et al., 2016). Animals in each group were divided into two batches ($n = 8$ for each batch). The first batch was used for cytoplasmic and SR Ca^{2+} level measurement. The second batch was used for molecular biology experiments, including protein extraction, western blot analysis, and protein co-localization analysis. At the end of surgical intervention, the animals were sacrificed by an overdose injection of sodium pentobarbital.

Cytoplasmic and SR Ca^{2+} Level Measurement

Muscle samples with tendons were dissected carefully from surrounding tissues and sarcolemma. The same volume of complete muscle from each type of skeletal muscle was separated along the longitudinal axis using tweezers (30-s process), then rinsed with 20 mL of phosphate-buffered saline (PBS, 137 mM sodium chloride, 4.3 mM disodium chloride, 2.7 mM potassium chloride, 1.4 mM monopotassium phosphate, pH 7.4), acutely dissociated with 3 mL of enzymatic digestion solution consisting of 0.35% collagenase I and 0.17% neutral protease (Sigma-Aldrich, Saint Quentin Fallavier, France), and finally incubated at 37°C on an orbital shaker for 2 h. The enzymatic digestion solution was saturated with 95% O_2 and 5% CO_2 gas mixture to ensure the muscle fibers were completely digested, after which the solution was removed with PBS and the muscles were agitated gently and repeatedly with pipettes (Wang et al., 2019). The dissociated single muscle fibers were set onto culture chamber slides and finally observed under an inverted microscope (Olympus, IX2-ILL100, Japan) (10-min process). One muscle fiber was separated on each slide in the incubator to avoid interaction of multiple muscle fibers during staining.

We used fluo-3-acetoxymethylester (Fluo-3/AM) (Invitrogen, Carlsbad, CA, United States), which demonstrates increased fluorescence upon Ca^{2+} binding, to determine cytoplasmic free Ca^{2+}. The experimental method is the same as that in our previous report (Zhang et al., 2019). Briefly, after washing the samples three times with fresh PBS, dye (5 mM Fluo-3/AM) was slowly added along the sides of the single muscle fibers, followed by incubation in the dark at 37°C for 30 min. After incubation, the glass slide-mounted Fluo-3/AM-loaded fibers were washed with fresh PBS three times (20 s/time, 1-min process). The slide was quickly placed on the microscope stage, with the fibers focused in the bright field (20-s process) and scanned via laser confocal microscopy in combination with an Olympus FV10-ASW system (Tokyo, Japan) under 488-nm krypton/argon laser illumination, with fluorescence detected at 526 nm. According to their length, three to five pictures were captured at 10 × objective magnification for each muscle fiber (10-s capture process for each picture). Six different areas were randomly selected for fluorescence intensity measurements in each image. Total fluorescence intensity/total area of the selected region was used as the average fluorescence intensity of the muscle fiber, which represented the relative concentration of Ca^{2+}. The average value of the measured result was taken as the fluorescence intensity of the muscle fiber cytosolic Ca^{2+} concentration. The average value of 10 muscle fibers was taken as the fluorescence intensity of the muscle fiber cytosolic Ca^{2+} concentration. Quantification analysis of the fluorescence intensity was performed with Image-Pro Plus 6.0.

Magnesium-Fluo-4-acetoxymethylester (mag-Fluo-4/AM) (M14206, Thermo Fisher Scientific, Rockford, IL, United States), which exhibits an increase in fluorescence upon binding to Ca^{2+}, was used to indicate SR free Ca^{2+}, as described previously (Park et al., 2000). Briefly, after washing samples twice with fresh PBS, dye (5 mM mag-Fluo-4/AM) was slowly added along the sides of the single muscle fibers, followed by incubation in the dark at 37°C for 30 min. After incubation, the glass slide-mounted mag-Fluo-4/AM-loaded fibers were washed with fresh PBS three times (20 s/time, 1-min process). The slide was then quickly placed on the microscope stage, with the fibers focused in the bright field (20-s process) and scanned via laser confocal microscopy in combination with an Olympus FV10-ASW system (Japan) under 488-nm krypton/argon laser illumination, with fluorescence detected at 526 nm. Analysis and statistical methods were similar to those used for the measurement of cytoplasmic Ca^{2+} mentioned above.

Western Blot

A Nuclear/Cytosol Fractionation Kit was used to extract cytoplasmic protein (Biovision, #K266-25, Mountain View, CA, United States). As described previously (Zhang et al., 2019; Wang et al., 2020b), soluble protein concentrations were then detected using a Pierce™ BCA Protein Quantification kit (Thermo Fisher

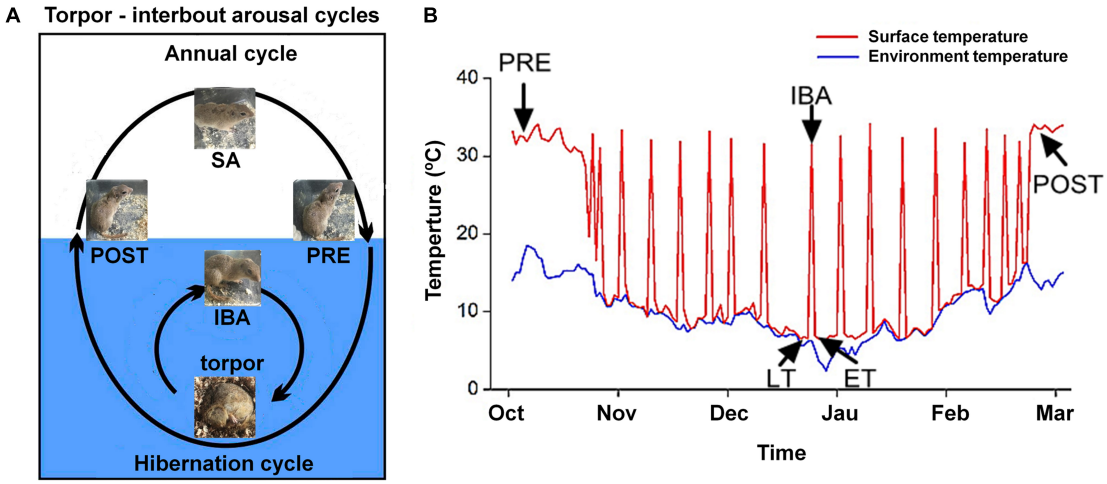

FIGURE 1 | Diagram of hibernation cycle and body surface temperature in ground squirrels. **(A)** Animal state of annual and hibernation (blue shading) cycles in ground squirrels. **(B)** Body surface temperature of Daurian ground squirrels (red line) and environmental temperature (blue line) during hibernation. SA, summer active; PRE, pre-hibernation; LT, late torpor; IBA, inter-bout arousal; ET, early torpor; POST, post-hibernation.

Scientific, 23227, United States). The supernatants were mixed with 1 × SDS loading buffer (100 mM Tris, 5% glycerol, 5% 2-β-mercaptoethanol, 4% SDS, and bromophenol blue, pH 6.8) at a 1:4 v/v ratio, followed by boiling and then storage at −20°C for further analysis.

The muscle protein extracts were then separated via SDS-PAGE [10% Laemmli gel with an acrylamide/bisacrylamide ratio of 29:1 and 98% 2,2,2-trichloroethanol (Aladdin, JI522028, China)]. After electrophoresis, the proteins were electrically transferred to polyvinylidene fluoride (PVDF) membranes (0.45-μm pore size) using a Bio-Rad semi-dry transfer apparatus. The blotted membranes were blocked with 1% BSA in Tris-buffered saline (TBS; 150 mM NaCl, 50 mM Tris-HCl, pH 7.5) and incubated with primary antibodies in TBS containing 0.1% BSA at 4°C overnight. The primary antibodies used for western blot analysis are listed in **Table 1**. The membranes were then incubated with Goat anti-Rabbit IgG (H + L) Secondary Antibody (1:5000, 31460, Thermo Fisher, United States) or Goat anti-Mouse IgG (H + L) Secondary Antibody (1:5000, 62-6520, Thermo Fisher, United States) for 90 min at room temperature, covered with West Pico Plus Chemiluminescent Substrate (34580, Thermo Fisher, United States), and visualized with an scanner (G: box, GBOX Cambridge, United Kingdom). Quantification analysis of the blots was performed using NIH Image J software. Immunoblot band density in each lane was standardized against the summed densities of total protein.

TABLE 1 | Primary and secondary antibodies used in western blot analysis.

Protein name	Antibody details
RyR1	1:1000, 8153S, CST, United States
DHPR	1:1000, SC-21781, Santa Cruz, United States
FKBP12	1:1000, ab58072, Abcam, United Kingdom
SERCA1	1:1000, 4219S, CST, United States
SLN	1:200, 18395-1-AP, Proteintech, China
PLB	1:1000, 8495S, CST, United States
P-PLB	1:1000, 8496S, CST, United States
β-AR2	1:500, ab182136, Abcam, United Kingdom
CaMK2	1:500, 3357S, CST, United States
P-CaMK2	1:1000, 12716S, CST, United States
CaM	1:1000, 4830S, CST, United States
CSQ1	1:10000, ab191564, Abcam, United Kingdom

Protein Co-localization Analysis

We cut 10-μm thick frozen muscle cross-sections from the mid-belly of each muscle at −20°C with a cryostat (Leica, Wetzlar, CM1850, Germany), followed by storage at −80°C for further staining (Wang et al., 2020a). Immunofluorescence was used to determine co-localization with dihydropyridine receptor (DHPR)/RyR1, CSQ1/RyR1, 12-kDa FK506 binding protein (FKBP12)/RyR1, and sarcolipin (SLN)/SERCA1. After air drying for 2 h, the sections were incubated in a blocking solution (5% BSA) (Boster, Wuhan, China) for 10 min at room temperature and then incubated in a primary antibody solution at 4°C overnight. The following day, the sections were incubated with secondary antibody at 37°C for 2 h. After this, the sections were incubated with another primary and secondary antibody under the same conditions. The primary and secondary antibodies are listed in **Table 2**. Finally, the glass slides were placed in 4′-6′-diamidino-2-phenylindole (DAPI) (1:100, D9542, Sigma-Aldrich, United States) at 37°C for 30 min. Images were visualized using a confocal laser scanning microscope by krypton/argon laser illumination at 350, 488, and 647 nm emitted light, and captured at 461, 526, and 665 nm. Six figures were analyzed in each sample and eight samples were analyzed in each group. The co-localization of two proteins was calculated by Pearson's correlation coefficients using Image-Pro Plus 6.0 (Lagache et al., 2015).

TABLE 2 | Primary and secondary antibodies used in protein co-localization.

Protein name	Primary antibody details	Secondary antibody details
DHPR/RyR1	Rabbit anti-RyR1 (1:200, 8153S, CST, United States)	Goat anti-rabbit Alexa Fluor 647 (1:200, A21245, Thermo Fisher Scientific, United States)
	Mouse anti-DHPR (1:200, SC-21781, Santa Cruz, United States)	Goat anti-mouse FITC (1:200, F1010, Sigma-Aldrich, France)
CSQ1/RyR1	Rabbit anti-RyR1	Goat anti-rabbit Alexa Fluor 647
	Rabbit anti-calsequestrin 1 (1:100, ab191564, Abcam, United Kingdom)	Goat anti-rabbit Alexa Fluor 488 (1:200, 11034, Thermo Fisher Scientific, United States)
FKBP12/RyR1	Rabbit anti-RyR1	Goat anti-rabbit Alexa Fluor 647
	Mouse anti-FKBP12 (1:200, ab58072, Abcam, United Kingdom)	Goat anti-mouse FITC
SLN/SERCA1	Rabbit anti-SERCA1 (1:200, 4219S, CST, United States)	Goat anti-rabbit Alexa Fluor 647
	Rabbit anti-SLN (1:200, 18395-1-AP, Proteintech, China)	Goat anti-rabbit Alexa Fluor 488

TABLE 3 | Effects of hibernation on body weight (BW), muscle wet weight (MWW), and ratio of MWW/BW in Daurian ground squirrels.

			MWW during experiment (mg)			MWW/BW during experiment (mg/g)		
Group	BW before experiment (g)	BW during experiment (g)	SOL	EDL	GAS	SOL	EDL	GAS
SA	325.24 ± 27.46	325.24 ± 27.46^{a}	131 ± 18	140 ± 18	257 ± 31^{a}	0.40 ± 0.05^{a}	0.43 ± 0.04^{bc}	0.79 ± 0.10^{b}
PRE	315.44 ± 21.82	315.44 ± 21.82^{a}	101 ± 23	123 ± 27	261 ± 41^{a}	0.32 ± 0.03^{b}	0.39 ± 0.05^{c}	0.82 ± 0.09^{b}
LT	322.71 ± 18.49	218.71 ± 30.4^{b}	99 ± 19	110 ± 32	211 ± 27^{ab}	0.45 ± 0.05^{a}	0.50 ± 0.06^{ab}	0.96 ± 0.12^{a}
IBA	330.14 ± 26.59	232.71 ± 32.07^{b}	113 ± 24	118 ± 22	225 ± 28^{ab}	0.49 ± 0.04^{a}	0.51 ± 0.07^{ab}	0.97 ± 0.11^{a}
ET	319.51 ± 24.90	217.83 ± 25.70^{b}	102 ± 18	114 ± 19	195 ± 32^{b}	0.47 ± 0.03^{a}	0.53 ± 0.04^{a}	0.90 ± 0.08^{b}
POST	319.39 ± 30.15	223.20 ± 31.43^{b}	101 ± 15	112 ± 23	200 ± 34^{ab}	0.45 ± 0.06^{a}	0.50 ± 0.04^{ab}	0.90 ± 0.08^{b}

SOL, soleus; GAS, gastrocnemius; EDL, extensor digitorum longus; SA, summer active; PRE, pre-hibernation; LT, late torpor; IBA, inter-bout arousal; ET, early torpor; POST, post-hibernation.

Data represent means ± SD; n = 16.

Different letters (such as a and b) indicate differences between period groups (P < 0.01), same letters (including a and ab) indicate no differences between period groups, and no letters indicate no differences among all six period groups.

Statistical Analyses

The normality of data and homogeneity of variance were tested by Levene tests. Single factor analysis of variance (one-way ANOVA) was used to determine group differences. The Tukey *post hoc* test was used for multiple comparisons among groups. Differences were considered significant at $P < 0.01$ because the Daurian ground squirrels were wild captured, and thus individual differences were larger. Data in the tables are expressed as means ± standard deviation (means ± SD); data in the figures are expressed as individual sample values, and median, average, upper and lower quartiles, upper and lower edges, and extreme outliers are reported. All statistical analyses were conducted using SPSS 19.0.

RESULTS

Body Weight, Skeletal Muscle Wet Weight (MWW), and Ratio of Skeletal Muscle Wet Weight to Body Weight (MWW/BW)

Compared with the body weights in the PRE group, the body weights during the experiment were 29–32% lower in the LT, IBA, ET, and POST groups. Compared with that in the SA group, the MWW showed no change in the SOL and EDL but a 22–25% decrease in the GAS in the LT, IBA, and ET groups. Moreover, compared with that in the PRE group, the skeletal muscle MWW/BW ratios were much higher in the other groups ($P < 0.01$). Thus, only slight skeletal muscle atrophy occurred in the different measured stages in hibernating ground squirrels (**Table 3**).

Cytoplasmic Ca^{2+} Level in Single Muscle Fibers

As shown in **Figure 2**, the same Ca^{2+} dynamics were observed in all three skeletal muscles. Compared with that in the SA and PRE groups, cytoplasmic Ca^{2+} was markedly elevated by 30–208% in the LT and IBA groups. During the torpor-arousal cycle, cytoplasmic Ca^{2+} decreased by 19–58% in the IBA and ET groups compared with that in the LT group. In addition, the levels were much lower in the ET group than that in the IBA group ($P < 0.01$). Overall, cytoplasmic Ca^{2+} was elevated to varying degrees in the different measured stages in hibernating ground squirrels (especially in the LT and IBA groups), but partially recovered when the animals aroused from and re-entered into torpor.

SR Ca^{2+} Level in Single Muscle Fibers

As shown in **Figure 3**, similar alternations in the SR Ca^{2+} levels were observed in the three different skeletal muscles. Compared with that in the SA group, SR Ca^{2+} levels in the SOL, EDL, and GAS muscles decreased by 20–80% in the PRE, LT, and

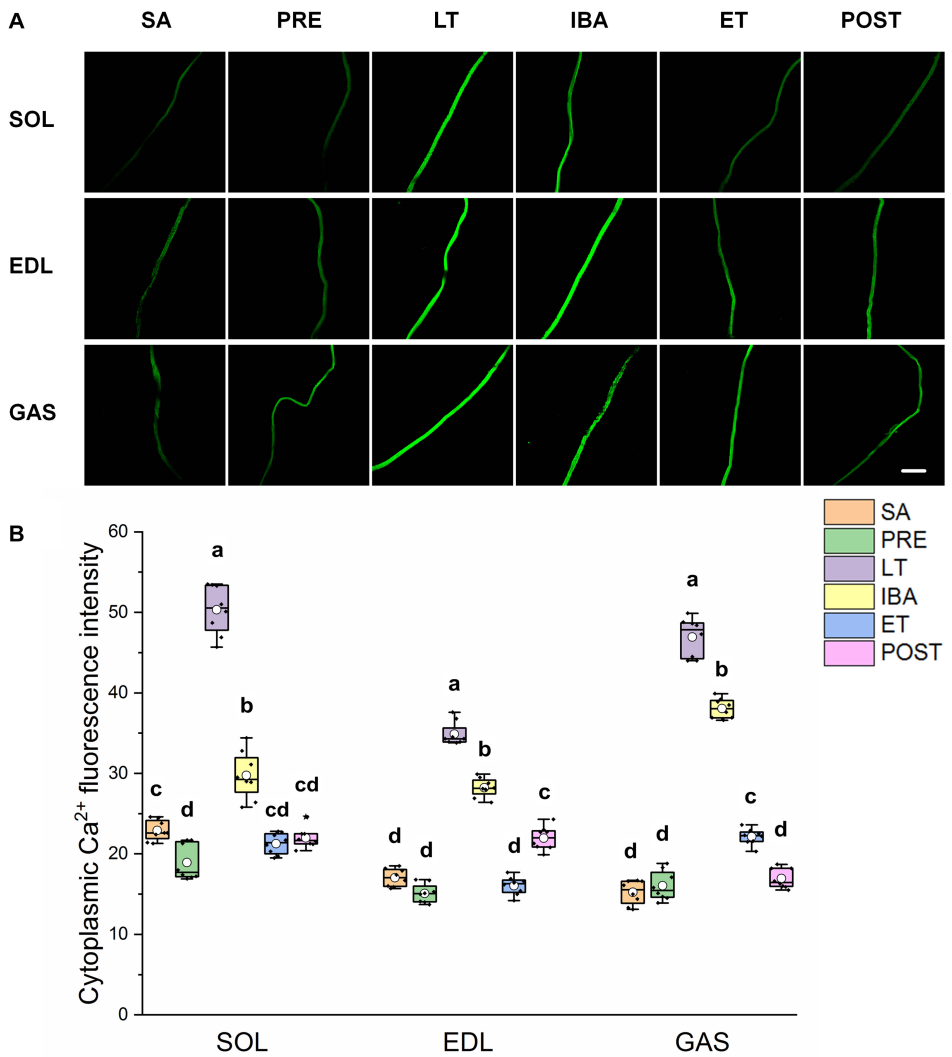

FIGURE 2 | Changes in cytoplasmic Ca^{2+} fluorescence intensity of single muscle fiber in skeletal muscles during different periods. **(A)** Representative fluorescence images of single muscle fiber loaded by Fluo-3/AM. Scale bar = 200 μm. **(B)** Box-plot depicting changes in mean intensity of cytoplasmic Ca^{2+} fluorescence. Boxes represent upper and lower quartiles, middle horizontal line represents median, hollow circle represents average, lines extending from upper and lower ends represent upper and lower edges, respectively, asterisks represent extreme outliers, and points represent individual sample values. $n = 8$. SOL, soleus muscle; EDL, extensor digitorum longus; GAS, gastrocnemius muscle; SA, summer active group; PRE, pre-hibernation group; LT, late torpor group; IBA, inter-bout arousal group; ET, early torpor group; POST, post-hibernation group. Different letters (such as a and b) indicate differences between period groups ($P < 0.01$), same letters (including a and ab) indicate no differences between period groups, and no letters indicate no differences among all six period groups.

IBA groups. Compared with that in the LT group, SR Ca^{2+} increased by 136–401% in the ET and POST groups. In addition, SR Ca^{2+} was 42–472% higher in the ET group relative to the IBA group ($P < 0.01$). Overall, SR Ca^{2+} decreased during torpor and recovered when animals aroused from and re-entered into torpor, opposite to the pattern observed for cytoplasmic Ca^{2+}.

Relative Protein Expression Involved in RyR1

A similar pattern of change in RyR1 protein expression in the different groups was observed in the SOL, EDL, and GAS muscles (**Figures 4A,B**). Compared with that in the SA and PRE groups, RyR1 protein expression increased by 20–107% in the LT, IBA, and ET groups, but then recovered in the POST group (**Figure 4C**). The DHPR protein expression levels in the SOL, EDL, and GAS muscles in the LT, IBA, and ET groups were lower than that in the SA group, with decrements of 31–33% (SOL), 34–39% (EDL), and 23–26% (GAS) (**Figure 4D**). A similar alternation pattern in FKBP12 protein expression was observed in the SOL and EDL muscles. Compared with that in the SA group, FKBP12 protein expression in the SOL and EDL muscles increased by 24–105% in the PRE and LT groups but decreased by 22–25% in the ET group. Compared with that in the LT group, FKBP12 protein expression decreased by 16–59% (SOL) and 30–43% (EDL) in the IBA, ET, and POST groups. However, compared

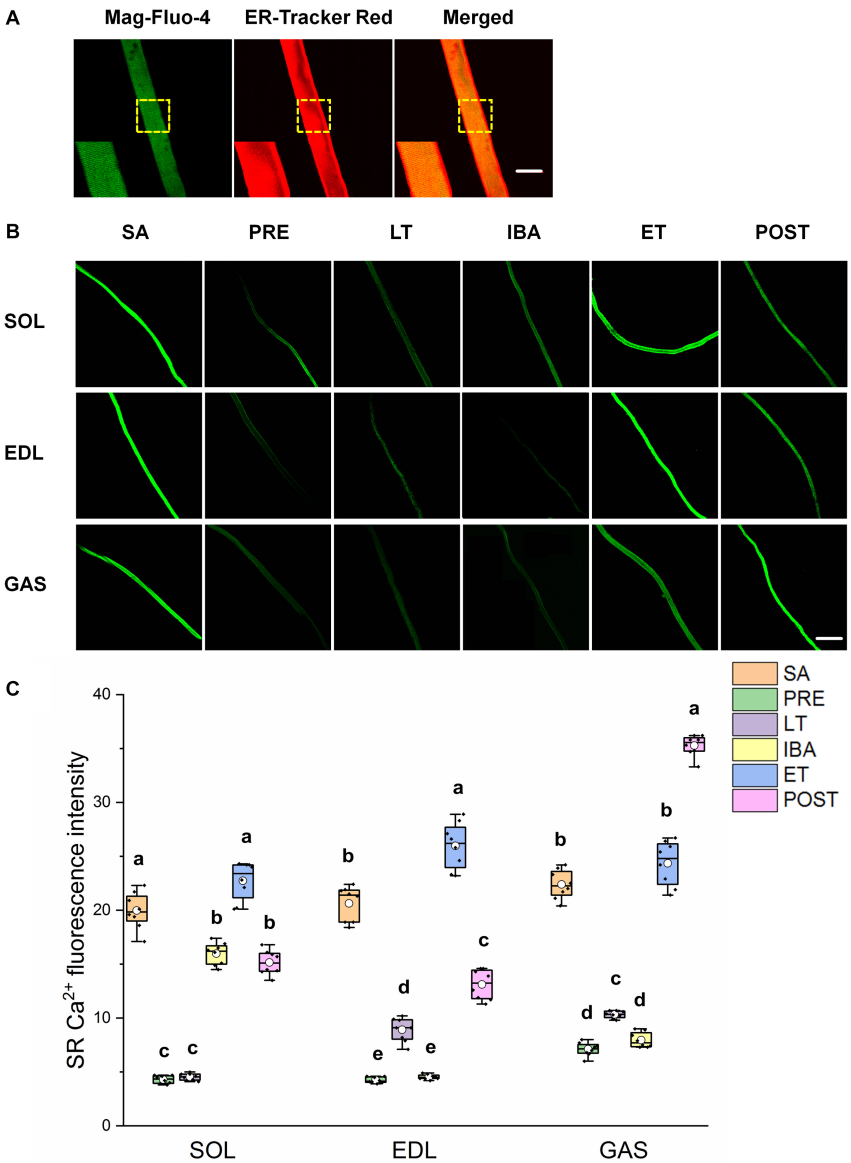

FIGURE 3 | Changes in sarcoplasmic reticulum (SR) Ca^{2+} fluorescence intensity of single muscle fibers in skeletal muscles during different periods. **(A)** Representative fluorescence images of single muscle fibers loaded by mag-Fluo-4/AM and SR-Tracker Red dye. Mag-Fluo-4/AM (green) for SR Ca^{2+}, SR-Tracker Red dye (red) for SR. Scale bar = 50 μm. **(B)** Representative fluorescence images of fluorescent SR Ca^{2+} in skeletal muscles during different periods. Scale bar = 200 μm. **(C)** Box-plot depicting changes in mean intensity of SR Ca^{2+} fluorescence. Boxes represent upper and lower quartiles, middle horizontal line represents median, hollow circle represents average, lines extending from upper and lower ends represent upper and lower edges, respectively, asterisks represent extreme outliers, and points represent individual sample values. $n = 8$. SOL, soleus muscle; EDL, extensor digitorum longus; GAS, gastrocnemius muscle; SA, summer active group; PRE, pre-hibernation group; LT, late torpor group; IBA, inter-bout arousal group; ET, early torpor group; POST, post-hibernation group. Different letters (such as a and b) indicate differences between period groups ($P < 0.01$), same letters (including a and ab) indicate no differences between period groups, and no letters indicate no differences among all six period groups.

with that in the SA group, FKBP12 protein expression in the GAS muscle declined by 19–38% in the PRE, LT, and ET groups ($P < 0.01$) (**Figure 4E**).

Relative Protein Expression Involved in SERCA1

In the SOL muscle, compared with that in the SA and PRE groups, SERCA1 protein expression increased by 23–40% in the IBA and ET groups. During the torpor-arousal cycle, SERCA1 protein expression in the IBA and ET groups was 28 and 16% higher than that in the LT group, respectively. In the EDL muscle, compared with that in the SA and PRE groups, SERCA1 protein expression increased by 38–64% in the LT, IBA, and ET groups. Furthermore, compared to that in the LT group, protein expression showed a 13 and 15% elevation in the IBA and ET groups, respectively. In the GAS muscle, compared with that in the SA group, SERCA1 protein expression increased by 50–100% in the PRE, LT, IBA,

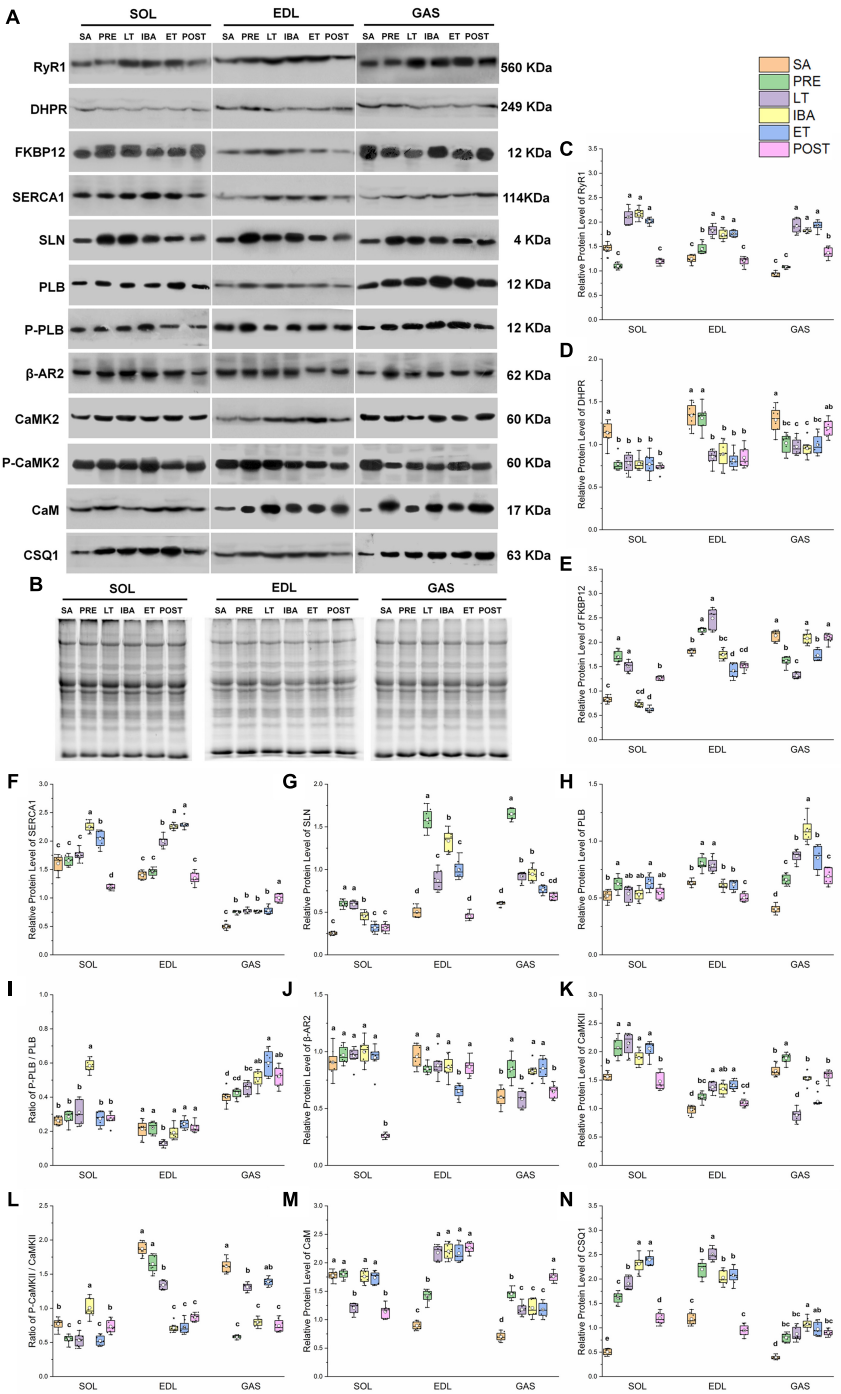

FIGURE 4 | Changes in protein levels of RyR1, DHPR, FKBP12, SERCA1, SLN, PLB, β-AR2, CaMK2, CaM, CSQ1, ratios of P-PLB/PLB and P-CaMK2/CaMK2 in skeletal muscles during different periods. **(A)** Representative immunoblots of RyR1, DHPR, FKBP12, SERCA1, SLN, P-PLB, PLB, β-AR2, P-CaMK2, CaMK2, CaM, and CSQ1 in three different types of skeletal muscles during different periods. **(B)** Representative polyacrylamide gel of total protein. **(C)** Relative protein expression of RyR1. **(D)** Relative protein expression of DHPR. **(E)** Relative protein expression of FKBP12. **(F)** Relative protein expression of SERCA1. **(G)** Relative protein expression of SLN. **(H)** Relative protein expression of PLB. **(I)** Ratio of P-PLB to PLB. **(J)** Relative protein expression of β-AR2. **(K)** Relative protein expression of CaMK2. **(L)** Ratio of P-CaMK2 to CaMK2. **(M)** Relative protein expression of CaM. **(N)** Relative protein expression of CSQ1. Boxes represent upper and lower quartiles, middle horizontal line represents median, hollow circle represents average, lines extending from upper and lower ends represent upper and lower edges, respectively, asterisks represent extreme outliers, and points represent individual sample values. $n = 8$. SOL, soleus muscle; EDL, extensor digitorum longus; GAS, gastrocnemius muscle; SA, summer active group; PRE, pre-hibernation group; LT, late torpor group; IBA, inter-bout arousal group; ET, early torpor group; POST, post-hibernation group. Different letters (such as a and b) indicate differences between period groups ($P < 0.01$), same letters (including a and ab) indicate no differences between period groups, and no letters indicate no differences among all six period groups.

ET, and POST groups (**Figure 4F**). SLN protein expression in the three muscles of the PRE, LT, IBA, and ET groups was higher than that in the SA group, and was 19–29% lower in the ET group than that in the IBA group (**Figure 4G**). Phospholamban (PLB) protein expression in the SOL (ET), EDL (LT), and GAS (all other groups) was higher than that in the SA group (**Figure 4H**). As shown in **Figure 4I**, the p-PLB/PLB ratio in the SOL muscle was higher in the IBA group than that in the SA, PRE, and LT groups, but showed a decrease in the LT group, then recovery in the IBA, ET, and POST groups in the EDL muscle. In the GAS muscle, compared with that in the SA group, the ratio was elevated in the IBA, ET, and POST groups, and was much higher in the ET group than that in the LT group (**Figure 4I**). β-adrenergic receptor2 (β-AR2) protein expression in the SOL showed no change in the LT, IBA, and ET groups compared with that in the SA group, but decreased in the POST group. Compared with that in the SA, PRE, LT, and IBA groups, β-AR2 protein expression declined in the EDL muscle in the ET group. In the GAS muscle, compared with that in the SA group, β-AR2 protein expression increased (38–42%) in the PRE, IBA, and ET groups. Expression was also much higher in the IBA and ET groups than that in the LT group (**Figure 4J**). A similar calmodulin kinase 2 (CaMK2) protein expression trend was found in the SOL and EDL, with higher levels in the PRE, LT, IBA, and ET groups than that in the SA group. In the GAS muscle, compared with that in the SA and PRE groups, CaMK2 protein expression decreased by 16–53% in the LT, IBA, ET, and POST groups (**Figure 4K**). Compared with that in the PRE and LT groups, the P-CaMK2/CaMK2 ratio in the SOL muscle increased. However, it decreased by 12–62% and 14–64% in the EDL and GAS muscles, respectively, in all groups compared with that in the SA group ($P < 0.01$) (**Figure 4L**).

Relative Protein Expression Involved in Ca^{2+}-Binding Proteins

In the SOL muscle, during the torpor-arousal cycle, CaM protein expression was 46 and 44% higher in the IBA and ET groups, respectively, than that in the LT group. Similar change trends in CaM protein expression were observed in the EDL and GAS muscles, with higher levels in all groups (EDL, 58–153%; GAS, 68–150%) compared with that in the SA group (**Figure 4M**). Similar changes in CSQ1 protein expression were observed in the three different skeletal muscles, with higher levels in all groups (SOL, 140–360%; EDL, 72–112%; GAS, 104–176%) compared with the SA group. In addition, compared with levels in the PRE, LT, IBA, and ET groups, CaM protein expression decreased by 26–50% (SOL) and 53–62% (EDL) in the POST group ($P < 0.01$) (**Figure 4N**).

Co-localization of Regulatory Proteins Involved in RyR1

As shown in **Figures 5A,B**, the co-localization levels of DHPR and RyR1 in the LT and ET groups were lower than that in the SA group in all three distinct skeletal muscles (**Figure 5C**). As shown in **Figure 6**, the co-localization levels of CSQ1 and RyR1 in the SOL muscle increased by 53% in the PRE group compared with that in the SA group. No change was found in the EDL muscle among all groups. In the GAS muscle, compared with that in the PRE group, levels decreased by 24 and 23% in the LT and ET groups, respectively ($P < 0.01$). The co-localization of RyR1 and FKBP12 was similarly measured and found to be unchanged among the six groups in all three skeletal muscles.

Co-localization of Regulatory Proteins Involved in SERCA1

The reticulate subcellular distributions of SLN and SERCA1 fluorescently labeled proteins are shown in **Figures 7A,B**. As seen in **Figure 7C**, compared with that in the SA and PRE groups, there was no change in the co-localization levels of SLN and SERCA1 in the three distinct skeletal muscles among the six groups; in the SOL muscle, however, levels were elevated in the POST group compared with that in the IBA and ET groups ($P < 0.01$) (**Figure 7C**).

DISCUSSION

An elevation in cytoplasmic Ca^{2+} concentration and a reduction in SR Ca^{2+} concentration were observed in the different skeletal muscles of the LT group compared to that of the SA group. This is similar to that found in non-hibernators under the disuse state (Ingalls et al., 2001; Hu et al., 2017), and indicates a degenerative change and loss of intracellular Ca^{2+} homeostasis. The elevation in Ca^{2+} concentration in all three skeletal muscles during late torpor was similar to the increase in cytoplasmic Ca^{2+} detected in the SOL of hibernating European hamsters (*Cricetus cricetus*) (Agostini et al., 1991). However, both Ca^{2+} concentrations recovered partially or completely in the ET group, thereby indicating the recovery of intracellular Ca^{2+} homeostasis. In addition, the changes in the cytoplasmic Ca^{2+} level were the opposite to those observed for SR Ca^{2+} during the "late torpor-inter-bout arousal-early torpor" cycle, indicating that the flow of Ca^{2+} between the cytoplasm and SR in skeletal muscle fibers was very active during the different stages in hibernating ground squirrels.

RyR1 protein expression increased in all three different skeletal muscles in the LT, IBA, and ET groups compared to levels in the SA and PRE groups, thus suggesting that SR Ca^{2+} release may have increased. The co-localization levels of DHPR and RyR1 in the three skeletal muscles decreased in the LT and ET groups compared to that in the SA and PRE groups. The structural combination of these two proteins is the basis for excitation-contraction coupling during skeletal muscle depolarization (Laver, 2018), and implies that the contraction function of skeletal muscle was weakened at this time, consistent with the fact that skeletal muscles are basically inactive during torpor. The co-localization levels of CSQ1 and RyR1 decreased, which may have increased the possibility of RyR1 channel opening to some extent, as CSQ1 is a negative regulator of RyR1 (Beard et al., 2002; Lee and Keener, 2008). Further, the co-localization levels of FKBP12 and RyR1 did not change in the three skeletal muscles in any of the six ground squirrel groups,

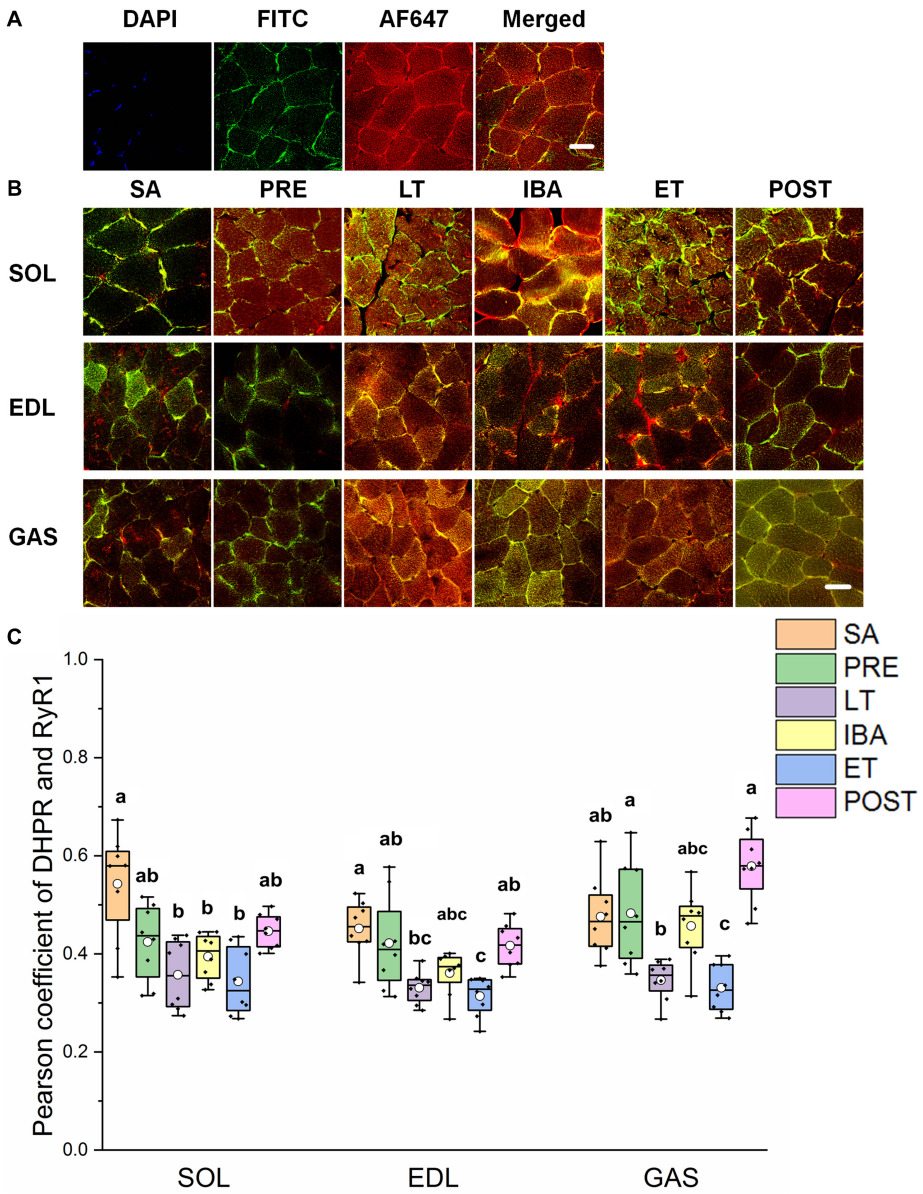

FIGURE 5 | Protein overlap levels of DHPR and RyR1 in skeletal muscles during different periods. **(A)** Reticulate subcellular distribution of DHPR and RyR1 fluorescently labeled proteins in skeletal muscles. DAPI (blue) for nuclei, FITC (green) for DHPR, 647 (red) for RyR1. Scale bar = 20 μm. **(B)** Representative immunofluorescence of protein overlap between DHPR and RyR1 in three different types of muscle during different periods. Scale bar = 20 μm. **(C)** Box-plot representing protein overlap level of DHPR and RyR1. Boxes represent upper and lower quartiles, middle horizontal line represents median, hollow circle represents average, lines extending from upper and lower ends represent upper and lower edges, respectively, asterisks represent extreme outliers, and points represent individual sample values. $n = 8$. SOL, soleus muscle; EDL, extensor digitorum longus; GAS, gastrocnemius muscle; SA, summer active group; PRE, pre-hibernation group; LT, late torpor group; IBA, inter-bout arousal group; ET, early torpor group; POST, post-hibernation group. Different letters (such as a and b) indicate differences between period groups ($P < 0.01$), same letters (including a and ab) indicate no differences between period groups, and no letters indicate no differences among all six period groups.

suggesting that the inhibition of FKBP12 on RyR1 was stable during these periods.

Unexpectedly, we found that SERCA1 protein expression increased in the different skeletal muscles in the LT, IBA, and ET groups. We previously found that SERCA activity in the skeletal muscles of ground squirrels is up-regulated during torpor (Guo et al., 2017). This up-regulation of SERCA1 protein expression or activity in skeletal muscles indicates that the potential ability of SR Ca^{2+} uptake increased in these periods. In contrast, earlier research found that SERCA activity decreases in the hindlimb skeletal muscles of long-tailed ground squirrels (*Spermophilus undulatus*) during torpor (Malysheva et al., 2001), contrary to our findings on Daurian ground squirrels. These different results may be due to the different living environments of these two

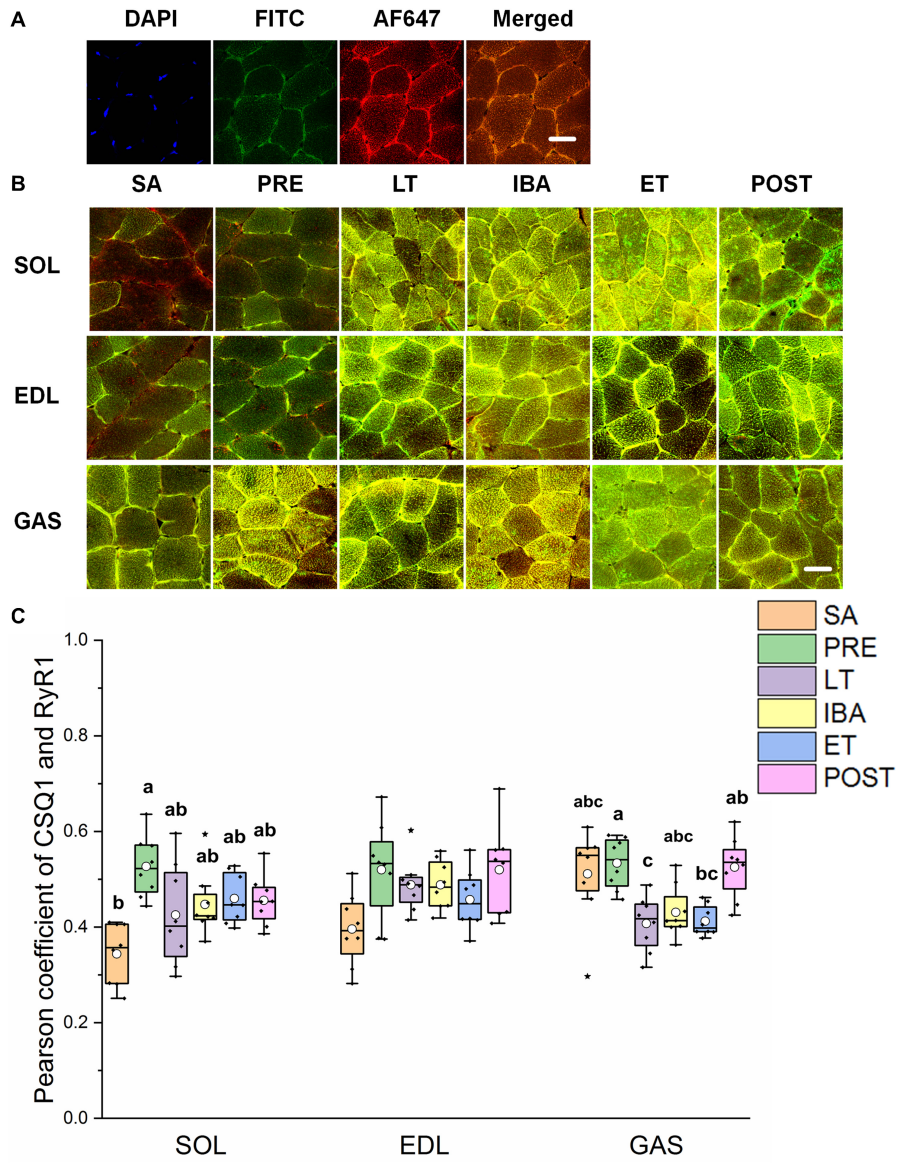

FIGURE 6 | Protein overlap levels of CSQ1 and RyR1 in three different types of muscle during different periods. **(A)** Reticulate subcellular distribution of CSQ1 and RyR1 fluorescently labeled proteins in three different types of muscle. DAPI (blue) for nuclei, AF488 (green) for CSQ1, 647 (red) for RyR1. Scale bar = 20 μm. **(B)** Representative immunofluorescence of protein overlap between CSQ1 and RyR1 in three different types of muscle during different periods. Scale bar = 20 μm. **(C)** Box-plot representing protein overlap level of CSQ1 and RyR1. Boxes represent upper and lower quartiles, middle horizontal line represents median, hollow circle represents average, lines extending from upper and lower ends represent upper and lower edges, respectively, asterisks represent extreme outliers, and points represent individual sample values. $n = 8$. SOL, soleus muscle; EDL, extensor digitorum longus; GAS, gastrocnemius muscle; SA, summer active group; PRE, pre-hibernation group; LT, late torpor group; IBA, inter-bout arousal group; ET, early torpor group; POST, post-hibernation group. Different letters (such as a and b) indicate differences between period groups ($P < 0.01$), same letters (including a and ab) indicate no differences between period groups, and no letters indicate no differences among all six period groups.

species. Long-tailed ground squirrels are mostly distributed in Siberia where the latitude is higher, winter is longer and colder, and the living environment is harsher. Therefore, the lower level of Ca^{2+} dynamic balance could reduce energy consumption and may be more conducive to survival. Phosphorylation of PLB, a key negative regulatory protein of SERCA, may reduce the inhibition effect of PLB on SERCA, resulting in the up-regulation of SERCA activity. The phosphorylation levels of PLB in the three different types of skeletal muscle (SOL in ET, EDL in PRE and LT, GAS in PRE, LT, IBA, ET, and POST) were increased, which may reduce the inhibition effect of PLB on SERCA (Asahi et al., 2003; Nicolaou et al., 2009; Shaikh et al., 2016). We found that β-AR2 protein expression in the GAS muscle increased in the other five groups compared with that in the SA group, which may explain the increased phosphorylation level of PLB (Hagemann and Xiao, 2002). SLN is another key negative regulatory protein

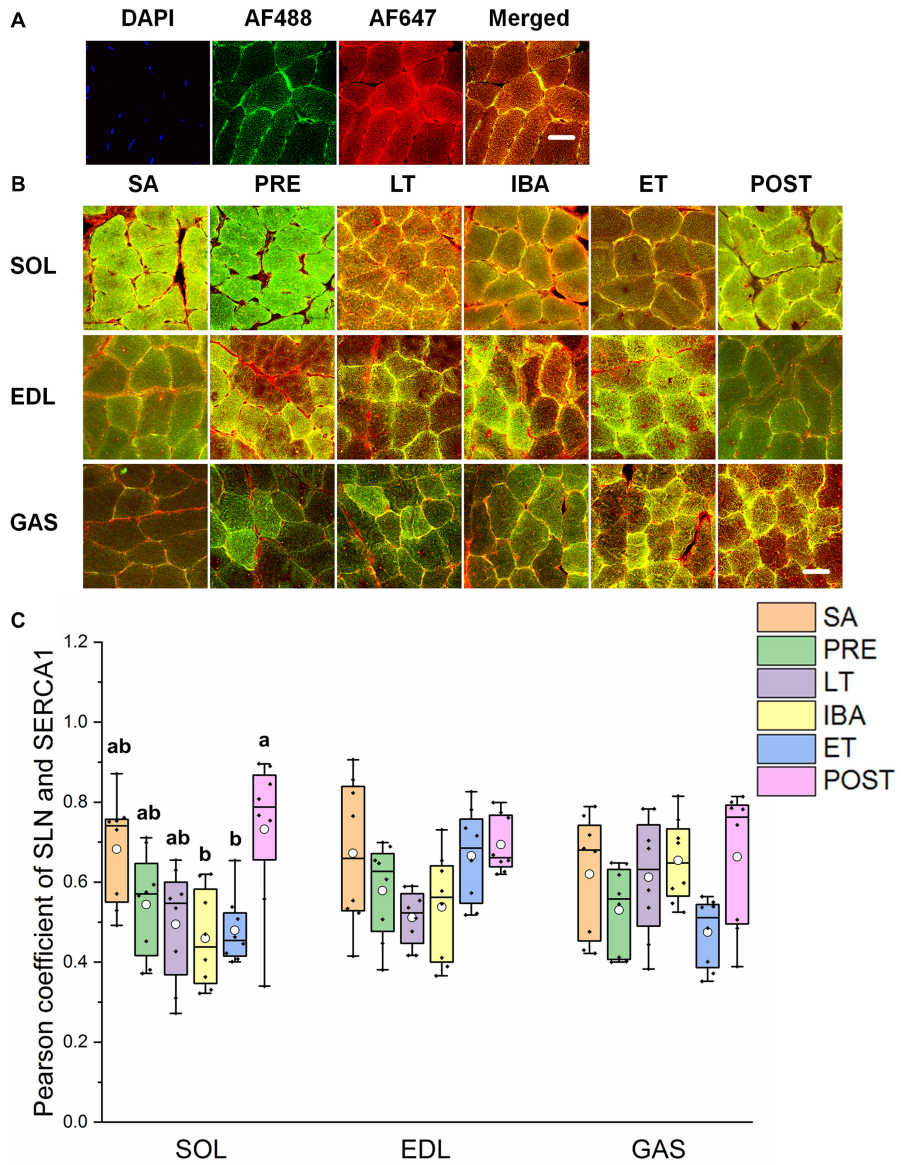

FIGURE 7 | Protein overlap levels of SLN and SERCA1 in three different types of muscle during different periods. **(A)** Reticulate subcellular distribution of SLN and SERCA1 fluorescently labeled proteins in three different types of muscle. DAPI (blue) for nuclei, AF488 (green) for SLN, 647 (red) for SERCA1. Scale bar = 20 μm. **(B)** Representative immunofluorescence of protein overlap between SERCA1 and SLN in three different types of muscle during different periods. Scale bar = 20 μm. **(C)** Box-plot representing protein overlap level of SERCA1 and SLN. Boxes represent upper and lower quartiles, middle horizontal line represents median, hollow circle represents average, lines extending from upper and lower ends represent upper and lower edges, respectively, asterisks represent extreme outliers, and points represent individual sample values. $n = 8$. SOL, soleus muscle; EDL, extensor digitorum longus; GAS, gastrocnemius muscle; SA, summer active group; PRE, pre-hibernation group; LT, late torpor group; IBA, inter-bout arousal group; ET, early torpor group; POST, post-hibernation group. Different letters (such as a and b) indicate differences between period groups ($P < 0.01$), same letters (including a and ab) indicate no differences between period groups, and no letters indicate no differences among all six period groups.

of SERCA (Asahi et al., 2002; Akin et al., 2010). Our results showed that the co-localization levels of SLN and SERCA1 did not change in the three skeletal muscles in any group, suggesting that SLN might not be involved in the regulation of SERCA activity during these periods. Calmodulin kinase 2 (CaMK2) can enhance SERCA activity through autophosphorylation (Narayanan and Xu, 1997; Vangheluwe et al., 2005). Here, results showed that the phosphorylation level of CaMK2 increased in the SOL muscle but remained unchanged/decreased in the GAS and EDL muscles in the IBA group. This suggests that the increased phosphorylation level of CaMK2 may be an upstream signaling factor for increased SERCA activity in the slow-twitch SOL muscle of the IBA group. Earlier studies have suggested that the composition of polyunsaturated fatty acids (PUFA) in the myocardial membrane of Syrian hamsters (*Mesocricetus auratus*) and dormice (*Dryomys nitedula*) participates in the

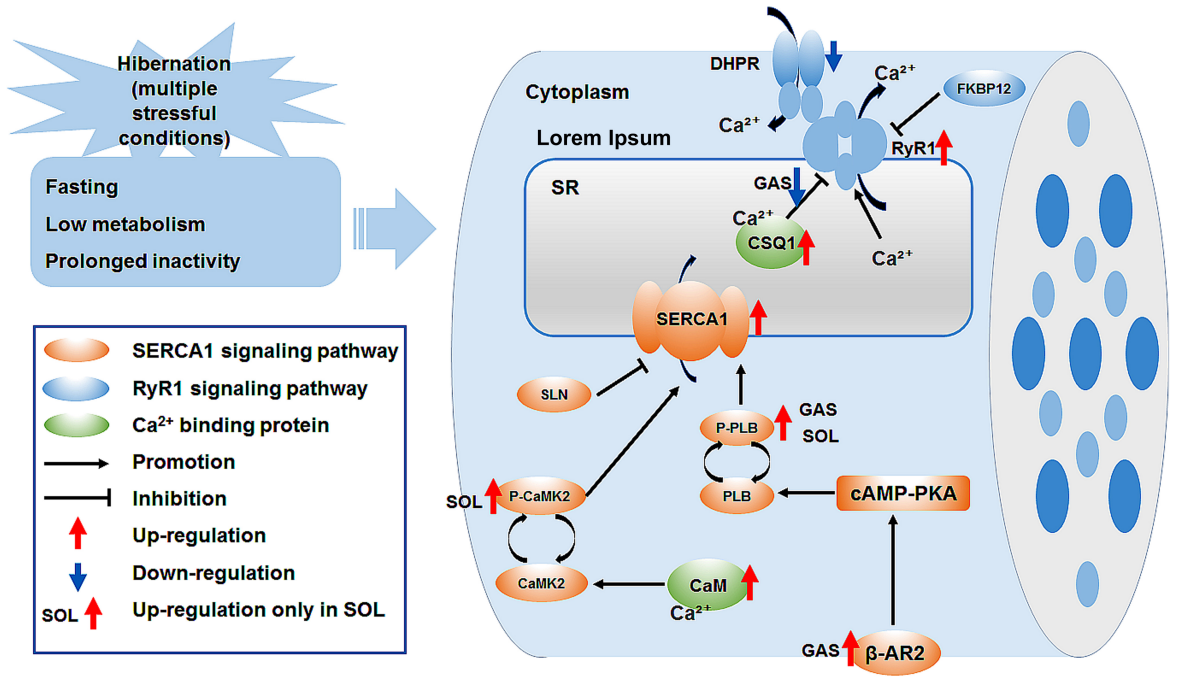

FIGURE 8 | Graphical summary of study. Ca^{2+}, calcium; SR, sarcoplasmic reticulum; DHPR, dihydropyridine receptor; FKBP12, 12kDa FK506 binding protein; RyR1, ryanodine receptor1; CSQ1, calsequestrin1; SERCA1, sarcoplasmic reticulum calcium ATPase; SLN, sarcolipin; PLB, phospholamban; P-PLB, phosphorylated phospholamban; CaM, calmodulin; CaMK2, calmodulin kinase2; P-CaMK2, phosphorylated calmodulin kinase2; β-AR2, β-adrenergic receptor 2; cAMP-PKA, cyclic adenosine monophosphate -protein kinase A signaling pathway.

regulation of SERCA activity (Giroud et al., 2013, 2018). We speculated that the up-regulation of SERCA activity in the skeletal muscle of hibernating animals may also be associated with the components of the sarcoplasmic membrane; however, this needs further study.

It should be noted that RyR1 and SERCA1 were up-regulated in all three skeletal muscles in the ET, LT, and IBA groups. This could not fully explain why the cytoplasmic Ca^{2+} level increased in the LT stage but decreased in the IBA and ET stages. This contradiction suggests that regulation of the RyR1 channel may mediate the rate of SR Ca^{2+} release, and that regulation of SERCA-mediated Ca^{2+} uptake may be another potential mechanism leading to cytoplasmic Ca^{2+} increase during certain periods of hibernation, rather than during all stages of hibernation. In addition, from the perspective of energetics (Lo Martire et al., 2018; Silvani et al., 2018), the increased cytoplasmic Ca^{2+} level in the LT group may represent an increase in futile Ca^{2+} cycling, while it is necessary to increase energy expenditure to restore Ca^{2+} homeostasis through the SERCA-RyR Ca^{2+} cycle. This may prompt the animals to arouse from torpor. In other words, the increase in cytoplasmic Ca^{2+} during LT may be one of the factors resulting in inter-bout arousal following prolonged torpor (Grabek et al., 2019). Conversely, the reduction in cytoplasmic Ca^{2+} during IBA and ET could represent a reduction in futile cycling meant to reduce energy expenditure. Therefore, further relevant experiments, including SR function and energetics, are required to explore the mechanisms involved in this interesting phenomenon.

Cytoplasmic Ca^{2+} is also involved in intracellular Ca^{2+}-binding proteins (Royer and Rios, 2009; Mekahli et al., 2011). Results showed that, compared with the SA group, the protein expression of CaM and CSQ1 in the different types of skeletal muscle increased by differing degrees, which would be beneficial for the decrease in cytoplasmic and SR free Ca^{2+} levels. This is similar to results reported in thirteen-lined ground squirrels, which show increases in protein expression in the SOL and GAS muscles during torpor (Zhang and Storey, 2016a,b).

CONCLUSION

In summary, the cytoplasmic Ca^{2+} level in skeletal muscle fiber increased, whereas the SR Ca^{2+} level decreased during late torpor. After inter-bout arousal and re-entry into torpor, the Ca^{2+} level recovered to varying degrees, indicating that intracellular Ca^{2+} is dynamic and the torpor-arousal cycle is very important for the recovery of intracellular Ca^{2+} homeostasis in the skeletal muscle of Daurian ground squirrels. The protein expression of RyR1 in skeletal muscles increased in the LT, IBA, and ET groups, suggesting that RyR1-mediated SR Ca^{2+} release may be elevated. The increase in SERCA1 and β-AR2 protein expression levels and P-PLB/PLB and P-CaMK2/CaMK2 ratios may have impacted the increase in SERCA-mediated SR Ca^{2+} uptake in the skeletal muscles of the IBA or ET groups. The high protein expression of Ca^{2+}-binding CaM and CSQ1 enhanced the free Ca^{2+}-binding capacity of skeletal

muscle in all five groups. These results suggest that the high expression of RyR1 and increased probability of RyR1 channel opening may be potential mechanisms of SR Ca^{2+} release in the cytoplasm, resulting in an increase in cytoplasmic Ca^{2+} level; while the enhanced protein expression level of SERCA1 and high expression of the two free Ca^{2+}-binding proteins may be possible mechanisms involved in the alleviation of the increase in cytoplasmic Ca^{2+} level and restoration of intracellular Ca^{2+} homeostasis (**Figure 8**).

LIMITATIONS

In this study, the protein expression levels of RyR and SERCA and their co-localization with regulatory factors only reflected the potential biological functions of the Ca^{2+} channel or pump and their possible role in cytoplasmic Ca^{2+} changes during the different stages in hibernating ground squirrels. The regulation of RyR channel-mediated SR Ca^{2+} release and SERCA-mediated Ca^{2+} uptake may be the potential mechanisms involved in the increase in Ca^{2+} observed during certain periods of hibernation, rather than in all stages of hibernation. Therefore, the biggest drawback of this study is the lack of functional RyR and SERCA data (SR Ca^{2+} release and uptake). In addition to several Ca^{2+}-handling-related proteins, cytoplasmic Ca^{2+} homeostasis is also affected by other Ca^{2+} stores (such as mitochondria) or Ca^{2+}-binding proteins (such as parvalbumin). However, as the remaining skeletal muscle samples could not satisfy the needs of these experiments, the effects of these factors on cytoplasmic Ca^{2+} homeostasis during hibernation will be explored in future work.

DATA AVAILABILITY STATEMENT

All datasets presented in this study are included in the article/ **Supplementary Material**.

ETHICS STATEMENT

Ethics approval and consent to participate all animal procedures and care and handling protocols were approved by the Committee on the Ethics of Animal Experiments of the Northwest University (Permit Number: SYXK 2010-004).

AUTHOR CONTRIBUTIONS

Y-FG, ZW, and H-PW conceived and designed the experiments. ZW, X-FM, JZ, HC, XP, and S-HX performed the experiments. ZW and X-FM analyzed the data. ZW, JZ, and Y-FG wrote the manuscript. All authors contributed to the article and approved the submitted version.

FUNDING

This work was supported by funds from the National Natural Science Foundation of China (No. 31772459) and Shaanxi Province Natural Science Basic Research Program (2018JM3015).

ACKNOWLEDGMENTS

This manuscript has been released as a pre-print at Research Square.

SUPPLEMENTARY MATERIAL

The Supplementary Material for this article can be found online at: https://www.frontiersin.org/articles/10.3389/fphys.2020.562080/full#supplementary-material

REFERENCES

Agostini, B., De Martino, L., Soltau, B., and Hasselbach, W. (1991). The modulation of the calcium transport by skeletal muscle sarcoplasmic reticulum in the hibernating European hamster. *Z. Naturforsch C J. Biosci.* 46, 1109–1126. doi: 10.1515/znc-1991-11-1229

Akin, B. L., Chen, Z., and Jones, L. R. (2010). Superinhibitory phospholamban mutants compete with Ca2+ for binding to SERCA2a by stabilizing a unique nucleotide-dependent conformational state. *J. Biol. Chem.* 285, 28540–28552. doi: 10.1074/jbc.m110.151779

Asahi, M., Kurzydlowski, K., Tada, M., and Maclennan, D. H. (2002). Sarcolipin inhibits polymerization of phospholamban to induce superinhibition of sarco(endo)plasmic reticulum Ca2+-ATPases (SERCAs). *J. Biol. Chem.* 277, 26725–26728. doi: 10.1074/jbc.c200269200

Asahi, M., Sugita, Y., Kurzydlowski, K., De Leon, S., Tada, M., Toyoshima, C., et al. (2003). Sarcolipin regulates sarco(endo)plasmic reticulum Ca2+-ATPase (SERCA) by binding to transmembrane helices alone or in association with phospholamban. *Proc. Natl. Acad. Sci. U. S. A.* 100, 5040–5045. doi: 10.1073/pnas.0330962100

Beard, N. A., Sakowska, M. M., Dulhunty, A. F., and Laver, D. R. (2002). Calsequestrin is an inhibitor of skeletal muscle ryanodine receptor calcium release channels. *Biophys. J.* 82, 310–320. doi: 10.1016/s0006-3495(02)75396-4

Donoghue, P., Ribaric, S., Moran, B., Cebasek, V., Erzen, I., and Ohlendieck, K. (2004). Early effects of denervation on Ca(2+)-handling proteins in skeletal muscle. *Int. J. Mol. Med.* 13, 767–772.

Fu, W. W., Hu, H. X., Dang, K., Chang, H., Du, B., Wu, X., et al. (2016). Remarkable preservation of Ca2+ homeostasis and inhibition of apoptosis contribute to anti-muscle atrophy effect in hibernating Daurian ground squirrels. *Sci. Rep.* 6:13.

Gao, Y. F., Arfat, Y., Wang, H. P., and Goswami, N. (2018). Muscle atrophy induced by mechanical unloading: mechanisms and potential countermeasures. *Front. Physiol.* 9:235. doi: 10.3389/fphys.2018.00235

Gao, Y. F., Wang, J., Wang, H. P., Feng, B., Dang, K., Wang, Q., et al. (2012). Skeletal muscle is protected from disuse in hibernating dauria ground squirrels. *Comp. Biochem. Physiol. A Mol. Integr. Physiol.* 161, 296–300. doi: 10.1016/j.cbpa.2011.11.009

Giroud, S., Frare, C., Strijkstra, A., Boerema, A., Arnold, W., and Ruf, T. (2013). Membrane phospholipid fatty acid composition regulates cardiac SERCA activity in a hibernator, the Syrian hamster (*Mesocricetus auratus*). *PLoS One* 8:e63111. doi: 10.1371/journal.pone.0063111

Giroud, S., Stalder, G., Gerritsmann, H., Kübber-Heiss, A., Kwak, J., Arnold, W., et al. (2018). Dietary lipids affect the onset of hibernation in the garden dormouse (*Eliomys quercinus*): implications for cardiac function. *Front. Physiol.* 9:1235. doi: 10.3389/fphys.2018.01235

Goll, D. E., Thompson, V. F., Li, H., Wei, W., and Cong, J. (2003). The calpain system. *Physiol. Rev.* 83, 731–801.

Grabek, K. R., Cooke, T. F., Epperson, L. E., Spees, K. K., Cabral, G. F., Sutton, S. C., et al. (2019). Genetic variation drives seasonal onset of hibernation in the 13-lined ground squirrel. *Commun. Biol.* 2:478.

Guo, Q., Mi, X., Sun, X., Li, X., Fu, W., Xu, S., et al. (2017). Remarkable plasticity of Na(+), K(+)-ATPase, Ca(2+)-ATPase and SERCA contributes to muscle disuse atrophy resistance in hibernating Daurian ground squirrels. *Sci. Rep.* 7:10509.

Hagemann, D., and Xiao, R. P. (2002). Dual site phospholamban phosphorylation and its physiological relevance in the heart. *Trends Cardiovasc. Med.* 12, 51–56. doi: 10.1016/s1050-1738(01)00145-1

Hindle, A. G., Otis, J. P., Epperson, L. E., Hornberger, T. A., Goodman, C. A., Carey, H. V., et al. (2015). Prioritization of skeletal muscle growth for emergence from hibernation. *J. Exp. Biol.* 218, 276–284. doi: 10.1242/jeb.109512

Hu, N. F., Chang, H., Du, B., Zhang, Q. W., Arfat, Y., Dang, K., et al. (2017). Tetramethylpyrazine ameliorated disuse-induced gastrocnemius muscle atrophy in hindlimb unloading rats through suppression of Ca2+/ROS-mediated apoptosis. *Appl. Physiol. Nutr. Metab.* 42, 117–127. doi: 10.1139/apnm-2016-0363

Hunter, R. B., Mitchell-Felton, H., Essig, D. A., and Kandarian, S. C. (2001). Expression of endoplasmic reticulum stress proteins during skeletal muscle disuse atrophy. *Am. J. Physiol. Cell Physiol.* 281, C1285–C1290.

Ingalls, C. P., Wenke, J. C., and Armstrong, R. B. (2001). Time course changes in [Ca2+]i, force, and protein content in hindlimb-suspended mouse soleus muscles. *Aviat. Space Environ. Med.* 72, 471–476.

Kraner, S. D., Wang, Q., Novak, K. R., Cheng, D., Cool, D. R., Peng, J., et al. (2011). Upregulation of the CaV 1.1-ryanodine receptor complex in a rat model of critical illness myopathy. *Am. J. Physiol. Regul. Integr. Comp. Physiol.* 300, R1384–R1391.

Lagache, T., Sauvonnet, N., Danglot, L., and Olivo-Marin, J. C. (2015). Statistical analysis of molecule colocalization in bioimaging. *Cytometry A* 87, 568–579. doi: 10.1002/cyto.a.22629

Laver, D. R. (2018). Regulation of the RyR channel gating by Ca(2+) and Mg(2). *Biophys. Rev.* 10, 1087–1095. doi: 10.1007/s12551-018-0433-4

Lee, Y. S., and Keener, J. P. (2008). A calcium-induced calcium release mechanism mediated by calsequestrin. *J. Theor. Biol.* 253, 668–679. doi: 10.1016/j.jtbi.2008.04.027

Lo Martire, V., Valli, A., Bingaman, M. J., Zoccoli, G., Silvani, A., and Swoap, S. J. (2018). Changes in blood glucose as a function of body temperature in laboratory mice: implications for daily torpor. *Am. J. Physiol. Endocrinol. Metab.* 315, E662–E670.

MacIntosh, B. R., Holash, R. J., and Renaud, J. M. (2012). Skeletal muscle fatigue - regulation of excitation-contraction coupling to avoid metabolic catastrophe. *J. Cell Sci.* 125, 2105–2114. doi: 10.1242/jcs.093674

Malysheva, A. N., Storey, K. B., Ziganshin, R. K., Lopina, O. D., and Rubtsov, A. M. (2001). Characteristics of sarcoplasmic reticulum membrane preparations isolated from skeletal muscles of active and hibernating ground squirrel *Spermophilus undulatus*. *Biochemistry* 66, 918–925.

Martin, S. L., and Yoder, A. D. (2014). Theme and variations: heterothermy in mammals. *Integr. Comp. Biol.* 54, 439–442. doi: 10.1093/icb/icu085

Mekahli, D., Bultynck, G., Parys, J. B., De Smedt, H., and Missiaen, L. (2011). Endoplasmic-reticulum calcium depletion and disease. *Cold Spring Harb. Perspect. Biol.* 3:a004317. doi: 10.1101/cshperspect.a004317

Narayanan, N., and Xu, A. (1997). Phosphorylation and regulation of the Ca(2+)-pumping ATPase in cardiac sarcoplasmic reticulum by calcium/calmodulin-dependent protein kinase. *Basic Res. Cardiol.* 92(Suppl. 1), 25–35. doi: 10.1007/bf00794065

Nicolaou, P., Hajjar, R. J., and Kranias, E. G. (2009). Role of protein phosphatase-1 inhibitor-1 in cardiac physiology and pathophysiology. *J. Mol. Cell Cardiol.* 47, 365–371. doi: 10.1016/j.yjmcc.2009.05.010

Nordeen, C. A., and Martin, S. L. (2019). Engineering human stasis for long-duration spaceflight. *Physiology* 34, 101–111. doi: 10.1152/physiol.00046.2018

Park, M. K., Petersen, O. H., and Tepikin, A. V. (2000). The endoplasmic reticulum as one continuous Ca2+ pool: visualization of rapid Ca2+ movements and equilibration. *EMBO J.* 19, 5729–5739. doi: 10.1093/emboj/19.21.5729

Royer, L., and Rios, E. (2009). Deconstructing calsequestrin. Complex buffering in the calcium store of skeletal muscle. *J. Physiol.* 587, 3101–3111. doi: 10.1113/jphysiol.2009.171934

Shaikh, S. A., Sahoo, S. K., and Periasamy, M. (2016). Phospholamban and sarcolipin: are they functionally redundant or distinct regulators of the Sarco(Endo)plasmic reticulum calcium ATPase? *J. Mol. Cell. Cardiol.* 91, 81–91. doi: 10.1016/j.yjmcc.2015.12.030

Silvani, A., Cerri, M., Zoccoli, G., and Swoap, S. J. (2018). Is adenosine action common ground for NREM sleep, torpor, and other hypometabolic states? *Physiology* 33, 182–196. doi: 10.1152/physiol.00007.2018

Thomas, A. P., Bird, G. S., Hajnoczky, G., Robb-Gaspers, L. D., Putney, J. W., Jr., (1996). Spatial and temporal aspects of cellular calcium signaling. *FASEB J.* 10, 1505–1517. doi: 10.1096/fasebj.10.13.8940296

van Breukelen, F., and Martin, S. L. (2015). The hibernation continuum: physiological and molecular aspects of metabolic plasticity in mammals. *Physiology* 30, 273–281. doi: 10.1152/physiol.00010.2015

Vangheluwe, P., Raeymaekers, L., Dode, L., and Wuytack, F. (2005). Modulating sarco(endo)plasmic reticulum Ca2+ ATPase 2 (SERCA2) activity: cell biological implications. *Cell Calcium* 38, 291–302. doi: 10.1016/j.ceca.2005.06.033

Wang, Z., Jiang, S. F., Cao, J., Liu, K., Xu, S. H., Arfat, Y., et al. (2019). Novel findings on ultrastructural protection of skeletal muscle fibers during hibernation of Daurian ground squirrels: mitochondria, nuclei, cytoskeleton, glycogen. *J. Cell Physiol.* 234, 13318–13331. doi: 10.1002/jcp.28008

Wang, Z., Xu, J. H., Mou, J. J., Kong, X. T., Wu, M., Xue, H. L., et al. (2020a). Photoperiod affects harderian gland morphology and secretion in female cricetulus barabensis: autophagy, apoptosis, and mitochondria. *Front. Physiol.* 11:408. doi: 10.3389/fphys.2020.00408

Wang, Z., Xu, J. H., Mou, J. J., Kong, X. T., Zou, J. W., Xue, H. L., et al. (2020b). Novel ultrastructural findings on cardiac mitochondria of huddling Brandt's voles in mild cold environment. *Comp. Biochem. Physiol. A Mol. Integr. Physiol.* 249:110766. doi: 10.1016/j.cbpa.2020.110766

Wu, X., Gao, Y. F., Zhao, X. H., and Cui, J. H. (2012). Effects of tetramethylpyrazine on nitric oxide synthase activity and calcium ion concentration of skeletal muscle in hindlimb unloading rats. *Zhonghua Yi Xue Za Zhi* 92, 2075–2077.

Zhang, J., Li, X., Ismail, F., Xu, S., Wang, Z., Peng, X., et al. (2019). Priority strategy of intracellular Ca(2+) Homeostasis in skeletal muscle fibers during the multiple stresses of hibernation. *Cells* 9:42. doi: 10.3390/cells9010042

Zhang, Y., and Storey, K. B. (2016a). Expression of nuclear factor of activated T cells (NFAT) and downstream muscle-specific proteins in ground squirrel skeletal and heart muscle during hibernation. *Mol. Cell Biochem.* 412, 27–40. doi: 10.1007/s11010-015-2605-x

Zhang, Y. C., and Storey, K. B. (2016b). Regulation of gene expression by NFAT transcription factors in hibernating ground squirrels is dependent on the cellular environment. *Cell Stress Chaperones* 21, 883–894. doi: 10.1007/s12192-016-0713-5

Conflict of Interest: The authors declare that the research was conducted in the absence of any commercial or financial relationships that could be construed as a potential conflict of interest.

frontiers in Physiology

ORIGINAL RESEARCH
published: 21 December 2020
doi: 10.3389/fphys.2020.615025

Regulation of Peroxisome Proliferator-Activated Receptor Pathway During Torpor in the Garden Dormouse, *Eliomys quercinus*

Alexander J. Watts[1], Samantha M. Logan[1], Anna Kübber-Heiss[2], Annika Posautz[2], Gabrielle Stalder[2], Johanna Painer[2], Kristina Gasch[2], Sylvain Giroud[2†] and Kenneth B. Storey[1*†]*

[1] Department of Biology, Carleton University, Ottawa, ON, Canada, [2] Department of Interdisciplinary Life Sciences, Research Institute of Wildlife Ecology, University of Veterinary Medicine Vienna, Vienna, Austria

OPEN ACCESS

Edited by:
Steven Swoap,
Williams College, United States

Reviewed by:
Cameron Schmidt,
East Carolina University, United States
Fritz Geiser,
University of New England, Australia

***Correspondence:**
Kenneth B Storey
kenneth.storey@carleton.ca;
KennethStorey@cunet.carleton.ca
Sylvain Giroud
sylvain.giroud@vetmeduni.ac.at

[†] These authors have contributed equally to this work

Specialty section:
This article was submitted to Integrative Physiology, a section of the journal Frontiers in Physiology

Received: 07 October 2020
Accepted: 03 December 2020
Published: 21 December 2020

Citation:
Watts AJ, Logan SM, Kübber-Heiss A, Posautz A, Stalder G, Painer J, Gasch K, Giroud S and Storey KB (2020) Regulation of Peroxisome Proliferator-Activated Receptor Pathway During Torpor in the Garden Dormouse, Eliomys quercinus. Front. Physiol. 11:615025. doi: 10.3389/fphys.2020.615025

Differential levels of n-6 and n-3 essential polyunsaturated fatty acids (PUFAs) are incorporated into the hibernator's diet in the fall season preceding prolonged, multi-days bouts of torpor, known as hibernation. Peroxisome proliferator-activated receptor (PPAR) transcriptional activators bind lipids and regulate genes involved in fatty acid transport, beta-oxidation, ketogenesis, and insulin sensitivity; essential processes for survival during torpor. Thus, the DNA-binding activity of PPARα, PPARδ, PPARγ, as well as the levels of PPARγ coactivator 1α (PGC-1α) and L-fatty acid binding protein (L-FABP) were investigated in the hibernating garden dormouse (*Eliomys quercinus*). We found that dormice were hibernating in a similar way regardless of the n-6/n-3 PUFA diets fed to the animals during the fattening phase prior to hibernation. Further, metabolic rates and body mass loss during hibernation did not differ between dietary groups, despite marked differences in fatty acid profiles observed in white adipose tissue prior and at mid-hibernation. Overall, maintenance of PPAR DNA-binding activity was observed during torpor, and across three n-6/n-3 ratios, suggesting alternate mechanisms for the prioritization of lipid catabolism during torpor. Additionally, while no change was seen in L-FABP, significantly altered levels of PGC-1α were observed within the white adipose tissue and likely contributes to enhanced lipid metabolism when the diet favors n-6 PUFAs, i.e., high n-6/n-3 ratio, in both the torpid and euthermic state. Altogether, the maintenance of lipid metabolism during torpor makes it likely that consistent activity or levels of the investigated proteins are in aid of this metabolic profile.

Keywords: PPAR, PGC-1 alpha, hibernation, fatty acids, adipose, liver

INTRODUCTION

Before the onset of predictable resource scarcity during winter, small mammals such as the garden dormouse (GD, *Eliomys quercinus*), prepare for entering a period of several bouts of multi-days torpor, i.e., hibernation, by engaging in hyperphagia and reducing their metabolic rate in the preceding fall season (Sheriff et al., 2012, 2013). Unique adaptations have evolved

to allow hibernators to suppress their global rate of metabolism while catabolizing mainly fatty acids and keeping carbohydrate stores reserved (Dark, 2005; Wu et al., 2013), in an effort to sustain themselves until spring; this is in contrast to food-storing mammals which survive on food caches (Weitten et al., 2016). By increasing their ingestion of fat-laden foods and altering circulating hormone levels, fat-storing mammalian hibernators increase their weight by around 40% usually before lowering activity levels and body temperature (T_b) in the late summer and early fall (Pengelley and Fisher, 1966; Mrosovsky, 1977; Geiser, 2016). During the hibernation season enhanced fat stores are utilized as metabolic fuels allowing them to survive the entire winter season. Notably, the enrichment of certain types of lipids, namely unsaturated fatty acids and especially n-6 polyunsaturated fatty acids (PUFA) are more beneficial for heterotherms than others and confer the ability to survive winter (see for reviews: Munro and Thomas, 2004; Dark, 2005; Ruf and Arnold, 2008; also from a large hibernator: Giroud et al., 2019); within adipocytes, due to the increased reliance on beta-oxidation for energy production, as well as in other tissues for the maintenance of membrane fluidity and proper protein functioning at low temperatures (for review, see Arnold et al., 2015; Staples, 2016; Giroud et al., 2018).

The ratio of certain fats within a mammalian hibernator's diet becomes consequential during their sustained dependence on lipid metabolism since these lipids also become incorporated and enriched in the cellular membranes of tissues that affect lipid catabolism (Geiser et al., 1994; Dark, 2005). Hibernators that consume a diet enriched with plant oils, which tend to be high in PUFAs, have lengthened torpor bouts and decreased torpid T_b, which could preserve energy for extended heterothermy (Geiser and Kenagy, 1987; Frank, 1992; Florant et al., 1993; Munro et al., 2005). Importantly, n-3 PUFAs (e.g., 18:3 n-3, i.e., α-linolenic acid, ALA) tend to effect hibernation in ways opposite to n-6 fatty acids (e.g., 18:2 n-6, i.e., linoleic acid, LA) PUFAs (Ruf and Arnold, 2008; Arnold et al., 2015). Hibernating species that are fed a diet high in n-6 but low in n-3 fatty acids are more likely to enter and remain in torpor than animals fed an equivalent amount of PUFAs but with a reversed ratio (low n-6/n-3) (Hill and Florant, 2000; Frank et al., 2008). Clearly then, the makeup of essential fatty acids consumed during the hibernator's preparatory period impacts the overall success of hibernation as a survival-strategy.

Indeed, the composition of phospholipid membranes can affect a number of intracellular pathways. One impact of lowered membrane n-3 levels is altered expression of the genes downstream of 2 transcription factor groups: the sterol-regulatory-element binding proteins (SREBPs) and peroxisome proliferator-activated receptors (PPARs) (for review see: Deckelbaum et al., 2006). Interestingly, these transcription factors are deeply involved in transcribing fatty-acid metabolism genes, as well as genes important in other processes such as inflammatory responses (Wahli and Michalik, 2012; Shimano and Sato, 2017). Given their influence over fatty acid metabolism, the regulation of PPARs has been explored in other hibernating species, including the little brown bat (*Myotis lucifugus*) and the 13-lined ground squirrel (*Ictidomys tridecemlineatus*) (Eddy and Storey, 2003; Eddy et al., 2005), wherein findings showed that PPARγ was upregulated during torpor. Upon binding a fatty acid ligand, PPARs bind a co-activator protein that allows transcription of genes containing a PPAR-response element. For instance, the cold-inducible PPARγ coactivator-1α (PGC-1α) regulates mitochondrial metabolism linking PPARα to the thermogenic capacity of tissues in a mechanism shown to be relevant in liver from hibernating jerboas (El Kebbaj et al., 2009). PPAR also regulates lipid and energy metabolism by inducing the expression of downstream genes such as fatty-acid binding protein (FABP), a key protein involved in facilitating lipid mobilization. Finally, PPAR protein and downstream gene expression is also relevant to the recruitment and activation of beige-like cells in white adipose tissue (WAT) (Chayama et al., 2018). In summary, PPARs are intricately involved in a variety of essential processes owing to the importance of this regulatory network in the context of mammalian hibernation.

When hibernators are in a hypometabolic state, gene expression for countless cellular pathways must be intricately regulated to prevent cell stress. A greater understanding of fatty acid metabolism during hibernation, when most tissues select lipids over carbohydrates as the preferred fuel source, has provided new perspectives into the survival of cells during hypometabolism and the treatment of metabolic disorders including insulin sensitivity (i.e., diabetes) and obesity (Wu et al., 2013; Logan et al., 2016). However, few studies to date have assessed the impact of diets containing different ratios of n-6 and n-3 PUFAs on fatty acid metabolism during torpor. Herein, liver, brown adipose tissue (BAT) and WAT from GD fed either a low, intermediate, or high n-6/n-3 ratio diet, were used to assess the impact of diet in the regulation of fatty acid metabolism during hibernation. Specifically, DNA binding activity of PPARs (PPARα, δ, and γ) were assessed in conjunction with total protein levels of the cofactor PGC1-α and downstream effector protein, liver-FABP (L-FABP). Altering the lipid composition of the GD's pre-hibernation diet has been shown to change the molecular phenotype displayed during hibernation in mammals (Logan et al., 2020), making it likely that molecular changes in fatty acid metabolism pathways will result from this difference.

METHODS

Animals

In total, 41 garden dormice (*Eliomys quercinus*) weighing prior to hibernation 140.0 ± 2.6 g [116-170 *g* CI] obtained from a breeding colony kept at the Research Institute of Wildlife Ecology (Vienna, Austria) were included in these experiments (**Table 1**). Animals were housed singly in cages (60 × 40 × 40 cm), each equipped with one nest, bedding and nesting material. Dormice were kept under natural fluctuations of ambient temperature (T_a) and photoperiod during their pre-hibernation fattening (September), until the hibernation period (October to January) under constant darkness, without food and water. During this time dormice were housed individually in standard laboratory cages (36 × 20 × 14 cm), each provided with a customized nest

TABLE 1 | Sample sizes of the different measurements and analyses conducted during the hibernation experiments.

Categories	Hibernation			Mid-hibernation		Dietary groups
	Metabolic rates	T_b patterns	Lipid profiles	Molecular assessments		
Group sample sizes	$n = 24$	$n = 32$		$n = 16$		$n = 8$ (4) Low $n = 8$ (7) Inter $n = 8$ (5) High
				–		$n = 2$ Low $n = 4$ Inter $n = 2$ High
	–	–		$n = 9$ with T_b only at mid-hibernation		$n = 3$ Low $n = 1$ Inter $n = 5$ High
Total analyses sample sizes	$n = 24$	$n = 32$		$n = 41$	$n = 25$	$n = 13$ (7) Low $n = 13$ (8) Inter $n = 15$ (10) High

Specific sample sizes are also indicated for each of the dietary groups, i.e., low n-6/n-3 ('Low'), intermediate n-6/n-3 ('Inter'), and high n-6/n-3 ('High') fatty acid diets. Numbers given in parentheses indicate sample sizes of the molecular analyses for each dietary group when different from the group sample sizes. Lipid profiles were assessed prior to hibernation and at mid-hibernation (sacrifices). In total, 41 garden dormice were included in the overall experiments.

and bedding material, and kept at 4°C in ventilated cooling units (Liebherr GKv 5730).

Ethics Statement

All procedures were approved by the institutional ethics committee and the national Austrian authority in accordance to the Austrian Animal Experimentation Act, 'Tierversuchsgesetz 2012' (BMBWF-68.205/0137-WF/V/3b/2014).

Protocol Overview

During the pre-hibernation fattening period, the 41 dormice were fed one of the three specific lipid diets (see below for further details), and then implanted with T_b transmitters prior to hibernation (see below for further details). After recovery from surgeries and once animals had spontaneously expressed torpor, hibernation was induced by housing the animals at 4°C without food and water. The readiness of dormice to enter prolonged torpor or hibernation was evaluated via measurements of the body mass and food intake of the individuals prior to hibernation. Once dormice attained a plateau for body mass and food intake was largely reduced, we considered that the individuals were extensively using torpor likely entering multiday torpor bouts, as previously shown in juvenile garden dormice prior to hibernation (Giroud et al., 2012, 2014; Mahlert et al., 2018). During the 3 months of experiments, core T_b via temperature transmitters was measured continuously in 32 dormice and metabolic rate (MR) using respirometry was recorded in 24 animals out of the 41 studied individuals, from which fatty acid compositions of WAT were determined at both pre- and mid-hibernation (see **Table 1** for details). Nine additional animals that were also implanted with T_b transmitters, were recorded for core T_b during at least two bouts before sacrifices at mid-hibernation. Molecular data were assessed in a subset ($n = 16$) of the 32 individuals continuously followed for T_b during hibernation, and from the extra-animals ($n = 9$) from which T_b was recorded shortly before sacrifices, leading to a total of 25 dormice investigated for molecular aspects (see **Table 1** for details). Animals were sacrificed at mid-winter (December to January), when torpor bout lengths are maximal, either in torpor or during interbout euthermia, by immediate decapitation (if torpid; T_b: 4.55 ± 0.15°C measured via implanted transmitters) or by CO_2-euthanasia then decapitation (if euthermic, T_b: 37.05 ± 0.13°C measured via implanted transmitters). Tissues were quickly sampled and immediately flash frozen in liquid nitrogen (−196°C) and stored at −80°C for 4-12 months until shipped to Carleton University on dry ice.

Diets

The fatty acid composition of the diets is summarized in Logan et al. (2020). During the fattening phase, dormice were fed one of the three specific diets, each differing in its lipid composition, made by adding either a 10% w/w of linseed oil as the source of n-3 fatty acids (notably ALA 18:3 n-3), or a 10% w/w of safflower oil as the source of n-6 fatty acids (mainly LA 18:2 n-6), or adding a 5% w/w of linseed oil and a 5% w/w of safflower oil to pellets the animals were accustomed to (Topix, Saturn Petcare GmbH, Bremen, Germany). Details of the exact composition of the colony diet is available in Mahlert et al. (2018). These preparations produced a chow with either low, intermediate or high amounts of LA or n-6 PUFAs, (described as such) but reversely mirrored by the contents of ALA or n-3 PUFAs (see **Table 2** for summary). Fresh pellets (kept in sealed bags filled with nitrogen at −80°C) were fed to the animals every 2 days, and uneaten food was discarded. During the September fattening phase, each group of dormice was fed their respective experimental diet for at least 14 days, which was previously shown to be sufficient to ensure maximum changes in the fatty acid composition of membranes and tissues in small rodents (Swanson and Kinsella, 1986; Swanson et al., 1987). Access to the specific lipid diets was maintained until dormice were moved to the hibernating cooling units where both food and

TABLE 2 | Proportions of Linoleic acid (LA) and Linolenic acid (ALA) of linseed oil- ('Low LA' or 'High ALA'), safflower oil- ('High LA' or 'Low ALA') and linseed/safflower oil ('Inter LA' or 'Inter ALA') -enriched diets as fed to garden dormice for at least two weeks prior to hibernation.

FATTY ACIDS	DIETS		
	Low LA or High ALA	Inter LA or Inter ALA	High LA or Low ALA
Linoleic acid (18:2 n-6)	19.28	35.55	52.95
Linolenic acid (18:3 n-3)	31.92	17.16	1.35
n-6 PUFA	19.62	35.87	53.29
n-3 PUFA	32.20	17.47	1.71
n-6/n-3	0.61	2.06	31.50
LA/ALA	0.61	2.08	41.22

The sums of n-6 or n-3 PUFA, as well as the ratios between n-6 and n-3 PUFA or LA and ALA of the three specific diets are also indicated. Fatty acid proportions are expressed as% of total fatty acids. Values are means from four analyses per diet. Data were extracted from ***Table 1*** *in Logan et al. (2020).*

water were entirely and permanently removed during the entire hibernation experiments.

Surgical Implantations of Transmitters and Body Temperature Measurements

Prior to hibernation experiments, the animals were implanted with small temperature transmitters and core T_b was monitored via a telemetry system. TA-F10 transmitters (1.1cc, 1.6g, accuracy: 0.15°C; Data Sciences International, St Paul, United States) were calibrated prior to implantation between 0 and 40°C in a temperature-controlled water bath. Surgery proceeded as previously described (Giroud et al., 2018). In short, transmitters were surgically implanted under anesthesia induced by subcutaneous 50 mg kg^{-1} ketamine (Ketamidor® 10%, Richter Pharma, Wels, Austria) and 5 mg kg^{-1} xylazine (Rompun® 2%, Bayer, Leverkusen, Germany) injection, which was maintained using 1.5% isoflurane via facemask. A subcutaneous administration of 5 mg kg^{-1} ketoprofen (Romefen® 10%, Merial S.A.S., Toulouse, France) was provided as post-operative analgesic. Upon surgical implantation of the temperature transmitters, a small amount (10-30 mg) of subcutaneous WAT were collected from each animal. WAT-samples were flash-frozen in liquid nitrogen and stored at −80°C until subsequent analysis of fatty acid composition. Following surgery, animals recovered for ten days before starting temperature recordings. An RPC-1 receiver board (Data Sciences International) was positioned under each individual cage to collect transmitter data. A 10s T_b measurement was recorded every 5 min, and data was analyzed using the Dataquest software (LabPro Data Sciences). Several parameters were derived from the temperature recordings. We assessed the onset of hibernation as the time between the food removal in cooling units at 4°C and entrance into the first torpor bout with a T_b threshold of 18°C and lasting at least for 24h. We further determined the number of arousals, mean and total arousal and torpor durations (with a T_b threshold of 18°C), as well as minimal T_b during torpor.

Metabolic Rate Measurement

Metabolic rate or oxygen consumption (VO_2 in ml O_2 h^{-1}) was assessed using an open-flow respirometry system, as previously described in Nowack et al. (2019) with the following modifications. We used a dual-channel electrochemical oxygen analyzer (FC-2 differential oxygen analyzer Oxzilla, Sable System, Las Vegas, United States[1]), which was calibrated once prior to the experiments with nitrogen for zero-oxygen value. During the hibernation experiments, we used the auto-calibration function of Oxzilla to reset the oxygen concentration to reference air at regular intervals. Air was pumped through the respirometry chamber (pulled mode) by mean of membrane pumps with a flow rate of ∼40 L h^{-1}. Relative humidity was measured in sampled air and used for correction within the calculations. VO_2 was measured in a group of 24 dormice (eight from each dietary group), where six individuals were measured in parallel. Oxygen measurements were corrected for drift of the analyzer by automated switching to reference air at regular intervals. MR was computed using a self-written R-program including the following equation VO_2 (L O_2 h^{-1}) = FD*(FIO_2-FEO_2)/(1-FIO_2*(1-RQ)), where FD = dry flow, FIO_2 = fraction O_2 concentration in the incoming airflow, FEO_2 = fraction O_2 concentration in the outgoing airflow, RQ = respiratory quotient, by Lighton (2008), assuming a RQ of 0.7. From VO_2 measurements, we visually determined interbout euthermic phases and computed the averaged MR during interbout euthermia ('mean euthermic MR'). Then, we defined a VO_2 threshold for torpor bouts as 25% of the mean euthermic MR and computed the averaged MR during torpor ('mean torpid MR') which includes VO_2 values below the threshold. We further calculated the averaged MR during the entire hibernation experiments, i.e., from multiday torpor-arousal cycles ('mean hibernating MR') over the experiments.

Lipid Analysis

Total lipids were extracted from WAT at both pre-hibernation (i.e., during surgeries) and mid-hibernation following the procedure of Folch et al. (1957). Since triglyceride fatty acids represent more than 95% of total lipids in rodent WAT (Florant et al., 1990), triglycerides and phospholipids in WAT were not separated prior to analysis. Samples were trans-esterified with a one-step method (Lepage and Roy, 1986; Eder, 1995). As previously described by Giroud et al. (2018), Fatty acid methyl esters (FAME) were identified by gas-liquid chromatography using a FID AutoSystem XL autosampler chromatograph (Perkin-Elmer, Traiskirchen, Austria) equipped with a 30 m × 0.25 mm × 0.25 µm HP INNOWax capillary column, using the following parameters: injector 240°C, column 130–180°C at 4°C/min, 180–200°C at 3°C/min, 200–240°C at 15°C/min, 240°C for 8 min. The relative fatty acid composition was quantified using Supelco external FAME standards (Sigma-Aldrich Handels GmbH, Vienna, Austria) run after every 20 samples and Turbochrom 6.3 software (Perkin Elmer). The concentrations of single fatty acids were calculated as mass% of total identified peaks for 13 fatty acids that had a chain

[1]https://www.sablesys.com

length of between 14 and 22. We further computed the sums of PUFAs, monounsaturated fatty acids (MUFA), saturated fatty acids (SFA), n-6 or n-3 PUFAs, as well as the ratio between n-6 and n-3 PUFA (n-6/n-3).

Total Protein Extraction

Total soluble protein was extracted from frozen liver, WAT and BAT. Frozen tissue was weighed (∼50-75 mg) and homogenized using a dounce-homogenizer in ice-cold cell lysis buffer (EMD Millipore, Billerica, MA; catalog No. 43-040) with added phosphatase (1 mM Na_3VO_4, 10 mM ß-glycerophosphate and 10 mM NaF) and protease (BioShop; catalog No. PIC001) inhibitors, using ratios of 1:5 (w/v) for liver and BAT and 1:3 (w/v) for WAT. Cell lysis was allowed to proceed on ice for 30 min with occasional agitation, before centrifuging for 20 min at 4°C and 12 000 × *g*. Total soluble protein was collected as the supernatant. A Bradford assay (Bio-Rad; catalog No. 500-0005) was employed to determine protein concentrations from tissue extracts and to standardize samples to 10 μg/μl before storage at −80°C.

Analysis of PPAR DNA-Binding Activity

The activity of several PPAR targets relevant to fatty acid metabolism were investigated in total protein extracts from aroused (control) and torpid garden dormouse. Measurements of DNA binding activity were conducted for PPARα, PPARδ, PPARγ (Abcam, Cambridge, MA, United States; catalog Nos. ab133107, ab133106, and ab133101, respectively), as previously published (Sharif et al., 2014; Ghosh et al., 2019; Jiang et al., 2020). DNA binding activity was measured according to the manufacturer's protocol. Following quality control and validation studies (i.e., determination of optimal protein load), consistent amounts of extracted protein (100 μg per well) were combined with the provided transcription factor binding buffer. Standardized total protein extracts were applied to microplate containing a specific double-stranded DNA probe containing the peroxisome proliferator response element (PPRE) immobilized in the bottom of the wells. Samples were incubated overnight at 4°C and provided primary and secondary antibodies were added following washes with the supplied wash buffer. Absorbance in each well was read at 450 nm using a Powerwave HT spectrophotometer (BioTek; Winooski, VT, United States). Wells with additional transcription factor binding buffer instead of protein extracts were run alongside the assay to act as negative controls as per the manufacturer's instructions.

Analysis of FABP and PGC-1 Levels

Protein levels of FABP and PGC-1α were also investigated in both aroused (control) and torpid conditions. FABP measurements were conducted in liver and made use of the Mouse Liver-FABP ELISA Kit (Abcam; catalog No. ab218262). For FABP measurements, 0.25 μg of protein per well was incubated with an antibody cocktail containing both primary and secondary antibodies for 1 h. Following the addition of TMB substrate for 10 min, the absorbance in each well was then read at 450 nm using a Powerwave HT spectrophotometer (BioTek, Winooski, VT, United States).

TABLE 3 | Parameters of linear mixed-effects models with animal ID as random factor for the effects of diet treatment ('Diet'), time ('Time,' pre-hibernation vs. mid-hibernation), and their interaction ('Diet*Time') on fatty acid proportions (% of total fatty acids) and ratios of certain fatty acid proportions from white adipose tissue total lipids of garden dormice fed one of the three diets contrasting in their n-6/n-3 PUFA ratio.

Fatty acids	Diet		Time		Diet*Time	
	***F*-Value**	***p*-Value**	***F*-Value**	***p*-Value**	***F*-Value**	***p*-Value**
C14:0	0.70	0.54	0.82	0.44	0.66	0.66
C15:0	3.14	0.07	0.75	0.44	2.64	0.24
C16:0	2.18	0.16	124.14	*<0.001*	0.18	0.89
C16:1 n-7	4.71	*0.026*	19.62	*<0.001*	1.23	0.48
C17:0	1.65	0.25	1.39	0.32	1.55	0.42
C18:0	0.04	0.96	32.63	*<0.001*	4.59	*0.06*
C18:1 n-9	17.21	*<0.001*	0.51	0.51	9.49	*<0.001*
C18:2 n-6	250.91	*<0.001*	72.60	*<0.001*	1.13	0.50
C18:3 n-3	797.18	*<0.001*	10.66	*0.003*	0.73	0.66
C20:4 n-6	9.85	*0.008*	17.97	*<0.001*	1.70	0.42
C20:5 n-3	5.43	*0.015*	20.07	*<0.001*	9.24	*<0.001*
C22:5 n-3	4.48	*0.029*	7.10	*0.015*	4.30	0.07
C22:6 n-3	4.36	*0.029*	17.35	*<0.001*	2.17	0.31
PUFA	17.05	*<0.001*	27.27	*<0.001*	10.34	*<0.001*
MUFA	16.32	*<0.001*	0.28	0.60	8.96	*<0.001*
SFA	1.34	0.30	51.11	*<0.001*	0.12	0.89
n-6	253.22	*<0.001*	69.14	*<0.001*	1.27	0.49
n-3	692.41	*<0.001*	11.87	*0.002*	0.55	0.69
n-6/n-3	699.08	*<0.001*	32.60	*<0.001*	0.22	0.89

'PUFA' refers to polyunsaturated fatty acids, 'MUFA' to monounsaturated fatty acids, 'SFA' to saturated fatty acids, 'n-6' to the sum of n-6 PUFA, 'n-3' to the sum of n-3 PUFA, and 'n-6/n-3' to the ratio between the sum of n-6 PUFA and the sum of n-3 PUFA. Significant p-Values are shown in italic.

PGC-1 measurements were conducted using 2.5 μg of protein per well; incubated for 2 h in pre-coated ELISA wells using the mouse PPARGC1A ELISA kit (MyBioSource, San Diego, CA, United States; catalog No. MBS707053). Manufacturer-provided primary and secondary antibodies were incubated for 1 h each following washes and well absorbance was detected at 450 nm using a Powerwave HT spectrophotometer (BioTek) following 7 min of color development with TMB. Wavelength correction was applied using additional readings at 540 nm and 570 nm. For both ELISA assays, wells with additional sample diluent buffer instead of protein extracts were assayed as negative controls as per the manufacturer's instructions.

Statistical Analysis

We used R 3.5.1 (R Core Team, 2018) to perform statistical analyses of fatty acid composition, hibernating patterns, MRs, body mass loss over the hibernation experiments. The distribution of statistical model residuals was assessed by inspecting quantile-quantile-plots and histograms. When necessary, response variables were Box-Cox transformed to achieve normality. We used linear mixed-effects models (R package 'nlme') (Pinheiro et al., 2014) with animal ID as random factor to test effects of dietary treatment (low, intermediate and high LA) and time (pre-hibernation vs.

TABLE 4 | Fatty acid proportions (% of total fatty acids), prior to and at mid-hibernation of white adipose tissue total lipids (means ± standard error), and ratios of certain fatty acid proportions of garden dormice fed diets of either low ('LOW'), intermediate ('INTER') or high n-6/n-3 PUFA ratio ('HIGH').

Fatty acid	Pre-hibernation			Mid-hibernation		
	LOW	INTER	HIGH	LOW	INTER	HIGH
C14:0	1.58 ± 0.14	1.63 ± 0.11	1.63 ± 0.07	1.58 ± 0.08	1.63 ± 0.05	1.59 ± 0.05
C15:0	0.03 ± 0.01	0.02 ± 0.01	0.01 ± 0.01	0.08 ± 0.05	0.06 ± 0.02	0.01 ± 0.01
C16:0	12.31 ± 0.82	12.96 ± 0.45	12.80 ± 0.37	9.89 ± 0.58*	10.65 ± 0.29*	10.66 ± 0.22*
C16:1 n-7	4.84 ± 0.12^{a}	5.26 ± 0.21^{a}	4.65 ± 0.23^{a}	4.56 ± 0.16^{ab}	4.65 ± 0.20^{a}	3.95 ± 0.16^{b}
C17:0	0.05 ± 0.02	0.06 ± 0.02	0.03 ± 0.01	0.14 ± 0.06	0.06 ± 0.02	0.03 ± 0.02
C18:0	2.15 ± 0.08^{a}	2.09 ± 0.07^{a}	1.95 ± 0.08^{a}	2.27 ± 0.08^{a}	2.28 ± 0.08^{a}	2.40 ± 0.11^{a*}
C18:1 n-9	46.57 ± 0.96^{a}	45.48 ± 0.70^{ab}	42.82 ± 1.05^{b}	49.46 ± 0.77^{a}	45.03 ± 0.44^{b}	41.68 ± 0.65^{b}
C18:2 n-6	14.04 ± 0.73^{a}	22.85 ± 0.69^{b}	34.76 ± 1.12^{c}	15.51 ± 0.48^{a}	26.71 ± 0.59^{b*}	39.79 ± 0.79^{c}
C18:3 n-3	17.85 ± 1.07^{a}	9.09 ± 0.56^{b}	0.91 ± 0.17^{c}	16.18 ± 0.51^{a}	8.54 ± 0.36^{b}	0.56 ± 0.04^{c}
C20:4 n-6	0.27 ± 0.02^{a}	0.29 ± 0.01^{ab}	0.38 ± 0.02^{b}	0.19 ± 0.02^{a}	0.26 ± 0.03^{ab}	0.28 ± 0.02^{b*}
C20:5 n-3	0.13 ± 0.04^{a}	0.09 ± 0.02^{a}	0.01 ± 0.01^{b}	0.04 ± 0.01^{a*}	0.04 ± 0.01^{a}	0.02 ± 0.01^{a}
C22:5 n-3	0.07 ± 0.02^{a}	0.07 ± 0.02^{a}	0.01 ± 0.01^{b}	0.04 ± 0.01^{a}	0.05 ± 0.01^{a}	0.02 ± 0.01^{a}
C22:6 n-3	0.09 ± 0.03^{ab}	0.11 ± 0.03^{a}	0.03 ± 0.01^{b}	0.04 ± 0.02^{a}	0.04 ± 0.02^{a*}	0.01 ± 0.01^{a}
PUFA	32.47 ± 0.82^{a}	32.51 ± 1.05^{a}	36.11 ± 1.05^{b}	32.54 ± 0.54^{a}	36.05 ± 0.79^{b}	40.33 ± 0.83^{c*}
MUFA	51.41 ± 1.02^{a}	50.74 ± 0.87^{b}	47.47 ± 1.22^{b}	54.02 ± 0.67^{a}	49.68 ± 0.58^{a}	45.63 ± 0.76^{b}
SFA	16.12 ± 0.98	16.76 ± 0.51	16.42 ± 0.47	13.96 ± 0.62*	14.68 ± 0.30*	14.69 ± 0.33*
Σ n-6	14.31 ± 0.74^{a}	23.14 ± 0.68^{b}	35.14 ± 1.13^{c}	15.70 ± 0.47^{a}	26.97 ± 0.59^{b*}	39.07 ± 0.79^{c*}
Σ n-3	18.14 ± 1.12^{a}	9.36 ± 0.62^{b}	0.96 ± 0.17^{c}	16.30 ± 0.51^{a}	8.67 ± 0.39^{b}	0.61 ± 0.05^{c}
n-6/n-3	0.85 ± 0.10^{a}	2.60 ± 0.18^{b}	46.78 ± 3.45^{c}	0.98 ± 0.06^{a}	3.19 ± 0.17^{b*}	70.21 ± 5.37^{c*}

'PUFA' refers to polyunsaturated fatty acids, 'MUFA' to monounsaturated fatty acids, 'SFA' to saturated fatty acids, 'n-6' to the sum of n-6 PUFA, 'n-3' to the sum of n-3 PUFA, and 'n-6/n-3' to the ratio between the sum of n-6 PUFA and the sum of n-3 PUFA. Groups differing significantly with $p < 0.05$ (Tukey-like post hoc comparisons) are denoted by different superscript letters for differences between diets and by stars for differences between times (pre- vs. mid-hibernation) when it applies.

TABLE 5 | Variables of hibernating patterns, metabolic rate (MR), and overwinter body mass (means ± standard error) of garden dormice fed diets of either low ('LOW'), intermediate ('INTER'), or high n-6/n-3 PUFA ratio ('HIGH').

Variables	LOW	INTER	HIGH	ANOVA	
				F-value	*p*-Value
Hibernation Onset (days)	1.5 ± 0.3	1.6 ± 0.2	1.5 ± 0.1	0.55	0.58
Number of arousals	10.8 ± 0.7	10.3 ± 0.7	11.6 ± 0.7	1.3	0.28
Mean arousal duration (h)	6.9 ± 0.3	7.0 ± 0.3	6.4 ± 0.2	1.74	0.19
Total arousal duration (h)	73.0 ± 5.3	71.1 ± 5.4	74.0 ± 6.2	0.01	0.90
Mean torpor duration (h)	192.6 ± 6.8	193.7 ± 6.4	183.1 ± 10.4	0.50	0.61
Total torpor duration (h)	2171.2 ± 169.7	2117.2 ± 163.3	2241.4 ± 185.6	0.01	0.79
Minimal body temperature (°C)	4.31 ± 0.58	4.83 ± 0.21	4.02 ± 0.11	1.87	0.20
Mean torpid MR (ml O_2 h^{-1})	6.1 ± 0.5	5.3 ± 0.6	6.4 ± 0.6	0.98	0.39
Mean euthermic MR (ml O_2 h^{-1})	321.0 ± 23.0	288.7 ± 23.7	319.6 ± 18.9	0.69	0.51
Mean hibernating MR (ml O_2 h^{-1})	18.1 ± 1.5	14.7 ± 1.9	17.5 ± 2.0	1.27	0.30
Mid-hibernation body mass (g)	110.4 ± 3.6	115.6 ± 4.0	112.7 ± 4.5	2.14	0.14

Pre-hibernation body mass was accounted as a random factor in models for hibernating patterns and as a fixed factor in the model for body mass at mid-hibernation. Body mass was also entered as random factor in models for MRs. Further, hibernation duration was included as a random factor in the model for number of arousals as well as for total arousal and torpor durations. Significant p-Values are shown in italic. Groups differing significantly with $p < 0.05$ (Tukey-like post hoc comparisons) are denoted by different superscript letters when it applies.

mid-hibernation) on WAT fatty acid composition. We reused previously published data of WAT fatty acid composition at pre-hibernation from Logan et al. (2020) into the analyses to compare changes in fatty acid composition during the experimental hibernation period. All *p*-values from linear mixed-effects models were adjusted for multi-comparisons between fatty acid proportions using False Discovery Rate (Benjamini and Hochberg, 1995). Tukey-like *post hoc* multiple comparison tests (R package 'multicomp') (Hothorn et al., 2008) were applied to test for specific differences between dietary groups and periods. Dietary effects on body mass loss over hibernation was also tested by using a linear mixed-effects model with post-hibernation bod mass as a response variable and pre-hibernation body mass along with diet treatment

as fixed factors. We further employed linear mixed-effects models with pre-hibernation body mass as a random factor to test effects of diets on variables derived from the hibernating patterns and MR measurements. Because dormice were sacrificed within a two-week period, individual duration of experimental hibernation was included as a random factor in the model for the number of arousals as well as total arousal and torpor durations.

Fold change values of molecular variables were calculated by comparing the difference between a particular diet (low, intermediate or high) to the euthermic intermediate value which is normalized to 1.0, or by comparing differences in the state (aroused or torpid) to the same. For example, the fold change for the low diet value was compared to the intermediate diet value, expressed as low/intermediate, and where a fold change > 1 represents an increase, while a fold decrease is expressed as the percentage decrease and represents a fold change < 1. All numerical data are expressed as mean with data points ($n = 4$ samples from independent animals) and were graphed using ggplot2 in R (v. 3.6.1) (Wickham, 2016). Statistical analysis of differences between experimental hibernation time-points was performed using a one-way ANOVA and *post hoc* Tukey tests using RBioPlot statistical package (Zhang and Storey, 2016) with $p < 0.05$ accepted as significant. All reported values are means ± SE.

RESULTS

WAT Lipid Profiles Prior to Hibernation and at Mid-Hibernation

After at least 14 days of feeding specific diets contrasting in their n-6 to n-3 PUFA ratio during the fattening phase, the pre-hibernation WAT fatty acid composition of dormice substantially differed between dietary groups (**Tables 3**, **4**). Specifically, proportions of 18:2 n-6 (LA) and 18:3 n-3 (ALA) were significantly higher and lower, respectively, in WAT of dormice fed diets with increased n-6/n-3 PUFA (**Table 3**). These differences led to contrasted sums of n-6 or n-3 PUFA and n-6/n-3 ratios between the three dietary groups. We further found lower proportions of 20:4 n-6 and higher levels of 18:1 n-9 in WAT of dormice fed a low n-6/n-3 diet compared to high n-6/n-3 diet-fed individuals, while proportions of those fatty acids in WAT of intermediate n-6/n-3 diet-fed individuals did not differ from the other two groups (**Table 3**). Also, long-chain n-3 fatty acids, namely 20:5 n-3, 22:5 n-3, and 22:6 n-3, were significantly in higher proportions in WAT of dormice

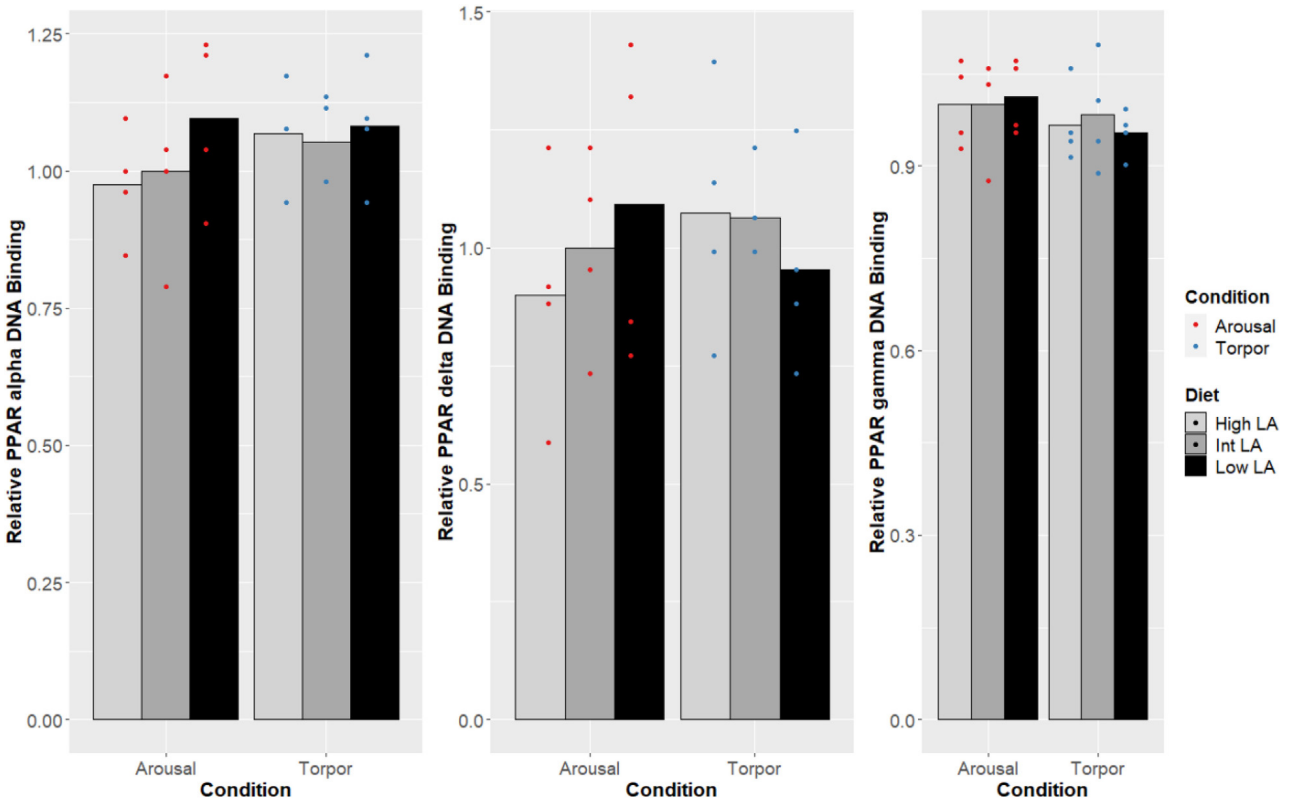

FIGURE 1 | Response of PPAR pathway targets in GD WAT to low, intermediate or high levels of LA (or of mirrored levels of ALA) within the pre-hibernation diet. Histogram shows the relative DNA-binding levels, assessed as the average absorbance of the intermediate diet in the euthermic animals relative to the other conditions. Data are presented as the mean along with individual data points ($n = 4$), where a significant difference is shown by a difference in the label above the corresponding bar, as assessed by one-way ANOVA and Tukey's *post hoc* analysis ($P < 0.05$). The absence of a label indicates no significant difference.

fed a low or an intermediate n-6/n-3 diet compared to those from individuals fed a high n-6/n-3 diet. Finally, WAT levels of all SFAs as well as the sum of SFA were similar across all dietary groups.

During hibernation and at mid-hibernation, both LA and ALA proportions in WAT were still differing significantly between the three dietary groups, with higher levels of LA and lower proportions of ALA in WAT of dormice fed a high n-6/n-3 diet, levels which were mirrored in WAT of low n-6/n-3 diet fed individuals (**Table 3**). Interestingly, LA proportions in WAT increased by 14% on average, during the hibernation experiments, across all three dietary groups, although LA proportions only significantly differed in dormice fed an intermediate n-6/n-3 diet (**Tables 3**, **4**). At mid-hibernation, the differences in the sum of n-6 or n-3 PUFA proportions as well as the n-6/n-3 ratio remained significant between the three dietary groups, while the sum of n-6 PUFAs and the n-6/n-3 ratio were increased by respectively 35% and 50% in WAT of dormice fed an intermediate or a high n-6/n-3 diet (**Table 4**). Further, proportions of 20:4 n-6 and 18:1 n-9 remained significantly lower and higher, respectively, in WAT of dormice fed a low n-6/n-3 diet than when fed a high n-6/n-3 diet, while WAT proportions of 20:4 n-6 were substantially reduced by 32% during hibernation in individuals fed a high n-6/n-3 lipid diet. Among SFAs, WAT proportions of several fatty acids were significantly affected, including 16:0 that decreased by 22% on average across all dietary groups, leading to 12% lowering of WAT proportions of the sum of SFA during the hibernation trial (**Tables 3**, **4**). Also, dormice fed a low or an intermediate n-6/n-3 diet substantially reduced along hibernation their WAT proportions of long-chain fatty acids, i.e., 20:5 n-3, 22:5 n-3, and 22:6 n-3; levels which did not differ anymore significantly between the three dietary groups at mid-hibernation.

Hibernating Patterns, Metabolic Rates, and Body Mass Loss

We found no significant differences of hibernating patterns during the experiments between dormice fed diets contrasting in their n-6/n-3 PUFA ratio during the fattening period (**Table 5**). Further, neither the mean torpid MR, nor the mean euthermic MR or hibernating MR, accounted for body mass variations, differed between the animals during the hibernation trial (**Table 5**). Although we observed a significant body mass loss in the hibernating dormice (pre- vs. mid-hibernation: 140.0 ± 2.6 g vs. 113.1 ± 2.3 g; F = 112.5, $p < 0.001$), the dietary treatment prior to hibernation did not affect body mass loss of the individuals over hibernation (**Table 5**).

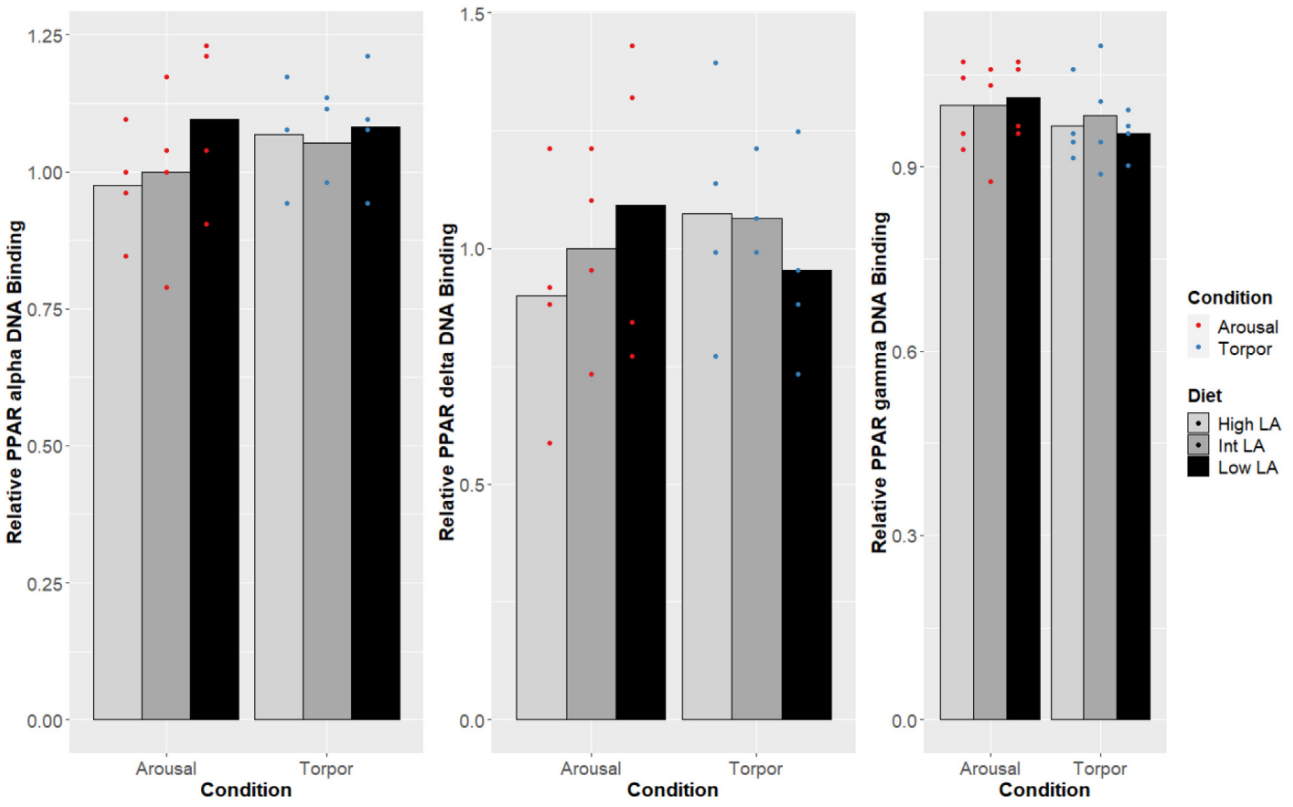

FIGURE 2 | Response of PPAR pathway targets in GD BAT to low, intermediate or high levels of LA (or of mirrored levels of ALA) within the pre-hibernation diet. Histogram shows the relative DNA-binding levels, assessed as the average absorbance of the intermediate diet in the euthermic animals relative to the other conditions. Data are presented as the mean along with individual data points ($n = 4$), where a significant difference is shown by a difference in the label above the corresponding bar, as assessed by one-way ANOVA and Tukey's *post hoc* analysis ($P < 0.05$). The absence of a label indicates no significant difference.

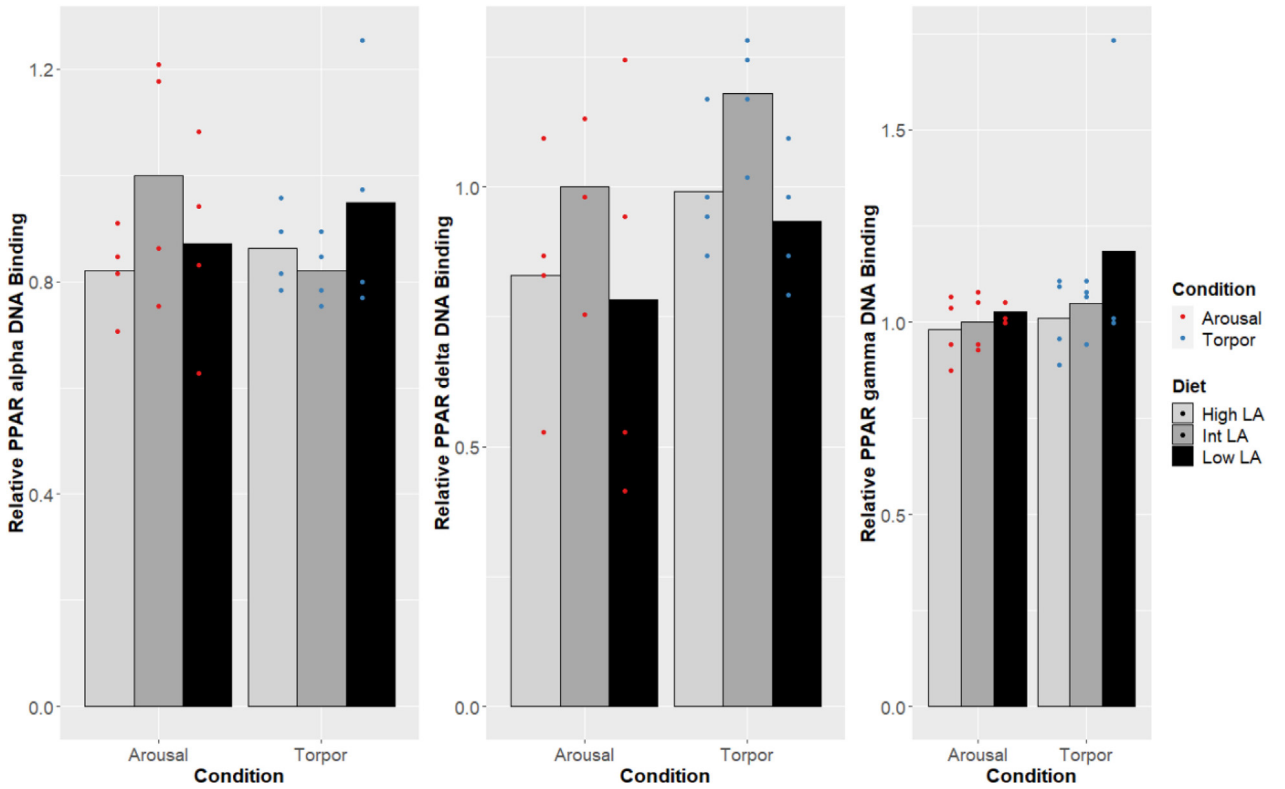

FIGURE 3 | Response of PPAR pathway targets in GD liver to low, intermediate or high levels of LA (or of mirrored levels of ALA) within the pre-hibernation diet Histogram shows the relative DNA-binding levels, assessed as the average absorbance of the intermediate diet in the euthermic animals relative to the other conditions. Data are presented as the mean along with individual data points ($n = 4$), where a significant difference is shown by a difference in the label above the corresponding bar, as assessed by one-way ANOVA and Tukey's *post hoc* analysis ($P < 0.05$). The absence of a label indicates no significant difference.

Expression and Activity Levels of PPARs, PGC-1 α, and L-FABP During Hibernation

Notably, no changes were seen in the DNA-binding activity of PPARα, PPARδ, PPARγ due to the GD's given diet and this was true during both the euthermic and torpid conditions in WAT (**Figure 1**), BAT (**Figure 2**), and liver (**Figure 3**). Similarly, comparing euthermic and torpid animals that were given the same diet condition, PPAR DNA-binding activity did not change.

The co-transcription factor PGC-1α was found to differ in WAT (**Figure 4**). The amount of protein expressed in the low LA (or high ALA) condition was significantly reduced from levels expressed when the dormouse is fed a diet enriched with additional LA (low ALA or high n-6/n-3). A significant increase in PGC-1 protein amount was observed in both euthermic and torpid GD fed a high LA (or low ALA) diet compared to GD fed a low LA (or high ALA) diet; however, PGC-1α protein levels in either of the enriched diets were not significantly different from the intermediate LA (or high ALA) diet condition. Additionally, this WAT-specific difference was visible in both euthermic and torpid animals. PGC-1α levels were not different between the aroused and torpid state in WAT, and so the diet-induced changes were seen in both states.

Finally, L-FABP displayed no changes across the different n-6/n-3 ratio diets (**Figure 5**), nor was a difference in the expression of FABP seen when comparing euthermic to torpid liver within a single diet condition.

DISCUSSION

In both torpid and euthermic GD, PGC-1α protein levels increased significantly within WAT in animals fed a high LA (or low ALA) diet compared to the animals fed a reduced amount of LA or increased level of ALA, while the intermediate group showed protein levels in between both groups (**Figure 4**). Interestingly, the pattern seen in torpid dormice was almost identical to that seen in euthermic animals, albeit at a slightly reduced signal level. Differences in PGC-1α protein levels induced by a high LA (or low ALA) diet suggest that induction of PPAR downstream targets is possible even though a difference in PPAR protein levels is not seen (Puigserver et al., 1998; for review, see Liang and Ward, 2006). As a co-activator of PPARγ target genes, PGC-1α is a central regulator of lipid-based energetics by stimulating mitochondrial metabolism in adipose tissue, and has been shown to play a role in the stimulation of a brown fat-like phenotype, or "beiging" within WAT (Puigserver and Spiegelman, 2003; Bargut et al., 2017), which is particularly interesting in the context of hibernation

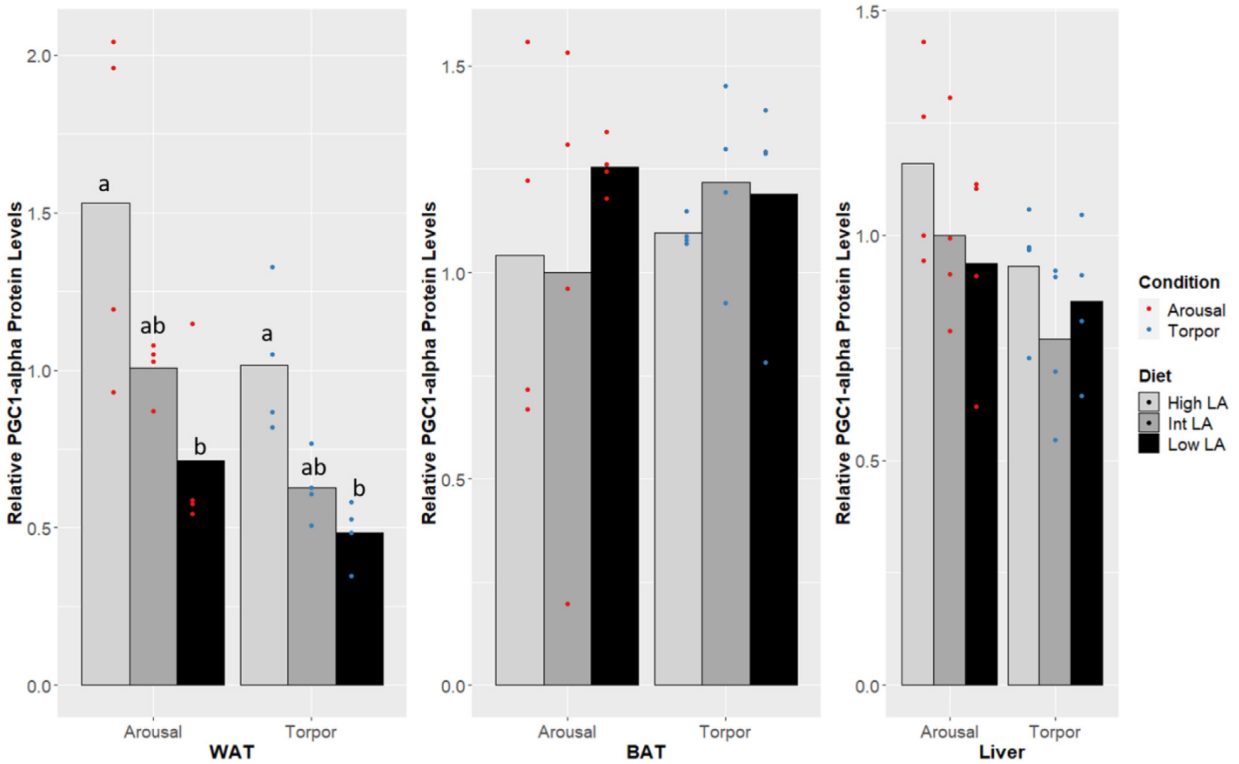

FIGURE 4 | Response of PGC-1α in GD to low, intermediate or high levels of LA (or of mirrored levels of ALA) within the pre-hibernation diet. Histogram shows the relative protein amount, assessed as the average absorbance of the intermediate diet in the euthermic animals relative to the other conditions. Data are presented as the mean along with individual data points ($n = 4$), where a significant difference is shown by a difference in the label above the corresponding bar, as assessed by one-way ANOVA and Tukey's *post hoc* analysis ($P < 0.05$). The absence of a label indicates no significant difference.

and warrants further study. For instance, increased levels of PGC-1α during hibernation in garden dormouse fed a high LA (or low ALA) diet could lead to co-activation of either PPARα or PPARγ, downstream activation of the mitochondrial transcription factor A (TFAM) and increased transcription of uncoupling protein-1 (UCP1); ultimately these changes would confer a more robust thermogenic capacity in animals fed a high LA (or low ALA) diet. This result is in line with finding from Logan et al. (2020) reporting increased levels of anti-oxidative and anti-apoptotic factors in the same dormice fed a high LA (or low ALA) diet compared to low or intermediate LA (or high or intermediate ALA) dietary levels during hibernation (euthermia). Further, PGC-1α in cooperation with PPARα, can increase PRD1-BF1-RIZ1 homologous domain-containing 16 (PRDM16) transcription, essential for the development and maintenance of "beige"-adipose tissue within WAT (Hondares et al., 2011; Ohno et al., 2012). PGC-1α levels are, therefore, deeply connected to the pre-hibernating diet choices in GD and its expression is likely consequential for WAT. Finally, the expression of PGC-1α is downstream of activated activating transcription factor-2 (ATF-2), which itself is downstream of activation by p38 mitogen-activated protein kinase (p38 MAPK) (Robidoux et al., 2005). Notably, p38 MAPK activation has previously been implicated in the maintenance of hibernating tissue (Eddy and Storey, 2007), and may potentially add to the protective effects elicited by PGC1α within hibernating tissues. Interestingly, UCP1 and electron transport chain protein levels are increased before the onset of hibernation within BAT, as shown in the 13-lined ground squirrel (Hindle and Martin, 2014), and remain heightened throughout the season, therefore hiding increases in the necessary upstream factors, such as PGC1α, from studies comparing protein levels between timepoints during hibernation.

The maintenance of PPAR DNA-binding activity across a range of LA or ALA levels within the diet during hibernation is intuitive given the dormouse's requirement for lipid-based metabolism; differences in PPAR DNA-binding activity were not observed when comparing animals fed an intermediate LA or ALA diet to animals fed a diet enriched for either LA or ALA (**Figures 2-4**). Such observation is corroborated by the significant decrease of all WAT-proportions of SFA, including that of palmitic acid (16:0), as short-chain SFAs are preferentially mobilized for oxidation at lower energetic costs during hibernation (for review, see Dark, 2005). Similarly, total, PPAR protein levels were expected to differ with torpor and diet conditions since PPARα protein levels have been shown to increase during torpor (Han et al., 2015), levels of PPARγ are known to favor increased thermogenic mechanisms during torpor in hibernating species (Eddy and Storey, 2003; Kabine et al., 2004; Eddy et al., 2005), and studies within hibernating jerboa (*Jaculus*

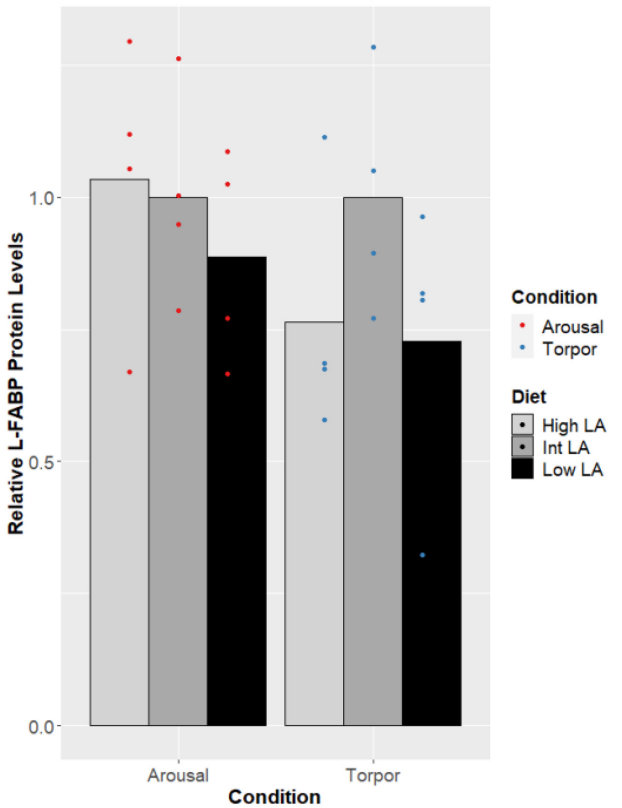

FIGURE 5 | Response of Liver FABP in GD to low, intermediate or high levels of LA within the pre-hibernation diet. Histogram shows the relative protein amount, assessed as the average absorbance of the intermediate diet in the euthermic animals relative to the other conditions. Data are presented as the mean along with individual data points ($n = 4$), where a significant difference is shown by a difference in the label above the corresponding bar, as assessed by one-way ANOVA and Tukey's *post hoc* analysis ($P < 0.05$). The absence of a label indicates no significant difference.

orientalis) show that a second truncated isoform, interferes with wild-type PPARα transcriptional activation during hibernation (Louet et al., 2001; El Kebbaj et al., 2009). Together, these results suggest that alternate mechanisms may be sufficient for prioritizing fatty acid catabolism during hibernation, without requiring changes to PPAR levels or DNA-binding activity. For instance, carbohydrate metabolism is inhibited via differential phosphorylation of metabolic enzymes and transcription factors in torpor (Buck et al., 2002; McMullen and Hallenbeck, 2010), forcing cellular metabolism to favor lipids as fuels. Similarly, differences in dietary preferences can partly explain the preferential catabolism of lipids as PPARδ-imposed suppression upon other PPARs is relieved by metabolites of LA catabolism, 13-S-hydroxyoctadecadienoic acid (13-S-HODE) (Shureiqi et al., 2003; Zuo et al., 2006). More specifically, LA is metabolized into arachidonic acid (AA), and AA-derived eicosanoids such as 13-S-HODE reduce PPARδ inhibition of other PPARs (Zuo et al., 2006). Furthermore, other AA-derived eicosanoids such as 8(S)-hydroxyeicosatetraenoic acid and Leukotriene B4 are more potent PPARα activators than n-3 lipids (Schmitz and Ecker, 2008). Therefore, our specific finding that LA 18:2 n-6 proportions increased significantly in dormice WAT during hibernation suggests that LA metabolites could regulate PPAR signaling pathways. Finally, the differential affinity of some PPAR co-activators for n-3 lipid-ligands over n-6 lipids (Schmitz and Ecker, 2008) could also affect PPAR target gene selection and is worth investigation in this model.

Finally, protein amounts of L-FABP were not changed by the GD's dietary lipid composition or by hibernation. Given the results from liver which show a lack of changes in PPAR protein levels and PGC levels, the consistency of L-FABP protein levels is unsurprising, since L-FABP is downstream of PPARα and PPARδ-activated transcription (Ramiah et al., 2015). Remarkably, research has shown that isolated L-FABP from ground squirrel has an increased capacity for binding fatty acids across the range of temperatures experienced during hibernation compared to L-FABP isolated from rat and this difference accommodates an increased palmitate (16:0) binding capacity at torpid temperatures compared to euthermic temperatures (Stewart et al., 1998). Whether L-FABP from GD shares similar modifications is yet to be explored although it is likely that these differences would be favored in a hibernating mammal given their dependence on lipid metabolism. Furthermore, rat L-FABP does not have a higher affinity for n-3 PUFAs over n-6 PUFAs but dormouse L-FABP function could be regulated by differential levels of fatty acid species or increases in absolute levels of fatty acids required for torpor (Norris and Spector, 2002).

The presence of n-3 fatty acids can adversely affect a mammal's hibernation and this has been demonstrated to be true within a number of hibernating species (Frank et al., 2004; Ruf and Arnold, 2008; Diedrich et al., 2014). Differences in the ratio of n-6 to n-3 fatty acids within hibernators' diets modulates the deposition of adipose within depots as well as the total amount of adipose tissue within the animal (Frank et al., 1998), that can lead to downstream effects on a hibernator's ability to adapt to winter. Marmots that ingest a higher amount of ALA relative to LA spend less time in hibernation, incorporate a higher amount of n-3 PUFAs into their WAT, and ingest more food in winter (Hill and Florant, 2000). This is in contrast with our observations in this study during which dormice hibernated in the same way without food supply and regardless of the dietary lipid manipulation applied prior to hibernation. Dormice of the present study were hibernating at T_a of 4°C, with a T_b of ∼0.5°C above ambient (barely above T_a for dormice fed a high LA diet). Then, animals were mostly thermoconforming during hibernation, and such thermal conditions might have been associated with rather small (not detectable) differences between dietary groups. Interestingly, such differences can become visible and significant when torpid individuals are exposed to low Ta (Geiser et al., 1997) when animals need to thermoregulate (Barnes and Buck, 2000; Buck and Barnes, 2000). In such case, the effects of dietary intake prior to hibernation might constrain hibernation performances with important ecological implications, including accelerated use of energetic fuels and a more rapid depletion of energy (fat) reserves, which can impair individual's survival during winter hibernation. Nevertheless, no such differences in thermal and metabolic patterns were reported under the hibernating

conditions of the dormice fed contrasted lipid diets during pre-hibernation in this study. Instead, animals seemed to have specifically remodeled their WAT lipid composition reducing levels of all n-3 PUFA, including long-chain fatty acids, along with enrichment of WAT-LA during hibernation. Such process of lipid remodeling independent of diets during hibernation has previously been observed in hibernating alpine marmots (Arnold et al., 2011) as well as in hibernating brown bears (Giroud et al., 2019). Nevertheless, feeding low n-6/n-3 diets (high ALA content) to dormice affected neither the torpor patterns nor the onset of hibernation of individuals in this study. This is again in contrast with our previous study where dormice that ingested a higher amount of docosahexaenoic acid (DHA, 22:3 n-3), relative to LA, during the fattening phase significantly delayed the onset of hibernation and had a higher proportion of n-3 fatty acid within their WAT and cardiac sarcoplasmic reticulum (SR) membranes (Giroud et al., 2018). This is important as low levels of n-6 PUFAs and/or high amounts of n-3 PUFAs can alter calcium reuptake within the heart (Swanson et al., 1989; Taffet et al., 1993), and prolong entrance into torpor due to inefficient cardiac maintenance and functioning (Hill and Florant, 2000; Ruf and Arnold, 2008). Such difference of an effect on hibernating patterns observed between our previous study (Giroud et al., 2018) and the present investigation would likely be explained by differential actions of DHA 22:6 n-3 and ALA 18:3 n-3 on oxidative metabolic pathways during hibernation. Clearly, further research is needed on how dietary lipids can affect hibernation performances of species, including modulations of both hibernating patterns and specific use of lipids or other energetic substrates.

In summary, PPAR transcriptional activation seems to be remarkably resilient to differences in the dietary n-6/n-3 ratio and to torpor. The overall molecular phenotype observed suggests that DNA binding activity is maintained within the family of PPAR transcription factors, and at levels similar to that seen in the euthermic GD. It is possible that the GD begins to increase PPAR activities and display a profile favoring lipid catabolism, possibly with preferential utilization of certain lipid types, across the entire hibernation season. If this were the case DNA-binding activity would likely show significant differences when comparing a euthermic GD during the active season, as seen in other hibernating species (Kabine et al., 2004; Chayama et al., 2018) although this comparison is out of the scope of the present study. Future studies should also address potential differences in peroxisomal lipid-metabolism in the hibernating GD given the mitochondria is less reliant on PPAR transcriptional activation, which was maintained across diets and torpor.

DATA AVAILABILITY STATEMENT

The original contributions presented in the study are included in the article/supplementary materials, further inquiries can be directed to the corresponding author/s.

ETHICS STATEMENT

The animal study was reviewed and approved by the institutional ethics committee and the national Austrian authority in accordance to the Austrian Animal Experimentation Act, "Tierversuchsgesetz 2012" (BMBWF-68.205/0137-WF/V/3b/2014).

AUTHOR CONTRIBUTIONS

AW, SL, SG, and KS did the conceptualization. AP, AK-H, and SG performed the methodology (model creation, animal setup, and experiments). JP and GS performed the surgeries. AW, SL, and KS performed the methodology (molecular analyses). AW, SL, and SG investigated the data. AW and SL validated the data. AW, KG, and SG carried out the formal analysis. AW visualized the data. SG and KS carried out the resources and funding acquisition and supervised the data. AW and SG prepared the manuscript. AW, SL, KG, SG, and KS reviewed and edited the manuscript. KS carried out the project administration. All authors commented and agreed on the final version of the manuscript and participated in revisions.

FUNDING

AW holds an Ontario Graduate Scholarship (OGS). SL holds an NSERC postgraduate scholarship. SG was financially supported by the Austrian Science Fund (FWF) (Grant No. P27267-B25 and P31577-B25). KS was supported by a discovery grant from the Natural Sciences and Engineering Research Council (NSERC) of Canada (Grant No. 6793) and the Canada Research Chairs Program.

ACKNOWLEDGMENTS

We thank P. Steiger and M. Salaba for their help with animal care, M. Hämmerle for the biochemical analyses of fatty acid composition.

REFERENCES

Arnold, W., Giroud, S., Valencak, T. G., and Ruf, T. (2015). Ecophysiology of omega Fatty acids: a lid for every jar. *Physiology* 30, 232–240. doi: 10.1152/physiol.00047.2014

Arnold, W., Ruf, T., Frey-Roos, F., and Bruns, U. (2011). Diet-independent remodeling of cellular membranes precedes seasonally changing body temperature in a hibernator. *PLoS One* 6:e18641. doi: 10.1371/journal.pone.0018641

Bargut, T. C. L., Souza-Mello, V., Aguila, M. B., and Mandarim-de-Lacerda, C. A. (2017). Browning of white adipose tissue: lessons from experimental models. *Horm. Mol. Biol. Clin. Invest.* 31:/j/hmbci.2017.31.issue-1/hmbci-2016-0051/hmbci-2016-0051.xml.

Barnes, B. M., and Buck, C. L. (2000). "Hibernation in the extreme: burrow and body temperatures, metabolism, and limits to torpor bout length in arctic ground squirrels," in *Life in the Cold*, eds G. Heldmaier and M. Klingenspor (Berlin: Springer), 65–72. doi: 10.1007/978-3-662-04162-8_7

Benjamini, Y., and Hochberg, Y. (1995). Controlling the false discovery rate: a practical and powerful approach to multiple testing on JSTOR. *J. R. Stat. Soc. Ser. B* 57, 289–300. doi: 10.1111/j.2517-6161.1995.tb02031.x

Buck, C. L., and Barnes, B. M. (2000). Effects of ambient temperature on metabolic rate, respiratory quotient, and torpor in an arctic hibernator. *Am. J. Physiol. Regul. Integr. Comp. Physiol.* 279, R255–R262.

Buck, M. J., Squire, T. L., and Andrews, M. T. (2002). Coordinate expression of the PDK4 gene: a means of regulating fuel selection in a hibernating mammal. *Physiol. Genomics* 8, 5–13. doi: 10.1152/physiolgenomics.00076.2001

Chayama, Y., Ando, L., and Sato, Y. (2018). Molecular basis of white adipose tissue remodeling that precedes and coincides with hibernation in the Syrian hamster, a food-storing hibernator. *Front. Physiol.* 9:1973. doi: 10.3389/fphys.2018.01973

Dark, J. (2005). Annual lipid cycles in hibernators: integration of physiology and behavior. *Annu. Rev. Nutr.* 25, 469–497. doi: 10.1146/annurev.nutr.25.050304.092514

Deckelbaum, R. J., Worgall, T. S., and Seo, T. (2006). n-3 fatty acids and gene expression. *Am. J. Clin. Nutr.* 83(6 Suppl.), 1520–1525.

Diedrich, V., Steinlechner, S., and Scherbarth, F. (2014). Effects of unsaturated fatty acids on torpor frequency and diet selection in Djungarian hamsters (*Phodopus sungorus*). *J. Exp. Biol.* 217(Pt 24), 4313–4319. doi: 10.1242/jeb.113217

Eddy, S. F., Morin, P., and Storey, K. B. (2005). Cloning and expression of PPAR-gamma and PGC-1alpha from the hibernating ground squirrel, *Spermophilus tridecemlineatus*. *Mol. Cell. Biochem.* 269, 175–182. doi: 10.1007/s11010-005-3459-4

Eddy, S. F., and Storey, K. B. (2003). Differential expression of Akt, PPARgamma, and PGC-1 during hibernation in bats. *Biochem. Cell Biol.* 81, 269–274. doi: 10.1139/o03-056

Eddy, S. F., and Storey, K. B. (2007). p38 MAPK regulation of transcription factor targets in muscle and heart of the hibernating bat, *Myotis lucifugus*. *Cell Biochem. Funct.* 25, 759–765. doi: 10.1002/cbf.1416

Eder, K. (1995). Gas chromatographic analysis of fatty acid methyl esters. *J. Chromatogr. B Biomed. Appl.* 671, 113–131.

El Kebbaj, Z., Andreoletti, P., Mountassif, D., Kabine, M., Schohn, H., Dauça, M., et al. (2009). Differential regulation of peroxisome proliferator-activated receptor (PPAR)-alpha1 and truncated PPARalpha2 as an adaptive response to fasting in the control of hepatic peroxisomal fatty acid beta-oxidation in the hibernating mammal. *Endocrinology* 150, 1192–1201. doi: 10.1210/en.2008-1394

Florant, G. L., Hester, L., Ameenuddin, S., and Rintoul, D. A. (1993). The effect of a low essential fatty acid diet on hibernation in marmots. *Am. J. Physiol.* 264(4 Pt 2), R747–R753.

Florant, G. L., Nuttle, L. C., Mullinex, D. E., and Rintoul, D. A. (1990). Plasma and white adipose tissue lipid composition in marmots. *Am. J. Physiol.* 258(5 Pt 2), R1123–R1131.

Folch, J., Lees, M., and Sloane Stanley, G. H. (1957). A simple method for the isolation and purification of total lipides from animal tissues. *J. Biol. Chem.* 226, 497–509.

Frank, C. L. (1992). The influence of dietary fatty acids on hibernation by golden-mantled ground squirrels (*Spermophilus lateralis*). *Physiol. Zool.* 65, 906–920. doi: 10.1086/physzool.65.5.30158549

Frank, C. L., Dierenfeld, E. S., and Storey, K. B. (1998). The relationship between lipid peroxidation, hibernation, and food selection in mammals. *Am. Zool.* 38, 341–349. doi: 10.1093/icb/38.2.341

Frank, C. L., Hood, W. R., and Donnelly, M. C. (2004). "The role of alpha-Linolenic acid (18:3) in mammalian torpor," in *Life in the Cold: Evolution, Mechanisms, Adaptation, and Application*, eds B. M. Barnes and H. V. Carey (Fairbanks, AK: Institute of Arctic Biology Press).

Frank, C. L., Karpovich, S., and Barnes, B. M. (2008). Dietary fatty acid composition and the hibernation patterns in free-ranging arctic ground squirrels. *Physiol. Biochem. Zool.* 81, 486–495. doi: 10.1086/589107

Geiser, F. (2016). Conserving energy during hibernation. *J. Exp. Biol.* 219(Pt 14), 2086–2087. doi: 10.1242/jeb.129171

Geiser, F., and Kenagy, G. J. (1987). Polyunsaturated lipid diet lengthens torpor and reduces body temperature in a hibernator. *Am. J. Physiol.* 252(5 Pt 2), R897–R901.

Geiser, F., Kenagy, G. J., and Wingfield, J. C. (1997). Dietary cholesterol enhances torpor in a rodent hibernator. *J. Comp. Physiol. B Biochem. Syst. Environ. Physiol.* 167, 416–422. doi: 10.1007/s003600050091

Geiser, F., McAllan, B. M., and Kenagy, G. J. (1994). The degree of dietary fatty acid unsaturation affects torpor patterns and lipid composition of a hibernator. *J. Comp. Physiol. B Biochem. Syst. Environ. Physiol.* 164, 299–305. doi: 10.1007/bf00346446

Ghosh, S., O'Connell, J. F., and Carlson, O. D. (2019). Linoleic acid in diets of mice increases total endocannabinoid levels in bowel and liver: modification by dietary glucose. *Obes. Sci. Pract.* 5, 383–394. doi: 10.1002/osp4.344

Giroud, S., Chery, I., and Bertile, F. (2019). Lipidomics reveals seasonal shifts in a large-bodied hibernator, the brown bear. *Front. Physiol.* 10:389. doi: 10.3389/fphys.2019.00389

Giroud, S., Stalder, G., and Gerritsmann, H. (2018). Dietary lipids affect the onset of hibernation in the garden dormouse (Eliomys quercinus): implications for cardiac function. *Front. Physiol.* 9:1235. doi: 10.3389/fphys.2018.01235

Giroud, S., Turbill, C., and Ruf, T. (2012). "Torpor use and body mass gain during pre-hibernation in late-born juvenile garden dormice exposed to food shortage," in *Living in a Seasonal World*, eds T. Ruf, C. Bieber, W. Arnold, and E. Millesi (Berlin: Springer), 481–491. doi: 10.1007/978-3-642-28678-0_42

Giroud, S., Zahn, S., Criscuolo, F., Chery, I., Blanc, S., Turbill, C., et al. (2014). Late-born intermittently fasted juvenile garden dormice use torpor to grow and fatten prior to hibernation: consequences for ageing processes. *Proc. Biol. Sci. R. Soc.* 281:20141131. doi: 10.1098/rspb.2014.1131

Han, Y., Zheng, G., Yang, T., Zhang, S., Dong, D., and Pan, Y.-H. (2015). Adaptation of peroxisome proliferator-activated receptor alpha to hibernation in bats. *BMC Evol. Biol.* 15:88. doi: 10.1186/s12862-015-0373-6

Hill, V. L., and Florant, G. L. (2000). The effect of a linseed oil diet on hibernation in yellow-bellied marmots (*Marmota flaviventris*). *Physiol. Behav.* 68, 431–437. doi: 10.1016/s0031-9384(99)00177-8

Hindle, A. G., and Martin, S. L. (2014). Intrinsic circannual regulation of brown adipose tissue form and function in tune with hibernation. *Am. J. Physiol. Endocrinol. Metab.* 306, E284–E299.

Hondares, E., Rosell, M., and Díaz-Delfín, J. (2011). Peroxisome proliferator-activated receptor α (PPARα) induces PPARγ coactivator 1α (PGC-1α) gene expression and contributes to thermogenic activation of brown fat: involvement of PRDM16. *J. Biol. Chem.* 286, 43112–43122. doi: 10.1074/jbc.m111.252775

Hothorn, T., Bretz, F., and Westfall, P. (2008). Simultaneous inference in general parametric models. *Biom. J.* 50, 346–363. doi: 10.1002/bimj.200810425

Jiang, Y., Lin, L., Liu, N., Wang, Q., Yuan, J., Li, Y., et al. (2020). FGF21 protects against aggravated blood-brain barrier disruption after ischemic focal stroke in diabetic db/db male mice via cerebrovascular PPARγ activation. *Int. J. Mol. Sci.* 21:824. doi: 10.3390/ijms21030824

Kabine, M., El Kebbaj, Z., and Oaxaca-Castillo, D. (2004). Peroxisome proliferator-activated receptors as regulators of lipid metabolism; tissue differential expression in adipose tissues during cold acclimatization and hibernation of jerboa (*Jaculus orientalis*). *Biochimie* 86, 763–770.

Lepage, G., and Roy, C. C. (1986). Direct transesterification of all classes of lipids in a one-step reaction. *J. Lipid Res.* 27, 114–120.

Liang, H., and Ward, W. F. (2006). PGC-1alpha: a key regulator of energy metabolism. *Adv. Physiol. Educ.* 30, 145–151. doi: 10.1152/advan.00052.2006

Lighton, J. R. B. (2008). *Measuring Metabolic Rates*. Oxford: Oxford University Press.

Logan, S. M., Luu, B. E., and Storey, K. B. (2016). Turn down genes for WAT? Activation of anti-apoptosis pathways protects white adipose tissue in metabolically depressed thirteen-lined ground squirrels. *Mol. Cell. Biochem.* 416, 47–62. doi: 10.1007/s11010-016-2695-0

Logan, S. M., Watts, A. J., and Posautz, A. (2020). The ratio of linoleic and linolenic acid in the pre-hibernation diet influences NFκB signaling in garden dormice during torpor. *Front. Mol. Biosci.* 7:97. doi: 10.3389/fmolb.2020.00097

Louet, J. F., Chatelain, F., Decaux, J. F., Park, E. A., Kohl, C., Pineau, T., et al. (2001). Long-chain fatty acids regulate liver carnitine palmitoyltransferase I gene (L-CPT I) expression through a peroxisome-proliferator-activated receptor alpha (PPARalpha)-independent pathway. *Biochem. J.* 354(Pt 1), 189–197. doi: 10.1042/bj3540189

Mahlert, B., Gerritsmann, H., and Stalder, G. (2018). Implications of being born late in the active season for growth, fattening, torpor use, winter survival and fecundity. *eLife* 7:e31225. doi: 10.7554/eLife.31225

McMullen, D. C., and Hallenbeck, J. M. (2010). Regulation of Akt during torpor in the hibernating ground squirrel, *Ictidomys tridecemlineatus*. *J. Comp. Physiol. B Biochem. Syst. Environ. Physiol.* 180, 927–934. doi: 10.1007/s00360-010-0468-8

Mrosovsky, N. (1977). Hibernation and body weight in dormice: a new type of endogenous cycle. *Science* 196, 902–903. doi: 10.1126/science.860123

Munro, D., and Thomas, D. W. (2004). The role of polyunsaturated fatty acids in the expression of torpor by mammals: a review. *Zoology* 107, 29–48. doi: 10.1016/j.zool.2003.12.001

Munro, D., Thomas, D. W., and Humphries, M. M. (2005). Torpor patterns of hibernating eastern chipmunks *Tamias striatus* vary in response to the size and fatty acid composition of food hoards. *J. Anim. Ecol.* 74, 692–700. doi: 10.1111/j.1365-2656.2005.00968.x

Norris, A. W., and Spector, A. A. (2002). Very long chain n-3 and n-6 polyunsaturated fatty acids bind strongly to liver fatty acid-binding protein. *J. Lipid Res.* 43, 646–653.

Nowack, J., Tarmann, I., Hoelzl, F., Smith, S., Giroud, S., and Ruf, T. (2019). Always a price to pay: hibernation at low temperatures comes with a trade-off between energy savings and telomere damage. *Biol. Lett.* 15:20190466. doi: 10.1098/rsbl.2019.0466

Ohno, H., Shinoda, K., Spiegelman, B. M., and Kajimura, S. (2012). PPARγ agonists induce a white-to-brown fat conversion through stabilization of PRDM16 protein. *Cell Metab.* 15, 395–404. doi: 10.1016/j.cmet.2012.01.019

Pengelley, E. T., and Fisher, K. C. (1966). Locomotor activity patterns and their relation to hibernation in the golden-mantled ground squirrel. *J. Mammal.* 47:63. doi: 10.2307/1378069

Pinheiro, J., Bates, D., DebRoy, S., Sarkar, D., and R Core team. (2014). nlme: linear and nonlinear mixed effects models. *R Packag Version* 3, 1–117.

Puigserver, P., and Spiegelman, B. M. (2003). Peroxisome proliferator-activated receptor-gamma coactivator 1 alpha (PGC-1 alpha): transcriptional coactivator and metabolic regulator. *Endocr. Rev.* 24, 78–90. doi: 10.1210/er.2002-0012

Puigserver, P., Wu, Z., Park, C. W., Graves, R., Wright, M., and Spiegelman, B. M. (1998). A cold-inducible coactivator of nuclear receptors linked to adaptive thermogenesis. *Cell* 92, 829–839. doi: 10.1016/s0092-8674(00)81410-5

R Core Team (2018). *R: A Language and Environment for Statistical Computing*. Vienna: R Foundation for Statistical Computing.

Ramiah, S. K., Meng, G. Y., and Ebrahimi, M. (2015). Upregulation of peroxisome proliferator-activated receptors and liver fatty acid binding protein in hepatic cells of broiler chicken supplemented with conjugated linoleic acids. *Ital. J. Anim. Sci.* 14:3846. doi: 10.4081/ijas.2015.3846

Robidoux, J., Cao, W., and Quan, H. (2005). Selective activation of mitogen-activated protein (MAP) kinase kinase 3 and p38alpha MAP kinase is essential for cyclic AMP-dependent UCP1 expression in adipocytes. *Mol. Cell. Biol.* 25, 5466–5479. doi: 10.1128/mcb.25.13.5466-5479.2005

Ruf, T., and Arnold, W. (2008). Effects of polyunsaturated fatty acids on hibernation and torpor: a review and hypothesis. *Am. J. Physiol. Regul. Integr. Comp. Physiol.* 294, R1044–R1052.

Schmitz, G., and Ecker, J. (2008). The opposing effects of n-3 and n-6 fatty acids. *Prog. Lipid Res.* 47, 147–155. doi: 10.1016/j.plipres.2007.12.004

Sharif, O., Gawish, R., and Warszawska, J. M. (2014). The triggering receptor expressed on myeloid cells 2 inhibits complement component 1q effector mechanisms and exerts detrimental effects during pneumococcal pneumonia. *PLoS Pathog.* 10:e1004167. doi: 10.1371/journal.ppat.1004167

Sheriff, M. J., Fridinger, R. W., Tøien, Ø, Barnes, B. M., and Buck, C. L. (2013). Metabolic rate and prehibernation fattening in free-living arctic ground squirrels. *Physiol. Biochem. Zool.* 86, 515–527. doi: 10.1086/673092

Sheriff, M. J., Williams, C. T., Kenagy, G. J., Buck, C. L., and Barnes, B. M. (2012). Thermoregulatory changes anticipate hibernation onset by 45 days: data from free-living arctic ground squirrels. *J. Comp. Physiol. B Biochem. Syst. Environ. Physiol.* 182, 841–847. doi: 10.1007/s00360-012-0661-z

Shimano, H., and Sato, R. (2017). SREBP-regulated lipid metabolism: convergent physiology - divergent pathophysiology. *Nat. Rev. Endocrinol.* 13, 710–730. doi: 10.1038/nrendo.2017.91

Shureiqi, I., Jiang, W., and Zuo, X. (2003). The 15-lipoxygenase-1 product 13-S-hydroxyoctadecadienoic acid down-regulates PPAR-delta to induce apoptosis in colorectal cancer cells. *Proc. Natl. Acad. Sci. U.S.A.* 100, 9968–9973. doi: 10.1073/pnas.1631086100

Staples, J. F. (2016). Metabolic flexibility: hibernation, torpor, and estivation. *Compr. Physiol.* 6, 737–771. doi: 10.1002/cphy.c140064

Stewart, J. M., English, T. E., and Storey, K. B. (1998). Comparisons of the effects of temperature on the liver fatty acid binding proteins from hibernator and nonhibernator mammals. *Biochem. Cell Biol.* 76, 593–599. doi: 10.1139/o98-018

Swanson, J. E., Black, J. M., and Kinsella, J. E. (1987). Dietary n-3 polyunsaturated fatty acids: rate and extent of modification of fatty acyl composition of lipid classes of mouse lung and kidney. *J. Nutr.* 117, 824–832. doi: 10.1093/jn/117.5.824

Swanson, J. E., and Kinsella, J. E. (1986). Dietary n-3 polyunsaturated fatty acids: modification of rat cardiac lipids and fatty acid composition. *J. Nutr.* 116, 514–523. doi: 10.1093/jn/116.4.514

Swanson, J. E., Lokesh, B. R., and Kinsella, J. E. (1989). Ca2+-Mg2+ ATPase of mouse cardiac sarcoplasmic reticulum is affected by membrane n-6 and n-3 polyunsaturated fatty acid content. *J. Nutr.* 119, 364–372. doi: 10.1093/jn/119.3.364

Taffet, G. E., Pham, T. T., Bick, D. L., Entman, M. L., Pownall, H. J., and Bick, R. J. (1993). The calcium uptake of the rat heart sarcoplasmic reticulum is altered by dietary lipid. *J. Membr. Biol.* 131, 35–42. doi: 10.1007/bf02258532

Wahli, W., and Michalik, L. (2012). PPARs at the crossroads of lipid signaling and inflammation. *Trends Endocrinol. Metab.* 23, 351–363. doi: 10.1016/j.tem.2012.05.001

Weitten, M., Oudart, H., and Habold, C. (2016). Maintenance of a fully functional digestive system during hibernation in the European hamster, a food-storing hibernator. *Comp. Biochem. Physiol. Part A Mol. Integr. Physiol.* 193, 45–51. doi: 10.1016/j.cbpa.2016.01.006

Wickham, H. (2016). *ggplot2 - Elegant Graphics for Data Analysis*. New York, NY: Springer-Verlag.

Wu, C. W., Biggar, K. K., and Storey, K. B. (2013). Biochemical adaptations of mammalian hibernation: exploring squirrels as a perspective model for naturally induced reversible insulin resistance. *Braz. J. Med. Biol. Res.* 46, 1–13. doi: 10.1590/1414-431x20122388

Zhang, J., and Storey, K. B. (2016). RBioplot: an easy-to-use R pipeline for automated statistical analysis and data visualization in molecular biology and biochemistry. *PeerJ* 4:e2436. doi: 10.7717/peerj.2436

Zuo, X., Wu, Y., Morris, J. S., Stimmel, J. B., Leesnitzer, L. M., Fischer, S. M., et al. (2006). Oxidative metabolism of linoleic acid modulates PPAR-beta/delta suppression of PPAR-gamma activity. *Oncogene* 25, 1225–1241. doi: 10.1038/sj.onc.1209160

Conflict of Interest: The authors declare that the research was conducted in the absence of any commercial or financial relationships that could be construed as a potential conflict of interest.

frontiers in Physiology

ORIGINAL RESEARCH
published: 18 January 2021
doi: 10.3389/fphys.2020.624677

Dynamic RNA Regulation in the Brain Underlies Physiological Plasticity in a Hibernating Mammal

Rui Fu[1†], Austin E. Gillen[1†], Katharine R. Grabek[2,3], Kent A. Riemondy[1], L. Elaine Epperson[4], Carlos D. Bustamante[3], Jay R. Hesselberth[1,5] and Sandra L. Martin[1,6]*

[1] RNA Bioscience Initiative, University of Colorado School of Medicine, Aurora, CO, United States, [2] Fauna Bio Incorporated, Emeryville, CA, United States, [3] Department of Biomedical Data Science, Stanford University, Stanford, CA, United States, [4] Center for Genes, Environment & Health, National Jewish Health, Denver, CO, United States, [5] Department of Biochemistry and Molecular Genetics, School of Medicine, University of Colorado, Aurora, CO, United States, [6] Department of Cell & Developmental Biology, School of Medicine, University of Colorado, Aurora, CO, United States

OPEN ACCESS

Edited by:
Steven Swoap,
Williams College, United States

Reviewed by:
Marshall Hampton,
University of Minnesota Duluth, United States
Christine Schwartz,
University of Wisconsin–La Crosse, United States
Henrik Oster,
University of Lübeck, Germany

***Correspondence:**
Sandra L. Martin
sandy.martin@cuanschutz.edu

[†] These authors have contributed equally to this work and share first authorship

Specialty section:
This article was submitted to Systems Biology, a section of the journal Frontiers in Physiology

Received: 10 November 2020
Accepted: 29 December 2020
Published: 18 January 2021

Citation:
Fu R, Gillen AE, Grabek KR, Riemondy KA, Epperson LE, Bustamante CD, Hesselberth JR and Martin SL (2021) Dynamic RNA Regulation in the Brain Underlies Physiological Plasticity in a Hibernating Mammal. Front. Physiol. 11:624677. doi: 10.3389/fphys.2020.624677

Hibernation is a physiological and behavioral phenotype that minimizes energy expenditure. Hibernators cycle between profound depression and rapid hyperactivation of multiple physiological processes, challenging our concept of mammalian homeostasis. How the hibernator orchestrates and survives these extremes while maintaining cell to organismal viability is unknown. Here, we enhance the genome integrity and annotation of a model hibernator, the 13-lined ground squirrel. Our new assembly brings this genome to near chromosome-level contiguity and adds thousands of previously unannotated genes. These new genomic resources were used to identify 6,505 hibernation-related, differentially-expressed and processed transcripts using RNA-seq data from three brain regions in animals whose physiological status was precisely defined using body temperature telemetry. A software tool, squirrelBox, was developed to foster further data analyses and visualization. SquirrelBox includes a comprehensive toolset for rapid visualization of gene level and cluster group dynamics, sequence scanning of *k*-mer and domains, and interactive exploration of gene lists. Using these new tools and data, we deconvolute seasonal from temperature-dependent effects on the brain transcriptome during hibernation for the first time, highlighting the importance of carefully timed samples for studies of differential gene expression in hibernation. The identified genes include a regulatory network of RNA binding proteins that are dynamic in hibernation along with the composition of the RNA pool. In addition to passive effects of temperature, we provide evidence for regulated transcription and RNA turnover during hibernation. Significant alternative splicing, largely temperature dependent, also occurs during hibernation. These findings form a crucial first step and provide a roadmap for future work toward defining novel mechanisms of tissue protection and metabolic depression that may 1 day be applied toward improving human health.

Keywords: AU-rich element (ARE), ARE binding proteins, forebrain, hypothalamus, *Ictidomys tridecemlineatus*, medulla, pre-miRNA, RNA binding protein

INTRODUCTION

Hibernating mammals exhibit extreme and highly predictable physiological plasticity across daily, seasonal and annual cycles. Most impressively, they temporarily suspend the mammalian trait of homeothermy by suppressing metabolic heat production. This block allows body temperature (Tb) to drop to near freezing, and the animal to enter a state of deep torpor. By spending much of their fall and winter months in torpor, hibernators achieve profound energetic savings compared to what would be required to maintain Tb at 37°C when environmental temperatures are near or below freezing (reviewed in Staples, 2016). It is noteworthy that torpor is typically discontinuous over the period of hibernation; prolonged bouts (days to weeks) of torpor are periodically and regularly interrupted by short periods (<24 h) of energy-intense reactivation of metabolism and Tb called interbout arousal (IBA). Cycles between torpor and IBA give rise to a pattern of seasonal heterothermy (**Figure 1**). Although hibernation patterns among mammals vary in detail (van Breukelen and Martin, 2015), the behavior typically occurs on a near annual, i.e., circannual, cycle. *Ictidomys tridecemlineatus* (13-lined ground squirrels) alternate between a spring and summer active period of reproduction, growth and fattening, and the fall and winter hibernation period (Carey et al., 2003).

The extraordinary phenotypic dynamics of the mammalian hibernator is orchestrated via a pattern of differential gene expression (Srere et al., 1992). In circannual hibernators, like the 13-lined ground squirrel, at least two key phenotypic cycles comprise hibernation (Epperson et al., 2011). The first is the seasonal cycle between permissive and not permissive for torpor, which enhances fat utilization (Martin, 2008), neuron function in the cold (Hoffstaetter et al., 2018) and tissue protection, including neuroprotection (Frerichs and Hallenbeck, 1998; Schwartz et al., 2015), during the many months of hibernation. The second is the cycle between the state of profoundly suppressed metabolic activity that results in cold Tb during torpor, and the rapid, intense physiologic and metabolic activation that rewarms the animal in IBA (**Figure 1**). Importantly, the animals first slow metabolic rate to reversibly enter the torpid state. Likewise, they must first reactivate metabolism despite very low Tb to rewarm for each interbout arousal (Wilz and Heldmaier, 2000). Mechanisms that protect cells, tissues and organs from damage due to the profound fluctuations of Tb and oxygen delivery, especially during the hyperactive metabolism that drives Tb recovery at the end of a torpor bout (i.e., during arousal from torpor), are likely equally critical for the hibernating phenotype. We expect that the molecular mechanisms underlying metabolic suppression and reactivation, as well as those responsible for seasonal tissue protection, will be revealed by identifying differentially-expressed (DE) genes among the distinct physiological stages of these two phenotypic cycles.

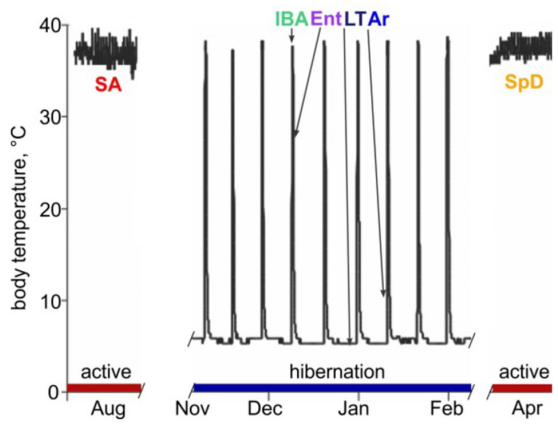

FIGURE 1 | Abdominal body temperature and hibernation behavior in 13-lined ground squirrels. Schematic of Tb vs. time shows heterothermic (hibernation, blue) and homeothermic (active, red) portions of a year and physiological states sampled for RNA-seq: SA, summer active; IBA, interbout aroused; Ent, entrance; LT, late in a torpor bout; Ar, arousing from torpor; SpD, spring dark. See Section "Materials and Methods" for additional details.

While a full understanding of hibernation will require defining differential expression in tissues throughout the body, here we focus on three brain regions: forebrain, hypothalamus and medulla. The forebrain is quiescent during entrance into torpor and remains so throughout the torpor bout and as animals initiate arousal from torpor (Kilduff et al., 1990). Despite inactivity, forebrain neurons undergo morphological changes during the prolonged period at low Tb that are rapidly reversed on rewarming (von der Ohe et al., 2006). In contrast, neuronal activity is more apparent in the hypothalamus and medulla as animals enter, maintain and arouse from torpor (Kilduff et al., 1990). This activity is consistent with the importance of at least a subset of neurons in both of these areas for autonomic functions with key roles in the torpor-arousal cycle, including body temperature, metabolic, respiratory and heart rate control (Bratincsák et al., 2007; Russell et al., 2019).

Few studies to date have attempted to discover the molecular mechanisms of hibernation or torpor in the brain using RNA-seq. The earliest considered two brain regions, cortex and hypothalamus, and four collection points from 13-lined ground squirrels: two from active animals before and after hibernation (October and April) plus torpid and interbout-aroused hibernators (Schwartz et al., 2013). But the majority of studies consider simply paired comparisons of winter torpid hibernators vs. summer active. These paired RNA-seq studies have been done using whole brain from *Rhinolophus ferrumequinum* (greater horseshoe bats) (Lei et al., 2014) and *Dromiciops gliroides* (Monito del Montes, a marsupial Nespolo et al., 2018), as well as medullary respiratory centers in pre-adapted vs. winter adapted *Mesocricetus auratus* (Syrian hamsters, Russell et al., 2019). Hypothalamus gene expression between animals entering daily torpor vs. those remaining euthermic in winter-adapted *Phodopus sungorus* (Djungarian hamsters) have also been compared by RNA-seq (Cubuk et al., 2017). All of the above studies were limited by infrequent and imprecise sampling across the phenotypic complexity of

hibernation, small sample sizes, and incomplete genomes with sparse annotation.

To address these limitations, we first improved the 13-lined ground squirrel genome and its annotation and then used this enhanced genomic resource to define quantitative and qualitative changes in the transcriptome. Key to this study are the use of samples for RNA-seq that were precisely collected from ground squirrels in four physiologically distinct phases of hibernation based on body temperature telemetry, in addition to the two sample groups from the active phase that bracket hibernation. Our sample collection strategy (Epperson et al., 2011), combined with a relatively large sample size (n = 5 individuals in each group) and enhanced 13-lined ground squirrel genome and annotation, allow separation of seasonal and torpor-arousal effects on gene expression for the first time. These data highlight the importance of precise sample collection for discovery research on hibernation and provide strong evidence for both season and temperature-related effects on the transcriptome. As initially discovered in a study of brown adipose tissue (Grabek et al., 2015), a subset of transcripts in all three brain regions are particularly stabilized across the torpor bout when transcription effectively ceases (van Breukelen and Martin, 2002). We propose a model whereby the surviving transcripts set up a transcriptional cycle that instructs torpor-arousal cycle dynamics.

RESULTS

Improved 13-Lined Ground Squirrel Genome and Annotation

Sensitive differential expression testing requires an accurate and complete transcriptome annotation. For this study on gene expression dynamics in hibernation, we built an improved 13-lined ground squirrel genome and annotated it using a novel pipeline (see section "Materials and Methods"). The new genome, HiC_Itri_2, exhibits little change in its total length of 2.5 Gb compared to the publicly available SpeTri2.0. The contiguity of the new genome is greatly improved, however, having just 15 N90 scaffolds of 67.94 Mb relative to the SpeTri2.0 N90 with 98 scaffolds of 4.762 Mb. The NCBI annotation (release 102 gff file) reports 24,612 genes across 1,160 SpeTri2.0 scaffolds for the 13-lined ground squirrel. We combined the 21,998 best-annotated genes from the NCBI transcriptome with 6,527 non-overlapping Ensembl annotations and added an additional 14,356 novel genes with 22,061 novel transcripts to create our new combined annotations (**Figure 2A** and **Supplementary Figures 1A,B**). We then refined these annotations using blastn. Including both novel transcripts and re-annotation of reference transcripts with cryptic gene symbols (e.g., c1orf1, LOC123, etc.), we were able to add gene symbols or a likely gene symbols for 5,093 genes and 7,336 transcripts. In sum, our new transcriptome assembly contains a total of 42,881 genes and 71,149 transcripts, with 96.3% of annotated genes located on the 17 longest contigs (**Figure 2A**), which approaches chromosome level contiguity for this female with 16 autosomes (Lemskaya et al., 2018). Based on the location of Xist and the large majority of regions syntenic (Grabherr et al., 2010) with the mouse X chromosome, Itri10 is the ground squirrel X chromosome (**Supplementary Figure 1C**).

Differential Gene Expression in Hibernation

Next, we reanalyzed the strand-specific, paired-end RNA-seq data from 90 brain samples that were collected for a study of RNA editing in 13-lined ground squirrels (Riemondy et al., 2018, **Supplementary Table 1**). The dataset comprised five individuals from each of six states (**Figure 2B**) for three brain regions: forebrain, hypothalamus and medulla. We found 13,035 genes passed the count filter in at least one of these regions, with most (85%) detected in all three (**Figure 2C**). Genes were analyzed for differential expression by physiological state (**Supplementary Datasheets 2–4** and **Supplementary Tables 2–4**). Three complementary but independent analytical approaches were used to interrogate this complex data set: random forest classification (Breiman, 2001), linear regression (Love et al., 2014), and weighted correlation network analysis (Langfelder and Horvath, 2008) followed by pattern clustering. The RNA-seq data from all three brain regions were also analyzed for state-specific changes in RNA structure caused by alternative splicing.

Unsupervised clustering of the gene-based relative abundance data from each brain region by random forests revealed that the transcriptome in IBA was the most distinct of these six physiological states in all three brain regions (**Figure 3**). The remaining hibernation groups, Ent, LT and Ar, were more closely juxtaposed. Animals from the two homeothermic groups, SpD and SA, also clustered closely together, but were generally well separated from the hibernators, including IBA despite its similarly warm Tb. These findings indicate that both seasonal and torpor-arousal cycles exert strong effects on the transcriptome in all three brain regions and reveal an extensive shift in the transcriptome within 2 h after Tb recovery during IBA compared to all other states.

We next considered pairwise DE genes among the contiguous physiological states (**Figures 4A–C** and **Supplementary Figure 2**). Consistent with the random forest findings, a relatively large number of DE genes distinguished IBA from both states in the homeothermic group (SpD and SA) as well as from Ar and Ent hibernators in all three brain regions. The transcriptome was most altered as the hibernating animals transitioned out of torpor into the first 2 h of the short euthermic period (Ar to IBA), where a large increase of transcripts was observed. The transcriptome also changed substantially across the 12-h euthermic period of the interbout arousal (IBA to Ent), and between active and hibernation seasons (compare the IBA hibernator to either SpD or SA active animals). A far smaller fraction of the transcriptome was altered between Ent and LT, or especially LT and Ar, hibernators, or between the two active states, SpD and SA. Among the three brain regions, the hypothalamus exhibited the greatest proportion of DE genes, 41%, followed by forebrain and medulla with 27 and 23% DE, respectively. Significantly, despite the high qualitative similarity of the transcriptome across the three brain regions, there was far less quantitative similarity. We observed large differences

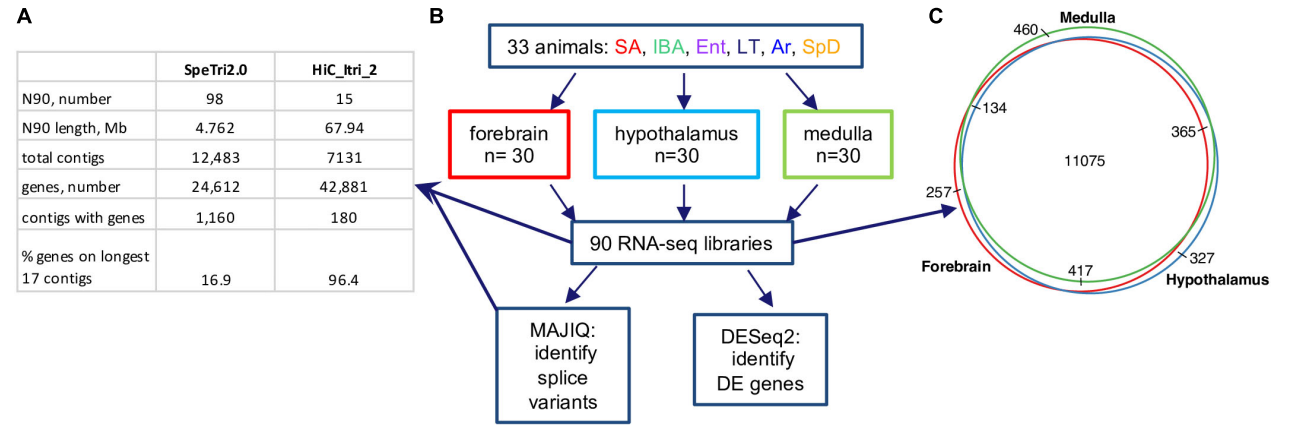

	SpeTri2.0	HiC_Itri_2
N90, number	98	15
N90 length, Mb	4.762	67.94
total contigs	12,483	7131
genes, number	24,612	42,881
contigs with genes	1,160	180
% genes on longest 17 contigs	16.9	96.4

FIGURE 2 | 13-lined ground squirrel genome and RNA-seq data. **(A)** Comparison of original (SpeTri2.0) and new genomes. Note that there are 16 autosomes in the 13-lined ground squirrel (Lemskaya et al., 2018) and the sequenced individual was female. **(B)** Schematic of RNA-seq data, collection and use. For each brain region the 30 animals comprised $n = 5$ individuals from each of the six physiological groups defined in **Figure 1**; DE, differential expression. **(C)** Transcripts for most genes (11075/13035, 85%) were detected in all three brain regions.

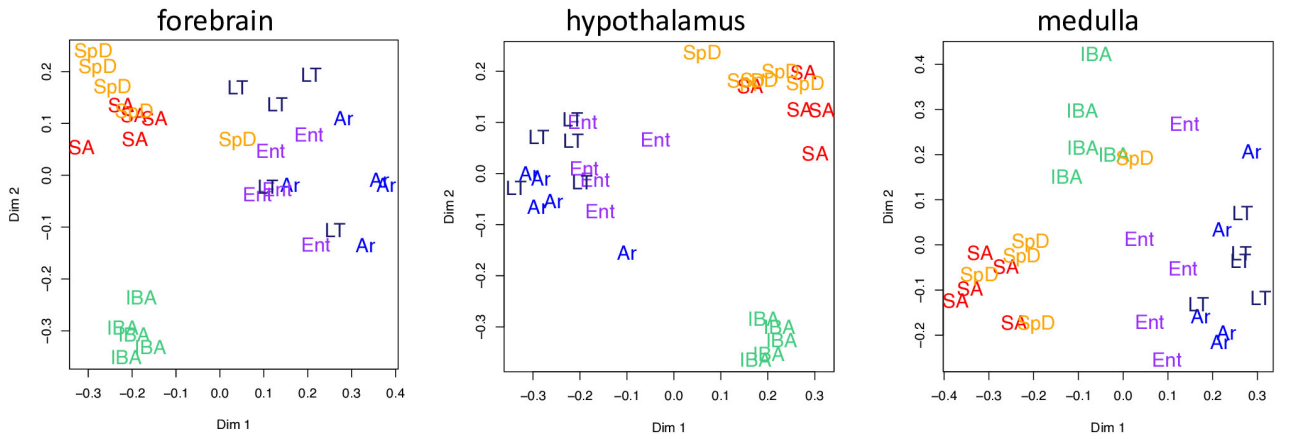

FIGURE 3 | Two dimensional scaling plots following unsupervised random forest clustering of all pass-filter pseudocounts for each brain region as indicated. States are as defined in **Figure 1** and individual animals are represented by their group name and color.

in the DE genes among regions (**Figure 4D**) — just 20% were common to all three regions in contrast to 85% of all genes detected (**Figure 2C**). The enhanced proportion of DE genes in hypothalamus can only partially explain this skew. Rather the large shift in the proportion of DE genes common to all three brain regions suggests unique roles or responses of forebrain, hypothalamus and medulla in hibernation physiology, consistent with previous findings (Schwartz et al., 2013).

A closer inspection of the DE genes across the pairwise transitions most relevant to hibernation physiology provides additional insight (**Supplementary Figure 2**). The relative proportion of increased and decreased DE genes varied depending on the physiological states compared. Pairwise comparisons between IBA and the neighboring winter states of Ent or Ar reveal an excess of genes with increased relative transcript abundance in IBA in all three brain regions, indicating an elevated burst of transcription when Tb recovers after torpor.

A more region-specific response was found in comparisons between IBA and either of the two, warm homeothermic states, SA and SpD. In forebrain, the number of genes increased in IBA slightly outnumbered those increased in either SA or SpD. In contrast, more genes were increased in SA and SpD than in IBA in hypothalamus (i.e., decreased for hibernation), and an even larger skew toward more genes with increased abundance in the two homeothermic states compared to IBA occurred in medulla. The maximum observed log2 fold change for any DE gene in any pairwise comparison varied from as low as −0.47 to as high as −5.15, but only a small fraction of genes (<5%) changed their relative abundance in the RNA pool by at least 2-fold (log2value ≥ 1 or ≤ -1) and by far the largest number of these were seen in the comparison of IBA to Ar animals in all three brain regions (**Supplementary Figure 2**), a comparison that also included a large number of novel, i.e., unnamed (G#), genes.

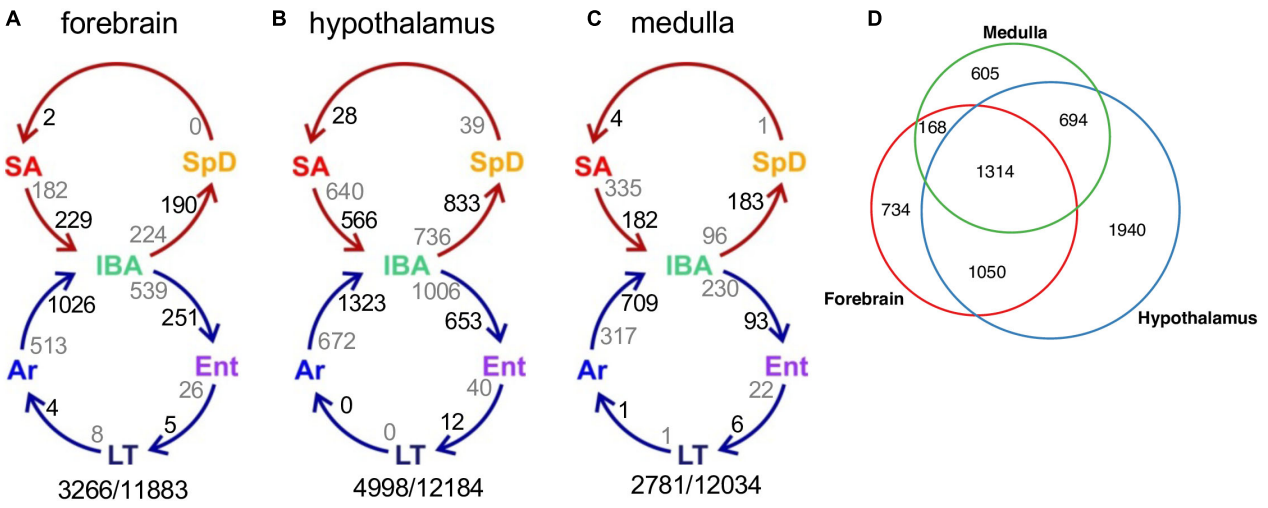

FIGURE 4 | Differentially-expressed genes across circannual rhythm of hibernation in three brain regions. **(A–C)** Circles represent the homeothermic (red) and heterothermic (blue) portions of the hibernator's year, arrows the sequence of physiological transitions. Two numbers are given on the inside of each arrow, decreasing in gray, increasing in black; their sum is the total DE between those two states (**Supplementary Figure 2**). Numbers outside the circles are the total number of DE genes ($q < 0.001$)/number of pass-filter genes detected in that brain region. **(D)** Venn diagram of common and unique DE genes among the three brain regions.

The DE genes increased in IBA-stage hibernators are expected to include a mix of those driving and responding to both season and the torpor-arousal cycle. In an attempt to deconvolute these effects, we next applied weighted gene correlation network analysis (WGCNA, Langfelder and Horvath, 2008) to the full dataset for each brain region. This method identifies modules of genes with correlated relative RNA abundance patterns across all six physiological states. WGCNA can further correlate those modules with phenotypes, in this case a panel of attributes related to hibernation (**Supplementary Table 1**). Modules highly correlated (>0.8) to heterothermy, Tb and IBA were found in all three brain regions (**Supplementary Figures 3–5**), consistent with the random forest and linear regression results described above. Because we (and others, e.g., Botía et al., 2017) found WGCNA frequently failed to assign genes to the module where they were best correlated, we modeled specific patterns to capture the bulk of gene expression changes and reassigned DE genes to their best fit cluster (see section "Materials and Methods"). Just ten clusters captured 83, 86, and 84% of the DE genes in forebrain, hypothalamus and medulla, respectively (**Figure 5A** and **Supplementary Figure 6**). The cluster pattern with the greatest number of genes in each brain region was Cold_low_EM, i.e., decreased in the low Tb animals (LT and Ar) from intermediate levels during Ent (EM), whereas the fewest number of genes had the pattern, Cold_high_EL, i.e., were increased at low Tb despite having low relative abundance when animals entered torpor (EL), **Figure 5B** and **Supplementary Figure 6**.

As noted above, the DE genes were relatively brain region-specific among forebrain, hypothalamus and medulla (**Figure 4D**); thus, it is not unexpected that the genes found in analogous clusters were also largely distinct among the three brain regions (**Supplementary Figure 6**). Despite this apparent uniqueness, their functional enrichments were nonetheless similar or identical, revealing general patterns linked to phenotype (**Supplementary Figures 7–9**). Genes encoding proteins that bind polyA RNA and function in ubiquitin-mediated proteolysis were increased throughout the winter (Winter_high), contrasting with genes exhibiting the Winter_low pattern, which were biased in structural components including cell junction and extracellular matrix. All three of the patterns with increased relative abundance at low Tb (Cold_high_ with Ent either high, medium or low, i.e., EH, EM or EL) were enriched in terms related to mitochondrial structure and function, whereas those decreased at low Tb (Cold_low) were strongly enriched for proteins involved in transcription. Finally, polyA binding proteins were again enriched in the transcripts increased in IBA in all three brain regions whereas those decreased in IBA were related to axon or synaptic function and cell adhesion in forebrain and hypothalamus (**Supplementary Figures 7–9** and **Supplementary Table 5**). Genes encoding proteins involved in mRNA translation/protein biosynthesis were also enriched in RNAs elevated at low Tb (Cold_high_) in both forebrain (EH) and hypothalamus (EM), but not medulla, which had substantially fewer DE genes than the other two brain regions and thus fewer significant enrichments were found.

Genes Exhibiting High Fold-Change

The large number of DE genes revealed by this study precludes specific detailed discussion of each, although the custom data browser, squirrelBox, provides easy access to explore the full set of DE genes on both an individual and group (pairwise and clusters) basis. Here we illustrate some of squirrelBox's capabilities by focusing on the small subset of genes with the largest fold changes (≥2-fold) between pairs of states (**Supplementary Tables 2–4**). A previous study of brown adipose tissue in these hibernators concluded that specific regulatory mechanisms are needed to

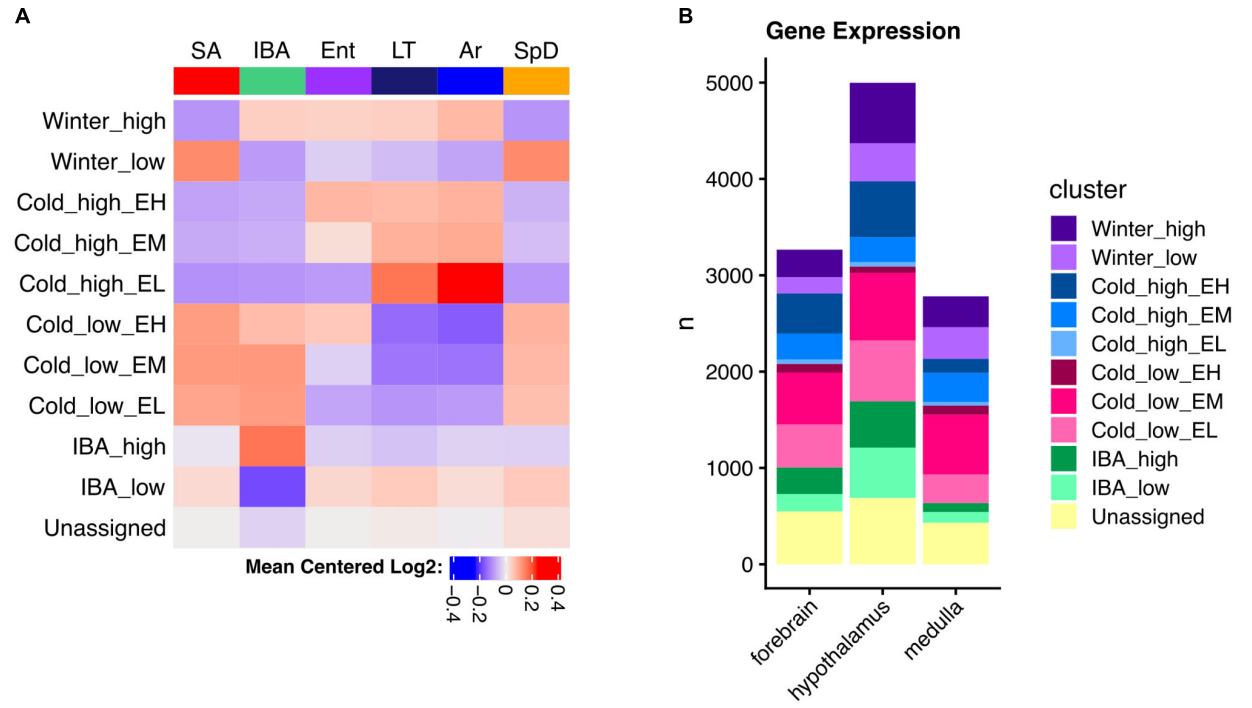

FIGURE 5 | Clustered brain DE genes in hibernation. **(A)** Mean gene expression patterns for each cluster in hypothalamus; EH, EM, and EL indicate the relative abundance during entrance into torpor – high, medium or low, respectively. **(B)** Comparison of the number of genes in each cluster among three brain regions as indicated. See also **Supplementary Figure 6**.

account for ≥2-fold relative changes in transcript abundance, whereas intrinsic mRNA half-life differences can fully explain the majority of smaller fold-changes (Grabek et al., 2015). Because the high cell-type complexity in the brain (documented here for hypothalamus, **Supplementary Table 6**) likely means that regulated transcripts in small subsets of specialized cells are effectively diluted (Epperson et al., 2010), ≥2-fold DE changes in these brain regions are of particular interest.

A set of miRNA-containing precursors that decreased 8 to 25-fold in LT and Ar compared to IBA in all three brain regions were among the highest fold-changes observed, including MIR656 (**Figure 6A**), MIR29B2CHG, MIRLET7D, MIR101-1, MIR138-1 and ENSSTOG00000034702 (**Figure 6B**). In stark contrast, another pair of miRNA precursors, ENSSTOG00000021167 and MIR493_containing (**Figure 6C**), increased dramatically (the highest in our dataset) during the cold stages, LT and Ar, particularly in hypothalamus. While their expression dynamics were generally smaller, several protein-coding genes were also ≥2-fold DE in all three brain regions, including: Chi3l1 (Winter_high), Unc13c (Winter_low), Dusp1 (Cold_high, note the relative abundance during entrance, EM, EL or EH, was variable among regions and is thus omitted), Clp1, Fadd, Kcnj2, Lig4, Lins1, Mex3c (**Figure 6D**), Pdk4, Slitrk6, and Znf646 (Cold_low; again, Ent variable), and Shisa2 (IBA_high).

Transcripts from additional genes that differed by at least 2-fold between at least one pair of states in one brain region included: Arc, Btg2, Fos (**Figure 6E**), Junb and Npas4 (Cold_low_EL), Entpd8 (IBA_high), and Piwil4 (Cold_high_EH) in forebrain; FosB, G21802, Txnip, Zfp36 (Cold_high_EL), Lysmd3 (Cold_low_EL), Pcdh18 (Cold_low_EM), Col11a1, Col19a1, Col2a1, Fzd2 (Winter_low) and Cga, Crym, Dio2, Hif3a (unassigned) in hypothalamus; and Hspa1a, Hspa1b (unassigned), B3gnt7 (Cold_high_EH), Tob2 (Cold_low_EL) and Ticam1 (Winter_low) in medulla. Taken together these genes provide a glimpse into the complexity of brain gene expression dynamics during hibernation.

Factors Influencing RNA Stability

The cohort of transcripts that increased in abundance across the torpor bout when Q10 effects virtually halt transcription (van Breukelen and Martin, 2002), present an interesting enigma. These relative abundance measurements reflect the balance between transcript synthesis and decay; in the absence of transcription, increased abundance must reflect increased stability. Our data provide numerous examples of transcripts that were stable or even increased over the prolonged period of low Tb (Cold_high_ EH, or EL and EM clusters, respectively, in **Figure 5**, **Supplementary Figures 6–9**, and **Supplementary Tables 2–4**), despite the profound depression of transcription at these temperatures. Moreover, we observed an enrichment of polyA RNA binding proteins in the IBA and Winter_high clusters. The presence or absence of *cis*-acting AU-rich elements (AREs, García-Mauriño et al., 2017; Otsuka et al., 2019), binding sites for other RNA binding proteins and miRNA target sites in 3′UTRs (Rissland, 2017), as well as the nucleotide composition of a transcript's coding sequence and 3′UTR (Courel et al., 2019),

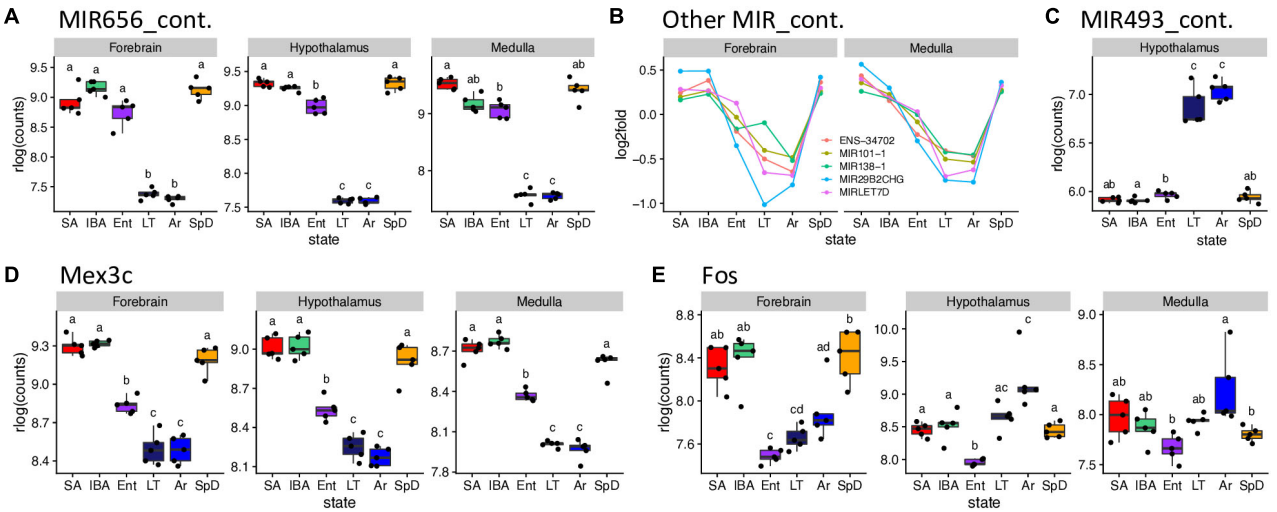

FIGURE 6 | Selected DE genes with large fold changes in hibernation. RNA-seq pseudocounts for **(A)** MIR656_containing RNA from three brain regions. **(B)** Line plots of five other MIR_containing DE genes for forebrain and medulla: hypothalamus, not shown, is similar. **(C)** Boxplot of MIR493_containing miRNA precursor gene counts in hypothalamus. **(D,E)** Boxplots for the protein coding genes, Mex3C and Fos, respectively, in the three brain regions. For boxplots, dots represent log2 values for individual samples, boxes delineate the interquartile range, horizontal lines mark the group median, whiskers indicate the boundaries where sample dots lying outside are outliers, lowercase letters define different groups ($q < 0.001$). For line plots, dots represent the log2 fold change of mean value of expression for each state over overall mean expression. Full names for the genes in **(B)** are: ENSSTOG00000034702, MIR101-1_containing, MIR29B2CHG_containing_G39119 and MIRLET7D_containing. See squirrelBox for additional information.

all affect mRNA translation, storage and stability. Therefore, we analyzed the GC and ARE content of significantly up- or down-regulated genes. Among the three brain regions, the hypothalamus showed the clearest effect of GC content on the relative RNA abundance– the genes increased as Tb began to decrease and further increased as Tb remained low, i.e., increased in the second state in the pairwise comparisons IBAvsEnt, EntvsLT and EntvsAr, had significantly higher GC content than the genes whose relative abundance increased when Tb increased (IBA increased in the ArvsIBA comparison, **Figure 7A**). Medulla but not forebrain exhibited a similar pattern (**Supplementary Figure 10A**), and not surprisingly, the ARE scores were reciprocal to the GC content (**Supplementary Figure 10B**). Comparing transcripts with no AREs to those with high ARE scores revealed a strong bias of transcripts lacking AREs in Cold_high_EH and Winter_high clusters. In contrast, transcripts with high ARE scores were enriched in the Cold_low_EL and Cold_low_EM clusters (**Figure 7B** and **Supplementary Figure 10C**). Mex3c, another RNA binding protein involved in post-transcriptional regulation of its target RNAs, is one of the strongest DE protein coding genes in our dataset (**Figure 6D**) and a member of the Cold_low_EM cluster across all three brain regions. In contrast to the ARE binding proteins, the mechanism of action of Mex3c has not yet been revealed in detail; nevertheless, it is known to be involved in a number of physiological processes, including energy expenditure (Jiao et al., 2012), and a recognition sequence has been described (Yang et al., 2017). We again find Mex3c motifs enriched in transcripts elevated in IBA compared to other hibernation states (**Figure 7C** and **Supplementary Figure 10D**). Finally, mRNAs that encode several ARE binding proteins are also DE in hibernation; these were most dynamic in hypothalamus and cycle asynchronously (**Figure 7D** and **Supplementary Figure 10E**). Taken together, these data are consistent with a complex and dynamic regulation of RNA stability during torpor-arousal cycles of hibernation.

Alternative Splicing in Hibernation

We used MAJIQ (Vaquero-Garcia et al., 2016) to identify alternative splicing events, both to improve transcript annotation (see section "Materials and Methods," **Figure 2B**) and to explore state-specific splicing changes. MAJIQ models alternative splicing in terms of local splicing variations (LSVs). A MAJIQ LSV consists of all possible junctions observed for a given source (upstream) or target (downstream) sequence. MAJIQ quantifies the relative abundance (percent spliced in, PSI) of all junctions in an LSV and then identifies significant changes in relative abundance (dPSI) between pairs of samples. We ran MAJIQ on all pairwise state comparisons, and clustered significant LSVs ($q \leq 0.001$) into the 10 most commonly observed patterns, as described above for the gene expression data. We found that alternative splicing, defined here as a significant increase in the PSI of all alternative junctions relative to the "summer-dominant junction" (most common junction in SA), is largely temperature dependent and most prevalent in Cold_high_EH and EM genes (**Figures 8A,B**). Intron retention, in particular, is highly temperature dependent and most prevalent in Cold_low_EM and EL genes (**Figures 8C,D**). However, rather than being 'alternative' splicing events as defined above, intron retention is the default homeothermic state at most significant LSVs that involve a retained intron (i.e., the retained intron has the highest PSI in SA). We observed multiple common classes of temperature-dependent alternative splicing events, including the

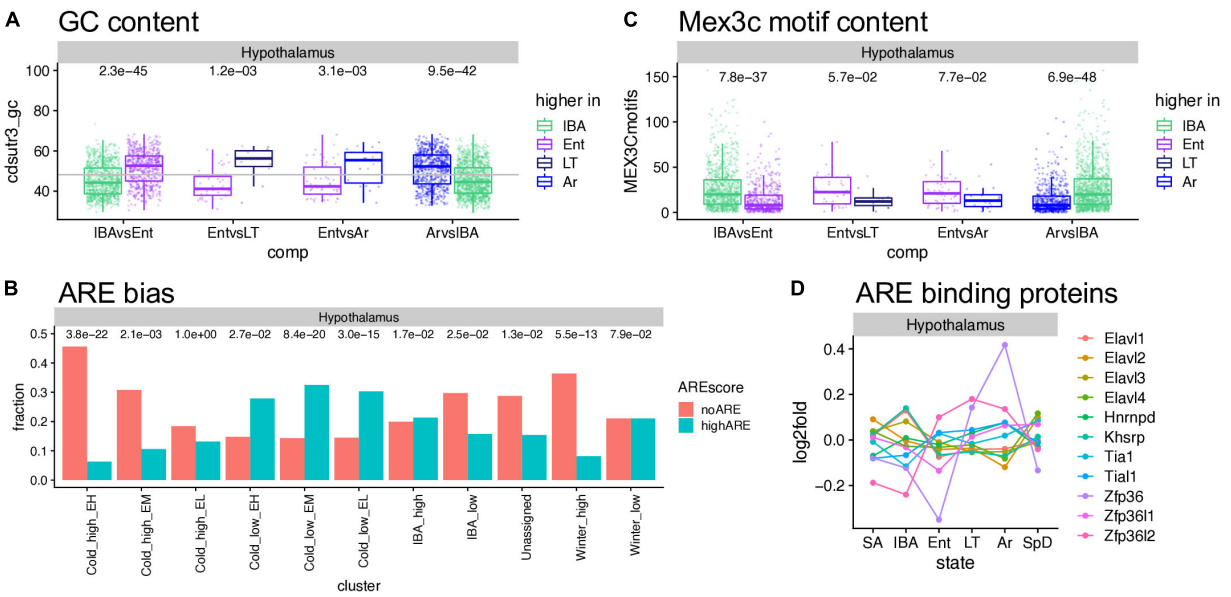

FIGURE 7 | Sequence features affecting RNA stability and utilization. **(A)** GC content in hypothalamus varies across the torpor-arousal cycle; dots represent DE genes in the pairwise comparison indicated below, each assigned to the state where it increased; numbers above are the Wilcoxon test *p*-values. **(B)** The fraction of genes in each cluster that completely lack A-rich elements (ARE) compared to those with ARE scores of at least 8; numbers above are p values (Fisher exact test) comparing the number of genes in each category to the overall gene counts in that cluster. **(C)** Mex3c motif content varies across the torpor-arousal cycle, plot and numbers are as described for panel **(A)**. **(D)** Differential expression of mRNAs encoding ARE binding proteins. See **Supplementary Figure 10**.

aforementioned intron retention in warm states at the alternative splicing-related SRSF6 locus (**Figure 8E** and **Supplementary Figure 11A**), exon skipping in the cold states at the mTORC1-regulating Pip4k2c locus (**Supplementary Figure 11B**), and the use of alternative 5′ splice sites at the brain development-related Cttnbp2 locus (**Supplementary Figure 11C**). In addition to temperature-dependent events, we also captured smaller numbers of seasonal and IBA-specific events. These included a complicated event at the ACSM1_like locus in which intron retention in the summer and spring is replaced with exon skipping in the winter (**Supplementary Figure 11D**), and IBA-specific intron retention at the Sec31a locus (**Supplementary Figure 11E**). Notably, these examples are all in the coding sequence of the transcript and predict an altered protein product.

The three brain regions shared a pattern of increased alternative splicing in the cold, but very few significant LSVs were common among regions (**Supplementary Figure 12**). Interestingly, the greatest overlap occurred in the large Cold_high_EH cluster, which most aggressively segregated the warm and cold states (23–32% of the significant LSVs in each region were common to all three brain regions in this cluster). This is in stark contrast to the other large cluster, Cold_high_EM, where only 4–7% of the significant LSVs were common across regions. LSVs in individual genes in each brain region are plotted in **Supplementary Figures 13–15**.

We also observed that intron retention events were common among the significant LSVs identified by MAJIQ. **Figure 8D** summarizes the state-dependent patterns of intron retention in these samples, demonstrating a consistent decrease of retained introns in the cold states. This is notably inverted relative to the alternative splicing patterns and demonstrates that intron retention is the default state of these LSVs when the animals are warm. This common cold-specific excision of introns may be the result of suboptimal *cis*-acting splicing sequences being recognized more frequently by the splicing machinery in the cold states than the warm states, as the splice sites flanking introns excised in the cold are statistically significantly weaker than those flanking all non-overlapping, non-significant introns (**Supplementary Figure 16**). As in the general alternative splicing analysis, the most significant overlap between the brain regions occurred in the cluster that most aggressively segregates the warm and cold states, "Cold_low_EL" (**Supplementary Figure 17**). In this cluster, 24–40% of the significant intron retention events in each region were shared among regions. Individual genes with intron retention events in each brain region are plotted in **Supplementary Figures 18–20**.

Comparison to Earlier Work

Very few datasets that examine differential gene expression in hibernator brain using high-throughput screening methodology are available for comparison to these data. A 2013 study of hypothalamus and cortex, also in 13-lined ground squirrels (Schwartz et al., 2013) is the most comparable. RNA-seq data were collected from three biological replicates (each a pool of one male and one female) in four physiological groups: non-hibernators in October and April and mid-season hibernators during torpor and IBA. We re-filtered our hypothalamus and forebrain data to include all DE genes with pairwise differences (padj < 0.05) between IBA and SpD, SpD and SA, SA and IBA, and IBA and LT, to allow direct comparison to the pairwise

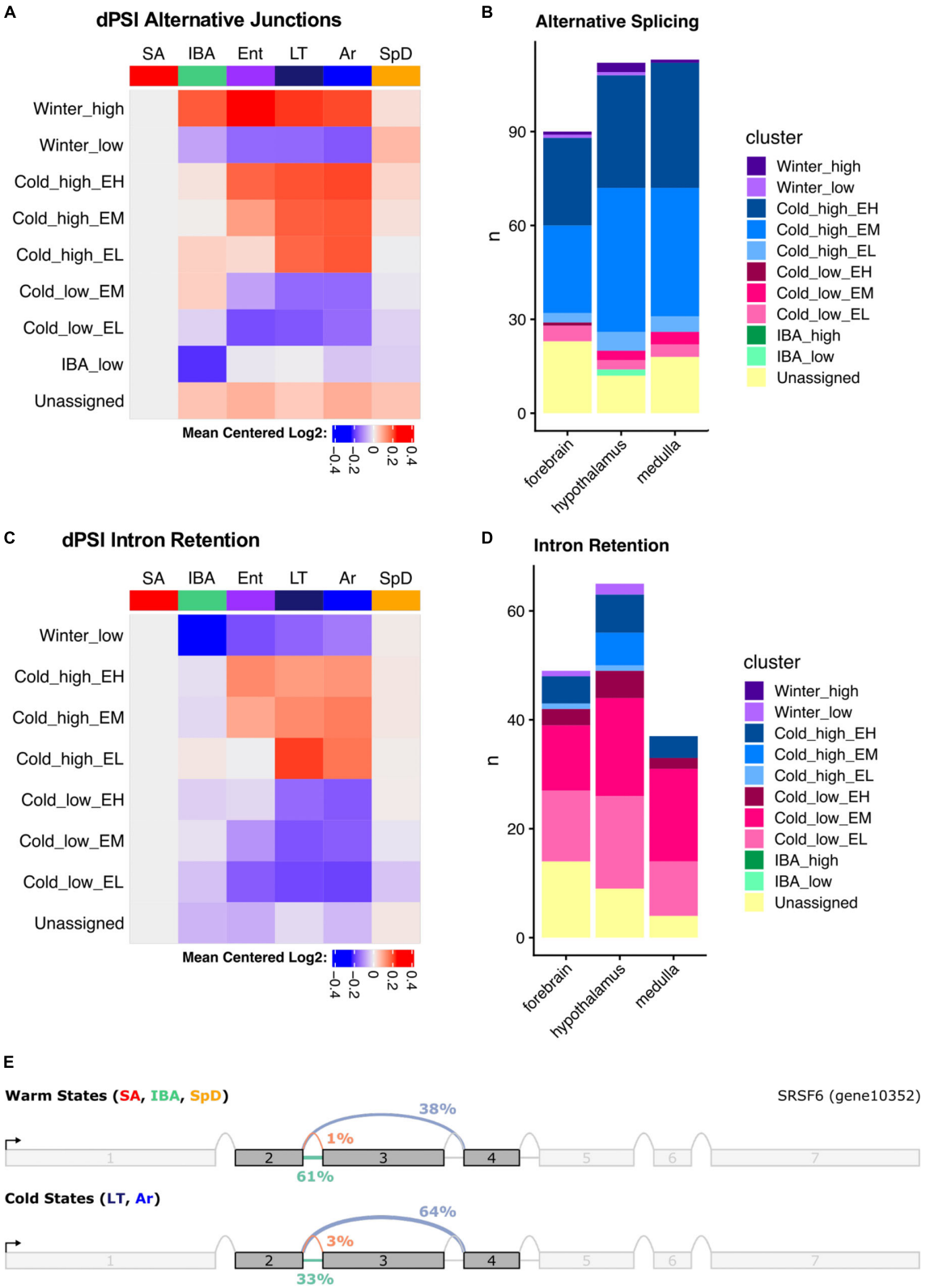

FIGURE 8 | Summary of alternative splicing in the hypothalamus. **(A)** Mean dPSI patterns relative to SA and **(B)** summary of clusters for alternative junctions. **(C)** Mean dPSI patterns relative to SA and **(D)** summary of clusters for retained introns. In **(B,D)**, brain regions are indicated below each bar, n is the number of genes, colors differentiate clusters. **(E)** SRSF6 splice graph from MAJIQ analysis illustrates temperature-dependent alternative splicing.

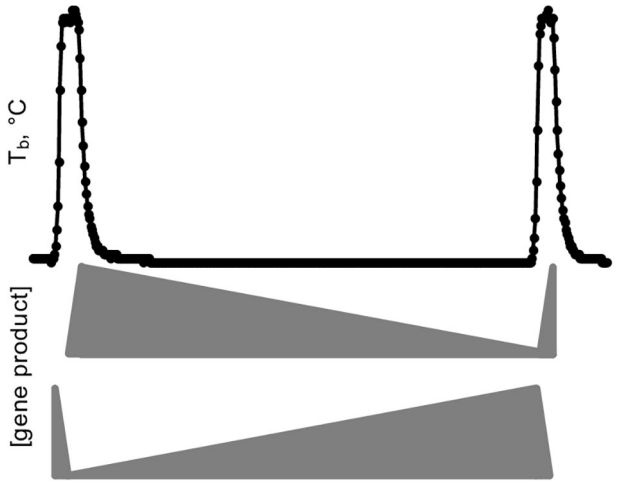

FIGURE 9 | Simplified model of gene expression dynamics during a torpor-arousal cycle in hibernation. Body temperature (Tb) trace plots two IBAs flanking one torpor bout. Middle, the relative abundance of a hypothetical "hibernation gene" that is transcribed during IBA and degraded during torpor, eventually reaching a threshold value that triggers arousal, where it can be replenished and start the cycle anew. Meanwhile a different gene product (bottom) protected from degradation and hence accumulates during torpor initiates the synchronized cascade of gene expression that ultimately leads to the next torpor bout, including correct timing for synthesis of the hibernation gene.

differences reported between IBA and April, April and October, October and IBA, and IBA and torpor (Schwartz et al., 2013), respectively. The gene count distributions were similar between the two datasets (**Supplementary Figure 21**, top panels), but the increased read depth in our study uncovered many additional DE genes. In hypothalamus, approximately half of the DE genes in Schwartz et al. (2013) were recaptured in the present dataset, and the common DE genes were well correlated. The comparison of forebrain to cortex also showed strong correlation of DE genes from the two datasets, although these were fewer, likely reflecting anatomical differences between the tissues used for RNA isolation. The largest fold change in relative transcript abundance (increased throughout winter hibernation) that was common to the two datasets in both brain regions (bottom panels, **Supplementary Figure 21**) was Chi3L1.

DISCUSSION

The goal of this study was to characterize gene expression variation across the spectrum of the hibernator's extraordinary physiology. We hypothesized that genes involved in tissue protection and metabolic suppression during hibernation are differentially expressed by timing in the seasonal or body temperature cycle, respectively, and thus would be revealed by the relative abundance of their transcripts in our sample groups. While ours is not the first study with this goal (Schwartz et al., 2013; Lei et al., 2014; Nespolo et al., 2018), it uses a more precisely defined and larger set of samples, as well as an improved genome and annotation, to separate for the first time seasonal from torpor-arousal cycle effects on the transcriptome in forebrain, hypothalamus and medulla. We document that both season and body temperature have large quantitative (**Figures 3–5** and **Supplementary Figures 2–9**) and smaller qualitative effects on the transcriptome (**Figure 8** and **Supplementary Figures 12–15**, **17–20**) in all three brain regions examined.

The vast majority of transcripts were detected in all three brain regions (**Figure 2C**), yet transcriptome dynamics during circannual hibernation were substantially more region specific (**Figure 4D**). This view is supported by results of both the pairwise (**Figure 4D**) and cluster (**Supplementary Figure 6**) based analyses and is consistent with earlier findings in hypothalamus and cortex from the same species (Schwartz et al., 2013). Some of the brain region-specific differences are likely due to bona fide functional differences. For example, the critical role of the hypothalamus in reproduction, feeding behavior, metabolism and thermoregulation, all variable across the timepoints studied, likely contribute to the large number of DE genes compared to medulla and cortex. Moreover, the hypothalamus remains active throughout the torpor-arousal cycle compared to the neocortex (a substantial component of our forebrain region) which is the first region to become inactive during entrance into torpor and the last to be reactivated upon arousal (Sonntag and Arendt, 2019). Differences among brain regions in neuronal activity as measured by 2-deoxyglucose uptake, blood flow dynamics and c-fos gene expression are well documented in hibernators (Kilduff et al., 1990; Frerichs et al., 1994; Bratincsák et al., 2007). But a closer inspection of many individual genes using squirrelBox suggests that these analyses also amplify subtle quantitative differences in transcripts that are qualitatively more similar among regions. Where the same transcript reaches our expression limit for detection in all three brain regions, an exaggeration of regional differences is often attributable to smaller fold changes and higher within group variability, e.g., Wnk4, a $[Cl^-]$-sensitive kinase that regulates cation/Cl^- cotransporters (Tang, 2016), is clustered with Winter_low in forebrain, IBA_low in hypothalamus and unassigned in medulla (squirrelBox). Yet the transcript varies similarly across the six physiological groups with different within group variability among brain regions. The brain's cell-type complexity likely also contributes to variability in our data, e.g., small variations in macroscopic dissection of hypothalamus and medulla, or subsampling of the pulverized forebrain could alter the cell composition of the tissue and thus the relative abundance of transcripts that are highly cell-type specific in the extracted RNA population, introducing variability.

A simple schematic illustrates the crucial importance of sample collection in capturing DE genes during hibernation (**Figure 9**). A hypothetical gene product critical for torpor is synthesized during IBA, but, in the absence of transcription at low Tb (van Breukelen and Martin, 2002), slowly degrades during the torpor bout. Alternatively, a gene product important for arousal is stabilized during torpor and degrades during IBA. It is clear from these examples that sampling several torpid or aroused hibernators without precise knowledge of their timing would

average to the same relative abundance and thus leave both types of DE genes undiscovered.

The simplified example in **Figure 9** falls far short of explaining the gene expression dynamics of hibernation as captured in our dataset, however, which reveals a complex integration of transcription and RNA turnover rates. The importance of regulating both is broadly reflected by the cluster gene enrichments showing unique differential expression of positive and negative transcription factors and RNA binding proteins. While RNA-seq measures steady-state RNA and not transcription, the profound temperature sensitivity of the transcription machinery (van Breukelen and Martin, 2002) likely means transcripts that maintained their abundance across the entire torpor bout (Winter_high, Cold_high_EH, IBA_low) have average stability compared to the overall transcript pool. In contrast, RNAs that decreased across the torpor bout, i.e., in the clusters Cold_low_EH and EM, are particularly unstable. Finally, the small group of RNAs that actually increased in the absence of transcription (Cold_high_EH and EM), are likely specifically stabilized, newly polyadenylated during torpor, or a combination of the two (Grabek et al., 2015), although we cannot rule out the possibility that very low rates of transcription at the low Tb of torpor can account for the increase in a few transcripts.

Fos provides a noteworthy example of a transcript that increased across the torpor bout, i.e., from Ent to LT to Ar in all three brain regions (**Figure 6E**). Its pattern is unassigned in hypothalamus and medulla but is Cold_low_EL in forebrain. This pattern suggests that Fos mRNA is particularly well-stabilized across the torpor bout or possibly even transcribed in limited cell types, with the latter view consistent with in previous situ hybridization results in hypothalamus (Bratincsák et al., 2007). Its further increase in Ar may reflect the onset of new transcription as Tb recovers, with the brain warming significantly faster during Ar (MacCannell et al., 2019) than the animal's abdominally measured Tb. This view is supported by the outlier arousing ground squirrel in all three brain regions whose Tb is significantly higher than that of the other Ar animals (#53 with Tb = 12.8 vs. 7.9 $\pm$ 0.5°C, squirrelBox), suggesting it is farther along in the process of arousing from torpor than the other Ar individuals studied here. Other immediate early genes with kinetics similar to Fos are the transcription factors Jun and Junb, and Zfp36, which destabilizes transcripts containing AREs, including itself. The rapid increase and then decrease of these transcripts indicate that additional precisely-collected timepoints later during the rewarming process and during the IBA are needed to fully capture the transcriptional program of the torpor-arousal cycle.

It is reasonable to postulate that the genes exhibiting larger fold changes reflect specific regulation because of their involvement in the hibernation phenotype rather than simple, intrinsic variation of RNA stability. In our dataset, relatively few of the 6,505 DE genes changed by greater than 2-fold, likely because the high cell-type complexity in the brain masks larger fold changes that occur in smaller subsets of cells (Epperson et al., 2010). The largest fold changes observed were in a set of miRNA precursor genes common to all three brain regions (**Figures 6A,B**). These decreased dramatically when the animals were at low Tb (Cold_low_EM or_EH). Further work is needed to determine whether their loss reflects processing and increased abundance of their embedded miRNAs and to identify the regulatory targets of those miRNAs. Interestingly two other miRNA precursors accumulated (**Figure 6C**, and ENSSTOG000000021167 in hypothalamus and medulla) equally dramatically in the cold, consistent with these high fold changes reflecting regulated processes rather than a general uncoupling of synthesis and processing at low temperature, as shown previously to occur during hibernation torpor for transcripts degraded by the nuclear exosome (Grabek et al., 2015).

Changes in the relative abundance of transcripts of known protein coding genes were of smaller magnitude than these miRNA precursors, but several with $\geq$2-fold change have plausible roles in hibernation. Two seasonally DE genes in all three brain regions have known functions that would contribute to the hibernator's enhanced neuroprotection. Chi3L1, increased throughout winter (**Supplementary Figures 21B, C**), induces oligodendrogenesis after inflammatory damage (Starossom et al., 2019) and Unc13c, decreased throughout winter, lowers synaptic activity (Palfreyman and Jorgensen, 2017). In torpor arousal cycles, the inwardly rectifying potassium channel, Kcnj2, is decreased in the cold. This channel modifies the excitability of neurons (Trimmer, 2015) and drives vasodilation to alter regional blood flow (Longden et al., 2017), a feature of hibernation (Frerichs et al., 1994). Other genes that altered by at least 2-fold in one or two of these brain regions may also contribute to the hibernators enhanced neuroprotection. Three non-fibrillar collagens decreased throughout winter in hypothalamus, Col11a1, Col2a1, and Col19a1 (and the first two were also altered similarly in medulla); these localize to the extracellular matrix and may facilitate synapse formation (Su et al., 2010). In forebrain, Arc and Npas4 decreased in the cold with the pattern Cold_low_EL, Arc mediates synaptic plasticity (Barylko et al., 2018) and may help reestablish synapses that retract during torpor but re-form, apparently early, during IBA (von der Ohe et al., 2006). Npas4 is neuroprotective after ischemia (Choy et al., 2015) which occurs transiently with minimal damage each time the hibernator arouses from torpor (Dave et al., 2012). In hypothalamus, Fzd2 which decreased in winter, attenuates pathological Ca^{++} increase in a rat model of traumatic brain injury (Niu et al., 2012). Also in hypothalamus, accumulation of Txnip1 during torpor could beneficially signal redox stress during arousal, with its quick drop again in IBA blunting its potential for damaging effects (Nasoohi et al., 2018), and the drop of Hif3a in IBA could help assure a robust transcriptional response to hypoxia. In medulla, the winter decreased Ticam1 reduces microglia activation, lowers proinflammatory cytokines and enhances neuron survival (Wang et al., 2018). Id2 is lowest in IBA; when this gene is silenced, hypoxia/ischemia-induced neuronal injury is attenuated because neuronal apoptosis is inhibited (Guo et al., 2015).

The transcripts of several genes linked to functions other than neuroprotection were also highly DE in our dataset. Dusp1, which negatively regulates of cell proliferation and responds to cellular stress, was dynamic across the torpor-arousal cycle, increasing during torpor to 2$\times$ higher in Ar than IBA in hypothalamus and medulla. Tob2 and Btg2, both

antiproliferative (Ezzeddine et al., 2012; Micheli et al., 2015), were decreased in torpor (Cold_low_EL or EM) in all three brain regions, as was Lig4, a DNA repair enzyme. Fadd, initially found to function as an adaptor molecule for death receptor-mediated apoptosis, but now known to be involved in non-apoptotic cellular processes including proliferation and cell-cycle control as well as regulation of gene expression and control of metabolic pathways (Marín-Rubio et al., 2019), likewise exhibits decreased expression in the cold. PiwiL4 increased from IBA to Ent in all three regions, it is an RNA mediated transcriptional repressor, consistent with the generalized repression of transcription during the torpor bout. Among the more region-specific genes Entpd8 is a diphosphatase that alters extracellular nucleotide abundance (Fausther et al., 2007), including of the hibernation-relevant adenosine (Jinka et al., 2011), which is elevated in medulla during IBA. Three genes related to thyroid hormone action are ≥2fold increased in the hypothalamus of SpD compared to SA animals: Cga, Crym and Dio2. Thyroid hormone action is important for both reproduction and metabolism – high reproductive hormones are incompatible with hibernation (Darrow et al., 1988; Richter et al., 2017), and there is a clear depression of metabolic rate prior to the onset of heterothermy (Concannon et al., 1999; Sheriff et al., 2012). Because the relative abundances of Cga and Crym transcripts in the reproductively active SpD animals were indistinguishable from the reproductively quiescent hibernators, these genes are likely more important for the metabolic effects of thyroid hormone in the hypothalamus. In contrast, the low levels of Dio2 in the 20 hibernators were more similar to the SA animals, suggesting it is more important for reproduction, a view bolstered by the outlier male ground squirrel in IBA whose tissue was collected in late March (#78, squirrelBox), at least one full month later in the year than all of the other hibernators in this study. Elevated protein chaperones Hspa1a and Hspa1b in medulla during SA may reflect a seasonal remodeling of electrophysiological properties to protect against respiratory failure at low temperatures, as shown for hamsters prior to hibernation (Russell et al., 2019). Of course, for all of these protein-coding genes, their biological activity will further depend on the synthesis, stability and post-translational modifications of their corresponding proteins.

In addition to previously annotated genes, there are multiple transcripts that remain unannotated that are also ≥2-fold DE in our dataset and hence may reflect regulated processes of particular interest to understanding mechanisms important for hibernation. Some of these, e.g., *G21802* in hypothalamus, likely reflect accumulation of intermediates that would not be seen but for differential effects on RNA synthesis and processing caused by the prolonged time at low Tb. G21802 is a U2 snoRNA that is processed from an intron in a protein coding gene, *Cep295*, which was not differentially expressed. Others of these, however, likely warrant further investigation, including G14950, which is decreased at low Tb in all three brain regions (Cold_low_EM) and is predicted to host a micropeptide (squirrelBox). Interestingly, this gene lacks homology to transcripts in human or mouse, despite sequence similarity to, and hence the presence, of the likely corresponding chromosomal region in the human genome, which is peppered by transposable element insertions. If the ability to hibernate is ancestral to mammals but lost among species that no longer hibernate (Srere et al., 1992), the remnants of the critical genes should be present to varying extents in non-hibernators including humans and mice, due to the relaxation of selective pressure for function. However, if a homologous, intact gene is found in other hibernators, it would be particularly interesting for follow-up functional analyses.

The transcriptome dynamics of the individual genes discussed above likely reflect molecular mechanisms controlling both RNA transcription and turnover. A relatively synchronized burst of transcription occurs as Tb recovers during arousal, and then the transcriptome changes dramatically over the 12-h euthermic period and again over the much longer period of torpor. Suppressed translation at low Tb (van Breukelen and Martin, 2001) would protect GC-rich, optimally translated mRNAs from their normal rates of degradation (Courel et al., 2019), allowing their increase across the torpor bout. The enrichment of RNA binding proteins among the DE genes uncovered by this study, and their complex abundance dynamics reveal a rich regulatory network that controls RNA stability seasonally and during the torpor-arousal cycle. Although ARE elements and their binding proteins were initially discovered for their role in promoting rapid turnover of transcripts that require tight regulation, i.e., genes with roles in cell proliferation or immune response, they are now known to operate with far more finesse. Some ARE binding proteins stabilize transcripts rather than cause their degradation, and signaling via post-translational modification may specifically stabilize or destabilize a given transcript (García-Mauriño et al., 2017; Otsuka et al., 2019). Taken together, the observations support a role for both transcriptional and post-transcriptional mechanisms in sculpting transcriptome dynamics during hibernation.

We also provide evidence for hibernation-associated RNA structural variation. Modeling the exact effect of the observed differential splicing on the corresponding protein is difficult because it is impossible to faithfully reconstruct mRNA isoforms from short-read sequencing at complex loci (Vaquero-Garcia et al., 2016). Nonetheless, two of these loci, *SRSF6* and *Pip4k2c*, are simple enough to make reasonable predictions about the proteins produced by alternative splicing.

In the cold states, the SRSF6 protein is 342 amino acids long and contains two highly conserved N-terminal RNA recognition motifs (RRM1 and RRM2). In the warm states, retention of the second intron (**Figure 8E**) results in a frameshift that truncates the protein to 192 amino acids and removes the RRM2 domain. Recent evidence shows that the RRM2 domain is required for SRSF6 to regulate alternative splicing (Wan et al., 2019), suggesting that temperature-dependent splicing of SRSF6 itself may be directly involved in the increase in alternative splicing observed in the cold states. Similar intron retention events that remove the RRM2 domain in SRSF6 are observed in several species, including *Drosophila melanogaster* and *Caenorhabditis elegans*, but not in humans (Shao et al., 2012). A similar cold-specific intron excision event is also observed at the closely related Srsf5 locus in all three brain regions (**Supplementary Figures 18–20**). Retention of this Srsf5 intron

in the warm states would also eliminate the RRM2 domain and introduce a premature stop codon. The temperature-dependence of these two events is particularly interesting, as unproductive splicing events leading to non-sense-mediated decay (NMD) is a highly conserved regulatory mechanism employed by SR-family transcripts across evolution (Lareau and Brenner, 2015).

The result of the exon skipping event in Pip4k2c (**Supplementary Figure 11B**) is much more subtle than the SRSF6 intron retention event; there is an in-frame deletion of 13 amino acids in the cold states relative to the warm states. This deletion occurs in the middle of the only known functional domain in the protein, a phosphatidylinositol phosphate kinase (PIPK) domain, but the effect on kinase activity is unknown. The PIPK domain is identified in both isoforms, albeit with a lower score in the shorter isoform. However, if the cold-dominant shorter isoform does have altered kinase activity it may play an important role in hibernation, as Pip4k2c modulates mTORC1 activity (Shim et al., 2016) and mTORC1-dependent translational control is known to play multiple roles in brain development and function (Santini and Klann, 2011).

Alternative splicing may also play an important role in controlling gene expression dynamics during hibernation. The majority of the alternative splicing events in our data are clearly temperature dependent, and thus may reflect a passive response rather than a regulated process. The data suggest that lower affinity splice sites are being recognized more efficiently by the spliceosome in the cold. This may simply reflect slowed molecular activity, including dramatically slowed transcription at lower temperatures; transcription rates are known to affect splicing (Saldi et al., 2016). Nonetheless, as discussed above at least some of the observed alternative splicing events, including cold-dependent intron excision, would alter the coding sequence of proteins plausibly connected to hibernation. Robust cold state-specific intron-excision at the Srsf5 and SRSF6 loci, in particular, may be directly involved in modulating other alternative splicing events. Unfortunately, the use of short-read RNA-seq limits our ability to reconstruct transcript isoforms, especially those from complex loci. The per-junction events that we do observe, however, strongly suggest that long-read RNA-sequencing is likely to reveal substantial transcript isoform diversity as a function of hibernation physiology.

This analysis provides one early step toward unraveling the complex gene expression dynamics that orchestrate and enable hibernation's extreme physiology. Importantly, these data demonstrate the utility and necessity of precisely timed samples for such work. The success of future experiments to discover key hibernation genes by exploiting their differential expression in the brain requires additional carefully collected samples to capture the complex dynamics of gene expression changes that occur later in the process of arousal, and at several timepoints across the IBA. Single-nucleus RNA-seq would help overcome problems caused by the high cell-type complexity in the brain. Nevertheless, the robust DE genes revealed in this study provide a rich set of gene-based hypotheses for guiding future work. The strongly DE, but presently uncharacterized genes, whether they likely encode proteins, lncRNAs or miRNAs, are of particular interest for future work that could lead to hibernation-based strategies for tissue protection or reversible metabolic depression.

MATERIALS AND METHODS

Genome Enhancement

The existing 2011 SpeTri2.0 genome was further assembled using HiC (Dovetail genomics), resulting in a substantially improved genome. For this, a Chicago library was prepared as described (Putnam et al., 2016). Briefly, ∼500 ng of HMW gDNA (mean fragment length ≥50 kbp) were reconstituted into chromatin *in vitro* and fixed with formaldehyde. Fixed chromatin was digested with *Dpn*II, the 5′ overhangs filled in with biotinylated nucleotides and free blunt ends were ligated. After ligation, crosslinks were reversed and protein was removed, as was biotin that was not internal to ligated fragments. The purified DNA was then sheared to ∼350 bp mean fragment size and sequencing libraries were generated using NEBNext Ultra enzymes and Illumina-compatible adapters. Biotin-containing fragments were isolated using streptavidin beads before PCR enrichment of each library. The libraries were sequenced on an Illumina HiSeq 2500 (rapid run mode) to produce 150 million 2 × 101bp paired-end reads, which provided 52.6× physical coverage of the genome (1–50 kb pairs). Three Dovetail HiC libraries were prepared in a similar manner as described previously (Lieberman-Aiden et al., 2009). Briefly, for each library, chromatin was fixed in place with formaldehyde in the nucleus and then extracted. Fixed chromatin was digested with *Dpn*II, the 5′ overhangs filled in with biotinylated nucleotides, and then free blunt ends were ligated. After ligation, crosslinks were reversed, and the DNA purified from protein. Purified DNA was treated to remove biotin that was not internal to ligated fragments. The DNA was then sheared to ∼350 bp mean fragment size and sequencing libraries were generated using NEBNext Ultra enzymes and Illumina-compatible adapters. Biotin-containing fragments were isolated using streptavidin beads before PCR enrichment of each library. The libraries were sequenced on an Illumina HiSeq X. The number and length of read pairs produced for each library was: 130 million, 2 × 150 bp for library 1; 175 million, 2 × 150 bp for library 2; 211 million, 2 × 150 bp for library 3. Together, these Dovetail HiC library reads provided 8,356.58× physical coverage of the genome (10–10,000 kb pairs). Finally, the *de novo* assembly (SpeTri2.0), Chicago library reads, and Dovetail HiC library reads were used as input data for HiRise, a software pipeline designed specifically for using proximity ligation data to scaffold genome assemblies (Putnam et al., 2016). An iterative analysis was conducted. First, Chicago library sequences were aligned to the draft input assembly using a modified SNAP read mapper[1]. The separations of Chicago read pairs mapped within draft scaffolds were analyzed by HiRise to produce a likelihood model for genomic distance between read pairs, and the model was used to identify and break putative mis-joins, to score prospective joins, and make joins above a threshold. After aligning and scaffolding Chicago data, Dovetail HiC library sequences were aligned and

[1]http://snap.cs.berkeley.edu

scaffolded following the same method. We named this genome HiC_Itri_2, reflecting the assembly method and that this is the second super-assembly of SpeTri2.0 (Grabek et al., 2019).

RNA Isolation and RNA-Seq

RNA was isolated from frozen (−80°C) brain regions dissected as described in **Supplementary Datasheet 1** from five individuals (Hindle and Martin, 2013) representing each of six, precisely defined hibernation states based on time of year and Tb measured using implanted telemeter or iButton, or rectal probe, at time of tissue collection (**Figure 1** and **Supplementary Table 1**): SA, summer active (08 August); IBA, interbout aroused (17 December–26 March, 2–3 h after Tb reached 30°C following >5 days torpid with Tb < 6.5°C, all with Tb 30.6–37.4°C); Ent, entrance (03 January–31 January, 23–27°C after 10–14 h with Tb > 30°C); LT, late in a torpor bout (31 January–26 February, Tb 5.5–7.2°C, with near constant, low Tb for 80–95% of the length of the previous torpor bout); Ar, arousing from torpor (28 December–22 January, with Tb spontaneously increasing to 7–12.8°C after multiple days in hibernation with near constant, low Tb); SpD, spring dark (21 March–30 April, after at least 10 consecutive days with Tb 35.6–37°C). Strand-specific RNA-sequencing libraries were prepared (TruSeq Stranded mRNA Library Prep Kit, Illumina) and sequenced as described (Riemondy et al., 2018). The raw read data were deposited at GEO (accession number GSE106947), after analysis for RNA editing (Riemondy et al., 2018), but here are analyzed for differential gene expression and isoform variation across hibernation states for the first time.

HiC Genome Annotation

First, we leveraged our extensive RNA-seq data to create a custom annotation of the new genome assembly, HiC_Itri_2. For this, three independent annotations: (1) the NCBI Release 102 annotation; (2) Ensembl 90 annotation; and (3) a merge of all confidently expressed regions of the genome based on our RNA-seq data, were merged stepwise onto the HiC assembly. The last comprised strand-specific, paired-end RNA-seq data collected from the 90 brain samples in the present study, plus samples from neonate and testes as described (Riemondy et al., 2018) and an additional 25 liver, 9 adrenal and 9 kidney samples to further enhance transcript discovery and annotation. Trimmed, high quality RNA-seq reads from all 138 samples were first mapped to the 13-lined ground squirrel mitochondrial genome (**Supplementary Table 1**). The remaining non-mitochondrial reads (92.2 ± 2.3%) were then mapped to the HiC genome using HISAT2 (Pertea et al., 2016). Next, the deduplicated, uniquely mapping reads from each sample were assembled into a transcriptome with StringTie [-j 3 –c3, -rf, (Pertea et al., 2015)], these were merged across all samples and annotated (NCBI annotation release 102) using TACO (Niknafs et al., 2017), as described (Riemondy et al., 2018).

Comparison of the three annotations revealed that the NCBI annotation often better reflected the transcripts detected in our merged RNA-seq based annotation than the Ensembl annotation. This is likely because the NCBI annotation includes cDNA and RNA-seq data deposited in GenBank together with Ensembl's homology-based annotation. But many loci in the Ensembl (Release 90) annotation, particularly small RNAs, were absent from the NCBI annotation. Because these were also detected in our ground squirrel RNA-seq data, all Ensembl transcripts that had no exon overlap with those from NCBI as well as short (<1 kb), single-exon Ensembl transcripts that had <90% reciprocal overlap with any NCBI transcripts were added (to retain the ability to capture primary transcripts of processed short RNAs). Finally, we added any remaining novel annotations from our merged RNA-seq data to the new Ensembl-supplemented NCBI annotations using the same rules as above.

We next used MAJIQ (v2.0, Vaquero-Garcia et al., 2016) in a novel application to complete the annotation and better integrate the previously unannotated transcripts represented in the data, which included fragments of retained introns, read-through events, and novel exons, with the reference annotations. After running MAJIQ Builder on the combined annotations (NCBI + Ensembl + novel transcripts), we extracted exon and intron retention information from the MAJIQ splicegraph and used these data to reassign or remove many novel transcripts and genes. In this step, the novel transcripts with evidence for splicing to a reference transcript (≥1 spliced read required) were re-assigned the gene ID of the reference transcript, and novel transcripts without evidence of splicing to a reference transcript and contained within a retained intron were removed from the annotations. Finally, we attempted to assign gene symbols to novel transcripts based on homology to human or squirrel RefSeq annotations. For this, we took all blastn results against the human RefSeq database with $e \leq$ 1e-20 and assigned the most significant gene symbol to each query transcript. The suffix "_like" was appended to the gene symbol if the query coverage was less than 90%, but higher than 50%, and the "_containing" suffix was appended if the coverage was less than 50%. Query transcripts with no blastn matches (e ≤ 1e-20) in human RefSeq were blasted against the *I. tridecemlineatus* RefSeq database (e ≤ 1e-20), which contains many predicted transcripts with no genome location information. Gene symbols were assigned as described above for the human blastn matches. See **Supplementary Figure 22**.

smORF Annotation

Sequences from all annotated transcripts were processed via the micropeptide prediction tool MiPepid. Reported short open reading frames of length ≥10 aa, in the MiPepid classification class of "coding," and probability ≥0.9 were labeled as "MiPepid_predicted." The similarities of these sequences to high confidence smORFs documented in the SmProt database were then calculated using blastp-short parameters for sequences of length ≤30 aa and default parameters on longer sequences. Homologous smORFs were annotated with the SmProt micropeptide when blastp results escore ≤ e−10, percentage identical ≥90, and alignment coverage of the subject sequence ≥0.9. These analyses are provided as columns in the squirrelBox gene summary table for exploration.

Transcript and DE Quantification

After demultiplexing, the reads were trimmed with cutadapt (Martin, 2011) to remove adaptor sequences and low-quality

bases ($Q < 10$). All reads that were at least 20 nt after trimming were assigned to transcripts in the newly constructed *I. tridecemlineatus* transcriptome described above using Salmon (Patro et al., 2017) with –numBootstraps 50 (Additional File 7). The Salmon assignments were imported into R (Team, 2019) and summarized at the gene level using tximport (Soneson et al., 2015). We filtered the data, retaining only those genes in each brain region where rlog was ≥7 in at least 4/5 individuals from at least one group. These values were used as input for random forests (Breiman, 2001), plotting, WGCNA (Langfelder and Horvath, 2008) and clustering algorithms. DESeq2 (Love et al., 2014) was then used to identify differentially expressed genes (DE genes), defined as those with likelihood ratio test (LRT) adjusted p-value of ≤0.001 across all states. Models for both tests included a term to control for the effect of sex. DESeq2 was also used to calculate "shrunken" log2 fold-changes (Stephens, 2017) for differentially expressed genes and normalized, transformed (rlog) count matrices (**Supplementary Tables 2–4**).

Exploratory Cluster Analyses

After processing via ComBat (Johnson et al., 2006) to remove effects of sex, expression data from each tissue were passed to WGCNA (Langfelder and Horvath, 2008) v1.68 for module detection. Parameters were optimized for constructing a signed network (TOMType = "signed," networkType = "signed"), high sensitivity (deepSplit = 3), and more aggressive than default merging and reassignment (mergeCutHeight = 0.25, reassignThreshold = 1). Additional settings were: minModuleSize = 30, minCoreKME = 0.5, minKMEtoStay = 0.4. Genes from each module were inspected in comparison to their summary profile eigengene. Then, module–trait associations quantification was performed to identify modules that were significantly associated with the measured traits. Modules and module-trait correlation values were color coded in plotting.

Reference Pattern Clustering

Gene expression patterns were assigned to their final reference clusters by calculating Pearson correlation coefficients. For each brain region, mean expression values were calculated for each gene in each state, and these average expression values were tested for correlation with the ten most common patterns observed in WGCNA modules. Correlated genes ($r \geq 0.8$) were assigned to the cluster with the highest correlation coefficient; no ties were observed. The remaining genes ($r < 0.8$ to any reference cluster) were grouped into the 'Unassigned' cluster. Cluster gene overlaps among brain regions were visualized using VennDiagram (Chen and Boutros, 2011) in R.

Alternative Splicing Analysis

All reads that were at least 20 nt after trimming (described above) were aligned to the HiC genome using STAR (Dobin et al., 2012) in two-pass mode with settings: –limitSjdbInsertNsj 2000000, –outSAMattributes NH HI AS nM MD, –alignSJoverhangMin 8 on the second pass. The STAR alignments were then analyzed using MAJIQ Builder to assemble splice graphs and MAJIQ Quantifier to identify changes in relative local splice variation (LSV) abundance (delta PSI = dPSI) between states (Vaquero-Garcia et al., 2016). LSVs with significant changes, defined as a 99.9% probability of a dPSI of at least 0.2 in any pairwise state comparison, were visualized by separately plotting the abundance of the SA-dominant splice junction and retained intron (if present) relative to SA using ComplexHeatmap (Gu et al., 2016) in R. Reference pattern clustering was performed as described for gene expression data. Protein domains in alternative splicing isoforms were identified using HMMER version 3.3[2] on version 32.0 of the PFAM database (El-Gebali et al., 2018). For intron retention splice site analysis, temperature-dependent retained intron events with 90% probability of a dPSI of at least 0.2 were identified and the sequences surrounding their 5′ and 3′ splice sites were passed to splice site strength prediction algorithms MaxEntScan (Yeo and Burge, 2004) and HBond (Erkelenz et al., 2018). All non-overlapping non-differentially retained introns described by MAJIQ were used as the control.

Data Exploration

In addition to data availability in the **Supplementary Datasheets 2–4** and **Supplementary Tables 2–4**, the RNA sequencing analyses as described above are integrated with the new genome assembly, and transcriptome annotation into an interactive R Shiny browser, squirrelBox,which is hosted online[3] or can be run locally[4,5]. squirrelBox enables data filtering, query, high quality plotting, and basic GO-term and *k*-mer enrichment analyses. Gene set distribution along the newly improved genome is powered by genomic interval manipulation via valr (Riemondy et al., 2017) and JavaScript-interfacing via Biocircos (Cui et al., 2016). squirrelBox is intentionally designed to be flexible to input datasets and is easily adaptable to other data exploration needs.

Sequence/Motif Analysis and Gene Ontology Enrichment

Additional analyses were carried out in R, heavily utilizing Bioconductor packages. The newly built genome assembly was forged into a BSgenome data package, which enables quick queries of coding and untranslated sequences. In addition, *k*-mer counting and enrichment statistical analysis are achieved through the R package transite (Krismer et al., 2020). Annotations of *k*-mer and motifs for potentially linked RNA-binding proteins or miRNAs were collected from multiple publicly available annotation databases. For AU-rich element analysis, AREscores (Spasic et al., 2012) were calculated for 3′UTR sequences of at least 200 nt in length via the web interface[6]. Initial GO-term enrichments were found using DAVID for comparison of individual cluster gene lists to the human gene background (**Supplementary Table 6**, Huang et al., 2009); these were used to annotate the cluster heatmaps. GO-term enrichment analysis in squirrelBox is conducted via Fisher exact test on GO-term collections from the Molecular Signatures Database with three

[2]hmmer.org

[3]https://raysinensis.shinyapps.io/squirrelBox/

[4]https://github.com/rnabioco/squirrelbox

[5]https://hub.docker.com/r/raysinensis/squirrelbox

[6]http://arescore.dkfz.de/arescore.pl

background choices: all human, all annotated ground squirrel, and pass-filter brain-detected genes.

Data Re-calculations for Comparison to Previous Work

Gene names and log2FC_ashr values for all pairwise DE genes with wald_padj < 0.05 were selected and log2_FC values converted to values for IBA_vs_SpD, SA_vs_SpD, IBA_vs_SA and IBA_vs_LT. Mean values for gene counts for APR, OCT, TOR, and IBA and their pairwise *p*-values were merged [**Supplementary Tables 1**, **2** in Schwartz et al. (2013)], and then selected for the appropriate Benjamini-adjusted pvalue according to the values in **Supplementary Table 3** to get padj < 0.05. The mean fold change was calculated for pairs IBA/APR, OCT/APR, IBA/OCT and IBA/TOR. Correlation and *p*-values were determined in R using cor.test for the DE hypothalamus genes recovered in both studies, as well as for common genes DE in forebrain (this study) and cortex (Schwartz et al., 2013).

DATA AVAILABILITY STATEMENT

The datasets presented in this study can be found in online repositories. The names of the repository/repositories and accession number(s) can be found in the article/ **Supplementary Material**.

ETHICS STATEMENT

Ethical review and approval was not required for the animal study because all of the materials used for this work came from a frozen tissue bank.

AUTHOR CONTRIBUTIONS

RF and AG analyzed data and drafted and reviewed manuscript. KG prepared DNA, analyzed data, and drafted and reviewed manuscript. KR analyzed data and reviewed manuscript. LE collected tissues and reviewed manuscript. JH supervised data analysis and reviewed manuscript. CB reviewed manuscript. SM designed study, prepared RNA, analyzed data, and drafted and reviewed manuscript. All authors contributed to the article and approved the submitted version.

FUNDING

This work was funded by NIH grants R01 HL089049 and R21 NS088315 to SM for tissue bank and RNA-seq data collection, R35 GM119550 to JH for supervision of data analysis, and NSF grant 1642184 to CB for HiC data and analysis as well as by the RNA Bioscience Initiative at the University of Colorado School of Medicine for data analysis. The University of Colorado Cancer Center Genomics Resource, where RNA-seq libraries were prepared and sequenced, is supported by NIH grant P30 CA046934.

ACKNOWLEDGMENTS

We thank R. Russell, P. O'Neill, and L. Bogren for help with RNA isolations, L. Bogren for early exploration of these data and K. Diener at the University of Colorado Cancer Center Genomics Resource for expert assistance with RNA-seq library construction and sequencing.

SUPPLEMENTARY MATERIAL

The Supplementary Material for this article can be found online at: https://www.frontiersin.org/articles/10.3389/fphys.2020.624677/full#supplementary-material

REFERENCES

Barylko, B., Wilkerson, J. R., Cavalier, S. H., Binns, D. D., James, N. G., Jameson, D. M., et al. (2018). Palmitoylation and membrane binding of Arc/Arg3.1: a potential role in synaptic depression. *Biochemistry* 57, 520–524. doi: 10.1021/acs.biochem.7b00959

Botía, J. A., Vandrovcova, J., Forabosco, P., Guelfi, S., D'sa, K., Hardy, J., et al. (2017). An additional k-means clustering step improves the biological features of WGCNA gene co-expression networks. *BMC Syst. Biol.* 11:47. doi: 10.1186/s12918-017-0420-6

Bratincsák, A., Mcmullen, D., Miyake, S., Tóth, Z. E., Hallenbeck, J. M., and Palkovits, M. (2007). Spatial and temporal activation of brain regions in hibernation: c-fos expression during the hibernation bout in thirteen-lined ground squirrel. *J. Comp. Neurol.* 505, 443–458. doi: 10.1002/cne.21507

Breiman, L. (2001). Random forests. *Mach. Learn.* 45, 5–32.

Carey, H. V., Andrews, M. T., and Martin, S. L. (2003). Mammalian hibernation: cellular and molecular responses to depressed metabolism and low temperature. *Physiol. Rev.* 83, 1153–1181. doi: 10.1152/physrev.00008.2003

Chen, H., and Boutros, P. C. (2011). VennDiagram: a package for the generation of highly-customizable Venn and Euler diagrams in R. *BMC Bioinform.* 12:35. doi: 10.1186/1471-2105-12-35

Choy, F. C., Klarić, T. S., Koblar, S. A., and Lewis, M. D. (2015). The role of the neuroprotective factor Npas4 in Cerebral Ischemia. *Int. J. Mol. Sci.* 16, 29011–29028. doi: 10.3390/ijms161226144

Concannon, P. W., Castracane, V. D., Rawson, R. E., and Tennant, B. C. (1999). Circannual changes in free thyroxine, prolactin, testes, and relative food intake in woodchucks, *Marmota monax*. *Am. J. Physiol.* 277, R1401–R1409.

Courel, M., Clément, Y., Bossevain, C., Foretek, D., Vidal Cruchez, O., Yi, Z., et al. (2019). GC content shapes mRNA storage and decay in human cells. *eLife* 8:e49708.

Cubuk, C., Kemmling, J., Fabrizius, A., and Herwig, A. (2017). Transcriptome analysis of hypothalamic gene expression during daily torpor in djungarian hamsters (Phodopus sungorus). *Front. Neurosci.* 11:122. doi: 10.3389/fnins.2017.00122

Cui, Y., Chen, X., Luo, H., Fan, Z., Luo, J., He, S., et al. (2016). BioCircos.js: an interactive Circos JavaScript library for biological data visualization on web applications. *Bioinformatics* 32, 1740–1742. doi: 10.1093/bioinformatics/btw041

Darrow, J. M., Duncan, M. J., Bartke, A., Bona-Gallo, A., and Goldman, B. D. (1988). Influence of photoperiod and gonadal steroids on hibernation in the European hamster. *J. Comp. Physiol. A* 163, 339–348. doi: 10.1007/bf00604009

Dave, K. R., Christian, S. L., Perez-Pinzon, M. A., and Drew, K. L. (2012). Neuroprotection: lessons from hibernators. *Comp. Biochem. Physiol. B Biochem. Mol. Biol.* 162, 1–9. doi: 10.1016/j.cbpb.2012.01.008

Dobin, A., Davis, C. A., Schlesinger, F., Drenkow, J., Zaleski, C., Jha, S., et al. (2012). STAR: ultrafast universal RNA-seq aligner. *Bioinformatics* 29, 15–21. doi: 10.1093/bioinformatics/bts635

El-Gebali, S., Mistry, J., Bateman, A., Eddy, S. R., Luciani, A., Potter, S. C., et al. (2018). The Pfam protein families database in 2019. *Nucleic Acids Res.* 47, D427–D432.

Epperson, L. E., Karimpour-Fard, A., Hunter, L. E., and Martin, S. L. (2011). Metabolic cycles in a circannual hibernator. *Physiol. Genomics* 43, 799–807. doi: 10.1152/physiolgenomics.00028.2011

Epperson, L. E., Rose, J. C., Russell, R. L., Nikrad, M. P., Carey, H. V., and Martin, S. L. (2010). Seasonal protein changes support rapid energy production in hibernator brainstem. *J. Comp. Physiol. B* 180, 599–617. doi: 10.1007/s00360-009-0422-9

Erkelenz, S., Theiss, S., Kaisers, W., Ptok, J., Walotka, L., Müller, L., et al. (2018). Ranking noncanonical 5' splice site usage by genome-wide RNA-seq analysis and splicing reporter assays. *Genome Res.* 28, 1826–1840. doi: 10.1101/gr.235861.118

Ezzeddine, N., Chen, C.-Y. A., and Shyu, A.-B. (2012). Evidence providing new insights into TOB-promoted deadenylation and supporting a link between TOB's deadenylation-enhancing and antiproliferative activities. *Mol. Cell. Biol.* 32, 1089–1098. doi: 10.1128/mcb.06370-11

Fausther, M., Lecka, J., Kukulski, F., Lévesque, S. A., Pelletier, J., Zimmermann, H., et al. (2007). Cloning, purification, and identification of the liver canalicular ecto-ATPase as NTPDase8. *Am. J. Physiol. Gastrointest. Liver Physiol.* 292, G785–G795.

Frerichs, K. U., and Hallenbeck, J. M. (1998). Hibernation in ground squirrels induces state and species-specific tolerance to hypoxia and aglycemia: an in vitro study in hippocampal slices. *J. Cereb. Blood Flow Metab.* 18, 168–175. doi: 10.1097/00004647-199802000-00007

Frerichs, K. U., Kennedy, C., Sokoloff, L., and Hallenbeck, J. M. (1994). Local cerebral blood flow during hibernation, a model of natural tolerance to "cerebral ischemia". *J. Cereb. Blood Flow Metab.* 14, 193–205. doi: 10.1038/jcbfm.1994.26

García-Mauriño, S. M., Rivero-Rodríguez, F., Velázquez-Cruz, A., Hernández-Vellisca, M., Díaz-Quintana, A., De La Rosa, M. A., et al. (2017). RNA binding protein regulation and cross-talk in the control of AU-rich mRNA fate. *Front. Mol. Biosci.* 4:71. doi: 10.3389/fmolb.2017.00071

Grabek, K. R., Cooke, T. F., Epperson, L. E., Spees, K. K., Cabral, G. F., Sutton, S. C., et al. (2019). Genetic variation drives seasonal onset of hibernation in the 13-lined ground squirrel. *Commun. Biol.* 2, 478–478.

Grabek, K. R., Diniz Behn, C., Barsh, G. S., Hesselberth, J. R., and Martin, S. L. (2015). Enhanced stability and polyadenylation of select mRNAs support rapid thermogenesis in the brown fat of a hibernator. *Elife* 4:e04517.

Grabherr, M. G., Russell, P., Meyer, M., Mauceli, E., Alföldi, J., Di Palma, F., et al. (2010). Genome-wide synteny through highly sensitive sequence alignment: satsuma. *Bioinformatics* 26, 1145–1151. doi: 10.1093/bioinformatics/btq102

Gu, Z., Eils, R., and Schlesner, M. (2016). Complex heatmaps reveal patterns and correlations in multidimensional genomic data. *Bioinformatics* 32, 2847–2849. doi: 10.1093/bioinformatics/btw313

Guo, L., Yang, X., Lin, X., Lin, Y., Shen, L., Nie, Q., et al. (2015). Silencing of Id2 attenuates hypoxia/ischemia-induced neuronal injury via inhibition of neuronal apoptosis. *Behav. Brain Res.* 292, 528–536. doi: 10.1016/j.bbr.2015.07.018

Hindle, A. G., and Martin, S. L. (2013). Cytoskeletal regulation dominates temperature-sensitive proteomic changes of hibernation in forebrain of 13-lined ground squirrels. *PLoS One* 8:e71627. doi: 10.1371/journal.pone.0071627

Hoffstaetter, L. J., Mastrotto, M., Merriman, D. K., Dib-Hajj, S. D., Waxman, S. G., Bagriantsev, S. N., et al. (2018). Somatosensory neurons enter a state of Altered excitability during hibernation. *Curr. Biol.* 28, 2998–3004.e3.

Huang, D. W., Sherman, B. T., and Lempicki, R. A. (2009). Systematic and integrative analysis of large gene lists using DAVID bioinformatics resources. *Nat. Protoc.* 4, 44–57. doi: 10.1038/nprot.2008.211

Jiao, Y., George, S. K., Zhao, Q., Hulver, M. W., Hutson, S. M., Bishop, C. E., et al. (2012). Mex3c mutation reduces adiposity and increases energy expenditure. *Mol. Cell. Biol.* 32, 4350–4362. doi: 10.1128/mcb.00452-12

Jinka, T. R., Toien, O., and Drew, K. L. (2011). Season primes the brain in an arctic hibernator to facilitate entrance into torpor mediated by adenosine A1 receptors. *J. Neurosci.* 31, 10752–10758. doi: 10.1523/jneurosci.1240-11.2011

Johnson, W. E., Li, C., and Rabinovic, A. (2006). Adjusting batch effects in microarray expression data using empirical Bayes methods. *Biostatistics* 8, 118–127. doi: 10.1093/biostatistics/kxj037

Kilduff, T. S., Miller, J. D., Radeke, C. M., Sharp, F. R., and Heller, H. C. (1990). 14C-2-deoxyglucose uptake in the ground squirrel brain during entrance to and arousal from hibernation. *J. Neurosci.* 10, 2463–2475. doi: 10.1523/jneurosci.10-07-02463.1990

Krismer, K., Bird, M. A., Varmeh, S., Handly, E. D., Gattinger, A., Bernwinkler, T., et al. (2020). Transite: a computational motif-based analysis platform that identifies RNA-binding proteins modulating changes in gene expression. *Cell Rep.* 32:108064. doi: 10.1016/j.celrep.2020.108064

Langfelder, P., and Horvath, S. (2008). WGCNA: an R package for weighted correlation network analysis. *BMC Bioinform.* 9:559. doi: 10.1186/1471-2105-9-559

Lareau, L. F., and Brenner, S. E. (2015). Regulation of splicing factors by alternative splicing and NMD Is conserved between kingdoms yet evolutionarily flexible. *Mol. Biol. Evol.* 32, 1072–1079. doi: 10.1093/molbev/msv002

Lei, M., Dong, D., Mu, S., Pan, Y.-H., and Zhang, S. (2014). Comparison of brain transcriptome of the greater horseshoe bats (Rhinolophus ferrumequinum) in active and torpid episodes. *PLoS One* 9:e107746. doi: 10.1371/journal.pone.0107746

Lemskaya, N. A., Kulemzina, A. I., Beklemisheva, V. R., Biltueva, L. S., Proskuryakova, A. A., Hallenbeck, J. M., et al. (2018). A combined banding method that allows the reliable identification of chromosomes as well as differentiation of AT- and GC-rich heterochromatin. *Chromosome Res.* 26, 307–315. doi: 10.1007/s10577-018-9589-9

Lieberman-Aiden, E., Van Berkum, N. L., Williams, L., Imakaev, M., Ragoczy, T., Telling, A., et al. (2009). Comprehensive mapping of long-range interactions reveals folding principles of the human genome. *Science* 326, 289–293. doi: 10.1126/science.1181369

Longden, T. A., Dabertrand, F., Koide, M., Gonzales, A. L., Tykocki, N. R., Brayden, J. E., et al. (2017). Capillary K+-sensing initiates retrograde hyperpolarization to increase local cerebral blood flow. *Nat. Neurosci.* 20, 717–726. doi: 10.1038/nn.4533

Love, M. I., Huber, W., and Anders, S. (2014). Moderated estimation of fold change and dispersion for RNA-seq data with DESeq2. *Genome Biol.* 15:550.

MacCannell, A. D. V., Sinclair, K. J., Tattersall, G. J., Mckenzie, C. A., and Staples, J. F. (2019). Identification of a lipid-rich depot in the orbital cavity of the thirteen-lined ground squirrel. *J. Exp. Biol.* 222:jeb195750. doi: 10.1242/jeb.195750

Marín-Rubio, J. L., Vela-Martín, L., Fernández-Piqueras, J., and Villa-Morales, M. (2019). FADD in Cancer: mechanisms of altered expression and function, and clinical implications. *Cancers (Basel)* 11:1462. doi: 10.3390/cancers11101462

Martin, M. (2011). Cutadapt removes adapter sequences from high-throughput sequencing reads. *EMBnet J.* 17:3.

Martin, S. L. (2008). Mammalian hibernation: a naturally reversible model for insulin resistance in man? *Diab. Vasc. Dis. Res.* 5, 76–81. doi: 10.3132/dvdr.2008.013

Micheli, L., Ceccarelli, M., Farioli-Vecchioli, S., and Tirone, F. (2015). Control of the normal and pathological development of neural stem and progenitor cells by the PC3/Tis21/Btg2 and Btg1 Genes. *J. Cell. Physiol.* 230, 2881–2890. doi: 10.1002/jcp.25038

Nasoohi, S., Ismael, S., and Ishrat, T. (2018). Thioredoxin-Interacting Protein (TXNIP) in cerebrovascular and neurodegenerative diseases: regulation and implication. *Mol. Neurobiol.* 55, 7900–7920. doi: 10.1007/s12035-018-0917-z

Nespolo, R. F., Gaitan-Espitia, J. D., Quintero-Galvis, J. F., Fernandez, F. V., Silva, A. X., Molina, C., et al. (2018). A functional transcriptomic analysis in the relict marsupial Dromiciops gliroides reveals adaptive regulation of protective functions during hibernation. *Mol. Ecol.* 27, 4489–4500. doi: 10.1111/mec.14876

Niknafs, Y. S., Pandian, B., Iyer, H. K., Chinnaiyan, A. M., and Iyer, M. K. (2017). TACO produces robust multisample transcriptome assemblies from RNA-seq. *Nat. Meth.* 14, 68–70. doi: 10.1038/nmeth.4078

Niu, L. J., Xu, R. X., Zhang, P., Du, M. X., and Jiang, X. D. (2012). Suppression of Frizzled-2-mediated Wnt/Ca2+ signaling significantly attenuates intracellular

calcium accumulation in vitro and in a rat model of traumatic brain injury. *Neuroscience* 213, 19–28. doi: 10.1016/j.neuroscience.2012.03.057

Ohe, C. G., Darian-Smith, C., Garner, C. C., and Heller, H. C. (2006). Ubiquitous and temperature-dependent neural plasticity in hibernators. *J. Neurosci.* 26, 10590–10598. doi: 10.1523/jneurosci.2874-06.2006

Otsuka, H., Fukao, A., Funakami, Y., Duncan, K. E., and Fujiwara, T. (2019). Emerging evidence of translational control by AU-rich element-binding proteins. *Front. Genet.* 10:332. doi: 10.3389/fgene.2019.00332

Palfreyman, M. T., and Jorgensen, E. M. (2017). Unc13 Aligns SNAREs and superprimes synaptic vesicles. *Neuron* 95, 473–475. doi: 10.1016/j.neuron.2017.07.017

Patro, R., Duggal, G., Love, M. I., Irizarry, R. A., and Kingsford, C. (2017). Salmon provides fast and bias-aware quantification of transcript expression. *Nat. Methods* 14:417. doi: 10.1038/nmeth.4197

Pertea, M., Kim, D., Pertea, G. M., Leek, J. T., and Salzberg, S. L. (2016). Transcript-level expression analysis of RNA-seq experiments with HISAT, StringTie and Ballgown. *Nat. Protocols* 11, 1650–1667. doi: 10.1038/nprot.2016.095

Pertea, M., Pertea, G. M., Antonescu, C. M., Chang, T.-C., Mendell, J. T., and Salzberg, S. L. (2015). StringTie enables improved reconstruction of a transcriptome from RNA-seq reads. *Nat. Biotech.* 33, 290–295. doi: 10.1038/nbt.3122

Putnam, N. H., O'connell, B. L., Stites, J. C., Rice, B. J., Blanchette, M., Calef, R., et al. (2016). Chromosome-scale shotgun assembly using an in vitro method for long-range linkage. *Genome Res.* 26, 342–350. doi: 10.1101/gr.193474.115

Richter, M. M., Barnes, B. M., O'reilly, K. M., Fenn, A. M., and Buck, C. L. (2017). The influence of androgens on hibernation phenology of free-living male arctic ground squirrels. *Horm. Behav.* 89, 92–97. doi: 10.1016/j.yhbeh.2016.12.007

Riemondy, K. A., Gillen, A. E., White, E. A., Bogren, L. K., Hesselberth, J. R., and Martin, S. L. (2018). Dynamic temperature-sensitive A-to-I RNA editing in the brain of a heterothermic mammal during hibernation. *RNA* 24, 1481–1495. doi: 10.1261/rna.066522.118

Riemondy, K. A., Sheridan, R. M., Gillen, A., Yu, Y., Bennett, C. G., and Hesselberth, J. R. (2017). valr: reproducible genome interval analysis in R. *F1000Res.* 6:1025. doi: 10.12688/f1000research.11997.1

Rissland, O. S. (2017). The organization and regulation of mRNA–protein complexes. *WIREs RNA* 8:e1369. doi: 10.1002/wrna.1369

Russell, T. L., Zhang, J., Okoniewski, M., Franke, F., Bichet, S., and Hierlemann, A. (2019). Medullary respiratory circuit is reorganized by a seasonally-induced program in preparation for hibernation. *Front. Neurosci.* 13:376. doi: 10.3389/fnins.2019.00376

Saldi, T., Cortazar, M. A., Sheridan, R. M., and Bentley, D. L. (2016). Coupling of RNA Polymerase II transcription elongation with Pre-mRNA splicing. *J. Mol. Biol.* 428, 2623–2635. doi: 10.1016/j.jmb.2016.04.017

Santini, E., and Klann, E. (2011). Dysregulated mTORC1-dependent translational control: from brain disorders to psychoactive drugs. *Front. Behav. Neurosci.* 5:76. doi: 10.3389/fnbeh.2011.00076

Schwartz, C., Ballinger, M. A., and Andrews, M. T. (2015). Melatonin receptor signaling contributes to neuroprotection upon arousal from torpor in thirteen-lined ground squirrels. *Am. J. Physiol. Regul. Integr. Comp. Physiol.* 309, R1292–R1300. doi: 10.2307/1377818

Schwartz, C., Hampton, M., and Andrews, M. T. (2013). Seasonal and regional differences in gene expression in the brain of a hibernating mammal. *PLoS One* 8:e58427. doi: 10.1371/journal.pone.0058427

Shao, W., Zhao, Q.-Y., Wang, X.-Y., Xu, X.-Y., Tang, Q., Li, M., et al. (2012). Alternative splicing and trans-splicing events revealed by analysis of the Bombyx mori transcriptome. *RNA* 18, 1395–1407. doi: 10.1261/rna.029751.111

Sheriff, M. J., Williams, C. T., Kenagy, G. J., Buck, C. L., and Barnes, B. M. (2012). Thermoregulatory changes anticipate hibernation onset by 45 days: data from free-living arctic ground squirrels. *J. Comp. Physiol. B* 182, 841–847. doi: 10.1007/s00360-012-0661-z

Shim, H., Wu, C., Ramsamooj, S., Bosch, K. N., Chen, Z., Emerling, B. M., et al. (2016). Deletion of the gene Pip4k2c a novel phosphatidylinositol kinase, results in hyperactivation of the immune system. *Proc. Natl. Acad. Sci. U. S. A.* 113, 7596–7601. doi: 10.1073/pnas.1600934113

Soneson, C., Love, M. I., and Robinson, M. D. (2015). Differential analyses for RNA-seq: transcript-level estimates improve gene-level inferences. *F1000Res* 4:1521. doi: 10.12688/f1000research.7563.2

Sonntag, M., and Arendt, T. (2019). Neuronal activity in the hibernating brain. *Front. Neuroanat.* 13:71. doi: 10.3389/fnana.2019.00071

Spasic, M., Friedel, C. C., Schott, J., Kreth, J., Leppek, K., Hofmann, S., et al. (2012). Genome-wide assessment of AU-rich elements by the AREScore Algorithm. *PLoS Genet.* 8:e1002433. doi: 10.1371/journal.pgen.1002433

Srere, H. K., Wang, L. C. H., and Martin, S. L. (1992). Central role for differential gene expression in mammalian hibernation. *Proc. Natl. Acad. Sci. U. S. A.* 89, 7119–7123. doi: 10.1073/pnas.89.15.7119

Staples, J. F. (2016). Metabolic flexibility: hibernation, torpor, and estivation. *Compr. Physiol.* 6, 737–771. doi: 10.1002/cphy.c140064

Starossom, S. C., Campo Garcia, J., Woelfle, T., Romero-Suarez, S., Olah, M., Watanabe, F., et al. (2019). Chi3l3 induces oligodendrogenesis in an experimental model of autoimmune neuroinflammation. *Nat. Commun.* 10:217.

Stephens, M. (2017). False discovery rates: a new deal. *Biostatistics* 18, 275–294.

Su, J., Gorse, K., Ramirez, F., and Fox, M. A. (2010). Collagen XIX is expressed by interneurons and contributes to the formation of hippocampal synapses. *J. Comp. Neurol.* 518, 229–253. doi: 10.1002/cne.22228

Tang, B. L. (2016). (WNK)ing at death: with-no-lysine (Wnk) kinases in neuropathies and neuronal survival. *Brain Res. Bull.* 125, 92–98. doi: 10.1016/j.brainresbull.2016.04.017

Team, R. C. (2019). *R: A Language and Environment for Statistical Computing* [Online]. Vienna: R Foundation of Statistical Computing.

Trimmer, J. S. (2015). Subcellular localization of K+ channels in mammalian brain neurons: remarkable precision in the midst of extraordinary complexity. *Neuron* 85, 238–256. doi: 10.1016/j.neuron.2014.12.042

van Breukelen, F., and Martin, S. L. (2001). Translational initiation is uncoupled from elongation at 18 degrees C during mammalian hibernation. *Am. J. Physiol. Regul. Integr. Comp. Physiol.* 281, R1374–R1379.

van Breukelen, F., and Martin, S. L. (2002). Reversible depression of transcription during hibernation. *J. Comp. Physiol.* 172, 355–361. doi: 10.1007/s00360-002-0256-1

van Breukelen, F., and Martin, S. L. (2015). The hibernation continuum: physiological and molecular aspects of metabolic plasticity in mammals. *Physiology (Bethesda)* 30, 273–281. doi: 10.1152/physiol.00010.2015

Vaquero-Garcia, J., Barrera, A., Gazzara, M. R., GonzaìLez-Vallinas, J., Lahens, N. F., Hogenesch, J. B., et al. (2016). A new view of transcriptome complexity and regulation through the lens of local splicing variations. *eLife* 5:e11752.

Wan, L., Yu, W., Shen, E., Sun, W., Liu, Y., Kong, J., et al. (2019). SRSF6-regulated alternative splicing that promotes tumour progression offers a therapy target for colorectal cancer. *Gut* 68, 118–129. doi: 10.1136/gutjnl-2017-314983

Wang, F.-X., Yang, X.-L., Ma, Y.-S., Wei, Y.-J., Yang, M.-H., Chen, X., et al. (2018). TRIF contributes to epileptogenesis in temporal lobe epilepsy during TLR4 activation. *Brain Behav. Immun.* 67, 65–76. doi: 10.1016/j.bbi.2017.07.157

Wilz, M., and Heldmaier, G. (2000). Comparison of hibernation, estivation and daily torpor in the edible dormouse, Glis glis. *J. Comp. Physiol. [B]* 170, 511–521. doi: 10.1007/s003600000129

Yang, L., Wang, C., Li, F., Zhang, J., Nayab, A., Wu, J., et al. (2017). The human RNA-binding protein and E3 ligase MEX-3C binds the MEX-3–recognition element (MRE) motif with high affinity. *J. Biol. Chem.* 292, 16221–16234. doi: 10.1074/jbc.m117.797746

Yeo, G., and Burge, C. B. (2004). Maximum entropy modeling of short sequence motifs with applications to RNA splicing signals. *J. Comput. Biol.* 11, 377–394. doi: 10.1089/1066527041410418

Conflict of Interest: KG is CSO for Fauna Bio and SM and CB serve on its SAB.

The remaining authors declare that the research was conducted in the absence of any commercial or financial relationships that could be construed as a potential conflict of interest.

frontiers in Physiology

REVIEW
published: 20 January 2021
doi: 10.3389/fphys.2020.623665

The Torpid State: Recent Advances in Metabolic Adaptations and Protective Mechanisms†

Sylvain Giroud[1], Caroline Habold[2], Roberto F. Nespolo[3,4], Carlos Mejías[3,4], Jérémy Terrien[5], Samantha M. Logan[6], Robert H. Henning[7] and Kenneth B. Storey[6]*

[1] Research Institute of Wildlife Ecology, Department of Interdisciplinary Life Sciences, University of Veterinary Medicine, Vienna, Austria, [2] University of Strasbourg, CNRS, IPHC, UMR 7178, Strasbourg, France, [3] Instituto de Ciencias Ambientales y Evolutivas, Universidad Austral de Chile, ANID – Millennium Science Initiative Program-iBio, Valdivia, Chile, [4] Center of Applied Ecology and Sustainability, Departamento de Ecología, Facultad de Ciencias Biológicas, Pontificia Universidad Católica de Chile, Santiago, Chile, [5] Unité Mécanismes Adaptatifs et Evolution (MECADEV), UMR 7179, CNRS, Muséum National d'Histoire Naturelle, Brunoy, France, [6] Department of Biology, Carleton University, Ottawa, ON, Canada, [7] Department of Clinical Pharmacy and Pharmacology, University Medical Center Groningen, Groningen, Netherlands

OPEN ACCESS

Edited by:
Steven Swoap, Williams College, United States

Reviewed by:
Giovanna Zoccoli, University of Bologna, Italy
Peter R. Corridon, Khalifa University, United Arab Emirates

****Correspondence:***
Sylvain Giroud
sylvain.giroud@vetmeduni.ac.at

Specialty section:
This article was submitted to Integrative Physiology, a section of the journal Frontiers in Physiology

Received: *30 October 2020*
Accepted: *21 December 2020*
Published: *20 January 2021*

Citation:
Giroud S, Habold C, Nespolo RF, Mejías C, Terrien J, Logan SM, Henning RH and Storey KB (2021) The Torpid State: Recent Advances in Metabolic Adaptations and Protective Mechanisms. Front. Physiol. 11:623665. doi: 10.3389/fphys.2020.623665

Torpor and hibernation are powerful strategies enabling animals to survive periods of low resource availability. The state of torpor results from an active and drastic reduction of an individual's metabolic rate (MR) associated with a relatively pronounced decrease in body temperature. To date, several forms of torpor have been described in all three mammalian subclasses, i.e., monotremes, marsupials, and placentals, as well as in a few avian orders. This review highlights some of the characteristics, from the whole organism down to cellular and molecular aspects, associated with the torpor phenotype. The first part of this review focuses on the specific metabolic adaptations of torpor, as it is used by many species from temperate zones. This notably includes the endocrine changes involved in fat- and food-storing hibernating species, explaining biomedical implications of MR depression. We further compare adaptive mechanisms occurring in opportunistic vs. seasonal heterotherms, such as tropical and sub-tropical species. Such comparisons bring new insights into the metabolic origins of hibernation among tropical species, including resistance mechanisms to oxidative stress. The second section of this review emphasizes the mechanisms enabling heterotherms to protect their key organs against potential threats, such as reactive oxygen species, associated with the torpid state. We notably address the mechanisms of cellular rehabilitation and protection during torpor and hibernation, with an emphasis on the brain, a central organ requiring protection during torpor and recovery. Also, a special focus is given to the role of an ubiquitous and readily-diffusing molecule, hydrogen sulfide (H_2S), in protecting against ischemia-reperfusion damage in various organs over the torpor-arousal cycle and during the torpid state. We conclude that (i) the flexibility of torpor use as an adaptive strategy enables different heterothermic species to substantially suppress their energy needs during periods of severely reduced food availability, (ii) the torpor phenotype implies marked metabolic adaptations from the whole organism

down to cellular and molecular levels, and (iii) the torpid state is associated with highly efficient rehabilitation and protective mechanisms ensuring the continuity of proper bodily functions. Comparison of mechanisms in monotremes and marsupials is warranted for understanding the origin and evolution of mammalian torpor.

Keywords: body temperature, metabolic depression, hibernation, hormones, lipids, non-Holarctic heterotherms, antioxidant, H_2S

INTRODUCTION

Torpor and hibernation represent powerful strategies that enable animals to survive periods of low resource availability in their environment. The state of torpor results from an active and drastic reduction of metabolic rate (MR) associated with an accompanying decrease in body temperature (T_b) after passive cooling (Heldmaier et al., 2004; Jastroch et al., 2016). According to several authors (Ruf and Geiser, 2015; Geiser, 2020), two different forms of torpor, also called heterothermy, can be distinguished based on the duration of the hypometabolic state. In daily torpor, animals show average minimum torpid MR of ∼19% of basal rates and lower their T_b to usually between 12 and 25°C during torpor; torpor lasts less than 24 h and is accompanied by continued foraging (Ruf and Geiser, 2015). On the other hand, during hibernation, individuals achieve a minimum torpid MR of 4% of basal rates, along with a variable reduction of their T_b ranging on average for most species between 0 and 10°C (Ruf and Geiser, 2015). Hence, hibernation corresponds to multiple and successive torpor bouts lasting for days to few weeks, during which animals rely entirely on fuel stores, such as body fat and/or food caches (Humphries et al., 2003a,b; Dark, 2005). Torpor is employed by all three mammalian subclasses, i.e., monotremes, marsupial, and placentals, as well as several avian orders (Ruf and Geiser, 2015) whereas hibernation is documented in mammals from all three subclasses but is known for only one bird species. Daily torpor is diverse in both mammals and birds, and is typically not as seasonal as hibernation (Geiser, 2020). The use of torpor is often associated with species inhabiting cold and seasonal habitats, such as temperate and arctic zones, but torpor is also used by many non-Holarctic species, i.e., the tropics and southern hemisphere (Nowack et al., 2020).

Most seasonal heterothermic eutherian species enter an obligatory physiological and behavioral preparation period when days become shorter, i.e., announcing the winter season. Such remodeling is controlled by the hypothalamus, operates at multiple levels (reviewed in Auld et al., 2010), and comprises a variety of physiological, biochemical, and molecular changes such as regulations of metabolic processes, erythropoiesis, protein transcription, membrane composition, and thermogenesis (Klug and Brigham, 2015; Ruf and Geiser, 2015; Jastroch et al., 2016). This leads to drastic changes in most of biological functions, including metabolic (Jastroch et al., 2016) and reproductive (Clarke and Caraty, 2013) signaling pathways. Actually, the physiological preparations for harsh winter conditions is probably explained by an adjustment of the thermoneutral zone combined with a decrease in basal MR (Kobbe et al., 2014), which contributes to the accumulation of energy body (fat) stores. Additionally, heterothermic species adjust the onset of torpor or hibernation periods to environmental factors, including food availability and/or quality (notably in terms of lipid composition), and T_a (Boyles et al., 2007; Geiser, 2013; Giroud et al., 2018), therefore introducing some flexibility to these syndromes. Further, diverse phenology of hibernation was described among different age classes, i.e., juveniles, yearlings, and adults (Michener, 1978; French, 1990; Kart Gür and Gür, 2015; Siutz et al., 2016), but also in aged individuals compared to younger ones (e.g., Bieber et al., 2018). These differences were mostly linked to ecological cues, including developmental constraints, rather than physiological or molecular mechanistic aspects. For instance, it is known that juveniles, especially those born late in the reproductive season, delay hibernation onset compared to yearlings or adult individuals (Boag and Murie, 1981; Stumpfel et al., 2017), due to their need to further grow and develop and extra time needed to accumulate sufficient fat reserves prior to hibernation (Mahlert et al., 2018); a process that strongly determines the overwintering survival of the individuals. The demonstration that the use of torpor and the physiological remodeling required for the setup of the torpor phenotype is a deeply conserved feature in species living in seasonal environments comes from the variety of studies both from wild and captive conditions. Indeed, organisms maintained under captive environment, with stable and favorable conditions, show persistent circannual rhythms even after more than fifty generations (Perret and Aujard, 2001; Terrien et al., 2017), indicating the deep genetic imprinting of the control of biological clocks on metabolism and reproduction (Dardente et al., 2019).

During the hysteresis of the torpor-arousal cycle over hibernation, the whole organism including organs, tissues, cells, and molecules experience major metabolic transitions triggered by extreme changes in MR and T_b. This is notably the case during the transition phase of arousal from torpor when individual's MR shows a drastic several-fold increase allowing T_b to return to normothermia. Periodic arousals represent the highest proportion of energy expended during the hibernation process, e.g., 70–80% in temperate species (Wang, 1978), and arousals are accompanied with increases in oxidative stress levels, as supported by substantial shortening of telomere lengths in individuals over winter hibernation (Turbill et al., 2013; Giroud et al., 2014; Hoelzl et al., 2016; Nowack et al., 2019). Prior to

[†]This review was written by the different authors and is partially based on oral presentations given during the symposium "Living at low pace: From the whole organism to the molecule" at the 10th International Congress of Comparative Physiology and Biochemistry (ICCPB) held in Ottawa, Canada.

hibernation, antioxidant defenses, and other specific regulatory processes are also upregulated to ensure the integrity of body organs, tissues, and cells (for review, see Carey et al., 2003). During the torpid state, specific protective mechanisms enter into play to ensure the continuity of key physiological functions, including heart, lung, muscle, and brain activity, to sustain life at low pace (for reviews, see Johansson, 1996; Ruf and Arnold, 2008; Talaei et al., 2012; Jastroch et al., 2016; Chanon et al., 2018; Nespolo et al., 2018).

Despite the threatening side associated with the torpid state, some progress has been made to further understand the mechanisms underlying the onset, maintenance and arousal from torpor, notably by pharmacological induction of hypometabolism in non-heterothermic species (Bouma et al., 2012). Several molecules and compounds for the induction and the maintenance of a torpor-like state in non-heterotherms have so far received special attention, including 5′-AMP and hydrogen sulfide (H_2S). In particular, the latter seems to be involved in the metabolic maintenance and protective mechanisms of the torpid state in hibernators (see section below for further details). Recently, it has been established that fasting and cold are the most important proximate determinants of torpor in mice, acting by a hypothalamic neuronal circuit as a feedback between fasting, cold, and brown adipose tissue (BAT) activity. Using "designer receptors exclusively activated by designer drugs" (DREADDs) systems, specific hypothalamic neurons were identified and were shown to be involved in the occurrence of either a short-term (daily) torpor (Hrvatin et al., 2020) or a long-term, multi-days hypometabolic state in mice similar to hibernation (Takahashi et al., 2020). Interestingly, a light-sensitive receptor protein expressed in neurons of the preoptic area inhibits BAT metabolism, thus demonstrating a strong link between light and metabolism in animals (Zhang et al., 2020). These results, however, open the question as to how this could work in heterothermic animals with no functional descriptions of BAT, i.e., marsupials and monotremes (Gaudry and Campbell, 2017). One mechanism and its evolutionary implications for heat generation as an alternative to uncoupling processes in BAT could be linked to non-shivering thermogenesis (NST) in muscle (reviewed in Nowack et al., 2017). Recently, this has been demonstrated to occur in wild boar piglets, a species lacking BAT, but which demonstrates marked thermoregulatory adaptive responses (Nowack et al., 2019).

The objective of the present review is then to highlight some of the characteristics associated with the torpor phenotype. In the first section, we focus on specific adaptations for torpor occurring in heterotherms that show contrasting heterothermic patterns. This includes (i) metabolic and endocrine changes involved in fat-storing vs. food-storing hibernating species, and (ii) adaptive mechanisms occurring in opportunistic vs. seasonal heterotherms, such as tropical and sub-tropical species. The latter notably brings, based on recent data on molecular aspects, new insights on the metabolic origins of hibernation among tropical species, and on the view of daily torpor and hibernation as a continuum of hypometabolic responses. In the second section of this review we emphasize the molecular mechanisms enabling heterotherms to protect key organs against potential threats, such as reactive oxygen species, associated with the torpid state. We notably address mechanisms of cellular rehabilitation and protection during torpor and hibernation, with (i) an emphasis on the brain, a central organ to be protected during torpor and recovery after, and (ii) the role of a ubiquitous and readily-diffusing molecule, H_2S, in protecting the integrity of organs against damage occurring over the torpor-arousal cycle and during the torpid state.

METABOLIC ADAPTATIONS DURING TORPOR AND HIBERNATION

Fat-Storing vs. Food-Storing Hibernators: Hibernating Patterns, Lipid, and Energy Metabolism

Hibernators are generally classified as either (i) fat-storing species, i.e., animals that do not feed during hibernation and rely entirely on body fat reserves accumulated prior to hibernation to cover winter energy requirements, or (ii) food-storing species that feed during periodic arousals between deep torpor bouts and therefore hoard large amounts of food prior to winter (mainly seeds) in their burrow (French, 1988). Due to these different strategies of energy acquisition, fat- and food-storing species show contrasting physiological and behavioral adaptations that we will review in this section.

Fat-storing species typically undergo an intense period of hyperphagia to build up large amounts of internal fat reserves during several weeks to months before hibernation. As example, golden-mantled ground squirrels (*Callospermophilus lateralis*) show respectively a two and threefold increase in body and fat mass, in only 5–7 weeks prior to hibernation (Kenagy and Barnes, 1988). Yellow-bellied marmots (*Marmota flaviventris*) also increase their body mass up to 150% through accumulating 3–4.5 kg body fat during their active period in summer (Florant et al., 2004). The accumulation of large internal fat stores associated with long and deep torpor bouts (as long as 15 days), and sometimes social thermoregulation, enable fat-storing animals to fast throughout winter. By contrast, food-storing species store large amounts of food in a burrow. These species are mainly granivorous, because seeds are the only food items that can be stored several months without rotting (Humphries et al., 2003b). Only a few species are food-storing hibernators, mainly hamsters and chipmunks and individuals typically weigh between 10 and 300 g and are solitary. During hibernation, food-storing animals undergo shorter torpor bouts than fat-storing species, but have longer interbout euthermic episodes during which individuals consume their food hoards (Wollnik and Schmidt, 1995; Humphries et al., 2001; **Table 1**).

Metabolic Changes in Fat-Storing Hibernating Species According to Body Fat Mass Changes and Activity

Fat-storing species show an increase in body (fat) mass prior to hibernation (**Figures 1A**, **3** left panel). Since individuals do not feed during the whole hibernation period, fat-storing hibernators

TABLE 1 | Hibernation parameters of the common hamster (*Cricetus cricetus*), a food-storing species, and the garden dormouse (*Eliomys quercinus*), a fat-storing species, under controlled conditions of ambient temperature (T_a) and photoperiod.

Hibernation parameters	Food-storing	Fat-storing
	Common hamster	Garden dormouse
Hibernation duration (h)	2385.6 ± 494.4**	3908.1 ± 32.6
Number of torpor bouts*	26.6 ± 0.6	19.4 ± 2.4
Mean duration of torpor bouts* (h)	90.5 ± 2.1	195.1 ± 21.4
Mean duration of IBE* (h)	29.4 ± 1.9	5.5 ± 1.0
Minimal body temperature (°C)	0.97***	6.0 ± 0.8

Conditions were for common hamsters (except for minimal body temperature): T_a ~ 8°C, LD 10/14 h; and for garden dormice: T_a ~ 5.3°C, LD 0/24 h, i.e., constant darkness. Results are presented as mean values ± SE. Data originated from Mahlert et al. (2018) for the garden dormouse, and from Waßmer and Wollnik (1997) (**) and Wassmer (2004) (***) for the common hamster.
**Body temperature threshold for torpor bouts or phases of interbout euthermia (IBE) is of 32°C for common hamsters or 18°C for garden dormice.*

rely on their fat stores to cover their energy requirements during winter. Plasma profiles of these animals during hibernation are characterized by a decrease in triglycerides, whereas plasma levels of ketone bodies increase (Rauch and Behrisch, 1981; Krilowicz, 1985; Nizielski et al., 1989). Lipid use and, more precisely, oxidation of non-esterified fatty acids (NEFAs) during hibernation are also supported by a respiratory quotient (RQ) close to 0.7 during torpor episodes (Lyman and Chatfield, 1955; Mokrasch et al., 1960; Snapp and Heller, 1981). Glycemia is maintained throughout hibernation thanks to the activation of gluconeogenic pathways (Twente and Twente, 1967; Tashima et al., 1970; Krilowicz, 1985; Florant et al., 1986; Nizielski et al., 1989). All these findings were recently confirmed via RNA sequencing and proteomic analyses in hibernating 13-lined ground squirrels (Hampton et al., 2011, 2013; Vermillion et al., 2015).

In fat-storing hibernators, the tissue showing the greatest changes during hibernation is probably the white adipose tissue (WAT). Therefore, it was interesting to look at adipokine levels over the seasons. Leptin is secreted proportionally to the amount of WAT. Hence, not surprising, plasma leptin levels are substantially high after fat accumulation, just before hibernation, compared to summer levels (*Marmota monax*: Concannon et al., 2001; *M. flaviventris:* Florant et al., 2004; *Dromiciops gliroides*: Franco et al., 2017; **Table 2**). However, this hormone is known to increase energy expenditure and to inhibit the initiation of torpor (Freeman et al., 2004). In the woodchuck, a large fat-storing species, it seems that plasma leptin levels and hypothalamic sensitivity to this hormone are uncoupled during the preparatory fattening phase prior to the hibernation onset (Concannon et al., 2001). In small hibernating species, uncoupling also exists, but

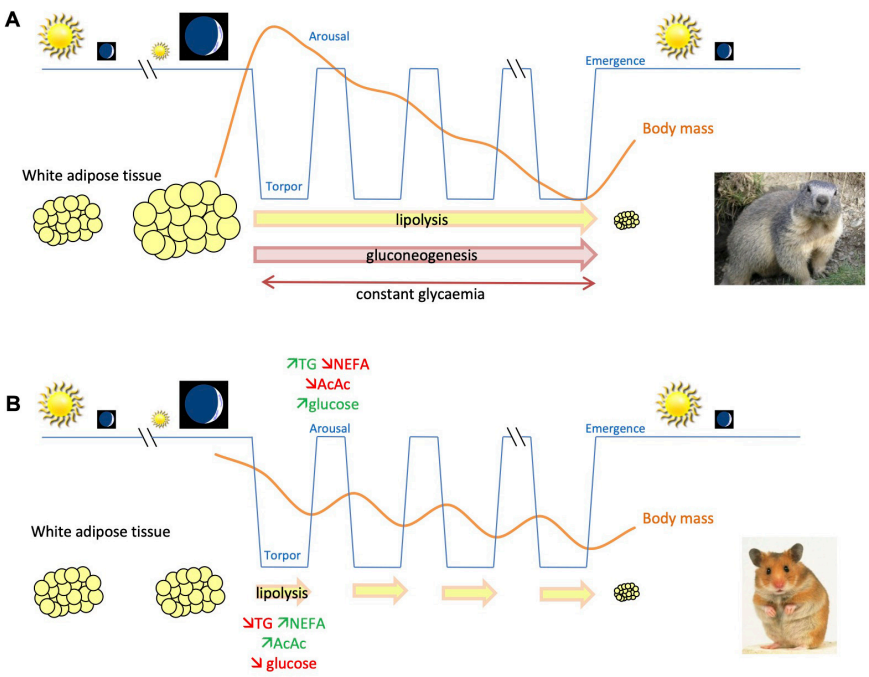

FIGURE 1 | Schematic representation for comparison of body mass changes and use of energy substrates throughout hibernation in fat-storing and food-storing species. **(A)** In fat-storing hibernators, e.g., marmots, animals undergo a long-term fast during winter by mobilizing mainly lipids, accumulated prior to winter in white adipose tissue, to sustain their energy requirements. This leads to a substantial reduction of body (fat) mass of individuals over their winter hibernation fast. Energy can also come from gluconeogenesis, i.e., the synthesis of glucose from non-carbohydrate substrates during hibernation. **(B)** In contrast, food-storing hibernators, e.g., Syrian hamsters, experience a state of intermittent fasting during winter hibernation. Animals mobilize lipid stores during the torpor phases, but feed during interbout arousals, using glucose as main source of energy, and partially restore their body lipid/glycogen stores. In contrast to fat-storing species, glycemia decreases during torpor, which could constitute an endogenous signal for food-storing hibernators to arise from torpor and feed during interbout euthermia.

TABLE 2 | Plasma hormone concentrations (means ± SEM) of fat-storing species during long photoperiod ("LP"), short photoperiod ("SP") hibernation at temperate ("SP warm") or low ("SP cold") ambient temperatures.

Hormones	LP	SP warm	SP cold		Species	Photoperiod/temperature	References
			Torpor	Re-warm	Arousal			
Insulin (pg.mL^{-1})	–	–	2.26 ± 0.38^{a}	12.7 ± 3.5^{b}	3.2 ± 0.9^{a}	*Glis glis*	LP LD natural/SP LD_9:17 (5°C)	Castex et al., 1984
	–	–	0.73 ± 0.14^{a}	0.90 ± 0.10^{a}	0.73 ± 0.10^{a}	*Marmota flaviventris*	SP LD_8:16 (5 ± 2°C)	Florant et al., 1986
Glucagon (pg.mL^{-1})	–	–	206 ± 14^{a}	334 ± 36^{b}	268 ± 21^{b}	*Glis glis*	LP LD natural/SP LD_8:16 (5°C)	Hoo-Paris et al., 1985
	–	–	82 ± 9^{a}	75 ± 8^{a}	94 ± 6^{a}	*Marmota flaviventris*	SP LD_8:16 (5 ± 2°C)	Florant et al., 1986
Adiponectin (AU)	1.2	1.2	–	–	–	*Marmota flaviventris*	LP LD natural (20 ± 3°C)/SP LD_0:24 (5°C)	Florant et al., 2004
Leptin (ng.mL^{-1})	3.2^{a}	–	10.7^{b}			*Marmota flaviventris*	LP LD natural (20 ± 3°C)/SP LD_0:24 (5°C)	Florant et al., 2004
Ghrelin (ng.mL^{-1})	3.6$^{a\prime}$	5.6$^{b\prime}$	~3^{a}	–	~4^{b}	*Citellus lateralis*	LD natural (20 ± 2°C)/SP LD_0:24 (5°C)	Healy et al., 2010
Cortisol (ng.mL^{-1})	77.3 ± 20.3	51.2 ± 3.8	19.2 ± 0.5^{a}	–	36.2 ± 2.2^{b}	*Citellus citellus*	LP LD natural (16-26°C)/SP LD_0:24 (7 ± 1°C)	Shivatcheva et al., 1988

Different superscripts indicate significant differences ($p < 0.05$) between columns from the same raw. Adapted from Weitten et al. (2013).

between adiposity and plasma leptin levels, as shown in the little brown bat (*Myotis luciferus*: Kronfeld-Schor et al., 2000). Similar patterns have been observed in golden-mantled ground squirrels (*C. lateralis*: Healy et al., 2008) and arctic ground squirrels (*Urocitellus parryii:* Ormseth et al., 1996; Boyer et al., 1997). Concerning adiponectin, an adipokine that is secreted inversely proportional to lipid stores (Lafontan and Viguerie, 2006), only one study has assessed its variations during the annual cycle of a hibernating species (Florant et al., 2004). This study conducted in marmots (*M. flaviventris*) showed that adiponectin is low at the beginning of fat accumulation and elevated during hibernation (Florant et al., 2004). This seems consistent with the role of adiponectin in stimulating fatty acid oxidation (Fruebis et al., 2001; Masaki et al., 2003). Other hormones controlling metabolic pathways have been measured during hibernation compared to the active season in fat-storing species. Pancreatic hormone levels are low during hibernation in deep torpor, but increase during the rewarming phase (*Erinaceus europaeus*: Hoo-Paris and Sutter, 1980; Hoo-Paris et al., 1982; *Glis glis*: Castex et al., 1984; Hoo-Paris et al., 1985; *C. lateralis:* Bauman et al., 1987). Glucagon level remains high during arousals whereas insulin level decreases, probably to sustain glycemia during this phase of euthermia (Hoo-Paris et al., 1985). In larger species, pancreatic hormone levels remain low throughout hibernation (*M. flaviventris*: Florant et al., 1986). The orexigenic hormone ghrelin increases before hibernation and may stimulate food ingestion during this period of fat accumulation (*Citellus lateralis*: Healy et al., 2010). Plasma ghrelin concentration is low during hibernation in deep torpor and increases again upon arousal from torpor, as generally observed during stages of starvation (Cummings, 2006). Cortisol decreases during deep torpor and increases again during arousal phases, but stays lower than during the active foraging phase (Popova and Koryakina, 1981; *Citellus citellus*: Shivatcheva et al., 1988). This might prevent the induction of catabolic pathways, especially of body proteins, during hibernation.

Metabolic Changes in Food-Storing Hibernating Species

Contrary to fat-storing hibernators, food-storing species do not gain weight before hibernation, or if they do, to a much lesser extent than fat-storing species. However, food-storing hibernators consume body fat (retroperitoneal and peri-epididymal fat pads) during hibernating bouts, as indicated by RQ close to 0.7 in torpor (**Figure 2**), and a decrease in triglyceridaemia, whereas plasma NEFA concentration increases (*Mesocricetus auratus*: Weitten et al., 2013). These NEFAs are mainly converted into acetoacetate. In contrast to fat-storing species, glycemia decreases during deep torpor, which could constitute an endogenous signal for food-storing hibernators to arise from torpor and feed during interbout euthermia. During arousals, the plasma profile of hamsters is characterized by a post-prandial state, with an increase in glycemia and triglyceridaemia and a decrease in plasma concentrations of both NEFAs and ketone bodies (**Figure 1B**). As described above, in fat-storing species, most hormones are at their nadir during hibernating

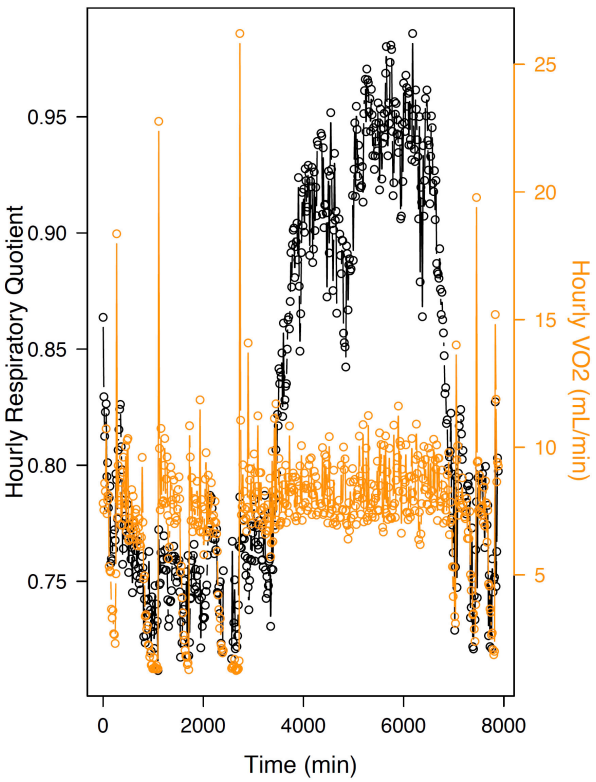

FIGURE 2 | Hourly variations in MR ("VO_2") and respiratory quotient ("RQ") toward the end of hibernation and after emergence in the common hamster, a food-storing hibernator. During torpor, VO_2 decreases substantially and RQ drops to values close to 0.7, indicating the primary oxidation of lipid to fuel energy requirements at low temperatures. Upon arousals, RQ increases to intermittent values or ∼0.8 (indicating oxidation of mixed substrates), whereas values rise to ∼0.9 at emergence from hibernation and further (0.95) toward the active season. The arrow represents the termination of hibernation, indicating an almost exclusive metabolization of carbohydrates.

bouts. This is also the case for food-storing species (**Table 3**). As an example, pancreatic hormone levels are low during deep torpor in the Syrian hamster (*M. auratus*) during hibernation but also during the pre-hibernation phase and upon arousal (Weitten et al., 2013). This is surprising because these animals are consuming stored food during arousal phases, leading to changes in plasma metabolite levels and especially glycemia that should trigger changes in pancreatic hormone secretion. However, activity of the pancreas seems to remain low in food-storing species under short photoperiod conditions, which is known to induce a winter-like phenotype in the individuals. The gut regulatory peptides GLP-1 and GIP also decrease significantly under short photoperiod (non-hibernating) conditions and during hibernation in deep torpor, but show a slight increase after food ingestion during arousal phases (Weitten et al., 2013). In fact, these peptides are generally secreted in response to food ingestion to enhance anabolic pathways (Baggio and Drucker, 2007). In food-storing species, a decrease in corticosteronemia during torpor probably prevents body protein catabolism, like in fat-storing species (Weitten et al., 2013). This latter hypothesis may be supported by an absence of increase in uremia during torpor. As in small fat-storing species, leptinemia decreases in the pre-hibernation phase (Weitten et al., 2013), suggesting an uncoupling between adiposity and leptin secretion, probably to induce a torpid state. Also, as in fat-storing animals, plasma adiponectin levels remain high throughout hibernation (Weitten et al., 2013), probably to stimulate NEFA oxidation. Adiponectin is also known to play a role in thermogenesis (Masaki et al., 2003) and could therefore enable food-storing species to maintain T_b at a few degrees above ambient temperature (T_a) during hibernation in deep torpor.

Gastro-Intestinal Adaptations of Food-Storing Species

Complete atrophy of the intestinal mucosa occurs in fat-storing species during hibernation (*Ictidomys tridecemlineatus:* Carey, 1990, 1995); *Marmota marmota*: Hume et al., 2002). In food-storing species, however, intestinal morphology is preserved and jejunal villi length even increases during torpor, as described in Syrian hamsters (*M. auratus*; Weitten et al., 2013). Despite mucosal atrophy during hibernation, fat-storing species show a maintenance of the expression of some intestinal enzymes and transporters such as those involved in glucose absorption (Carey and Martin, 1996). Similarly, Galluser et al. (1988) observed that enzymes involved in protein and sugar hydrolysis were expressed throughout hibernation in the common hamster (*Cricetus cricetus*), a food-storing species. A further study of common hamsters even showed that intestinal hydrolysis

TABLE 3 | Plasma hormone concentrations (means ± SEM) of Syrian hamsters (*Mesocricetus auratus*) under long photoperiod at 20°C ("LP20"), short photoperiod at 20°C ("SP20"), and short photoperiod at 8°C in torpor ("Torpor") or during arousal phases ("Arousal").

Hormones	LP20	SP20	Torpor	Arousal
Insulin ($ng.mL^{-1}$)	1.60 ± 0.34^{a}	0.44 ± 0.06^{b}	0.86 ± 0.08^{ab}	0.39 ± 0.04^{b}
Glucagon ($pg.mL^{-1}$)	238.4 ± 62.3^{a}	51.8 ± 23.2^{b}	53.2 ± 13.7^{ab}	38.2 ± 12.0^{b}
GLP-1 ($pg.mL^{-1}$)	108.53 ± 24.50^{a}	6.31 ± 3.25^{b}	2.24 ± 0.26^{b}	14.39 ± 3.49^{bc}
GIP ($pg.mL^{-1}$)	21.79 ± 4.90^{a}	6.62 ± 2.09^{a}	5.35 ± 1.03^{a}	13.09 ± 5.15^{a}
Leptin ($ng.mL^{-1}$)	1.61 ± 0.10^{a}	0.58 ± 0.02^{b}	0.80 ± 0.09^{ab}	0.78 ± 0.06^{ab}
Adiponectin ($ng.mL^{-1}$)	89.4 ± 2.3^{a}	95.1 ± 3.8^{a}	125.6 ± 6.6^{a}	75.9 ± 2.0^{a}
Corticosterone ($ng.mL^{-1}$)	5.93 ± 0.45^{ab}	9.23 ± 0.42^{a}	1.00 ± 0.06^{b}	8.39 ± 0.67^{a}

Different superscripts indicate significant differences ($p < 0.05$) between photoperiodic and physiological states. Adapted from Weitten et al. (2013).

of triglycerides, starch, and protein was maintained during hibernation as well as NEFA and glucose absorption (Weitten et al., 2016). Glucose absorption was even increased in hibernating hamsters, certainly to restore glycemia and glycogen stores for the subsequent hibernating bout. In another food-storing species, the eastern chipmunk (*Tamias striatus*), digestive efficiency was positively correlated to torpor use (Humphries et al., 2001). According to these authors, food-storing species could acquire a twofold advantage in undergoing a torpid state: energy sparing and increased efficiency for assimilating fuel reserves.

Biomedical and Evolutionary Implications of Contrasted Hibernation Strategies: The Case of Fat- vs. Food-Storing Hibernators

One can consider hibernation in fat-storing species as a continuous state of long-term fasting, whereas food-storing hibernators alternate short fasting and feeding bouts, which resembles intermittent fasting. These two types of fasting, i.e., continuous and intermittent, could have major biomedical implications in terms of depression of MR and positive effects of fasting on human health and longevity, as highlighted by a number of studies in this field (for reviews, see Martin et al., 2006; Golbidi et al., 2017; Patterson and Sears, 2017; de Cabo and Mattson, 2019). Indeed, these contrasted responses to metabolic depression and intermittent or long-term fully reduced calorie intake are transduced into specific metabolic adaptations, including the maintenance of a fully-functional digestive tract in food-storing species throughout the hibernating season. Such a strategy should lead to a more positive energy balance in these individuals during hibernation compared to fat-storing species.

Beyond biomedical considerations, what do these contrasted hibernation behaviors imply in terms of evolutionary perspectives? This can be addressed by comparing different life-history traits between fat- and food-storing hibernators. At first, overwintering survival was assumed to be worse in food-storing species because of a risk of rotting or pilfering of food hoards (Davis, 1976; Vander Wall, 1990). However, food-storing animals should have a better body condition upon emergence from hibernation, due to their ability to assimilate food along winter hibernation (Humphries et al., 2001). Therefore, food-storing animals can immediately mate after hibernation, and are able to produce more litters per year compared to fat-storing species. These litters are generally composed of more offspring that grow more rapidly and become fertile earlier (sometimes within their year of birth), leading to a better reproductive success in food-storing than in fat-storing species. However, the maximum lifespan is higher in fat-storing hibernators than in food storing species or non-heterotherms (Wolf et al., 2007; Careau et al., 2009; Turbill et al., 2011; Ruf et al., 2012). Hence, from an evolutionary perspective, the fat-storing strategy might correspond to a slow life history, with a trade-off in favor of survival, whereas the food-storing strategy might be in line with a fast life history, with short life expectancy and a trade-off in favor of reproduction.

Torpor in the Tropics – Opportunistic (Daily) Torpor vs. Seasonal Hibernation

Another case of contrasted use of heterothermy and its ecological and evolutionary implications is highlighted by adaptive mechanisms occurring in opportunistic and seasonal heterotherms. In particular, comparisons of the gray mouse lemur (*Microcebus murinus*) and the "monito del monte" (*D. gliroides*) are expected to bring new insights on the metabolic origins of hibernation among tropical and sub-tropical species, and notably based on molecular aspects supporting the view of the existence of a continuum of hypometabolic responses between daily torpor and hibernation.

Two Cases of Opportunistic Heterotherms: Lemurs and Monitos

In this section, we will refer to "hibernation" as a synonym for "seasonal obligatory long-lasting torpor bouts," occurring in a predictable manner, to distinguish it from "daily opportunistic torpor," which occurs among species that perform short (few hours) and shallow torpor events (T_b reduction to 15–18°C) (Song and Geiser, 1997; Bartels et al., 1998; Bozinovic et al., 2007), and generally occurs as an adaptation to unpredictable environments (Ruf and Geiser, 2015; Geiser, 2020). These authors maintain that the evolutionary origin and functional meaning of daily opportunistic torpor is different from that of seasonal torpor, and they classify species separately between "daily heterotherms" or "seasonal heterotherms," but not without debate (Boyles et al., 2013; Nowack et al., 2020). With this criterion, more than 50% of Australian mammal species appear to exhibit some form of heterothermy, showing great physiological diversity, ranging from the long hibernation bouts of echidnas (7 months) to the short torpor bouts of Dasyurid marsupials and bats (Geiser and Körtner, 2010). African heterotherms include Madagascar tenrecs (*Echinops telfari*) that display seasonal torpor (Lovegrove and Genin, 2008), elephant shrews (*Elephantulus*) with random patterns of hibernation-daily torpor (Lovegrove et al., 2001), Cheirogaleidae lemurs (Storey, 2015; Faherty et al., 2016) that show daily torpor even at "warm" temperatures, and the mouse lemur (*M. murinus*) that shows flexible heterothermic phenotypes (Schmid and Ganzhorn, 2009). Daily torpor has been described for a few South American species including hummingbirds (Carpenter, 1974; Wolf et al., 2020), bats (Bozinovic et al., 1985), rodents (Bozinovic and Marquet, 1991), and didelphid marsupials (Bozinovic et al., 2007; Geiser and Martin, 2013). However, seasonal torpor is only known in the Microbiotherian "monito del monte," *D. gliroides* (Bozinovic et al., 2004).

Monito del Monte, a Flexible Hibernator

The "monito del monte" ("monitos," hereafter) is a hibernating South American marsupial (Bozinovic et al., 2004) phylogenetically more related to Australian marsupials than to other South and North American marsupial species (Mitchell et al., 2014). This species is distributed in a latitudinal range of about 1000 km, closely associated with the temperate rainforests of Southern South America ("Valdivian" forests) in Chile and Argentina and covering altitudes ranging from

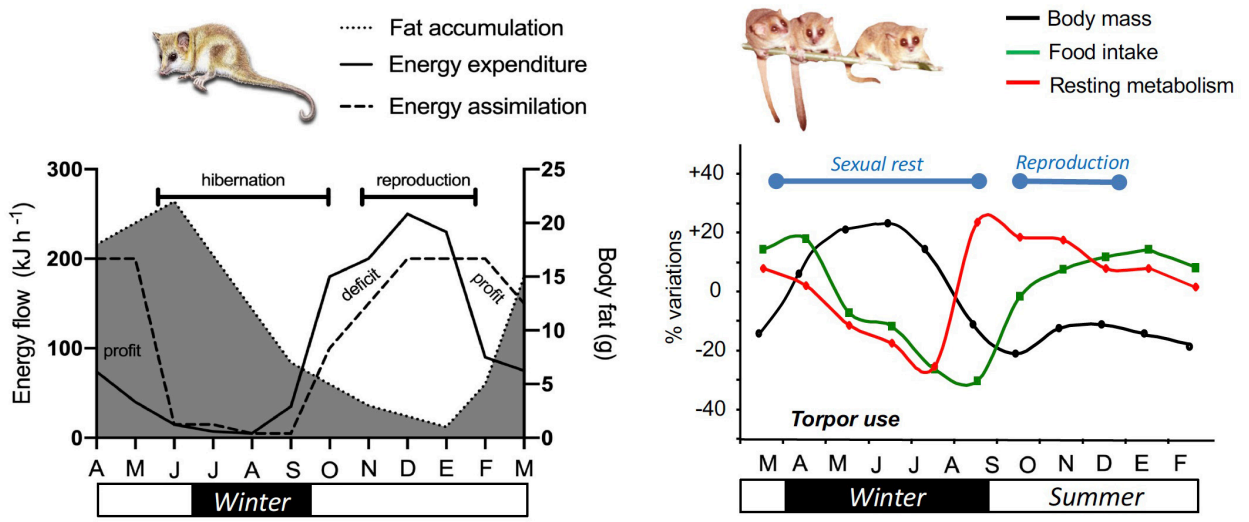

FIGURE 3 | Hypothetical (but realistic) annual budget of energy and activity in monitos and mouse lemurs. Curves for South American monito del monte (*Dromiciops gliroides*) (left panel) are based on several descriptions of the reproductive cycle (Muñoz-Pedreros et al., 2005), seasonal variations in activity, adiposity and body mass (Celis-Diez et al., 2012; Franco et al., 2017) and food availability (Franco et al., 2011; di Virgilio et al., 2014). After reproduction in March (end of summer), monitos start to reduce activity and energy expenditure, and accumulate almost twice their body size in fat (Franco et al., 2017). The net annual energy balance is usually close to zero and varies depending on cold winter temperatures, allowing torpor to occur. Annual variations of body mass, MR (Perret, 1997) and food intake in captive male mouse lemurs (*Microcebus murinus*) native to Madagascar (right panel) show drastic changes across seasons, similar to that observed in wild conditions. At the beginning of winter, male mouse lemurs make extensive use of daily torpor to save energy and therefore fatten to increase their body mass by ∼40%. They reach a plateau in the middle of winter and spontaneously increase their MR while food intake is still low. Such changes coincide with the recrudescence of the reproductive axis, and lead to body mass loss. High MRs during and after mating season are supported by increased foraging, thus leading to stable body mass throughout the summer.

200 m.a.s.l. in coastal forests to 1600 m.a.s.l. in high Andean *Nothofagus pumilio* ("lenga") forests (Martin, 2010; Valladares-Gómez et al., 2019). Hibernation in monitos extends from approximately May to September and animals show a marked seasonality in fat deposits and energy expenditure (**Figure 3**). They are strictly arboreal (Godoy-Güinao et al., 2018), social and omnivorous with great preference for fruits which make them important dispersers of several native plants (Amico and Aizen, 2000; Amico et al., 2009). Monitos hibernate in clusters of four to nine individuals in elaborate nests that they build using mosses and South American bamboo (*Chusquea quila*); these potentially represent a strategy for heat conservation in winter (Celis-Diez et al., 2012; Nespolo et al., 2020). Although initially described as seasonal heterotherms (Bozinovic et al., 2004), recent field studies using miniature data loggers for simultaneously recordings of T_a and T_b over the whole hibernation cycle, revealed that monitos can experience long torpor bouts in winter (**Figure 4A**), but can also undergo short daily torpor episodes in any time of year, even at mild temperatures (T_a = 20°C, see Nespolo et al., 2010). While in deep torpor, monitos defend a critical T_b of about 5°C and thermoregulate in torpor (**Figure 4B**, black line). Interestingly, animals show the typical endothermic increase in MR when active and exposed to low T_a (**Figure 4B**, red line), but at the same time can experience torpor bouts at any T_a above the critical defended temperature. Monitos cluster together in hibernacula, which permit them to limit heat loss (**Figure 4C**) but, when food supplemented, individuals experience frequent arousals in winter (**Figure 4D**). At the same time, animals can experience long torpor episodes of up to 31 days without feeding and showing collective arousals and euthermic periods of 24–48 h (**Figure 4E**). Thus, monitos represent a case of a species experiencing both daily torpor and hibernation, and that modulate the use of heterothermy on a day-to-day basis depending on food supply (Nespolo et al., 2020). This flexible hibernator has been one of the best studied marsupial models of heterothermy from the molecular point of view.

Monitos as a Model of Marsupial Torpor

Although hundreds of studies have described the physiological underpinnings of heterothermy in marsupials, especially for Australian species (summarized in Geiser and Körtner, 2010), the molecular biology and biochemistry of marsupial heterothermy has been particularly well described in monitos, a South American marsupial. Monitos trigger their heterothermic state primarily due to a drop in T_a, in food-deprived individuals with photoperiod and fat stores also being important modulators of torpor susceptibility (Nespolo et al., 2010, 2020). The transition from endothermy to heterothermy is characterized by passive cooling after a sudden reduction in MR, to a limit of about 1–2°C, when monitos start defending T_b by active thermoregulation (**Figure 4B**). It is highly likely that monitos hibernate at freezing temperatures, since several populations in Chile and Argentina are distributed in Andean locations where temperatures go below zero in winter (Balazote-Oliver et al., 2017; Valladares-Gómez et al., 2019). During torpor in monitos, usually T_b remains one or two degrees above T_a, and animals could spend several weeks

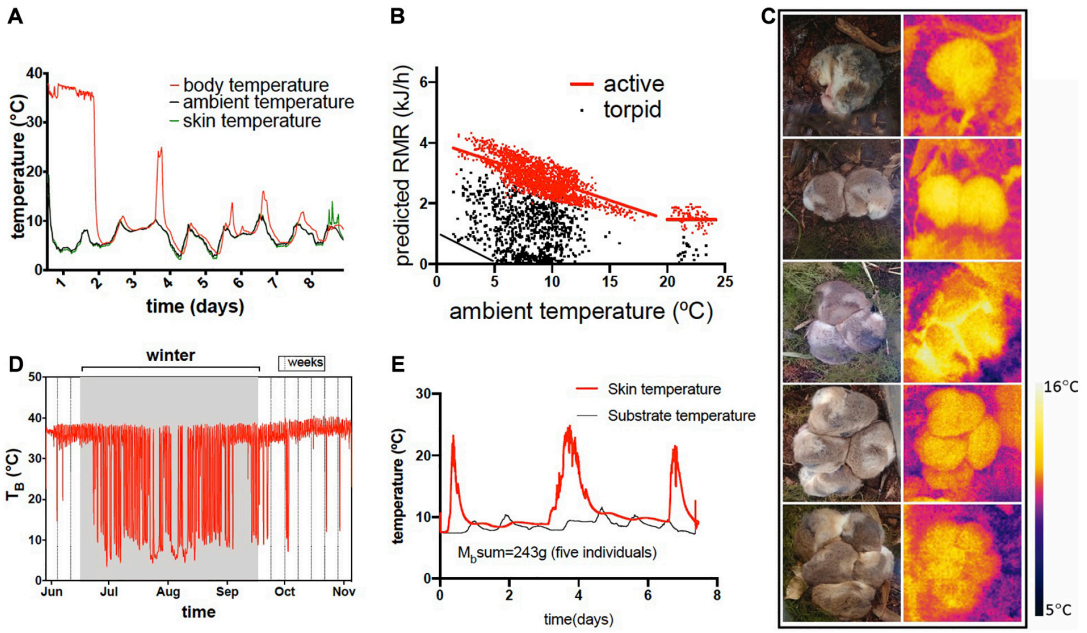

FIGURE 4 | Flexible hibernation in *Dromiciops gliroides*. **(A)** a single torpor bout of 8 days in one individual; **(B)** predicted resting metabolic rate (RMR) in one individual followed during one winter, using the formula RMR = $c(T_b–T_a)$; from an intraperitoneal data logger) where c = minimum thermal conductance for *D. gliroides* (c = 3.49 J $g^{-1}h^{-1}°C^{-1}$), from Bozinovic et al. (2004) showing the frequent torpor episodes at relatively warm temperature except when reaching the critical T_A = 5°C, when thermoregulation in torpor begins (black line); **(C)** social hibernation showing animals in torpor and thermographic images of the groups; **(D)** body temperatures in a single individual during one hibernating cycle in the field showing the frequent arousals (this animal received supplementary food) and, **(E)** skin temperature (red) of a cluster of five individuals that were in torpor during 3 weeks (no food available); this plot shows the last 8 days (animals remained in the same site during these normothermic episodes).

in this condition, where MRs are of about 5% of normothermic values, heart frequency can reach 3 beats per minute and breathing frequency could be less than 1 per minute (Nespolo et al., 2010). Deep torpor is common in winter, but monitos often experience daily torpor in summer and spring (**Figure 4C**).

The Gray Mouse Lemur, a Primate Model of Flexible Heterothermy

The gray mouse lemur (*M. murinus*; Strepsirrhini; Lemuriformes; Cheirogaleidae) is a small nocturnal primate species (body mass: 60–90 g) originating from Madagascar. Half-life expectancy is around 5.7 years but animals can live for 8–10 years in captivity (Perret, 1997). The species as been widely used as a model for aging studies (Languille et al., 2012) and exhibits robust changes in body composition that are synchronized on photoperiodic cycles, a feature that is conserved in captivity (Perret and Aujard, 2001). These variations in body composition result from deep changes in physiological characteristics during winter, in particular the use of hypometabolism, even in captivity (**Figure 5**). Mouse lemurs adjust the depth and duration of torpor bouts according to feeding status and T_a (**Figures 5A,B**), and show an interesting inter-variability in their response (**Figure 5C**). Recent work (Terrien et al., 2017) has shown that captive male mouse lemurs acclimated to winter-like photoperiod (10 h/day) for 6 months and maintained in constant favorable housing conditions exhibit large changes in body mass explained by variations in metabolic levels and food intake. Such changes result in a biphasic phenotype: a phase of massive body mass gain followed by the spontaneous arrest of fattening. Strikingly, mouse lemurs are protected against glucose intolerance during fattening, but not during the second half of winter when they lose fat and exhibit increased fasting insulin levels. Most importantly, these natural transitions are fully reversible, and never reach pathological levels, as reflected by the apparent absence of an inflammatory response (Terrien et al., 2017). The second half of winter corresponds (only for male mouse lemurs) to the recrudescence of the reproductive system, which is completely regressed during the first half of winter (Perret and Aujard, 2001). This regression/recruitment phenotype can be interpreted as a yearly puberty that could repeatedly occur in both males and females (read below), year after year.

Although generally considered to be a daily heterotherm, records of hibernation episodes (up to 30 days) have been reported in wild female gray mouse lemurs (Schmid and Ganzhorn, 2009). There seems to have a strong inter-individual variability in this feature, probably due to differences in habitat structure (habitat fragmentation), nutritional state (food availability), and body composition (fat stores). Torpor is triggered to save energy and water (Humphries et al., 2003b) but is somehow also a costly process, as highlighted by recent work on telomere dynamics during hibernation (Giroud et al., 2014; Hoelzl et al., 2016; Nowack et al., 2019). Although supported by behavioral strategies (Terrien et al., 2011), arousals from torpor are very demanding as they require the activation of NST in

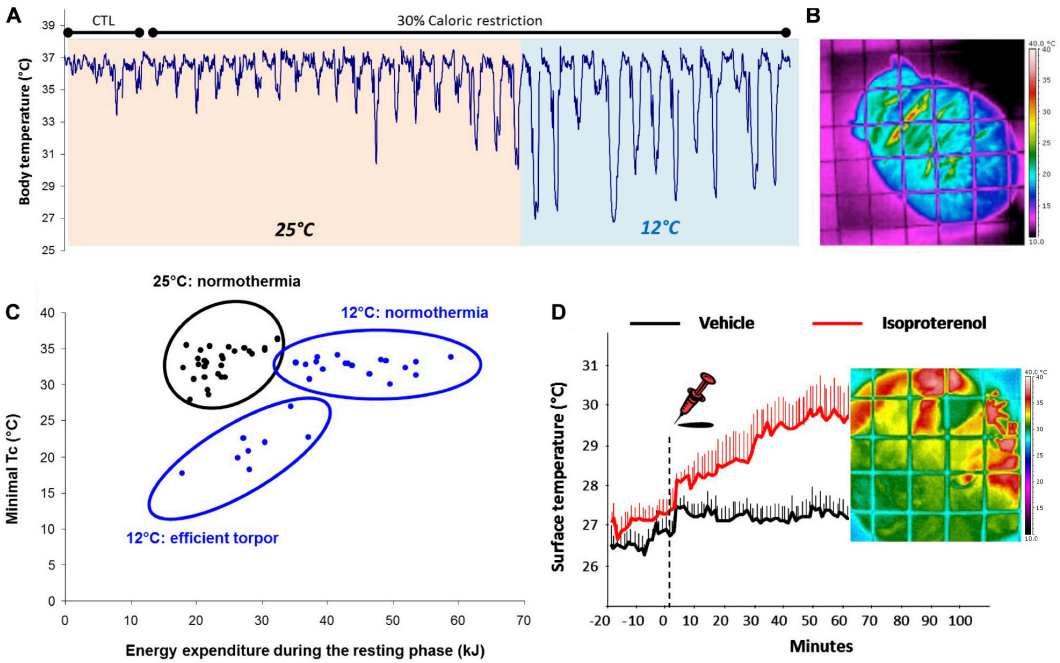

FIGURE 5 | Flexibility of heterothermy in captive *Microcebus murinus*. **(A)** Captive mouse lemurs adjust the depth and duration of torpor bouts depending on food supply (control CTL vs. 30% caloric restriction CR) and ambient temperature (25 vs. 12°C); **(B)** Example of thermographic image of a mouse lemur acclimated to 12°C; the surface temperature is maintained very low, witnessing the insulating capacity of the animal, except at the inter-capsular region where brown adipose tissue is present; **(C)** Graph showing the relationship between minimal core temperature and energy expenditure during the resting phase recorded in animals acclimated to 25 and 12°C; the data clearly demonstrate the existence of an inter-individual variability in the response to cold (either maintenance of normothermia or deep torpor bouts); **(D)** Data showing the rise of surface temperature (heat dissipation mostly through hands and feet) following the injection of isoproterenol, a chemical that stimulates non-shivering thermogenesis.

BAT. The activation of such process induces rapid and efficient production of body heat (**Figure 5D**), but also consumes fat reserves. The balance between the energy saved during torpor vs. the energetic costs of arousal is known to be altered by the aging process. Indeed, aged mouse lemurs display deficiencies in controlling the drop in T_b when exposed to low T_a (Terrien et al., 2008), thereby necessitating higher energy input for subsequent rewarming (Terrien et al., 2009). This leads to a faster exhaustion of fuel reserves, notably in BAT (Terrien et al., 2010a). These results are further supported by the enhanced use of behavioral adjustments during aging in this species (Terrien et al., 2010b) as a compensation for age-related deficiencies in physiological responses to cold exposure.

An additional parameter, quite neglected in the literature, that introduces variability in the heterothermic response is sex (Vuarin et al., 2015). Indeed, hibernation episodes during the dry season have only been reported in females but not males (Schmid and Kappeler, 1998; Schmid, 1999), supporting the "female thrifty hypothesis" that confers to females an enhanced capacity to display hypometabolism (Jonasson and Willis, 2011). Such sex bias could be linked to the phenological shift that exists between males and females in the yearly period during which they invest energy in reproduction. Female reproductive investment centers on gestation, lactation, and juvenile care and occurs during the wet favorable season. By contrast, male mouse lemur reproductive investment centers on male-to-male competition at the mating season (early summer) and, most importantly, on spermatogenesis that is a long-lasting process and has to start at the end of the dry season to ensure male readiness at the mating season. Such phenological differences between males and females might determine the flexibility of torpor bouts in mouse lemurs. There are a number of indications of enhanced torpor efficiency in females as compared to males. Indeed, although hibernation episodes have never been observed in captivity, captive female mouse lemurs are capable of using torpor during gestation and lactation when facing food shortage (Canale et al., 2012), whereas the male response to a comparable stress shows a relative inefficiency to maintain body mass by using torpor (Giroud et al., 2008; Villain et al., 2016). In addition, female mouse lemurs show enhanced mitochondrial and antioxidant capacities (Noiret et al., 2020).

Monitos and Mouse Lemurs: Daily and Seasonal Heterotherms in the Same Species

Torpor use in its depth and duration seems to be highly flexible in mouse lemurs and monitos and such flexibility probably requires specific physiological characteristics and are highly constrained by life-history traits and environmental conditions. For example, it is well referenced that hibernation capacities rely on the ability to store enough fat in order to sustain long periods of foraging and/or metabolic inactivity. As a consequence, such a phenotype is mostly expressed by larger heterotherms

(Ruf and Geiser, 2015). However, among small heterotherms, including monitos and mouse lemurs, individuals showing the best body condition, i.e., the highest fat stores, also have the capacity to extend their periods of hibernation to several weeks. By contrast, inappropriate use of daily torpor or hibernation, i.e., when extrinsic (environmental) or intrinsic (body condition) factors are not favorable, might not bring the expected benefits of using hypometabolism. Indeed, a recent perspective paper proposes that physiological flexibility, including hypometabolic response to environmental constraints, not only offers ecological and physiological benefits, but also induces important costs, e.g., oxidative damage and immunodeficiency (Landes et al., 2020). Comparable observations of torpor flexibility have been made in lesser hedgehog tenrecs, *Echinops telfairi* (Lovegrove and Genin, 2008) and stripe-faced dunnarts (*Sminthopsis macroura*, Körtner and Geiser, 2009; for review see Nowack et al., 2020). Such physiological features, i.e., being able to either display short daily torpor bouts or longer weekly hibernating periods in the same species, contribute to the view that rather than being two distinct functional traits, hibernation, and daily torpor are probably extremes of a continuum (Boyles et al., 2013).

Daily Torpor and Hibernation as a Continuum of Hypometabolic Responses: Insights From Molecular Analyses

Based on observations from molecular analyses of the torpid state (for reviews, see Van Breukelen and Martin, 2002; Storey and Storey, 2004, 2007; Staples, 2011; van Breukelen and Martin, 2015), it appears that the daily expression of torpor and the successive use of multi-day or weeks-long torpor, also defined as hibernation, stand as two extremes along the continuum of hypometabolic responses. Indeed, a range of molecular experiments done with *D. gliroides* -a species expressing both daily torpor and seasonal hibernation- reveal that monitos experience immunological depression and muscle atrophy during torpor (Franco et al., 2013, 2017), whereas other analyses suggest the existence of tissue-specific responses regulating key molecular pathways by microRNAs to limit oxidative damage and muscle atrophy (Hadj-Moussa et al., 2016), and overexpressing cryoprotective proteins against ischemia/reperfusion stress (e.g., heat shock proteins) in the liver, heart, and brain (Nespolo et al., 2018). Interestingly, these authors found a single transcript encoding for the thioredoxin interacting protein (*TXNIP*) that was strongly overexpressed in several tissues, but especially in the brain. This is a potent antioxidant protein involved in regulating mitochondrial function to help suppress oxidative metabolism when oxygen is limiting and regulating a metabolic shift to anaerobic glucose catabolism by mediating inhibition of pyruvate dehydrogenase (Spindel et al., 2012; Chong et al., 2014; Yoshioka and Lee, 2014). In mice, the *TXNIP* gene is overexpressed in the hypothalamus, liver, and white and brown adipose during induced-torpor experiments as well as in natural torpor in Siberian hamsters, *Phodopus sungorus* (Hand et al., 2013; DeBalsi et al., 2014; Jastroch et al., 2016).

In the same vein, recent data show that some genes regulating daily and prolonged torpor in mouse lemurs, although altered in a much less extensive manner, are shared with that of classical hibernating species, but can also show some specificities. For example, miRNAs are known regulators of metabolic flexibility in hibernating mammals (Hadj-Moussa et al., 2016; Arfat et al., 2018; Biggar and Storey, 2018) and are particularly involved in growth processes. Such regulation of gene expression also seems to be involved in the torpor response of mouse lemurs (Biggar et al., 2018; Hadj-Moussa et al., 2020). In particular, mouse lemur torpor use involves miRNA inhibition of gene transcripts related to energetically-unfavorable cellular processes in order to facilitate metabolic suppression (Hadj-Moussa et al., 2020). For instance, small RNA sequencing of lemur miRNAs in skeletal muscle revealed that muscle-specific miR-1 and miR-133 are downregulated in mouse lemurs during daily torpor. These "myomiRs" are likely to have important roles in preventing disuse-induced muscle atrophy by targeting genes involved in regulating muscle development and energy use. For example, mir-1 and miR-133 are generally upregulated in skeletal muscles of warm-hibernating Swedish brown bears (Luu et al., 2020), the daily- or seasonally-torpid marsupial, monito del monte (Hadj-Moussa et al., 2016), and in the foot muscle of anoxia- and freeze-tolerant sea snails (Biggar et al., 2012), likely helping to protect their muscles from sustaining damage as they lie dormant. A decrease in these miRNAs in lemurs is significant and emphasizes the need to study molecular adaptations in a range of species capable of metabolic suppression, especially through the unbiased approach of sequencing all available small non-coding RNAs. Regulation of energy homeostasis through AMPK signaling, especially to promote ATP sparing and partitioning, also seems to be similar in the mouse lemur to that of classic hibernators (Zhang et al., 2015). Protein kinases involved in MAPK cascades also showed comparable regulation of expression and relative protein phosphorylation between mouse lemurs and hibernators (Biggar et al., 2015b). For instance, phosphorylation for ERK1/2 and MEK was strongly negatively regulated in skeletal muscle during torpor in the mouse lemur and in the heart of hibernating ground squirrels (Childers et al., 2019). In addition, suppression of the immune system during torpor was observed in the mouse lemur, in line with what was already known in hibernators (Franco et al., 2013; Tessier et al., 2015a). Epigenetic regulation is also involved since miR-222 was reduced during torpor in the mouse lemur as well during hibernation in ground squirrels (Wu et al., 2014). By contrast, it seems that the regulation of heat shock proteins or proteins involved in the antioxidant machinery do not change as much during daily torpor (Biggar et al., 2015a) as during hibernation (Carey et al., 1999; Morin and Storey, 2007). Furthermore, hepatic regulation of the phosphorylation state of the insulin receptor showed contrasting effects, increasing in torpid mouse lemurs (Tessier et al., 2015b), and therefore potentially reflecting an inhibition of gluconeogenesis although this process that is known to be sustained during hibernation (Green et al., 1984).

Taken together, all the data for these two small mammal models (mouse lemurs and monitos) point toward specific molecular and cellular mechanisms for the adjustment of metabolic processes and protective functions during the extreme hypometabolic down-state of torpor. These adaptive mechanisms seem to be conserved in evolution among diverse heterothermic

species known to date. Taking inspiration from natural adaptations constitutes a necessity in the current world of ongoing climate change and spreading pathophysiological pandemics. Therefore, exploring these outstanding mechanisms occurring naturally in heterothermic models constitutes a unique opportunity to develop efficient responses, tools and treatments to address major environmental and health concerns. Specifically, the study of these mechanisms have potential for a better understanding of (i) protective responses against metabolic disorders such as obesity or sarcopenia (Cotton, 2016), (ii) the homeostasis of neuronal functions, e.g., the maintenance of hyper-phosphorylation of Tau proteins involved in resistance to neuro-degenerative diseases (Härtig et al., 2007; Luppi et al., 2019), and (iii) the underlying mechanisms for a state of hypothermia in humans, also called "synthetic torpor," for therapeutic goals (Cerri, 2017) or space exploration (Choukèr et al., 2019). In the context of the latter, the study of protective mechanisms for the torpid brain is of particular interest as well as the implications for the gaseous molecule H_2S involved in the potential control and maintenance of metabolic depression and protective mechanisms in the torpid state.

PROTECTIVE MECHANISMS DURING THE STATE OF METABOLIC DEPRESSION

Mechanisms to Protect the Torpid Brain

During torpor, hibernators may suppress their brain activity to the point where no electrical activity can be observed (Chatfield et al., 1951; Frerichs et al., 1994), but behind closed eyes, hibernating species coordinate the expression and activities of thousands of proteins (via changes in gene and protein expression, post-translational modification, and epigenetic controls) to ensure that one of the most important organs, the brain, is viable upon arousal (see **Figure 6** for overview).

Regulation of Protein Translation and Tau Phosphorylation During Torpor

Most species suppress energetically expensive molecular processes during torpor to avoid metabolic disruption, when cellular resources of substrates to produce ATP may be limited. For example, protein translation is suppressed in brain of 13-lined ground squirrels (*Ictidomys tridecemlineatus*) to just 0.04% of euthermic levels (Frerichs et al., 1998) which was expected to correlate with a significant decrease in the relative expression levels of translated proteins during hibernation. However, multiple studies focusing on translational regulation in a range of hibernator tissues, including brain, indicate that hibernators use a much more rapid and reversible process to throttle translation: protein phosphorylation (Frerichs et al., 1998; Miyake et al., 2015; Logan et al., 2019). For example, ribosomal protein S6 is less phosphorylated at Ser235 during torpor, reducing its ability to bind the 5′-cap of mRNA and initiate translation (Miyake et al., 2015; Logan et al., 2019).

Consistent with these observations, hibernators including European ground squirrels (*Spermophilus citellus*), Arctic ground squirrels (*U. parryii*), black bears (*Ursus americanus*), and Syrian hamsters (*M. auratus*) use reversible phosphorylation of structural proteins such as Tau, to facilitate dendritic retraction and reduce neuronal cell signaling (Bullmann et al., 2016). Tau phosphorylation is a common feature of many tauopathies, which are neurodegenerative disorders associated with the build-up of proteinaceous plaques including tau, but fascinatingly, hibernators can reverse tau phosphorylation and clear protein aggregates upon arousal from deep torpor. Glycogen synthase kinase 3 beta (GSK3β) was postulated to regulate hibernator tau phosphorylation because it targets the specific phospho-sites that were differentially affected in hibernating Syrian hamster brain (Bullmann et al., 2016). However, new data from the Storey group indicates that GSK3β is inhibited during deep torpor in the forebrain and cerebellum of hibernating 13-lined ground squirrels (*Ictidomys tridecemlineatus*), based on increases in p-GSK3β (S9) during torpor (Tessier et al., 2019). As a result, it is unlikely that GSK3β is part of a conserved mechanism governing hibernator tau phosphorylation across species.

Regulation of Inflammation and Apoptosis During Hibernation

In addition to their purported importance in reducing brain activity and maintaining brain functionality during hibernation, the neurons of cold-bodied hibernators pull their dendrites back into the cell bodies that sprouted them. This appears to be an effort to reduce tissue damage to the delicate, filamentous protrusions that are responsible for accepting information from the axons of other neurons and relaying those messages to the cell body (Popov et al., 1992). Microglia (neuronal immune cells) also change their morphology during torpor in hibernating hamsters such that their protrusions are thinned and appear disconnected from the main cell body (Cogut et al., 2018; León-Espinosa et al., 2018). Microglia have important roles in regulating dendrite elongation, neuronal plasticity and synaptic transmission of signals, in addition to producing inflammatory signaling molecules. Together, changes in dendrite and microglia morphology with a decrease in core T_b could serve to inhibit neuronal activity, and possibly inflammatory signaling during deep torpor. Hibernating animals may also facilitate changes in brain structure by differentially expressing genes involved in extracellular matrix plasticity and maintenance including collagens, laminins, integrins, and matrix metalloproteinases (Schwartz et al., 2013). Matrix metalloproteinases are also differentially expressed during torpor in hibernating hamster lung (Talaei et al., 2012), suggesting a role for tissue remodeling in the survival strategies of a range of hibernating species.

Interestingly, the enzyme GSK3β may regulate the DNA binding of transcription factors that suppress neuronal apoptosis and neuroinflammation. Specifically, GSK3β activation is required for control of signal transducer and activator of transcription (STAT) 3 and STAT5 activity but is not necessary for STAT1 or STAT6 activity in astrocytes (Beurel and Jope, 2008). Neither STAT3 nor STAT5 were differentially phosphorylated during hibernation in *I. tridecemlineatus* forebrain, cerebellum,

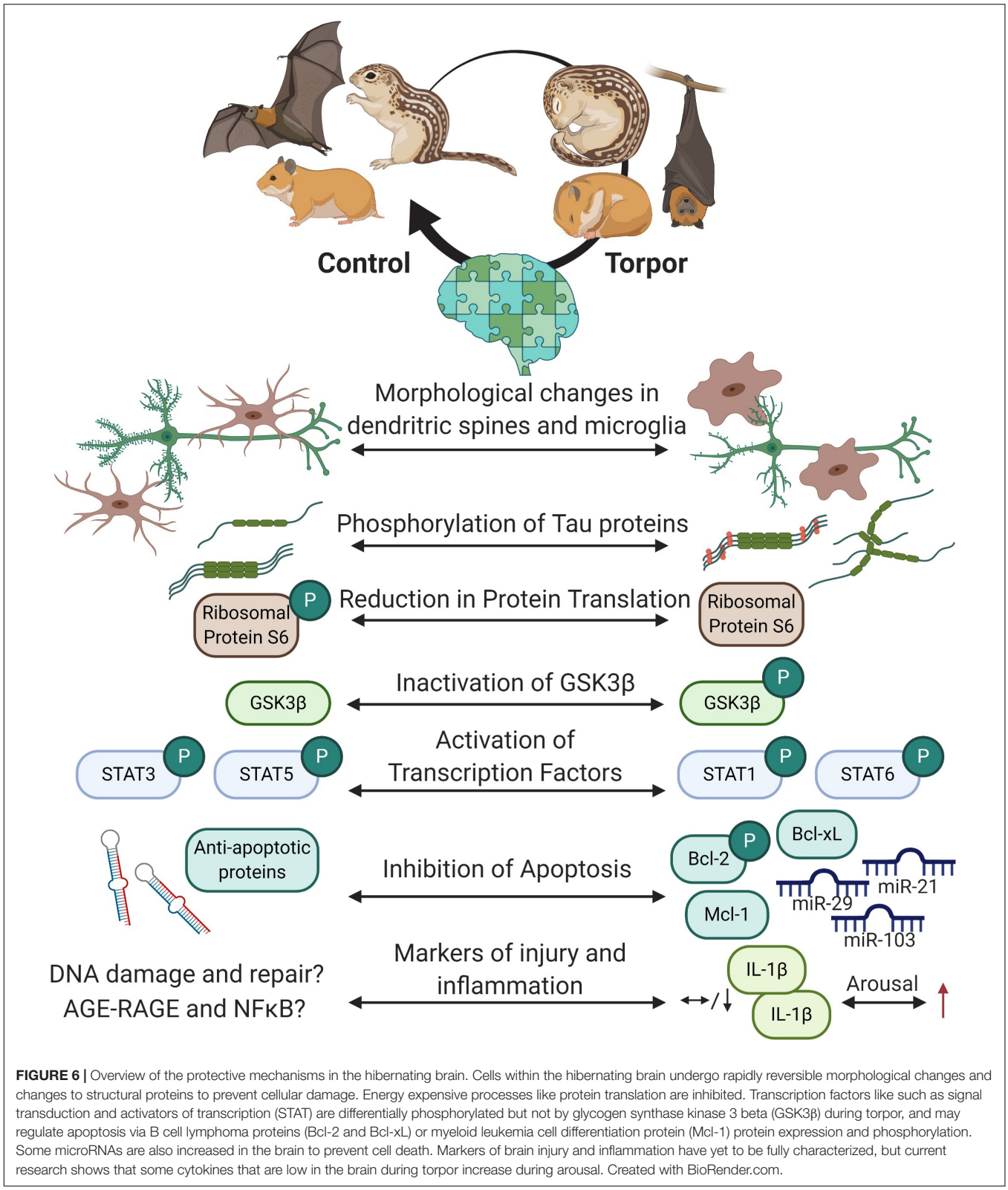

FIGURE 6 | Overview of the protective mechanisms in the hibernating brain. Cells within the hibernating brain undergo rapidly reversible morphological changes and changes to structural proteins to prevent cellular damage. Energy expensive processes like protein translation are inhibited. Transcription factors like such as signal transduction and activators of transcription (STAT) are differentially phosphorylated but not by glycogen synthase kinase 3 beta (GSK3β) during torpor, and may regulate apoptosis via B cell lymphoma proteins (Bcl-2 and Bcl-xL) or myeloid leukemia cell differentiation protein (Mcl-1) protein expression and phosphorylation. Some microRNAs are also increased in the brain to prevent cell death. Markers of brain injury and inflammation have yet to be fully characterized, but current research shows that some cytokines that are low in the brain during torpor increase during arousal. Created with BioRender.com.

or brainstem, suggesting that GSK3β inhibition during torpor could correlate with a decrease in the translocation of STAT3 and STAT5 to the nucleus (Tessier et al., 2019). By contrast, compared to winter euthermic and summer euthermic controls, respectively, forebrain and brainstem STAT1 was more phosphorylated during hibernation in deep torpor.

In addition, both the cerebellum and brainstem of hibernating ground squirrels exhibit increased STAT6 phosphorylation levels at Y641 during deep torpor, compared with summer active and interbout aroused animals (Tessier et al., 2019). This transcription factor may play an important role in upregulating anti-apoptotic genes such as B-cell lymphoma 2 (Bcl-2) (Lee et al., 2018). Indeed, whole brain from hibernating ground squirrels shows a significant increase in the protein and phosphorylation levels of multiple anti-apoptotic proteins including Bcl-2, Bcl-xL, Bax-inhibitor 1, and Mcl-1 (Rouble et al., 2013). These molecular responses during torpor could help hibernating ground squirrels prevent brain damage during times of nutrient limitation.

Signal transducer and activator of transcription 6 has been implicated in mediating inflammation by facilitating macrophage recruitment, mucus production, and smooth muscle contractility, suggesting that its upregulation in the hibernating ground squirrel brain may help regulate neuroinflammation during natural torpor. Hibernators including hamsters and ground squirrels can mount inflammatory responses during deep torpor (Kurtz and Carey, 2007). At the molecular level, hibernators increase the local levels of pro- and anti-inflammatory cytokines (IL-1β, IL-4, IL-6, IL-10, TNFα, interferon γ) and potentially, leukocytes, based on increases in the relative levels of cell surface markers, in order to rapidly respond to exogenous and/or endogenous damage markers as they arouse from a hibernation bout (Kurtz and Carey, 2007; Cogut et al., 2018). Endogenous markers of damage can be sensed by receptors such as the receptor for advanced glycation end products (RAGE), that can then activate MAPK and JAK/STAT signaling cascades to increase the expression of pro-inflammatory transcription factors like NFκB. RAGE expression was recently discovered to be upregulated in hibernating ground squirrel adipose tissues, particularly as they enter or exit a hibernating bout (Logan and Storey, 2018). An increase in RAGE expression during entrance into deep torpor is consistent with a suppression of mitochondrial activity and therefore a potential for less efficient electron transport through the electron transport chain leading to ROS formation. Additionally, an increase in RAGE levels in arousing animals, when ROS levels increase as a result of increased breathing and MRs and elevated mitochondrial activity, suggest that RAGE is able to sense and respond to biomarkers of oxidative stress. Consistently, BAT in hibernating arctic ground squirrels shows increased levels of lipid peroxides and protein carbonyls during the rewarming period, and these oxidized lipids and proteins may be sensed by receptors such as RAGE to trigger their removal during interbout arousal (Orr et al., 2009). In addition, NFκB signaling is upregulated during deep torpor and arousal in ground squirrel cardiac muscle, skeletal muscle, and intestine, as well as hamster lung, which could contribute to increased pro-inflammatory gene expression (Carey et al., 2000; Allan and Storey, 2012; Talaei et al., 2012; Wei et al., 2018a). Interestingly, studies show that deep hibernators injected with inflammatory stimulants only respond to the exogenous markers of cell stress (e.g., *Escherichia coli* lipopolysaccharide) during interbout arousals, measured as an increase in T_b relative to saline-injected ground squirrels (Prendergast et al., 2002). By contrast, forebrain shows no signs of oxidized proteins (endogenous damage markers) during deep torpor, compared with euthermic controls, suggesting that brain may use molecular mechanisms such as elevated antioxidant capacity to prevent the accumulation of damaged proteins during hibernation (Orr et al., 2009). Other damage markers such as 8-hydroxy-2′-deoxyguanosine or markers of mitochondrial dysfunction have yet to be assessed in brain cells, in conjunction with an analysis of pro-inflammatory signaling cascades. However, an analysis of CD16–CD32 and CD68 expression as markers of microglia activity revealed that hibernating hamsters do not increase microglial activity (León-Espinosa et al., 2018). Though microglia do not display advanced morphological changes associated with microglial activation, the retraction of microglial dendrites and increases in microglial cell body to cell size ratio during deep torpor, as well as increases in the relative transcript levels of pro-inflammatory IL-1β and IL-6 upon arousal point to a role for microglia in the regulation of neuronal inflammation (Cogut et al., 2018). Together, these results suggest that hibernators may induce inflammation at particular time points of the torpor-arousal cycle, but much has yet to be explored with regard to the molecular mechanisms controlling hibernator neuroinflammation.

Other Brain Protective Mechanisms in Hibernation

Neuroprotection may also be facilitated through epigenetic mechanisms, including differential microRNA expression. In a study that focused on miRNAs that are commonly dysregulated in neurodegenerative conditions, hibernating little brown bats (*Myotis lucifugus*) showed significant increases in microRNAs during deep torpor that were involved in regulating focal adhesion, a process that involves changes in neuronal cell cytoskeletal structure, cell cycle progression, and cell death (Biggar and Storey, 2014). For example, miR-21, -29, and -103 were all significantly increased in brain of hibernating *M. lucifugus* and all have important roles in decreasing apoptosis (Roshan et al., 2014; Zhou and Zhang, 2014). These data, in conjunction with protein/phosphorylation data from *I. tridecemlineatus* studies and gene transcript data from hibernating greater horseshoe bats (*Rhinolophus ferrumequinum*) (Lei et al., 2014), suggest that hibernators may use conserved regulatory mechanisms acting at multiple levels (non-coding RNA, gene, protein, and post-translational) to limit neuronal cell death during hibernation in deep torpor.

Role of H2S in Protective Mechanisms During Hibernation

Ever since the paper by Blackstone et al. (2005) that showed that inhalation of low concentrations of H_2S confers a reversible metabolic suppression in mice, people have wondered whether H_2S is involved in hibernation, for instance by inducing or maintaining torpor. Mechanistically, there are good reasons to explore this, since H_2S can profoundly reduce mitochondrial respiration through inhibition of complex IV (cytochrome *c* oxidase) (Khan et al., 1990). Moreover, the past 15 years of H_2S research has disclosed an array of protective effects that

may be highly instrumental in hibernation to safeguard organ function and integrity in the face of hypoxia and/or excess reactive oxygen species production (Carey et al., 2000; Orr et al., 2009; Wu and Storey, 2014).

Endogenous H_2S Production and Physiological Effects

Involvement of H_2S in hibernation, be it as a metabolic suppressor or cell protective agent, requires it to be generated by the animal. In mammals, endogenous H_2S is produced by three enzymes embedded in the trans-sulfuration pathway, i.e., cystathionine β-synthase (CBS), cystathionine γ-lyase (CSE), and 3-mercaptopyruvate sulfur transferase (3MST). The trans-sulfuration pathway generates H_2S as a byproduct of methionine to cysteine conversion (reviewed in Zuhra et al., 2020), the latter amino acid being a crucial component of the antioxidant, glutathione. CBS and 3-MST are the major H_2S producing enzymes in the nervous system (Abe and Kimura, 1996; Bruintjes et al., 2014), whereas CSE is more abundant in the cardiovascular system (Yang et al., 2008). CBS and CSE are also secreted by endothelial cells and hepatocytes, and confers H_2S production in plasma (Bearden et al., 2010). Next to enzymatic synthesis, endogenous H_2S may also be derived from "sulfide" pools. Pathways are detailed in **Figure 7** (left panels).

Hydrogen sulfide confers a wide array of physiological effects. Firstly, it affects mitochondria in a concentration-dependent manner. In brief, at low concentrations, the prevailing effect is stimulation of oxygen consumption and ATP production, whereas high H_2S concentrations inhibit mitochondrial respiration. Secondly, H_2S confers potent antioxidant effects, both directly through scavenging of free radicals and indirectly by upregulation of various antioxidant pathways. Mechanisms of these and additional protective pathways are detailed in **Figure 7** (right panels).

H_2S in Hibernation

Despite the booming number of publications on H_2S over the past decade (Szabo, 2018), there is a surprising paucity of data on the involvement of H_2S in hibernation. To date only two studies have reported on the subject. Talaei et al. (2012) reported an increase in CBS abundance with increased production of H_2S in lung tissue of torpid Syrian hamster (*M. auratus*), that was rapidly reversed to summer levels during interbout arousal. Increased H_2S levels were shown to quench Zn^{2+}, and possibly drive torpor related lung remodeling (Talaei et al., 2011b) by lowering activity of Zn^{2+}-dependent enzymes including metalloproteases and angiotensin converting enzyme (ACE). In addition, Revsbech et al. (2014) showed a change in H_2S metabolism in plasma and red blood cells of hibernating Scandinavian brown bears (*Ursus arctos*), with a shift toward higher levels of bound sulfane sulfur (thiosulfate and polysulfides), lower levels of free sulfide (H_2S and HS^-) and a likely increase in H_2S producing capacity in plasma and red blood cells. Furthermore, analysis of plasma metabolomics in hibernating 13-lined squirrels showed substantial regulation of substrates and products of the trans-sulfuration pathway, consistent with increased H_2S synthesis during late torpor and early arousal (D'Alessandro et al., 2017), as found in hamster lung.

The question is whether there is additional indirect evidence for a role of H_2S in hibernation. Regarding involvement of H_2S in suppression of metabolism, i.e., initiation or maintenance of torpor, there is little evidence. It should be noted that the original Blackstone et al. (2005) experiments reporting on H_2S conferring metabolic suppression in mice were performed under hypoxic conditions (17.5% of O_2). When the experiment was repeated with 21% O_2, H_2S failed to induce hypothermia (Baumgart et al., 2010; Hemelrijk et al., 2018), whereas it was successful at 17.5% O_2, albeit with a much slower onset (Hemelrijk et al., 2018). Further, exposure to severe hypoxia (5% O_2) reduced T_b close to T_a (Hemelrijk et al., 2018). Consequently, the authors attribute the observed hypothermia to hypoxemia induced vasodilation, rather than suppression of metabolism. Such a view may be supported by the absence of H_2S reduction of metabolism in other, larger animal species (Haouzi et al., 2008; Dirkes et al., 2015). As the above studies employ exogenous administration of H_2S, differences between species may also arise because of differences in pharmacokinetics and diffusion route length. Thus, a pertinent question is what the effect would be from enhancing endogenous production of H_2S. Overexpression of CBS and CSE confer longevity in Drosophila (Shaposhnikov et al., 2018), but effects on metabolism were not reported. Further, dopamine treatment strongly increases CBS expression and H_2S production in cells (Talaei et al., 2011a) and in rats *in vivo* (Dugbartey et al., 2015). However, neither in these experiments, nor in the literature, has a torpor-like reduction of metabolism been noted following treatment with dopamine. Finally, changes in mitochondrial function during torpor have been explored. Compared with arousal, torpor leads to a 40% lower activity of ETC complex I, a 60% lower activity of ETC complex II, but does not affect the activity of ETC complexes III, IV, or V, as measured in isolated mitochondria derived from 13-lined ground squirrel liver (Muleme et al., 2006; Brown et al., 2012; Mathers et al., 2017). Given that metabolic suppression by H_2S is through inhibition of complex IV, these data do not lend support to a prominent role of H_2S in induction or maintenance of torpor. However, a finite verdict awaits the development of (inducible) knock-out animals and/or development of selective inhibitors of H_2S producing enzymes.

On the other hand, cellular protective effects induced by H_2S may well play a role in hibernation associated antioxidant and cell protective adaptations outlined in previous sections. Notably, consistent with a prominent antioxidant effect of H_2S (**Figure 7**), hibernation features a strong upregulation of antioxidant mechanisms through the Nrf2 pathway (Morin et al., 2008; Ni and Storey, 2010; Wu and Storey, 2014; Yin et al., 2016; Frigault et al., 2018; Wei et al., 2018b). These and other studies report upregulation or activation of downstream genes and proteins, including, but not limited to, phosphorylated Nrf2, superoxide dismutase, glutathione reductase and peroxidase, catalase, thioredoxin, and miRNA miR-200a. Further, a number of the above studies document higher levels of glutathione in various organs, which may be compatible with enhanced flux

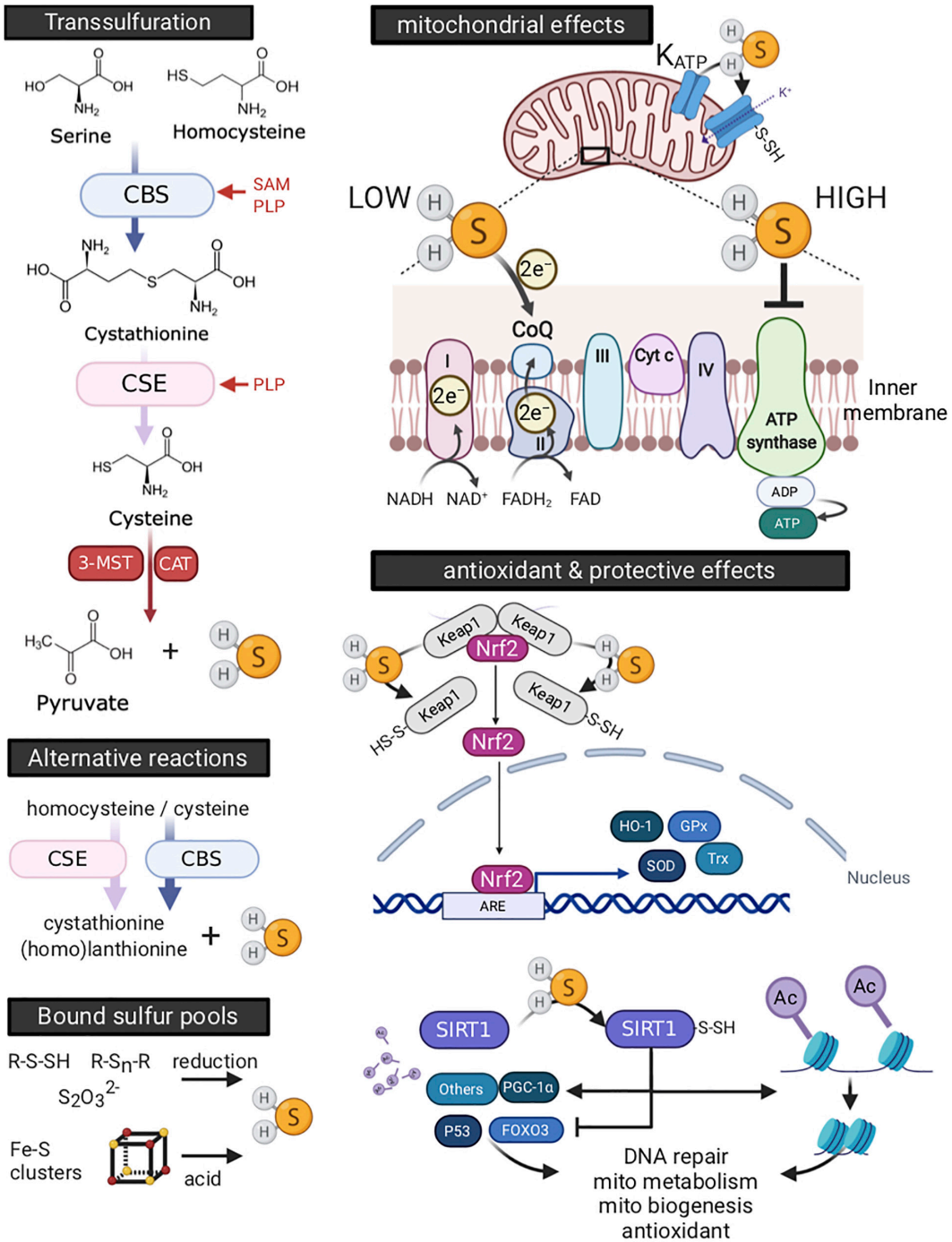

FIGURE 7 | Endogenous production and physiology of hydrogen sulfide (H_2S). H_2S is enzymatically produced by the trans-sulfuration pathway or by alternative reactions, or derived from compounds binding sulfur (left side panels). H_2S producing enzymes differ in various ways, including their dependence on co-factors, cellular, and tissue distribution. Optimal function for both cystathionine β-synthase (CBS) and cystathionine γ-lyase (CSE) is dependent on binding of pyridoxal-5′-phosphate (PLP, or vitamin B6) as a co-factor. In addition, S-adenosyl-L-methionine (SAM), the universal methyl group donor synthesized as an intermediate in the conversion of methionine to homocysteine, serves as a potent allosteric activator of CBS. The cellular localization of CBS and CSE is mainly cytosolic, yet they translocate to mitochondria under stressful conditions (Fu et al., 2012; Teng et al., 2013). 3-mercaptopyruvate sulfur transferase (3-MST) is located in both cytosol and mitochondria, with its activity increasing threefold in mitochondria (Nagahara et al., 1998). Endogenous H_2S may also be derived non-enzymatically from "bound sulfur" pools. Upper compounds are sulfane sulfurs, such as thiosulfate ($S_2O_3^{2-}$), persulfides (R-S-SH) and polysulfides (R-S_n-R), which release H_2S in the presence of reducing substances including glutathione (GSH) and cysteine (Ishigami et al., 2009) or by the action of 3-MST (Shibuya et al., 2009). Lower depicted compounds are acid-labile sulfides, which consist mainly of iron-sulfur clusters, of which the cubane-type [4Fe-4S] cluster is most common

(Continued)

FIGURE 7 | Continued
(Johnson et al., 2005). They are best known for their presence in proteins involved in oxidation-reduction reactions, including those of the electron transport chain in mitochondria. While degradation of iron-sulfur clusters releases H_2S, this occurs at strong acidic conditions (pH < 5.4), likely limiting their contribution to endogenous H_2S generation even under pathological conditions (Ishigami et al., 2009). H_2S affects mitochondria (upper right panel) and produces antioxidant defense (lower right panel). Stimulation of oxygen consumption and ATP production occurs at low H_2S concentration and originates from electron donation at coenzyme Q (CoQ) between complexes II and III (Goubern et al., 2007; Módis et al., 2013). At high concentrations, H_2S competitively and reversibly inhibits cytochrome c oxidase (complex IV) (Khan et al., 1990; Módis et al., 2014). Moreover, high concentrations of H_2S still donate electrons at coenzyme Q, which now reversely flow to complex II, reducing fumarate into succinate (Fu et al., 2012). Moreover, H_2S activates the mitochondrial K_{ATP} channel (Zhao et al., 2001; Lu et al., 2019) and blocks the Ca^{2+}-mediated opening of the mitochondria permeability transition pore (MPTP) channel, thus supporting maintenance of mitochondrial membrane potential (Yao et al., 2010; Lu et al., 2019; Papu John et al., 2019). In addition, H_2S serves as an antioxidant and increases glutathione levels. Further, H_2S activates the prominent antioxidant master switch, nuclear factor−erythroid 2−related factor 2 (Nrf2), by sulfhydration of cysteine residues of Kelch-like ECH-associated protein 1 (Keap1) dimer. This breaks Keap1 inhibitory binding to Nrf2 and allows for Nrf2 to translocate to the nucleus (Hourihan et al., 2012; Yang et al., 2012), where it activates expression of antioxidant and cytoprotective genes, such as glutathione peroxidase (Gpx), thioredoxin (Trx), superoxide dismutase (SOD), and heme oxygenase-1 (HO-1). H_2S mediated sulfhydration of other proteins confers additional cell protective effects (Mustafa et al., 2009; Zhao et al., 2014). For example, H_2S activates the histone deacetylase sirtuin-1 (SIRT1) through its sulfhydration, leading to deacetylation of histones and condensation of chromatin, affecting an array of transcription and nuclear receptors. SIRT1 activation thus influences abundant cellular functions, including stimulation of mitochondrial metabolism and biogenesis, antioxidant pathways, DNA repair and inflammation (Du et al., 2018). ARE, antioxidant response element; Cyt C, cytochrome c, FOXO3, Forkhead box protein O3; PGC-1α, proliferator-activated receptor gamma coactivator 1-alpha. Created with BioRender.com.

in the trans-sulfuration pathway (D'Alessandro et al., 2017) and a coupled increase in H_2S production (**Figure 7**). Interestingly, hibernator cells seem to display cell-autonomous adaptations that enable upkeep of mitochondrial function during cold stress, thus safeguarding ATP production and strongly limiting oxygen radical production, as demonstrated in Syrian hamster kidney cell lines (Hendriks et al., 2017, 2020) and in neurons differentiated from pluripotent stem cells of ground squirrels (Ou et al., 2018), possibly by mild inhibition of complex I. In addition, cooled Syrian hamster kidney cells harnessed their glutathione production, thus effectively precluding ferroptotic cell death (Hendriks et al., 2020). Hibernators have been described to have developed natural resistance to chronic kidney disease (CKD), often associated with cardiovascular impairments in humans (for reviews, see Romagnani et al., 2017; Sarnak et al., 2019), despite their long hibernation fast during winter. Indeed, it was recently reported that markers of CKD differed significantly between animal species with different feeding habits and thermoregulatory behaviors, and that hibernating brown bears and garden dormice displayed higher levels of betaine and choline (known to be cardioprotective) and lower, sometimes even non-detectable, levels of trimethylamine N-oxide (TMAO), a marker of CDK in human and animals (Ebert et al., 2020). Hence, the betaine endogenously produced by the organism may protect organs (notably kidney) of bears, dormice, and other hibernators from oxidative or other damages during the hibernation period of depressed metabolism. Similarly, previous research showed that cooled hibernator kidney cells maintained production of H_2S and that dopamine induction of CBS precludes cooling-induced cell death in non-hibernator kidney cells (Talaei et al., 2011a). Together, these observations suggest that H_2S may play a role in the cell-autonomous effects observed in hibernator cells.

Taken together it appears that research efforts into the role of H_2S in hibernation need to be intensified. To date, the evidence that H_2S confers entrance or maintenance of torpor is very limited. Conversely, cell protective adaptations by H_2S have a close resemblance to those documented in hibernation, which makes H_2S involvement herein likely.

CONCLUSION

The flexibility of torpor use as an adaptive strategy enables different heterothermic mammals to substantially suppress their energy requirements during periods of severely reduced food availability. The phenotype of torpor is associated with marked metabolic adaptations, at the whole organism and cellular/molecular levels, that contrast with (i) the behavior of hibernation, e.g., food- vs. fat-storing hibernators, and (ii) the form of hypometabolic responses, i.e., opportunistic (daily) torpor vs. seasonal hibernation, even within one species. The torpid state is also associated with highly efficient rehabilitation and protective mechanisms ensuring continuity of proper functions in the animal, including key organs such as the brain or the heart. There are clear perspectives to be drawn out from the torpor and hibernation phenotypes, notably in terms of models for calorie restriction or intermittent fasting, e.g., fat vs. food storing species, but also for organ (e.g., brain) and tissue resistance to oxidative stress or cell protective adaptations to challenges such as ischemia-reperfusion. Given that most of these mechanisms have been addressed with placental mammals, future work comparing placentals with monotremes, marsupials and birds in a phylogenetic context would reveal convergent evolutionary pathways.

AUTHOR CONTRIBUTIONS

All authors drafted and critically revised the manuscript.

FUNDING

SG was financially supported by the Austrian Science Fund (FWF, Grant Nos. P27267-B25 and P31577-B25); KS and SL were funded by NSERC Canada. RH was financially supported by a grant from the European Space Agency (Research agreement collaboration 4000123556 attributed to RH). RN thanks a Fondecyt grant No. 1180917, ANID PIA/BASAL grant No. FB-0002, and Instituto Milenio de Biología Integrativa (iBio).

ACKNOWLEDGMENTS

This review is based partially on oral presentations given during the symposium "Living at low pace: From the whole organism to the molecule" organized by SG and KS at the 10th International Congress of Comparative Physiology and Biochemistry (ICCPB) held in August 2019 in Ottawa, Canada. The authors thank Renate Hengsberger for her help with literature search and formatting of the manuscript, and the two reviewers for their helpful comments and suggestions, which greatly contributed to improve the overall quality of this review.

REFERENCES

Abe, K., and Kimura, H. (1996). The possible role of hydrogen sulfide as an endogenous neuromodulator. *J. Neurosci.* 16, 1066–1071. doi: 10.1523/JNEUROSCI.16-03-01066.1996

Allan, M. E., and Storey, K. B. (2012). Expression of NF-κB and downstream antioxidant genes in skeletal muscle of hibernating ground squirrels, *Spermophilus tridecemlineatus*. *Cell Biochem. Funct.* 30, 166–174. doi: 10.1002/cbf.1832

Amico, G., and Aizen, M. A. (2000). Ecology. Mistletoe seed dispersal by a marsupial. *Nature* 408, 929–930. doi: 10.1038/35050170

Amico, G. C., Rodriguez-Cabal, M. A., and Aizen, M. A. (2009). The potential key seed-dispersing role of the arboreal marsupial *Dromiciops gliroides*. *Acta Oecol.* 35, 8–13. doi: 10.1016/j.actao.2008.07.003

Arfat, Y., Chang, H., and Gao, Y. (2018). Stress-responsive microRNAs are involved in re-programming of metabolic functions in hibernators. *J. Cell. Physiol.* 233, 2695–2704. doi: 10.1002/jcp.26034

Auld, J. R., Agrawal, A. A., and Relyea, R. A. (2010). Re-evaluating the costs and limits of adaptive phenotypic plasticity. *Proc. R. Soc. B* 277, 503–511. doi: 10.1098/rspb.2009.1355

Baggio, L. L., and Drucker, D. J. (2007). Biology of Incretins: GLP-1 and GIP. *Gastroenterology* 132, 2131–2157. doi: 10.1053/j.gastro.2007.03.054

Balazote-Oliver, A., Amico, G. C., Rivarola, M. D., and Morales, J. M. (2017). Population dynamics of *Dromiciops gliroides* (*Microbiotheriidae*) in an austral temperate forest. *J. Mammal.* 98, 1179–1184. doi: 10.1093/jmammal/gyx051

Bartels, W., Law, B. S., and Geiser, F. (1998). Daily torpor and energetics in a tropical mammal, the northern blossom-bat *Macroglossus minimus* (Megachiroptera). *J. Comp. Physiol. B* 168, 233–239. doi: 10.1007/s003600050141

Bauman, W. A., Meryn, S., and Florant, G. L. (1987). Pancreatic hormones in the nonhibernating and hibernating golden- mantled ground squirrel. *Comp. Biochem. Physiol. A Mol. Integr. Physiol.* 86, 241–244. doi: 10.1016/0300-9629(87)90324-0

Baumgart, K., Wagner, F., Gröger, M., Weber, S., Barth, E., Vogt, J. A., et al. (2010). Cardiac and metabolic effects of hypothermia and inhaled hydrogen sulfide in anesthetized and ventilated mice. *Crit. Care Med.* 38, 588–595. doi: 10.1097/CCM.0b013e3181b9ed2e

Bearden, S. E., Beard, R. S. Jr., and Pfau, J. C. (2010). Extracellular transsulfuration generates hydrogen sulfide from homocysteine and protects endothelium from redox stress. *Am. J. Physiol. Heart Circ. Physiol.* 299, H1568–H1576. doi: 10.1152/ajpheart.00555.2010

Beurel, E., and Jope, R. S. (2008). Differential regulation of STAT family members by glycogen synthase kinase-3. *J. Biol. Chem.* 283, 21934–21944. doi: 10.1074/jbc.M802481200

Bieber, C., Turbill, C., and Ruf, T. (2018). Effects of aging on timing of hibernation and reproduction. *Sci. Rep.* 8:13881. doi: 10.1038/s41598-018-32311-7

Biggar, K. K., Kornfeld, S. F., Maistrovski, Y., and Storey, K. B. (2012). MicroRNA regulation in extreme environments: differential expression of MicroRNAs in the intertidal snail *Littorina littorea* during extended periods of freezing and anoxia. *Genomics Proteomics Bioinformatics* 10, 302–309. doi: 10.1016/j.gpb.2012.09.002

Biggar, K. K., Luu, B. E., Wu, C. W., Pifferi, F., Perret, M., and Storey, K. B. (2018). Identification of novel and conserved microRNA and their expression in the gray mouse lemur. *Microcebus murinus*, a primate capable of daily torpor. *Gene* 677, 332–339. doi: 10.1016/j.gene.2018.08.014

Biggar, K. K., and Storey, K. B. (2014). Identification and expression of microRNA in the brain of hibernating bats. *Myotis lucifugus*. *Gene* 544, 67–74. doi: 10.1016/j.gene.2014.04.048

Biggar, K. K., and Storey, K. B. (2018). Functional impact of microRNA regulation in models of extreme stress adaptation. *J. Mol Cell Biol* 10, 93–101. doi: 10.1093/jmcb/mjx053

Biggar, K. K., Wu, C. W., Tessier, S. N., Zhang, J., Pifferi, F., Perret, M., et al. (2015a). Modulation of gene expression in key survival pathways during daily torpor in the gray mouse lemur. *Microcebus murinus*. *Genomics Proteomics Bioinformatics* 13, 111–118. doi: 10.1016/j.gpb.2015.03.001

Biggar, K. K., Wu, C. W., Tessier, S. N., Zhang, J., Pifferi, F., Perret, M., et al. (2015b). Primate torpor: regulation of stress-activated protein kinases during daily torpor in the gray mouse lemur. *Microcebus murinus*. *Genomics Proteomics Bioinformatics* 13, 81–90. doi: 10.1016/j.gpb.2015.03.002

Blackstone, E., Morrison, M., and Roth, M. B. (2005). H2S induces a suspended animation-like state in mice. *Science* 308, 518. doi: 10.1126/science.1108581

Boag, D. A., and Murie, J. O. (1981). Weight in relation to sex, age, and season in Columbian ground squirrels (*Sciuridae*. *Rodentia*). Can. J. Zool. 59, 999–1004. doi: 10.1139/z81-139

Bouma, H. R., Verhaag, E. M., Otis, J. P., Heldmaier, G., Swoap, S. J., Strijkstra, A. M., et al. (2012). Induction of torpor: mimicking natural metabolic suppression for biomedical applications. *J. Cell. Physiol.* 227, 1285–1290. doi: 10.1002/jcp.22850

Boyer, B. B., Ormseth, O. A., Buck, L., Nicolson, M., Pelleymounter, M. A., and Barnes, B. M. (1997). Leptin prevents posthibernation weight gain but does not reduce energy expenditure in arctic ground squirrels. *Comp. Biochem. Physiol. C* 118, 405–412. doi: 10.1016/S0742-8413(97)00172-2

Boyles, J. G., Dunbar, M. B., Storm, J. J., and Brack, V. Jr. (2007). Energy availability influences microclimate selection of hibernating bats. *J. Exp. Biol.* 210(Pt 24), 4345–4350. doi: 10.1242/jeb.007294

Boyles, J. G., Thompson, A. B., McKechnie, A. E., Malan, E., Humphries, M. M., and Careau, V. (2013). A global heterothermic continuum in mammals. *Global Ecol. Biogeogr.* 22, 1029–1039. doi: 10.1111/Geb.12077

Bozinovic, F., Contreras, L., Rosenmann, M., and Torres-Mura, J. C. (1985). Bioenergética de *Myotis chiloensis* (*Quiroptera*: *Vespertilionidae*). *Rev. Chil. Hist. Nat.* 58, 39–45.

Bozinovic, F., and Marquet, P. A. (1991). Energetics and torpor in the Atacama desert-dwelling rodent *Phyllotis darwini rupestris*. *J. Mammal.* 72, 734–738. doi: 10.2307/1381835

Bozinovic, F., Muñoz, J. L. P., Naya, D. E., and Cruz-Neto, A. P. (2007). Adjusting energy expenditures to energy supply: food availability regulates torpor use and organ size in the Chilean mouse-opossum *Thylamys elegans*. *J. Comp. Physiol. B* 177, 393–400. doi: 10.1007/s00360-006-0137-0

Bozinovic, F., Ruiz, G., and Rosenmann, M. (2004). Energetics and torpor of a South American "living fossil", the microbiotheriid *Dromiciops gliroides*. *J. Comp. Physiol. B* 174, 293–297. doi: 10.1007/s00360-004-0414-8

Brown, J. C. L., Chung, D. J., Belgrave, K. R., and Staples, J. F. (2012). Mitochondrial metabolic suppression and reactive oxygen species production in liver and skeletal muscle of hibernating thirteen-lined ground squirrels. *Am. J. Physiol. Reg. Int. Comp. Physiol.* 302, R15–R28. doi: 10.1152/ajpregu.00230.2011

Bruintjes, J. J., Henning, R. H., Douwenga, W., and van der Zee, E. A. (2014). Hippocampal cystathionine beta synthase in young and aged mice. *Neurosci. Lett.* 563, 135–139. doi: 10.1016/j.neulet.2014.01.049

Bullmann, T., Seeger, G., Stieler, J., Hanics, J., Reimann, K., Kretzschmann, T. P., et al. (2016). Tau phosphorylation-associated spine regression does not impair hippocampal-dependent memory in hibernating golden hamsters. *Hippocampus* 26, 301–318. doi: 10.1002/hipo.22522

Canale, C. I., Perret, M., and Henry, P. Y. (2012). Torpor use during gestation and lactation in a primate. *Naturwissenschaften* 99, 159–163. doi: 10.1007/s00114-011-0872-2

Careau, V., Bininda-Emonds, O. R. P., Thomas, D. W., Reale, D., and Humphries, M. M. (2009). Exploration strategies map along fast-slow metabolic and life-history continua in muroid rodents. *Funct. Ecol.* 23, 150–156. doi: 10.1111/j.1365-2435.2008.01468.x

Carey, H. V. (1990). Seasonal changes in mucosal structure and function in ground squirrel intestine. *Am. J. Physiol. Reg. Int. Comp. Physiol.* 259, R385–R392. doi: 10.1152/ajpregu.1990.259.2.R385

Carey, H. V. (1995). Gut feelings about hibernation. *Physiology* 10, 55–61. doi: 10.1152/physiologyonline.1995.10.2.55

Carey, H. V., Andrews, M. T., and Martin, S. L. (2003). Mammalian hibernation: cellular and molecular responses to depressed metabolism and low temperature. *Physiol. Rev.* 83, 1153–1181. doi: 10.1152/physrev.00008.2003

Carey, H. V., Frank, C. L., and Seifert, J. P. (2000). Hibernation induces oxidative stress and activation of NF-κB in ground squirrel intestine. *J. Comp. Physiol. B* 170, 551–559. doi: 10.1007/s003600000135

Carey, H. V., and Martin, S. L. (1996). Preservation of intestinal gene expression during hibernation. *Am. J. Physiol. Gastro. Liver Physiol.* 271, G804–G813. doi: 10.1152/ajpgi.1996.271.5.G805

Carey, H. V., Sills, N. S., and Gorham, D. A. (1999). Stress proteins in mammalian hibernation. *Am. Zool.* 39, 825–835. doi: 10.1093/icb/39.6.825

Carpenter, F. L. (1974). Torpor in an andean hummingbird: its ecological significance. *Science* 183, 545–547. doi: 10.1126/science.183.4124.545

Castex, C., Tahri, A., Hoo-Paris, R., and Sutter, B. C. J. (1984). Insulin secretion in the hibernating edible dormouse (*Glis glis*): *in vivo* and *in vitro* studies. *Comp. Biochem. Physiol. A* 79, 179–183. doi: 10.1016/0300-9629(84)90729-1

Celis-Diez, J. L., Hetz, J., Marín-Vial, P. A., Fuster, G., Necochea, P., Vásquez, R. A., et al. (2012). Population abundance, natural history, and habitat use by the arboreal marsupial *Dromiciops gliroides* in rural Chiloé Island. *Chile. J. Mammal.* 93, 134–148. doi: 10.1644/10-MAMM-A-406.1

Cerri, M. (2017). The central control of energy expenditure: exploiting torpor for medical applications. *Annu. Rev. Physiol.* 79, 167–186. doi: 10.1146/annurev-physiol-022516-034133

Chanon, S., Chazarin, B., Toubhans, B., Durand, C., Chery, I., Robert, M., et al. (2018). Proteolysis inhibition by hibernating bear serum leads to increased protein content in human muscle cells. *Sci. Rep.* 8:5525. doi: 10.1038/s41598-018-23891-5

Chatfield, P. O., Lyman, C. P., and Purpura, D. P. (1951). The effects of temperature on the spontaneous and induced electrical activity in the cerebral cortex of the golden hamster. *Electroencephalogr. Clin. Neurophysiol.* 3, 225–230. doi: 10.1016/0013-4694(51)90015-6

Childers, C. L., Tessier, S. N., and Storey, K. B. (2019). The heart of a hibernator: EGFR and MAPK signaling in cardiac muscle during the hibernation of thirteen-lined ground squirrels. *Ictidomys tridecemlineatus*. *PeerJ* 7:e7587. doi: 10.7717/peerj.7587

Chong, C. R., Chan, W. P. A., Nguyen, T. H., Liu, S. F., Procter, N. E. K., Ngo, D. T., et al. (2014). Thioredoxin-interacting protein: pathophysiology and emerging pharmacotherapeutics in cardiovascular disease and diabetes. *Cardiovasc. Drugs Ther.* 28, 347–360. doi: 10.1007/s10557-014-6538-5

Choukèr, A., Bereiter-Hahn, J., Singer, D., and Heldmaier, G. (2019). Hibernating astronauts-science or fiction? *Pflugers Arch. Eur. J. Physiol.* 471, 819–828. doi: 10.1007/s00424-018-2244-7

Clarke, I. J., and Caraty, A. (2013). Kisspeptin and seasonality of reproduction. *Adv. Exp. Med. Biol.* 784, 411–430. doi: 10.1007/978-1-4614-6199-9_19

Cogut, V., Bruintjes, J. J., Eggen, B. J. L., van der Zee, E. A., and Henning, R. H. (2018). Brain inflammatory cytokines and microglia morphology changes throughout hibernation phases in Syrian hamster. *Brain Behav Immun.* 68, 17–22. doi: 10.1016/j.bbi.2017.10.009

Concannon, P., Levac, K., Rawson, R., Tennant, B., and Bensadoun, A. (2001). Seasonal changes in serum leptin, food intake, and body weight in photoentrained woodchucks. *Am. J. Physiol. Reg. Int. Comp. Physiol.* 281, R951–R959. doi: 10.1152/ajpregu.2001.281.3.R951

Cotton, C. J. (2016). Skeletal muscle mass and composition during mammalian hibernation. *J. Exp. Biol.* 219, 226–234. doi: 10.1242/jeb.125401

Cummings, D. E. (2006). Ghrelin and the short- and long-term regulation of appetite and body weight. *Physiol. Behav.* 89, 71–84. doi: 10.1016/j.physbeh.2006.05.022

D'Alessandro, A., Nemkov, T., Bogren, L. K., Martin, S. L., and Hansen, K. C. (2017). Comfortably numb and back: plasma metabolomics reveals biochemical adaptations in the hibernating 13-lined ground squirrel. *J. Proteome Res.* 16, 958–969. doi: 10.1021/acs.jproteome.6b00884

Dardente, H., Wood, S., Ebling, F., and Sáenz de Miera, C. (2019). An integrative view of mammalian seasonal neuroendocrinology. *J. Neuroendocrinol* 31:e12729. doi: 10.1111/jne.12729

Dark, J. (2005). Annual lipid cycles in hibernators: integration of physiology and behavior. *Annu. Rev. Nutr.* 25, 469–497. doi: 10.1146/annurev.nutr.25.050304.092514

Davis, D. E. (1976). Hibernation and circannual rhythms of food consumption in marmots and ground squirrels. *Q. Rev. Biol.* 51, 477–514. doi: 10.1086/409594

de Cabo, R., and Mattson, M. P. (2019). Effects of intermittent fasting on health. Aging, and Disease. *New Engl. J. Med.* 381, 2541–2551. doi: 10.1056/NEJMra1905136

DeBalsi, K. L., Wong, K. E., Koves, T. R., Slentz, D. H., Seiler, S. E., Wittmann, A. H., et al. (2014). Targeted metabolomics connects thioredoxin-interacting protein (TXNIP) to mitochondrial fuel selection and regulation of specific oxidoreductase enzymes in skeletal muscle. *J. Biol. Chem.* 289, 8106–8120. doi: 10.1074/jbc.M113.511535

di Virgilio, A., Amico, G. C., and Morales, J. M. (2014). Behavioral traits of the arboreal marsupial *Dromiciops gliroides* during *Tristerix corymbosus* fruiting season. *J. Mammal.* 95, 1189–1198. doi: 10.1644/13-MAMM-A-281

Dirkes, M. C., Milstein, D. M. J., Heger, M., and van Gulik, T. M. (2015). Absence of hydrogen sulfide-induced hypometabolism in pigs: a mechanistic explanation in relation to small nonhibernating mammals. *Eur. Surg. Res.* 54, 178–191. doi: 10.1159/000369795

Du, C., Lin, X., Xu, W., Zheng, F., Cai, J., Yang, J., et al. (2018). Sulfhydrated Sirtuin-1 increasing its deacetylation activity is an essential epigenetics mechanism of anti-atherogenesis by hydrogen sulfide. *Antioxid. Redox. Signal.* 30, 184–197. doi: 10.1089/ars.2017.7195

Dugbartey, G. J., Talaei, F., Houwertjes, M. C., Goris, M., Epema, A. H., Bouma, H. R., et al. (2015). Dopamine treatment attenuates acute kidney injury in a rat model of deep hypothermia and rewarming – The role of renal H2S-producing enzymes. *Eur. J. Pharmacol.* 769, 225–233. doi: 10.1016/j.ejphar.2015.11.022

Ebert, T., Painer, J., Bergman, P., Qureshi, A. R., Giroud, S., Stalder, G., et al. (2020). Insights in the regulation of trimetylamine N-oxide production using a comparative biomimetic approach suggest a metabolic switch in hibernating bears. *Sci. Rep.* 10:20323. doi: 10.1038/s41598-020-76346-1

Faherty, S. L., Villanueva-Cañas, J. L., Klopfer, P. H., Albà, M. M., and Yoder, A. D. (2016). Gene expression profiling in the hibernating primate. *Cheirogaleus Medius*. *Genome Biol. Evol.* 8, 2413–2426. doi: 10.1093/gbe/evw163

Florant, G. L., Hoo-Paris, R., Castex, C., Bauman, W. A., and Sutter, B. C. (1986). Pancreatic A and B cell stimulation in euthermic and hibernating marmots (*Marmota flaviventris*): effects of glucose and arginine administration. *J. Comp. Physiol. B* 156, 309–314. doi: 10.1007/BF01101092

Florant, G. L., Porst, H., Pfeiffer, A., Hudachek, S. F., Pittman, C., Summers, S. A., et al. (2004). Fat-cell mass, serum leptin and adiponectin changes during weight gain and loss in yellow-bellied marmots (*Marmota flaviventris*). *J. Comp. Physiol. B* 174, 633–639. doi: 10.1007/s00360-004-0454-0

Franco, M., Contreras, C., and Nespolo, R. F. (2013). Profound changes in blood parameters during torpor in a South American marsupial. *Comp. Biochem. Physiol. A* 166, 338–342. doi: 10.1016/j.cbpa.2013.07.010

Franco, M., Contreras, C., Place, N. J., Bozinovic, F., and Nespolo, R. F. (2017). Leptin levels, seasonality and thermal acclimation in the Microbiotherid marsupial *Dromiciops gliroides*: does photoperiod play a role? *Comp. Biochem. Physiol. A* 203, 233–240. doi: 10.1016/j.cbpa.2016.09.025

Franco, M., Quijano, A., and Soto-Gamboa, M. (2011). Communal nesting, activity patterns, and population characteristics in the near-threatened monito del monte. *Dromiciops gliroides*. *J. Mammal.* 92, 994–1004. doi: 10.1644/10-MAMM-A-256.1

Freeman, D. A., Lewis, D. A., Kauffman, A. S., Blum, R. M., and Dark, J. (2004). Reduced leptin concentrations are permissive for display of torpor in Siberian hamsters. *Am. J. Physiol. Reg. Int. Comp. Physiol.* 287, R97–R103. doi: 10.1152/ajpregu.00716.2003

French, A. R. (1988). The patterns of mammalian hibernation. *Am. Sci.* 76, 569–575.

French, A. R. (1990). Age-class differences in the pattern of hibernation in yellow-bellied marmots. *Marmota flaviventris*. *Oecologia* 82, 93–96. doi: 10.1007/BF00318538

Frerichs, K. U., Kennedy, C., Sokoloff, L., and Hallenbeck, J. M. (1994). local cerebral blood flow during hibernation, a model of natural tolerance to "Cerebral Ischemia". *J. Cereb. Blood Flow Metab.* 14, 193–205. doi: 10.1038/jcbfm.1994.26

Frerichs, K. U., Smith, C. B., Brenner, M., DeGracia, D. J., Krause, G. S., Marrone, L., et al. (1998). Suppression of protein synthesis in brain during hibernation involves inhibition of protein initiation and elongation. *Proc. Natl. Acad. Sci. U.S.A.* 95, 14511–14516. doi: 10.1073/pnas.95.24.14511

Frigault, J. J., Gaudet, J. D., and Morin, P. Jr. (2018). Investigating Nrf2-associated non-coding RNAs in the hibernating ground squirrel, *Ictidomys tridecemlineatus*. *J. Therm. Biol.* 75, 38–44. doi: 10.1016/j.jtherbio.2018.05.008

Fruebis, J., Tsao, T. S., Javorschi, S., Ebbets-Reed, D., Erickson, M. R., Yen, F. T., et al. (2001). Proteolytic cleavage product of 30-kDa adipocyte complement-related protein increases fatty acid oxidation in muscle and causes weight loss in mice. *Proc. Natl. Acad. Sci. U.S.A.* 98, 2005–2010. doi: 10.1073/pnas.041591798

Fu, M., Zhang, W., Wu, L., Yang, G., Li, H., and Wang, R. (2012). Hydrogen sulfide (H2S) metabolism in mitochondria and its regulatory role in energy production. *Proc. Natl. Acad. Sci. U.S.A.* 109, 2943–2948. doi: 10.1073/pnas.1115634109

Galluser, M., Raul, F., and Canguilhem, B. (1988). Adaptation of intestinal enzymes to seasonal and dietary changes in a hibernator: the European hamster (*Cricetus cricetus*). *J. Comp. Physiol. B* 158, 143–149. doi: 10.1007/bf01075827

Gaudry, M. J., and Campbell, K. L. (2017). Evolution of *UCP1* transcriptional regulatory elements across the mammalian phylogeny. *Front. Physiol.* 8:670. doi: 10.3389/fphys.2017.00670

Geiser, F. (2013). Hibernation. *Curr. Biol.* 23, R188–R193. doi: 10.1016/j.cub.2013.01.062

Geiser, F. (2020). Seasonal expression of avian and mammalian daily torpor and hibernation: not a simple summer-winter affair. *Front. Physiol.* 11:436. doi: 10.3389/fphys.2020.00436

Geiser, F., and Körtner, G. (2010). Hibernation and daily torpor in Australian mammals. *Aust. Zool.* 35, 204–215. doi: 10.7882/AZ.2010.009

Geiser, F., and Martin, G. M. (2013). Torpor in the Patagonian opossum (*Lestodelphys halli*): implications for the evolution of daily torpor and hibernation. *Naturwissenschaften* 100, 975–981. doi: 10.1007/s00114-013-1098-2

Giroud, S., Blanc, S., Aujard, F., Bertrand, F., Gilbert, C., and Perret, M. (2008). Chronic food shortage and seasonal modulations of daily torpor and locomotor activity in the grey mouse lemur (*Microcebus murinus*). *Am. J. Physiol. Reg. Int. Comp. Physiol.* 294, R1958–R1967. doi: 10.1152/ajpregu.00794.2007

Giroud, S., Stalder, G., Gerritsmann, H., Kübber-Heiss, A., Kwak, J., Arnold, W., et al. (2018). Dietary lipids affect the onset of hibernation in the garden dormouse (*Eliomys quercinus*): implications for cardiac function. *Front. Physiol.* 9:1235. doi: 10.3389/fphys.2018.01235

Giroud, S., Zahn, S., Criscuolo, F., Chery, I., Blanc, S., Turbill, C., et al. (2014). Late-born intermittently fasted juvenile garden dormice use torpor to grow and fatten prior to hibernation: consequences for ageing processes. *Proc. R. Soc. B* 281:20141131. doi: 10.1098/rspb.2014.1131

Godoy-Güinao, J., Díaz, I. A., and Celis-Diez, J. L. (2018). Confirmation of arboreal habits in *Dromiciops gliroides*: a key role in chilean temperate rainforests. *Ecosphere* 9:e02424. doi: 10.1002/ecs2.2424

Golbidi, S., Daiber, A., Korac, B., Li, H., Essop, M. F., and Laher, I. (2017). Health benefits of fasting and caloric restriction. *Curr. Diab. Rep.* 17:123. doi: 10.1007/s11892-017-0951-7

Goubern, M., Andriamihaja, M., Nübel, T., Blachier, F., and Bouillaud, F. (2007). Sulfide, the first inorganic substrate for human cells. *FASEB J.* 21, 1699–1706. doi: 10.1096/fj.06-7407com

Green, C. J., Brosman, J. T., Fuller, B. J., Lowry, M., Stubbs, M., and Ross, B. C. (1984). Effect of hibernation on liver and kidney metabolism in 13-lined ground squirrels. *Comp. Biochem. Phys. B* 79, 167–171. doi: 10.1016/0305-0491(84)90009-9

Hadj-Moussa, H., Moggridge, J. A., Luu, B. E., Quintero-Galvis, J. F., Gaitán-Espitia, J. D., Nespolo, R. F., et al. (2016). The hibernating South American marsupial, *Dromiciops gliroides*, displays torpor-sensitive microRNA expression patterns. *Sci. Rep.* 6:24627. doi: 10.1038/srep24627

Hadj-Moussa, H., Zhang, J., Pifferi, F., Perret, M., and Storey, K. B. (2020). Profiling torpor-responsive microRNAs in muscles of the hibernating primate *Microcebus murinus*. *BBA Gene Struct. Exp.* 1863:194473. doi: 10.1016/j.bbagrm.2019.194473

Hampton, M., Melvin, R. G., and Andrews, M. T. (2013). Transcriptomic analysis of brown adipose tissue across the physiological extremes of natural hibernation. *PLoS One* 8:e85157. doi: 10.1371/journal.pone.0085157

Hampton, M., Melvin, R. G., Kendall, A. H., Kirkpatrick, B. R., Peterson, N., and Andrews, M. T. (2011). Deep sequencing the transcriptome reveals seasonal adaptive mechanisms in a hibernating mammal. *PLoS One* 6:e27021. doi: 10.1371/journal.pone.0027021

Hand, L. E., Saer, B. R. C., Hui, S. T., Jinnah, H. A., Steinlechner, S., Loudon, A. S. I., et al. (2013). Induction of the metabolic regulator Txnip in fasting-induced and natural torpor. *Endocrinology* 154, 2081–2091. doi: 10.1210/En.2012-2051

Haouzi, P., Notet, V., Chenuel, B., Chalon, B., Sponne, I., Ogier, V., et al. (2008). H2S induced hypometabolism in mice is missing in sedated sheep. *Resp. Physiol. Neurobiol.* 160, 109–115. doi: 10.1016/j.resp.2007.09.001

Härtig, W., Stieler, J., Boerema, A. S., Wolf, J., Schmidt, U., Weißfuß, J., et al. (2007). Hibernation model of tau phosphorylation in hamsters: selective vulnerability of cholinergic basal forebrain neurons – implications for Alzheimer's disease. *Eur. J. Neurosci.* 25, 69–80. doi: 10.1111/j.1460-9568.2006.05250.x

Healy, J. E., Ostrom, C. E., Wilkerson, G. K., and Florant, G. L. (2010). Plasma ghrelin concentrations change with physiological state in a sciurid hibernator (*Spermophilus lateralis*). *Gen. Comp. Endocrinol.* 166, 372–378. doi: 10.1016/j.ygcen.2009.12.006

Healy, J. E., Richter, M. M., Suu, L., Fried, S. K., and Florant, G. L. (2008). "Changes in serum leptin concentrations with fat mass in golden-mantled ground squirrels (*Spermophilus lateralis*)," in *Hypometabolism in Animals: Hibernation, Torpor and Cryobiology*, eds B. G. Lovegrove and A. E. McKechnie (Pietermaritzburg: University of KwaZulu-Natal).

Heldmaier, G., Ortmann, S., and Elvert, R. (2004). Natural hypometabolism during hibernation and daily torpor in mammals. *Resp. Physiol. Neurobiol.* 141, 317–329. doi: 10.1016/j.resp.2004.03.014

Hemelrijk, S. D., Dirkes, M. C., van Velzen, M. H. N., Bezemer, R., van Gulik, T. M., and Heger, M. (2018). Exogenous hydrogen sulfide gas does not induce hypothermia in normoxic mice. *Sci. Rep.* 8:3855. doi: 10.1038/s41598-018-21729-8

Hendriks, K. D. W., Joschko, C. P., Hoogstra-Berends, F., Heegsma, J., Faber, K.-N., and Henning, R. H. (2020). Hibernator-derived cells show superior protection and survival in hypothermia compared to non-hibernator cells. *Int. J. Mol. Sci.* 21:1864. doi: 10.3390/ijms21051864

Hendriks, K. D. W., Lupi, E., Hardenberg, M. C., Hoogstra-Berends, F., Deelman, L. E., and Henning, R. H. (2017). Differences in mitochondrial function and morphology during cooling and rewarming between hibernator and non-hibernator derived kidney epithelial cells. *Sci. Rep.* 7:15482. doi: 10.1038/s41598-017-15606-z

Hoelzl, F., Cornils, J. S., Smith, S., Moodley, Y., and Ruf, T. (2016). Telomere dynamics in free-living edible dormice (*Glis glis*): the impact of hibernation and food supply. *J. Exp. Biol.* 219(Pt 16), 2469–2474. doi: 10.1242/jeb.140871

Hoo-Paris, R., Castex, C., Hamsany, M., Thari, A., and Sutter, B. (1985). Glucagon secretion in the hibernating edible dormouse (*Glis glis*). *Comp. Biochem. Physiol. A* 81, 277–281. doi: 10.1016/0300-9629(85)90135-5

Hoo-Paris, R., Hamsany, M., Sutter, B. C. J., Assan, R., and Boillot, J. (1982). Plasma glucose and glucagon concentrations in the hibernating hedgehog. *Gen. Comp. Endocrinol.* 46, 246–254. doi: 10.1016/0016-6480(82)90206-4

Hoo-Paris, R., and Sutter, B. C. J. (1980). Blood glucose control by insulin in the lethargic and arousing hedgehog (*Erinaceus europaeus*). *Comp. Biochem. Physiol. A Physiol.* 66, 141–143. doi: 10.1016/0300-9629(80)90371-0

Hourihan, J. M., Kenna, J. G., and Hayes, J. D. (2012). The gasotransmitter hydrogen sulfide induces Nrf2-target genes by inactivating the Keap1 ubiquitin ligase substrate adaptor through formation of a disulfide bond between Cys-226 and Cys-613. *Antioxid. Redox. Signal.* 19, 465–481. doi: 10.1089/ars.2012.4944

Hrvatin, S., Sun, S., Wilcox, O. F., Yao, H., Lavin-Peter, A. J., Cicconet, M., et al. (2020). Neurons that regulate mouse torpor. *Nature* 583, 115–121. doi: 10.1038/s41586-020-2387-5

Hume, I. D., Beiglböck, C., Ruf, T., Frey-Roos, F., Bruns, U., and Arnold, W. (2002). Seasonal changes in morphology and function of the gastrointestinal tract of free-living alpine marmots (*Marmota marmota*). *J. Comp. Physiol. B* 172, 197–207. doi: 10.1007/s00360-001-0240-1

Humphries, M. M., Kramer, D. L., and Thomas, D. W. (2003a). The role of energy availability in mammalian hibernation: an experimental test in free-ranging eastern chipmunks. *Physiol. Biochem. Zool.* 76, 180–186. doi: 10.1086/367949

Humphries, M. M., Thomas, D. W., and Kramer, D. L. (2003b). The role of energy availability in mammalian hibernation: a cost-benefit approach. *Physiol. Biochem. Zool.* 76, 165–179. doi: 10.1086/367950

Humphries, M. M., Thomas, D. W., and Kramer, D. L. (2001). Torpor and digestion in food-storing hibernators. *Physiol. Biochem. Zool.* 74, 283–292. doi: 10.1086/319659

Ishigami, M., Hiraki, K., Umemura, K., Ogasawara, Y., Ishii, K., and Kimura, H. (2009). A source of hydrogen sulfide and a mechanism of its release in the brain. *Antioxid. Redox. Signal.* 11, 205–214. doi: 10.1089/ars.2008.2132

Jastroch, M., Giroud, S., Barrett, P., Geiser, F., Heldmaier, G., and Herwig, A. (2016). Seasonal control of mammalian energy balance: recent advances in the understanding of daily torpor and hibernation. *J. Neuroendocrinol* 28. doi: 10.1111/jne.12437

Johansson, B. W. (1996). The hibernator heart - Nature's model of resistance to ventricular fibrillation. *Cardiovasc. Res.* 31, 826–832. doi: 10.1016/0008-6363(95)00192-1

Johnson, D. C., Dean, D. R., Smith, A. D., and Johnson, M. K. (2005). Structure, function, and formation of biological iron-sulfur clusters. *Annu. Rev. Biochem.* 74, 247–281. doi: 10.1146/annurev.biochem.74.082803.133518

Jonasson, K. A., and Willis, C. K. (2011). Changes in body condition of hibernating bats support the thrifty female hypothesis and predict consequences for populations with white-nose syndrome. *PLoS One* 6:e21061. doi: 10.1371/journal.pone.0021061

Kart Gür, M., and Gür, H. (2015). Age and sex differences in hibernation patterns in free-living Anatolian ground squirrels. *Mamm. Biol.* 80, 265–272. doi: 10.1016/j.mambio.2015.02.006

Kenagy, G. J., and Barnes, B. M. (1988). Seasonal reproductive patterns in four coexisting rodent species from the Cascade Mountains, Washington. *J. Mammal.* 69, 274–292. doi: 10.2307/1381378

Khan, A. A., Schuler, M. M., Prior, M. G., Yong, S., Coppock, R. W., Florence, L. Z., et al. (1990). Effects of hydrogen sulfide exposure on lung mitochondrial respiratory chain enzymes in rats. *Toxicol. Appl. Pharm.* 103, 482–490. doi: 10.1016/0041-008X(90)90321-K

Klug, B. J., and Brigham, R. M. (2015). Changes to metabolism and cell physiology that enable mammalian hibernation. *Springer Sci. Rev.* 3, 39–56. doi: 10.1007/s40362-015-0030-x

Kobbe, S., Nowack, J., and Dausmann, K. H. (2014). Torpor is not the only option: seasonal variations of the thermoneutral zone in a small primate. *J. Comp. Physiol. B* 184, 789–797. doi: 10.1007/s00360-014-0834-z

Körtner, G., and Geiser, F. (2009). The key to winter survival: daily torpor in a small arid-zone marsupial. *Naturwissenschaften* 96, 525–530. doi: 10.1007/s00114-008-0492-7

Krilowicz, B. L. (1985). Ketone body metabolism in a ground squirrel during hibernation and fasting. *Am. J. Physiol. Reg. Int. Comp. Physiol.* 249, R462–R470. doi: 10.1152/ajpregu.1985.249.4.R462

Kronfeld-Schor, N., Richardson, C., Silvia, B. A., Kunz, T. H., and Widmaier, E. P. (2000). Dissociation of leptin secretion and adiposity during perhibernatory fattening in little brown bats. *Am. J. Physiol. Reg. Int. Comp. Physiol.* 279, R1277–R1281. doi: 10.1152/ajpregu.2000.279.4.R1277

Kurtz, C. C., and Carey, H. V. (2007). Seasonal changes in the intestinal immune system of hibernating ground squirrels. *Dev. Comp. Immunol.* 31, 415–428. doi: 10.1016/j.dci.2006.07.003

Lafontan, M., and Viguerie, N. (2006). Role of adipokines in the control of energy metabolism: focus on adiponectin. *Curr. Opin. Pharmacol.* 6, 580–585. doi: 10.1016/j.coph.2006.08.002

Landes, J., Pavard, S., Henry, P. Y., and Terrien, J. (2020). Flexibility is costly: hidden physiological damage from seasonal phenotypic transitions in Heterothermic species. *Front. Physiol.* 11:985. doi: 10.3389/Fphys.2020.00985

Languille, S., Blanc, S., Blin, O., Canale, C. I., Dal-Pan, A., Devau, G., et al. (2012). The grey mouse lemur: a non-human primate model for ageing studies. *Ageing Res. Rev.* 11, 150–162. doi: 10.1016/j.arr.2011.07.001

Lee, H. K., Koh, S., Lo, D. C., and Marchuk, D. A. (2018). Neuronal IL-4R modulates neuronal apoptosis and cell viability during the acute phases of cerebral ischemia. *FEBS J.* 285, 2785–2798. doi: 10.1111/febs.14498

Lei, M., Dong, D., Mu, S., Pan, Y. H., and Zhang, S. Y. (2014). Comparison of brain transcriptome of the greater horseshoe bats (*Rhinolophus ferrumequinum*) in active and torpid episodes. *PLoS One* 9:e107746. doi: 10.1371/journal.pone.0107746

León-Espinosa, G., Regalado-Reyes, M., DeFelipe, J., and Muñoz, A. (2018). Changes in neocortical and hippocampal microglial cells during hibernation. *Brain Struct. Funct.* 223, 1881–1895. doi: 10.1007/s00429-017-1596-7

Logan, S. M., and Storey, K. B. (2018). Pro-inflammatory AGE-RAGE signaling is activated during arousal from hibernation in ground squirrel adipose. *PeerJ* 6:e4911. doi: 10.7717/peerj.4911

Logan, S. M., Wu, C.-W., and Storey, K. B. (2019). The squirrel with the lagging eIF2: global suppression of protein synthesis during torpor. *Comp. Biochem. Physiol. A* 227, 161–171. doi: 10.1016/j.cbpa.2018.10.014

Lovegrove, B. G., and Genin, F. (2008). Torpor and hibernation in a basal placental mammal, the lesser hedgehog tenrec *Echinops telfairi*. *J. Comp. Physiol. B* 178, 691–698. doi: 10.1007/s00360-008-0257-9

Lovegrove, B. G., Raman, J., and Perrin, M. R. (2001). Heterothermy in elephant shrews, Elephantulus spp. (Macroscelidea): daily torpor or hibernation? *J. Comp. Physiol. B* 171, 1–10. doi: 10.1007/s003600000139

Lu, A., Chu, C., Mulvihill, E., Wang, R., and Liang, W. (2019). ATP-sensitive K+ channels and mitochondrial permeability transition pore mediate effects of hydrogen sulfide on cytosolic Ca2+ homeostasis and insulin secretion in β-cells. *Pflügers Arch. Eur. J. Physiol.* 471, 1551–1564. doi: 10.1007/s00424-019-02325-9

Luppi, M., Hitrec, T., Di Cristoforo, A., Squarcio, F., Stanzani, A., Occhinegro, A., et al. (2019). Phosphorylation and dephosphorylation of tau protein during synthetic torpor. *Front. Neuroanat* 13:57. doi: 10.3389/fnana.2019.00057

Luu, B. E., Lefai, E., Giroud, S., Swenson, J. E., Chazarin, B., Gauquelin-Koch, G., et al. (2020). MicroRNAs facilitate skeletal muscle maintenance and metabolic suppression in hibernating brown bears. *J. Cell. Physiol.* 235, 3984–3993. doi: 10.1002/jcp.29294

Lyman, C. P., and Chatfield, P. O. (1955). Physiology of hibernation in mammals. *Physiol. Rev.* 35, 403–425. doi: 10.1152/physrev.1955.35.2.403

Mahlert, B., Gerritsmann, H., Stalder, G., Ruf, T., Zahariev, A., Blanc, S., et al. (2018). Implications of being born late in the active season for growth, fattening, torpor use, winter survival and fecundity. *eLife* 7:e31225. doi: 10.7554/eLife.31225

Martin, B., Mattson, M. P., and Maudsley, S. (2006). Caloric restriction and intermittent fasting: Two potential diets for successful brain aging. *Ageing Res. Rev.* 5, 332–353. doi: 10.1016/j.arr.2006.04.002

Martin, G. M. (2010). Geographic distribution and historical occurrence of *Dromiciops gliroides* Thomas (*Metatheria*: *Microbiotheria*). *J. Mammal.* 91, 1025–1035. doi: 10.1644/09-mamm-a-347.1

Masaki, T., Chiba, S., Yasuda, T., Tsubone, T., Kakuma, T., Shimomura, I., et al. (2003). Peripheral, But not central, administration ofadiponectin reduces visceral adiposity andupregulates the expression of uncoupling proteinin agouti yellow (*Ay/a*) obese mice. *Diabetes* 52, 2266–2273. doi: 10.2337/diabetes.52.9.2266

Mathers, K. E., McFarlane, S. V., Zhao, L., and Staples, J. F. (2017). Regulation of mitochondrial metabolism during hibernation by reversible suppression of electron transport system enzymes. *J. Comp. Physiol. B* 187, 227–234. doi: 10.1007/s00360-016-1022-0

Michener, G. R. (1978). Effect of age and parity on weight gain and entry into hibernation in Richardson's ground squirrels. *Can. J. Zool.* 56, 2573–2577. doi: 10.1139/z78-345

Mitchell, K. J., Pratt, R. C., Watson, L. N., Gibb, G. C., Llamas, B., Kasper, M., et al. (2014). Molecular phylogeny, biogeography, and habitat preference evolution of marsupials. *Mol. Biol. Evol.* 31, 2322–2330. doi: 10.1093/molbev/msu176

Miyake, S.-I., Wakita, H., Bernstock, J. D., Castri, P., Ruetzler, C., Miyake, J., et al. (2015). Hypophosphorylation of ribosomal protein S6 is a molecular mechanism underlying ischemic tolerance induced by either hibernation or preconditioning. *J. Neurochem.* 135, 943–957. doi: 10.1111/jnc.13368

Módis, K., Bos, E. M., Calzia, E., van Goor, H., Coletta, C., Papapetropoulos, A., et al. (2014). Regulation of mitochondrial bioenergetic function by hydrogen sulfide. Part II. Pathophysiological and therapeutic aspects. *Br. J. Pharmacol.* 171, 2123–2146. doi: 10.1111/bph.12368

Módis, K., Coletta, C., Erdélyi, K., Papapetropoulos, A., and Szabo, C. (2013). Intramitochondrial hydrogen sulfide production by 3-mercaptopyruvate sulfurtransferase maintains mitochondrial electron flow and supports cellular bioenergetics. *FASEB J.* 27, 601–611. doi: 10.1096/fj.12-216507

Mokrasch, L. C., Grady, H. J., and Grisolia, S. (1960). Thermogenic and adaptive mechanisms in hibernation and arousal from hibernation. *Am. J. Physiol. Legacy Content* 199, 945–949. doi: 10.1152/ajplegacy.1960.199.5.945

Morin, P. Jr., Ni, Z., McMullen, D. C., and Storey, K. B. (2008). Expression of Nrf2 and its downstream gene targets in hibernating 13-lined ground squirrels, *Spermophilus tridecemlineatus*. *Mol. Cell. Biochem.* 312, 121–129. doi: 10.1007/s11010-008-9727-3

Morin, P. Jr., and Storey, K. B. (2007). Antioxidant defense in hibernation: cloning and expression of peroxiredoxins from hibernating ground squirrels, *Spermophilus tridecemlineatus*. *Arch. Biochem. Biophys.* 461, 59–65. doi: 10.1016/j.abb.2007.01.035

Muleme, H. M., Walpole, A. C., and Staples, J. F. (2006). Mitochondrial metabolism in hibernation: metabolic suppression, temperature effects, and substrate preferences. *Physiol. Biochem. Zool.* 79, 474–483. doi: 10.1086/501053

Muñoz-Pedreros, A., Lang, B. K., Bretos, M., and Meserve, P. L. (2005). Reproduction and development of *Dromiciops gliroides* (*Marsupialia*: *Microbiotheriidae*) in temperate rainforests of southern Chile. *Gayana* 69, 225–233. doi: 10.4067/S0717-65382005000200002

Mustafa, A. K., Gadalla, M. M., Sen, N., Kim, S., Mu, W., Gazi, S. K., et al. (2009). H2S signals through protein S-sulfhydration. *Sci. Signal.* 2:ra72. doi: 10.1126/scisignal.2000464

Nagahara, N., Ito, T., Kitamura, H., and Nishino, T. (1998). Tissue and subcellular distribution of mercaptopyruvate sulfurtransferase in the rat: confocal laser fluorescence and immunoelectron microscopic studies combined with biochemical analysis. *Histochem. Cell Biol.* 110, 243–250. doi: 10.1007/s004180050286

Nespolo, R. F., Fontúrbel, F. E., Mejias, C., Contreras, R., Gutierrez, P., Oda, E., et al. (2020). A mesocosm experiment in ecological physiology: adaptive modulation of energy budget in a hibernating marsupial under chronic caloric restriction. *bioRxiv* [Preprint]. doi: 10.1101/2020.06.05.136028

Nespolo, R. F., Gaitan-Espitia, J. D., Quintero-Galvis, J. F., Fernandez, F. V., Silva, A. X., Molina, C., et al. (2018). A functional transcriptomic analysis in the relict marsupial *Dromiciops gliroides* reveals adaptive regulation of protective functions during hibernation. *Mol. Ecol.* 27, 4489–4500. doi: 10.1111/mec.14876

Nespolo, R. F., Verdugo, C., Cortes, P. A., and Bacigalupe, L. D. (2010). Bioenergetics of torpor in the Microbiotherid marsupial, Monito del Monte (*Dromiciops gliroides*): the role of temperature and food availability. *J. Comp. Physiol. B* 180, 767–773. doi: 10.1007/s00360-010-0449-y

Ni, Z. L., and Storey, K. B. (2010). Heme oxygenase expression and Nrf2 signaling during hibernation in ground squirrels. *Can. J. Physiol. Pharmacol.* 88, 379–387. doi: 10.1139/Y10-017

Nizielski, S. E., Billington, C. J., and Levine, A. S. (1989). Brown fat GDP binding and circulating metabolites during hibernation and arousal. *Am. J. Physiol. Reg. Int. Comp. Physiol.* 257, R536–R541. doi: 10.1152/ajpregu.1989.257.3.R536

Noiret, A., Puch, L., Riffaud, C., Costantini, D., Riou, J. F., Aujard, F., et al. (2020). Sex-specific response to caloric restriction after reproductive investment in *Microcebus murinus*: an integrative approach. *Front. Physiol.* 11:506. doi: 10.3389/fphys.2020.00506

Nowack, J., Giroud, S., Arnold, W., and Ruf, T. (2017). Muscle non-shivering thermogenesis and its role in the evolution of endothermy. *Front. Physiol.* 8:889. doi: 10.3389/fphys.2017.00889

Nowack, J., Levesque, D. L., Reher, S., and Dausmann, K. H. (2020). Variable climates lead to varying phenotypes: "Weird" mammalian torpor and lessons from non-holarctic species. *Front. Ecol. Evol.* 8:60. doi: 10.3389/fevo.2020.00060

Nowack, J., Tarmann, I., Hoelzl, F., Smith, S., Giroud, S., and Ruf, T. (2019). Always a price to pay: hibernation at low temperatures comes with a trade-off between energy savings and telomere damage. *Biol. Lett.* 15:20190466. doi: 10.1098/rsbl.2019.0466

Ormseth, O. A., Nicolson, M., Pelleymounter, M. A., and Boyer, B. B. (1996). Leptin inhibits prehibernation hyperphagia and reduces body weight in arctic ground squirrels. *Am. J. Physiol. Reg. Int. Comp. Physiol.* 271, R1775–R1779. doi: 10.1152/ajpregu.1996.271.6.R1775

Orr, A. L., Lohse, L. A., Drew, K. L., and Hermes-Lima, M. (2009). Physiological oxidative stress after arousal from hibernation in Arctic ground squirrel. *Comp. Biochem. Physiol. A Mol. Integr. Physiol.* 153, 213–221. doi: 10.1016/j.cbpa.2009.02.016

Ou, J., Ball, J. M., Luan, Y., Zhao, T., Miyagishima, K. J., Xu, Y., et al. (2018). iPSCs from a hibernator provide a platform for studying cold adaptation and its potential medical applications. *Cell* 173, 851.e16–863.e16. doi: 10.1016/j.cell.2018.03.010

Papu John, A. S., Kundu, S., Pushpakumar, S., Amin, M., Tyagi, S. C., and Sen, U. (2019). Hydrogen sulfide inhibits Ca2+-induced mitochondrial permeability transition pore opening in type-1 diabetes. *Am. J. Physiol. Endocrinol. Metab.* 317, E269–E283. doi: 10.1152/ajpendo.00251.2018

Patterson, R. E., and Sears, D. D. (2017). Metabolic effects of intermittent fasting. *Annu. Rev. Nutr.* 37, 371–393. doi: 10.1146/annurev-nutr-071816-064634

Perret, M. (1997). Change in photoperiodic cycle affects life spanin a prosimian primate (*Microcebus murinus*). *J. Biol. Rhythms* 12, 136–145. doi: 10.1177/074873049701200205

Perret, M., and Aujard, F. (2001). Regulation by photoperiod of seasonal changes inBody mass and reproductive function in GrayMouse Lemurs (*Microcebus murinus*): differential responses by sex. *Int. J. Primatol.* 22, 5–24. doi: 10.1023/A:1026457813626

Popov, V. I., Bocharova, L. S., and Bragin, A. G. (1992). Repeated changes of dendritic morphology in the hippocampus of ground squirrels in the course of hibernation. *Neuroscience* 48, 45–51. doi: 10.1016/0306-4522(92)90336-Z

Popova, N. K., and Koryakina, L. A. (1981). Seasonal changes in pituitary-adrenal reactivity in hibernating spermophiles. *Endocrinol. Exp.* 15, 269–276.

Prendergast, B. J., Freeman, D. A., Zucker, I., and Nelson, R. J. (2002). Periodic arousal from hibernation is necessary for initiation of immune responses in ground squirrels. *Am. J. Physiol. Reg. Int. Comp. Physiol.* 282, R1054–R1082. doi: 10.1152/ajpregu.00562.2001

Rauch, J. C., and Behrisch, H. W. (1981). Ketone bodies: a source of energy during hibernation. *Can. J. Zool.* 59, 754–760. doi: 10.1139/z81-108

Revsbech, I. G., Shen, X., Chakravarti, R., Jensen, F. B., Thiel, B., Evans, A. L., et al. (2014). Hydrogen sulfide and nitric oxide metabolites in the blood of free-ranging brown bears and their potential roles in hibernation. *Free Rad. Biol. Med.* 73, 349–357. doi: 10.1016/j.freeradbiomed.2014.05.025

Romagnani, P., Remuzzi, G., Glassock, R., Levin, A., Jager, K. J., Tonelli, M., et al. (2017). Chronic kidney disease. *Nat. Rev. Dis. Primers* 3:17088. doi: 10.1038/nrdp.2017.88

Roshan, R., Shridhar, S., Sarangdhar, M. A., Banik, A., Chawla, M., Garg, M., et al. (2014). Brain-specific knockdown of miR-29 results in neuronal cell death and ataxia in mice. *RNA* 20, 1287–1297. doi: 10.1261/rna.044008.113

Rouble, A. N., Hefler, J., Mamady, H., Storey, K. B., and Tessier, S. N. (2013). Anti-apoptotic signaling as a cytoprotective mechanism in mammalian hibernation. *PeerJ* 1:e29. doi: 10.7717/peerj.29

Ruf, T., and Arnold, W. (2008). Effects of polyunsaturated fatty acids on hibernation and torpor: a review and hypothesis. *Am. J. Physiol. Reg. Int. Comp. Physiol.* 294, R1044–R1052. doi: 10.1152/ajpregu.00688.2007

Ruf, T., Bieber, C., and Turbill, C. (2012). "Survival, aging, and life-history tactics in mammalian hibernators," in *Living in a Seasonal World. Thermoregulatory and Metabolic Adaptations*, eds T. Ruf, C. Bieber, W. Arnold, and E. Millesi (Heidelberg: Springer Verlag), 123–132. doi: 10.1007/978-3-642-28678-0_11

Ruf, T., and Geiser, F. (2015). Daily torpor and hibernation in birds and mammals. *Biol. Rev.* 90, 891–926. doi: 10.1111/brv.12137

Sarnak, M. J., Amann, K., Bangalore, S., Cavalcante, J. L., Charytan, D. M., Craig, J. C., et al. (2019). Chronic kidney disease and coronary artery disease: JACC State-of-the-art review. *J. Am. Coll. Cardiol.* 74, 1823–1838. doi: 10.1016/j.jacc.2019.08.1017

Schmid, J. (1999). Sex-specific differences in activity patterns and fattening in the gray mouse lemur (*Microcebus murinus*) in Madagascar. *J. Mammal.* 80, 749–757. doi: 10.2307/1383244

Schmid, J., and Ganzhorn, J. U. (2009). Optional strategies for reduced metabolism in gray mouse lemurs. *Naturwissenschaften* 96, 737–741. doi: 10.1007/s00114-009-0523-z

Schmid, J., and Kappeler, P. M. (1998). Fluctuating sexual dimorphism and differential hibernation by sex in a primate, the gray mouse lemur (*Microcebus murinus*). *Behav. Ecol. Sociobiol.* 43, 125–132. doi: 10.1007/s002650050474

Schwartz, C., Hampton, M., and Andrews, M. T. (2013). Seasonal and regional differences in gene expression in the brain of a hibernating mammal. *PLoS One* 8:e58427. doi: 10.1371/journal.pone.0058427

Shaposhnikov, M., Proshkina, E., Koval, L., Zemskaya, N., Zhavoronkov, A., and Moskalev, A. (2018). Overexpression of *CBS* and *CSE* genes affects lifespan,

stress resistance and locomotor activity in *Drosophila melanogaster*. *Aging* 10, 3260–3272. doi: 10.18632/aging.101630

Shibuya, N., Mikami, Y., Kimura, Y., Nagahara, N., and Kimura, H. (2009). Vascular endothelium expresses 3-mercaptopyruvate sulfurtransferase and produces hydrogen sulfide. *J. Biochem.* 146, 623–626. doi: 10.1093/jb/mvp111

Shivatcheva, T. M., Ankov, V. K., and Hadjioloff, A. I. (1988). Circannual fluctuations of the serum cortisol in the European ground squirrel, *Citellus citellus* L. *Comp. Biochem. Physiol. A* 90, 515–518. doi: 10.1016/0300-9629(88)90229-0

Siutz, C., Franceschini, C., and Millesi, E. (2016). Sex and age differences in hibernation patterns of common hamsters: adult females hibernate for shorter periods than males. *J. Comp. Physiol. B* 186, 801–811. doi: 10.1007/s00360-016-0995-z

Snapp, B. D., and Heller, H. C. (1981). Suppression of metabolism during hibernation in ground squirrels (*Citellus lateralis*). *Physiol. Zool.* 54, 297–307. doi: 10.1086/physzool.54.3.30159944

Song, X., and Geiser, F. (1997). Daily torpor and energy expenditure in *sminthopsis macroura*: interactions between food and water availability and temperature. *Physiol. Zool.* 70, 331–337. doi: 10.1086/639610

Spindel, O. N., World, C., and Berk, B. C. (2012). Thioredoxin interacting protein: redox dependent and independent regulatory mechanisms. *Antioxid. Redox. Signal.* 16, 587–596. doi: 10.1089/ars.2011.4137

Staples, J. F. (2011). "Metabolic flexibility: hibernation, torpor, and estivation," in *Comprehensive Physiology*, ed. D. M. Pollock (Hoboken, NJ: John Wiley & Sons, Inc), 737–771. doi: 10.1002/cphy.c140064

Storey, K. B. (2015). The gray mouse lemur: a model for studies of primate metabolic rate depression. *Genomics Proteomics Bioinformatics* 13, 77–80. doi: 10.1016/j.gpb.2015.06.001

Storey, K. B., and Storey, J. M. (2004). Metabolic rate depression in animals: transcriptional and translational controls. *Biol. Rev.* 79, 207–233. doi: 10.1017/S1464793103006195

Storey, K. B., and Storey, J. M. (2007). Tribute to P. L. Lutz: putting life on 'pause' - molecular regulation of hypometabolism. *J. Exp. Biol.* 210, 1700–1714. doi: 10.1242/jeb.02716

Stumpfel, S., Bieber, C., Blanc, S., Ruf, T., and Giroud, S. (2017). Differences in growth rates and pre-hibernation body mass gain between early and late-born juvenile garden dormice. *J. Comp. Physiol. B* 187, 253–263. doi: 10.1007/s00360-016-1017-x

Szabo, C. (2018). A timeline of hydrogen sulfide (H2S) research: from environmental toxin to biological mediator. *Biochem. Pharmacol.* 149, 5–19. doi: 10.1016/j.bcp.2017.09.010

Takahashi, T. M., Sunagawa, G. A., Soya, S., Abe, M., Sakurai, K., Ishikawa, K., et al. (2020). A discrete neuronal circuit induces a hibernation-lile state in rodents. *Nature* 583, 109–114. doi: 10.1038/s41586-020-2163-6

Talaei, F., Bouma, H. R., Hylkema, M. N., Strijkstra, A. M., Boerema, A. S., Schmidt, M., et al. (2012). The role of endogenous H2S formation in reversible remodeling of lung tissue during hibernation in the Syrian hamster. *J. Exp. Biol.* 215, 2912–2919. doi: 10.1242/jeb.067363

Talaei, F., Bouma, H. R., Van der Graaf, A. C., Strijkstra, A. M., Schmidt, M., and Henning, R. H. (2011a). Serotonin and dopamine protect from Hypothermia/Rewarming damage through the CBS/ H2S Pathway. *PLoS One* 6:e22568. doi: 10.1371/journal.pone.0022568

Talaei, F., Hylkema, M. N., Bouma, H. R., Boerema, A. S., Strijkstra, A. M., Henning, R. H., et al. (2011b). Reversible remodeling of lung tissue during hibernation in the Syrian hamster. *J. Exp. Biol.* 214(Pt 8), 1276–1282. doi: 10.1242/jeb.052704

Tashima, L. S., Adelstein, S. J., and Lyman, C. P. (1970). Radioglucose utilization by active, hibernating, and arousing ground squirrels. *Am. J. Physiol. Legacy Content* 218, 303–309. doi: 10.1152/ajplegacy.1970.218.1.303

Teng, H., Wu, B., Zhao, K., Yang, G., Wu, L., and Wang, R. (2013). Oxygen-sensitive mitochondrial accumulation of cystathionine β-synthase mediated by Lon protease. *Proc. Natl. Acad. Sci. U.S.A.* 110, 12679–12684. doi: 10.1073/pnas.1308487110

Terrien, J., Ambid, L., Nibbelink, M., Saint-Charles, A., and Aujard, F. (2010a). Non-shivering thermogenesis activation and maintenance in the aging gray mouse lemur (*Microcebus murinus*). *Exp. Gerontol.* 45, 442–448. doi: 10.1016/j.exger.2010.03.013

Terrien, J., Perret, M., and Aujard, F. (2010b). Gender markedly modulates behavioral thermoregulation in a non-human primate species, the mouse lemur (*Microcebus murinus*). *Physiol. Behav.* 101, 469–473. doi: 10.1016/j.physbeh.2010.07.012

Terrien, J., Gaudubois, M., Champeval, D., Zaninotto, V., Roger, L., Riou, J. F., et al. (2017). Metabolic and genomic adaptations to winter fattening in a primate species, the grey mouse lemur (*Microcebus murinus*). *Int. J. Obes.* 42, 211–230. doi: 10.1038/ijo.2017.195

Terrien, J., Perret, M., and Aujard, F. (2011). Behavioral thermoregulation in mammals: a review. *Front. Biosci.* 16:1428–1444. doi: 10.2741/3797

Terrien, J., Zahariev, A., Blanc, S., and Aujard, F. (2009). Impaired control of body cooling during heterothermia represents the major energetic constraint in an aging non-human primate exposed to cold. *PLoS One* 4:e7587. doi: 10.1371/journal.pone.0007587

Terrien, J., Zizzari, P., Bluet-Pajot, M. T., Henry, P. Y., Perret, M., Epelbaum, J., et al. (2008). Effects of age on thermoregulatory responses during cold exposure in a nonhuman primate. *Microcebus murinus*. *Am. J. Physiol. Reg. Int. Comp. Physiol.* 295, R696–R703. doi: 10.1152/ajpregu.00629.2007

Tessier, S. N., Katzenback, B. A., Pifferi, F., Perret, M., and Storey, K. B. (2015a). Cytokine and antioxidant regulation in the intestine of the gray mouse lemur (*Microcebus murinus*) during torpor. *Genomics Proteomics Bioinformatics* 13, 127–135. doi: 10.1016/j.gpb.2015.03.005

Tessier, S. N., Zhang, J., Biggar, K. K., Wu, C. W., Pifferi, F., Perret, M., et al. (2015b). Regulation of the PI3K/AKT pathway and fuel utilization during primate torpor in the grey mouse lemur. *Microcebus murinus*. *Genomics Proteomics Bioinformatics* 13, 91–102. doi: 10.1016/j.gpb.2015.03.006

Tessier, S. N., Wu, C.-W., and Storey, K. B. (2019). Molecular control of protein synthesis, glucose metabolism, and apoptosis in the brain of hibernating thirteen-lined ground squirrels. *Biochem. Cell Biol.* 97, 536–544. doi: 10.1139/bcb-2018-0256

Turbill, C., Bieber, C., and Ruf, T. (2011). Hibernation is associated with increased survival and the evolution of slow life histories among mammals. *Proc. R. Soc. B* 278, 3355–3363. doi: 10.1098/rspb.2011.0190

Turbill, C., Ruf, T., Smith, S., and Bieber, C. (2013). Seasonal variation in telomere length of a hibernating rodent. *Biol. Lett.* 9:20121095. doi: 10.1098/rsbl.2012.1095

Twente, J. W., and Twente, J. A. (1967). Concentrations of *d*-glucose in the blood of *Citellus lateralis* after known intervals of hbernating priods. *J. Mammal.* 48, 381–386. doi: 10.2307/1377770

Valladares-Gómez, A., Celis-Diez, J. L., Sepúlveda-Rodríguez, C., Inostroza-Michael, O., Hernández, C. E., and Palma, R. E. (2019). genetic diversity, population structure, and migration scenarios of the marsupial "Monito del Monte" in south-central chile. *J. Hered.* 110, 651–661. doi: 10.1093/jhered/esz049

Van Breukelen, F., and Martin, S. L. (2002). Invited review: molecular adaptations in mammalian hibernators: unique adaptations or generalized responses? *J. Appl. Physiol* 92, 2640–2647. doi: 10.1152/japplphysiol.01007.2001

van Breukelen, F., and Martin, S. L. (2015). The hibernation continuum: physiological and molecular aspects of metabolic plasticity in mammals. *Physiology* 30, 273–281. doi: 10.1152/physiol.00010.2015

Vander Wall, S. B. (1990). *Food Hoarding in Animals*. Chicago, IL: The University of Chicago Press.

Vermillion, K. L., Jagtap, P., Johnson, J. E., Griffin, T. J., and Andrews, M. T. (2015). Characterizing cardiac molecular mechanisms of mammalian hibernation via quantitative proteogenomics. *J. Proteome Res.* 14, 4792–4804. doi: 10.1021/acs.jproteome.5b00575

Villain, N., Picq, J. L., Aujard, F., and Pifferi, F. (2016). Body mass loss correlates with cognitive performance in primates under acute caloric restriction conditions. *Behav. Brain Res.* 305, 157–163. doi: 10.1016/j.bbr.2016.02.037

Vuarin, P., Dammhahn, M., Kappeler, P. M., and Henry, P. Y. (2015). When to initiate torpor use? Food availability times the transition to winter phenotype in a tropical heterotherm. *Oecologia* 179, 43–53. doi: 10.1007/s00442-015-3328-0

Wang, L. C. H. (1978). "Energetic and field aspects of mammalian torpor: the Richardson's ground squirrel," in *Strategies in Cold: Natural Torpidity and Thermogenesis*, eds L. C. H. Wang and J. W. Hudson (New York, NY: Academic Press), 109–145. doi: 10.1016/b978-0-12-734550-5.50009-0

Wassmer, T. (2004). Body temperature and above-ground patterns during hibernation in European hamsters (*Cricetus cricetus* L.). *J. Zool.* 262, 281–288. doi: 10.1017/S0952836903004643

Waßmer, T., and Wollnik, F. (1997). Timing of torpor bouts during hibernation in European hamsters (*Cricetus cricetus* L.). *J. Comp. Physiol. B* 167, 270–279. doi: 10.1007/s003600050074

Wei, Y., Gong, L., Fu, W., Xu, S., Wang, Z., Zhang, J., et al. (2018a). Unexpected regulation pattern of the IKKβ/NF-κB/MuRF1 pathway with remarkable muscle plasticity in the Daurian ground squirrel (*Spermophilus dauricus*). *J. Cell. Physiol.* 233, 8711–8722. doi: 10.1002/jcp.26751

Wei, Y., Zhang, J., Xu, S., Peng, X., Yan, X., Li, X., et al. (2018b). Controllable oxidative stress and tissue specificity in major tissues during the torpor–arousal cycle in hibernating Daurian ground squirrels. *Open Biol.* 8:180068. doi: 10.1098/rsob.180068

Weitten, M., Oudart, H., and Habold, C. (2016). Maintenance of a fully functional digestive system during hibernation in the European hamster, a food-storing hibernator. *Comp. Biochem. Physiol. A* 193, 45–51. doi: 10.1016/j.cbpa.2016.01.006

Weitten, M., Robin, J. P., Oudart, H., Pevet, P., and Habold, C. (2013). Hormonal changes and energy substrate availability during the hibernation cycle of Syrian hamsters. *Horm. Behav.* 64, 611–617. doi: 10.1016/j.yhbeh.2013.08.015

Wolf, B. O., McKechnie, A. E., Schmitt, C. J., Czenze, Z. J., Johnson, A. B., and Witt, C. C. (2020). Extreme and variable torpor among high-elevation Andean hummingbird species. *Biol. Lett.* 16:20200428. doi: 10.1098/rsbl.2020.0428

Wolf, M., van Doorn, G. S., Leimar, O., and Weissing, F. J. (2007). Life-history trade-offs favour the evolution of animal personalities. *Nature* 447, 581–584. doi: 10.1038/nature05835

Wollnik, F., and Schmidt, B. (1995). Seasonal and daily rhythms of body temperature in the European hamster (*Cricetus cricetus*) under semi-natural conditions. *J. Comp. Physiol. B* 165, 171–182. doi: 10.1007/BF00260808

Wu, C. W., Biggar, K. K., and Storey, K. B. (2014). Expression profiling and structural characterization of MicroRNAs in adipose tissues of hibernating ground squirrels. *Genomics Proteomics Bioinformatics* 12, 284–291. doi: 10.1016/j.gpb.2014.08.003

Wu, C.-W., and Storey, K. B. (2014). FoxO3a-mediated activation of stress responsive genes during early torpor in a mammalian hibernator. *Mol. Cell. Biochem.* 390, 185–195. doi: 10.1007/s11010-014-1969-7

Yang, G., Wu, L., Jiang, B., Yang, W., Qi, J., Cao, K., et al. (2008). H2S as a physiologic vasorelaxant: hypertension in mice with deletion of cystathionine gamma-lyase. *Science* 322, 587–590. doi: 10.1126/science.1162667

Yang, G., Zhao, K., Ju, Y., Mani, S., Cao, Q., Puukila, S., et al. (2012). Hydrogen sulfide protects against cellular senescence *via* S-Sulfhydration of Keap1 and Activation of Nrf2. *Antioxid. Redox. Signal.* 18, 1906–1919. doi: 10.1089/ars.2012.4645

Yao, L.-L., Huang, X.-W., Wang, Y.-G., Cao, Y.-X., Zhang, C.-C., and Zhu, Y.-C. (2010). Hydrogen sulfide protects cardiomyocytes from hypoxia/reoxygenation-induced apoptosis by preventing GSK-3β-dependent opening of mPTP. *Am. J. Physiol. Heart Circ. Physiol.* 298, H1310–H1319. doi: 10.1152/ajpheart.00339.2009

Yin, Q., Ge, H., Liao, C.-C., Liu, D., Zhang, S., and Pan, Y.-H. (2016). Antioxidant defenses in the brains of bats during hibernation. *PLoS One* 11:e0152135. doi: 10.1371/journal.pone.0152135

Yoshioka, J., and Lee, R. T. (2014). Thioredoxin-interacting protein and myocardial mitochondrial function in ischemia-reperfusion injury. *Trends Cardiovasc. Med.* 24, 75–80. doi: 10.1016/j.tcm.2013.06.007

Zhang, J., Tessier, S. N., Biggar, K. K., Wu, C. W., Pifferi, F., Perret, M., et al. (2015). Regulation of torpor in the gray mouse lemur: transcriptional and translational controls and role of AMPK signaling. *Genomics Proteomics Bioinformatics* 13, 103–110. doi: 10.1016/j.gpb.2015.03.003

Zhang, K. X., D'Souza, S., Upton, B. A., Kernodle, S., Vemaraju, S., Nayak, G., et al. (2020). Violet-light suppression o thermogenesis by opsin 5 hypothalamic neurons. *Nature* 585, 420–425. doi: 10.1038/s41586-020-2683-0

Zhao, K., Ju, Y., Li, S., Altaany, Z., Wang, R., and Yang, G. (2014). S-sulfhydration of MEK1 leads to PARP-1 activation and DNA damage repair. *EMBO Rep.* 15, 792–800. doi: 10.1002/embr.201338213

Zhao, W., Zhang, J., Lu, Y., and Wang, R. (2001). The vasorelaxant effect of H2S as a novel endogenous gaseous KATP channel opener. *EMBO J.* 20, 6008–6016. doi: 10.1093/emboj/20.21.6008

Zhou, J., and Zhang, J. (2014). Identification of miRNA-21 and miRNA-24 in plasma as potential early stage markers of acute cerebral infarction. *Mol. Med. Rep.* 10, 971–976. doi: 10.3892/mmr.2014.2245

Zuhra, K., Augsburger, F., Majtan, T., and Szabo, C. (2020). Cystathionine-β-synthase: molecular regulation and pharmacological inhibition. *Biomolecules* 10:697. doi: 10.3390/biom10050697

Conflict of Interest: The authors declare that the research was conducted in the absence of any commercial or financial relationships that could be construed as a potential conflict of interest.

frontiers in Physiology

REVIEW
published: 18 February 2021
doi: 10.3389/fphys.2021.634953

Body Protein Sparing in Hibernators: A Source for Biomedical Innovation

Fabrice Bertile[1]*, *Caroline Habold*[2], *Yvon Le Maho*[2,3†] and *Sylvain Giroud*[4*†]

[1] University of Strasbourg, CNRS, IPHC UMR 7178, Laboratoire de Spectrométrie de Masse Bio-Organique, Strasbourg, France, [2] University of Strasbourg, CNRS, IPHC UMR 7178, Ecology, Physiology & Ethology Department, Strasbourg, France, [3] Centre Scientifique de Monaco, Monaco, Monaco, [4] Research Institute of Wildlife Ecology, Department of Interdisciplinary Life Sciences, University of Veterinary Medicine Vienna, Vienna, Austria

Proteins are not only the major structural components of living cells but also ensure essential physiological functions within the organism. Any change in protein abundance and/or structure is at risk for the proper body functioning and/or survival of organisms. Death following starvation is attributed to a loss of about half of total body proteins, and body protein loss induced by muscle disuse is responsible for major metabolic disorders in immobilized patients, and sedentary or elderly people. Basic knowledge of the molecular and cellular mechanisms that control proteostasis is continuously growing. Yet, finding and developing efficient treatments to limit body/muscle protein loss in humans remain a medical challenge, physical exercise and nutritional programs managing to only partially compensate for it. This is notably a major challenge for the treatment of obesity, where therapies should promote fat loss while preserving body proteins. In this context, hibernating species preserve their lean body mass, including muscles, despite total physical inactivity and low energy consumption during torpor, a state of drastic reduction in metabolic rate associated with a more or less pronounced hypothermia. The present review introduces metabolic, physiological, and behavioral adaptations, e.g., energetics, body temperature, and nutrition, of the torpor or hibernation phenotype from small to large mammals. Hibernating strategies could be linked to allometry aspects, the need for periodic rewarming from torpor, and/or the ability of animals to fast for more or less time, thus determining the capacity of individuals to save proteins. Both fat- and food-storing hibernators rely mostly on their body fat reserves during the torpid state, while minimizing body protein utilization. A number of them may also replenish lost proteins during arousals by consuming food. The review takes stock of the physiological, molecular, and cellular mechanisms that promote body protein and muscle sparing during the inactive state of hibernation. Finally, the review outlines how the detailed understanding of these mechanisms at play in various hibernators is expected to provide innovative solutions to fight human muscle atrophy, to better help the management of obese patients, or to improve the *ex vivo* preservation of organs.

Keywords: hibernation, fasting, lean mass, metabolic depression, muscles, obesity, biomimicry

OPEN ACCESS

Edited by:
Jean-Pierre Montani,
Université de Fribourg, Switzerland

Reviewed by:
Toshio Tsubota,
Hokkaido University, Japan
Vadim Fedorov,
University of Alaska Fairbanks,
United States

***Correspondence:**
Fabrice Bertile
fbertile@unistra.fr
Sylvain Giroud
Sylvain.Giroud@vetmeduni.ac.at

†These authors have contributed equally to this work

Specialty section:
This article was submitted to Integrative Physiology, a section of the journal Frontiers in Physiology

Received: *30 November 2020*
Accepted: *12 January 2021*
Published: *18 February 2021*

Citation:
Bertile F, Habold C, Le Maho Y and Giroud S (2021) Body Protein Sparing in Hibernators: A Source for Biomedical Innovation. Front. Physiol. 12:634953. doi: 10.3389/fphys.2021.634953

INTRODUCTION

The maintenance of a stable body composition is essential to ensure overall health and performance. Each organism can roughly be separated into a fat and a lean compartment, healthy proportions in humans ranging from 12 to 30% of fat and 70 to 88% of fat-free mass (Abernathy and Black, 1996). The lean compartment is composed of mainly water (73%) and proteins (20%) (Wagner and Heyward, 2000), and excessive loss of lean body or protein mass has been associated with a myriad of adverse effects (Willoughby et al., 2018). It is estimated that the loss of 30–50% of total body proteins is directly responsible for death (Silber, 1984).

Although ubiquitous in the body, proteins are predominantly found in muscles, which in humans represent ∼40% of total body weight (Janssen et al., 2000). Besides their obvious importance for posture maintenance, locomotion, and any movement from the cellular scale to the whole body, muscles are nowadays regarded as important modulators of the whole-body energy metabolism and interorgan cross-talks (Argiles et al., 2016). Muscles ensure organs to be continuously supplied with oxygen and nutrients while waste products are excreted not only by supporting the respiratory and circulatory systems but also through their endocrine/paracrine functions (Karstoft and Pedersen, 2016; Giudice and Taylor, 2017; Graf and Ferrari, 2019). Muscles are important consumers of lipids and carbohydrates and store glycogen to be mobilized in case of reduced glucose availability in food supply (Frontera and Ochala, 2015; Argiles et al., 2016). Further, the high protein content of muscles makes up a large reservoir of amino acids for protein synthesis within the body (Wolfe, 2006; Argiles et al., 2016) and for hepatic gluconeogenesis during starvation (Ruderman, 1975; Argiles et al., 2016). Finally, muscle shivering or non-shivering thermogenesis has also been involved in tuning body temperature (T_b) and energy expenditure, with an ultimate control on body weight (Periasamy et al., 2017; Fuller-Jackson and Henry, 2018). Given such essential roles, it is not surprising that metabolic health relies on the maintenance of muscle structure and function (Hunt, 2003; Wolfe, 2006; McLeod et al., 2016; Deutz et al., 2019).

Muscle atrophy, or muscle wasting, can be defined as a loss of muscle mass, strength, and mobility. Causes of muscle atrophy in humans are multiple and notably include aging (McCormick and Vasilaki, 2018), malnutrition (Roy et al., 2016), prolonged fasting (Ibrahim et al., 2020b), disuse observed in immobilized patients or due to sedentary lifestyles (Rudrappa et al., 2016), denervation (Carlson, 2014), microgravity environments (Gao et al., 2018), and a variety of diseases (Schardong et al., 2018; Sisto et al., 2018; Song et al., 2018; Yang et al., 2018; Zhang et al., 2018). Contrary to humans, hibernating animals usually lose no or very little muscle mass during winter in metabolic depression, despite several months of complete food deprivation and physical inactivity after a nearly doubling level of fat mass (see below). In this review, a brief description of the main features of torpor and hibernation is followed by a detailed compilation of the available data on the preservation of body and skeletal muscle proteins during hibernation. Then, it elaborates on the various mechanisms that may help sustain protein homeostasis, involving the mechanisms of metabolic rate depression, muscle shivering, urea and nitrogen recycling, the role played by a number of humoral factors, and the regulation of intracellular pathways. Finally, this review also presents how the outstanding performances of hibernators can very likely fuel innovative solutions for humans to fight muscle atrophy and promote therapies for preserving body proteins.

Abbreviations: AMPD1, AMP deaminase 1; BAT, brown adipose tissue; CO_2, carbon dioxide; DHA, docosahexaenoic acid; GH, growth hormone; H_2S, hydrogen sulfide; IGF1, insulin-like growth factor 1; LED, low energy diet; MR, metabolic rate; mTOR, mammalian target of rapamycin; mTORC1, mammalian target of rapamycin complex 1; *p*-Akt1, phosphorylated AKT1; *p*-FOXO1, phosphorylated FOXO1; *p*-mTOR, phosphorylated mTOR; RQ, respiratory quotient; SERCA, sarcoplasmic/endoplasmic reticulum Ca^{2+} ATPase; SGK1, serum/glucocorticoid-induced kinase; T_a, ambient temperature; T_b, body temperature; VLED, very low energy diet.

MAINTENANCE OF LEAN BODY MASS IN HIBERNATORS DURING WINTER

Torpor and Hibernation

Torpor is an energy-saving strategy used by small heterothermic mammals and birds, involving a controlled reduction of metabolic rate (MR) and T_b, which enables animals to survive periods of energetic bottleneck (Lyman et al., 1982). Heterothermic species can be differentiated in the so-called "daily heterotherms," i.e., species undergoing rather shallow (12–25°C) bouts of torpor of less than 24 h, and "hibernators" that undergo long and deep (<10°C) bouts of torpor lasting for days or weeks (Ruf and Geiser, 2015). Hibernation is documented in mammals from all three subclasses but is known for only one bird species (Ruf and Geiser, 2015). It is often associated with species inhabiting cold and seasonal habitats, such as temperate and arctic zones, but it is also used by many non-Holarctic species, i.e., in the tropics and southern hemisphere (Nowack et al., 2020). During hibernation, animals reach minimum torpid MR of ∼ 4% of basal MR, in association with a more or less pronounced reduction of their T_b ranging on average for most hibernators between 0°C and 10°C (Ruf and Geiser, 2015). However, the occurrence of subfreezing T_b has been documented in some hibernating species, e.g., in Arctic ground squirrels (*Urocitellus parryii*), which allow their peripheral T_b to drop to −2.9°C (Barnes, 1989).

In most species, hibernation is structured by successive torpor bouts and periodic interbout arousals with euthermia (Twente et al., 1977; French, 1982, 1985; Barnes et al., 1986; Carey et al., 2003b). In small mammals, MR increases drastically during arousals and T_b returns to normothermic levels of about 35–37°C for a few hours (Carey et al., 2003a; Heldmaier et al., 2004). These arousals represent the highest proportion of energy expended during the hibernation process, e.g., 70–80% in temperate species (Wang, 1978). In Arctic ground squirrels (*U. parryii*) hibernating at 2°C, arousal episodes can even account for up to 86% of the estimated energetic costs during the hibernation season (Karpovich et al., 2009). A few hibernating species do not fatten prior to winter and must therefore feed during these arousal phases (Humphries et al., 2003b). However,

for the others, i.e., the majority of hibernating species, that fast throughout hibernation, the exact purposes of these periodic arousals remain a mystery. Many hypotheses have been put forward, some of which have fairly convincing experimental data: a restoration of metabolic homeostasis (Osborne and Hashimoto, 2003; Epperson et al., 2011), a prevention of excessive accumulation of oxidative damage during torpor and arousal bouts (Buzadzic et al., 1990), the elimination of metabolic waste by renal function (e.g., Clausen and Storesund, 1971), the replenishment of carbohydrate supplies (Wang, 1989), the restoration of functional protein pools (Carey et al., 2003a), the reactivation of immune function (Prendergast et al., 2002), a pH regulation linked to the accumulation of carbon dioxide (CO_2) (Malan et al., 1988), or to allow animals to sleep (Daan et al., 1991). However, for the latter hypothesis, accumulation of sleep need during torpor bouts has been challenged by several studies. It was notably shown that sleep deprivation during the first few hours of euthermia following arousal in ground squirrels resulted in the disappearance of the classically observed peak level of slow-wave activity at this stage, without any compensatory rebound when sleep deprivation was terminated (Larkin and Heller, 1996, 1999; Strijkstra and Daan, 1998). Hence, the early peak of slow-wave activity during arousals does not appear as a homeostatic response to an accumulated sleep debt. Similarly, the reactivation of the immune function may not be a purpose of torpor arousals, but secondary to rewarming. During the rewarming process of arousals, non-shivering thermogenesis from brown adipose tissue (BAT) is crucial until T_b reaches 15°C. Then, the rewarming continues *via* muscle shivering thermogenesis until the muscles are warm enough (Hashimoto et al., 2002). In the case of some tropical and subtropical species, rewarming is generally diurnal and thus passive with rising ambient temperatures (T_a), then becoming active *via* the heat production from BAT (Geiser and Drury, 2003). Non-shivering thermogenesis can also occur within muscles *via* futile cycles of calcium (Rowland et al., 2015) and has been postulated as an alternative mechanism for heat production in all those heterotherms that completely lack BAT, e.g., heterothermic marsupials and birds (Nowack et al., 2017). Because skeletal muscle accounts for approximately 40% of the dry mass of the typical mammalian body, downregulating skeletal muscle non-shivering thermogenesis would allow for whole-body cooling and long-term maintenance of a depressed core T_b during the steady state of torpor. In their review dealing with thermoregulation in hibernating mammals, Oliver et al. (2019) notably highlighted the importance of skeletal muscle and sarcolipin, a peptide regulating sarcoplasmic/endoplasmic reticulum Ca^{2+} ATPase (SERCA) activity, as a major thermogenic target.

In few other heterotherms, hibernation constitutes a continuous torpid state, showing a lack of arousals in, e.g., hibernating *Ursus arctos* (Evans et al., 2016), *Tenrec ecaudatus* (Lovegrove et al., 2014), and free-ranging *Cheirogaleus medius* (Dausmann et al., 2005), the latter nevertheless possibly having multiday torpor bouts interrupted with metabolic heat production when hibernating in well-insulated tree holes (Dausmann et al., 2004). Historically, due to a definition based not only on metabolic depression but also on characteristics that are secondary to it (Watts et al., 1981), mammalian hibernation has been restrictively attributed to only those animal species of less than 5–10 kg for which not only MR is reduced by 90–95% during the hibernation period but also T_b is lowered below 10°C (Nedergaard and Cannon, 1990; Geiser, 2011). One of the main reasons resides in the allometric scaling of MR with body mass, which has been greatly discussed elsewhere (Geiser, 2004; Heldmaier et al., 2004; Staples, 2016). Briefly, larger animals have lower basal MR per unit of body mass than smaller ones. Animals' surface area-to-volume ratio may contribute to explain this difference, larger animals having less body surface—across which heat is exchanged with the environment—relative to their volume, representing the amount of tissue that produces heat *via* metabolism. As a result, larger animals, with low surface area-to-volume ratios, lose less heat than smaller animals in a cool environment, and less energy, i.e., a lower MR, is needed to maintain T_b. In addition, if an important cooling would occur in large animals, a huge amount of energy would be required thereafter for body rewarming, which could not be achievable in a hibernation context. Therefore, hibernation could be expected to be of lower advantage for larger animals in terms of energy savings. Today, we know that large animals, such as bears (family *Ursidae*), undergo hibernation as they exhibit features of metabolic depression very similar to those found in small hibernators (Staples, 2014). Similar values of minimal specific MR around 0.03 ml $O_2.g^{-1}.h^{-1}$ are in fact observed in all small and large hibernators during the hibernation period (Heldmaier et al., 2004), thus indicating that the allometric scaling of MR with body mass is disrupted during torpor. Similar values are also observed in the largest animals on Earth, elephants and blue whales (Singer, 2006). As suggested earlier, minimal specific MR reached during hibernation may therefore represent a lower limit to ensure that cell viability is maintained. With a specific MR similarly lowered in small and large hibernators, it has been calculated that the low surface area-to-volume ratio of large hibernators implies a limited drop in T_b, such as of a few degrees Celsius only for bears (Hochachka and Guppy, 1987). Accordingly, hibernating bears exhibit a 75–85% decline in MR but a T_b decreased by only few degrees Celsius compared to values during the summer-active season, hence remaining at around 32–33°C (Watts et al., 1981; Hissa et al., 1994; Toien et al., 2011; Evans et al., 2016). Thermoregulatory mechanisms could explain the maintenance of a relatively high T_b in bears. Indeed, previous studies have revealed that hibernating grizzly (*U. arctos horribilis*) and polar bears (*U. maritimus*) still express a circadian rhythm in locomotor activity (Jansen et al., 2016; Ware et al., 2020), whereas other reports showed that black bears (*U. americanus*) replace their circadian rhythm of activity and body temperature by multi-day cycle during hibernation (Toien et al., 2011). In addition to reflecting putative thermoregulatory mechanisms, multi-day cycles may suggest a unique capacity to slow down MRs and ultimately biological time (Malan et al., 2018). Not only changes in body surface temperature have suggested that black bears engage in bouts of muscle activity during hibernation (Harlow et al., 2004), but bursts of shivering have also directly been measured in another study (Toien et al., 2011). The muscles from captive grizzly bears have also been

reported to shudder during hibernation for periods lasting greater than 1 h (Lin et al., 2004). However, thermoregulation may not be of major importance to support hibernation at only mild hypothermia in bears. First, increased body insulation in hibernating bears due to important fur covering (Scholander et al., 1950b) and subcutaneous fat accumulation (Svihla and Bowman, 1954) is expected to drastically lower heat loss. Second, T_a in the dens of Colorado black bears (*Ursus americanus*) has been reported to be +10°C on average despite outside T_a fluctuating from −20°C to +5°C (Harlow et al., 2004), and similar values have been reported for black bears in Canada (Watts et al., 1981). Comparable climate conditions have been reported for Scandinavian brown bears (*U. arctos*) (Evans et al., 2016). Hence, since the manipulation of den temperature in black bears (*U. americanus*) has revealed a lower critical temperature close to 0°C (Toien et al., 2015) and since a similar value has been reported for polar bears (*Ursus maritimus*) (Scholander et al., 1950a), ursids are expected to hibernate under thermoneutral conditions. In addition, it is noteworthy that, although one study has reported the presence of BAT in bears in the early 1990s (Davis et al., 1990), no BAT has later been found in bears (Jones et al., 1999; Rigano et al., 2017). Whether beige adipocytes, which also possess thermogenic properties (Ikeda et al., 2018), are present in bears is still not known.

Energy Substrate Use During Hibernation

Most of the hibernators, i.e., fat-storing species, do not feed during hibernation and rely entirely on body fat reserves accumulated prior to hibernation (Dark, 2005). Some other hibernators, e.g., food-storing species, feed during interbout arousals and therefore hoard large amounts of food (mainly seeds) prior to winter in their burrow (French, 1988; Humphries et al., 2003b). Only a few species are food-storing hibernators, mainly hamsters and chipmunks; they undergo shorter torpor bouts than fat-storing species but have longer arousal phases during which individuals consume their food hoards (Wollnik and Schmidt, 1995; Humphries et al., 2001). Thus, fat- and food-storing species show different metabolic and digestive adaptations throughout their annual life cycle (Humphries et al., 2001, 2003a; Weitten et al., 2013; Giroud et al., 2020).

In small hibernators, the measurement of respiratory quotient (RQ) values close to 0.7 during torpor shows that the coverage of energy expenditure is provided almost exclusively by the oxidation of lipids (Kayser, 1952; Buck and Barnes, 2000). Variations in T_a, in particular a decrease, can however trigger thermoregulatory responses (thermoregulation is not abolished during hibernation), and one can then observe higher RQ (Buck and Barnes, 2000), indicating an increase in the oxidation of carbohydrates and/or proteins. Plasma profiles during torpor are similar to those observed during fasting, with a decrease in blood glucose and triglyceride levels and an increase in blood free fatty acid and ketone body levels in most fat-storing hibernators [Belding's ground squirrels (Krilowicz, 1985), golden-mantled ground squirrels (Tashima et al., 1970; Lovegrove and McKechnie, 2008)], and food-storing species [golden hamster (Weitten et al., 2013)]. The use of proteomics has revealed changes in skeletal muscles of hibernating thirteen-lined ground squirrels, which were consistent with their reliance on lipids for energy during hibernation (Anderson et al., 2016). Measurements of the activity of key enzymes involved in metabolic pathways and of the level of gene expression during and outside the hibernation period in a number of studies have confirmed that the use of glucose is reduced in favor of that of lipids during hibernation (Dark, 2005), with the exception of glucose-dependent tissues like kidneys and brain (South and House, 1967; Rauch and Behrisch, 1981). At the beginning of the rewarming phase in small hibernators, the major substrate of BAT for non-shivering thermogenesis is still fatty acids. Then, the increase in T_b up to 12–16°C is accompanied by an increase in RQ to 1.0, indicating oxidation of carbohydrates, mainly by muscles for shivering thermogenesis (Mokrasch et al., 1960; Castex and Hoo-Paris, 1987; Heldmaier et al., 2004), and/or an evacuation of the CO_2 accumulated during torpor (Malan et al., 1988). A recent study has deepened the analysis in hibernating thirteen-lined ground squirrels (Regan et al., 2019). It has shown that a combination of lipids and carbohydrates is used during the initial ∼60 min of arousal before switching to predominantly lipid oxidation. To compensate for glucose utilization and to maintain glycemia during hibernation, glucose is provided by liver glycogenolysis and gluconeogenesis (Burlington and Klain, 1967; Green et al., 1984). The major gluconeogenic substrate is glycerol, whereas amino acid and lactate contribute only moderately to endogenous glucose production (Burlington and Klain, 1967; Galster and Morrison, 1975). In food-storing hibernating species, glucose is provided by food ingestion. Increased digestive efficiency and in particular upregulated intestinal glucose absorption rates during hibernation, e.g., in eastern chipmunks (Humphries et al., 2001) and common hamsters (Weitten et al., 2016), might rapidly restore blood glucose levels upon arousal phases (Serkova et al., 2007; Weitten et al., 2013).

Numerous reports have shown that black (*U. americanus*) and brown (*U. arctos*) bears remain not only physically inactive, but they also do not eat, drink, defecate, or urinate during the whole duration of the denning period (Craighead and Craighead, 1972; Nelson et al., 1975; Craighead et al., 1976; Folk et al., 1976, 1980; Hellgren et al., 1989; Hissa et al., 1994; Hellgren, 1998). Mobilization of body fuel reserves promotes survival during hibernation, essentially from body fat stored prior to denning (Nelson et al., 1975; Lundberg et al., 1976; Barboza et al., 1997). This is supported by the loss of 15–25% of bear body mass over the hibernating season (Hissa et al., 1994; Swenson et al., 2007), an RQ value close to 0.7 or slightly below (Nelson et al., 1973; Hellgren, 1998), and an increase in concentrations of circulating fatty acids (Nelson, 1973; LeBlanc et al., 2001; Chazarin et al., 2019a; Giroud et al., 2019). Plasma total ketone bodies have also been found higher in March than in June and November in Japanese black bears (Shimozuru et al., 2016), and we have observed a significant increase in 3-hydroxybutyrate in hibernating brown bears (Chazarin et al., 2019a), thus suggesting its use instead of glucose by, e.g., the brain. Liver gluconeogenesis has notably been proposed to be fueled from glycerol, which is released by white adipose cells due to lipolysis, but its plasma

concentration remains unchanged due to liver uptake (Chazarin et al., 2019a). Lactate has also been suggested as a precursor for the hepatic neo-synthesis of glucose (Shimozuru et al., 2016; Chazarin et al., 2019a).

Preservation of Body and Skeletal Muscle Proteins During Hibernation

Strikingly, black (*U. americanus*) and brown (*U. arctos*) bears exhibit no significant loss in their lean body mass during hibernation (Nelson et al., 1975; Lundberg et al., 1976; Barboza et al., 1997; Hilderbrand et al., 2000). Accordingly, whole-body protein turnover rates have been found at similar (Barboza et al., 1997) or higher (Lundberg et al., 1976) levels in bears during hibernation (winter) compared to the pre-denning period of hyperphagia (autumn), protein synthesis and breakdown being elevated in winter. Ketone body production and the preferential utilization of fatty acids and ketone bodies likely contribute to the sparing of amino acids and glucose during fasting (Owen et al., 1998). Body protein conservation is improved when lipid reserves are larger in fasting laboratory rodents (Goodman et al., 1984; Lowell and Goodman, 1987; Cherel et al., 1992), and the same mechanism may operate in hibernating bears as suggested by the fact that fatness of polar bears is inversely correlated to body protein breakdown (Atkinson et al., 1996). In this context, body protein sparing is also supported by the transcriptional downregulation of amino acid catabolism-related genes and upregulation of gluconeogenesis- and ketogenesis-related genes in the liver from hibernating Japanese black bears (*U. thibetanus japonicas*) (Shimozuru et al., 2012), American black bears (Fedorov et al., 2011), and grizzly bears (Jansen et al., 2019). Moreover, RQ values below 0.7 suggest that metabolic CO_2 serves for anabolic processes (Nelson et al., 1973; Hellgren, 1998).

Both skeletal muscle strength and mass appear to be retained in hibernating bears. Indeed, black bears (*U. americanus*) have been shown to lose no more than 29% of tibialis anterior strength over 2 months of hibernation (Harlow et al., 2001; Lohuis et al., 2007b), while skeletal muscle cell number or size (cross-sectional area) and contractile properties remained unchanged in various skeletal muscles during hibernation (Tinker et al., 1998; Harlow et al., 2001). Two different studies have observed an increase in the proportion of fast-twitch fibers (type II) for the biceps femoris muscle from hibernating black bears, which was accompanied by decreased activity of citrate synthase, whereas no change was observed for the gastrocnemius muscle (Tinker et al., 1998; Rourke et al., 2006). In brown bears (*U. arctos*), similar results were obtained in the biceps femoris for fiber cross-sectional area, the relative proportion of fast and slow fibers, and contractile properties, which remained essentially unchanged during hibernation compared to the summer-active season (Hershey et al., 2008). Giant sarcomeric proteins (titin, nebulin) have notably been shown to be roughly maintained at normal levels during hibernation in striated muscles of brown bears (*U. arctos*) and Himalayan black bears (*Ursus thibetanus ussuricus*) (Salmov et al., 2015). Recently, a 26% decrease in sartorius muscle fiber size following hibernation has nevertheless been reported in the Japanese black bear (*Ursus thibetanus japonicus*) (Miyazaki et al., 2015). Besides the various fast muscles mentioned above, maintenance of slow oxidative soleus muscle during hibernation has been documented recently in black bears (Riley et al., 2018). It was notably shown that soleus fiber type proportions, size, average fiber cross-sectional area-to-body mass ratio, and muscle-specific tension and normalized power were not altered by the hibernating state.

Changes in protein concentrations of bear hind limb muscles may differ according to the muscle considered; they either remain stable from the period prior to hibernation to spring arousal (Koebel et al., 1991; Harlow et al., 2001) or decrease by a maximum of generally 4–10%, notably in lactating females during denning (Tinker et al., 1998; Hershey et al., 2008). One study in black bears has reported a 15% loss in the protein content of the vastus lateralis muscle after 1 month of denning, this same value having been measured again 3.5 months later (Lohuis et al., 2007a). Moreover, muscle nitrogen content was unchanged in winter compared to summer, thus indicating moderate protein loss at the transitions between the summer-active and winter-resting periods but the striking maintenance of muscle integrity over long periods of hibernation. In fact, reduced protein turnover in skeletal muscles during hibernation (decreased levels of both protein synthesis and breakdown) supports muscle preservation.

Small hibernators also spare their body proteins during hibernation, as suggested by low uremia levels [e.g., of fat-storing species: golden-mantled ground squirrels (Wit and Twente, 1983); e.g., of food-storing species: Syrian hamsters (Weitten et al., 2013)] and limited muscle atrophy (e.g., Cotton and Harlow, 2010; Nowell et al., 2011; Hindle et al., 2015). In the common hamster, a food-storing hibernator, diet quality strongly influences body composition and particularly fat-free mass during hibernation (Weitten et al., 2018). Indeed, hamsters fed a high-protein diet spent more time in torpor during hibernation than hamsters fed a high-lipid diet, thus losing less body mass and particularly no fat-free mass. The extent of muscle atrophy during hibernation is relatively small compared to inactive non-hibernating rodents, e.g., the hind limb-suspended rat model (Musacchia et al., 1988). When it occurs, atrophy develops at the beginning of hibernation in fat-storing species, regardless of T_a (5 or 23°C), such as, e.g., in golden-mantled ground squirrels (Steffen et al., 1991; Wickler et al., 1991; Nowell et al., 2011), and it does not progress but on the contrary, it can even disappear before the end of hibernation (Hindle et al., 2015). It is characterized by a decrease in muscle mass, i.e., muscle proteins, due mainly to a decrease in cell size and not cell number, since muscle DNA content is not altered (Steffen et al., 1991) and apoptosis is decreased (Xu et al., 2013). Even when muscle atrophy is observed during torpor, oxidative capacity is increased (Wickler et al., 1987, 1991; Steffen et al., 1991) probably because slow oxidative fibers are preserved, whereas fast-glycolytic fibers are atrophied (Hindle et al., 2015). A shift in skeletal muscle composition from fast-glycolytic to slow-oxidative fibers has also been observed (Rourke et al., 2004; Nowell et al., 2011; Gao et al., 2012). This enables heat production during rewarming from torpor and locomotor activity during interbout arousal phases and favors emergence from hibernation (Nowell et al., 2011).

Contrasting with a decrease in mass of some skeletal muscles, cardiac muscle mass is increased during hibernation in golden-mantled ground squirrels (Wickler et al., 1991). In the liver also, proteolysis is reduced during hibernation (Velickovska et al., 2005).

Metabolic Rate Depression Contributes to Protein Sparing During Hibernation

The regulatory mechanisms involved in energy savings and metabolic flexibility characterized by dropped MR during hibernation likely contribute to cell and organ preservation (**Figure 1**). Physiologically, energy savings during hibernation involve specific changes, i.e., reduced allocation of energy to vital and energy-costly functions such as blood circulation, respiration, digestion, immunity, and kidney waste excretion.

In black and brown bears, a significant decline in the average heart rate from 50 to 80 beats per minute during the summer-active period to 10–30 beats per minute during winter months has been reported (Folk et al., 1980; Nelson et al., 2008; Nelson and Robbins, 2010, 2015; Laske et al., 2011; Toien et al., 2011; Evans et al., 2012; Jorgensen et al., 2014, 2020). Also in bears, the respiratory rate drops from 10 to 12 breaths per minute during summer to 5–7 breaths per minute in bears during the winter (Laske et al., 2011; Evans et al., 2012). Similarly in small mammals, extremely low heart rates of 3–10 beats per minute have been recorded during hibernation compared with 200–400 beats per minute when the animals are active (Lyman et al., 1982; Hampton et al., 2010). Breathing also drops from greater than 40 to less than one breath per minute in small hibernating mammals, and breathing patterns in many species can include long periods of apnea, ranging from minutes to hours. It has been claimed that there is no gut atrophy in denning bears but a decrease in gut motility and of metabolic activity of the gut flora that may be essential to the adaptation of the bear's physiology to hibernation (Jones and Zollman, 1997). A suppression of the innate immune system has been reported in small hibernating mammals (Bouma et al., 2010, 2011) and in hibernating brown bears (*U. arctos*) (Sahdo et al., 2013; Graesli et al., 2015). However, the immune competence may be maintained in black bears (*U. americanus*) (Chow et al., 2013). Such discrepancies between bear species highlight the need for further studies to definitely conclude. At the kidney level, bear glomerular filtration rate is decreased from 117 ml per minute in the summer-active state to 37 ml per minute during bear hibernation (Brown et al., 1971), thus resulting in the production of very low amounts of urine that are reabsorbed from the bladder urothelium (Nelson et al., 1973, 1975), and hibernating bears are therefore anuric. It is noteworthy to mention that paradoxical energy-demanding processes are activated in pregnant female bears during the denning period for gestation and cub lactation (Matson, 1954; Wimsatt, 1963; Tsubota et al., 1987; Sandell, 1990; Oftedal et al., 1993; Farley and Robbins, 1995; Spady et al., 2007; Friebe et al., 2013, 2014). Nevertheless, related energetics costs are limited by a gestation period reduced to about 2 months, calving of small cubs of only 300–400 g, and a low production of fat-rich milk ranging from 2.5 to 5 g/kg.

Various mechanisms are involved in metabolic suppression, which may contribute to the sparing of (muscle) proteins during hibernation. Forty years ago, Malan (1980) highlighted that MR reduction during hibernation is likely induced by body cooling and the resulting slowing down of enzymatic rates according to the Arrhenius law, but he also stressed the superimposition of additional temperature-independent mechanisms actively contributing to hypometabolism. Since then, the majority of metabolic suppression to 25% of basal rates in hibernating black bears (*U. amercicanus*) has been reported to be independent of lowered T_b (Toien et al., 2011). The active mechanisms underlying metabolic depression in hibernators have been discussed several times (Carey et al., 2003a; Storey, 2010; Storey and Storey, 2010; Quinones et al., 2014; Staples, 2014, 2016; Klug and Brigham, 2015). In golden-mantled ground squirrels, liver transcription and translation are largely suspended during deep torpor and are restored upon periodic arousals (Van Breukelen and Martin, 2001; Epperson and Martin, 2002). Regulation of transcription–translation appears peculiar in bears vs. small hibernators. Liver microarray analysis in the liver from hibernating golden-mantled ground squirrel (*Spermophilus lateralis*) has revealed that 90% of differentially expressed genes are downregulated (Williams et al., 2005), whereas more balanced proportions of downregulated and upregulated genes have been reported in the liver from hibernating black bears (*U. americanus*) and protein synthesis genes were shown to be upregulated (Fedorov et al., 2009, 2011). These specific adaptive mechanisms of bear liver compared to small hibernators may be linked to hibernation at higher T_b and MR. It should also be noted that transcript global analysis in skeletal muscles has revealed that hibernation induces a common transcriptional programming in Arctic ground squirrels (*U. parryii*) and black bears (*U. americanus*), including coordinated induction of protein biosynthesis (translation) genes and suppression of genes involved in oxidation–reduction and glucose metabolism (Fedorov et al., 2014). In addition, protein turnover is reduced but remains at equilibrium during hibernation, both protein synthesis and breakdown rates being lower in winter compared to summer in the muscles of black bear (Lohuis et al., 2007a). Signs of reduced protein translation (Van Breukelen and Martin, 2001) and of protein catabolism have also been reported in the liver of hibernating small mammals (Velickovska et al., 2005). Reduced levels of miR-24 transcripts have been reported in heart and skeletal muscle of torpid ground squirrels as was a lowering of miR-122a levels in the muscle (Morin et al., 2008). In bears, increased levels of mir-27, mir29, and mir33 have also been recorded (Luu et al., 2020). These miR data provide a mechanism for a reversible gene silencing during torpor, rapidly reversed upon arousals, and for an active suppression of metabolism during the torpid state.

Reduction of enzyme activities due to posttranslational modifications like phosphorylation is a mechanism prone to lower the rate of ATP turnover during hibernation in small mammals (MacDonald and Storey, 1999; Lee et al., 2010). For instance, ion fluxes through membranes *via* ATPase pumps constitute a major energy-demanding process (Rolfe and Brown, 1997). In most tissues, including liver and muscle, the Na^+/K^+

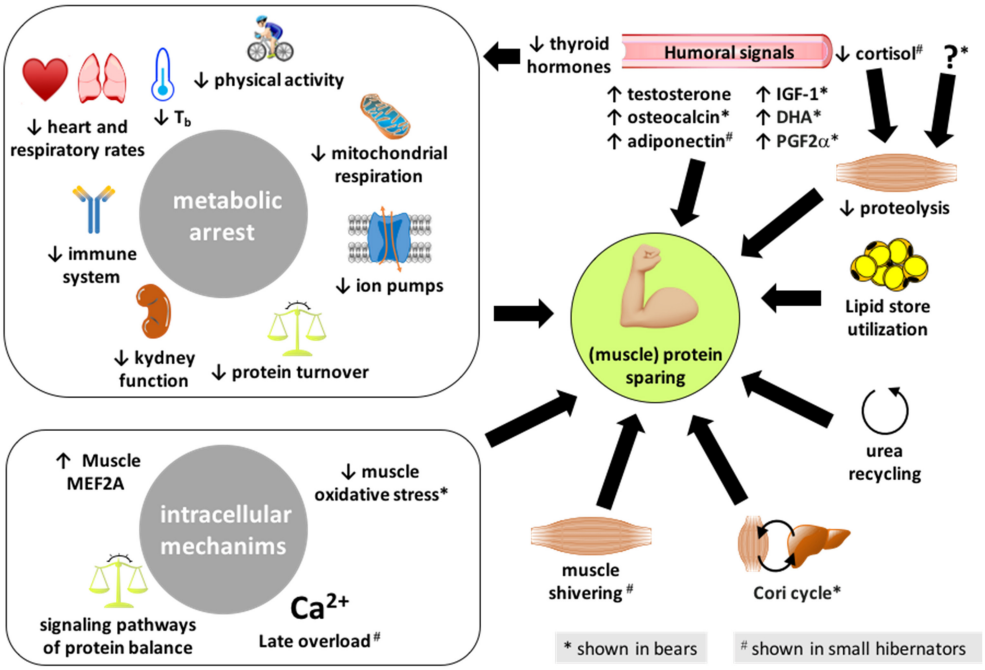

FIGURE 1 | Summary of the different processes enabling hibernators to spare their (muscle) proteins. The mechanisms presented here have been reported in both bears and small mammal hibernators, except those highlighted with an * or a # that are shown or believed to be involved, respectively, in bears only or small hibernators only. IGF-1, insulin-like growth factor-1; DHA, docosahexaenoic acid; PG2α, prostaglandin F2α.

and some calcium ATPases are downregulated in small mammals (Storey, 2010). Hibernation notably induces a 60% decrease of Na^+/K^+ ATPase activity in muscles of ground squirrels (*S. lateralis*), which appears regulated *via* reversible protein phosphorylation (MacDonald and Storey, 1999). Surprisingly, sarcoplasmic reticulum RyR1 and SERCA1 protein expression levels are higher, and major RyR1 and SERCA1 signaling pathway-related factors are active during torpor in Daurian ground squirrels (Wang et al., 2020) probably to handle the overload of calcium associated with complete inactivity and notably *via* periodic elevation in cytoplasmic calcium levels, which is normalized when individuals go back into torpor (see below). In black bear red blood cells, energy-saving mechanisms have been reported to involve decreased activities of Ca^{2+}/Mg^{2+} ATPase and Na^+/K^+ ATPase (Chauhan et al., 2002). Possible inhibition of muscle Na^+/K^+ ATPase activity in hibernating brown bears (*U. arctos*) has been recently discussed, and abundance of the three isoforms of SERCA was shown to remain unchanged (Chazarin et al., 2019a). The possible modulation of SERCA activity by endogenous protein effectors like sarcolipin, by posttranslational modifications, or in relation with the lipid composition of the sarcoplasmic reticulum membrane having not been studied to date in hibernating bears.

Mitochondria is responsible for 90% of whole-animal oxygen consumption (Rolfe and Brown, 1997), therefore being an obvious target to study in relation with changes in MR (Staples and Brown, 2008; Staples, 2014). Mitochondria morphology is preserved in skeletal muscle of edible dormice during hibernation (Malatesta et al., 2009). However, mitochondrial respiration has been shown to drop during hibernation in small mammals (Staples, 2014), this suppression being 2- to 3-fold greater in intermyofibrillar than sub-sarcolemmal mitochondria in skeletal muscles from thirteen-lined ground squirrels (*Ictidomys tridecemlineatus*) (Brown and Staples, 2014). The investigation of mitochondrial respiration is still lacking for bears, however, the expression levels of nearly all mitochondrial respiratory chain complexes have been shown to drop in muscles from hibernating brown bears, in accordance with depressed metabolism (Chazarin et al., 2019a). Downregulation of muscle mitochondrial metabolism is also supported by a reduction of substrate oxidation during hibernation (Chazarin et al., 2019a). Hydrogen sulfide (H_2S) is an endogenous gaseous molecule synthetized at the mitochondrial level, which has profound effects on mitochondrial respiration, either stimulatory at low dose or inhibitory at high dose (Murphy et al., 2019). By inhibiting the respiratory chain complex IV, exogenous H_2S is able to induce a "hibernation-like" state in mice (Blackstone et al., 2005), reducing oxygen consumption without changes in T_b (Volpato et al., 2008). Stable total sulfide concentration in the μM range has been shown in the plasma from hibernating vs. active brown bears (Revsbech et al., 2014), thus suggesting H_2S might help sustain a certain amount of mitochondrial electron chain activity during bear hibernation (Giroud et al., 2020). A role for respiratory acidosis in the inhibition of enzyme activities from the mitochondrial respiratory chain resulting in MR depression during hibernation has been hypothesized earlier

(Malan, 1986, 2014), however, it has not been specifically studied in bears.

Muscle Shivering and Protein Sparing During Hibernation

In humans, during bed rest of medium duration, physical exercise, and notably resistive vibration-induced small movements of muscles are able, when combined with whey/alkalizing salt supplementation, to prevent skeletal muscle protein changes, i.e., to limit muscle atrophy, and to maintain insulin sensitivity (Kenny et al., 2020). For small mammals, periodic arousals in deep hibernators, i.e., the return to euthermia and reactivation of major metabolic functions, and in particular the massive myofiber recruitment and elevated motor signaling during shivering in the early phase of arousals likely contribute to explain how, e.g., hibernating bats do not lose muscle mass relative to body mass during winter (Lee et al., 2010) (**Figure 1**). Although bears do not interrupt their fast and do not arouse during hibernation, it has already been hypothesized that the muscle preservation they exhibit may involve comparable mechanisms. It has already been mentioned above that muscle shivering occurs in hibernating bears (Harlow et al., 2004; Lin et al., 2004; Toien et al., 2011). Moreover, the nervous system exerts key control over skeletal muscles notably to maintain muscle tone and trigger muscle contraction, and the main consequence of muscle denervation is actually atrophy (Bongers et al., 2013). Bear skeletal muscles are sensitive to the atrophic effects of denervation during the summer-active period, however, not during hibernation (Lin et al., 2012). Therefore, the nervous system and, possibly, muscle shivering do not seem to be primarily involved in the resistance to muscle atrophy in hibernating bears.

Urea Recycling and Protein Sparing During Hibernation

The limited decrease in muscle protein content may be at the origin of an elevation of 3-methylhistidine observed in the serum of hibernating vs. active brown bears (Hissa, 1997; Stenvinkel et al., 2013). However, unchanged or decreased levels of circulating urea, the main end product of protein catabolism, likely reflect low protein mobilization and recycling mechanisms for urea in bears during winter (Folk et al., 1976; Barboza et al., 1997; Hissa, 1997; Stenvinkel et al., 2013) (**Figure 1**). The coordinated underexpression of liver genes involved in the urea cycle during hibernation in black bears argues in favor of reduced urea production (Fedorov et al., 2009). Reduced expression of genes involved in urea production has also been recently reported in skeletal muscle from hibernating grizzly bears (*U. arctos horribilis*) (Jansen et al., 2019). In addition to decreased urea production due to limited protein catabolism, a rapid degradation of urea has been shown in hibernating bears (Wolfe et al., 1982; Stenvinkel et al., 2013), indicating the synthesis of essential amino acids, which can be used for gluconeogenesis (Nelson et al., 1975; Ahlquist et al., 1984). Finally, urea reabsorption, together with water and other substances, from the bladder epithelium to the bloodstream has been shown (Nelson et al., 1973, 1975). Many studies suggest that urea recycling also occurs in hibernating rodents (Galster and Morrison, 1975), urea cycle intermediates remaining at stable levels during torpor, which is consistent with the suppression of the urea cycle (Rice et al., 2020). Accordingly, genes involved in the urea cycle have been shown to be downregulated in the liver of torpid golden-mantled ground squirrel (Williams et al., 2005). The expression of urea cycle enzymes has also been shown to be less abundant and posttranslationally inactivated during hibernation in the liver of thirteen-lined ground squirrels (Epperson et al., 2010; Hindle et al., 2014), thus facilitating amino acid sparing during torpor. A potential for protein conservation through a urea recycling by the microbiome has been suggested in fasted and water-deprived golden-mantled ground squirrel (Riedesel and Steffen, 1980) (**Figure 1**).

Nitrogen recycling is suggested in hibernating bears by the greatly reduced amounts of urinary nitrogen and ammonia, which exceed changes in the blood (Nelson, 1973; Nelson et al., 1973; Folk et al., 1976) but also by normal concentration of blood total amino acids (Nelson et al., 1973; Hissa, 1997; Stenvinkel et al., 2013) and the absence of intestinal storage (Nelson et al., 1973). The nitrogen produced from amino acid and urea metabolism is likely used for amino acid synthesis and is incorporated in newly synthesized proteins (Lundberg et al., 1976; Nelson, 1978; Hellgren, 1998), a process likely involving glycerol released from mobilization of adipose fat stores (Ahlquist et al., 1984). In hibernating thirteen-lined squirrels, low levels of skeletal muscle AMP deaminase 1 (AMPD1), a protein regulating the AMP/ATP ratio, have been interpreted as reflecting an alteration in the production of nitrogenous waste (Anderson et al., 2016). Moreover, a selective enrichment of several essential amino acids in the plasma from hibernating ground squirrels has led the authors to hypothesize a mechanism whereby they are spared and recycled for use in new protein synthesis during the winter fast (Epperson et al., 2011). Nitrogen recycling has been investigated recently in hibernating arctic ground squirrels (Rice et al., 2020). It was notably shown that slow rates of skeletal muscle protein breakdown during torpor may provide a source of (essential) amino acids and that the free nitrogen released during protein breakdown is recycled and buffered by transamination, with accumulation in glutamine, glutamate, and alanine. After the infusion of [^{15}N]ammonium acetate, the incorporation of nitrogen in amino acids and key energy metabolites during interbout arousals was in agreement with a *de novo* synthesis of amino acids and ultimately of proteins.

Humoral Control of Muscle Protein Sparing During Hibernation

Together with metabolic hormones, a number of circulating factors are known to control muscle protein balance (Bonaldo and Sandri, 2013; Martin et al., 2018; Krause et al., 2019; Ibrahim et al., 2020b). They may therefore mediate protein sparing during hibernation (**Figure 1**). The serum concentration of testosterone is elevated during the second half of the hibernation period and then until mid-July, low values being thereafter

recorded from mid-July to November–December (McMillin et al., 1976; Palmer et al., 1988; Garshelis and Hellgren, 1994; Tsubota et al., 1999). Similar results have been found in captive Hokkaido brown bears (*U. arctos yesoensis*) that are devoid of torpor, serum testosterone levels being gradually increased from February to April–May, then low baseline values being restored and remaining stable from the middle of the mating season (June) to January (Tsubota and Kanagawa, 1989). From these different studies, elevated levels of testosterone in the second half of hibernation period have been associated with testicular and spermatogenesis recrudescence in male bears. An increase in testosterone secretion also occurs in hibernating rodents before emergence (Barnes et al., 1988), which has also been associated with changes in spermatogenesis. Moreover, the increase in testosterone levels during hibernation is concomitant with an increase in skeletal muscle volume (Hindle et al., 2015). Testosterone, being known to promote protein synthesis (Dubois et al., 2012), has also been suggested to play a role in the control of blood urea and maintenance of the hibernating state in black bears (*U. americanus*) (Nelson et al., 1978).

In fat- and food-storing rodents, the secretion of most anabolic hormones, such as, e.g., insulin (Castex et al., 1984; Florant et al., 1986; Weitten et al., 2013) and insulin-like growth factor 1 (IGF1) (Schmidt and Kelley, 2001), is low during torpor. Insulinemia is also lower in hibernating bears compared to during the fall period of hyperphagia, while circulating glucagon levels tend to be higher during early hibernation (Palumbo et al., 1983; McGee-Lawrence et al., 2015). One study has found higher levels of circulating insulin in wild American black bears during hibernation (McCain et al., 2013), a characteristic that could be at the origin of the development of insulin resistance in bears (Rigano et al., 2017). Discrepant data concerning insulin concentrations may however be due to the absence of insulin assays specific to bear insulin. In addition, decreased expression of genes involved in muscle insulin signaling has also been recently shown in grizzly bears during hibernation (Jansen et al., 2019). Hence, the anabolic effects of insulin, in particular concerning protein synthesis, may therefore not be of key importance during bear hibernation. Decreased insulinemia may rather favor lipolysis during hibernation, as it is the case in response to fasting in non-hibernating rodents (Ibrahim et al., 2020a). Hibernating bears remain responsive to growth hormone (GH) treatment, but IGF1 serum levels decline in autumn to reach lowest values during early denning before they are increased in late denning to reach the highest values during summer (Donahue et al., 2006; Blumenthal et al., 2011; Seger et al., 2011). A role for the GH–IGF1 axis in fat accretion prior to denning and in the prevention of excessive lipolysis in early hibernation has thus been suggested in black bears. Because IGF1 is known to protect against muscle atrophy, notably *via* the control of intracellular protein balance (Timmer et al., 2018), such regulations may favor (muscle) protein sparing during bear hibernation.

Adiponectin is both an adipokine and myokine that is able to modulate metabolism and insulin sensitivity in skeletal muscle (Liu and Sweeney, 2014). Adiponectin has also been shown to protect skeletal muscles against atrophy, notably rodents *in vivo* and in C2C12 cells *in vitro* (Krause et al., 2019), a mechanism that does not seem to play a role in hibernating bears. Indeed, serum adiponectin levels have been shown to be related to body fat percentage in black bears, increasing gradually during the active season to reach highest values in the hyperphagic pre-denning period, then values were decreased back during hibernation (McGee-Lawrence et al., 2015; Rigano et al., 2017). Decreased adiponectinemia has also been shown in Scandinavian brown bears during hibernation vs. the summer-active season (Welinder et al., 2016). On the contrary, adiponectin is low at the beginning of fat accumulation and elevated during hibernation in fat- and food-storing rodents (Florant et al., 2004; Weitten et al., 2013), which could trigger fatty acid oxidation and inhibit gluconeogenesis during torpor (Fruebis et al., 2001; Masaki et al., 2003) and help to protect muscles.

Since total and free concentrations of thyroid hormones T3 and T4 have been shown to decline from October through March in the serum of American black bears, elevated levels being restored in April–May, it has been suggested that hibernating bears have a hypothalamic hypothyroidism (Azizi et al., 1979; Tomasi et al., 1998). Similar results have been found in Finnish brown bears (Hissa et al., 1994). Such a drop in thyroid hormone levels during denning is likely linked to depressed metabolism during hibernation. Because thyroid hormones are known to increase the number and diameter of muscle fibers (Salvatore et al., 2014) and muscle wasting is induced when they are deficient (Carneiro et al., 2008), it is difficult to understand if and how the regulation of the thyroid function during hibernation is involved or not in the control of bear muscle metabolism. Finally, osteocalcin, a bone-derived hormone, has been shown to promote muscle mass maintenance in aging mice, an effect likely due to stimulation of protein synthesis (Mera et al., 2016). Opposite results have been found in black and brown bears during hibernation, an increase in serum osteocalcin being observed for the former (McGee-Lawrence et al., 2015), whereas decreased osteocalcinemia was reported for the latter (Vestergaard et al., 2011). Osteocalcin might then play a role in muscle maintenance during hibernation in black bears, however not in brown bears. The reasons for such a difference between bear species are not understood.

Yet, the secret of muscle protein sparing in hibernating bears could be in proteolysis inhibition. The *ex vivo* incubation of rat skeletal muscle (extensor digitorum longus) for 120 min in a supplemented medium containing 5% of hibernating bear plasma has indeed resulted in the reduction of muscle net proteolytic rate (−40%) and of the levels of proteolytic-related mRNAs (cathepsin B, ubiquitin) as compared with rat muscles incubated with the plasma from non-hibernating bears (Fuster et al., 2007). The exposure of cultured human differentiated muscle cells to brown bear serum collected during winter and summer periods later confirmed that the anti-proteolytic properties of hibernating bear plasma/serum also affect human cells (Chanon et al., 2018). The protein turnover rate of human myotubes was reduced when they were incubated during 48 h with the serum from hibernating vs. summer-active bears, a dramatic inhibition of proteolysis involving both proteasomal and lysosomal systems being observed, which resulted in an

increase in muscle cell protein content. Therefore, the plasma from hibernating bears appears to contain one or several proteolytic inhibitors that may modulate muscle intracellular pathways to attenuate muscle loss during hibernation. Cortisol (or corticosterone) is the main steroid hormone that is involved in protein degradation (Schiaffino et al., 2013). In fat-storing rodents, plasma concentrations of cortisol are low during hibernation compared to the active season, which might help prevent protein catabolism (Shivatcheva et al., 1988; Armitage, 1991). In bears, however, values of corticosteroids were observed to be higher during fall hyperphagia and hibernation periods than during the summer-active phase (Palumbo et al., 1983; Harlow et al., 1990; Hellgren et al., 1993; Donahue et al., 2003a,b), which has been proposed to be involved in lipolysis promotion, rather than gluconeogenesis from the use of amino acids (Harlow et al., 1990). Other anti-proteolytic factors remain therefore to be found.

Intracellular Pathways of Muscle Protein Sparing During Hibernation

Several intracellular signaling pathways that could be involved in the regulation of muscle protein balance in hibernators have been listed elsewhere (Tessier and Storey, 2016; Gonzalez-Bernardo et al., 2020). In bears, the elevated expression of multiple genes involved in protein biosynthesis and ribosome biogenesis has been consistently documented in skeletal muscles from hibernating black bears (Fedorov et al., 2009, 2014) and grizzly bears (Jansen et al., 2019). Moreover, an increased level for the phosphorylated form of S6K1 was observed in the skeletal muscles of hibernating Japanese black bears (*Ursus thibetanus japonicus*) (Miyazaki et al., 2019), suggesting an activation of mammalian target of rapamycin (mTOR) complex 1 (mTORC1) signaling. Accordingly, the gene expression of myostatin, a negative regulator of skeletal muscle growth that reduces mTORC1 activity *via* Smad2/3 signaling (Trendelenburg et al., 2009; Welle, 2009), was significantly downregulated following hibernation. In thirteen-lined ground squirrels (*Spermophilus tridecemlineatus*), no significant change of myostatin expression was observed during entrance into torpor and early or late torpor (Brooks et al., 2011). There was, however, approximately a 6-fold increase in myostatin protein levels as squirrels arose from torpor. If the absence of variation during torpor goes in the direction of muscle preservation, the increase during arousal phases does not support the hypothesis that shivering thermogenesis promotes muscle anabolic pathways (Lee et al., 2010). Mechanisms that could release the suppression or promote increased levels of myostatin involved the upregulation of both Smad2 and phosphorylated Smad2 during early torpor, but only that of phosphorylated Smad2 during arousals (Brooks et al., 2011). Overall, these regulations likely enhance muscle growth following hibernation and counteract an excessive loss of muscle during hibernation. Transcriptional changes affecting genes associated with insulin–Akt–mTOR signaling in skeletal muscle of hibernating grizzly bear and changes in non-essential amino acid levels have recently been suggested as cooperating mechanisms that may explain the increase in mTOR activity during hibernation (Mugahid et al., 2019). Whereas unchanged transcriptional level of protein catabolism genes was recorded in black bears (Fedorov et al., 2009, 2014), increased mRNA levels have been reported for key factors of the ubiquitin-proteasome and autophagy degradation pathways in sartorius muscle of Japanese black bears at the end of the hibernation period, which may contribute to the decrease in mass of this muscle (see above) (Miyazaki et al., 2019). In grizzly bears, skeletal muscle mRNA levels have been observed decreased for muscle protein degradation pathways (Jansen et al., 2019). A coordinated downregulation of atrogenes during arousal has also been reported in arctic ground squirrels (Goropashnaya et al., 2020). Overall, these data suggest that, if an inhibition of proteolysis is involved in muscle protein sparing during hibernation (see above), part of the regulation is made at the transcriptional level for brown bears and arctic ground squirrels, albeit not for black bears.

In small mammal hibernators, a previous study examined some parameters of transcriptional control in skeletal muscle of thirteen-lined ground squirrels that could be used to provide reversible suppression of transcription during torpor (Morin and Storey, 2006). The authors notably reported a significant reduction of maximal activity of RNA polymerase II in muscles during hibernation to just 58% of the activity in euthermic muscle despite a constant total amount of Pol II protein. Moreover, RNA content is decreased during small mammal hibernation, suggesting a loss of functional ribosomes as observed in suspended rats (Steffen and Musacchia, 1984), impairing protein synthesis. Recent studies show, however, that this seems to be dependent on the species and muscle studied, and that it evolves during hibernation. Indeed, a recent study did not support an arrest of transcription during low-temperature torpor in quadriceps muscle of hibernating arctic ground squirrels but supported a transcriptional elevation of protein biosynthesis (Goropashnaya et al., 2020). The reduction of the levels of AMPD1 preceding and during hibernation in thirteen-lined squirrels, by reducing the ability to clear cellular AMP, could lead to increased AMPK activity and could thereafter induce a reduction of muscle mass *via* an inhibition of protein synthesis (Anderson et al., 2016). This said, if muscle protein synthesis decreases at the start of hibernation, it then increases again during late hibernation through the activation of the mTOR signaling cascade, as shown in hibernating bats and rodents (Lee et al., 2010; Nowell et al., 2011; Fedorov et al., 2014), leading to an increase in skeletal muscle volume before emergence (Hindle et al., 2015). A role for fibromodulin in the muscle maintenance seen during hibernation has also been hypothesized in thirteen-lined squirrels (Anderson et al., 2016). The activation of serum/glucocorticoid-induced kinase 1 (SGK1), an activator of mTOR signaling, has also been shown in hibernating thirteen-lined ground squirrels (Andres-Mateos et al., 2013). Moreover, the phosphorylation levels of Akt1 (*p*-Akt1) and mTOR (*p*-mTOR) are reduced significantly in bats during hibernation compared to summer-active bats (Lee et al., 2010). Upon arousals, little variations of *p*-Akt1 occur, but *p*-mTOR exhibits biphasic oscillations. These findings suggest that the resistance to atrophy in small deep hibernators might be attained primarily

by relatively constant or decreased proteolysis (see below) in combination with oscillatory anabolic activity (e.g., *p*-mTOR) during arousals. This response is not restricted to skeletal muscle, as both cardiac (Wu and Storey, 2012) and smooth muscle (Talaei, 2014) also show increases in mTOR activity upon arousal from torpor. Muscle preservation during torpor in thirteen-lined ground squirrels may also involve an increase in the percentage of satellite cells favoring growth processes (Brooks et al., 2015). Finally, an activation of the endurance exercise pathway involving PGC-1α has been shown in hibernating 13-lined ground squirrels (Xu et al., 2013), and this might therefore be an important mechanism for the preservation of skeletal muscle during hibernation.

Protein degradation has been reported either to decrease during small mammal hibernation, thus contributing to protein sparing, or to remain unaltered. Indeed, the activity of the ubiquitin-proteasome system is largely suppressed at low T_b during small mammal torpor (Velickovska et al., 2005), which is expected to greatly reduce muscle catabolism during torpor bouts. Muscle calpain activity also appears inhibited possibly due to elevated levels of its specific inhibitor, calpastatin, in hibernating Daurian ground squirrels (Yang et al., 2014). Moreover, the skeletal muscles of hibernating Daurian ground squirrels maintain protein sialylation homeostasis by restoring sialylation modification upon periodic arousals, which might help prevent disuse atrophy (Zhou et al., 1997). A decrease in protein degradation can be attributed to the downregulation of the FOXO1 proteolytic pathway (Nowell et al., 2011). In this context, the levels of proteolysis-related factors in skeletal muscles, including phosphorylated FOXO1 (*p*-FOXO1), atrogin-1, MuRF1, Skp2, and calpain-1, seem to remain constant during hibernation in bats (Lee et al., 2010). In addition, SGK1 activation in hibernating thirteen-lined ground squirrels has been involved in downregulation of proteolysis and autophagy (Andres-Mateos et al., 2013). In the Daurian ground squirrel during hibernation, the expression of IKKβ and MuRF1 remains stable in little atrophied soleus and extensor digitorum longus muscles, whereas an increase in MuRF1 mRNA level in the soleus and MuRF1 protein level in the extensor digitorum longus is observed upon arousals (Wei et al., 2018). Stress conditions experienced by animals can trigger excessive endoplasmic reticulum stress, which can lead to the activation of the unfolded protein response to adapt cellular folding capacity, but it can also drive cell death (Karagoz et al., 2019). In this regard, the upregulation of *p*-eIF2α and GRP78 mediated by PERK signaling pathway has been identified in torpid Daurian ground squirrels as possibly alleviating elevated endoplasmic reticulum stress, hence preventing skeletal muscle cell apoptosis during hibernation (Zhang et al., 2019b). There was also an indication for an inhibitory role of apoptosis during the torpid state, as suggested by a reduced Bax/Bcl-2 protein ratio in muscles of torpid Daurian ground squirrels, which was recovered upon interbout arousals (Fu et al., 2016).

Intracellular calcium overload plays an important role in the mechanisms of disuse-induced muscle atrophy. Increased intracellular calcium concentration can activate some proteases (e.g., calpains) and trigger the catabolism of myofibrillar proteins (Costelli et al., 2005; Goll et al., 2008; Fu et al., 2016). Prolonged skeletal muscle disuse (e.g., during spaceflight, hind limb unloading, and bed rest) can notably lead to disturbance of intracellular calcium homeostasis, mainly exhibited by cytoplasmic calcium overload (Goll et al., 2003; Costelli et al., 2005; Shenkman and Nemirovskaya, 2008). Interestingly, hibernators might regulate intracellular calcium homeostasis during hibernation *via* transient cytosolic overload of calcium upon arousals. For instance, a previous study in Daurian ground squirrels showed increased cytoplasmic calcium levels in skeletal muscle fibers during late torpor and upon interbout arousals and partial recovery when the animals entered torpor again (Zhang et al., 2019a; Wang et al., 2020).

The resistance to muscle atrophy in hibernating bears has also been shown to involve other mechanisms. The expression levels of pyruvate dehydrogenase kinase 4, a protein known to inhibit the activity of pyruvate dehydrogenase, thereby limiting the entry of glycolytic intermediates into the Krebs cycle, is increased in skeletal muscles from hibernating Japanese black bears (Shimozuru et al., 2016) and hibernating Scandinavian and American brown bears (Chazarin et al., 2019a; Mugahid et al., 2019). These data, together with the increase in muscle lactate dehydrogenase activity levels and either maintained or reduced plasma lactate levels (Ahlquist et al., 1984; Evans et al., 2012; Chazarin et al., 2019a), have led some authors to suggest that the Cori cycle is active in bears during hibernation, therefore helping to spare muscle protein during hibernation (Shimozuru et al., 2016; Chazarin et al., 2019a). Previous data indicated an enhancement, *via* a COX-2-dependent pathway, of *in vitro* skeletal muscle growth in C2C12 myotubes where the supplementation with arachidonic acid triggers increased secretion of prostaglandin F2a and prostaglandin E2 (Markworth and Cameron-Smith, 2013). Accordingly, the maintenance of prostaglandin levels in skeletal muscles from hibernating brown bears has been proposed to play a role in muscle sparing (Giroud et al., 2018). Moreover, a role for increased levels of omega-3 fatty acids like docosahexaenoic acid (DHA) and docosapentaenoic acid has been suggested recently in hibernating brown bears (Chazarin et al., 2019a). DHA-enriched diets are known to help preserve muscle integrity in various catabolic conditions (Smith et al., 2015; Deval et al., 2016) and to induce muscle protein synthesis (Wei et al., 2013). DHA itself also prevents palmitate-induced proteolysis *in vitro* (Woodworth-Hobbs et al., 2017). Furthermore, hibernation has been shown to elicit a myogenic microRNA, or "myomiR," response *via* MEF2A-mediated signaling in skeletal muscle from hibernating brown bears, consisting of an upregulation of miR-1 and miR-206 and respective downregulation of pax7 and id2 mRNAs (Luu et al., 2020). Increased levels of miR-206, miR-221, and miR-31 were also indicative of stimulated muscle regeneration process, and higher levels of miR-33, miR-23a, and miR-29b suggested suppression of ubiquitin ligase expression. A significant role for MEF2-mediated gene transcription has also been suggested in hibernating ground squirrels (Tessier and Storey, 2010). MEF2 protein levels significantly increased when animals were in torpor and the amount of phosphorylated (Thr312) active MEF2A increased during entrance into torpor. MEF2C levels also rose

significantly during entrance into torpor and torpor as did the amount of phosphorylated MEF2C Ser387.

Finally, because oxidative stress promotes muscle proteolysis and inhibits protein synthesis in catabolic conditions (Powers et al., 2016), its limitation in skeletal muscle from hibernating brown bears has been proposed to favor resistance to atrophy (Chazarin et al., 2019b). More precisely, increased gene expression for the cold-inducible proteins CIRBP and RBM3 was observed and could favor muscle mass maintenance and alleviate oxidative stress during hibernation. In addition, a possible reduction of the production of reactive oxygen species in the hibernating muscle could be hypothesized from indices of reduced mitochondrial content. It was paralleled by a coordinated induction of cytosolic antioxidant systems, under the control of the transcription factor NRF2, and the maintenance of the GSH/GSSG ratio. H_2S is known to have antioxidant properties (Murphy et al., 2019). It has been suggested previously that remodeling of H_2S metabolism could be involved in the synthesis of GSH found in high quantity in hibernating bear erythrocytes (Revsbech et al., 2014). In bear muscles, the GSH/GSSG ratio was maintained stable during hibernation due to decreased levels of both glutathione forms (Chazarin et al., 2019b), and an eventual role for H_2S therefore remains undetermined. Lower levels of oxidative damage were recorded in hibernating bear skeletal muscles (Chazarin et al., 2019b). Enhanced expression of chaperones and heat shock proteins in bear skeletal muscle during hibernation may also help maintain the integrity of muscle proteins (Chazarin et al., 2019b). It is noteworthy to mention that antioxidant-rich berries (Rimando et al., 2004; Zifkin et al., 2012) are consumed in large amounts by bears during the summer and autumn (Stenset et al., 2016). Whether and to what extent such a diet prior to denning has an influence on bear muscle protection against oxidative stress during hibernation are not yet known. Antioxidant mechanisms have also been hypothesized in small hibernating mammals, involving, for example, allantoin and ascorbate (Epperson et al., 2011).

Altogether, along the hibernation period in small as well as in large hibernators, these molecular and subcellular mechanisms contribute to the sparing of muscles *via* tight controls of both the synthesis and the catabolism of proteins (**Figure 1**).

HIBERNATORS AS GOOD MODELS TO STUDY THE MAINTENANCE OF MUSCLE MASS

Bernard (1865) and Krogh (1929) were among the first, if not the first, to develop the idea that the solution to solve a problem in biology or medicine is necessarily hidden in an animal species, hence pioneering the biomimicry concept. Hundred years later, and particularly since the discovery that mole rats have anticancer mechanisms that do not exist in mice or rats, i.e., the so-called standard models, there is an increasing interest for "exotic" animals as a source of biomedical innovation (Sedivy, 2009). In this context, hibernation is a unique metabolic condition, since it is superimposing an important drop in both energy expenditure and physical activity to a usually long fast. From the pioneering work of Cahill (1970), it is well-known that the main adaptation to tolerate a long fast in humans is a decrease in protein breakdown, the so-called "protein sparing" through the mobilization of body fat. But, in contrast, inactivity results in an important reduction in muscles (Rudrappa et al., 2016).

Protein Sparing and Fasting Abilities in Hibernators

The first remarkable feature of hibernators is, as indicated above, that they are able to rely essentially on their body fat despite inactivity. They consistently emerge from winter with very little atrophy despite conditions that would typically result in muscle atrophy combined with a loss of oxidative fibers (Cotton, 2016). A major question was whether the extent of the drop in T_b, i.e., torpor vs. deep hibernation, interferes with this protein sparing. Quantitative data are limited to answer this question, particularly in small hibernators, due to the difficulty in monitoring small changes in body condition. Importantly, therefore, in shallow- and deep-hypothermal fasting hedgehogs (Cherel et al., 1995), despite the different levels in energy expenditure of about 2.5 and 1 $W.kg^{-1}$, respectively, the energy sources were found identical in both groups, neutral lipid contributing similarly as the main fuel (about 90%) and body protein accounting for the same remainder (about 10%). In the fat-storing arctic ground squirrel, the contribution of body protein to energy expenditure during hibernation is also about 10% (Galster and Morrison, 1976). It therefore suggests that the extent of the drop of energy expenditure does not interfere with the efficiency in protein sparing.

The maintenance of body protein, and particularly muscle mass, is critical, as human death occurs when about 50% of body proteins have been depleted (Silber, 1984). As for hibernating species during torpor, obese and non-obese humans are very efficient in their ability to spare body proteins during food deprivation, and they may safely undergo therapeutic fasts of 1 to 3 weeks (Wilhelmi de Toledo et al., 2019). However, due to the high caloric value of fat compared to body protein, severely obese humans would not be able to undergo such a fast as long as necessary to deplete their excessive fat. Long before, they would have reached this critical stage where about 50% of body protein have disappeared and die (Le Maho et al., 1988). One way for severely obese humans to rapidly lose fat in excess while reducing protein loss is therefore by undertaking a very low energy diet (VLED) providing protein. The ambition is not to totally preserve body protein but to minimize its loss, and it is more efficient with a behavioral program that involves increased locomotor activity (Asher et al., 2013; Parretti et al., 2016). In this biomedical context, it is therefore of particular interest that food-storing hibernators, such as golden-mantled ground squirrels (*Citellus lateralis*), which can survive for months without eating, have a very low food intake during their episodes of arousals (Mrosovsky and Sherry, 1980; Kauffman et al., 2004). This spontaneous drop in food intake is not specific of hibernators, since it also occurs in non-hibernator animals, such as, for birds, the female of the red junglefowl (*Gallus gallus*) when incubating

its eggs (Mrosovsky and Sherry, 1980). It is a spontaneous fast, i.e., an anorexia, since the squirrel and the bird do not eat more when food is nearby *ad libitum*. In both cases, food intake is progressively decreasing from a figure, which corresponds to a low energy diet (LED) to a value that can be later considered as a spontaneous VLED, since food intake is reduced by 80% or more. Consequently, body mass is decreasing during the entire period when torpor occurs in squirrels and all throughout the incubation for the junglefowl. If food is removed, which therefore corresponds to a zero energy diet, there is obviously an accelerated drop in body mass (**Figure 2A**) (Karmann et al., 1994). When food is again available, food intake is temporarily larger than it was before. It is however quite remarkable that food intake returns to the previous spontaneous very low caloric value once body mass has reached not its value at the onset of the zero-calorie diet but the lower value it would have reached at that time without any interruption of the VLED. This means therefore that there is a sliding set point in the defense in body mass during spontaneous VLED.

Considering the physiological mechanisms involved in this regulated drop in body mass, it was therefore interesting to determine the metabolic consequences of the spontaneous VLED. Indeed, in obese humans, the aim of VLEDs is to minimize body protein depletion in association with a reduced calorie intake in order to reduce excessive fat. Again, as indicated above, although fat contributes to most of the energy expenditure in obese humans under a zero-calorie diet, the low caloric value of body protein would result in a critical loss in lean body mass while fat is still in excess (Le Maho et al., 1988). Moreover, as documented in this review, hibernators, as birds before breeding or migration, generally store a huge amount of fat. Metabolic flexibility appears therefore as a prerequisite for body protein savings during hibernation.

The most accurate way to determine individual changes in body protein is through a nitrogen balance, i.e., a comparison of nitrogen intake and output. This has been done during the season of torpor in ground squirrels (**Figure 2B**) (Karmann et al., 1994). It shows that all through that period, the spontaneous LED and then VLED that occur during each arousal compensate for the loss in body protein during the previous episodes of torpor. On a zero-energy diet, there is obviously a significant loss in body protein, although much smaller than that in rats, which, in contrast to the squirrels, are not hibernators. There is an initial high food intake once food is again available. It allows to restore this larger than usual body protein loss. But the return of body mass to the defended value corresponds again to the situation when the spontaneous VLED allows to compensate for the protein loss during torpor. It accords with the observation that dry fat-free body mass is maintained in those hibernators hoarding food, which allows them to feed during arousals (Jameson and Mead, 1964). It is unfortunate that, to our knowledge, there are no more investigations on the nitrogen balance of food-storing hibernators. Based on the similar contribution of body protein and fat in torpid and hibernating hedgehogs (Cherel et al., 1995), we might however assume that fat-storing deep hibernators manage as well as the squirrels after torpor episodes

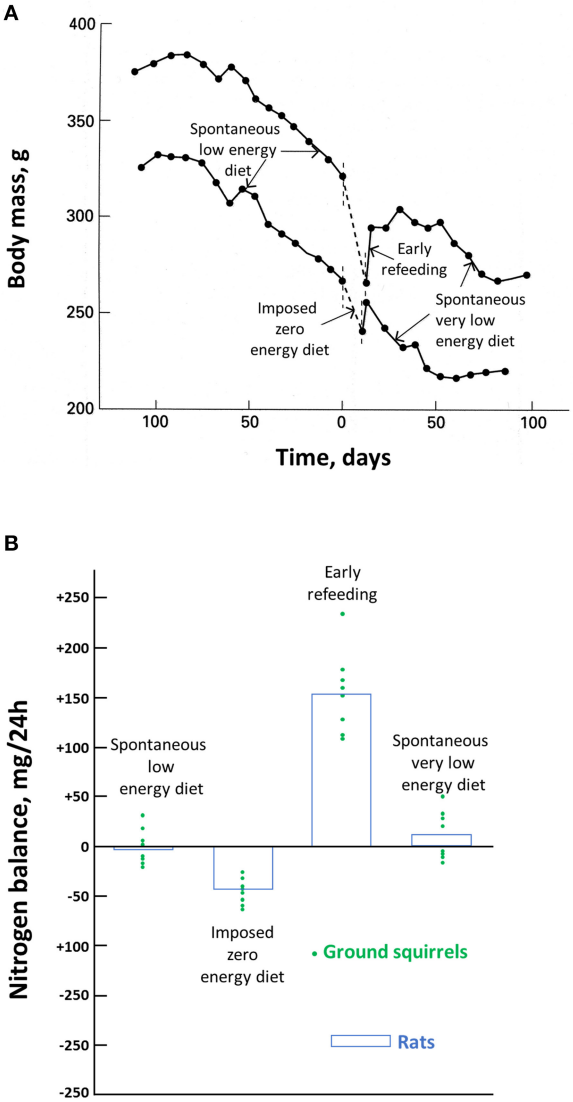

FIGURE 2 | Effects of food deprivation in ground squirrels and rats. Body mass changes in two hibernating ground squirrels before, during, and after an experimental fast are shown in **(A)** and the nitrogen balance in hibernating ground squirrels before, during, and after an experimental fast, and in experimentally fasted rats are shown in **(B)**. Modified from Karmann et al. (1994).

to compensate from the protein loss that has occurred during deep hibernation and arousal. In the absence of nutrient intake, provision of amino acids and prevention of ammonia toxicity in hibernating arctic ground squirrels have recently been shown to involve buffering and recycling of free nitrogen released from skeletal muscle protein breakdown during torpor into newly synthesized amino acids and proteins during interbout arousals (Rice et al., 2020).

Finally, by relying on a reduced energy diet during the episodes of arousal, food-storing hibernators seem to be able to achieve the same goal, as do the hibernating bears in maintaining

body protein and only relying on fat without eating. Elucidating how small and larger hibernators manage to be so efficient is therefore an important biomedical goal.

Transfer of Hibernator Protein-Sparing Abilities to Humans

Apart from the deprivation of food, innovations inspired from the study of hibernation can be expected to improve a number of other situations where (muscle) proteins are lost in humans, including, e.g., during aging, sedentary lifestyle, and life in space and for the preservation of tissues and organs for transplantation (**Figure 3**). In the context of translational research, some of the aspects and benefits of considering hibernators as models of choice to better understanding and managing diseases (e.g., ischemia–reperfusion injury, chronic kidney disease, cardiovascular diseases, obesity/diabetes) or pathophysiological situations (e.g., muscle disuse) in humans have been discussed elsewhere (Carey et al., 2003a; Bodine, 2013; von Linde et al., 2015; Stenvinkel et al., 2018).

Millions of people suffer from muscle atrophy worldwide (Ding et al., 2018), and this number is expected to increase rapidly. Apart from the widespread chronic diseases like cardiovascular diseases or cancers, the main causes of muscle loss remain aging, malnutrition (in the form of undernourishment or overeating), and physical inactivity, the prevalence of which is continuously growing. First, there is a general trend toward population aging throughout the world, with the number of persons aged 80 years or over being projected to increase more than 3-fold between 2017 and 2050, rising from 137 to 425 million (United Nations, 2017). Second, almost 690 million people in the world (∼9% of the world population) were estimated to have been undernourished in 2019, and projected values indicate that more than 840 million people could be undernourished in 2030 (FAO et al., 2020). Third, global obesity has more than doubled since the 1980s, with more than 1.5 billion overweight adults, and current estimates are not optimistic as they still predict an increase in the prevalence of obesity of 33 and 130% for severe obesity by 2030 (Finkelstein et al., 2012). Fourth, sedentary lifestyles and the lack of physical activity have become a threat to public health, reaching pandemic proportions, making it now considered the fourth leading cause of morbidity and mortality in the world (Kohl et al., 2012). Weightlessness is also a well-known cause for skeletal muscle atrophy (Narici and de Boer, 2011), which for now remains among the limiting factors in the context of the human exploratory missions to the moon or Mars, which are today envisioned by almost all major national and international space agencies in the world as well as private companies (Patel et al., 2020).

The high prevalence of muscle wasting and its consequences such as impairment of health and life quality, the induction of weakness, fatigability, frailty, reduced activity, and metabolic alterations, and delayed recovery from diseases have led to decades of research dedicated to a better understanding of associated mechanisms (Powers et al., 2016; Ji and Yeo, 2019; Vainshtein and Sandri, 2020). Physical inactivity has been reported as a primary cause for developing metabolic inflexibility during bed-rest studies (Bergouignan et al., 2011), disuse-induced muscle atrophy being associated with the development of insulin resistance, hyperlipidemia, and a decreased capacity for oxidizing lipids (Stein and Wade, 2005). Insulin resistance and impairment in muscle lipid oxidation are also well-known features of obesity (Houmard, 2008). Although lean body mass is generally higher in overweight or obese individuals compared to their lean counterparts (Forbes and Welle, 1983), muscle quality and function are generally deteriorated (Cava et al., 2017). Moreover, obesity has been shown to progressively induce muscle atrophy, notably due to decreased physical activity, muscle inflammation, and impairment of muscle protein synthesis (Kim et al., 2014, 2016; Roy et al., 2016; Cava et al., 2017). Defining sarcopenia as the loss of muscle mass and strength and, ultimately, function, muscle wasting associated with obesity has led to the notion of sarcopenic obesity (Baumgartner, 2000). In obese individuals, sarcopenia is notably exacerbated by lipotoxicity to muscle cells due to increased fat levels (Prado et al., 2012). Sarcopenic obesity adverse effects are multiple, with notably increased risks of developing insulin resistance, metabolic syndrome, dyslipidemia, inflammation, and cardiovascular diseases in comparison with obesity or sarcopenia alone (Roh and Choi, 2020). Given the actual pandemic of obesity and its associated comorbidities, it is of crucial interest to develop efficient therapies and treatments for ensuring human health. Weight loss therapy is generally at the forefront to resolve obesity. However, body weight loss is usually achieved *via* a reduction in both fat mass and lean body mass (Cava et al., 2017; Willoughby et al., 2018). A substantial loss of lean body mass can negatively affect overall metabolism, muscle function, and other physiological processes, and it may worsen body fat accretion (Cava et al., 2017; Willoughby et al., 2018). The use of food deprivation to treat obesity has proven successful in some cases (Stewart and Fleming, 1973); however, the occurrence of several sudden deaths has been recorded (Cubberley et al., 1965). As with anorexia nervosa (Silber, 1984), the cause of these deaths has been attributed to excessive loss of body proteins (Le Maho et al., 1988). Therefore, adequate therapies should trigger fat mass loss in a sustainable way while preserving muscle mass and strength. As already stressed in this review, the continuously growing basic knowledge of the cellular and molecular mechanisms of muscle atrophy (Bonaldo and Sandri, 2013) and a myriad of wasting conditions including, e.g., prolonged fasting (Ibrahim et al., 2020b), physical inactivity (Rudrappa et al., 2016), and microgravity (Tascher et al., 2017) could be a way to identify possible anti-atrophy targets. From such studies, clinical therapies to fight muscle atrophy have been developed, notably including physical exercise, nutritional supplements, and a series of drugs (Carraro et al., 2018; Cretoiu and Zugravu, 2018; Kern et al., 2018; Owens, 2018; Rabelo et al., 2018; Sakuma and Yamaguchi, 2018; Shen et al., 2018). Nonetheless, no effective treatments have been proven to fully prevent loss of muscle mass (Ding et al., 2018; Duan et al., 2020).

On the reverse, hibernators are naturally resistant to large changes in adiposity levels (obesity is a necessary part of life for most hibernating animals) and to skeletal muscle atrophy despite long periods of dropped MR accompanied by fasting

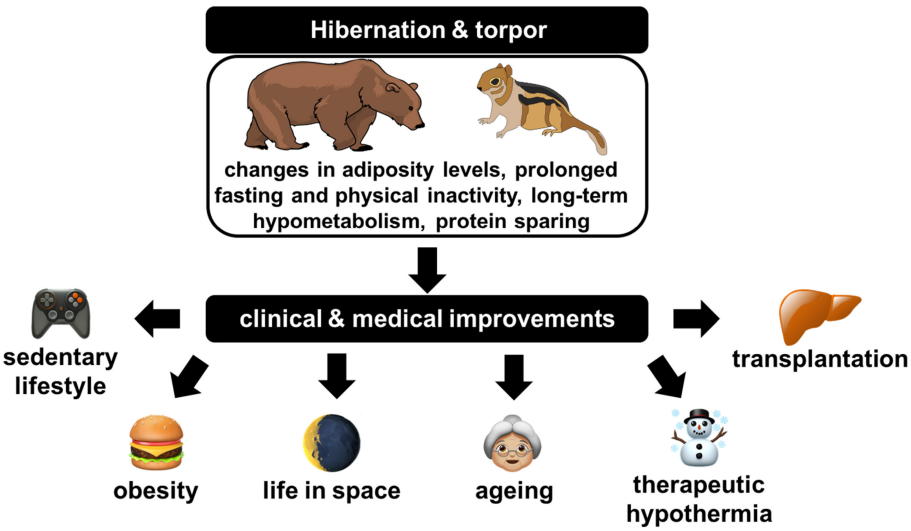

FIGURE 3 | Illustration of the clinical and medical improvements that could likely originate from a deep understanding of physiological, cellular, and molecular regulations at play in hibernators.

and physical inactivity, abilities that likely have an evolutionary origin. We should therefore get inspired from the "turning on" of specific regulatory programs involved in the control of energy and protein metabolism in hibernating animals (see above) and the "turning off" of other programs involved in the development of obesity comorbidities (**Figure 3**). Hence, molecular studies in hibernating mammals have already been proven successful in identifying potential therapeutic targets for combatting loss of skeletal muscle mass associated with muscle degeneration and atrophy. It has been demonstrated that SGK1, which appears involved in muscle preservation of hibernating 13-lined ground squirrels, is also critical for the maintenance of skeletal muscle homeostasis and function in non-hibernating mammals in normal and atrophic conditions such as starvation and immobilization (Andres-Mateos et al., 2013). Research in hibernating mammals will probably bring a wealth of new knowledge in the future, and it may result 1 day to the application of critical hibernator strategies to human wasting conditions. Therapeutic hypothermia has already been designed in various clinical contexts (Turban et al., 2001; Lee and Ding, 2020). Going further, i.e., by mimicking a hibernation-like state or inducing relevant hibernation features in humans could be of great help to favor healthy aging, improve health outcomes in critical patients, long-term immobilized patients, sedentary and obese people, and to promote healthy spaceflight to deep space (Martin, 2008; Johnson et al., 2013; Wu et al., 2013; Gorr, 2017; Chouker et al., 2019; Ferris and Gregg, 2019; Al-attar and Storey, 2020) (**Figure 3**).

Proteolysis is one of the main limitations for the preservation of allografts (Calmus et al., 1995), and suppression of major metabolic functions is a goal to reach to allow extending preservation times (Guibert et al., 2011). Apart from their natural resistance to muscle atrophy, hibernators are also able to preserve the functionality of their organs over the long-term while into a hypometabolic state notably through body protein sparing *via* inhibition of protein degradation (see above). They therefore constitute very good models for the improvement of the preservation of tissues and organs for transplantation (Ratigan and McKay, 2016; Soo et al., 2020) (**Figure 3**). If interbout arousals during hibernation in small mammals have a lot to teach regarding notably ischemia–reperfusion injury problems in the context of the cold storage of organs (Zancanaro et al., 1999; Soo et al., 2020), the concept of normothermic or sub-normothermic organ preservation has gained much attention in recent years. Not only normothermic organ conservation overcomes the main weaknesses of cold storage, e.g., by avoiding ischemia–reperfusion injury (Vogel et al., 2012), but it also allows much longer preservation times. It therefore appears as a very promising way to overcome the current shortage of organ donors worldwide while enabling to provide transplantation for a greatly increased number of patients (Brockmann et al., 2009; Nasralla et al., 2018). As they hibernate with a slight T_b lowering, bears and lemurs appear as very good models to help improve the field of warm (sub-normothermic to normothermic) organ preservation (Hadj-Moussa and Storey, 2019). With a core T_b greater than 30°C during hibernation, bears are indeed not confronted with the need for periodic body rewarming to revert deep hypothermia and associated adverse effects of torpor such as in small hibernators (see above). Neither they arouse nor return to euthermia after entering torpor, but they have been proven to be successful in preserving organ functionality over several months while into the torpor state.

CONCLUSION

Based on the description above, it clearly appears that hibernators constitute unique animal models to study energy

and substrate metabolism associated with muscle preservation under extreme conditions of complete inactivity and/or food deprivation. They provide avenues for further investigations with obvious biomedical interests, including treatments for obesity and cardiovascular diseases, and for improving health conditions during space travels. Bears seem to be unique models to develop new ways of organ preservation and to study the preservation of skeletal muscle during complete inactivity at mild T_b. Some hibernating primate species, as, e.g., lemurs from the *Cheirogaleus* family, including fat-tailed dwarf lemur (*Cheirogaleus medius*) and greater dwarf lemur (*Cheirogaleus major*), may also represent good models to that respect due to their phylogenetic proximity with humans. Small hibernating rodents appear as useful models to discover new ways to improve therapeutic hypothermia due to very low T_b during torpor. As they repeatedly experience periodic arousals that seem to interfere with protein metabolism, their study is also expected to improve the understanding of metabolic depression and muscle preservation. The small size of deep hibernators may also represent an advantage due to a usually easy handling compared to large hibernators or other heterothermic primates.

The underlying mechanisms of muscle preservation at the molecular/cellular level and at the more integrative level during the torpor state appear to slightly differ, if not substantially, between the two types of hibernators. Muscle preservation involves mechanisms of protein sparing that are specific to hibernating bears and a combination of reduced energy expenditure and protein synthesis-related compensatory processes in small hibernators. Therefore, the development of comparative studies investigating these mechanisms in a variety of heterotherms (present across a large spectrum of species from mammals, birds, and marsupials) and considering the diverse forms of hibernation or torpor known to date would largely contribute to elucidating the extraordinary ability of some hibernators to spare protein and conserve their muscles during hibernation.

AUTHOR CONTRIBUTIONS

All authors listed have made a substantial, direct and intellectual contribution to the work, and approved it for publication.

FUNDING

FB was financially supported by the CNRS (PEPS ExoMod; MyoBears program), University of Strasbourg (ProjEx H2E), and French space agency (CNES, Grant Nos. 4800000865, 800000874, 4800000974, 4800001006, and 4800001052), and SG by the Austrian Science Fund (FWF, Grant Nos. P27267-B25 and P31577-B25) and the University of Veterinary Medicine Vienna.

REFERENCES

Abernathy, R. P., and Black, D. R. (1996). Healthy body weights: an alternative perspective. *Am. J. Clin. Nutr.* 63(3 Suppl.), 448S—451S. doi: 10.1093/ajcn/63.3.448

Ahlquist, D. A., Nelson, R. A., Steiger, D. L., Jones, J. D., and Ellefson, R. D. (1984). Glycerol metabolism in the hibernating black bear. *J. Comp. Physiol. B* 155, 75–79. doi: 10.1007/Bf00688794

Al-attar, R., and Storey, K. B. (2020). Suspended in time: molecular responses to hibernation also promote longevity. *Exp. Gerontol.* 134:110889. doi: 10.1016/J.Exger.2020.110889

Anderson, K. J., Vermillion, K. L., Jagtap, P., Johnson, J. E., Griffin, T. J., and Andrews, M. T. (2016). Proteogenomic analysis of a hibernating mammal indicates contribution of skeletal muscle physiology to the hibernation phenotype. *J. Proteome Res.* 15, 1253–1261. doi: 10.1021/acs.jproteome.5b01138

Andres-Mateos, E., Brinkmeier, H., Burks, T. N., Mejias, R., Files, D. C., Steinberger, M., et al. (2013). Activation of serum/glucocorticoid-induced kinase 1 (SGK1) is important to maintain skeletal muscle homeostasis and prevent atrophy. *EMBO Mol. Med.* 5, 80–91. doi: 10.1002/emmm.201201443

Argiles, J. M., Campos, N., Lopez-Pedrosa, J. M., Rueda, R., and Rodriguez-Manas, L. (2016). Skeletal muscle regulates metabolism via interorgan crosstalk: roles in health and disease. *J. Am. Med. Dir. Assoc.* 17, 789–796. doi: 10.1016/j.jamda.2016.04.019

Armitage, K. B. (1991). Factors affecting corticosteroid concentrations in yellow-bellied marmots. *Comp. Biochem. Physiol. A Comp. Physiol.* 98, 47–54. doi: 10.1016/0300-9629(91)90576-x

Asher, R. C. Z., Burrows, T. L., and Collins, C. E. (2013). Very low-energy diets for weight loss in adults: a review. *Nutr. Diet.* 70, 101–112. doi: 10.1111/j.1747-0080.2012.01628.x

Atkinson, S. N., Nelson, R. A., and Ramsay, M. A. (1996). Changes in the body composition of fasting polar bears (*Ursus maritimus*): the effect of relative fatness on protein conservation. *Physiol. Zool.* 69, 304–316. doi: 10.1086/physzool.69.2.30164186

Azizi, F., Mannix, J. E., Howard, D., and Nelson, R. A. (1979). Effect of winter sleep on pituitary-thyroid axis in American black bear. *Am. J. Physiol.* 237, E227–E230. doi: 10.1152/ajpendo.1979.237.3.E227

Barboza, P. S., Farley, S. D., and Robbins, C. T. (1997). Whole-body urea cycling and protein turnover during hyperphagia and dormancy in growing bears (*Ursus americanus* and *U-arctos*). *Can. J. Zool.* 75, 2129–2136. doi: 10.1139/Z97-848

Barnes, B. M. (1989). Freeze avoidance in a mammal - body temperatures below 0-Degrees-C in an Arctic hibernator. *Science* 244, 1593–1595. doi: 10.1126/science.2740905

Barnes, B. M., Kretzmann, M., Licht, P., and Zucker, I. (1986). The influence of hibernation on testis growth and spermatogenesis in the golden-mantled ground-Squirrel, Spermophilus-Lateralis. *Biol. Reprod.* 35, 1289–1297. doi: 10.1095/biolreprod35.5.1289

Barnes, B. M., Kretzmann, M., Zucker, I., and Licht, P. (1988). Plasma androgen and gonadotropin levels during hibernation and testicular maturation in golden-mantled ground squirrels. *Biol. Reprod.* 38, 616–622. doi: 10.1095/biolreprod38.3.616

Baumgartner, R. N. (2000). Body composition in healthy aging. *Ann. N. Y. Acad. Sci.* 904, 437–448. doi: 10.1111/j.1749-6632.2000.tb06498.x

Bergouignan, A., Rudwill, F., Simon, C., and Blanc, S. (2011). Physical inactivity as the culprit of metabolic inflexibility: evidence from bed-rest studies. *J. Appl. Physiol.* 111, 1201–1210. doi: 10.1152/japplphysiol.00698.2011

Bernard, C. (1865). *Introduction à l'Etude de la Médecine Expérimentale*. Paris: J.B. Baillière et Fils.

Blackstone, E., Morrison, M., and Roth, M. B. (2005). H2S induces a suspended animation-like state in mice. *Science* 308, 518–518. doi: 10.1126/science.1108581

Blumenthal, S., Morgan-Boyd, R., Nelson, R., Garshelis, D. L., Turyk, M. E., and Unterman, T. (2011). Seasonal regulation of the growth hormone-insulin-like growth factor-I axis in the American black bear (*Ursus americanus*). *Am. J. Physiol. Endocrinol. Metab.* 301, E628–E636. doi: 10.1152/ajpendo.00082.2011

Bodine, S. C. (2013). Hibernation: the search for treatments to prevent disuse-induced skeletal muscle atrophy. *Exp. Neurol.* 248, 129–135. doi: 10.1016/j.expneurol.2013.06.003

Bonaldo, P., and Sandri, M. (2013). Cellular and molecular mechanisms of muscle atrophy. *Dis. Model. Mech.* 6, 25–39. doi: 10.1242/dmm.010389

Bongers, K. S., Fox, D. K., Ebert, S. M., Kunkel, S. D., Dyle, M. C., Bullard, S. A., et al. (2013). Skeletal muscle denervation causes skeletal muscle atrophy through a pathway that involves both Gadd45a and HDAC4. *Am. J. Physiol. Endocrinol. Metab.* 305, E907–E915. doi: 10.1152/ajpendo.00380.2013

Bouma, H. R., Carey, H. V., and Kroese, F. G. M. (2010). Hibernation: the immune system at rest? *J. Leukoc. Biol.* 88, 619–624. doi: 10.1189/jlb.0310174

Bouma, H. R., Kroese, F. G. M., Kok, J. W., Talaei, F., Boerema, A. S., Herwig, A., et al. (2011). Low body temperature governs the decline of circulating lymphocytes during hibernation through sphingosine-1-phosphate. *Proc. Natl. Acad. Sci. U.S.A.* 108, 2052–2057. doi: 10.1073/pnas.1008823108

Brockmann, J., Reddy, S., Coussios, C., Pigott, D., Guirriero, D., Hughes, D., et al. (2009). Normothermic perfusion: a new paradigm for organ preservation. *Ann. Surg.* 250, 1–6. doi: 10.1097/SLA.0b013e3181a63c10

Brooks, N. E., Myburgh, K. H., and Storey, K. B. (2011). Myostatin levels in skeletal muscle of hibernating ground squirrels. *J. Exp. Biol.* 214(Pt 15), 2522–2527. doi: 10.1242/jeb.055764

Brooks, N. E., Myburgh, K. H., and Storey, K. B. (2015). Muscle satellite cells increase during hibernation in ground squirrels. *Comp. Biochem. Physiol. B Biochem. Mol. Biol.* 189, 55–61. doi: 10.1016/j.cbpb.2015.07.006

Brown, D. C., Mulhausen, R. O., Andrew, D. J., and Seal, U. S. (1971). Renal function in anesthetized dormant and active bears. *Am. J. Physiol.* 220, 293–298. doi: 10.1152/ajplegacy.1971.220.1.293

Brown, J. C., and Staples, J. F. (2014). Substrate-specific changes in mitochondrial respiration in skeletal and cardiac muscle of hibernating thirteen-lined ground squirrels. *J. Comp. Physiol. B* 184, 401–414. doi: 10.1007/s00360-013-0799-3

Buck, C. L., and Barnes, B. M. (2000). Effects of ambient temperature on metabolic rate, respiratory quotient, and torpor in an arctic hibernator. *Am. J. Physiol. Regul. Integr. Comp. Physiol.* 279, R255–R262. doi: 10.1152/ajpregu.2000.279.1.R255

Burlington, R. F., and Klain, G. J. (1967). Gluconeogenesis during hibernation and arousal from hibernation. *Comp. Biochem. Physiol.* 22, 701–708. doi: 10.1016/0010-406x(67)90763-3

Buzadzic, B., Spasic, M., Saicic, Z. S., Radojicic, R., Petrovic, V. M., and Halliwell, B. (1990). Antioxidant defenses in the ground squirrel *Citellus citellus*. 2. The effect of hibernation. *Free Radic. Biol. Med.* 9, 407–413.

Cahill, G. F. Jr. (1970). Starvation in man. *N. Engl. J. Med.* 282, 668–675. doi: 10.1056/NEJM197003192821209

Calmus, Y., Cynober, L., Dousset, B., Lim, S. K., Soubrane, O., Conti, F., et al. (1995). Evidence for the detrimental role of proteolysis during liver preservation in humans. *Gastroenterology* 108, 1510–1516. doi: 10.1016/0016-5085(95)90701-7

Carey, H. V., Andrews, M. T., and Martin, S. L. (2003a). Mammalian hibernation: cellular and molecular responses to depressed metabolism and low temperature. *Physiol. Rev.* 83, 1153–1181. doi: 10.1152/physrev.00008.2003

Carey, H. V., Rhoads, C. A., and Aw, T. Y. (2003b). Hibernation induces glutathione redox imbalance in ground squirrel intestine. *J. Comp. Physiol. B* 173, 269–276. doi: 10.1007/s00360-003-0330-3

Carlson, B. M. (2014). The biology of long-term denervated skeletal muscle. *Eur. J. Transl. Myol.* 24:3293. doi: 10.4081/ejtm.2014.3293

Carneiro, I., Castro-Piedras, I., Munoz, A., Labandeira-Garcia, J. L., Devesa, J., and Arce, V. M. (2008). Hypothyroidism is associated with increased myostatin expression in rats. *J. Endocrinol. Invest.* 31, 773–778. doi: 10.1007/Bf033 49256

Carraro, U., Gava, K., Baba, A., Marcante, A., and Piccione, F. (2018). To contrast and reverse skeletal muscle atrophy by full-body in-bed gym, a mandatory lifestyle for older olds and borderline mobility-impaired persons. *Adv. Exp. Med. Biol.* 1088, 549–560. doi: 10.1007/978-981-13-1435-3_25

Castex, C., and Hoo-Paris, R. (1987). Regulation of endocrine pancreas secretions (insulin and glucagon) during the periodic lethargy-waking cycle of the hibernating mammal. *Diabete Metab.* 13, 176–181.

Castex, C., Tahri, A., Hooparis, R., and Sutter, B. C. J. (1984). Insulin-secretion in the hibernating edible dormouse (Glis-glis) – *in vivo* and *in vitro* studies. *Comp. Biochem. Physiol. A Physiol.* 79, 179–183. doi: 10.1016/0300-9629(84)90729-1

Cava, E., Yeat, N. C., and Mittendorfer, B. (2017). Preserving healthy muscle during weight loss. *Adv. Nutr.* 8, 511–519. doi: 10.3945/an.116.014506

Chanon, S., Chazarin, B., Toubhans, B., Durand, C., Chery, I., Robert, M., et al. (2018). Proteolysis inhibition by hibernating bear serum leads to increased protein content in human muscle cells. *Sci. Rep.* 8:5525. doi: 10.1038/s41598-018-23891-5

Chauhan, V. P., Tsiouris, J. A., Chauhan, A., Sheikh, A. M., Brown, W. T., and Vaughan, M. (2002). Increased oxidative stress and decreased activities of Ca(2+)/Mg(2+)-ATPase and Na(+)/K(+)-ATPase in the red blood cells of the hibernating black bear. *Life Sci.* 71, 153–161. doi: 10.1016/s0024-3205(02)01619-3

Chazarin, B., Storey, K. B., Ziemianin, A., Chanon, S., Plumel, M., Chery, I., et al. (2019a). Metabolic reprogramming involving glycolysis in the hibernating brown bear skeletal muscle. *Front. Zool.* 16:12. doi: 10.1186/s12983-019-0312-2

Chazarin, B., Ziemianin, A., Evans, A. L., Meugnier, E., Loizon, E., Chery, I., et al. (2019b). Limited oxidative stress favors resistance to skeletal muscle atrophy in hibernating brown bears (*Ursus arctos*). *Antioxidants* 8:334. doi: 10.3390/antiox8090334

Cherel, Y., El Omari, B., Le Maho, Y., and Saboureau, M. (1995). Protein and lipid utilization during fasting with shallow and deep hypothermia in the European hedgehog (*Erinaceus europaeus*). *J. Comp. Physiol. B* 164, 653–658. doi: 10.1007/BF00389807

Cherel, Y., Robin, J. P., Heitz, A., Calgari, C., and Le Maho, Y. (1992). Relationships between lipid availability and protein utilization during prolonged fasting. *J. Comp. Physiol. B* 162, 305–313. doi: 10.1007/BF00260757

Chouker, A., Bereiter-Hahn, J., Singer, D., and Heldmaier, G. (2019). Hibernating astronauts-science or fiction? *Pflugers Arch.* 471, 819–828. doi: 10.1007/s00424-018-2244-7

Chow, B. A., Donahue, S. W., Vaughan, M. R., McConkey, B., and Vijayan, M. M. (2013). Serum immune-related proteins are differentially expressed during hibernation in the American black bear. *PLoS ONE* 8:e66119. doi: 10.1371/journal.pone.0066119

Clausen, G., and Storesund, A. (1971). Electrolyte distribution and renal function in the hibernating hedgehog. *Acta Physiol. Scand.* 83, 4–12. doi: 10.1111/j.1748-1716.1971.tb05045.x

Costelli, P., Reffo, P., Penna, F., Autelli, R., Bonelli, G., and Baccino, F. A. (2005). Ca2+-dependent proteolysis in muscle wasting. *Int. J. Biochem. Cell Biol.* 37, 2134–2146. doi: 10.1016/j.biocel.2005.03.010

Cotton, C. J. (2016). Skeletal muscle mass and composition during mammalian hibernation. *J. Exp. Biol.* 219(Pt 2), 226–234. doi: 10.1242/jeb.125401

Cotton, C. J., and Harlow, H. J. (2010). Avoidance of skeletal muscle atrophy in spontaneous and facultative hibernators. *Physiol. Biochem. Zool.* 83, 551–560. doi: 10.1086/650471

Craighead, F. C., and Craighead, J. J. (1972). "Data on grizzly bear denning activities and behavior obtained by using wildlife telemetry," in *Bears: Their Biology and Management 2*, ed S. Herrero (Morges: International Association for Bear Research and Management Publisher), 84–106.

Craighead, J. J., Varney, J. R., and Summer, J. S. (1976). "Telemetry experiments with hibernating black bears", in *Bears: Their Biology and Management*, eds M. R. Pelton, J. W. Lentfer, and G. E. Folk (Morges: International Union for Conservation of Nature and Natural Resources), 357–371.

Cretoiu, S. M., and Zugravu, C. A. (2018). Nutritional considerations in preventing muscle atrophy. *Adv. Exp. Med. Biol.* 1088, 497–528. doi: 10.1007/978-981-13-1435-3_23

Cubberley, P. T., Polster, S. A., and Schulman, C. L. (1965). Lactic acidosis and death after the treatment of obesity by fasting. *N. Engl. J. Med.* 272, 628–630. doi: 10.1056/NEJM196503252721208

Daan, S., Barnes, B. M., and Strijkstra, A. M. (1991). Warming up for sleep? Ground squirrels sleep during arousals from hibernation. *Neurosci. Lett.* 128, 265–268.

Dark, J. (2005). Annual lipid cycles in hibernators: integration of physiology and behavior. *Annu. Rev. Nutr.* 25, 469–497. doi: 10.1146/annurev.nutr.25.050304.092514

Dausmann, K. H., Glos, J., Ganzhorn, J. U., and Heldmaier, G. (2004). Physiology: hibernation in a tropical primate. *Nature* 429, 825–826. doi: 10.1038/429825a

Dausmann, K. H., Glos, J., Ganzhorn, J. U., and Heldmaier, G. (2005). Hibernation in the tropics: lessons from a primate. *J. Comp. Physiol. B* 175, 147–155. doi: 10.1007/s00360-004-0470-0

Davis, W. L., Goodman, D. B., Crawford, L. A., Cooper, O. J., and Matthews, J. L. (1990). Hibernation activates glyoxylate cycle and gluconeogenesis in black bear brown adipose tissue. *Biochim. Biophys. Acta* 1051, 276–278. doi: 10.1016/0167-4889(90)90133-x

Deutz, N. E. P., Ashurst, I., Ballesteros, M. D., Bear, D. E., Cruz-Jentoft, A. J., Genton, L., et al. (2019). The underappreciated role of low muscle mass in the management of malnutrition. *J. Am. Med. Dir. Assoc.* 20, 22–27. doi: 10.1016/j.jamda.2018.11.021

Deval, C., Capel, F., Laillet, B., Polge, C., Bechet, D., Taillandier, D., et al. (2016). Docosahexaenoic acid-supplementation prior to fasting prevents muscle atrophy in mice. *J. Cachexia Sarcopenia Muscle* 7, 587–603. doi: 10.1002/jcsm.12103

Ding, S., Dai, Q., Huang, H., Xu, Y., and Zhong, C. (2018). An overview of muscle atrophy. *Adv. Exp. Med. Biol.* 1088, 3–19. doi: 10.1007/978-981-13-1435-3_1

Donahue, S. W., Galley, S. A., Vaughan, M. R., Patterson-Buckendahl, P., Demers, L. M., Vance, J. L., et al. (2006). Parathyroid hormone may maintain bone formation in hibernating black bears (*Ursus americanus*) to prevent disuse osteoporosis. *J. Exp. Biol.* 209, 1630–1638. doi: 10.1242/jeb.02185

Donahue, S. W., Vaughan, M. R., Demers, L. M., and Donahue, H. J. (2003a). Bone formation is not impaired by hibernation (disuse) in black bears Ursus americanus. *J. Exp. Biol.* 206, 4233–4239. doi: 10.1242/jeb.00671

Donahue, S. W., Vaughan, M. R., Demers, L. M., and Donahue, H. J. (2003b). Serum markers of bone metabolism show bone loss in hibernating bears. *Clin. Orthop. Relat. Res.* 408, 295–301. doi: 10.1097/01.blo.0000038054.29678.6b

Duan, K., Gao, X., and Zhu, D. (2020). The clinical relevance and mechanism of skeletal muscle wasting. *Clin. Nutr.* 40, 27–37. doi: 10.1016/j.clnu.2020.07.029

Dubois, V., Laurent, M., Boonen, S., Vanderschueren, D., and Claessens, F. (2012). Androgens and skeletal muscle: cellular and molecular action mechanisms underlying the anabolic actions. *Cell. Mol. Life Sci.* 69, 1651–1667. doi: 10.1007/s00018-011-0883-3

Epperson, L. E., Karimpour-Fard, A., Hunter, L. E., and Martin, S. L. (2011). Metabolic cycles in a circannual hibernator. *Physiol. Genomics* 43, 799–807. doi: 10.1152/physiolgenomics.00028.2011

Epperson, L. E., and Martin, S. L. (2002). Quantitative assessment of ground squirrel mRNA levels in multiple stages of hibernation. *Physiol. Genomics* 10, 93–102. doi: 10.1152/physiolgenomics.00004.2002

Epperson, L. E., Rose, J. C., Carey, H. V., and Martin, S. L. (2010). Seasonal proteomic changes reveal molecular adaptations to preserve and replenish liver proteins during ground squirrel hibernation. *Am. J. Physiol. Regul. Integr. Comp. Physiol.* 298, R329–R340. doi: 10.1152/ajpregu.00416.2009

Evans, A. L., Sahlen, V., Stoen, O. G., Fahlman, A., Brunberg, S., Madslien, K., et al. (2012). Capture, anesthesia, and disturbance of free-ranging brown bears (*Ursus arctos*) during hibernation. *PLoS ONE* 7:e40520. doi: 10.1371/journal.pone.0040520

Evans, A. L., Singh, N. J., Friebe, A., Arnemo, J. M., Laske, T. G., Frobert, O., et al. (2016). Drivers of hibernation in the brown bear. *Front. Zool.* 13:7. doi: 10.1186/s12983-016-0140-6

FAO, IFAD, UNICEF, WFP, and WHO. (2020). *The State of Food Security and Nutrition in the World 2020. Transforming Food Systems for Affordable Healthy Diets*. Rome: FAO.

Farley, S. D., and Robbins, C. T. (1995). Lactation, hibernation, and mass dynamics of American black bears and grizzly bears. *Can. J. Zool.* 73, 2216–2222. doi: 10.1139/Z95-262

Fedorov, V. B., Goropashnaya, A. V., Stewart, N. C., Toien, O., Chang, C., Wang, H., et al. (2014). Comparative functional genomics of adaptation to muscular disuse in hibernating mammals. *Mol. Ecol.* 23, 5524–5537. doi: 10.1111/mec.12963

Fedorov, V. B., Goropashnaya, A. V., Toien, O., Stewart, N. C., Chang, C., Wang, H., et al. (2011). Modulation of gene expression in heart and liver of hibernating black bears (*Ursus americanus*). *BMC Genomics* 12:171. doi: 10.1186/1471-2164-12-171

Fedorov, V. B., Goropashnaya, A. V., Toien, O., Stewart, N. C., Gracey, A. Y., Chang, C., et al. (2009). Elevated expression of protein biosynthesis genes in liver and muscle of hibernating black bears (*Ursus americanus*). *Physiol. Genomics* 37, 108–118. doi: 10.1152/physiolgenomics.90398.2008

Ferris, E., and Gregg, C. (2019). Parallel accelerated evolution in distant hibernators reveals candidate cis elements and genetic circuits regulating mammalian obesity. *Cell Rep.* 29, 2608–2620 e2604. doi: 10.1016/j.celrep.2019.10.102

Finkelstein, E. A., Khavjou, O. A., Thompson, H., Trogdon, J. G., Pan, L., Sherry, B., et al. (2012). Obesity and severe obesity forecasts through 2030. *Am. J. Prev. Med.* 42, 563–570. doi: 10.1016/j.amepre.2011.10.026

Florant, G. L., Hoo-Paris, R., Castex, C., Bauman, W. A., and Sutter, B. C. (1986). Pancreatic A and B cell stimulation in euthermic and hibernating marmots (*Marmota flaviventris*): effects of glucose and arginine administration. *J. Comp. Physiol. B* 156, 309–314. doi: 10.1007/BF01101092

Florant, G. L., Porst, H., Peiffer, A., Hudachek, S. F., Pittman, C., Summers, S. A., et al. (2004). Fat-cell mass, serum leptin and adiponectin changes during weight gain and loss in yellow-bellied marmots (*Marmota flaviventris*). *J. Comp. Physiol. B* 174, 633–639. doi: 10.1007/s00360-004-0454-0

Folk, G. E., Larson, A., and Folk, M. A. (1976). "Physiology of hibernating bears," in *Bears: Their Biology And Management*, eds M. R. Pelton, J. W. Lentfer, and G. E. Folk (Morges: International Union for Conservation of Nature and Natural Resources), 373–380.

Folk, L. C., Hunt, J. M., and Folk, M. A. (1980). "Further evidence for hibernation of bears," in *Bears: Their Biology and Management 4*, eds C. J. Martinka and K. L. Mc Arthur (Morges: International Union for Conservation of Nature and Natural Resources), 43–47. doi: 10.2307/3872841

Forbes, G. B., and Welle, S. L. (1983). Lean body mass in obesity. *Int. J. Obes.* 7, 99–107.

French, A. R. (1982). Effects of temperature on the duration of arousal episodes during hibernation. *J. Appl. Physiol.* 52, 216–220. doi: 10.1152/jappl.1982.52.1.216

French, A. R. (1985). Allometries of the durations of torpid and euthermic intervals during mammalian hibernation - a test of the theory of metabolic control of the timing of changes in body-temperature. *J. Comp. Physiol. B* 156, 13–19. doi: 10.1007/Bf00692921

French, A. R. (1988). The patterns of mammalian hibernation. *Am. Sci.* 76, 568–575.

Friebe, A., Evans, A. L., Arnemo, J. M., Blanc, S., Brunberg, S., Fleissner, G., et al. (2014). Factors affecting date of implantation, parturition, and den entry estimated from activity and body temperature in free-ranging brown bears. *PLoS ONE* 9:e101410. doi: 10.1371/journal.pone.0101410

Friebe, A., Zedrosser, A., and Swenson, J. E. (2013). Detection of pregnancy in a hibernator based on activity data. *Eur. J. Wild Res.* 59, 731–741. doi: 10.1007/s10344-013-0728-5

Frontera, W. R., and Ochala, J. (2015). Skeletal muscle: a brief review of structure and function. *Calcif. Tissue Int.* 96, 183–195. doi: 10.1007/s00223-014-9915-y

Fruebis, S., Javorschi, S., Ebbets-Reed, D., Erickson, M. R., Yen, F. T., Bihain, B. E., et al. (2001). Proteolytic cleavage product of 30-kDa adipocyte complement-related protein increases fatty acid oxidation in muscle and causes weight loss in mice. *Proc. Natl. Acad. Sci. U.S.A.* 98, 2005–2010. doi: 10.1073/pnas.041591798

Fu, W. W., Hu, H. X., Dang, K., Chang, H., Du, B., Wu, X., et al. (2016). Remarkable preservation of Ca^{2+} homeostasis and inhibition of apoptosis contribute to anti-muscle atrophy effect in hibernating Daurian ground squirrels. *Sci. Rep.* 6:27020. doi: 10.1038/Srep27020

Fuller-Jackson, J. P., and Henry, B. A. (2018). Adipose and skeletal muscle thermogenesis: studies from large animals. *J. Endocrinol.* 237, R99–R115. doi: 10.1530/JOE-18-0090

Fuster, G., Busquets, S., Almendro, V., Lopez-Soriano, F. J., and Argiles, J. M. (2007). Antiproteolytic effects of plasma from hibernating bears: a new approach for muscle wasting therapy? *Clin. Nutr.* 26, 658–661. doi: 10.1016/j.clnu.2007.07.003

Galster, W., and Morrison, P. (1976). Seasonal changes in body composition of the arctic ground squirrel, *Citellus undulatus*. *Can. J. Zool.* 54, 74–78. doi: 10.1139/z76-008

Galster, W., and Morrison, P. R. (1975). Gluconeogenesis in arctic ground squirrels between periods of hibernation. *Am. J. Physiol.* 228, 325–330. doi: 10.1152/ajplegacy.1975.228.1.325

Gao, Y., Arfat, Y., Wang, H., and Goswami, N. (2018). Muscle atrophy induced by mechanical unloading: mechanisms and potential countermeasures. *Front. Physiol.* 9:235. doi: 10.3389/fphys.2018.00235

Gao, Y. F., Wang, J., Wang, H. P., Feng, B., Dang, K., Wang, Q., et al. (2012). Skeletal muscle is protected from disuse in hibernating dauria ground squirrels. *Comp. Biochem. Physiol. A Mol. Integr. Physiol.* 161, 296–300. doi: 10.1016/j.cbpa.2011.11.009

Garshelis, D. L., and Hellgren, E. C. (1994). Variation in reproductive-biology of male black bears. *J. Mammal.* 75, 175–188. doi: 10.2307/1382249

Geiser, F. (2004). Metabolic rate and body temperature reduction during hibernation and daily torpor. *Annu. Rev. Physiol.* 66, 239–274. doi: 10.1146/annurev.physiol.66.032102.115105

Geiser, F. (2011). "Hibernation: endotherms," in *eLS subject area: Ecology*, eds J. Wiley & sons, Ltd (Chichester: John Wiley and Sons, Ltd). doi: 10.1002/9780470015902.a0003215.pub2

Geiser, F., and Drury, R. L. (2003). Radiant heat affects thermoregulation and energy expenditure during rewarming from torpor. *J. Comp. Physiol. B* 173, 55–60. doi: 10.1007/s00360-002-0311-y

Giroud, S., Chery, I., Bertile, F., Bertrand-Michel, J., Tascher, G., Gauquelin-Koch, G., et al. (2019). Lipidomics reveals seasonal shifts in a large-bodied hibernator, the brown bear. *Front. Physiol.* 10:389. doi: 10.3389/fphys.2019.00389

Giroud, S., Evans, A. L., Chery, I., Bertile, F., Tascher, G., Bertrand-Michel, J., et al. (2018). Seasonal changes in eicosanoid metabolism in the brown bear. *Sci. Nat.* 105:58. doi: 10.1007/s00114-018-1583-8

Giroud, S., Habold, C., Nespolo, R. F., Mejias, C., Terrien, J., Logan, S. M., et al. (2020). The torpid state: recent advances in metabolic adaptations and protective mechanisms. *Front. Physiol.* 11:623665. doi: 10.3389/fphys.2020.623665

Giudice, J., and Taylor, J. M. (2017). Muscle as a paracrine and endocrine organ. *Curr. Opin. Pharmacol.* 34, 49–55. doi: 10.1016/j.coph.2017.05.005

Goll, D. E., Neti, G., Mares, S. W., and Thompson, V. F. (2008). Myofibrillar protein turnover: the proteasome and the calpains. *J. Anim. Sci.* 86, E19–E35. doi: 10.2527/jas.2007-0395

Goll, D. E., Thompson, V. F., Li, H., Wei, W., and Cong, J. (2003). The calpain system. *Physiol. Rev.* 83, 731–801. doi: 10.1152/physrev.00029.2002

Gonzalez-Bernardo, E., Russo, L. F., Valderrabano, E., Fernandez, A., and Penteriani, V. (2020). Denning in brown bears. *Ecol. Evol.* 10, 6844–6862. doi: 10.1002/ece3.6372

Goodman, M. N., Lowell, B., Belur, E., and Ruderman, N. B. (1984). Sites of protein conservation and loss during starvation: influence of adiposity. *Am. J. Physiol.* 246(5 Pt 1), E383–E390. doi: 10.1152/ajpendo.1984.246.5.E383

Goropashnaya, A. V., Barnes, B. M., and Fedorov, V. B. (2020). Transcriptional changes in muscle of hibernating arctic ground squirrels (*Urocitellus parryii*): implications for attenuation of disuse muscle atrophy. *Sci. Rep.* 10:9010. doi: 10.1038/s41598-020-66030-9

Gorr, T. A. (2017). Hypometabolism as the ultimate defence in stress response: how the comparative approach helps understanding of medically relevant questions. *Acta Physiol.* 219, 409–440. doi: 10.1111/apha.12747

Graesli, A. R., Evans, A. L., Fahlman, A., Bertelsen, M. F., Blanc, S., and Arnemo, J. M. (2015). Seasonal variation in haematological and biochemical variables in free-ranging subadult brown bears (*Ursus arctos*) in Sweden. *BMC Vet. Res.* 11:301. doi: 10.1186/s12917-015-0615-2

Graf, C., and Ferrari, N. (2019). Metabolic health-the role of adipo-myokines. *Int. J. Mol. Sci.* 20:6159. doi: 10.3390/ijms20246159

Green, C. J., Brosnan, J. T., Fuller, B. J., Lowry, M., Stubbs, M., and Ross, B. D. (1984). Effect of hibernation on liver and kidney metabolism in 13-lined ground squirrels. *Comp. Biochem. Physiol. B* 79, 167–171. doi: 10.1016/0305-0491(84)90009-9

Guibert, E. E., Petrenko, A. Y., Balaban, C. L., Somov, A. Y., Rodriguez, J. V., and Fuller, B. J. (2011). Organ preservation: current concepts and new strategies for the next decade. *Transfus. Med. Hemother.* 38, 125–142. doi: 10.1159/000327033

Hadj-Moussa, H., and Storey, K. B. (2019). Bringing nature back: using hibernation to reboot organ preservation. *FEBS J.* 286, 1094–1100. doi: 10.1111/febs.14683

Hampton, M., Nelson, B. T., and Andrews, M. T. (2010). Circulation and metabolic rates in a natural hibernator: an integrative physiological model. *Am. J. Physiol. Regul. Integr. Comp. Physiol.* 299, R1478–R1488. doi: 10.1152/ajpregu.00273.2010

Harlow, H. J., Beck, T. D. I., Walters, L. M., and Greenhouse, S. S. (1990). Seasonal serum glucose, progesterone, and cortisol-levels of black bears (*Ursus-americanus*). *Can. J. Zool.* 68, 183–187. doi: 10.1139/Z90-025

Harlow, H. J., Lohuis, T., Anderson-Sprecher, R. C., and Beck, T. D. I. (2004). Body surface temperature of hibernating black bears may be related to periodic muscle activity. *J. Mammal.* 85, 414–419. doi: 10.1644/1545-1542(2004)085<0414:Bstohb>2.0.Co;2

Harlow, H. J., Lohuis, T., Beck, T. D., and Iaizzo, P. A. (2001). Muscle strength in overwintering bears. *Nature* 409:997. doi: 10.1038/35059165

Hashimoto, M., Gao, B. H., Kikuchi-Utsumi, K., Ohinata, H., and Osborne, P. G. (2002). Arousal from hibernation and BAT thermogenesis against cold: central mechanism and molecular basis. *J. Therm. Biol.* 27, 503–515. doi: 10.1016/S0306-4565(02)00024-4

Heldmaier, G., Ortmann, S., and Elvert, R. (2004). Natural hypometabolism during hibernation and daily torpor in mammals. *Respir. Physiol. Neurobiol.* 141, 317–329. doi: 10.1016/j.resp.2004.03.014

Hellgren, E. C. (1998). Physiology of hibernation in bears. *Ursus* 10, 467–477.

Hellgren, E. C., Rogers, L. L., and Seal, U. S. (1993). Serum chemistry and hematology of black bears - physiological indexes of habitat quality or seasonal patterns. *J. Mammal.* 74, 304–315. doi: 10.2307/1382385

Hellgren, E. C., Vaughan, M. R., and Kirkpatrick, R. L. (1989). Seasonal patterns in physiology and nutrition of black bears in great dismal swamp, Virginia - North-Carolina. *Can. J. Zool.* 67, 1837–1850. doi: 10.1139/Z89-262

Hershey, J. D., Robbins, C. T., Nelson, O. L., and Lin, D. C. (2008). Minimal seasonal alterations in the skeletal muscle of captive brown bears. *Physiol. Biochem. Zool.* 81, 138–147. doi: 10.1086/524391

Hilderbrand, G. V., Schwartz, C. C., Robbins, C. T., and Hanley, T. A. (2000). Effect of hibernation and reproductive status on body mass and condition of coastal brown bears. *J. Wildl. Manage.* 64, 178–183. doi: 10.2307/3802988

Hindle, A. G., Grabek, K. R., Epperson, L. E., Karimpour-Fard, A., and Martin, S. L. (2014). Metabolic changes associated with the long winter fast dominate the liver proteome in 13-lined ground squirrels. *Physiol. Genomics* 46, 348–361. doi: 10.1152/physiolgenomics.00190.2013

Hindle, A. G., Otis, J. P., Epperson, L. E., Hornberger, T. A., Goodman, C. A., Carey, H. V., et al. (2015). Prioritization of skeletal muscle growth for emergence from hibernation. *J. Exp. Biol.* 218(Pt 2), 276–284. doi: 10.1242/jeb.109512

Hissa, R. (1997). Physiology of the European brown bear (*Ursus arctos arctos*). *Ann. Zool. Fenn.* 34, 267–287.

Hissa, R., Siekkinen, J., Hohtola, E., Saarela, S., Hakala, A., and Pudas, J. (1994). Seasonal patterns in the physiology of the European brown bear (*Ursus-arctos arctos*) in Finland. *Comp. Biochem. Physiol. A Physiol.* 109, 781–791. doi: 10.1016/0300-9629(94)90222-4

Hochachka, P. W., and Guppy, M. (1987). *Metabolic Arrest and the Control of Biological Time.* Cambridge, MA: Harvard University Press.

Houmard, J. A. (2008). Intramuscular lipid oxidation and obesity. *Am. J. Physiol. Regul. Integr. Comp. Physiol.* 294, R1111–R1116. doi: 10.1152/ajpregu.00396.2007

Humphries, M. M., Kramer, D. L., and Thomas, D. W. (2003a). The role of energy availability in Mammalian hibernation: an experimental test in free-ranging eastern chipmunks. *Physiol. Biochem. Zool.* 76, 180–186. doi: 10.1086/367949

Humphries, M. M., Thomas, D. W., and Kramer, D. L. (2001). Torpor and digestion in food-storing hibernators. *Physiol. Biochem. Zool.* 74, 283–292. doi: 10.1086/319659

Humphries, M. M., Thomas, D. W., and Kramer, D. L. (2003b). The role of energy availability in Mammalian hibernation: a cost-benefit approach. *Physiol. Biochem. Zool.* 76, 165–179. doi: 10.1086/367950

Hunt, A. (2003). Musculoskeletal fitness: the keystone in overall well-being and injury prevention. *Clin. Orthop. Relat. Res.* 409, 96–105. doi: 10.1097/01.blo.0000057787.10364.4e

Ibrahim, M., Ayoub, D., Wasselin, T., Van Dorsselaer, A., Le Maho, Y., Raclot, T., et al. (2020a). Alterations in rat adipose tissue transcriptome and proteome in response to prolonged fasting. *Biol. Chem.* 401, 389–405. doi: 10.1515/hsz-2019-0184

Ibrahim, M., Wasselin, T., Challet, E., Van Dorsselaer, A., Le Maho, Y., Raclot, T., et al. (2020b). Transcriptional changes involved in atrophying muscles during prolonged fasting in rats. *Int. J. Mol. Sci.* 21:5984. doi: 10.3390/ijms21175984

Ikeda, K., Maretich, P., and Kajimura, S. (2018). The common and distinct features of brown and beige adipocytes. *Trends Endocrinol. Metab.* 29, 191–200. doi: 10.1016/j.tem.2018.01.001

Jameson, E. W., and Mead, R. A. (1964). Seasonal changes in body fat, water and basic weight in *Citellus lateralis*, *Eutamias Speciosus* and *E. Amoenus*. *J. Mammal.* 45, 359–365. doi: 10.2307/1377407

Jansen, H. T., Leise, T., Stenhouse, G., Pigeon, K., Kasworm, W., Teisberg, J., et al. (2016). The bear circadian clock doesn't 'sleep' during winter dormancy. *Front. Zool.* 13:42. doi: 10.1186/s12983-016-0173-x

Jansen, H. T., Trojahn, S., Saxton, M. W., Quackenbush, C. R., Evans Hutzenbiler, B. D., Nelson, O. L., et al. (2019). Hibernation induces widespread transcriptional remodeling in metabolic tissues of the grizzly bear. *Commun. Biol.* 2:336. doi: 10.1038/s42003-019-0574-4

Janssen, I., Heymsfield, S. B., Wang, Z. M., and Ross, R. (2000). Skeletal muscle mass and distribution in 468 men and women aged 18-88 yr. *J. Appl. Physiol.* 89, 81–88. doi: 10.1152/jappl.2000.89.1.81

Ji, L. L., and Yeo, D. (2019). Mitochondrial dysregulation and muscle disuse atrophy. *F1000Res.* 8:F1000 Faculty Rev-1621. doi: 10.12688/f1000research.19139.1

Johnson, R. J., Stenvinkel, P., Martin, S. L., Jani, A., Sanchez-Lozada, L. G., Hill, J. O., et al. (2013). Redefining metabolic syndrome as a fat storage condition based on studies of comparative physiology. *Obesity* 21, 659–664. doi: 10.1002/oby.20026

Jones, J. D., Burnett, P., and Zollman, P. (1999). The glyoxylate cycle: does it function in the dormant or active bear? *Comp. Biochem. Physiol. B Biochem. Mol. Biol.* 124, 177–179. doi: 10.1016/S0305-0491(99)00109-1

Jones, J. D., and Zollman, P. E. (1997). Black bear (*Ursus americanus*) bile composition: seasonal changes. *Comp. Biochem. Physiol. C Pharmacol. Toxicol. Endocrinol.* 118, 387–390. doi: 10.1016/s0742-8413(97)00176-x

Jorgensen, P. G., Arnemo, J., Swenson, J. E., Jensen, J. S., Galatius, S., and Frobert, O. (2014). Low cardiac output as physiological phenomenon in hibernating, free-ranging Scandinavian brown bears (*Ursus arctos*) - an observational study. *Cardiovasc. Ultrasound* 12:36. doi: 10.1186/1476-7120-12-36

Jorgensen, P. G., Evans, A., Kindberg, J., Olsen, L. H., Galatius, S., and Frobert, O. (2020). Cardiac adaptation in hibernating, free-ranging scandinavian brown bears (*Ursus arctos*). *Sci. Rep.* 10:247. doi: 10.1038/s41598-019-57126-y

Karagoz, G. E., Acosta-Alvear, D., and Walter, P. (2019). The unfolded protein response: detecting and responding to fluctuations in the protein-folding capacity of the endoplasmic reticulum. *Cold Spring Harb. Perspect. Biol.* 11:a033886. doi: 10.1101/cshperspect.a033886

Karmann, H., Mrosovsky, N., Heitz, A., and Lemaho, Y. (1994). Protein sparing on very-low-calorie diets - ground-squirrels succeed where obese people fail. *Int. J. Obes.* 18, 351–353.

Karpovich, S. A., Toien, O., Buck, C. L., and Barnes, B. M. (2009). Energetics of arousal episodes in hibernating arctic ground squirrels. *J. Comp. Physiol. B* 179, 691–700. doi: 10.1007/s00360-009-0350-8

Karstoft, K., and Pedersen, B. K. (2016). Skeletal muscle as a gene regulatory endocrine organ. *Curr. Opin. Clin. Nutr. Metab. Care* 19, 270–275. doi: 10.1097/Mco.0000000000000283

Kauffman, A. S., Paul, M. J., and Zucker, I. (2004). Increased heat loss affects hibernation in golden-mantled ground squirrels. *Am. J. Physiol. Regul. Integr. Comp. Physiol.* 287, R167–R173. doi: 10.1152/ajpregu.00670.2003

Kayser, C. (1952). Les échanges respiratoires du hamster doré (*Mesocricetus auratus*) en léthargie hivernale. *C. R. Seances Soc. Biol. Fil. CXLVI*, 929.

Kenny, H. C., Tascher, G., Ziemianin, A., Rudwill, F., Zahariev, A., Chery, I., et al. (2020). Effectiveness of resistive vibration exercise and whey protein supplementation plus alkaline salt on the skeletal muscle proteome following 21 days of bed rest in healthy males. *J. Proteome Res.* 19, 3438–3451. doi: 10.1021/acs.jproteome.0c00256

Kern, H., Gargiulo, P., Pond, A., Albertin, G., Marcante, A., and Carraro, U. (2018). To reverse atrophy of human muscles in complete SCI lower motor neuron denervation by home-based functional electrical stimulation. *Adv. Exp. Med. Biol.* 1088, 585–591. doi: 10.1007/978-981-13-1435-3_27

Kim, J. E., O'Connor, L. E., Sands, L. P., Slebodnik, M. B., and Campbell, W. W. (2016). Effects of dietary protein intake on body composition changes after weight loss in older adults: a systematic review and meta-analysis. *Nutr. Rev.* 74, 210–224. doi: 10.1093/nutrit/nuv065

Kim, T. N., Park, M. S., Ryu, J. Y., Choi, H. Y., Hong, H. C., Yoo, H. J., et al. (2014). Impact of visceral fat on skeletal muscle mass and vice versa in a prospective cohort study: the Korean Sarcopenic Obesity Study (KSOS). *PLoS ONE* 9:e115407. doi: 10.1371/journal.pone.0115407

Klug, B. J., and Brigham, R. M. (2015). Changes to metabolism and cell physiology that enable mammalian hibernation. *Sci. Rev.* 3, 39–56. doi: 10.1007/s40362-015-0030-x

Koebel, D. A., Miers, P. G., Nelson, R. A., and Steffen, J. M. (1991). Biochemical changes in skeletal muscles of denning bears (*Ursus americanus*). *Comp. Biochem. Physiol. B* 100, 377–380. doi: 10.1016/0305-0491(91)90390-Y

Kohl, H. W. III., Craig, C. L., Lambert, E. V., Inoue, S., Alkandari, J. R., Leetongin, G., et al. (2012). The pandemic of physical inactivity: global action for public health. *Lancet* 380, 294–305. doi: 10.1016/S0140-6736(12)60898-8

Krause, M. P., Milne, K. J., and Hawke, T. J. (2019). Adiponectin-consideration for its role in skeletal muscle health. *Int. J. Mol. Sci.* 20:1528. doi: 10.3390/ijms20071528

Krilowicz, B. L. (1985). Ketone body metabolism in a ground squirrel during hibernation and fasting. *Am. J. Physiol.* 249(4 Pt 2), R462–R470. doi: 10.1152/ajpregu.1985.249.4.R462

Krogh, A. (1929). The progress of physiology. *Science* 70, 200–204. doi: 10.1126/science.70.1809.200

Larkin, J. E., and Heller, H. C. (1996). Temperature sensitivity of sleep homeostasis during hibernation in the golden-mantled ground squirrel. *Am. J. Physiol. Regul. Integr. Comp. Physiol.* 270, R777–R784. doi: 10.1152/ajpregu.1996.270.4.R777

Larkin, J. E., and Heller, H. C. (1999). Sleep after arousal from hibernation is not homeostatically regulated. *Am. J. Physiol. Regul. Integr. Comp. Physiol.* 276, R522–R529. doi: 10.1152/ajpregu.1999.276.2.R522

Laske, T. G., Garshelis, D. L., and Iaizzo, P. A. (2011). Monitoring the wild black bear's reaction to human and environmental stressors. *BMC Physiol.* 11:13. doi: 10.1186/1472-6793-11-13

Le Maho, Y., Robin, J. P., and Cherel, Y. (1988). Starvation as a treatment for obesity: the need to conserve body protein. *News Physiol. Sci.* 3, 21–24. doi: 10.1152/physiologyonline.1988.3.1.21

LeBlanc, P. J., Obbard, M., Battersby, B. J., Felskie, A. K., Brown, L., Wright, P. A., et al. (2001). Correlations of plasma lipid metabolites with hibernation and lactation in wild black bears *Ursus americanus*. *J. Comp. Physiol. B* 171, 327–334. doi: 10.1007/s003600100180

Lee, H., and Ding, Y. C. (2020). Temporal limits of therapeutic hypothermia onset in clinical trials for acute ischemic stroke: how early is early enough? *Brain Circ.* 6, 139–144. doi: 10.4103/bc.bc_31_20

Lee, K., So, H., Gwag, T., Ju, H., Lee, J. W., Yamashita, M., et al. (2010). Molecular mechanism underlying muscle mass retention in hibernating bats: role of periodic arousal. *J. Cell. Physiol.* 222, 313–319. doi: 10.1002/jcp.21952

Lin, D. C., Egeland, L. A., Schertenleib, K. W., Nelson, O. L., and Robbins, C. T. (2004). "Intermittent muscle activation in grizzly bears during hibernation: a strategy to prevent muscle atrophy?" in *Society for Neuroscience Annual Meeting Program* (San Diego, CA: Society for Neuroscience).

Lin, D. C., Hershey, J. D., Mattoon, J. S., and Robbins, C. T. (2012). Skeletal muscles of hibernating brown bears are unusually resistant to effects of denervation. *J. Exp. Biol.* 215(Pt 12), 2081–2087. doi: 10.1242/jeb.066134

Liu, Y., and Sweeney, G. (2014). Adiponectin action in skeletal muscle. *Best Pract. Res. Clin. Endocrinol. Metab.* 28, 33–41. doi: 10.1016/j.beem.2013.08.003

Lohuis, T. D., Harlow, H. J., and Beck, T. D. (2007a). Hibernating black bears (*Ursus americanus*) experience skeletal muscle protein balance during winter anorexia. *Comp. Biochem. Physiol. B Biochem. Mol. Biol.* 147, 20–28. doi: 10.1016/j.cbpb.2006.12.020

Lohuis, T. D., Harlow, H. J., Beck, T. D., and Iaizzo, P. A. (2007b). Hibernating bears conserve muscle strength and maintain fatigue resistance. *Physiol. Biochem. Zool.* 80, 257–269. doi: 10.1086/513190

Lovegrove, B. G., Lobban, K. D., and Levesque, D. L. (2014). Mammal survival at the Cretaceous-Palaeogene boundary: metabolic homeostasis in prolonged tropical hibernation in tenrecs. *Proc. Biol. Sci.* 281:20141304. doi: 10.1098/rspb.2014.1304

Lovegrove, B. G., and McKechnie, A. E. (2008). *Hypometabolism in Animals: Torpor, Hibernation and Cryobiology*. Pietermaritzburg: University of KwaZulu-Natal.

Lowell, B. B., and Goodman, M. N. (1987). Protein sparing in skeletal muscle during prolonged starvation. Dependence on lipid fuel availability. *Diabetes* 36, 14–19. doi: 10.2337/diab.36.1.14

Lundberg, D. A., Nelson, R. A., Wahner, H. W., and Jones, J. D. (1976). Protein metabolism in the black bear before and during hibernation. *Mayo Clin. Proc.* 51, 716–722.

Luu, B. E., Lefai, E., Giroud, S., Swenson, J. E., Chazarin, B., Gauquelin-Koch, G., et al. (2020). MicroRNAs facilitate skeletal muscle maintenance and metabolic suppression in hibernating brown bears. *J. Cell. Physiol.* 235, 3984–3993. doi: 10.1002/jcp.29294

Lyman, C. P., Willis, J. S., Malan, A., and Wang, L. C. H. (1982). *Hibernation and Torpor in Mammals and Birds*. New York, NY: Academic Press. doi: 10.1016/C2012-0-01593-1

MacDonald, J. A., and Storey, K. B. (1999). Regulation of ground squirrel Na+K+-ATPase activity by reversible phosphorylation during hibernation. *Biochem. Biophys. Res. Commun.* 254, 424–429. doi: 10.1006/bbrc.1998.9960

Malan, A. (1980). "Enzyme regulation, metabolic rate and acid-base state in hibernation," in *Animals and Environmental Fitness*, ed R. Gilles (Oxford: Pergamon Press), 487–501.

Malan, A. (1986). "pH as a control factor in hibernation," in *Living in the Cold*, eds H. C. Heller, X. J. Musacchia, and L. C. H. Wang (New York, NY: Elsevier), 61–70.

Malan, A. (2014). The evolution of mammalian hibernation: lessons from comparative acid-base physiology. *Integr. Comp. Biol.* 54, 484–496. doi: 10.1093/icb/icu002

Malan, A., Ciocca, D., Challet, E., and Pevet, P. (2018). Implicating a temperature-dependent clock in the regulation of torpor bout duration in classic hibernation. *J. Biol. Rhythms* 33, 626–636. doi: 10.1177/0748730418797820

Malan, A., Mioskowski, E., and Calgari, C. (1988). Time-course of blood acid-base state during arousal from hibernation in the European hamster. *J. Comp. Physiol. B* 158, 495–500. doi: 10.1007/BF00691147

Malatesta, M., Perdoni, F., Battistelli, S., Muller, S., and Zancanaro, C. (2009). The cell nuclei of skeletal muscle cells are transcriptionally active in hibernating edible dormice. *BMC Cell Biol.* 10:19. doi: 10.1186/1471-2121-10-19

Markworth, J. F., and Cameron-Smith, D. (2013). Arachidonic acid supplementation enhances *in vitro* skeletal muscle cell growth via a COX-2-dependent pathway. *Am. J. Physiol. Cell Physiol.* 304, C56–C67. doi: 10.1152/ajpcell.00038.2012

Martin, A. I., Priego, T., and Lopez-Calderon, A. (2018). Hormones and muscle atrophy. *Adv. Exp. Med. Biol.* 1088, 207–233. doi: 10.1007/978-981-13-1435-3_9

Martin, S. L. (2008). Mammalian hibernation: a naturally reversible model for insulin resistance in man? *Diab. Vasc. Dis. Res.* 5, 76–81. doi: 10.3132/dvdr.2008.013

Masaki, T., Chiba, S., Yasuda, T., Tsubone, T., Kakuma, T., Shimomura, I., et al. (2003). Peripheral, but not central, administration of adiponectin reduces visceral adiposity and upregulates the expression of uncoupling protein in agouti yellow (Ay/a) obese mice. *Diabetes* 52, 2266–2273. doi: 10.2337/diabetes.52.9.2266

Matson, J. R. (1954). Observations on the dormant phase of a female black bear. *J. Mammal.* 35, 28–35. doi: 10.2307/1376069

McCain, S., Ramsay, E., and Kirk, C. (2013). The effects of hibernation and captivity on glucose metabolism and thyroid hormones in American black bear (*Ursus americanus*). *J. Zoo Wildl. Med.* 44, 324–332. doi: 10.1638/2012-0146R1.1

McCormick, R., and Vasilaki, A. (2018). Age-related changes in skeletal muscle: changes to life-style as a therapy. *Biogerontology* 19, 519–536. doi: 10.1007/s10522-018-9775-3

McGee-Lawrence, M., Buckendahl, P., Carpenter, C., Henriksen, K., Vaughan, M., and Donahue, S. (2015). Suppressed bone remodeling in black bears conserves energy and bone mass during hibernation. *J. Exp. Biol.* 218(Pt 13), 2067–2074. doi: 10.1242/jeb.120725

McLeod, M., Breen, L., Hamilton, D. L., and Philp, A. (2016). Live strong and prosper: the importance of skeletal muscle strength for healthy ageing. *Biogerontology* 17, 497–510. doi: 10.1007/s10522-015-9631-7

McMillin, J. M., Seal, U. S., Rogers, L., and Erickson, A. W. (1976). Annual testosterone rhythm in the black bear (*Ursus americanus*). *Biol. Reprod.* 15, 163–167. doi: 10.1095/biolreprod15.2.163

Mera, P., Laue, K., Wei, J. W., Berger, J. M., and Karsenty, G. (2016). Osteocalcin is necessary and sufficient to maintain muscle mass in older mice. *Mol. Metab.* 5, 1042–1047. doi: 10.1016/j.molmet.2016.07.002

Miyazaki, M., Shimozuru, M., and Tsubota, T. (2015). Altered signaling pathway governing protein metabolism in skeletal muscle of the Japanese black bear during hibernation. *FASEB J.* 29:LB698. doi: 10.1096/fasebj.29.1_supplement.lb698

Miyazaki, M., Shimozuru, M., and Tsubota, T. (2019). Skeletal muscles of hibernating black bears show minimal atrophy and phenotype shifting despite prolonged physical inactivity and starvation. *PLoS ONE* 14:e0215489. doi: 10.1371/journal.pone.0215489

Mokrasch, L. C., Grady, H. J., and Grisolia, S. (1960). Thermogenic and adaptive mechanisms in hibernation and arousal from hibernation. *Am. J. Physiol.* 199, 945–949. doi: 10.1152/ajplegacy.1960.199.5.945

Morin, P. J., and Storey, K. B. (2006). Evidence for a reduced transcriptional state during hibernation in ground squirrels. *Cryobiology* 53, 310–318. doi: 10.1016/j.cryobiol.2006.08.002

Morin, P. Jr., Dubuc, A., and Storey, K. B. (2008). Differential expression of microRNA species in organs of hibernating ground squirrels: a role in translational suppression during torpor. *Biochim. Biophys. Acta* 1779, 628–633. doi: 10.1016/j.bbagrm.2008.07.011

Mrosovsky, N., and Sherry, D. F. (1980). Animal anorexias. *Science* 207, 837–842. doi: 10.1126/science.6928327

Mugahid, D. A., Sengul, T. G., You, X., Wang, Y., Steil, L., Bergmann, N., et al. (2019). Proteomic and transcriptomic changes in hibernating grizzly bears reveal metabolic and signaling pathways that protect against muscle atrophy. *Sci. Rep.* 9:19976. doi: 10.1038/s41598-019-56007-8

Murphy, B., Bhattacharya, R., and Mukherjee, P. (2019). Hydrogen sulfide signaling in mitochondria and disease. *FASEB J.* 33, 13098–13125. doi: 10.1096/fj.201901304R

Musacchia, X. J., Steffen, J. M., and Fell, R. D. (1988). Disuse atrophy of skeletal muscle: animal models. *Exerc. Sport Sci. Rev.* 16, 61–87.

Narici, M. V., and de Boer, M. D. (2011). Disuse of the musculo-skeletal system in space and on earth. *Eur. J. Appl. Physiol.* 111, 403–420. doi: 10.1007/s00421-010-1556-x

Nasralla, D., Coussios, C. C., Mergental, H., Akhtar, M. Z., Butler, A. J., Ceresa, C. D. L., et al. (2018). A randomized trial of normothermic preservation in liver transplantation. *Nature* 557, 50–56. doi: 10.1038/s41586-018-0047-9

Nedergaard, J., and Cannon, B. (1990). Mammalian hibernation. *Philos. Trans. R Soc. Lond. B Biol. Sci.* 326, 669–685, discussion 685–666. doi: 10.1098/rstb.1990.0038

Nelson, O. L., and Robbins, C. T. (2010). Cardiac function adaptations in hibernating grizzly bears (*Ursus arctos horribilis*). *J. Comp. Physiol. B* 180, 465–473. doi: 10.1007/s00360-009-0421-x

Nelson, O. L., and Robbins, C. T. (2015). Cardiovascular function in large to small hibernators: bears to ground squirrels. *J. Comp. Physiol. B* 185, 265–279. doi: 10.1007/s00360-014-0881-5

Nelson, O. L., Robbins, C. T., Wu, Y., and Granzier, H. (2008). Titin isoform switching is a major cardiac adaptive response in hibernating grizzly bears. *Am. J. Physiol. Heart Circ. Physiol.* 295, H366–H371. doi: 10.1152/ajpheart.00234.2008

Nelson, R. A. (1973). Winter sleep in the black bear. A physiologic and metabolic marvel. *Mayo Clin. Proc.* 48, 733–737.

Nelson, R. A. (1978). Urea metabolism in the hibernating black bear. *Kidney Int. Suppl.* 8, S177–S179.

Nelson, R. A., Jones, J. D., Wahner, H. W., McGill, D. B., and Code, C. F. (1975). Nitrogen metabolism in bears: urea metabolism in summer starvation and in winter sleep and role of urinary bladder in water and nitrogen conservation. *Mayo Clin. Proc.* 50, 141–146.

Nelson, R. A., Wahner, H. W., Jones, J. D., Ellefson, R. D., and Zollman, P. E. (1973). Metabolism of bears before, during, and after winter sleep. *Am. J. Physiol.* 224, 491–496. doi: 10.1152/ajplegacy.1973.224.2.491

Nelson, R. A., Wellik, D. L., McMillin, J. M., and Palumbo, P. J. (1978). Role of testosterone in hibernating black bears. *Physiologist* 21:84.

Nowack, J., Giroud, S., Arnold, W., and Ruf, T. (2017). Muscle non-shivering thermogenesis and its role in the evolution of endothermy. *Front. Physiol.* 8:889. doi: 10.3389/Fphys.2017.00889

Nowack, J., Levesque, D. L., Reher, S., and Daussmann, K. H. (2020). Variable climates lead to varying phenotypes: 'weird' mammalian torpor and lessons from lower latitudes. *Front. Ecol. Evol.* 8:60. doi: 10.3389/fevo.2020.00060

Nowell, M. M., Choi, H., and Rourke, B. C. (2011). Muscle plasticity in hibernating ground squirrels (*Spermophilus lateralis*) is induced by seasonal, but not low-temperature, mechanisms. *J. Comp. Physiol. B* 181, 147–164. doi: 10.1007/s00360-010-0505-7

Oftedal, O. T., Alt, G. L., Widdowson, E. M., and Jakubasz, M. R. (1993). Nutrition and growth of suckling black bears (*Ursus-americanus*) during their mothers winter fast. *Br. J. Nutr.* 70, 59–79. doi: 10.1079/Bjn19930105

Oliver, S. R., Anderson, K. J., Hunstiger, M. M., and Andrews, M. T. (2019). Turning down the heat: down-regulation of sarcolipin in a hibernating mammal. *Neurosci. Lett.* 696, 13–19. doi: 10.1016/j.neulet.2018.11.059

Osborne, P. G., and Hashimoto, M. (2003). State-dependent regulation of cortical blood flow and respiration in hamsters: response to hypercapnia during arousal from hibernation. *J. Physiol.* 547(Pt 3), 963–970. doi: 10.1113/jphysiol.2002.033571

Owen, O. E., Smalley, K. J., D'Alessio, D. A., Mozzoli, M. A., and Dawson, E. K. (1998). Protein, fat, and carbohydrate requirements during starvation: anaplerosis and cataplerosis. *Am. J. Clin. Nutr.* 68, 12–34. doi: 10.1093/ajcn/68.1.12

Owens, D. J. (2018). Nutritional support to counteract muscle atrophy. *Adv. Exp. Med. Biol.* 1088, 483–495. doi: 10.1007/978-981-13-1435-3_22

Palmer, S. S., Nelson, R. A., Ramsay, M. A., Stirling, I., and Bahr, J. M. (1988). Annual changes in serum sex steroids in male and female black (*Ursus-americanus*) and polar (*Ursus-maritimus*) bears. *Biol. Reprod.* 38, 1044–1050. doi: 10.1095/biolreprod38.5.1044

Palumbo, P. J., Wellik, D. L., Bagley, N. A., and Nelson, R. A. (1983). Insulin and glucagon responses in the hibernating black bear. *Int. Conf. Bear Res. Manage.* 5, 291–296. doi: 10.2307/3872552

Parretti, H. M., Jebb, S. A., Johns, D. J., Lewis, A. L., Christian-Brown, A. M., and Aveyard, P. (2016). Clinical effectiveness of very-low-energy diets in the management of weight loss: a systematic review and meta-analysis of randomized controlled trials. *Obes. Rev.* 17, 225–234. doi: 10.1111/obr.12366

Patel, Z. S., Brunstetter, T. J., Tarver, W. J., Whitmire, A. M., Zwart, S. R., Smith, S. M., et al. (2020). Red risks for a journey to the red planet: the highest priority human health risks for a mission to Mars. *NPJ Microgravity* 6:33. doi: 10.1038/s41526-020-00124-6

Periasamy, M., Herrera, J. L., and Reis, F. C. G. (2017). Skeletal muscle thermogenesis and its role in whole body energy metabolism. *Diabetes Metab. J.* 41, 327–336. doi: 10.4093/dmj.2017.41.5.327

Powers, S. K., Morton, A. B., Ahn, B., and Smuder, A. J. (2016). Redox control of skeletal muscle atrophy. *Free Radic. Biol. Med.* 98, 208–217. doi: 10.1016/j.freeradbiomed.2016.02.021

Prado, C. M., Wells, J. C., Smith, S. R., Stephan, B. C., and Siervo, M. (2012). Sarcopenic obesity: a critical appraisal of the current evidence. *Clin. Nutr.* 31, 583–601. doi: 10.1016/j.clnu.2012.06.010

Prendergast, B. J., Freeman, D. A., Zucker, I., and Nelson, R. J. (2002). Periodic arousal from hibernation is necessary for initiation of immune responses in ground squirrels. *Am. J. Physiol. Regul. Integr. Comp. Physiol.* 282, R1054–R1062. doi: 10.1152/ajpregu.00562.2001

Quinones, Q. J., Ma, Q., Zhang, Z. Q., Barnes, B. M., and Podgoreanu, M. V. (2014). Organ protective mechanisms common to extremes of physiology: a window through hibernation biology. *Integr. Comp. Biol.* 54, 497–515. doi: 10.1093/icb/icu047

Rabelo, M., de Moura Juca, R. V. B., Lima, L. A. O., Resende-Martins, H., Bo, A. P. L., Fattal, C., et al. (2018). Overview of FES-assisted cycling approaches and their benefits on functional rehabilitation and muscle atrophy. *Adv. Exp. Med. Biol.* 1088, 561–583. doi: 10.1007/978-981-13-1435-3_26

Ratigan, E. D., and McKay, D. B. (2016). Exploring principles of hibernation for organ preservation. *Transplant. Rev.* 30, 13–19. doi: 10.1016/j.trre.2015.08.002

Rauch, J. C., and Behrisch, H. W. (1981). Ketone-bodies - a source of energy during hibernation. *Can. J. Zool.* 59, 754–760. doi: 10.1139/Z81-108

Regan, M. I., Chiang, E., Martin, S. L., Porte, W. P., Assadi-Porter, F. M., and Carey, H. V. (2019). Shifts in metabolic fuel use coincide with maximal rates of ventilation and body surface rewarming in an arousing hibernator. *Am. J. Physiol. Regul. Integr. Comp. Physiol.* 316, R764–R775. doi: 10.1152/ajpregu.00379.2018

Revsbech, I. G., Shen, X., Chakravarti, R., Jensen, F. B., Thiel, B., Evans, A. L., et al. (2014). Hydrogen sulfide and nitric oxide metabolites in the blood of free-ranging brown bears and their potential roles in hibernation. *Free Radic. Biol. Med.* 73, 349–357. doi: 10.1016/j.freeradbiomed.2014.05.025

Rice, S. A., Ten Have, G. A. M., Reisz, J. A., Gehrke, S., Stefanoni, D., Frare, C., et al. (2020). Nitrogen recycling buffers against ammonia toxicity from skeletal muscle breakdown in hibernating arctic ground squirrels. *Nat. Metab.* 2, 1459–1471. doi: 10.1038/s42255-020-00312-4

Riedesel, M. L., and Steffen, J. M. (1980). Protein metabolism and urea recycling in rodent hibernators. *Fed. Proc.* 39, 2959–2963.

Rigano, K. S., Gehring, J. L., Hutzenbiler, B. D. E., Chen, A. V., Nelson, O. L., Vella, C. A., et al. (2017). Life in the fat lane: seasonal regulation of insulin sensitivity, food intake, and adipose biology in brown bears. *J. Comp. Physiol. B* 187, 649–676. doi: 10.1007/s00360-016-1050-9

Riley, D. A., Van Dyke, J. M., Vogel, V., Curry, B. D., Bain, J. L. W., Schuett, R., et al. (2018). Soleus muscle stability in wild hibernating black bears. *Am. J. Physiol. Regul. Integr. Comp. Physiol.* 315, R369–R379. doi: 10.1152/ajpregu.00060.2018

Rimando, A. M., Kalt, W., Magee, J. B., Dewey, J., and Ballington, J. R. (2004). Resveratrol, pterostilbene, and piceatannol in vaccinium berries. *J. Agric. Food Chem.* 52, 4713–4719. doi: 10.1021/jf040095e

Roh, E., and Choi, K. M. (2020). Health consequences of sarcopenic obesity: a narrative review. *Front. Endocrinol.* 11:332. doi: 10.3389/fendo.2020.00332

Rolfe, D. F., and Brown, G. C. (1997). Cellular energy utilization and molecular origin of standard metabolic rate in mammals. *Physiol. Rev.* 77, 731–758. doi: 10.1152/physrev.1997.77.3.731

Rourke, B. C., Cotton, C. J., Harlow, H. J., and Caiozzo, V. J. (2006). Maintenance of slow type I myosin protein and mRNA expression in overwintering prairie dogs (*Cynomys leucurus* and ludovicianus) and black bears (*Ursus americanus*). *J. Comp. Physiol. B* 176, 709–720. doi: 10.1007/s00360-006-0093-8

Rourke, B. C., Yokoyama, Y., Milsom, W. K., and Caiozzo, V. J. (2004). Myosin isoform expression and MAFbx mRNA levels in hibernating golden-mantled ground squirrels (*Spermophilus lateralis*). *Physiol. Biochem. Zool.* 77, 582–593. doi: 10.1086/421753

Rowland, L. A., Bal, N. C., and Periasamy, M. (2015). The role of skeletal-muscle-based thermogenic mechanisms in vertebrate endothermy. *Biol. Rev.* 90, 1279–1297. doi: 10.1111/brv.12157

Roy, B., Curtis, M. E., Fears, L. S., Nahashon, S. N., and Fentress, H. M. (2016). Molecular mechanisms of obesity-induced osteoporosis and muscle atrophy. *Front. Physiol.* 7:439. doi: 10.3389/fphys.2016.00439

Ruderman, N. B. (1975). Muscle amino acid metabolism and gluconeogenesis. *Annu. Rev. Med.* 26, 245–258. doi: 10.1146/annurev.me.26.020175.001333

Rudrappa, S. S., Wilkinson, D. J., Greenhaff, P. L., Smith, K., Idris, I., and Atherton, P. J. (2016). Human skeletal muscle disuse atrophy: effects on muscle protein synthesis, breakdown, and insulin resistance-a qualitative review. *Front. Physiol.* 7:361. doi: 10.3389/fphys.2016.00361

Ruf, T., and Geiser, F. (2015). Daily torpor and hibernation in birds and mammals. *Biol. Rev. Camb. Philos. Soc.* 90, 891–926. doi: 10.1111/brv.12137

Sahdo, B., Evans, A. L., Arnemo, J. M., Frobert, O., Sarndahl, E., and Blanc, S. (2013). Body temperature during hibernation is highly correlated with a decrease in circulating innate immune cells in the brown bear (*Ursus arctos*): a common feature among hibernators? *Int. J. Med. Sci.* 10, 508–514. doi: 10.7150/ijms.4476

Sakuma, K., and Yamaguchi, A. (2018). Drugs of muscle wasting and their therapeutic targets. *Adv. Exp. Med. Biol.* 1088, 463–481. doi: 10.1007/978-981-13-1435-3_21

Salmov, N. N., Vikhlyantsev, I. M., Ulanova, A. D., Gritsyna, Y. V., Bobylev, A. G., Saveljev, A. P., et al. (2015). Seasonal changes in isoform composition of giant proteins of thick and thin filaments and titin (connectin) phosphorylation level in striated muscles of bears (Ursidae, Mammalia). *Biochemistry* 80, 343–355. doi: 10.1134/S0006297915030098

Salvatore, D., Simonides, W. S., Dentice, M., Zavacki, A. M., and Larsen, P. R. (2014). Thyroid hormones and skeletal muscle-new insights and potential implications. *Nat. Rev. Endocrinol.* 10, 206–214. doi: 10.1038/nrendo.2013.238

Sandell, M. (1990). The evolution of seasonal delayed implantation. *Q. Rev. Biol.* 65, 23–42. doi: 10.1086/416583

Schardong, J., Marcolino, M. A. Z., and Plentz, R. D. M. (2018). Muscle atrophy in chronic kidney disease. *Adv. Exp. Med. Biol.* 1088, 393–412. doi: 10.1007/978-981-13-1435-3_18

Schiaffino, S., Dyar, K. A., Ciciliot, S., Blaauw, B., and Sandri, M. (2013). Mechanisms regulating skeletal muscle growth and atrophy. *FEBS J.* 280, 4294–4314. doi: 10.1111/febs.12253

Schmidt, K. E., and Kelley, K. M. (2001). Down-regulation in the insulin-like growth factor (IGP) axis during hibernation in the golden-mantled ground squirrel, *Spermophilus lateralis*: IG-F-I and the IGF-binding proteins (IGFBPs). *J. Exp. Zool.* 289, 66–73. doi: 10.1002/1097-010x(20010101/31)289:1<66::Aid-Jez7>3.0.Co;2-Q

Scholander, P. F., Hock, R., Walters, V., Johnson, F., and Irving, L. (1950a). Heat regulation in some arctic and tropical mammals and birds. *Biol. Bull.* 99, 237–258. doi: 10.2307/1538741

Scholander, P. F., Walters, V., Hock, R., and Irving, L. (1950b). Body insulation of some arctic and tropical mammals and birds. *Biol. Bull.* 99, 225–236. doi: 10.2307/1538740

Sedivy, J. M. (2009). How to learn new and interesting things from model systems based on "exotic" biological species. *Proc. Natl. Acad. Sci. U.S.A.* 106, 19207–19208. doi: 10.1073/pnas.0911232106

Seger, R. L., Cross, R. A., Rosen, C. J., Causey, R. C., Gundberg, C. M., Carpenter, T. O., et al. (2011). Investigating the mechanism for maintaining eucalcemia despite immobility and anuria in the hibernating American black bear (*Ursus americanus*). *Bone* 49, 1205–1212. doi: 10.1016/j.bone.2011.08.017

Serkova, N. J., Rose, J. C., Epperson, L. E., Carey, H. V., and Martin, S. L. (2007). Quantitative analysis of liver metabolites in three stages of the circannual hibernation cycle in 13-lined ground squirrels by NMR. *Physiol. Genomics* 31, 15–24. doi: 10.1152/physiolgenomics.00028.2007

Shen, L., Meng, X., Zhang, Z., and Wang, T. (2018). Physical exercise for muscle atrophy. *Adv. Exp. Med. Biol.* 1088, 529–545. doi: 10.1007/978-981-13-1435-3_24

Shenkman, B. S., and Nemirovskaya, T. L. (2008). Calcium-dependent signaling mechanisms and soleus fiber remodeling under gravitational unloading. *J. Muscle Res. Cell Motil.* 29, 221–230. doi: 10.1007/s10974-008-9164-7

Shimozuru, M., Kamine, A., and Tsubota, T. (2012). Changes in expression of hepatic genes involved in energy metabolism during hibernation in captive, adult, female Japanese black bears (*Ursus thibetanus japonicus*). *Comp. Biochem. Physiol. B Biochem. Mol. Biol.* 163, 254–261. doi: 10.1016/j.cbpb.2012.06.007

Shimozuru, M., Nagashima, A., Tanaka, J., and Tsubota, T. (2016). Seasonal changes in the expression of energy metabolism-related genes in white adipose tissue and skeletal muscle in female Japanese black bears. *Comp. Biochem. Physiol. B Biochem. Mol. Biol.* 196-197, 38–47. doi: 10.1016/j.cbpb.2016.02.001

Shivatcheva, T. M., Ankov, V. K., and Hadjioloff, A. I. (1988). Circannual fluctuations of the serum cortisol in the European ground squirrel, *Citellus citellus* L. *Comp. Biochem. Physiol. A Comp. Physiol.* 90, 515–518. doi: 10.1016/0300-9629(88)90229-0

Silber, T. (1984). Anorexia nervosa: morbidity and mortality. *Pediatr. Ann.* 13, 851, 855–859.

Singer, D. (2006). Human hibernation for space flight: utopistic vision or realistic possibility? *J. Br. Interplanet.* 59, 139–143.

Sisto, I. R., Hauck, M., and Plentz, R. D. M. (2018). Muscular atrophy in cardiovascular disease. *Adv. Exp. Med. Biol.* 1088, 369–391. doi: 10.1007/978-981-13-1435-3_17

Smith, G. I., Julliand, S., Reeds, D. N., Sinacore, D. R., Klein, S., and Mittendorfer, B. (2015). Fish oil-derived n-3 PUFA therapy increases muscle mass and function in healthy older adults. *Am. J. Clin. Nutr.* 102, 115–122. doi: 10.3945/ajcn.114.105833

Song, M., Xia, L., Liu, Q., Sun, M., Wang, F., and Yang, C. (2018). Sarcopenia in liver disease: current evidence and issues to be resolved. *Adv Exp Med Biol* 1088, 413–433. doi: 10.1007/978-981-13-1435-3_19

Soo, E., Welch, A., Marsh, C., and McKay, D. B. (2020). Molecular strategies used by hibernators: Potential therapeutic directions for ischemia reperfusion injury and preservation of human donor organs. *Transplant. Rev.* 34:100512. doi: 10.1016/J.Trre.2019.100512

South, F. E., and House, W. A. (1967). "Energy metabolism in hibernation," in *Mammalian Hibernation III*, eds K. C. Fisher, A. R. Dawe, C. P. Lyman, E. Schonbaum, and F. E. South (London: Oliver and Boyd), 305–324.

Spady, T. J., Lindburg, D. G., and Durrant, B. S. (2007). Evolution of reproductive seasonality in bears. *Mamm. Rev.* 37, 21–53. doi: 10.1111/j.1365-2907.2007.00096.x

Staples, J. F. (2014). Metabolic suppression in mammalian hibernation: the role of mitochondria. *J. Exp. Biol.* 217(Pt 12), 2032–2036. doi: 10.1242/jeb.092973

Staples, J. F. (2016). Metabolic flexibility: hibernation, torpor, and estivation. *Compr. Physiol.* 6, 737–771. doi: 10.1002/cphy.c140064

Staples, J. F., and Brown, J. C. (2008). Mitochondrial metabolism in hibernation and daily torpor: a review. *J. Comp. Physiol. B* 178, 811–827. doi: 10.1007/s00360-008-0282-8

Steffen, J. M., Koebel, D. A., Musacchia, X. J., and Milsom, W. K. (1991). Morphometric and metabolic indexes of disuse in muscles of hibernating ground-squirrels. *Comp. Biochem. Physiol. B Biochem. Mol. Biol.* 99, 815–819. doi: 10.1016/0305-0491(91)90147-6

Steffen, J. M., and Musacchia, X. J. (1984). Effect of hypokinesia and hypodynamia on protein, RNA, and DNA in rat hindlimb muscles. *Am. J. Physiol.* 247(4 Pt 2), R728–732. doi: 10.1152/ajpregu.1984.247.4.R728

Stein, T. P., and Wade, C. E. (2005). Metabolic consequences of muscle disuse atrophy. *J. Nutr.* 135, 1824S−1828S. doi: 10.1093/jn/135.7.1824S

Stenset, N. E., Lutnaes, P. N., Bjarnadottir, V., Dahle, B., Fossum, K. H., Jigsved, P., et al. (2016). Seasonal and annual variation in the diet of brown bears Ursus arctos in the boreal forest of southcentral Sweden. *Wild. Biol.* 22, 107–116. doi: 10.2981/wlb.00194

Stenvinkel, P., Frobert, O., Anderstam, B., Palm, F., Eriksson, M., Bragfors-Helin, A. C., et al. (2013). Metabolic changes in summer active and anuric hibernating free-ranging brown bears (*Ursus arctos*). *PLoS ONE* 8:e72934. doi: 10.1371/journal.pone.0072934

Stenvinkel, P., Painer, J., Kuro-o, M., Lanaspa, M., Arnold, W., Ruf, T., et al. (2018). Novel treatment strategies for chronic kidney disease: insights from the animal kingdom. *Nat. Rev. Nephrol.* 14, 265–284. doi: 10.1038/nrneph.2017.169

Stewart, W. K., and Fleming, L. B. (1973). Features of successful therapeutic fast of 382 days' duration. *Postgrad. Med. J.* 49, 203–209. doi: 10.1136/pgmj.49.569.203

Storey, K. B. (2010). Out cold: biochemical regulation of mammalian hibernation - a mini-review. *Gerontology* 56, 220–230. doi: 10.1159/000228829

Storey, K. B., and Storey, J. M. (2010). Metabolic rate depression: the biochemistry of mammalian hibernation. *Adv. Clin. Chem.* 52, 77–108.

Strijkstra, A. M., and Daan, S. (1998). Dissimilarity of slow-wave activity enhancement by torpor and sleep deprivation in a hibernator. *Am. J. Physiol. Regul. Integr. Comp. Physiol.* 275, R1110–R1117. doi: 10.1152/ajpregu.1998.275.4.R1110

Svihla, A., and Bowman, H. S. (1954). Hibernation in the American Black Bear. *Am. Midl. Nat.* 52, 248–252. doi: 10.2307/2422063

Swenson, J. E., Adamic, M., Huber, D., and Stokke, S. (2007). Brown bear body mass and growth in northern and southern Europe. *Oecologia* 153, 37–47. doi: 10.1007/s00442-007-0715-1

Talaei, F. (2014). Modulation of mTOR and autophagy in hibernating hamster lung and the application of the potential mechanism to improve the recellularization process of decellularized lung scaffolds. *J. Regener. Med. Tissue Eng.* 3, 1–10. doi: 10.7243/2050-1218-3-1

Tascher, G., Brioche, T., Maes, P., Chopard, A., O'Gorman, D., Gauquelin-Koch, G., et al. (2017). Proteome-wide adaptations of mouse skeletal muscles during a full month in space. *J. Proteome Res.* 16, 2623–2638. doi: 10.1021/acs.jproteome.7b00201

Tashima, L. S., Adelstein, S. J., and Lyman, C. P. (1970). Radioglucose utilization by active, hibernating, and arousing ground squirrels. *Am. J. Physiol.* 218, 303–309. doi: 10.1152/ajplegacy.1970.218.1.303

Tessier, S. N., and Storey, K. B. (2010). Expression of myocyte enhancer factor-2 and downstream genes in ground squirrel skeletal muscle during hibernation. *Mol. Cell. Biochem.* 344, 151–162. doi: 10.1007/s11010-010-0538-y

Tessier, S. N., and Storey, K. B. (2016). Lessons from mammalian hibernators: molecular insights into striated muscle plasticity and remodeling. *Biomol. Concepts* 7, 69–92. doi: 10.1515/bmc-2015-0031

Timmer, L. T., Hoogaars, W. M. H., and Jaspers, R. T. (2018). The role of IGF-1 signaling in skeletal muscle atrophy. *Adv. Exp. Med. Biol.* 1088, 109–137. doi: 10.1007/978-981-13-1435-3_6

Tinker, D. B., Harlow, H. J., and Beck, T. D. I. (1998). Protein use and muscle-fiber changes in free-ranging, hibernating black bears. *Physiol. Zool.* 71, 414–424. doi: 10.1086/515429

Toien, O., Blake, J., and Barnes, B. M. (2015). Thermoregulation and energetics in hibernating black bears: metabolic rate and the mystery of multi-day body temperature cycles. *J. Comp. Physiol. B Biochem. Syst. Environ. Physiol.* 185, 447–461. doi: 10.1007/s00360-015-0891-y

Toien, O., Blake, J., Edgar, D. M., Grahn, D. A., Heller, H. C., and Barnes, B. M. (2011). Hibernation in black bears: independence of metabolic suppression from body temperature. *Science* 331, 906–909. doi: 10.1126/science.1199435

Tomasi, T. E., Hellgren, E. C., and Tucker, T. J. (1998). Thyroid hormone concentrations in black bears (*Ursus americanus*): hibernation and pregnancy effects. *Gen. Comp. Endocrinol.* 109, 192–199. doi: 10.1006/gcen.1997.7018

Trendelenburg, A. U., Meyer, A., Rohner, D., Boyle, J., Hatakeyama, S., and Glass, D. J. (2009). Myostatin reduces Akt/TORC1/p70S6K signaling, inhibiting myoblast differentiation and myotube size. *Am. J. Physiol. Cell Physiol.* 296, C1258–C1270. doi: 10.1152/ajpcell.00105.2009

Tsubota, T., Garshelis, D. L., Nelson, R. A., and Bahr, J. M. (1999). Sex steroid and prolactin profiles in male American black bears (*Ursus americanus*) during denning. *J. Vet. Med. Sci.* 61, 81–83. doi: 10.1292/Jvms.61.81

Tsubota, T., and Kanagawa, H. (1989). Annual changes in serum testosterone levels and spermatogenesis in the Hokkaido brown bear, *Ursus arctos yesoensis*. *J. Mamm. Soc. Jpn.* 14, 11–17. doi: 10.11238/jmammsocjapan1987.14.11

Tsubota, T., Takahashi, Y., and Kanagawa, H. (1987). Changes in serum progesterone levels and growth of fetuses in Hokkaido brown bears. *Int. Conf. Bear Res. Manage.* 7, 355–358. doi: 10.2307/3872643

Turban, S., Hainault, I., Andre, J., Ferre, P., Quignard-Boulange, A., and Guerre-Millo, M. (2001). Molecular and cellular mechanisms of adipose secretion: comparison of leptin and angiotensinogen. *J. Cell. Biochem.* 82, 666–673. doi: 10.1002/jcb.1187

Twente, J. W., Twente, J., and Moy, R. M. (1977). Regulation of arousal from hibernation by temperature in three species of Citellus. *J. Appl. Physiol. Respir. Environ. Exerc. Physiol.* 42, 191–195. doi: 10.1152/jappl.1977.42.2.191

United Nations, Department of Economic and Social Affairs, and Population Division (2017). *World Population Ageing 2017 - Highlights (ST/ESA/SER.A/397)*. Available online at: https://www.un.org/en/development/desa/population/publications/pdf/ageing/WPA2017_Highlights.pdf (accessed November 27, 2020)

Vainshtein, A., and Sandri, M. (2020). Signaling pathways that control muscle mass. *Int. J. Mol. Sci.* 21:4759. doi: 10.3390/Ijms21134759

Van Breukelen, F., and Martin, S. L. (2001). Translational initiation is uncoupled from elongation at 18 degrees C during mammalian hibernation. *Am. J. Physiol. Regul. Integr. Comp. Physiol.* 281, R1374–R1379. doi: 10.1152/ajpregu.2001.281.5.R1374

Velickovska, V., Lloyd, B. P., Qureshi, S., and van Breukelen, F. (2005). Proteolysis is depressed during torpor in hibernators at the level of the 20S core protease. *J. Comp. Physiol. B Biochem. Syst. Environ. Physiol.* 175, 329–335. doi: 10.1007/s00360-005-0489-x

Vestergaard, P., Stoen, O. G., Swenson, J. E., Mosekilde, L., Heickendorff, L., and Frobert, O. (2011). Vitamin D status and bone and connective tissue turnover in brown bears (*Ursus arctos*) during hibernation and the active state. *PLoS ONE* 6:e21483. doi: 10.1371/journal.pone.0021483

Vogel, T., Brockmann, J. G., Coussios, C., and Friend, P. J. (2012). The role of normothermic extracorporeal perfusion in minimizing ischemia reperfusion injury. *Transplant. Rev.* 26, 156–162. doi: 10.1016/j.trre.2011.02.004

Volpato, G. P., Searles, R., Yu, B., Scherrer-Crosbie, M., Bloch, K. D., Ichinose, F., et al. (2008). Inhaled hydrogen sulfide: a rapidly reversible inhibitor of cardiac and metabolic function in the mouse. *Anesthesiology* 108, 659–668. doi: 10.1097/ALN.0b013e318167af0d

von Linde, M. B., Arevstrom, L., and Frobert, O. (2015). Insights from the den: how hibernating bears may help us understand and treat human disease. *Clin. Transl. Sci.* 8, 601–605. doi: 10.1111/cts.12279

Wagner, D. R., and Heyward, V. H. (2000). Measures of body composition in blacks and whites: a comparative review. *Am. J. Clin. Nutr.* 71, 1392–1402. doi: 10.1093/ajcn/71.6.1392

Wang, L. C. H. (1978). "Energetic and field aspects of mammalian torpor: the Richardson's ground squirrel," in *Strategies in Cold*, eds L. C. Wang and H. Hudson (New York, NY: Academic Press), 109–145.

Wang, L. C. H. (1989). "Ecological, physiological, and biochemical aspects of torpor in mammals and birds," in *Advances in Comparative and Environmenandd Physiology 4,* eds L. C. H. Wang (Berlin: Springer-Verlag), 361–401.

Wang, Z., Zhang, J., Ma, X. F., Chang, H., Peng, X., Xu, S. H., et al. (2020). A temporal examination of cytoplasmic Ca(2 +) levels, sarcoplasmic reticulum Ca(2 +) levels, and Ca(2 +) -handling-related proteins in different skeletal muscles of hibernating daurian ground squirrels. *Front. Physiol.* 11:562080. doi: 10.3389/fphys.2020.562080

Ware, J. V., Rode, K. D., Robbins, C. T., Leise, T., Weil, C. R., and Jansen, H. T. (2020). The clock keeps ticking: circadian rhythms of free-ranging polar bears. *J. Biol. Rhythms* 35, 180–194. doi: 10.1177/0748730419900877

Watts, P. D., Oritsland, N. A., Jonkel, C., and Ronald, K. (1981). Mammalian hibernation and the oxygen-consumption of a denning black bear (*Ursus americanas*). *Comp. Biochem. Physiol. A Physiol.* 69, 121–123. doi: 10.1016/0300-9629(81)90645-9

Wei, H. K., Zhou, Y. F., Jiang, S. Z., Tao, Y. X., Sun, H. Q., Peng, J., et al. (2013). Feeding a DHA-enriched diet increases skeletal muscle protein synthesis in growing pigs: association with increased skeletal muscle insulin action and local mRNA expression of insulin-like growth factor 1. *Br. J. Nutr.* 110, 671–680. doi: 10.1017/S0007114512005740

Wei, Y. H., Gong, L. C., Fu, W. W., Xu, S. H., Wang, Z., Zhang, J., et al. (2018). Unexpected regulation pattern of the IKK/NF-B/MuRF1 pathway with remarkable muscle plasticity in the Daurian ground squirrel (*Spermophilus dauricus*). *J. Cell. Physiol.* 233, 8711–8722. doi: 10.1002/jcp.26751

Weitten, M., Oudart, H., and Habold, C. (2016). Maintenance of a fully functional digestive system during hibernation in the European hamster, a food-storing hibernator. *Comp. Biochem. Physiol. A Mol. Integr. Physiol.* 193, 45–51. doi: 10.1016/j.cbpa.2016.01.006

Weitten, M., Robin, J. P., Oudart, H., Pevet, P., and Habold, C. (2013). Hormonal changes and energy substrate availability during the hibernation cycle of Syrian hamsters. *Horm. Behav.* 64, 611–617. doi: 10.1016/j.yhbeh.2013.08.015

Weitten, M., Tissier, M. L., Robin, J. P., and Habold, C. (2018). Dietary proteins improve hibernation and subsequent reproduction in the European hamster, *Cricetus cricetus*. *Am. J. Physiol. Regul. Integr. Comp. Physiol.* 315, R848–R855. doi: 10.1152/ajpregu.00146.2018

Welinder, K. G., Hansen, R., Overgaard, M. T., Brohus, M., Sonderkaer, M., von Bergen, M., et al. (2016). Biochemical foundations of health and energy conservation in hibernating free-ranging subadult brown bear *Ursus arctos*. *J. Biol. Chem.* 291, 22509–22523. doi: 10.1074/jbc.M116.742916

Welle, S. L. (2009). Myostatin and muscle fiber size. Focus on "Smad2 and 3 transcription factors control muscle mass in adulthood" and "Myostatin reduces Akt/TORC1/p70S6K signaling, inhibiting myoblast differentiation and myotube size". *Am. J. Physiol. Cell Physiol.* 296, C1245–C1247. doi: 10.1152/ajpcell.00154.2009

Wickler, S. J., Horwitz, B. A., and Kott, K. S. (1987). Muscle function in hibernating hamsters - a natural analog to bed rest. *J. Therm. Biol.* 12, 163–166. doi: 10.1016/0306-4565(87)90058-1

Wickler, S. J., Hoyt, D. F., and van Breukelen, F. (1991). Disuse atrophy in the hibernating golden-mantled ground squirrel, *Spermophilus lateralis*. *Am. J. Physiol.* 261(5 Pt 2), R1214–R1217. doi: 10.1152/ajpregu.1991.261.5.R1214

Wilhelmi de Toledo, F., Grundler, F., Bergouignan, A., Drinda, S., and Michalsen, A. (2019). Safety, health improvement and well-being during a 4 to 21-day fasting period in an observational study including 1422 subjects. *PLoS ONE* 14:e0209353. doi: 10.1371/journal.pone.0209353

Williams, D. R., Epperson, L. E., Li, W. Z., Hughes, M. A., Taylor, R., Rogers, J., et al. (2005). Seasonally hibernating phenotype assessed through transcript screening. *Physiol. Genomics* 24, 13–22. doi: 10.1152/physiolgenomics.00301.2004

Willoughby, D., Hewlings, S., and Kalman, D. (2018). Body composition changes in weight loss: strategies and supplementation for maintaining lean body mass, a brief review. *Nutrients* 10:1876. doi: 10.3390/nu10121876

Wimsatt, W. A. (1963). "Delayed implantation in the Ursidae, with particular reference to the black bear," in *Delayed Implantation*, ed A. C. Enders (Chicago, IL: University of Chicago Press), 49–76.

Wit, L. C., and Twente, J. W. (1983). Metabolic responses of hibernating golden-mantled ground squirrels *Citellus lateralis* to lowered environmental temperatures. *Comp. Biochem. Physiol. A Comp. Physiol.* 74, 823–827. doi: 10.1016/0300-9629(83)90353-5

Wolfe, R. R. (2006). The underappreciated role of muscle in health and disease. *Am. J. Clin. Nutr.* 84, 475–482. doi: 10.1093/ajcn/84.3.475

Wolfe, R. R., Nelson, R. A., Stein, T. P., Rogers, L., and Wolfe, M. H. (1982). Urea nitrogen reutilization in hibernating bears. *Fed. Proc.* 41, 1623–1623

Wollnik, F., and Schmidt, B. (1995). Seasonal and daily rhythms of body temperature in the European hamster (*Cricetus cricetus*) under semi-natural conditions. *J. Comp. Physiol. B* 165, 171–182. doi: 10.1007/BF00260808

Woodworth-Hobbs, M. E., Perry, B. D., Rahnert, J. A., Hudson, M. B., Zheng, B., and Russ Price, S. (2017). Docosahexaenoic acid counteracts palmitate-induced endoplasmic reticulum stress in C2C12 myotubes: impact on muscle atrophy. *Physiol. Rep.* 5:e13530. doi: 10.14814/phy2.13530

Wu, C. W., Biggar, K. K., and Storey, K. B. (2013). Biochemical adaptations of mammalian hibernation: exploring squirrels as a perspective model for naturally induced reversible insulin resistance. *Braz. J. Med. Biol. Res.* 46, 1–13. doi: 10.1590/1414-431x20122388

Wu, C. W., and Storey, K. B. (2012). Regulation of the mTOR signaling network in hibernating thirteen-lined ground squirrels. *J. Exp. Biol.* 215(Pt 10), 1720–1727. doi: 10.1242/jeb.066225

Xu, R., Andres-Mateos, E., Mejias, R., MacDonald, E. M., Leinwand, L. A., Merriman, D. K., et al. (2013). Hibernating squirrel muscle activates the endurance exercise pathway despite prolonged immobilization. *Exp. Neurol.* 247, 392–401. doi: 10.1016/j.expneurol.2013.01.005

Yang, C. X., He, Y., Gao, Y. F., Wang, H. P., and Goswami, N. (2014). Changes in calpains and calpastatin in the soleus muscle of Daurian ground squirrels during hibernation. *Comp. Biochem. Physiol. A Mol. Integr. Physiol.* 176, 26–31. doi: 10.1016/j.cbpa.2014.05.022

Yang, J., Cao, R. Y., Li, Q., and Zhu, F. (2018). Muscle atrophy in cancer. *Adv. Exp. Med. Biol.* 1088, 329–346. doi: 10.1007/978-981-13-1435-3_15

Zancanaro, C., Malatesta, M., Mannello, F., Vogel, P., and Fakan, S. (1999). The kidney during hibernation and arousal from hibernation. A natural model of organ preservation during cold ischaemia and reperfusion. *Nephrol. Dial. Transplant.* 14, 1982–1990. doi: 10.1093/ndt/14.8.1982

Zhang, J., Li, X., Ismail, F., Xu, S., Wang, Z., Peng, X., et al. (2019a). Priority strategy of intracellular Ca(2+) homeostasis in skeletal muscle fibers during the multiple stresses of hibernation. *Cells* 9:42. doi: 10.3390/cells9010042

Zhang, J., Wei, Y. H., Qu, T., Wang, Z., Xu, S. H., Peng, X., et al. (2019b). Prosurvival roles mediated by the PERK signaling pathway effectively prevent excessive endoplasmic reticulum stress-induced skeletal muscle loss during high-stress conditions of hibernation. *J. Cell. Physiol.* 234, 19728–19739. doi: 10.1002/jcp.28572

Zhang, Y., Pan, X., Sun, Y., Geng, Y. J., Yu, X. Y., and Li, Y. (2018). The molecular mechanisms and prevention principles of muscle atrophy in aging. *Adv. Exp. Med. Biol.* 1088, 347–368. doi: 10.1007/978-981-13-1435-3_16

Zhou, Y. T., Shimabukuro, M., Lee, Y., Koyama, K., Trieu, F., and Unger, R. H. (1997). Leptin normalizes the impaired response of proinsulin mRNA to long chain fatty acids in heterozygous Zucker diabetic fatty rats. *J. Biol. Chem.* 272, 25648–25651. doi: 10.1074/jbc.272.41.25648

Zifkin, M., Jin, A., Ozga, J. A., Zaharia, L. I., Schernthaner, J. P., Gesell, A., et al. (2012). Gene expression and metabolite profiling of developing highbush blueberry fruit indicates transcriptional regulation of flavonoid metabolism and activation of abscisic acid metabolism. *Plant. Physiol.* 158, 200–224. doi: 10.1104/pp.111.180950

Conflict of Interest: The authors declare that the research was conducted in the absence of any commercial or financial relationships that could be construed as a potential conflict of interest.

frontiers in Physiology

ORIGINAL RESEARCH
published: 04 March 2021
doi: 10.3389/fphys.2021.620614

Dynamic Function and Composition Shift in Circulating Innate Immune Cells in Hibernating Garden Dormice

Nikolaus Huber[1,2], Sebastian Vetter[3], Gabrielle Stalder[1], Hanno Gerritsmann[1] and Sylvain Giroud[1]**

[1] Research Institute of Wildlife Ecology, Department of Interdisciplinary Life Sciences, University of Veterinary Medicine Vienna, Vienna, Austria, [2] Unit of Veterinary Public Health and Epidemiology, Institute of Food Safety, Food Technology and Veterinary Public Health Department for Farm Animals and Veterinary Public Health, University of Veterinary Medicine Vienna, Vienna, Austria, [3] Institute of Animal Welfare Science, Department for Farm Animals and Veterinary Public Health, University of Veterinary Medicine Vienna, Vienna, Austria

Hibernation is characterized by successive torpor bouts during which metabolic rate is down-regulated to 2–4% of euthermic levels along with core body temperatures (T_b) ranging between 0 and 10°C. One characteristic of the torpid state, which is periodically interrupted by a few hours of euthermic phases or arousals during hibernation, resides in an overall impairment of the immune system. The most striking change during torpor is the reduction of circulating white blood cells up to 90%, while their numbers rise to near summer euthermic level upon rewarming. However, potential changes in responsiveness and function of neutrophil granulocytes, accounting for the primary cellular innate immune defense, are unknown. Here we present the first data on shifts in oxidative burst capacity, i.e., the ability to produce reactive oxygen species (ROS), of neutrophils during hibernation. Using a chemiluminescence assay, we measured real-time ROS production in whole blood of hibernating garden dormice (*Eliomys quercinus*) in early or late torpor, and upon arousals. Accounting for changes in neutrophil numbers along the torpor-arousal cycle, we found significant differences, between torpid and euthermic states, in the neutrophil oxidative burst capacity (NOC), with shallow cell responses during torpor and a highly significant increase by up to 30-fold during arousals. Further, we observed a significant reduction of NOC from aroused animals with euthermic T_b of 36.95 ± 0.37°C, when tested at 6°C, whereas no change occurred in NOC from torpid individuals reaching constant T_b of 4.67 ± 0.42°C, when measured at 35°C. This dynamic indicates that the reduction in NOC during torpor may be temperature-compensated. These results linked to the understanding of immune function during the torpor-arousal cycle might have clinical relevance in the context of therapeutic hypothermia and reperfusion injury.

Keywords: torpor, metabolic depression, arousal, oxidative burst, immunity, hibernator, ROS

OPEN ACCESS

Edited by:
Alessandro Silvani, University of Bologna, Italy

Reviewed by:
Allyson Hindle, University of Nevada, Las Vegas, United States
Laura Thompson, Sea Research Foundation, United States
Robert Henning, University Medical Center Groningen, Netherlands

****Correspondence:***
Nikolaus Huber
nikolaus.huber@vetmeduni.ac.at
Sylvain Giroud
sylvain.giroud@vetmeduni.ac.at

Specialty section:
This article was submitted to Integrative Physiology, a section of the journal Frontiers in Physiology

Received: *27 October 2020*
Accepted: *09 February 2021*
Published: *04 March 2021*

Citation:
Huber N, Vetter S, Stalder G, Gerritsmann H and Giroud S (2021) Dynamic Function and Composition Shift in Circulating Innate Immune Cells in Hibernating Garden Dormice. Front. Physiol. 12:620614. doi: 10.3389/fphys.2021.620614

INTRODUCTION

Endothermic vertebrates sustain a high basal metabolism to maintain a stabilized body temperature (T_b). Confronted with large fluctuations in ambient temperature (T_a) and bottlenecks in food (energy) and water availabilities a wide array of physiological and behavioral adaptations to conserve energy have evolved (Terrien et al., 2011; Boyles et al., 2016). The prime example of these

adaptive strategies is hibernation or multi-day torpor (Lane, 2012; Ruf and Geiser, 2015) which is described in a surprisingly wide range of species and is considered the most effective means of energy conservation in endotherms (Geiser, 2013; Boyles et al., 2020). Hibernation is characterized by successive bouts of torpor, lasting for days or even weeks, where the metabolic rate is actively down-regulated to 2–4% of euthermic rates with a subsequent drop of core T_b reaching values between 0 and 10°C during torpor. During the ultra-metabolic downstate of torpor, all essential physiological systems including the cardiovascular function, respiration, digestive system, brain and renal metabolism as well as cellular mitosis are profoundly reduced (Carey et al., 2003; Storey, 2010; Jastroch et al., 2016; Jørgensen et al., 2020). Remarkably, in most hibernators, hibernation is interspersed by short periods of less than a day, called interbout arousals, during which animals quickly (<90 min) increase their metabolism and return to euthermic T_b levels while restoring their main physiological functions (Carey et al., 2003; Heldmaier et al., 2004; Ruf and Geiser, 2015; Jastroch et al., 2016). Although the organism of hibernating mammals undergoes these extreme and rapid metabolic and temperature changes, no evidence of organ injury can be found (Dugbartey et al., 2018). Therefore it has been suggested that hibernating mammals represent a natural model to study tissue injury following surgery, trauma or transplantation in the context of ischemia and reperfusion injury. The primary pathomechanism of ischemia and reperfusion injury is the recruitment of innate immune cells such as leukocytes and the formation of cytotoxic reactive oxygen species (ROS; Thiele et al., 2018).

The immune system is one of the vital physiological compartments that is severely affected by extreme shifts in physiological states during the torpor-arousal cycle (Bouma et al., 2010a; Bouma et al., 2011). Several studies reported an overall impaired function of the innate as well as the cellular and humoral adaptive immunity during torpor, including lower complement levels, reduced macrophage phagocytic capacity, diminished lymphocyte proliferation as well as decreased cytokine and antibody production (reviewed by Bouma et al., 2010a, 2012, 2013b). In this context, the most striking immunological change is the drop of circulating white blood cells (WBC) by up to 90%. In all investigated torpid or hibernating animals WBCs including neutrophil granulocytes, lymphocytes and monocytes are decreased, whereby neutrophil granulocytes, hereafter referred to 'neutrophils', remain the most abundant (Bouma et al., 2010a; Sahdo et al., 2013; Uzenbaeva et al., 2019).

In mammals, neutrophils are part of the first line of cellular innate immune defense against invading pathogens (Mantovani et al., 2011; Dahlgren et al., 2019). Activated neutrophils generate and release superoxide molecules, also called oxygen free radicals, as the basis for several anti-pathogenic and highly ROS which are also involved in other biomedical aspects such as the integration and resolution of inflammation and tissue injury and repair (Thiele et al., 2018; Yang et al., 2019; Dinauer, 2020). The induced ROS production is accompanied by a steep increase in cellular oxygen consumption, also referred to as "oxidative burst." In particular, the use of whole blood chemiluminescence is a highly effective means for quantifying leukocyte (neutrophil) function, as reported by several studies measuring the production of ROS species (Lilius and Marnila, 1992; Kukovetz et al., 1997; Shelton-Rayner et al., 2012; Dahlgren et al., 2020).

During hibernation, the extreme up-shift in metabolic functions upon interbout arousal is paralleled by a vast increase in circulating WBCs, close to levels observed during summer euthermia (Bouma et al., 2011, 2013a). Contrary to shifts in WBC abundance and composition, there is, however, very little known on their responsiveness and functionality along the torpor-arousal cycle. Novoselova et al. (2000) showed in Arctic Yakutian ground squirrels (*Citellus undulatus Pallas*) that the production of tumor necrosis factor-alpha (TNFα) of macrophages, another circulating cellular component of the innate immune system, is significantly reduced during torpor, but restored to summer euthermic levels upon arousals. Further, the authors reported no change in the production of TNFα over the entire season in splenic T-lymphocytes (Novoselova et al., 2000). To the best of our knowledge, insight on the responsiveness and function in one of the most abundant circulating immune cells, i.e., neutrophils, during hibernation is lacking.

Therefore, in the present study, we aimed at (i) quantifying the number of different circulating WBC populations and (ii) determining the responsiveness of neutrophils within the torpor-arousal cycle as it occurs at mid-hibernation. Specifically, we hypothesized that, along with the marked reduction of neutrophils during torpor, the ability of neutrophils to produce oxygen free radicals would be dampened to a minimal level at low T_b. We further hypothesized that the function of neutrophils would be recovered to a certain degree upon arousals. To test these hypotheses, we used a whole blood chemiluminescence assay to measure real-time neutrophil oxidative burst capacity (NOC) along the torpor-arousal cycle of the garden dormouse (*Eliomys quercinus*), a medium-sized hibernating rodent. To assess differences in circulating WBC composition and potential shifts in neutrophil function, we collected blood samples and measured NOC at three different physiological states within the torpor-arousal cycle: (i) early torpor, (ii) late torpor, and (iii) during interbout arousal upon arousals. With the intention of testing for a possible effect of temperatures on neutrophil function, we additionally reversed the respective NOC assay temperature (low torpid vs high euthermic) for each hibernating state. As we expected a substantial reduction of WBCs in torpor and a vast increase upon arousals, we additionally predicted that NOC would be significantly diminished at both temperatures during torpor followed by a reversal to a certain degree during interbout arousal.

MATERIALS AND METHODS

Experimental Animals

Twenty-five garden dormice (11 males, 14 females), 1.5 to 2.5 years old, issued from a breeding colony kept at the Research Institute of Wildlife Ecology (Vienna, Austria), were included in the experiment. Garden dormice are small fat storing and omnivorous hibernators endemic to Europe (Mrosovsky and Lang, 1980). They are known for their naturally long hibernation

periods which can be induced by decreasing their housing temperature and by limiting food availability. Garden dormice show very regular rhythms of torpor and arousal phases, another reason why this species is especially suited for hibernation research. In our main colony, animals are housed in large outdoor enclosures and exposed to natural fluctuations of T_a and photoperiod. During winter (October to March), dormice are naturally hibernating, and when T_a is low (<10°C), animals enter multi-days torpor bouts, i.e., hibernation, and do not feed or drink during several months (Giroud et al., 2014; Mahlert et al., 2018). For this particular experiment, animals were housed in individual cages (60 × 40 × 40 cm), each equipped with one nest, bedding and nesting material as well as branches with leaves, already during the pre-hibernation period. These cages were set up in a room under natural photoperiod, at a constant T_a of 20°C, with *ad libitum* access to food and water. For the actual winter hibernation period, garden dormice were transferred to individual standard laboratory cages (36 × 20 × 14 cm), each provided with a customized nest for proper hibernation kept at 4°C in ventilated cooling units (refrigerators; Liebherr GKv 5730) under constant darkness, without food and water, as previously described (Giroud et al., 2018; Logan et al., 2020).

Ethics Statement

All procedures were approved by the institutional ethics committee and the Austrian national authority according to §26 of the Animal Experimental law, Tierversuchsgesetz 2012 – TVG 2012 (BMWF – 68.205/0137-WF/V/3b/2014).

Protocol Overview

Before hibernation experiments, we implanted our study animals with small temperature transmitters, and core T_b was monitored via a telemetry system (read below for further details and specifications). Once animals were spontaneously entering prolonged (>24 h) torpor, hibernation was induced by housing the animals at 4°C without food and water. Hibernation was monitored during the next 3 months until animals were sacrificed at mid-winter (Dec 2014–Jan 2015) where torpor bout lengths were maximal (12.1 ± 1.4 [9.2 to 15.5 days CI]). Torpid animals were sacrificed by immediate decapitation. Euthermic animals were quickly removed from the cooling unit and were then incrementally exposed (flow rate regulator) to carbon dioxide (CO_2, 100%) in a standard makrolon cage (type II long) with a modified lid (Corbach, 2006). Exposure lasted for 20 s at 3 L/min, then 40 s at 6 L/min until loss of consciousness followed by decapitation.

Torpor was defined when T_b of the animals decreased below 18°C, which was also the threshold to consider individuals above this value as euthermic. Torpid animals were sacrificed either in early torpor (1.5 ± 0.3 days torpid), in late-torpor (9.5 ± 0.2 days torpid) or during interbout arousal when they were euthermic for 3.4 ± 1.2 h. Fresh blood was collected in lithium heparinized tubes (LiHep Micro-tube, 1.3 ml, Sarstedt, Germany) immediately after decapitation via the trunk of the animals for immediate measurements of NOC and subsequent assessments of hematological parameters.

Measurement of Core Body Temperature

Before implantation T_b transmitters (model: TA-10TA-F10, 1.1cc, 1.6 g, accuracy: 0.15°C; Data Sciences International, St Paul, MN, United States[1]) were calibrated for temperatures between 0 and 40°C in a temperature-controlled water bath. Transmitters were surgically implanted under anesthesia induced by subcutaneous injection of 50 mg kg^{-1} ketamine (Ketamidor 10%, Richter Pharma, Wels, Austria) and 5 mg kg^{-1} xylazine (Rompun 2%, Bayer, Leverkusen, Germany), as routinely performed in garden dormice (Logan and Storey, 2016; Giroud et al., 2018; Mahlert et al., 2018). Anesthesia was maintained with 1.5% isoflurane via an oxygen stream through a facemask. For postoperative analgesia 5 mg kg^{-1} ketoprofen (Romefen 10% Merial S.A.S., Toulouse, France) was administered subcutaneously. The operation field was prepared according to standard surgical procedures and covered by sterile surgical drapes. Animals were placed in dorsal recumbency, and the abdominal cavity was opened through a 1 cm incision in the *linea alba* to introduce the temperature transmitter into the abdomen. Peritoneum and abdominal muscles were sutured using synthetic absorbable surgical suture material USP 3/0 (Surgicryl PGA, SMI AG, Hünningen, Belgium) using a single-button suture technique. For the additional intra-cutaneous skin suture, we used synthetic absorbable surgical suture material USP 4/0 (Surgicryl PGA, SMI AG, Hünningen, Belgium). All standard vital parameters [respiration rate, peripheral hemoglobin oxygen saturation as measured by pulse oximetry (SpO_2), and heart rate] were monitored during the entire procedure. After surgery, all animals recovered for 10 days before starting temperature recordings. For real-time temperature readings, a receiver board (RPC-1; Data Sciences International, St Paul, MN, United States; see text footnote 1) was positioned under every individual cage to collect the radio frequency signals from transmitters. T_b was recorded for 10 sec every 5 min. The Dataquest software package (LabPro Data Sciences) was used to download and visualize the data for first inspections.

White Blood Cell Differential Count

An aliquot of lithium-heparinized full blood was sent to the *INVITRO* laboratory (*Invitro* – Laboratory for Veterinary Diagnostics and Hygiene GmbH, Vienna, Austria) for WBC-differential counts. WBC differential counts were done manually from Diff-quick stained blood smears by a clinical pathologist from the *INVITRO* laboratory. Total leukocytes were analyzed from all individuals (early torpor, n = 8; late torpor, n = 9; interbout arousal, n = 8). Due to hemolysis of some blood samples, neutrophils and lymphocytes (early torpor, n = 7) as well as monocytes (early torpor, n = 4; late torpor, n = 5; interbout arousal, n = 6) and eosinophils (early and late torpor, interbout arousal, n = 5) could not be differentiated and the sample size was reduced in these parameters.

[1]https://www.datasci.com

Neutrophil Oxidative Burst Capacity (NOC)

To measure individual baseline levels of ROS, i.e., unstimulated blood chemiluminescence levels as well as the oxidative burst capacity of neutrophils, we followed previously published protocols (Shelton-Rayner et al., 2012; Huber et al., 2019) which have been used for small rodents (Gelling et al., 2009, 2010). Briefly, 10 μl of lithium-heparinized whole blood was transferred into four silicon antireflective tubes (Lumivial, EG & G Berthold, Germany). We added 90 μl of 10^{-4} mol l^{-1} luminol (5-amino-2,3-dihydro-phthalazine-1,4-dione; VWR International, Stockholm, Sweden) dissolved in dimethyl sulfoxide (DMSO; Sigma-Aldrich (now Merck), Darmstadt, Germany) and diluted with phosphate-buffered saline (PBS, pH 7.4) in each tube. Luminol is excited by phagocyte-generated ROS, resulting in chemiluminescence (Merényi et al., 1990). Subsequently, in two tubes acting as the unstimulated individual control sample, 10 μl of PBS was added, and the tubes were swiveled gently for mixing. To measure full blood chemiluminescence produced in response to a chemical challenge 10 μl of 10^{-5} mol l^{-1} phorbol 12-myristate 13-acetate (PMA; Sigma-Aldrich (now Merck), Darmstadt, Germany) was added into the other two tubes instead of 10 μl PBS. PMA is a well-characterized activator of protein kinase C and neutrophil oxidative burst inducer (Karlsson et al., 2000). All measurements were carried out directly after the blood sample was collected in a closed experimental room, ensuring stable conditions at 20°C. Immediately after blood collection and preparation of the samples (<1 min), tubes were incubated for 2 min at either 6 or 35°C (one baseline and one challenge sample for each temperature regime) in a lightproof water bath before starting the measurements. Blood chemiluminescence was assessed using a portable high sensitivity chemiluminometer (Junior LB 9509, EG & G Berthold, Germany). Measurements for each tube were made at the start (i.e., 0 min) and every 5 min for a total of 30 s over 30 min, resulting in 7 measure time points expressed in relative light units (RLU) per individual and temperature treatment. When not in the chemiluminometer, tubes were incubated at the respective temperature regime, i.e., at 6°C ("low") or at 35°C ("high").

In order to correct for background noise, we subtracted the values of the control sample from that of the challenged sample measured at the same time-point. The obtained values were used for the subsequent statistical analysis.

Data Computations and Statistical Analysis

All statistical analyses were carried out in R 3.6.2 (R Core Team, 2019). To test for an effect of hibernating states on body temperature, the total number of WBCs, neutrophils, lymphocytes, monocytes and eosinophil granulocytes, we constructed separate linear models for each variable that only contained hibernation state as the solitary explanatory variable (function lm).

To analyse the NOC an integral of the area under the curve was calculated based on the seven measured chemiluminescence-assay time points for each individual at each temperature treatment, and was used for subsequent analyses (function "rollmean"; package "zoo"; Zeileis and Grothendieck, 2005). To test for a potential effect of the different hibernating states (early and late torpor as well as interbout arousal), the two different temperature treatments (6°C vs 35°C), and the interaction of these two variables on the NOC a linear mixed-effects model was constructed (function "lme"; package "nlme" Pinheiro et al., 2017). Within this model, we additionally included the number of neutrophils for the respective individual sample in order to correct for a potential mass effect on ROS production as well as animal ID as a random effect. For all models normal distribution of residuals was inspected using histograms and quantile–quantile plots. In case of deviations from normality, data were boxcox-transformed, as the respective retested models showed no violation of model assumptions thereafter.

All constructed models were analyzed statistically with ANOVAs with type II sum of squares (function Anova, package "car" Fox and Weisberg, 2018). *Post hoc* comparisons between hibernating states were carried out with Tukey-like tests (function "glht" package "multcomp" Hothorn et al., 2008). All reported values are expressed as means ± SD.

RESULTS

Body Temperatures of Hibernating Garden Dormice

During early torpor, dormice had a mean T_b of 4.73 ± 0.54°C which did not significantly differ from that of animals in late torpor with a T_b of 4.78 ± 0.51°C; **Figure 1**). As expected, interbout arousal euthermic animals showed a significant T_b increase of 36.96 ± 0.39°C compared to torpid individuals in early or late torpor (**Figure 1**).

Levels of White Blood Cells (WBC) of Hibernating Garden Dormice

We found significant shifts in total WBCs and WBC differential counts concerning neutrophils and lymphocytes. Range (minimum, maximum), means and standard deviations of circulating WBCs during the phases of early and late torpor as well as interbout arousal, are shown in the **Table 1**.

The number of total WBCs in average tripled during interbout arousal compared to torpid animals without difference between early and late torpor (**Table 2** and **Figure 2A**). Neutrophils increased 3.6-fold on average during interbout arousal compared to animals in the early or late phase of torpor with no significant difference between early and late torpor (**Table 2** and **Figure 2B**). Lymphocyte numbers were significantly lower only during late torpor compared to interbout arousal but were not different between interbout arousal and early torpor (**Table 2** and **Figure 2C**). Also, no significant differences between hibernating states were found for monocyte (**Table 2** and **Figure 2D**) or eosinophil counts (**Table 1**).

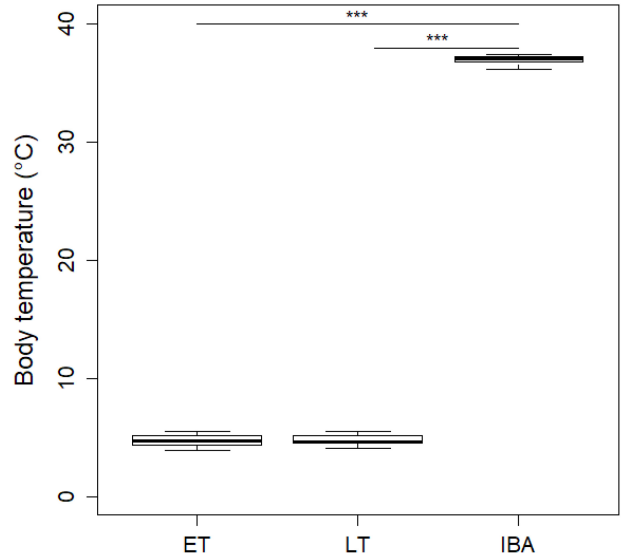

FIGURE 1 | Boxplot of mean core body temperatures (T_b) of hibernating garden dormice. Core T_b of animals in early torpor ("ET," $n = 8$) was 4.73 ± 0.54°C which did not significantly differ from that of animals in late torpor ("LT"; 4.78 ± 0.51°C; $n = 9$; estimate = 0.04 ± 0.24, $z = 0.16$, $p > 0.98$). In contrast, euthermic animals during interbout arousals ("IBA," $n = 8$) had significant higher T_b values of 36.96 ± 0.39°C compared to individuals in ET (estimate = 32.22 ± 0.24, $z = 132.24$, $p \leq 0.001$) or LT (estimate = 32.18 ± 0.24, $z = 135.91$, $p \leq 0.001$). Asterisks indicate significant differences ($p \leq 0.001$) between physiological hibernating states.

Neutrophil Oxidative Burst Capacity (NOC) of Hibernating Garden Dormice

We found a significant interaction between hibernating states and temperature treatments during the NOC assay (**Table 3** and **Figure 3**). *Post hoc* tests revealed significantly higher NOC levels in interbout arousal dormice, measured at 35°C, compared to those from torpid animals measured at 6°C. NOC Levels of animals in interbout arousal measured with the reversed temperature, i.e., at 6°C, significantly dropped compared to the measured levels at 35°C, and then did not significantly differ from the ones of the torpid animals (**Table 3** and **Figure 3**). Range (minimum, maximum), means and standard deviations for NOC values for the respective assay temperatures during in the phases of early and late torpor as well as interbout arousal are presented in **Table 1**. Interestingly, we observed no significant effects of the assay's temperature on NOC of either early or late-torpor individuals, all having the same low amplitudes (**Table 3** and **Figure 3**). The full NOC response curves over the 30-minute measure period including the baseline as well as the challenge sample for each assay temperature during early- and late torpor and during interbout arousal are presented in **Figure 4A–F**. Further, testing for a potential mass effect of neutrophils on NOC revealed that the NOC response was independent of the number of neutrophils ($X^2_{2,48} = 0.45$, $p = 0.50$; **Table 2**). However, we did observe a positive but non-significant correlation between the number of neutrophils and the NOC response in animals during interbout arousal (for visualization please see **Supplementary Figure 1**).

DISCUSSION

In this study, we assessed potential differences in the number and composition of WBC, as well as in the function, i.e., capacity to produce ROS, of neutrophils in garden dormice hibernating under controlled but natural conditions. We collected blood samples at three defined time-points within the torpor-arousal cycle, i.e., either early or late during the ultra-metabolic downstate of torpor, and after natural periodic arousal in interbout arousal. To test for a possible effect on NOC, beyond temperatures, we also reversed the respective NOC measurement temperature for each hibernating state. Besides a substantial drop in circulating WBCs accompanied by a shift in WBC composition during torpor reversible in interbout arousal, our results revealed a significant decrease in neutrophil function, i.e., NOC during torpor which was restored to a substantial degree in interbout arousal and the concomitant rise in T_b upon arousal.

TABLE 1 | Range (minimum and maximum), means and standard deviations of total and differential white blood cell counts as well as the neutrophil oxidative burst capacity (NOC, measured at 6 and 35°C) at three different physiological states within the torpor-arousal cycle of hibernating garden dormice.

State	ET ($n = 8$)				LT ($n = 9$)				IBA ($n = 8$)			
	min	max	mean	± SD	min	max	mean	± SD	min	max	mean	± SD
Leukocytes G/L	0.90	4.08	1.88	1.13	1.05	5.35	2.21	1.41	2.91	7.83	5.62	1.53
Neutrophils G/L*	0.03	0.60	0.32	0.23	0.15	1.93	0.84	0.61	1.28	5.25	2.87	1.32
Lymphocytes G/L*	0.38	3.28	1.49	1.15	0.49	3.32	1.24	0.95	1.38	4.52	2.58	0.99
Monocytes G/L**	0.02	0.04	0.03	0.01	0.02	0.11	0.06	0.04	0.05	0.54	0.17	0.19
Eosinophils G/L***	0.01	0.57	0.19	0.24	0.02	0.45	0.16	0.17	0.03	0.16	0.08	0.05
AUC_NOC_6°C	0.00	260.00	82.81	81.25	32.50	790.00	128.33	242.23	30.00	177.50	77.19	52.36
AUC_NOC_35°C	10.00	272.50	100.94	88.30	75.00	3550.00	608.33	1121.04	1057.50	6642.50	3768.44	2041.11

*Blood samples were collected during the states of early torpor ("ET"; 1–2 days torpid; T_b mean ± SD = 4.73 ± 0.54°C), late-torpor ("LT"; 9–10 days torpid; T_b = 4.78 ± 0.51°C), and interbout arousal ("IBA"; 3.4 ± 1.2 h after arousal; T_b = 36.96 ± 0.39°C). "AUC_NOC_6°C" and "AUC_NOC_35°C" represent the areas under the curve response of neutrophil reactive oxygen species production measured every 5 min over 30 min at either 6 or 35°C. G/L = 10^9/l. *n = 7 in ET. **n = 4 in ET, 5 in LT, 6 in IBA. ***n = 5 in ET, LT, and IBA.*

TABLE 2 | Differences in total and differential white blood cell count between three different measured time points within the torpor-arousal cycle in hibernating garden dormice.

	Estimate	Std. Error	*t*-value	*p*-value
Leukocytes				
$F_{2,51} = 18.642$, $p < 0.001$				
LT–ET	0.329	0.664	0.495	0.771
IBA–ET	3.742	0.683	5.473	**<0.001**
IBA–LT	3.413	0.664	5.137	**<0.001**
Neutrophils				
$F_{2,24} = 19.064$, $p < 0.001$				
LT–ET	0.518	0.434	1.192	0.471
IBA–ET	2.551	0.446	5.722	**<0.001**
IBA–LT	2.034	0.419	4.858	**<0.001**
Lymphocytes				
$F_{2,24} = 4.321$, $p = 0.026$				
LT–ET	−0.043	0.290	−0.145	0.878
IBA–ET	0.727	0.305	2.377	0.127
IBA–LT	0.770	0.287	2.682	**0.036**
Monocytes				
$F_{2,15} = 1.86$, $p = 0.198$				
Eosinophils				
$F_{2,15} = 0.545$, $p = 0.593$				

Lymphocyte numbers were boxcox transformed to meet the assumption of statistical normality. Differences are reported as partial effects accounting for the individual as a random effect. Blood samples were collected during the physiological states of early torpor ("ET," n = 8), late-torpor ("LT," n = 9), and interbout arousal ("IBA," n = 8). It was not possible to differentiate neutrophils and lymphocytes due to hemolysis in one blood sample and the sample size for these parameters during early torpor are reduced by one (n = 7). Significant differences are displayed in bold letters.

White Blood Cell Number and Composition Change Within the Torpor-Arousal Cycle

The observed extreme and transient leukopenia in our study animals during early and late torpor, including granulocytes (neutrophils, eosinophils), lymphocytes and monocytes, with a significant increase in WBCs to a certain level upon arousal (**Figure 2A**), confirms previous findings on WBC dynamics during hibernation from all hibernating species studied in this aspect to date (Bouma et al., 2010a,b, 2011, 2012, 2013b; Sahdo et al., 2013; Kuznetsova et al., 2016; Kizhina et al., 2018; Uzenbaeva et al., 2019). At this point, we would like to note that we did not measure summer euthermic animals in this study and, therefore, cannot draw any conclusions or comparisons on the seasonal aspect of blood cell counts or distribution.

Bouma et al. (2011) showed that lymphopenia, i.e., a marked drop of lymphocytes, during hibernation is driven by T_b, via altered erythrocyte generated plasma sphingosine-1-phosphate (S1P) levels inducing the storage of lymphocytes in secondary lymphoid organs. In another study, it was demonstrated that the reversible neutropenia during torpor is primarily caused by margination neutrophils, i.e., the reversible attachment of blood cells to the endothelial wall of the blood vessels and that this phenomenon is not restricted to hibernating species (Bouma et al., 2013a; Sahdo et al., 2013).

In contrast to previous studies, the number of lymphocytes observed in our studied dormice during early torpor was similar or only moderately reduced compared to interbout arousal and only decreased to a significant level during late torpor (**Figure 2C**). Hence our results in regards to WBC composition in hibernating garden dormice do not fully align with previous studies. Bouma et al. (2010a) noted in their review that the majority of the remaining WBCs during the state of torpor are neutrophils (90%), whereas in our study lymphocytes are the predominant WBC type during early (71%) as well as during late torpor (52%), which is likely to be species-specific (see also Uzenbaeva et al., 2019). The lymphocyte numbers in our study are not significantly different between interbout arousal and early torpor, i.e., 1–2 days after interbout arousal, but continue to decrease further along the torpor bout. One possible explanation may be that S1P levels in early torpor are only minimally lower compared to levels during interbout arousal but decrease over the course of torpor with the consequence of a further reduction of lymphocytes and the observed significant differences in lymphocyte abundance between late torpor and interbout arousal. A higher proportion of lymphocytes to phagocytes, i.e., neutrophils and monocytes, was also reported in edible dormouse (*Glis glis*) shortly after emergence from hibernation in spring (Havenstein and Fietz, 2013). Therefore, the higher proportion of lymphocytes during torpor in garden dormice may also have an immune protective role as shown for torpid 13-lined ground squirrels (*Ictidomys tridecemlineatus*), where the ability to mount a humoral immune response to a T-lymphocyte dependent antigen (NP-ovalbumin) remained optimal during hibernation (Bouma et al., 2013b). Moreover, the immunization of hibernating ground squirrels with NP-ovalbumin induced the production of antibodies and caused a disturbance of the hibernating pattern, i.e., an atypical (emergency) rewarming from torpor, along with increased mortality in this small hibernator (Bouma et al., 2013b). The results of the latter study demonstrate functional and responsive lymphocytes during torpor and the hibernation period and may partly explain the adaptive significance of maintaining a high proportion of lymphocytes during the hypo-metabolic downstate of torpor. Here we would like to note that the use of CO_2 for euthanasia can impact blood cell distribution with increasing number of lymphocytes with increasing CO_2 levels in the circulation (Pecaut et al., 2000). This may have influenced blood cell distribution in the interbout arousal group to a certain degree.

From an immunological perspective, our findings extend earlier work reporting that organismal immune cell responses are inhibited to varying degrees during torpor and restored close to summer euthermic levels during interbout arousal (Shivatcheva et al., 1988; Novoselova et al., 2000; Bouma et al., 2010b). In golden-mantled ground squirrels (*Spermophilus lateralis*) the acute phase response to bacterial lipopolysaccharide (LPS) was ultimately arrested during torpor but fully restored upon interbout arousal as animals developed a fever only during the subsequent interbout arousal which was additionally prolonged up to six times

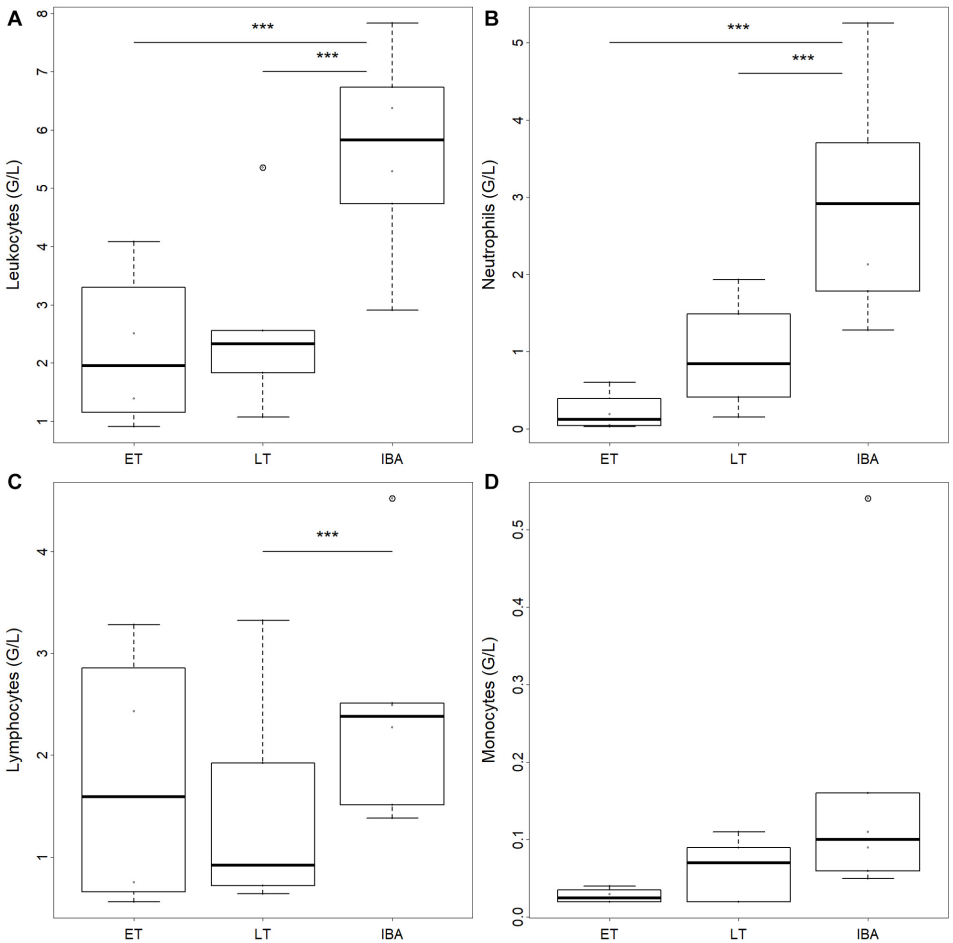

FIGURE 2 | Box plots of circulating **(A)** total leukocyte, **(B)** neutrophil, **(C)** lymphocyte, and **(D)** monocyte numbers in hibernating garden dormice under different physiological states within the torpor-arousal cycle. Hibernating states correspond to early torpor ("ET," $n = 8$), late-torpor ("LT," $n = 9$), and interbout arousal ("IBA," $n = 8$). Asterisks indicate significant differences between states (*Post hoc* Tukey-like test: $^{***}p < 0.001$). When not indicated, effects were non-significant.

compared to regular interbout arousal durations in this species (Prendergast et al., 2002). In the latter study, Prendergast et al. (2002) also tested the neuronal signaling pathways mediating febrile responses with intra-cerebro-ventricular infusions of prostaglandin-E2 and demonstrated that the underlying neuronal circuit is functional during torpor and thereby narrowed the absent response to LPS during torpor down to cellular immune processes including LPS binding and cytokine production.

Neutrophil Oxidative Burst Capacity (NOC) Reveals Restoration of Rapid Innate Immune Defense During Arousals

Studies on the NOC in non-hibernating species in mammals as well as in birds using the very same protocol as applied in present study observed a significant correlation between the number of neutrophils and NOC (Huber et al., 2019, 2020). The missing correlation in the current manuscript is likely explained, beyond the relatively small sample sizes, by the fact that a high number of neutrophils is only present in the IBA group (**Supplementary Figure 1**). Our results of NOC show a low to negligible ROS production in torpid animals when measured at a low temperature (close to torpid T_b) with no significant difference between early and late torpor. Interestingly, and following our prediction, NOC of animals in interbout arousal was significantly increased up to 30-fold compared to the one measured in torpid individuals (**Figure 3**). An early study comparing the effect of temperature on NOC using whole-blood chemiluminescence in two non-hibernating species, the ectothermic rainbow trout (*Salmo gairdneri*) and humans (endotherms), revealed that the chemiluminescence responses were approximately equivalent for the two species measured at their physiological T_b associated with their respective preferred T_a (Sohnle and Chusid, 1983). The highest magnitude in the oxidative burst of human neutrophils was attained from 23 to 37°C, and between 4 and 15°C in rainbow trout neutrophils. When assay temperatures were reversed, i.e., chemiluminescence of human cells was measured at 4°C and trout cells at 37°C, the responses were negligible in

TABLE 3 | Differences in neutrophil oxidative burst capacity (NOC) between three different time points, i.e., early torpor ("ET"), late-torpor ("LT"), and the interbout arousal ("IBA"), within the torpor-arousal cycle of hibernating garden dormice.

	Estimate	Std. Error	*z*-value	*p*-value
Hibernation state: Temperature				
$X^2_{2,48} = 38.96$, $p < 0.001$				
IBA 35°C–ET 6°C	7.14	1.30	5.48	**<0.001**
IBA 35°C–LT 6°C	5.41	1.14	4.75	**<0.001**
IBA 35°C–IBA 6°C	7.21	0.82	8.81	**<0.001**
IBA 35°C–ET 35°C	6.33	1.30	4.85	**<0.001**
IBA 35°C–LT 35°C	4.33	1.14	3.80	**0.001**
All other comparisons $p > 0.2$				
Neutrophils				
$X^2_{2,48} = 0.45$, $p = 0.50$				

NOC values were boxcox transformed to meet the statistical assumption of normality. Differences are reported as partial effects including the number of neutrophils for the respective individual to correct for a potential mass effect on ROS production as well as animals ID as random effect. NOC was measured at two different assay temperatures close to the core body temperature of either 35°C (euthermic) and 6°C (torpid). The number of neutrophils for the respective individual sample was included in the analysis in order to correct for a potential mass effect on NOC. Significant differences are displayed in bold letters.

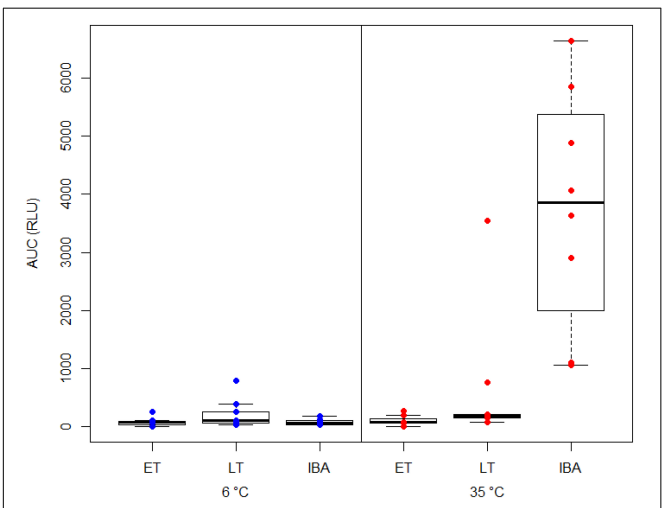

FIGURE 3 | Box plot showing the area under the curve response ("AUC") expressed in relative light units ("RLU") of the neutrophil oxidative burst capacity (NOC) in hibernating garden dormice under different physiological states within the torpor-arousal cycle. Blood samples from dormice in early torpor ("ET," $n = 8$), late-torpor ("LT," $n = 9$), and interbout arousal ("IBA," $n = 8$) were measured at both 6 and 35°C. NOC from IBA animals measured at 35°C is significantly higher compared to those from all other physiological states and measurement temperatures ($p < 0.001$). Please note the higher variability of NOC response from the blood of LT animals measured at 35°C.

both species (Sohnle and Chusid, 1983). Hence, the NOC appears to be temperature-sensitive but well adapted to the respective T_b and environmental T_a of each species. However, in mammals, the NOC response to soluble chemicals (e.g., PMA) as well as to phagocytic stimuli in general, has been shown to develop more rapidly and to a greater extent at higher T_b (Wenisch et al., 1996). Here we would like to remark, that also increased circulating CO_2 levels can negatively influence the NOC response as reported in rainbow trout (*Oncorhynchus mykiss*) tissues (Kaya et al., 2013). Hence the NOC response in interbout arousal animals in our study may have been higher as measured in our study until the animals were exposed to increased CO_2 levels (for 60 s) in the course of the sacrification procedure.

Also, in our system, the question regarding the drivers and the downstream mechanisms leading to the highly diminished NOC during the hypometabolic downstate of torpor arises. Reversing of the NOC measurement temperatures from animals in interbout arousal resulted in a significant reduction in NOC to an almost non-detectable level indicating a temperature dependence of the neutrophil oxidative burst response during euthermia (**Figure 3**). Conversely, the reversal of the measurement temperature from torpid animals, i.e., the rewarming of blood and measuring NOC close to euthermic temperatures, did not affect an increase in NOC and ROS production over the 30-min measurement period. The insignificant change of NOC in rewarmed blood from torpid animals let us speculate that the inhibition of NOC during torpor may be temperature-compensated. However, we would like to note that blood samples from animals were taken when animals had been euthermic for more than 3 h and the reversal (i.e., warming and cooling) of the assay temperatures occurred relatively fast and over only 32 min. This time difference (32 min vs 3 h) in cooling and rewarming rates may have influenced cell homeostasis and their ability to produce and release ROS differently, although the peak increase in metabolic rate, hence systemic oxidative burst, upon natural arousal from torpor occurs within the first 40 min of rewarming. In this context, the generation of microbicidal oxidants by neutrophils results from the assembly of the multiprotein enzyme complex nicotinamide-adenine-dinucleotide-phosphate- (NADPH) oxidase (NOX), which catalyzes the formation of superoxide anion, the primary molecule for various ROS (Babior, 1999; Quinn and Gauss, 2004). NOC by NOX is an NADPH-dependent process derived from the pentose phosphate shunt dependent on both glucose/glycogen and adenosine triphosphate for its formation (Ying, 2008). Therefore, one possible explanation for the diminished NOC in the torpid state could be the low substrate availability and the concomitant low levels of NADPH as a result of the extreme metabolic suppression during torpor.

The chemical stimulus PMA is a broad-spectrum protein kinase C (PKC) activator that bypasses receptor-mediated control of free radical production (Karlsson et al., 2000). PKC phosphorylates the NOX subunit $p47^{PHOX}$ and thereby contributes to the assembly of the NOX and the subsequent production of ROS (Dang et al., 2006; Rastogi et al., 2017). Although we cannot conclude on the exact cause of the reduction or suppression in NOC during torpor, the regulation could specifically act via an insensitivity of PKC to PMA, altered subsequent activation of the NOX enzyme complex, or a combination of both (Babior, 1999). Also, an alternative explanation for the low NOC during torpor may be the inhibiting effect of hydrogen sulfide (H_2S) on NOX and

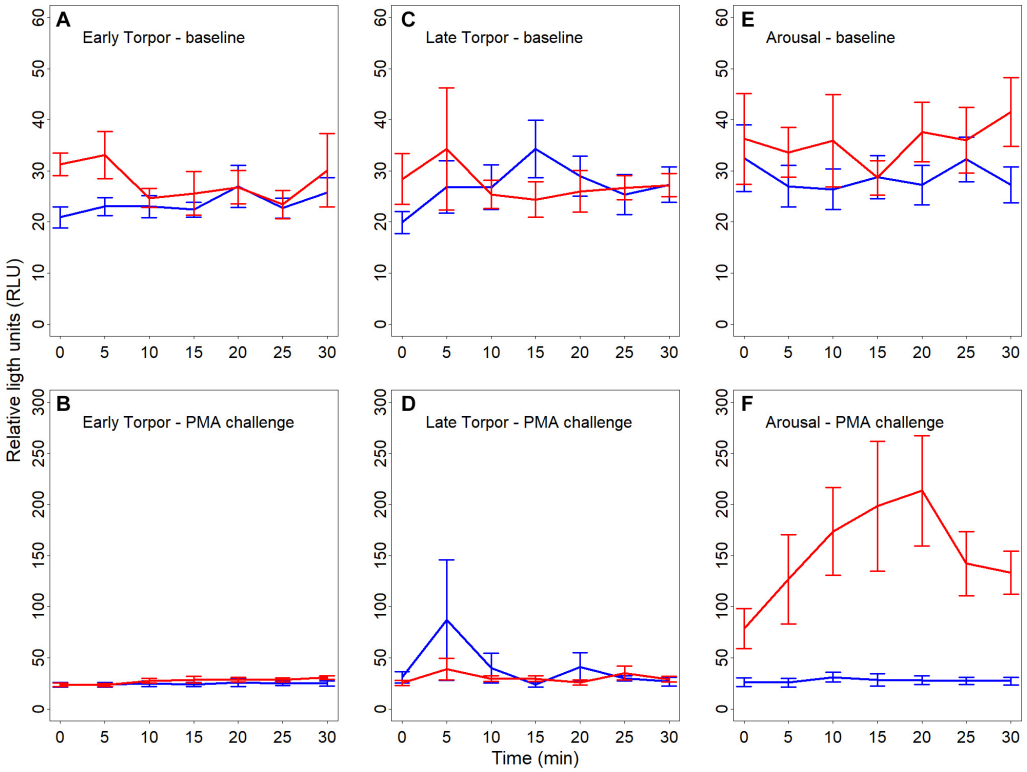

FIGURE 4 | (A–F) Line plots showing baseline reactive oxygen species (ROS; **A**,**C**,**E**) as well as challenge ROS levels **(B,F,F)** in full blood of hibernating garden dormice measured for 30 s every 5 min over 30 min and expressed in relative light units ("RLU"). Chemiluminescence was measured in different physiological states within the torpor-arousal cycle, i.e., in early torpor (**A**,**B**; $n = 8$), late-torpor (**C**,**D**; $n = 9$), and interbout arousal (**E**,**F**; $n = 8$) at both 6°C (blue lines) and 35°C (red lines). There was no significant difference in baseline chemiluminescence between the different states (all $p > 0.5$) with a small increase in baseline ROS in IBA animals when measured at 35°C. Error bars represent the standard error.

the linked ROS production (Muzaffar et al., 2008a,b; Al-Magableh et al., 2014; also see for review Giroud et al., 2020). Talaei et al. (2012) report endogenous production of H_2S in hibernating Syrian hamsters (*Mesocricetus auratus*), with increased levels during early and late torpor and a normalization, i.e., low levels, during interbout arousal. Hence, the observed dynamic in NOC during different hibernating states may result from a similar dynamic of H_2S levels along the torpor arousal cycle. Additionally, H_2S is limiting the migration of neutrophils through tissues, suppresses the inflammatory response and is acting as an endogenous regulator of the innate as well as the adaptive immune system (Faller et al., 2018).

Further Considerations on the Neutrophil Oxidative Burst Response During Hibernation

Luminol, the light enhancer used in this study, can diffuse across biological membranes and therefore allows the detection of both extra and intracellular ROS production (Briheim et al., 1984). However, several authors highlight that Luminol reflects intracellular ROS kinetic production rather than extracellular ROS detection (Müller-Peddinghaus, 1984; Caldefie-Chézet et al., 2002; Freitas et al., 2009). Furthermore, luminol chemiluminescence in full blood is a myeloperoxidase (MPO) requiring reaction and its presence and functionality depict another factor that could potentially interfere with the production and subsequent detection of ROS by neutrophils during the torpor-arousal cycle. In this context, it has also been shown that H_2S inhibits MPO activity and the production of ROS by neutrophils and thereby contributes to an anti-neutrophil (anti-inflammatory) state. To disentangle the involved pathways and down-stream mechanisms, further studies comprising the use of additional chemiluminescence amplifiers such as iso-luminol, which is not able to cross cell membranes, or lucigenin, which is highly specific to the activity of the NOX complex and the production of extracellular ROS, are warranted (Dahlgren and Karlsson, 1999; Dahlgren et al., 2020). Furthermore, we recommend including the measurement of intra- and extracellular MPO concentrations using flow cytometry (Peake et al., 2004) as well as H_2S levels as a promising candidate and underlying molecule regulating NOC along the torpor arousal cycle (Talaei et al., 2012; Dilek et al., 2020). Additionally, we suggest to include the measurement of PKC substrates such as $p47^{PHOX}$ and their activity into future experiments and investigate the underlying mechanisms more in depth.

CONCLUSION

To conclude, this study confirms changes in numbers, composition, and function of WBC during the alternating periods of extreme metabolic downregulation known as torpor and short euthermic periods of rapid and drastic increases in metabolic rate, called periodic arousals. Our study particularly reveals suppression of neutrophil function in terms of their capacity to produce oxygen radicals, a key-player of the innate immune system, which is reversed upon arousals when hibernators reactivate primary physiological functions, including the dormant immune system. Since WBCs and neutrophil granulocytes play a central role in the pathophysiology of tissue damage and organ injury, this dynamic may be obligatory to minimize inflammation and possibly organ injury during these extreme physiological shifts over the course of the torpor-arousal cycle and thereby to survive the hibernation period. Further studies are necessary to determine the underlying mechanisms and translate them into biomedical applications and therapies. Our findings highlight small hibernating species and natural hibernation in general as an excellent model to explore the adaptive value of immunological shifts during extreme hypometabolic and hypothermic states in the context of ischemia-reperfusion injury, organ preservation, and therapeutic hypothermia.

DATA AVAILABILITY STATEMENT

The raw data supporting the conclusions of this article will be made available by the authors, without undue reservation, to any qualified researcher upon request.

ETHICS STATEMENT

The animal study was reviewed and approved by the Institutional Ethics Committee and the Austrian National Authority.

AUTHOR CONTRIBUTIONS

NH and SG conceived and designed the study. HG and GS performed the temperature logger implantations. NH performed all chemiluminescence assays and drafted the manuscript. SG and SV analyzed the data with input from NH. SG edited and critically revised the manuscript. All co-authors commented on the manuscript. All authors contributed to the article and approved the submitted version.

FUNDING

NH was financially supported by a Ph.D. fellowship of the University of Veterinary Medicine Vienna (Austria). SG was financially supported by a post-doctoral fellowship of the University of Veterinary Medicine Vienna (Austria) and the Austrian Science Fund (FWF) (Grant Nos. P27267-B25 and P31577-B25).

ACKNOWLEDGMENTS

We would like to thank the animal caretakers of the Research Institute for Wildlife Ecology, especially P. Steiger and M. Salaba, for their invaluable help with the garden dormouse colony. M. Hämmerle for providing the cooling water bath, R. Hengsberger, for her help with literature search and formatting of the manuscript. Special thanks to Dr. Hilmar Bouma for valuable input and discussions regarding immunological changes during hibernation.

SUPPLEMENTARY MATERIAL

The Supplementary Material for this article can be found online at: https://www.frontiersin.org/articles/10.3389/fphys.2021.620614/full#supplementary-material

REFERENCES

Al-Magableh, M. R., Kemp-Harper, B. K., Ng, H. H., Miller, A. A., and Hart, J. L. (2014). Hydrogen sulfide protects endothelial nitric oxide function under conditions of acute oxidative stress in vitro. *Naunyn Schmiedeberg's Arch. Pharmacol.* 387, 67–74. doi: 10.1007/s00210-013-0920-x

Babior, B. M. (1999). NADPH Oxidase: An Update. *Blood* 93, 1464–1476. doi: 10.1182/blood.V93.5.1464

Bouma, H. R., Carey, H. V., and Kroese, F. G. M. (2010a). Hibernation: the immune system at rest? *J. Leukoc. Biol.* 88, 619–624. doi: 10.1189/Jlb.0310174

Bouma, H. R., Dugbartey, G. J., Boerema, A. S., Talaei, F., Herwig, A., Goris, M., et al. (2013a). Reduction of body temperature governs neutrophil retention in hibernating and nonhibernating animals by margination. *J. Leukoc. Biol.* 94, 431–437. doi: 10.1189/jlb.0611298

Bouma, H. R., Henning, R. H., Kroese, F. G. M., and Carey, H. V. (2013b). Hibernation is associated with depression of T-cell independent humoral immune responses in the 13-lined ground squirrel. *Dev. Comp. Immunol.* 39, 154–160. doi: 10.1016/j.dci.2012.11.004

Bouma, H. R., Kroese, F. G. M., Kok, J. W., Talaei, F., Boerema, A. S., Herwig, A., et al. (2011). Low body temperature governs the decline of circulating lymphocytes during hibernation through sphingosine-1-phosphate. *Proc. Natl. Acad. Sci. U S A.* 108, 2052–2057. doi: 10.1073/pnas.1008823108

Bouma, H. R., Strijkstra, A. M., Boerema, A. S., Deelman, L. E., Epema, A. H., Hut, R. A., et al. (2010b). Blood cell dynamics during hibernation in the European Ground Squirrel. *Vet. Immunol. Immunopathol.* 136, 319–323. doi: 10.1016/j.vetimm.2010.03.016

Bouma, H. R., Strijkstra, A. M., Talaei, F., Henning, R. H., Carey, H. V., and Kroese, F. G. M. (2012). "The Hibernating Immune System," in *Living in a Seasonal World: Thermoregulatory and Metabolic Adaptations*, eds T. Ruf, C. Bieber, W. Arnold, and E. Millesi (Berlin: Springer), 259–270. doi: 10.1007/978-3-642-28678-0_23

Boyles, J. G., Johnson, J. S., Blomberg, A., and Lilley, T. M. (2020). Optimal hibernation theory. *Mammal Rev.* 50, 91–100. doi: 10.1111/mam.12181

Boyles, J. G., McGuire, L. P., Boyles, E., Reimer, J. P., Brooks, C. A. C., Rutherford, R. W., et al. (2016). Physiological and behavioral adaptations in bats living at high latitudes. *Physiol. Behav.* 165, 322–327. doi: 10.1016/j.physbeh.2016.08.016

Briheim, G., Stendahl, O., and Dahlgren, C. (1984). Intra- and Extracellular Events in Luminol-Dependent Chemiluminescence of Polymorphonuclear Leukocytes. *Infect. Immun.* 45, 1–5. doi: 10.1128/iai.45.1.1-5.1984

Caldefie-Chézet, F., Walrand, S., Moinard, C., Tridon, A., Chassagne, J., and Vasson, M.-P. (2002). Is the neutrophil reactive oxygen species production measured by luminol and lucigenin chemiluminescence intra or extracellular? Comparison with DCFH-DA flow cytometry and cytochrome *c* reduction. *Clin. Chim. Acta* 319, 9–17. doi: 10.1016/S0009-8981(02)00015-3

Carey, H. V., Andrews, M. T., and Martin, S. L. (2003). Mammalian Hibernation: Cellular and Molecular Responses to Depressed Metabolism and Low Temperature. *Physiol. Rev.* 83, 1153–1181. doi: 10.1152/physrev.00008.2003

Corbach, S. (2006). *Untersuchung der CO_2-Euthanasie bei Labormäusen auf Tierschutzgerechtigkeit*. Ph. D. thesis, Hanover: Institut für Tierschutz und Verhalten.

Dahlgren, C., and Karlsson, A. (1999). Respiratory burst in human neutrophils. *J. Immunol. Methods* 232, 3–14. doi: 10.1016/S0022-1759(99)00146-5

Dahlgren, C., Björnsdottir, H., Sundqvist, M., Christenson, K., and Bylund, J. (2020). "Measurement of Respiratory Burst Products, Released or Retained, During Activation of Professional Phagocytes," in *Neutrophil. Methods and Protocols*, 3rd Edn, eds M. T. Quinn and F. R. DeLeo (New York: Humana Press), 301–324. doi: 10.1007/978-1-0716-0154-9_22

Dahlgren, C., Karlsson, A., and Bylund, J. (2019). Intracellular Neutrophil Oxidants: From Laboratory Curiosity to Clinical Reality. *J. Immunol.* 202, 3127–3134. doi: 10.4049/jimmunol.1900235

Dang, P. M. C., Stensballe, A., Boussetta, T., Raad, H., Dewas, C., Kroviarski, Y., et al. (2006). A specific p47 phox-serine phosphorylated by convergent MAPKs mediates neutrophil NADPH oxidase priming at inflammatory sites. *J. Clin. Investig.* 116, 2033–2043. doi: 10.1172/JCI27544

Dilek, N., Papapetropoulos, A., Toliver-Kinsky, T., and Szabo, C. (2020). Hydrogen sulfide: An endogenous regulator of the immune system. *Pharmacol. Res.* 161:105119. doi: 10.1016/j.phrs.2020.105119

Dinauer, M. C. (2020). "Neutrophil Defects and Diagnosis Disorders of Neutrophil Function: An Overview," in *Neutrophil: Methods and Protocols*, eds M. T. Quinn and F. R. DeLeo (New York, NY: Springer US), 11–29. doi: 10.1007/978-1-0716-0154-9_2

Dugbartey, G. J., Bouma, H. R., Saha, M. N., Lobb, I., Henning, R. H., and Sener, A. (2018). A hibernation-like state for transplantable organs: is hydrogen sulfide therapy the future of organ preservation? *Antioxidants Redox Signal.* 28, 1503–1515. doi: 10.1089/ars.2017.7127

Faller, S., Hausler, F., Goeft, A., von Itter, M.-N. A., Gyllenram, V., Hoetzel, A., et al. (2018). Hydrogen sulfide limits neutrophil transmigration, inflammation, and oxidative burst in lipopolysaccharide-induced acute lung injury. *Sci. Rep.* 8:14676. doi: 10.1038/s41598-018-33101-x

Fox, J., and Weisberg, S. (2018). *An R Companion to Applied Regression*. Thousand Oaks, CA: Sage.

Freitas, M., Lima, J. L. F. C., and Fernandes, E. (2009). Optical probes for detection and quantification of neutrophils' oxidative burst. *Rev. Anal. Chim. Acta* 649, 8–23. doi: 10.1016/j.aca.2009.06.063

Geiser, F. (2013). Hibernation. *Curr. Biol.* 23, R188–R193. doi: 10.1016/j.cub.2013.01.062

Gelling, M., McLaren, G. W., Mathews, F., Mian, R., and Macdonald, D. W. (2009). Impact of trapping and handling on Leukocyte Coping Capacity in bank votes (*Clethrionomys glareolus*) and wood mice (*Apodemus sylvaticus*). *Anim. Welfare* 18, 1–7.

Gelling, M., Montes, I., Moorhouse, T. P., and Macdonald, D. W. (2010). Captive Housing during Water Vole (*Arvicola terrestris*) Reintroduction: Does Short-Term Social Stress Impact on Animal Welfare? *PLoS One* 5:e9791. doi: 10.1371/journal.pone.0009791

Giroud, S., Habold, C., Nespolo, R. F., Mejías, C., Terrien, J., Logan, S. M., et al. (2020). The torpid state: Recent advances in metabolic adaptations and protective mechanisms. *Front. Physiol.* 11:1824. doi: 10.3389/fphys.2020.623665

Giroud, S., Stalder, G., Gerritsmann, H., Kübber-Heiss, A., Kwak, J., Arnold, W., et al. (2018). Dietary Lipids Affect the Onset of Hibernation in the Garden Dormouse (*Eliomys quercinus*): Implications for Cardiac Function. *Front. Physiol.* 9:1235. doi: 10.3389/fphys.2018.01235

Giroud, S., Zahn, S., Criscuolo, F., Chery, I., Blanc, S., Turbill, C., et al. (2014). Late-born intermittently fasted juvenile garden dormice use torpor to grow and fatten prior to hibernation: consequences for ageing processes. *Proc. R. Soc. B* 281:20141131. doi: 10.1098/rspb.2014.1131

Havenstein, N., and Fietz, J. (2013). Recovery of the immune system after hibernation in an obligate hibernator, the edible dormouse. *Brain Behav. Immun.* 29, S23–S24. doi: 10.1016/j.bbi.2013.01.072

Heldmaier, G., Ortmann, S., and Elvert, R. (2004). Natural hypometabolism during hibernation and daily torpor in mammals. *Resp. Physiol. Neurobiol.* 141, 317–329. doi: 10.1016/j.resp.2004.03.014

Hothorn, T., Bretz, F., and Westfall, P. (2008). Simultaneous Inference in General Parametric Models. *Biometr. J.* 50, 346–363. doi: 10.1002/bimj.200810425

Huber, N., Canoine, V., Cornils, J. S., Maggini, I., Cardinale, M., Ruf, T., et al. (2020). Leukocyte coping capacity as a complementary stress metric in migrating birds. *J. Ornithol.* 161, 909–913. doi: 10.1007/s10336-020-01774-9

Huber, N., Marasco, V., Painer, J., Vetter, S. G., Göritz, F., Kaczensky, P., et al. (2019). Leukocyte Coping Capacity: An Integrative Parameter for Wildlife Welfare Within Conservation Interventions. *Front. Vet. Sci.* 6:105. doi: 10.3389/fvets.2019.00105

Jastroch, M., Giroud, S., Barrett, P., Geiser, F., Heldmaier, G., and Herwig, A. (2016). Seasonal Control of Mammalian Energy Balance: Recent advances in the understanding of daily torpor and hibernation. *J. Neuroendocrinol.* 28:12437. doi: 10.1111/jne.12437

Jørgensen, P. G., Evans, A., Kindberg, J., Olsen, L. H., Galatius, S., and Fröbert, O. (2020). Cardiac adaptation in hibernating, free-ranging Scandinavian Brown Bears (*Ursus arctos*). *Sci. Rep.* 10:247. doi: 10.1038/s41598-019-57126-y

Karlsson, A., Nixon, J. B., and McPhail, L. C. (2000). Phorbol myristate acetate induces neutrophil NADPH-oxidase activity by two separate signal transduction pathways: dependent or independent of phosphatidylinositol 3-kinase. *J. Leukoc. Biol.* 67, 396–404. doi: 10.1002/jlb.67.3.396

Kaya, H., Yılmaz, S., Gürkan, M., and Hisar, O. (2013). Effects of environmental hypercapnia on hemato-immunological parameters, carbonic anhydrase, and Na+, K+-ATPase enzyme activities in rainbow trout (*Oncorhynchus mykiss*) tissues. *Toxicol. Environ. Chem.* 95, 1395–1407. doi: 10.1080/02772248.2014.887629)

Kizhina, A., Uzenbaeva, L., Antonova, E., Belkin, V., Ilyukha, V., and Khizhkin, E. (2018). Hematological Parameters in Hibernating *Eptesicus nilssonii* (Mammalia: Chiroptera) Collected in Northern European Russia. *Acta Chiropterol.* 20, 273–283. doi: 10.3161/15081109ACC2018.20.1.021

Kukovetz, E. M., Bratschitsch, G., Hofer, H. P., Egger, G., and Schaur, R. J. (1997). Influence of Age on the Release of Reactive Oxygen Species by Phagocytes as Measured by a Whole Blood Chemiluminescence Assay. *Free Radic. Bio. Med.* 22, 433–438. doi: 10.1016/S0891-5849(96)00334-6

Kuznetsova, E. V., Feoktistova, N. Y., Naidenko, S. V., Surov, A. V., Tikhonova, N. B., and Kozlovskii, J. E. (2016). Seasonal changes in blood cells and biochemical parameters in the Mongolian hamster (*Allocricetulus curtatus*). *Biol. Bull.* 43, 344–349. doi: 10.1134/S1062359016040087

Lane, J. E. (2012). "Evolutionary Ecology of Mammalian Hibernation Phenology," in *Living in a Seasonal World. Thermoregulatory and Metabolic Adaptations*, eds T. Ruf, C. Bieber, W. Arnold, and E. Millesi (Berlin: Springer), 51–61.

Lilius, E. M., and Marnila, P. (1992). Photon emission of phagocytes in relation to stress and disease. *Experientia* 48, 1082–1091.

Logan, S. M., and Storey, K. B. (2016). Avoiding apoptosis during mammalian hibernation. *Temperature* 4, 15–17. doi: 10.1080/23328940.2016.1211071

Logan, S., Watts, A., Posautz, A., Kübber-Heiss, A., Painer, J., Stalder, G., et al. (2020). The Ratio of Linoleic and Linolenic Acid in the Pre-hibernation Diet Influences NFκB Signaling in Garden Dormice During Torpor. *Front. Mol. Biosci.* 7:97. doi: 10.3389/fmolb.2020.00097

Mahlert, B., Gerritsmann, H., Stalder, G., Ruf, T., Zahariev, A., Blanc, S., et al. (2018). Implications of being born late in the active season for growth, fattening, torpor use, winter survival and fecundity. *eLife* 7:e31225. doi: 10.7554/eLife.31225

Mantovani, A., Cassatella, M. A., Costantini, C., and Jaillon, S. (2011). Neutrophils in the activation and regulation of innate and adaptive immunity. *Nat. Rev. Immunol.* 11, 519–531. doi: 10.1038/nri3024

Merényi, G., Lind, J., and Eriksen, T. E. (1990). Luminol Chemiluminescence: Chemistry, Excitation, Emitter. *J. Biolumin. Chemilumin.* 5, 53–56. doi: 10.1002/bio.1170050111

Mrosovsky, N., and Lang, K. (1980). Body weights of garden dormice, *Eliomys quercinus*, kept in constant conditions for two years. *Comp. Biochem. Physiol. A* 67, 667–669. doi: 10.1016/0300-9629(80)90257-1

Müller-Peddinghaus, R. (1984). *In vitro* determination of phagocyte activity by luminol- and lucigenin-amplified chemiluminescence. *Int. J. Immunopharmacol.* 6, 455–466. doi: 10.1016/0192-0561(84)90084-5

Muzaffar, S., Jeremy, J. Y., Sparatore, A., Del Soldato, P., Angelini, G. D., and Shukla, N. (2008a). H_2S-donating sildenafil (ACS6) inhibits superoxide formation and gp91^{phox} expression in arterial endothelial cells: role of protein kinases A and G. *Br. J. Pharmacol.* 155, 984–994. doi: 10.1038/bjp.2008.326

Muzaffar, S., Shukla, N., Bond, M., Newby, A. C., Angelini, G. D., Sparatore, A., et al. (2008b). Exogenous Hydrogen Sulfide Inhibits Superoxide Formation, NOX-1 Expression and Rac_1 Activity in Human Vascular Smooth Muscle Cells. *J. Vasc. Res.* 45, 521–528. doi: 10.1159/000129686

Novoselova, E. G., Kolaeva, S. G., Makar, V. R., and Agaphonova, T. A. (2000). Production of tumor necrosis factor in cells of hibernating ground squirrels *Citellus Undulatus* during annual cycle. *Life Sci.* 67, 1073–1080. doi: 10.1016/S0024-3205(00)00698-6

Peake, J., Wilson, G., Hordern, M., Suzuki, K., Yamaya, K., Nosaka, K., et al. (2004). Changes in neutrophil surface receptor expression, degranulation, and respiratory burst activity after moderate- and high-intensity exercise. *J. Appl. Physiol.* 97, 612–618. doi: 10.1152/japplphysiol.01331.2003

Pecaut, M. J., Smith, A. L., Jones, T. A., and Gridley, D. S. (2000). Modification of immunologic and hematologic variables by method of CO2 euthanasia. *Comparat. Med.* 50, 595–602.

Pinheiro, J., Bates, D., DebRoy, S., Sarkar, D., and R Development Core team. (2017). *nlme: Linear and Nonlinear Mixed Effects Models*. Vienna: R Core Team.

Prendergast, B. J., Freeman, D. A., Zucker, I., and Nelson, R. J. (2002). Periodic arousal from hibernation is necessary for initiation of immune responses in ground squirrels. *Am. J. Physiol. Reg. Int. Comp. Physiol.* 282, R1054–R1082. doi: 10.1152/ajpregu.00562.2001

Quinn, M. T., and Gauss, K. A. (2004). Structure and regulation of the neutrophil respiratory burst oxidase: comparison with nonphagocyte oxidases. *J. Leukoc. Biol.* 76, 760–781. doi: 10.1189/jlb.0404216

R Core Team (2019). *R: A language and environment for statistical computing*. Vienna: R Foundation for Statistical Computing.

Rastogi, R., Geng, X., Li, F., and Ding, Y. (2017). NOX Activation by Subunit Interaction and Underlying Mechanisms in Disease. *Front. Cell. Neurosci.* 10:301. doi: 10.3389/fncel.2016.00301

Ruf, T., and Geiser, F. (2015). Daily torpor and hibernation in birds and mammals. *Biol. Rev.* 90, 891–926. doi: 10.1111/brv.12137

Sahdo, B., Evans, A. L., Arnemo, J. M., Fröbert, O., Särndahl, E., and Blanc, S. (2013). Body temperature during hibernation Is highly correlated with a decrease in circulating innate immune cells in the brown bear (*Ursus arctos*): A common feature among hibernators? *Int. J. Med. Sci.* 10, 508–514. doi: 10.7150/ijms.4476

Shelton-Rayner, G. K., Mian, R., Chandler, S., Robertson, D., and Macdonald, D. W. (2012). Leukocyte responsiveness, a quantitative assay for subjective mental workload. *Int. J. Ind. Ergonom.* 42, 25–33. doi: 10.1016/j.ergon.2011.11.004

Shivatcheva, T. M., Ankov, V. K., and Hadjioloff, A. I. (1988). Circannual fluctuations of the serum cortisol in the European ground squirrel, *Citellus citellus* L. *Comp. Biochem. Physiol. A* 90, 515–518. doi: 10.1016/0300-9629(88)90229-0

Sohnle, P. G., and Chusid, M. J. (1983). The effect of temperature on the chemiluminescence response of neutrophils from rainbow trout and man. *J. Comp. Pathol.* 93, 493–497. doi: 10.1016/0021-9975(83)90054-3

Storey, K. B. (2010). Out cold: biochemical regulation of mammalian hibernation - a mini-review. *Gerontology* 56, 220–130. doi: 10.1159/000228829

Talaei, F., Bouma, H. R., Hylkema, M. N., Strijkstra, A. M., Boerema, A. S., Schmidt, M., et al. (2012). The role of endogenous H_2S formation in reversible remodeling of lung tissue during hibernation in the Syrian hamster. *J. Exp. Biol.* 215, 2912–2919. doi: 10.1242/jeb.067363

Terrien, J., Perret, M., and Aujard, F. (2011). Behavioral thermoregulation in mammals: a review. *Front. Biosci.* 16:1428–1444. doi: 10.2741/3797

Thiele, J. R., Zeller, J., Kiefer, J., Braig, D., Kreuzaler, S., Lenz, Y., et al. (2018). A conformational change in C-reactive protein enhances leukocyte recruitment and reactive oxygen species generation in ischemia/reperfusion injury. *Front. Immunol.* 9:675. doi: 10.3389/fimmu.2018.00675

Uzenbaeva, L. B., Kizhina, A. G., Ilyukha, V. A., Belkin, V. V., and Khizhkin, E. A. (2019). Morphology and Composition of Peripheral Blood Cells during Hibernation in Bats (Chiroptera, Vespertilionidae) of Northwestern Russia. *Biol. Bull.* 46, 398–406. doi: 10.1134/S1062359019030130

Wenisch, C., Narzt, E., Sessler, D. I., Parschalk, B., Lenhardt, R., Kurz, A., et al. (1996). Mild Intraoperative Hypothermia Reduces Production of Reactive Oxygen Intermediates by Polymorphonuclear Leukocytes. *Anesth. Analg.* 82:23. doi: 10.1097/00000539-199604000-00023

Yang, W., Tao, Y., Wu, Y., Zhao, X., Ye, W., Zhao, D., et al. (2019). Neutrophils promote the development of reparative macrophages mediated by ROS to orchestrate liver repair. *Nat. Commun.* 10:1076. doi: 10.1038/s41467-019-09046-8

Ying, W. (2008). NAD+/NADH and NADP+/NADPH in cellular functions and cell death: regulation and biological consequences. *Antioxid. Redox Signal.* 10, 179–206. doi: 10.1089/ars.2007.1672

Zeileis, A., and Grothendieck, G. (2005). zoo: S3 infrastructure for regular and irregular time series. *J. Stat. Softw.* 14, 1–27.

Conflict of Interest: The authors declare that the research was conducted in the absence of any commercial or financial relationships that could be construed as a potential conflict of interest.

frontiers in Physiology

ORIGINAL RESEARCH
published: 24 March 2021
doi: 10.3389/fphys.2021.623401

Discrepancies in the Time Course of Sleep Stage Dynamics, Electroencephalographic Activity and Heart Rate Variability Over Sleep Cycles in the Adaptation Night in Healthy Young Adults

*Ai Shirota[1], Mayo Kamimura[1], Akifumi Kishi[2], Hiroyoshi Adachi[3,4], Masako Taniike[3,5] and Takafumi Kato[1,3,5]**

[1] Department of Oral Physiology, Osaka University Graduate School of Dentistry, Suita, Japan, [2] Graduate School of Education, The University of Tokyo, Bunkyo-ku, Japan, [3] Osaka University Hospital, Sleep Medicine Center, Suita, Japan, [4] Osaka University Health and Counseling Center, Toyonaka, Japan, [5] Department of Child Development, Osaka University United Graduate School of Child Development, Suita, Japan

OPEN ACCESS

Edited by:
Alessandro Silvani, University of Bologna, Italy

Reviewed by:
Luigi De Gennaro, Sapienza University of Rome, Italy
Raffaele Manni, Fondazione Casimiro Mondino National Neurological Institute (IRCCS), Italy

***Correspondence:**
Takafumi Kato
takafumi@dent.osaka-u.ac.jp

Specialty section:
This article was submitted to Integrative Physiology, a section of the journal Frontiers in Physiology

Received: *30 October 2020*
Accepted: *12 February 2021*
Published: *24 March 2021*

Citation:
Shirota A, Kamimura M, Kishi A, Adachi H, Taniike M and Kato T (2021) Discrepancies in the Time Course of Sleep Stage Dynamics, Electroencephalographic Activity and Heart Rate Variability Over Sleep Cycles in the Adaptation Night in Healthy Young Adults. Front. Physiol. 12:623401. doi: 10.3389/fphys.2021.623401

Objective: The aim of the present study was to characterize the cyclic sleep processes of sleep-stage dynamics, cortical activity, and heart rate variability during sleep in the adaptation night in healthy young adults.

Methods: Seventy-four healthy adults participated in polysomnographic recordings on two consecutive nights. Conventional sleep variables were assessed according to standard criteria. Sleep-stage continuity and dynamics were evaluated by sleep runs and transitions, respectively. These variables were compared between the two nights. Electroencephalographic and cardiac activities were subjected to frequency domain analyses. Cycle-by-cycle analysis was performed for the above variables in 34 subjects with four sleep cycles and compared between the two nights.

Results: Conventional sleep variables reflected lower sleep quality in the adaptation night than in the experimental night. Bouts of stage N1 and stage N2 were shorter, and bouts of stage Wake were longer in the adaptation night than in the experimental night, but there was no difference in stage N3 or stage REM. The normalized transition probability from stage N2 to stage N1 was higher and that from stage N2 to N3 was lower in the adaptation night, whereas that from stage N3 to other stages did not differ between the nights. Cycle-by-cycle analysis revealed that sleep-stage distribution and cortical beta EEG power differed between the two nights in the first sleep cycle. However, the HF amplitude of the heart rate variability was lower over the four sleep cycles in the adaptation night than in the experimental night.

Conclusion: The results suggest the distinct vulnerability of the autonomic adaptation processes within the central nervous system in young healthy subjects while sleeping in a sleep laboratory for the first time.

Keywords: first-night effect, adaptation, sleep-stage transition, sleep-stage continuity, sleep cycle, EEG power, heart rate variability, sleep process

INTRODUCTION

The sleep architecture throughout the night is continuous, but heterogeneous, and characterized by cyclic fluctuations. Alternating non-rapid eye movement (NREM) sleep and rapid eye movement (REM) sleep constitute a series of sleep cycles, with the latter being related to the sleep cycle configuration (Vyazovskiy and Delogu, 2014). Sleep cycles last for approximately 90 min (Hartmann, 1968) and are repeated 3–5 times in one night (Hartmann, 1968; Hirshkowitz et al., 1992; Rosipal et al., 2013). Mutual interactions between the genesis of NREM and REM sleep underlie the stability of sleep cycles overnight (Kishi et al., 2011; Hayashi et al., 2015). Sleep processes and continuity within one sleep cycle are characterized by dynamic phenomena such as transitions among sleep stages (Lo et al., 2004; Kishi et al., 2008, 2011). Sleep stages are associated with cortical electroencephalography (EEG) and autonomic nervous system activities (Žemaitytė et al., 1984; Toscani et al., 1996; Brandenberger et al., 2001); slow-wave sleep is characterized by high cortical delta power, whereas light NREM sleep and REM sleep are characterized by low delta power (Brandenberger et al., 2001). Reciprocal changes in sympathetic and parasympathetic modulation tone are correlated with the cortical delta power within a sleep cycle (Brandenberger et al., 2001). The ratio of sleep stages and activity levels of cortical and autonomic systems in a sleep cycle gradually change from the initial to late periods of sleep cycles (Dement and Wolpert, 1958; Feinberg, 1974; Brandenberger et al., 2001; Versace et al., 2003). Therefore, the time-course changes in sleep variables over sleep cycles represent the progression of sleep processes in the integration of cortical and autonomic homeostatic sleep regulation overnight (Hayashi et al., 2015).

Previous studies demonstrated that the progression and stability of sleep can be altered when one sleeps in an unfamiliar environment. A typical example is the first-night effect, a phenomenon that is commonly observed in the first night of polysomnographic recordings for the purpose of adaptation to sleep laboratory settings (Agnew et al., 1966). Sleep in the adaptation night is characterized by poorer sleep quality than in subsequent nights due to increased sleep latency, less REM sleep, and frequent arousal (Hirshkowitz et al., 1992; Sforza et al., 2008; Rosipal et al., 2013). A difference in the sleep architecture overnight between the adaptation and experimental nights was generally detected during the initial period of sleep or in the first sleep cycle such as a delay in the onset of NREM sleep stages and REM sleep latency (Agnew et al., 1966; Tamaki et al., 2005a). We therefore hypothesized that the sleep architecture in the first sleep cycle is most influenced by the laboratory environment in the adaptation night and the influences on sleep decrease in the subsequent sleep cycles in healthy subjects.

The characteristics of sleep in the adaptation night were previously investigated by conventional analyses of sleep architecture such as the amount of each sleep stage. Recent studies analyzed sleep continuity and characterized the patterns of sleep-stage transitions in order to elucidate the dynamic nature of sleep regulation (Kishi et al., 2017, 2020). The analyses in these studies revealed the novel properties of sleep regulation that were not detected by the conventional sleep-stage variables (Norman et al., 2006; Kishi et al., 2011). Therefore, the quantification of sleep continuity and sleep-stage transitions will enable the further characterization of sleep in the adaptation night. In addition, sleep variables assessed by sleep-stage scoring may not be concordant with those by the quantitative analyses of EEG and heart rate variability (HRV) activities in the adaptation night (Toussaint et al., 1997; Le Bon et al., 2001; Curcio et al., 2004; Israel et al., 2012; Virtanen et al., 2018). As such, analysis of sleep-stage dynamics and the quantification of cortical/cardiac activities may provide physiological insights into sleep processes over sleep cycles in the adaptation night. Therefore, the aim of the present study was to investigate the time-course changes in sleep-stage transitions, cortical EEG power, and heart rate variability in the progress of sleep cycles in the adaptation night in comparison with the experimental night in healthy subjects.

MATERIALS AND METHODS

Participants

One hundred participants aged between 20 and 33 years (47 women and 53 men, mean age 24.3 ± 2.9 years) were enrolled in the PSG study at Osaka University between November 25th, 2013, and September 25th, 2019. The participants were recruited via flyers posted and word of mouth. They were compensated for participation (5,000 JPY). The sample size was determined by a prior power analysis in order to detect a medium effect size (dz = 0.5) with a power of 0.90 by a two-tailed paired *t*-test. All participants completed a written informed consent form approved by the Research Ethics Committee of Osaka University Graduate School of Dentistry and Osaka University Dental Hospital. This study was approved by the ethics committee of the Osaka University Dental Hospital and the Graduate School of Dentistry (H25-E9-5, H29-E48-3).

Polysomnography and Sleep Stages

Polysomnographic recordings were performed on two consecutive nights in a sleep laboratory at Osaka University Graduate School of Dentistry. All subjects completed the Pittsburgh Sleep Quality Index (PSQI) for Japanese (Doi et al., 2000) and Self-rating Depression Scale: SDS (Zung, 1965): the Japanese version of the SDS (Fukuda and Kobayashi, 1973). The PSQI is a subjective questionnaire to assess sleep quality and disturbances over a 1 month period, and the SDS is a self-administered survey to quantify the depressed status of a patient. Subjects were instructed to lead a regular life prior to participating in the recording evaluation. They were not allowed to nap, perform excessive exercise, or drink alcohol before coming to the sleep lab on the two nights. On the day of the PSG recording, participants arrived at our sleep lab at approximately 8:30 pm. The light was off between 10:30 and 11:00 p.m. and on in the next morning between 6:30 and 7:30 a.m. or when they woke up. The times for lights-on and -off were the same between the two nights. After waking up, participants answered the questionnaire on the quality of sleep; they were asked about sleep latency, number of periods of wakefulness after sleep onset, total sleep time and, sleep quality score (from 1 point: "bad" to 5 points: "good").

PSG recordings were performed using surface electroencephalography (EEGs: C3-A2, C4-A1, O1-A2, O2-A1, F3-A2, F4-A1, Fp1-A2, and Fp2-A1), bilateral electrooculography (EOG), lead II electrocardiography (ECG), and chin electromyography (EMG). Signals were amplified, filtered (EEG, EOG, and ECG: 0.3–70 Hz; EMG: > 10 Hz, with a 60 Hz hum filter), and recorded with a sampling frequency of 200 Hz using a software package (Embla N7000, REMbrandt^{TM} PSG software, Natus Medical, Pleasanton, CA). The stage was scored by one technician (registered polysomnographic technologist) blinded to the study aims (Nonoue et al., 2017). Oronasal thermal airflow, nasal pressure, chest, and abdominal movements, arterial oxygen saturation, and body position were also recorded. Audio and video recordings were performed simultaneously. Sleep stages and respiratory events were scored according to the American Academy of Sleep Medicine criteria version 2.1 (Berry et al., 2014). The apnea–hypopnea index (AHI) was calculated as the sum of all apneas and hypopneas with 3% O_2 desaturation and/or EEG arousal divided by the total sleep time. The AHI exclusion criteria followed the AASM criteria (Berry et al., 2014). Subjects with AHI $\geq$5 times/h were excluded from the analyses of this study; they may exhibit a lower quality of sleep than the others even though they did not exhibit signs or symptoms of sleep apnea (Okura et al., 2020).

Sleep Cycles

The sleep cycle was assessed with reference to the method proposed by Feinberg (1974). A sleep cycle was defined as the time from the end of REM sleep to the end of the next REM sleep. The first sleep cycle was defined as the time from sleep onset to the end of the first REM sleep. REM sleep was considered to be two separate REM sleep periods if it discontinued for more than 20 min and one REM sleep period if the gap was less than 20 min. Furthermore, participants were considered to have been in a REM sleep period if they woke up less than 10 min from the last REM sleep even if the sleep stage immediately before the end of the PSG recording was not REM sleep. Sleep cycles were considered to have been completed only if another sleep stage was continued more than 10 min from the last REM sleep and the number of complete cycles was measured accordingly. The number of REM sleep periods included those in which the last stage of the sleep cycle before waking up was REM sleep. In order to compare the variables (i.e., sleep stage, cortical activity, and heart rate variability) for sleep cycles between the adaptation night and the experimental night within a subject, the same number of sleep cycles was analyzed because the number of sleep cycles differed between the two nights in some subjects.

Sleep-Stage Transition

The number of sleep-stage transitions per night was measured for each participant, and the rate of stage transitions (%) was calculated by dividing the number of sleep transitions per night by the total number of epochs. The same method was used to calculate the percentage of sleep stages for each sleep cycle. Normalized transition probabilities between five sleep stages were calculated by dividing the number of transitions from the specific stage to one of the other stages by the total number of transitions from the specific stage to another stage (Kishi et al., 2008, 2011).

The continuity of sleep (regardless of sleep stage) and each sleep stage (N1, N2, N3, REM, and wake) were analyzed with the rules in the previous study (Kishi et al., 2017). A sleep run began with a transition from Wake to any stage of sleep and continued until Wake occurred. Separate from the sleep run, a run of each sleep stage (N1, N2, N3, REM, and Wake) was defined as consecutive epochs scored as the stage, terminated by one or more epochs scored as another stage.

Cortical and Cardiac Activities

During the night, continuous EEG (C4 referenced to the left ear) was digitized at 200 Hz and stored for off-line analysis. Prior to the analysis, epochs with artifacts were visually identified and removed. Spectral power was calculated using the fast Fourier transform (FFT) algorithm (Bio Trend Professional, NoruPro Light Systems). FFT windows of 2,048 points were used, and truncating error was reduced by applying a Hanning window. The frequency resolution was 0.25 Hz. The analysis window was 10.24 s with a 0.24 s overlap every 10 s, and the data for three units were averaged to obtain a value every 30 s. The limits for band frequencies were as follows: delta, 0.5–4 Hz; theta, 4–8 Hz; alpha, 8–12 Hz; sigma, 12–15 Hz; low beta, 15–23 Hz; high beta, 23–32 Hz.

Heart rate analysis was performed using complex demodulation (CD) (Shin et al., 1989). The oscillations can be characterized based on the heart rate accelerating or slowing, the wavelength, and/or the amplitude (Task Force of the European Society of Cardiology and the North American Society of Pacing and Electrophysiology, 1996). The correlations of frequency components of HRV, however, diminish as the wavelength of the oscillations and the recording duration increase. The CD method uses the techniques of interpolation and detrending (Shin et al., 1989; Hayano et al., 1993) and provides the time resolution necessary to detect short-term heart rate changes and to describe the amplitude and phase of particular frequency components as functions of time (Task Force of the European Society of Cardiology and the North American Society of Pacing and Electrophysiology, 1996). The mean value of the instantaneous amplitude (in ms) was calculated in 30 s windows using a computer program with a time scale of 0.1 s and a frequency resolution of 0.002 Hz (HRV LOG-Pro-DSA Analysis, NoruPro Light Systems). Following the removal of epochs with artifacts, frequency spectra in RR interval data were estimated for the range between zero and 0.40 Hz and were divided into three components depending on their central frequencies, i.e., the spectral domain with a central frequency of less than 0.04 Hz, between 0.04 and 0.15 Hz, and greater than 0.15 Hz but less than 0.40 Hz. These domains were labeled as bands with a very low frequency (VLF), low frequency (LF), and high frequency (HF), respectively (Malliani et al., 1991). HRV reflects autonomic modulation, whereas the average RR interval reflects autonomic tone. In the present study, HF amplitude was used as an index of alteration of parasympathetic nervous system activity.

Statistical Analysis

Paired *t*-tests were used to compare the adaptation and experimental nights, in addition to the mean duration of runs

for sleep and each sleep stage. The effect size was presented in Cohen's d, which was the mean preference index divided by the standard deviation. To individually assess variables that were significantly affected by the first-night effect, a three-way analysis of variance (ANOVA) for repeated measures [(night: two levels), (sleep stage: five levels), and (cycle: four levels)] was used. Moreover, a two-way analysis of variance (ANOVA) for repeated measures [(night: two levels) and (cycle: four levels)] was used to assess EEG and HRV parameters. The Greenhouse–Geisser ε correction was performed to evaluate *F*-ratios for repeated measures involving more than one degree of freedom and when the sphericity assumption was not met. The effect size was presented in partial η^2, which was the sum of squares for the effect of interest divided by the total sum of squares for all data variance. *Post hoc* comparisons between pairs of nights were conducted using the paired *t*-test. Results were considered to be significant when *p*-values were less than 0.05.

RESULTS

Participants

Data from 26 participants were excluded from the analysis for the following reasons: sleep apnea syndrome (AHI $\geq$ 5 for both nights) (n = 19) and TST/TIB < 70% or sleep latency > 60 min (N = 7). As a result, 74 participants were included (40 women and 34 men, 20–33 years old, mean age 23.8 $\pm$ 2.2 years, BMI 20.5 $\pm$ 1.6 kg/m^2). The sleep quality assessed by the PSQI in all participants was 4.6 $\pm$ 1.96 (range: 0–21, cutoff score: 5.5≥). The average score on the SDS was within the standard range (range: 20–80, cutoff score: 40>, average score in all participants: 39.2 $\pm$ 5.49).

Sleep Variables for the Entire Night

Sleep variables measured during the adaptation and experimental nights are shown in **Table 1**. Although the time in bed did not significantly differ between the two nights, the total sleep time was shorter ($p < 0.01$) and sleep efficiency was lower ($p < 0.001$) in the adaptation night than in the experimental night. The latencies of stage N1 (i.e., sleep latency), stage N3, and stage REM were significantly longer in the adaptation night than in the experimental night (all $p < 0.05$). In terms of sleep stages, the adaptation night was characterized by a longer time in WASO (wakefulness after sleep onset) and stage N1 (both $p < 0.01$), and a shorter time in stage REM ($p < 0.001$) than in the experimental night. The number of REM sleep periods increased from the adaptation night to the experimental night ($p < 0.05$).

The percentage of transitions per night (%) was significantly higher in the adaptation night than in the experimental night ($p < 0.001$, **Table 1**). The arousal index was significantly higher in the adaptation night than in the experimental night ($p < 0.001$), but the number of awakenings did not significantly differ between the two nights. No significant difference was observed in AHI between the two nights. The subjective sleep parameters were better in the experimental night than in the adaptation night (No. of WASO, total sleep time, and sleep quality) (all $p < 0.05$, **Table 1**).

Sleep-Stage Continuity and Sleep-Stage Transitions for the Entire Night

The mean continuity time for sleep and each sleep stage is shown in **Table 2**. The mean duration of sleep runs was significantly shorter in the adaptation night than in the experimental night ($p < 0.01$). Runs of stage N1 and stage N2 were shorter in the adaptation night than in the experimental night (both $p < 0.01$), but no significant difference was observed in stage N3 or stage REM. On the other hand, the runs of stage Wake were significantly longer in the adaptation night than in the experimental night ($p < 0.01$).

Normalized transition probabilities among the five vigilance states (Wake, N1, N2, N3, and REM) for the two nights are shown in **Table 3**. The transition from Wake to N1 (Wake → N1) in the adaptation night was significantly higher, whereas that from Wake to N2 (Wake → N2) was significantly lower in the adaptation night than in the experimental night ($p < 0.01$). Normalized transition probabilities from N1 to REM (N1 → REM) significantly decreased in the adaptation night than in the ($p < 0.01$). Normalized transition probabilities from N2 to N1 (N2 → N1) were significantly higher in the adaptation night than in the experimental night ($p < 0.01$), whereas those from N2 to N3 (N2 → N3) were lower in the adaptation night than in the experimental night ($p < 0.01$). No inter-night differences were found in transitions from stage N3 to other stages. The frequency of transition from REM to N1 (REM → N1) was significantly lower in the adaptation night than in the experimental night ($p < 0.05$), whereas that from REM to N2 (REM → N2) was higher in the adaptation night than in the experimental night ($p < 0.01$).

Sleep Variables for Each Sleep Cycle

The percentage of each sleep stage in each sleep cycle is shown in **Figure 1**. In order to compare the variables for sleep cycles between the adaptation night and the experimental night within a subject, the same number of sleep cycles was analyzed (cycle 1 and cycle 2: n = 74, cycle 3: n = 63, cycle 4: n = 34). The three-way repeated-measures ANOVA (nights: two levels × sleep stage: five levels × sleep cycle: four levels) demonstrated a significant interaction [$F_{(12,396)} = 2.82$, $p = 0.022$, $\varepsilon = 0.38$, partial $\eta^2 = 0.085$]. *Post hoc* comparisons between the two nights in the first sleep cycle revealed that the percentages of stage Wake and N1 were significantly higher ($p < 0.01$), and that of stage N3 was significantly lower ($p < 0.01$) in the adaptation night than in the experimental night. *Post hoc* comparisons between the two nights in the second sleep cycle revealed that the percentage of stage REM was significantly lower ($p < 0.05$) in the adaptation night than in the experimental night. There were no significant differences between the two nights in the third and fourth sleep cycles.

Quantitative EEG and HRV Analyses

The mean spectral parameters of the first four sleep cycles calculated on the adaptation night and experimental night are shown in **Figure 2**. The two-way repeated-measures ANOVA (nights: two levels × sleep cycle: four levels) demonstrated a

TABLE 1 | Sleep variables in adaptation and experimental nights.

	Adaptation night		Experimental night			
	Mean	***SD***	**Mean**	***SD***	**Cohen's d**	***p***
Sleep architecture						
Time in bed (min)	466.9	34.6	468.3	33.8	0.04	0.646
Sleep efficiency (%)	91.6	4.9	94.1	4.0	0.57	<0.001**
Latency (min)						
Sleep latency	7.8	7.8	6.0	5.6	0.26	0.047*
N2 latency	11.5	8.4	9.9	7.3	0.21	0.098
N3 latency	22.3	18.1	17.3	9.3	0.35	0.011*
REM latency	110.4	43.0	97.3	42.0	0.31	0.028*
Percentage of sleep stages (%)						
N1	11.5	4.9	10.2	4.1	0.30	0.003**
N2	43.8	7.4	44.4	6.6	0.09	0.456
N3	21.9	7.4	22.6	6.6	0.10	0.289
REM	16.3	4.2	18.5	4.1	0.51	<0.001**
WASO	6.5	4.5	4.3	3.5	0.54	<0.001**
Sleep cycles						
No. of REM sleep period	3.9	0.8	4.3	0.8	0.33	0.014*
Stage transitions (%)						
Percentage of stage transitions	20.7	4.2	18.9	3.9	0.45	<0.001**
Arousal events						
Arousal index	12.9	5.7	9.8	4.5	0.60	<0.001**
Respiratory events						
AHI (no./h)	2.4	2.1	2.1	1.7	0.16	0.196
Subjective sleep parameters						
Sleep latency (min)	20.0	17.7	15.0	11.0	0.34	0.017*
No. of WASO	2.9	1.8	2.3	1.4	0.41	0.003**
Total sleep time (min)	415.7	71.9	434.0	41.3	0.31	0.024*
Sleep quality	2.5	0.9	2.9	1.0	0.36	0.002**

*SD, standard deviation; WASO, wakefulness after sleep onset; REM, rapid eye movement; AHI, apnea hypopnea index. *p < 0.05, **p < 0.01 from the experimental night by a two-tailed paired t-test.*

significant interaction [$F_{(3,99)} = 3.49$, $p = 0.019$, partial $\eta^2 = 0.096$] only in the high Beta band in the NREM sleep period. *Post hoc* comparisons between the two nights revealed that the high Beta band in NREM of the first sleep cycle was significantly higher ($p < 0.01$) in the adaptation night than in the experimental night.

TABLE 2 | Mean continuity time for sleep and each sleep stage.

	Adaptation night		Experimental night			
	Mean	***SD***	**Mean**	***SD***	**Cohen's d**	***p***
Sleep runs (min)	19.1	9.1	22.8	11.1	0.36	0.001**
N1 runs (min)	0.9	0.2	1.0	0.2	0.45	0.007**
N2 runs (min)	3.4	1.1	3.9	1.1	0.42	<0.001**
N3 runs (min)	7.0	5.3	6.1	2.4	0.22	0.129
REM runs (min)	9.1	6.0	8.8	5.1	0.06	0.590
Wake runs (min)	1.1	0.7	0.9	0.4	0.40	0.004**

*Values are means and standard deviations, **p < 0.01 from the experimental night by a two-tailed paired t-test.*

There were no significant differences between the two nights in all other bands in NREM and REM sleep periods.

The mean HF band and RR intervals of the first four sleep cycles calculated on the adaptation night and experimental night are shown in **Figure 3**. In the NREM sleep period, the two-way repeated-measures ANOVA (nights: two levels × sleep cycle: four levels) revealed a significant interaction between nights and sleep cycles for the RR intervals and HF amplitude [RR intervals: $F_{(3, 99)} = 2.88$, $p = 0.040$, partial $\eta^2 = 0.080$; HF amplitude: $F_{(3, 99)} = 3.08$, $p = 0.031$, partial $\eta^2 = 0.085$]. *Post hoc* comparisons between the two nights revealed that RR intervals and HF amplitude were significantly lower over the four sleep cycles in the adaptation night than in the experimental night (both $p < 0.05$). There were no significant differences between the two nights in RR intervals or HF amplitude in the REM sleep periods.

DISCUSSION

The present study investigated the process to adaptation to sleeping in a sleep laboratory in healthy young adults. The objective and subjective sleep quality was lower in the

TABLE 3 | Normalized transition probabilities between five behavioral states within the sleep period time in the adaptation and experimental nights.

		Adaptation night							Experimental night						
		Followed stage							Followed stage						
	(%)	Wake	N1	N2	N3	REM			(%)	Wake	N1	N2	N3	REM	
Previous stage	Wake		76.6**	16.8**	1.9	4.7**	100%	Previous stage	Wake		71.1	21.1	1.3	6.5	100%
	N1	14.0		77.1	0.6	8.3	100%		N1	12.1		75.8	0.7	11.4	100%
	N2	19.0	44.9**		27.7**	8.4	100%		N2	18.1	38.9		33.6	9.4	100%
	N3	18.6	9.8	71.2		0.4	100%		N3	16.6	9.0	73.9		0.5	100%
	REM	32.7	45.4*	21.7**	0.2		100%		REM	32.7	52.0	15.3	0.0		100%

*Normalized transition probabilities between Wake, N1, N2, N3, and REM within the sleep period time in the adaptation and experimental nights. The labels in the rows denote the preceding states, and those in the columns denote the subsequent states of transitions. *p < 0.05, **p < 0.01 from the experimental night by a two-tailed paired t-test.*

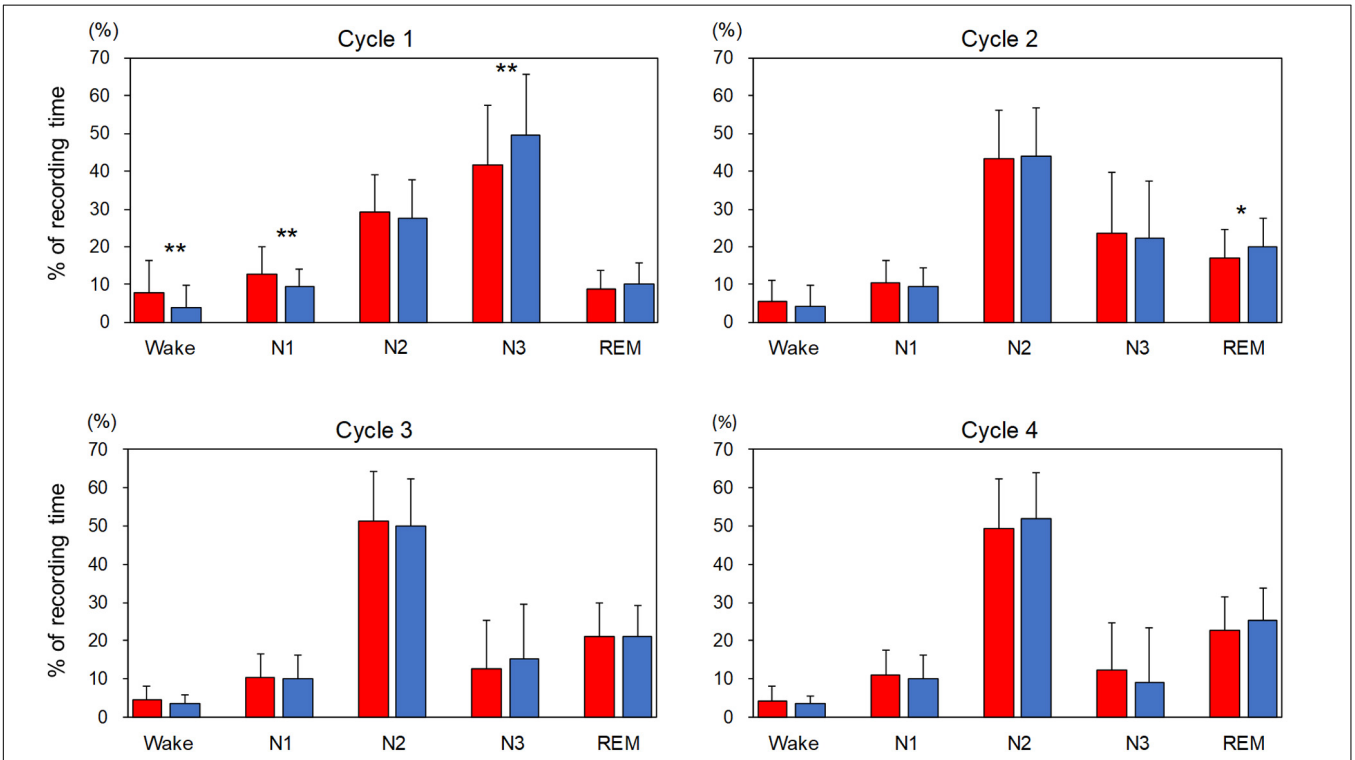

FIGURE 1 | Percentage of each sleep stage in each sleep cycle. The percentage of each sleep stage is present as mean and standard deviation (red box: adaptation night, blue box: experimental night). Values that significantly differed between nights are indicated by one ($p < 0.05$) or two stars ($p < 0.01$; two-tailed paired *t*-test). The numbers of subjects were 74 for cycles 1 and 2, 63 for cycle 3 and 34 for cycle 4.

adaptation night than in the experimental night and was characterized by low sleep continuity and high sleep-stage transitions in association with the changes in cortical EEG power and heart rate variability. Cycle-by-cycle analyses revealed differences in sleep-stage distribution and cortical beta EEG power in the first sleep cycle. However, heart rate variability differed in the four sleep cycles between the two nights. This suggested that the physiological systems representing sleep-stage dynamics, cortical activity, and heart rate variability were differentially altered during the progression of sleep cycles between the adaptation and experimental nights in healthy subjects.

Sleep-Stage Dynamics in the Entire Night and Sleep Cycles

The present study revealed that the sleep macrostructure on the adaptation night was characterized by reduced sleep efficiency, less REM sleep, more stage N1, more wakefulness, and more frequent arousal than in the experimental night (**Table 1**). This study supports previous findings on the so-called first-night effect (Agnew et al., 1966; Browman and Cartwright, 1980; Toussaint et al., 1995; Rotenberg et al., 1997; Le Bon et al., 2001; Curcio et al., 2004; Moser et al., 2010), although sleep architecture was of good quality for the two nights in this study population (e.g., sleep

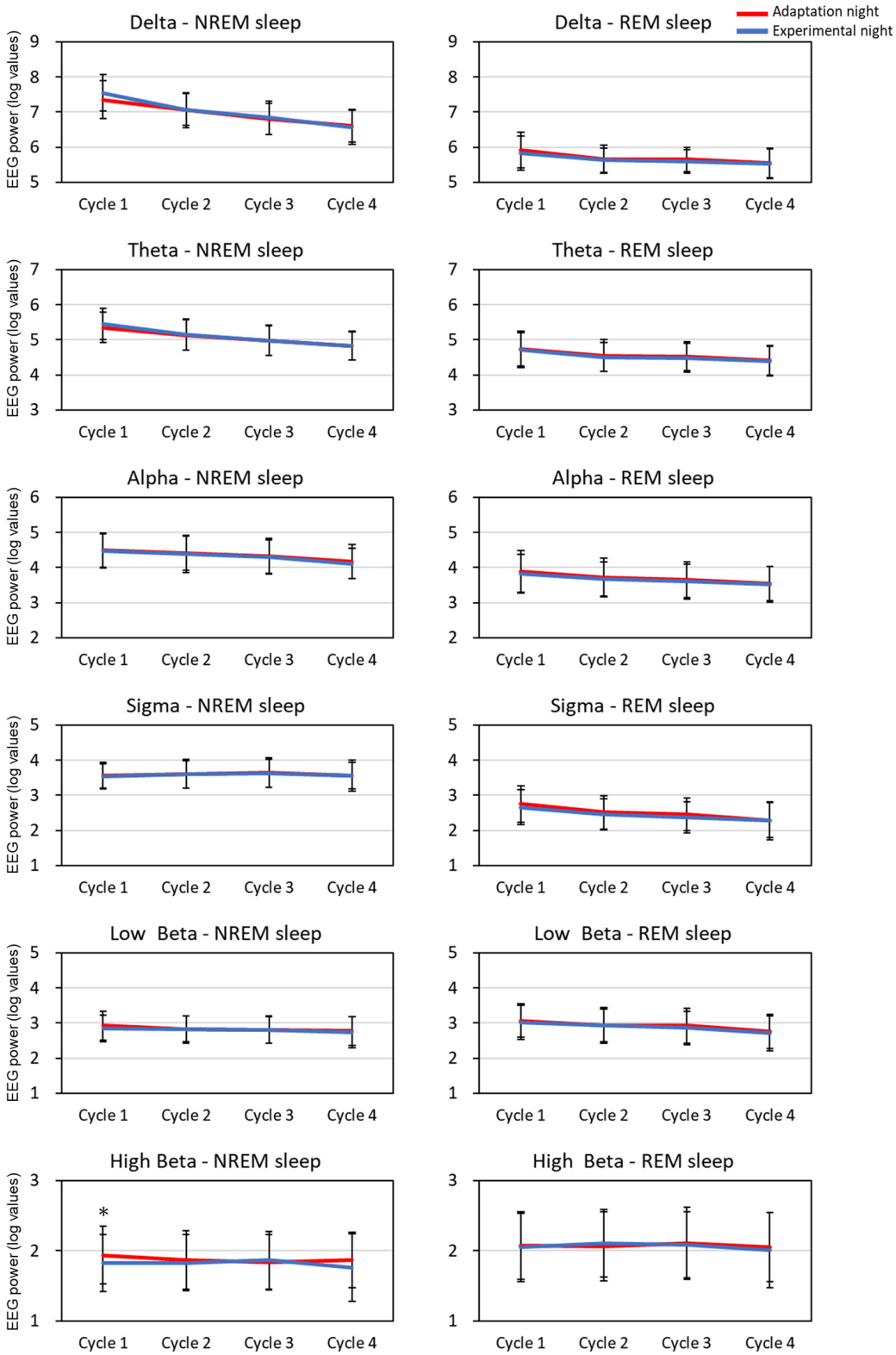

FIGURE 2 | EEG spectral power for each sleep cycle. EEG power was expressed as log-transformed values. The data is present as mean and standard deviation (red line: adaptation night, blue line: experimental night). Values that significantly differed between nights are indicated by one star ($p < 0.05$; two-tailed paired *t*-test). The frequency ranges were as follows: delta, 0.5–4 Hz; theta, 4–8 Hz; alpha, 8–12 Hz; sigma, 12–15 Hz; low beta, 15–23 Hz; high beta, 23–32 Hz. The numbers of subjects analyzed were the same as in **Figure 1**.

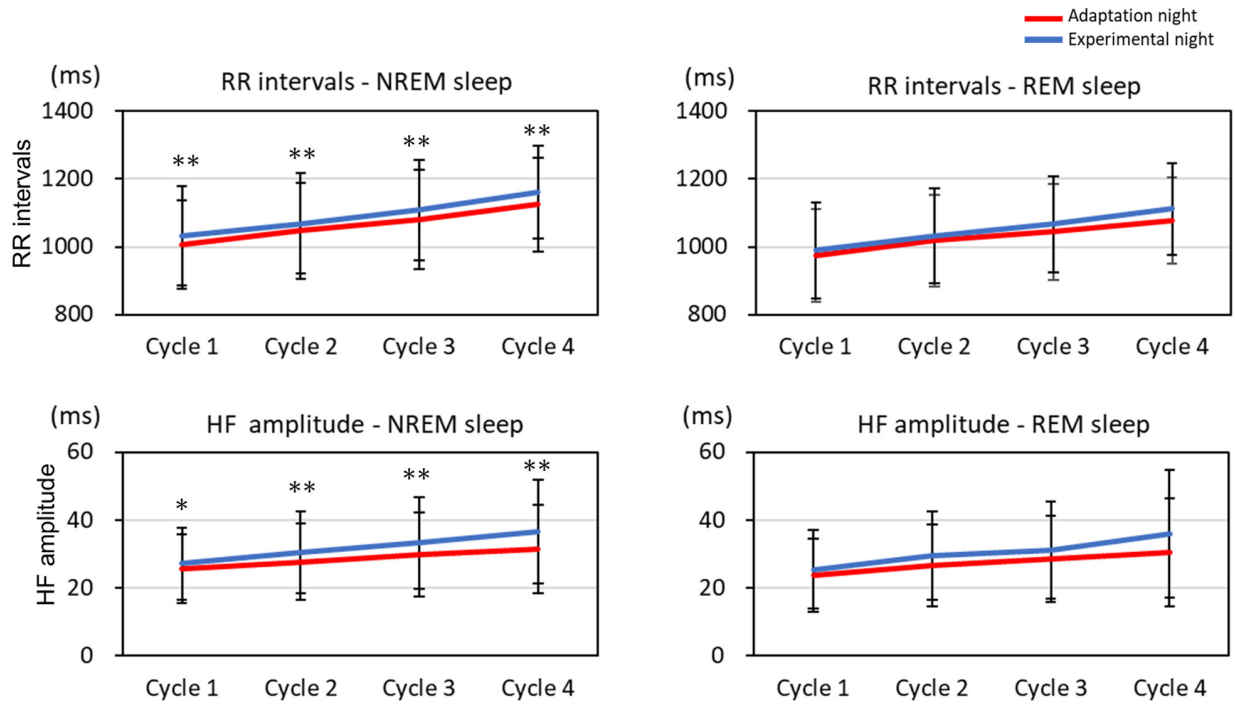

FIGURE 3 | RR intervals and HF amplitude for each sleep cycle. RR intervals and HF amplitude for each sleep cycle are present as mean and standard deviation (red line: adaptation night, blue line: experimental night). Values that significantly differed between nights are indicated by one ($p < 0.05$) or two stars ($p < 0.01$; two-tailed paired *t*-test). The numbers of subjects analyzed were the same as in **Figure 1**.

efficiency > 90%). In the adaptation night, the decreased stability of sleep stages can influence the sleep process. However, cycle-by-cycle analysis revealed that the first sleep cycle was most affected with higher percentage of time in stage N1 and stage Wake and lower percentage of stage N3 (**Figure 1**). Moreover, reduced sleep stability can disturb the progression of sleep stages in the first sleep cycle such as a delay in the onset of stage N3 and stage REM. However, in this study, the changes in sleep-stage dynamics in the adaptation night had no major impact on sleep architecture in the following sleep cycles. This suggests that the sleep in the first sleep cycle is susceptible to environmental changes in the adaptation night. However, environmental influences on sleep processes are not carried over to later sleep cycles because mutual interactions between homeostatic sleep regulation and ultradian rhythms may have functioned in young healthy participants in this study (Lorenzo and Barbanoj, 2002; Hayashi et al., 2015; Kishi et al., 2011, 2018).

Quantitative EEG and HRV Variables

Cortical EEG power, such as delta bands, autonomic nervous system function, and sleep-stage distribution fluctuate within a sleep cycle (Brandenberger et al., 2001; Borbély et al., 2016; de Zambotti et al., 2018). Previous studies reported the difference in the sleep architecture between the adaptation (first) and experimental (second) nights in healthy subjects, but the difference in sleep architecture was not clearly correlated with that in EEG power spectra (Toussaint et al., 1997; Curcio et al., 2004) or HRV (Israel et al., 2012; Virtanen et al., 2018) throughout the entire night. Based on the cycle-by-cycle analyses of both nights, the cortical EEG power for each frequency band and HRV of NREM sleep and REM sleep exhibited typical alterations across sleep cycles such as the decrease in delta EEG power and increase in RR intervals (Achermann and Borbély, 2017; Lanfranchi et al., 2017; de Zambotti et al., 2018). However, the time-course changes in sleep architecture, EEG activity, and HRV can differ among the sleep cycles since cyclic fluctuation within a sleep cycle is modulated by the homeostatic and circadian influences over the night (Åkerstedt et al., 1998). As addressed above, in the first sleep cycle, sleep architecture differed between the adaptation and experimental nights. Delta EEG power did not differ between the two nights, as reported previously (Toussaint et al., 1997), whereas the beta EEG power was higher and RR intervals and HF amplitude were lower in the first sleep cycle in the adaptation night than in the experimental night. In the following sleep cycles, however, the difference in sleep architecture and EEG power between the two nights disappeared, whereas the RR intervals and HF amplitude, as demonstrated previously (Virtanen et al., 2018), remained lower in the adaptation night than in the experimental night (**Figure 2**). Previous studies showed that the correlation between cortical and autonomic activities was found to be attenuated in the latter half of the night in healthy subjects (Thomas et al., 2014; Rothenberger et al., 2015). Therefore, the distinct time course of cortical and autonomic activity suggests that the homeostatic and circadian influences can differently modulate the reactivity of cortical and autonomic activity in the adaptation night. The

results also suggest the possibilities that the autonomic nervous system has lower adaptability than cortical system.

Physiological Significance of Sleep-Stage Dynamics and Cortical/Cardiac Activity

Previous studies proposed that changes in sleep in the adaptation night are related to alertness in order to ensure safety when sleeping in a new and potentially dangerous environment (Curcio et al., 2004; Tamaki et al., 2016; Tamaki and Sasaki, 2019). Therefore, alertness may enhance wake-promoting influences at the beginning of sleep and increase the latency of sleep onset and NREM sleep stages in the adaptation night (Tamaki et al., 2005a,b). High beta EEG power and low RR intervals and HF amplitude may be associated with hyperarousal and/or autonomic hyperactivation related to alertness, with an increase in phasic cortical events related to autonomic activation (i.e., arousal and EEG desynchronization) in the adaptation night (Trinder et al., 2003; Kato et al., 2004; de Zambotti et al., 2011; Silvani et al., 2015). These conditions were reported in patients with sleep disorders such as chronic pain (Lavigne et al., 2011) and insomnia (Bonnet and Arand, 1997; Jurysta et al., 2009). However, in the healthy subjects of the present study, high beta EEG power and low RR intervals and HF amplitude may have a role for sleep maintenance, rather than sleep disturbance. As sensory alertness remains functional during sleep (Oswald et al., 1960; Kato et al., 2004; Lavigne et al., 2004), sensory experience in a novel sleep environment may be processed, especially during the first sleep cycle, to ensure the safety of the sleep laboratory environment in healthy participants: autonomic activity remains functional in order to respond to the environment in subsequent cycles.

Study Limitations

The major factors causing altered sleep in a sleep laboratory have changed over time due to improvements in the sleep laboratory environment. However, disturbances cannot be completely eliminated by improving the comfort of the surrounding settings (Lorenzo and Barbanoj, 2002; Moser et al., 2010). In addition, sleep irregularity in the previous week negatively correlates with sleep efficiency during the adaptation night (Lee et al., 2016). In the present study, the possibility that sleep conditions prior to PSG recordings affected sleep in the laboratory recordings cannot be excluded because sleep–wake patterns on previous days were not fully controlled or monitored. Another limitation is that not all subjects had four sleep cycles in the adaptation and experimental nights. The results of cycle-by-cycle analysis performed on a limited number of subjects with four sleep cycles may be interpreted as the responses to the environmental influences in subjects whose sleep is more stable and regular than in those with fewer sleep cycles. Furthermore, psychological predisposition may play a role in the lower ability to adapt to a sleep laboratory environment. As the participants in the present study did not have self-rated depression, psychological effects on adaptability to the sleep laboratory environment were considered minimal.

CONCLUSION

The present study revealed that the time course of sleep-stage dynamics, electroencephalographic activity, and heart rate variability over sleep cycles are discrepant in the adaptation night in healthy young adults. The results suggest the distinct vulnerability of the adaptation processes within the central nervous system while sleeping in a sleep laboratory for the first time.

DATA AVAILABILITY STATEMENT

The original contributions presented in the study are included in the article/supplementary material, further inquiries can be directed to the corresponding author/s.

ETHICS STATEMENT

The studies involving human participants were reviewed and approved by the Research Ethics Committee of Osaka University Graduate School of Dentistry and Osaka University Dental Hospital (H25-E9-5, H29-E48-3). The patients/participants provided their written informed consent to participate in this study.

AUTHOR CONTRIBUTIONS

AS and TK designed the study and wrote the main manuscript. AS and MK prepared the data sets and analyzed the data. MK and TK contributed to the data collection. AK, HA, and MT revised and commented on the manuscript. All authors reviewed the manuscript and agreed with its content.

FUNDING

This study was funded by Grants-in-Aid for Scientific Research (B) (#25293393, #18H02965) and (A) (#25253102) from the Japan Society for the Promotion of Science (JSPS), by funds from the Intractable Oral Disease at Osaka University Graduate School of Dentistry and the Center of Innovation Science and Technology Based Radical Innovation and Entrepreneurship Program (COISTREAM), and partially by a Grant-in-Aid for Challenging Research (exploratory, #17K19753) from JSPS.

ACKNOWLEDGMENTS

We would like to thank the sleep laboratory members (Teruaki Nochino, Shingo Haraki, and Akiko Tsujisaka) for their helpful advice on this manuscript and technicians (Kataoka N, Takahashi C, Nakamura M, Teshima Y, Maekawa T, Yamamoto A, Koda S, Hirai N, Iwaki A, Nishida M, and Nakamura U) for their technical assistance. We also thank Mr. Nonoue S, RPSGT for his technical assistance on sleep scoring.

REFERENCES

Achermann, P., and Borbély, A. A. (2017). "Sleep homeostasis and models of sleep regulation," in *Principles and Practice of Sleep Medicine*, eds M. Kryger, T. Roth, and B. Dement (Philadelphia, PA: Elsevier Press), 377–387. doi: 10.1016/B978-0-323-24288-2.00179-3

Agnew, H. W. J., Webb, W. B., and Williams, R. L. (1966). The first night effect: an EEG study of sleep. *Psychophysiology* 2, 263–266.

Åkerstedt, T., Hume, K., Minors, D., and Waterhouse, J. (1998). Experimental separation of time of day and homeostatic influences on sleep. *Am. J. Physiol. Regul. Integr. Comp. Physiol.* 274, 1162–1168. doi: 10.1152/ajpregu.1998.274.4.r1162

Berry, R., Gamaldo, C., Hardig, S., Lloyd, R., Marcus, C., and Vaughn, B. (2014). *The AASM Manual for the Scoring of Sleep and Associated Events: Rules, Terminology and Technical Specifications, Version2.1*. Darien, IL: American Academy of Sleep Medicine

Bonnet, M. H., and Arand, D. L. (1997). Heart rate variability: sleep stage, time of night, and arousal influences. *Electroencephalogr. Clin. Neurophysiol.* 102, 390–396. doi: 10.1016/S0921-884X(96)96070-1

Borbély, A. A., Daan, S., Wirz-Justice, A., and Deboer, T. (2016). EEG beta power and heart rate variability describe the association between cortical and autonomic arousals across sleep. *J. Sleep Res.* 25, 131–143. doi: 10.1111/jsr.12371

Brandenberger, G., Ehrhart, J., Piquard, F., and Simon, C. (2001). Inverse coupling between ultradian oscillations in delta wave activity and heart rate variability during sleep. *Clin. Neurophysiol.* 112, 992–996. doi: 10.1016/S1388-2457(01)00507-7

Browman, C. P., and Cartwright, R. D. (1980). The first-night effect on sleep and dreams. *Biol. Psychiatry* 15, 809–812.

Curcio, G., Ferrara, M., Piergianni, A., Fratello, F., and De Gennaro, L. (2004). Paradoxes of the first-night effect: a quantitative analysis of antero-posterior EEG topography. *Clin. Neurophysiol.* 115, 1178–1188. doi: 10.1016/j.clinph.2003.12.018

de Zambotti, M., Covassin, N., De Min Tona, G., Sarlo, M., and Stegagno, L. (2011). Sleep onset and cardiovascular activity in primary insomnia. *J. Sleep Res.* 20, 318–325. doi: 10.1111/j.1365-2869.2010.00871.x

de Zambotti, M., Trinder, J., Silvani, A., Colrain, I. M., and Baker, F. C. (2018). Dynamic coupling between the central and autonomic nervous systems during sleep: a review. *Neurosci. Biobehav. Rev.* 90, 84–103. doi: 10.1016/j.neubiorev.2018.03.027

Dement, W., and Wolpert, E. A. (1958). The relation of eye movements, body motility, and external stimuli to dream content. *J. Exp. Psychol.* 55, 543–553.

Doi, Y., Minowa, M., Uchiyama, M., Okawa, M., Kim, K., Shibui, K., et al. (2000). Psychometric assessment of subjective sleep quality using the Japanese version of the Pittsburgh Sleep Quality Index (PSQI-J) in psychiatric disordered and control subjects. *Psychiatry Res.* 97, 165–172. doi: 10.1016/S0165-1781(00)00232-8

Feinberg, I. (1974). Changes in sleep cycle patterns with age. *J. Psychiatr. Res.* 10, 283–306. doi: 10.1016/0022-3956(74)90011-9

Fukuda, K., and Kobayashi, S. (1973). Jiko-hyoka-shiki yokuutsu-sei shakudo no kenkyuu (A study on a self-rating depression scale). *Psychiatr. Neurol. Jpn.* 75, 673–679.

Hartmann, E. (1968). The 90-minute sleep-dream cycle. *Arch. Gen. Psychiatry* 18, 280–286. doi: 10.1001/archpsyc.1968.01740030024004

Hayano, J., Taylor, J. A., Yamada, A., Mukai, S., Hori, R., Asakawa, T., et al. (1993). Continuous assessment of hemodynamic control by complex demodulation of cardiovascular variability. *Am. J. Physiol. Heart Circ. Physiol.* 264(4 Pt 2), H1229–H1238. doi: 10.1152/ajpheart.1993.264.4.h1229

Hayashi, Y., Kashiwagi, M., Yasuda, K., Ando, R., Kanuka, M., Sakai, K., et al. (2015). Cells of a common developmental origin regulate REM/non-REM sleep and wakefulness in mice. *Science* 350, 957–961. doi: 10.1126/science.aad1023

Hirshkowitz, M., Moore, C. A., Hamilton, C. R. III, Rando, K. C., and Karacan, I. (1992). Polysomnography of adults and elderly: sleep architecture, respiration, and leg movement. *J. Clin. Neurophysiol.* 9, 56–62.

Israel, B., Buysse, D. J., Krafty, R. T., Begley, A., Miewald, J., and Hall, M. (2012). Short-term stability of sleep and heart rate variability in good sleepers and patients with insomnia: for some measures, one night is enough. *Sleep* 35, 1285–1291. doi: 10.5665/sleep.2088

Jurysta, F., Lanquart, J.-P., Sputaels, V., Dumont, M., Migeotte, P.-F., Leistedt, S., et al. (2009). The impact of chronic primary insomnia on the heart rate – EEG variability link. *Clin. Neurophysiol.* 120, 1054–1060. doi: 10.1016/j.clinph.2009.03.019

Kato, T., Montplaisir, J., and Lavigne, G. (2004). Experimentally induced arousals during sleep: a cross-modality matching paradigm. *J. Sleep Res.* 13, 229–238. doi: 10.1111/j.1365-2869.2004.00409.x

Kishi, A., Haraki, S., Toyota, R., Shiraishi, Y., Kamimura, M., Taniike, M., et al. (2020). Sleep stage dynamics in young patients with sleep bruxism. *Sleep* 43:zsz202. doi: 10.1093/sleep/zsz202

Kishi, A., Struzik, Z. R., Natelson, B. H., and Yamamoto, Y. (2008). Dynamics of sleep stage transitions in healthy humans and patients with chronic fatigue syndrome. *Am. J. Physiol. Integr. Comp. Physiol.* 294, R1980–R1987. doi: 10.1152/ajpregu.00925.2007

Kishi, A., van Dongen, H. P. A., Natelson, B. H., Bender, A. M., Palombini, L. O., Bittencourt, L., et al. (2017). Sleep continuity is positively correlated with sleep duration in laboratory nighttime sleep recordings. *PLoS One* 12:e0175504. doi: 10.1371/journal.pone.0175504

Kishi, A., Yamaguchi, I., Togo, F., and Yamamoto, Y. (2018). Markov modeling of sleep stage transitions and ultradian REM sleep rhythm. *Physiol. Meas.* 39:84005. doi: 10.1088/1361-6579/aad900

Kishi, A., Yasuda, H., Matsumoto, T., Inami, Y., Horiguchi, J., Tamaki, M., et al. (2011). NREM sleep stage transitions control ultradian REM sleep rhythm. *Sleep* 34, 1423–1432. doi: 10.5665/SLEEP.1292

Lanfranchi, P. A., Pépin, J., and Somers, V. K. (2017). "Cardiovascular physiology: autonomic control in health and in sleep disorders," in *Principles and Practice of Sleep Medicine*, eds M. Kryger, T. Roth, and B. Dement (Philadelphia, PA: Elsevier Press), 142–154. doi: 10.1016/B978-0-323-24288-2.00179-3

Lavigne, G., Brousseau, M., Kato, T., Mayer, P., Manzini, C., Guitard, F., et al. (2004). Experimental pain perception remains equally active over all sleep stages. *Pain* 110, 646–655. doi: 10.1016/J.PAIN.2004.05.003

Lavigne, G. J., Okura, K., Abe, S., Colombo, R., Huynh, N., Montplaisir, J. Y., et al. (2011). Gender specificity of the slow wave sleep lost in chronic widespread musculoskeletal pain. *Sleep Med.* 12, 179–185. doi: 10.1016/j.sleep.2010.07.015

Le Bon, O., Staner, L., Hoffmann, G., Dramaix, M., and Sebastian, I. S. (2001). The first-night effect may last more than one night. *J. Psychiatr. Res.* 35, 165–172. doi: 10.1016/s0022-3956(01)00019-x

Lee, D., Cho, C., Han, C., Bok, K., and Moon, J. H. (2016). Sleep irregularity in the previous week influences the first-night effect in polysomnographic studies. *Psychiatry Investig.* 13, 203–209.

Lo, C., Chou, T., Penzel, T., Scammell, T. E., Strecker, R. E., Stanley, H. E., et al. (2004). Common scale-invariant patterns of sleep – wake transitions across mammalian species. *Proc. Natl. Acad. Sci. U.S.A.* 101, 17545–17548.

Lorenzo, J.-L., and Barbanoj, M.-J. (2002). Variability of sleep parameters across multiple laboratory sessions in healthy young subjects: the "very first night effect". *Psychophysiology* 39, 409–413.

Malliani, A., Pagani, M., Lombardi, F., and Cerutti, S. (1991). Cardiovascular neural regulation explored in the frequency domain. *Circulation* 84, 482–492. doi: 10.1161/01.CIR.84.2.482

Moser, D., Kloesch, G., Fischmeister, F. P., Bauer, H., and Zeitlhofer, J. (2010). Cyclic alternating pattern and sleep quality in healthy subjects—is there a first-night effect on different approaches of sleep quality? *Biol. Psychol.* 83, 20–26. doi: 10.1016/J.BIOPSYCHO.2009.09.009

Nonoue, S., Mashita, M., Haraki, S., Mikami, A., Adachi, H., Yatani, H., et al. (2017). Inter-scorer reliability of sleep assessment using EEG and EOG recording system in comparison to polysomnography. *Sleep Biol. Rhythms* 15, 39–48. doi: 10.1007/s41105-016-0078-2

Norman, R. G., Scott, M. A., Ayappa, I., Walsleben, J. A., and Rapoport, D. M. (2006). Sleep continuity measured by survival curve analysis. *Sleep* 29, 1625–1631. doi: 10.1093/sleep/29.12.1625

Okura, M., Nonoue, S., Tsujisaka, A., Haraki, S., Yokoe, C., Taniike, M., et al. (2020). Polysomnographic analysis of respiratory events during sleep in young nonobese Japanese adults without clinical complaints of sleep apnea. *J. Clin. Sleep Med.* 16, 1303–1310. doi: 10.5664/jcsm.8498

Oswald, I., Taylor, A. M., and Treisman, M. (1960). Discriminative responses to stimulation during human sleep. *Brain* 83, 440–453. doi: 10.1093/brain/83.3.440

Rosipal, R., Lewandowski, A., and Dorffner, G. (2013). In search of objective components for sleep quality indexing in normal sleep. *Biol. Psychol.* 94, 210–220. doi: 10.1016/j.biopsycho.2013.05.014

Rotenberg, V. S., Hadjez, J., Kimhi, R., Indurski, P., Sirota, P., Mosheva, T., et al. (1997). First night effect in depression: new data and a new approach. *Biol. Psychiatry* 42, 267–274. doi: 10.1016/S0006-3223(96)00343-5

Rothenberger, S. D., Krafty, R. T., Taylor, B. J., Cribbet, M. R., Thayer, J. F., Buysse, D. J., et al. (2015). Time-varying correlations between delta EEG power and heart rate variability in midlife women: the SWAN sleep study. *Psychophysiology* 52, 572–584. doi: 10.1111/psyp.12383

Sforza, E., Chapotot, F., Pigeau, R., and Buguet, A. (2008). Time of night and first night effects on arousal response in healthy adults. *Clin. Neurophysiol.* 119, 1590–1599. doi: 10.1016/j.clinph.2008

Shin, S. J., Tapp, W. N., Reisman, S. S., and Natelson, B. H. (1989). Assessment of autonomic regulation of heart rate variability by the method of complex demodulation. *IEEE Trans. Biomed. Eng.* 36, 274–283.

Silvani, A., Calandra-Buonaura, G., Benarroch, E. E., Dampney, R. A. L., and Cortelli, P. (2015). Bidirectional interactions between the baroreceptor reflex and arousal: an update. *Sleep Med.* 16, 210–216. doi: 10.1016/j.sleep.2014.10.011

Tamaki, M., Bang, J. W., Watanabe, T., and Sasaki, Y. (2016). Night watch in one brain hemisphere during sleep associated with the first-night effect in humans. *Curr. Biol.* 26, 1190–1194. doi: 10.1016/j.cub.2016.02.063

Tamaki, M., Nittono, H., Hayashi, M., and Hori, T. (2005a). Examination of the first-night effect during the sleep-onset period. *Sleep* 28, 195–202. doi: 10.1093/sleep/28.2.195

Tamaki, M., Nittono, H., Hayashi, M., and Hori, T. (2005b). Spectral analysis of the first-night effect on the sleep-onset period. *Sleep Biol. Rhythms* 3, 122–129. doi: 10.1111/j.1479-8425.2005.00173.x

Tamaki, M., and Sasaki, Y. (2019). Surveillance during REM sleep for the first-night effect. *Front. Neurosci.* 13:1161. doi: 10.3389/fnins.2019.01161

Task Force of the European Society of Cardiology and the North American Society of Pacing and Electrophysiology (1996). Heart rate variability: standards of measurement, physiological interpretation, and clinical use. *Eur. Heart J.* 17, 354–381.

Thomas, R. J., Mietus, J. E., Peng, C.-K., Guo, D., Gozal, D., Montgomery-Downs, H., et al. (2014). Relationship between delta power and the electrocardiogram-derived cardiopulmonary spectrogram: possible implications for assessing the effectiveness of sleep. *Sleep Med.* 15, 125–131. doi: 10.1016/j.sleep.2013.10.002

Toscani, L., Gangemi, P. F., Parigi, A., Silipo, R., Ragghianti, P., Sirabella, E., et al. (1996). Human heart rate variability and sleep stages. *Ital. J. Neurol. Sci.* 17, 437–439. doi: 10.1007/BF01997720

Toussaint, M., Luthringer, R., Schaltenbrand, N., Carelli, G., Lainey, E., Jacqmin, A., et al. (1995). First-night effect in normal subjects and psychiatric inpatients. *Sleep* 18, 463–469. doi: 10.1093/sleep/18.6.463

Toussaint, M., Luthringer, R., Schaltenbrand, N., Nicolas, A., Jacqmin, A., Carelli, G., et al. (1997). Changes in EEG power density during sleep laboratory adaptation. *Sleep* 20, 1201–1207. doi: 10.1093/sleep/20.12.1201

Trinder, J., Allen, N., Kleiman, J., Kralevski, V., Kleverlaan, D., Anson, K., et al. (2003). On the nature of cardiovascular activation at an arousal from sleep. *Sleep* 26, 543–551. doi: 10.1093/sleep/26.5.543

Versace, F., Mozzato, M., De Min Tona, G., Cavallero, C., and Stegagno, L. (2003). Heart rate variability during sleep as a function of the sleep cycle. *Biol. Psychol.* 63, 149–162. doi: 10.1016/S0301-0511(03)00052-8

Virtanen, I., Kalleinen, N., Urrila, A. S., and Polo-Kantola, P. (2018). Sleep and cardiovascular function first-night effect on cardiac autonomic function in different female reproductive states. *J. Sleep Res.* 27, 150–158. doi: 10.1111/jsr.12560

Vyazovskiy, V. V., and Delogu, A. (2014). NREM and REM sleep: complementary roles in recovery after wakefulness. *Neuroscientist* 20, 203–219. doi: 10.1177/1073858413518152

Žemaitytė, D., Varoneckas, G., and Sokolov, E. (1984). Heart rhythm control during sleep. *Psychophysiology* 21, 279–289. doi: 10.1111/j.1469-8986.1984.tb02935.x

Zung, W. W. (1965). A self-rating depression scale. *Arch. Gen. Psychiatry* 12, 63–70. doi: 10.1001/archpsyc.1965.01720310065008

Conflict of Interest: The authors declare that the research was conducted in the absence of any commercial or financial relationships that could be construed as a potential conflict of interest.

frontiers in Physiology

REVIEW
published: 01 April 2021
doi: 10.3389/fphys.2021.624950

Unraveling the Big Sleep: Molecular Aspects of Stem Cell Dormancy and Hibernation

*Itamar B. Dias[1], Hjalmar R. Bouma[1,2] and Robert H. Henning[1]**

[1] Department of Clinical Pharmacy and Pharmacology, University Medical Center Groningen, University of Groningen, Groningen, Netherlands, [2] Department of Internal Medicine, University Medical Center Groningen, University of Groningen, Groningen, Netherlands

Tissue-resident stem cells may enter a dormant state, also known as quiescence, which allows them to withstand metabolic stress and unfavorable conditions. Similarly, hibernating mammals can also enter a state of dormancy used to evade hostile circumstances, such as food shortage and low ambient temperatures. In hibernation, the dormant state of the individual and its cells is commonly known as torpor, and is characterized by metabolic suppression in individual cells. Given that both conditions represent cell survival strategies, we here compare the molecular aspects of cellular quiescence, particularly of well-studied hematopoietic stem cells, and torpor at the cellular level. Critical processes of dormancy are reviewed, including the suppression of the cell cycle, changes in metabolic characteristics, and cellular mechanisms of dealing with damage. Key factors shared by hematopoietic stem cell quiescence and torpor include a reversible activation of factors inhibiting the cell cycle, a shift in metabolism from glucose to fatty acid oxidation, downregulation of mitochondrial activity, key changes in hypoxia-inducible factor one alpha (HIF-1α), mTOR, reversible protein phosphorylation and autophagy, and increased radiation resistance. This similarity is remarkable in view of the difference in cell populations, as stem cell quiescence regards proliferating cells, while torpor mainly involves terminally differentiated cells. A future perspective is provided how to advance our understanding of the crucial pathways that allow stem cells and hibernating animals to engage in their 'great slumbers.'

Keywords: cell cycle, cell dormancy, hibernation, metabolism, torpor, quiescence

OPEN ACCESS

Edited by:
Alessandro Silvani, University of Bologna, Italy

Reviewed by:
Kelly Drew, University of Alaska Fairbanks, United States
Matteo Cerri, University of Bologna, Italy
Thomas Rando, Stanford University, United States
Toshio Suda, National University of Singapore, Singapore

****Correspondence:***
Robert H. Henning
r.h.henning@umcg.nl

Specialty section:
This article was submitted to Integrative Physiology, a section of the journal Frontiers in Physiology

Received: *01 November 2020*
Accepted: *11 March 2021*
Published: *01 April 2021*

Citation:
Dias IB, Bouma HR and Henning RH (2021) Unraveling the Big Sleep: Molecular Aspects of Stem Cell Dormancy and Hibernation. Front. Physiol. 12:624950. doi: 10.3389/fphys.2021.624950

INTRODUCTION

The difference between life and death of individual cells or animals depends on their ability to survive, particularly during periods of scarcity. When environmental conditions are unfavorable, or nutrients are scarce, individual cells may enter a dormant state (quiescence). Similarly, some mammals may hibernate to cope with such conditions by suppressing metabolism in a state called torpor. Given that they represent cell survival strategies triggered by external factors, cell quiescence and hibernation both deploy molecular adaptations to survive environmental stress such as low temperature and shortage of nutrients, and even increase their resistance to withstand periods of low oxygen supply. In both cases, phenotypic plasticity is of paramount importance to ensure survival, yet it is undocumented whether the mechanism governing entry or exit from cellular

dormancy and torpidity are similar. Here, we summarize mechanisms used in cellular quiescence and mammalian hibernation and use the collective findings to establish their resemblance.

Cellular Dormancy

Cellular dormancy is the ability to enter a quiescence state (reversible cellular arrest) by withdrawing from the cell cycle and entering the so called G_0 phase (Nakamura-Ishizu et al., 2014). The cell cycle is divided into four phases: G_1 phase (interphase), S phase (DNA synthesis), G_2 phase (interphase), and M phase (mitosis) (Yang and Sheridan, 2014). Cells that overcome the G_1 checkpoint commit to divide and proceed to the S phase, culminating in cell division. In the early G_1 phase, cells that are non-proliferating, undivided, senescent (permanent cell cycle arrest) or terminally differentiated, can withdraw from the cell cycle and enter a dormant or quiescent state (G_0) (Figel and Fenstermaker, 2018). Quiescent cells are characterized by low mobility, low metabolic activity and rare division (Rocheteau et al., 2014). Once quiescent, cells may either re-enter the G_1 phase in response to growth signals and commit to divide (reversible quiescence) or continue dormancy, which may or may not ultimately lead to senescence, i.e., a state of permanent cell cycle arrest with high metabolic activity and secretion of inflammatory factors (Sabbatinelli et al., 2019). In contrast, non-proliferating cells that are either terminally differentiated or senescent are irreversibly arrested.

In humans, reversible quiescence commonly occurs in many somatic cells including hematopoietic stem cells (Nakamura-Ishizu et al., 2014), muscle stem cells (Chakkalakal et al., 2012), epithelial stem cell (Coloff et al., 2016), neural stem cell (Kalamakis et al., 2019), and hair follicle stem cell (Wang et al., 2016). Although quiescence is a key characteristic of tissue-resident stem cells, which function as a dormant reserve to replenish the tissue loss throughout life, the discovery of highly proliferative stem cells in several tissues has challenged the concept that quiescence is an integral property of all stem cells (Clevers and Watt, 2018). Given the divergent mechanisms governing quiescence in different stem cells, this review will focus on the most extensively and well-characterized tissue-resident stem cells: hematopoietic stem cells (HSCs) (Richmond et al., 2016). Nevertheless, quiescence can also be found in non-stem cells such as endothelial cells (Sabbatinelli et al., 2019) and mature hepatocytes, the latter being considered long-term quiescent cells essential for liver regeneration (Zimmermann, 2004; Berasain and Avila, 2015). Although quiescence is not an inherent property that characterizes stem cells or distinguishes them from non-stem cells (e.g., consider mature hepatocytes), dysregulation and loss of quiescence affects homeostasis of many progenitor cell populations, ultimately leading to stem cell exhaustion, i.e., the depletion of stem cells with impact on health (Orford and Scadden, 2008). Stem cell exhaustion is particularly noticeable in HSCs, due to their multi-lineage capacity of differentiation and self-renewal potential (Pietras et al., 2011). HSCs give rise to progenitor cells that differentiate into all lineages of mature blood cells. However, continuous self-renewal of HSCs is insufficient for lifelong maintenance, as the inevitable accumulation of damage would result in dysfunctional hematopoiesis, leading to diseases such as leukemia (Riether et al., 2015). Hence quiescence is considered an essential feature to prevent HSCs exhaustion. To avoid this potential hazard, HSCs are kept quiescent in a unique microenvironment in the bone marrow. Quiescence is actively maintained in HSCs, in which the microenvironment plays a crucial role to assure their longevity and function. Furthermore, computational modeling of HSCs kinetics infers that human HSCs complete the cell cycle once every 18 years to self-renew and generate progenitor cells. Quiescence thus allows stem cells to prolong their lifespan to maintain critical physiological functions (Hao et al., 2016).

Animal Dormancy

Dormancy in animals can be subdivided into four subclasses: hibernation (Lee, 2009), diapause (Renfree and Shaw, 2000), estivation (Masaki, 2009; Storey and Storey, 2012), and brumation (McEachern et al., 2015). Hibernation is often described as winter dormancy and is adopted by both warm and cold-blooded vertebrates. Furthermore, hibernation is characterized by alternating periods of low metabolic activity (torpor), and normalization of metabolism and physiology (arousals) (Carey et al., 2003). Diapause refers to a spontaneous interruption of the development, characterized by a reduction of metabolic activity and is mainly observed in insects and a few mammalian species (Renfree and Shaw, 2000; Denlinger, 2002). Estivation occurs in vertebrates and invertebrates and is characterized by reduced metabolic rate and inactivity to avoid desiccation during hot periods with soaring temperatures (Masaki, 2009; Storey and Storey, 2012). Brumation is mostly seen in reptiles and strictly induced by low ambient temperatures. It is characterized by long periods of inactivity with lowered respiration rate, intersected by brief periods of activity required to drink (McEachern et al., 2015). Despite having evolved different forms of dormancy, the end goal of these animals is the same: survival of periods with low energy supply.

Between these forms of animal dormancy, hibernation is the best explored regarding molecular changes, which is why we will almost exclusively focus on hibernation in mammals. Depending on the species and environmental challenges hibernation takes different forms, mostly consisting of seasonal hibernation with multi-day torpor bouts and brief arousals (12–18 h) *versus* daily torpor during which metabolism is suppressed for 6–10 h (Turbill et al., 2011). Likely, similar molecular mechanisms govern both, as some species switch between multi-day and daily torpor (Wilz and Heldmaier, 2000; Dausmann et al., 2004). Hibernation consists of (daily) torpor phases that are characterized by low metabolism, which are interspersed by brief periods of arousal with restoration of metabolic rate to levels of non-hibernating animals. Torpidity is a state in which physical activity, development, growth and metabolism are transitorily and profoundly reduced in response to harsh environmental conditions and to reduce energy dissipation (Heldmaier et al., 2000). In this review, we discriminate between the two different forms of torpidity by using 'torpor' and 'daily torpor.'

During torpor, animals undergo profound physiological, morphological and behavioral changes. For example, body

temperature of seasonal hibernators in cold environments sharply declines to as low as 0–4°C, heart rate and respiration decreases by 95%, and renal function is significantly reduced (Carey et al., 2003). Most hibernators synchronize their dormancy with environmental changes, with some animals entering dormancy only after the start of unfavorable conditions (consequential dormancy, such as facultative hibernation in the Syrian hamster), while others have a yearly rhythmicity allowing them to enter in advance of harsh conditions (predictive dormancy, such as seasonal hibernation in ground squirrels) (Lee, 2009; Masaki, 2009; Ruf and Geiser, 2015).

Prerequisites for Dormancy

Cellular quiescence in HSC is associated with three key changes in cell physiology: (i) cell cycle arrest by inhibition of cyclin-dependent kinases (CDKs) upon an increase in expression of cyclin-dependent kinase inhibitors (CKIs), (ii) lowering of metabolism with a switch from carbohydrate to lipid-based metabolism and (iii) resistance to accumulating cellular damage conferred by differential expression of genes involved in apoptosis, proliferation and oxidative stress.

The exact signals that induce torpidity in mammals are still not known, yet reduction of metabolic rate is at its heart (Heldmaier et al., 2000; Storey and Storey, 2004). Torpor entry is achieved by active suppression of metabolism and by limiting ATP-expensive activities, ultimately leading to a change of physiology in cells, tissues and organs. In torpor, vital functions including respiratory and heart rate strongly decline secondary to the metabolic suppression, while temperature regulation is adjusted to accommodate lower body temperatures (Tsiouris, 2005; Ruf and Geiser, 2015). Moreover, reversible cell cycle arrest has been reported in hypoxic red-eared slider turtles and torpid 13-lined squirrels (Biggar and Storey, 2009; Wu and Storey, 2012a), in concert with the metabolic suppression and shift in energy source from carbohydrates to fatty acids (Storey et al., 2010).

Because of the similarity between the overall regulation of HSC quiescence and torpidity, it is conceivable that some form of reversible quiescence occurs during hibernation and might even be necessary for the induction of hibernation. The interaction between these mechanisms may set the stage for both reversible cellular quiescence and hibernation allowing them to withstand stress conditions and extend their life span. However, it must be underlined that the impact of mechanisms involved, particularly those regulating cell cycle, differ largely between quiescence in stem cells and torpidity. While in stem cells cell cycle regulation drives their proliferation and self-renewal, it is less clear what its role is in terminally differentiated cells, as studied in torpor.

CELL CYCLE REGULATION

General Regulation of the Cell Cycle

While numerous intrinsic and extrinsic factors regulate the cell cycle, they generally converge on the cell cycle master regulators, cyclin-dependent kinases, CDKs (Fisher, 1997; Coller et al., 2006; Valcourt et al., 2012; Cheung and Rando, 2013; Lim and Kaldis, 2013). CDK activation requires binding to the proper cyclin regulatory subunit (A, B, D, and E) and together they drive cell cycle progress (Murray, 2004; Garcia and Su, 2008; Figel and Fenstermaker, 2018). Differential gene expression of cyclins during specific cell cycle phases drives cell cycle progression or arrest (Malumbres and Barbacid, 2005; Camins et al., 2013). Cyclin-CDK complex formation is antagonized by CKIs that competitively bind to the catalytic site of the cyclin-CDK complex (Dai and Grant, 2003; Sánchez-Martínez et al., 2015). Two families of CKIs exist, namely INK4 ($p16^{INK4a}$, $p15^{INK4b}$, $p18^{INK4c}$, $p19^{INK4d}$) and CIP/KIP ($p21^{cip1}$, $p27^{kip1}$, $p57^{kip2}$). The balance between CDKs, cyclins and CKIs determines whether a cell will commit to proliferation or maintains cell cycle arrest. The major factors contributing to regulation of the cell cycle with relevancy to quiescence or torpor are depicted in **Figure 1**.

Mitogen-induced signaling pathways tightly regulate cell growth and proliferation. In the presence of plentiful nutrients, growth factors activate transmembrane receptors, eliciting downstream signaling cascades, including the rat sarcoma oncogene (RAS) (Beauséjour et al., 2003), myelocytomatosis (Myc) (Rahl et al., 2010) and the serine/threonine-protein kinase B (PI3K/Akt) pathways. This is followed by sequential activation of the mitogen-activated protein kinases (MAPKs), which induce the transcription of cyclin D that binds to cyclin-dependent kinases (CDK) 4 and 6, forming activated complexes that initiate the downstream phosphorylation of DNA synthesis associated proteins (Seger and Krebs, 1995; Pimienta and Pascual, 2007; Risal et al., 2016; Seger and Wexler, 2016). The cyclin-D-CDK(4,6) complex phosphorylates and inactivates the tumor suppressor retinoblastoma protein (Rb) and its homologs p107 and p130. Rb inhibition releases its inhibiting of the E2F transcription factor, thus activating E2F-binding to DNA promoter regions (Infante et al., 2008; Kent and Leone, 2019), allowing the transcription of E2F-dependent genes such as cyclin A and cyclin E. These cyclins form a complex with CDK-2, activating its kinase activity. Cyclin(A,E)-CDK-2 complexes further phosphorylate Rb resulting in its complete inactivation (Dyson, 1998; Harbour and Dean, 2000; Bracken et al., 2004). The increase in cyclins and the activated cyclin(D,E)-CDKs(2/4/6) complexes are essential to drive cells from G1 to the S phase and commit the cell to proliferation.

On the other hand, the absence of growth factors reduces the activity of the RAS (MAPKs) and PI3K/Akt pathways, thus leading to the activation of the glycogen synthase kinase 3 beta (GSK3β), which halts the cell cycle by phosphorylation and subsequent degradation of cyclin-D (Dong et al., 2005; Theeuwes et al., 2017; Tessier et al., 2019). Degradation of cyclin D reduces cyclin(D)-CDK(4,6) complex formation followed by an increase in activated Rb, leading to strong suppression of the E2F transcription factor and downstream genes. Cyclin D thus comprises a rate-limiting factor of cell cycle progression through G_1 (Trimarchi and Lees, 2002; Malumbres and Barbacid, 2009). Quiescent cells display low levels of activators of the cyclin-CDK-Rb-E2F pathway, such as cyclin D, CDK 2, 4, and 6, and high levels of the pathway repressors, including Rb protein and family homologs (p107 and p130) (Harbour and Dean, 2000; Bracken et al., 2004; Peng et al., 2015) and the CKIs p21 (Cheng et al., 2000) and p27 (Coats et al., 1996).

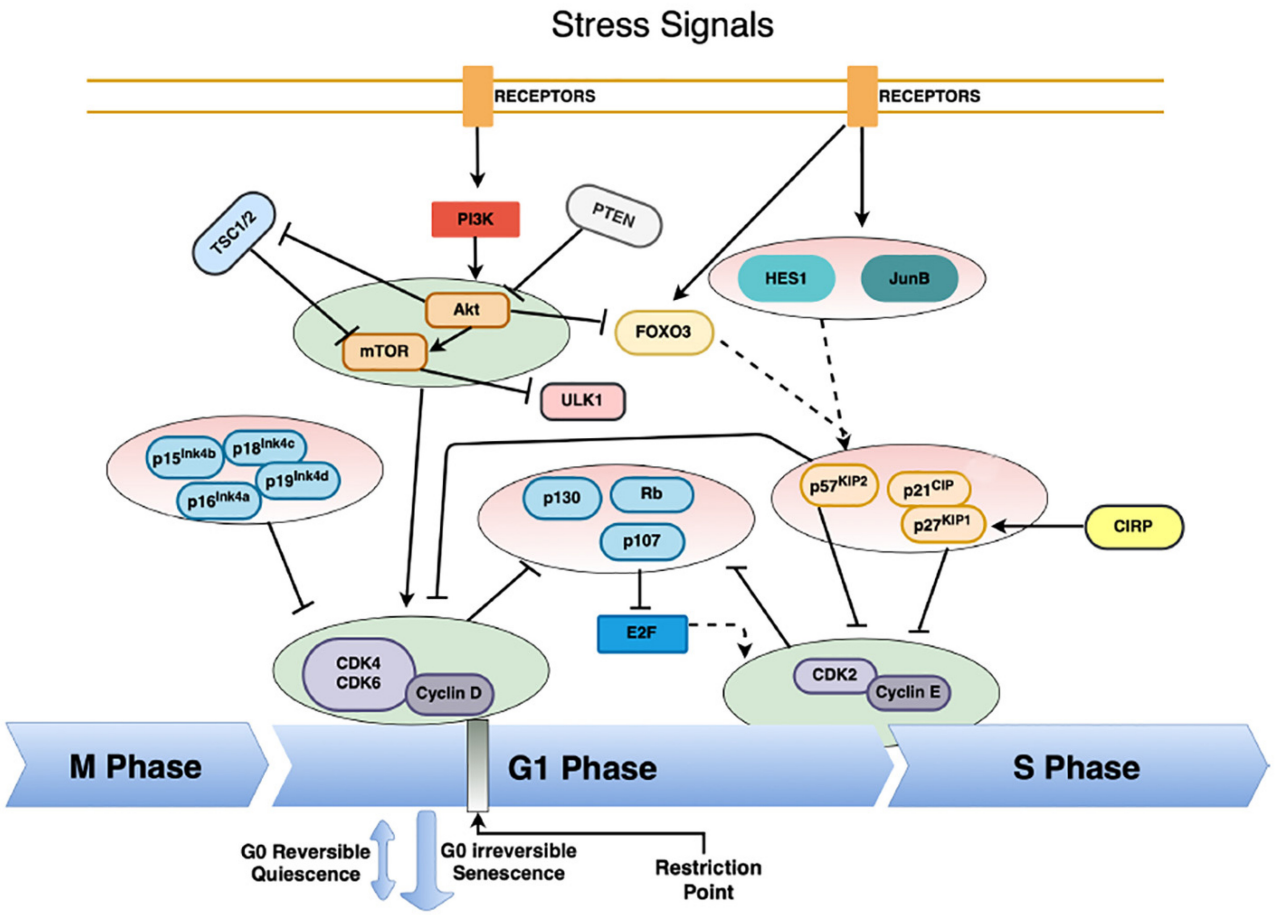

FIGURE 1 | The complex regulation of HSC – and possibly hibernators – cell cycle entry. Cyclin-CDK complexes drive the progression of the cell cycle. Their inhibition forces entry into quiescence from G_1 into the G_0 phase of the cell, mainly by the action of cyclin-dependent kinase inhibitors (CKI) from the INK and CIP/KIP family. Various pathways converge on the CKIs, thus instituting quiescence. Low activity of the PI3K/Akt/mTOR pathway is vital to enter quiescence, mainly through the inhibition of cyclin-D-CDK4/6 complexes and suppression of the Rb-E2F pathway. This pathway is massively regulated, primarily through inhibition by the tumor suppressors phosphatase and tensin homolog (PTEN) and tuberous sclerosis proteins 1 and 2 (TSC1/2). Furthermore, the activity of the cyclin D-CDK4/6 complexes is inhibited both by the Ink4 and CIP/KIP CKIs. The Cyclin E-CDK2 complex regulates progression from the G_1 to the S phase, and it is mainly regulated by the CIP/KIP family of CKIs, as well as by tumor suppressors from the retinoblastoma protein family (Rb, p107, p130). Extrinsic signals activate the transcription factors HES1, JunB and FOXO3a expression, which in turn regulate the transcription of the CIP/KIP family members. Moreover, entry into cellular quiescence is also subject to regulation via the tumor suppressor p53, as a response to cellular damage. Solid arrows indicate direct activation pathways, solid T-lines indicate inhibitory pathways and dashed arrows indicate transcriptional regulation activity.

However, when conditions turn favorable again, quiescent HSCs increase Cyclin D and E abundance, thus outcompeting CKIs and activating CDK2/4/6 (Murray, 2004; Choi and Anders, 2014; Figel and Fenstermaker, 2018).

Cell Cycle Regulation in Cell Quiescence

Cell Cycle Arrest in Quiescence

Hematopoietic stem cells quiescence primarily results from cell cycle arrest through inhibition of CDKs by an increase in the abundance of CKIs. When conditions for HSCs survival are unfavorable, intrinsic and extrinsic signals upregulate the expression of CKIs, modulating the formation of cyclin-CDK complexes and allowing the formation of the Rb-E2F complex, thus effectively halting the cell cycle. Meanwhile, quiescent HSCs ensure reversibility by upregulation of the chromatin remodeler helix-loop-helix protein 1 (HES1), which promotes transcriptional repression through alteration of chromatin recruiting histone deacetylases (HDACs) (Sang and Coller, 2009), promoting tight packaging of DNA into heterochromatin and downregulation of p21 (Yu et al., 2006; Sang et al., 2008), p27 (Murata et al., 2005), and E2F-dependent proteins (Hartman et al., 2004). Quiescent HSCs deploy additional mechanisms to protect DNA integrity by raising defense mechanisms against excessive oxidative stress to protect cells from accumulating damage and apoptosis. Low levels of reactive oxygen species (ROS) are tolerated by an increased antioxidant defense, including the NADPH-dependent glutathione reductase system (Hosokawa et al., 2006; Jang and Sharkis, 2007), FOXO3a (Miyamoto et al., 2008; Rimmelé et al., 2015), and Sirtuin1 (Ezoe et al., 2008; Matsui et al., 2012). Further, DNA repair systems

are enhanced in HSCs, including non-homologous end joining (NHEJ) and p53-mediated DNA damage response (Maynard et al., 2008; Mohrin et al., 2010; Dannenmann et al., 2015). In addition, increased expression of p53 serves to further enhance quiescence in HSCs by upregulation of downstream genes, including p21, Necdin, Gfi-1, BTG2, BAX, and PUMA (Lacorazza et al., 2006; Liu et al., 2009; Asai et al., 2012).

Reversing Cell Cycle Arrest in Quiescence

The ability to recommence the cell cycle following reversible arrest is crucial to the functionality of quiescent cells. Upon sufficient extrinsic growth stimulation, MAPKs activate the transcription factor Myc, which promotes the transcription of several cell-cycle promoting genes, including cyclin D, cyclin E, E2F2, and CDK4. Moreover, evidence suggests that the upregulation of Myc (Eilers et al., 1991; Kretzner et al., 1992), E2F (Johnson et al., 1993; Kowalik et al., 1995) and Cyclin E (Blomen and Boonstra, 2007; Fox et al., 2011) alone can drive a cell out of quiescence into cell cycle progression. Nevertheless, downregulation of CKIs activity, p21 (Cheng et al., 2000; Kippin et al., 2005) and p27 (Coats et al., 1996; Rivard et al., 1996), and downregulation of all three retinoblastoma protein family members (Rb, p107, p130) result in quiescence exit and cellular proliferation (Dannenberg et al., 2000; Sage et al., 2003; Viatour et al., 2008). Moreover, the upregulation of cell cycle progression genes leads to a shift in energy metabolism from lipid based oxidation (FAO) back to carbohydrate oxidation (glycolysis). This switch is essential to supply the demand of the ATP-expensive processes to meet the energy demand during proliferation (Valcourt et al., 2012; Takubo et al., 2013). It is of note that quiescent cells may resume cell proliferation only if they express a specific group of genes. One of the genes essential to the reversibility of quiescence is HES1. Hes1 is upregulated in quiescent cells and prevents premature senescence or terminal differentiation in response to specific signals (hypoxia, wnt signaling, Hedgehog pathways) (Baek et al., 2006; Sang et al., 2008). Although the exact mechanism by which Hes1 governs cell quiescence is still unknown, Hes1 can bind to the DNA enhancer site of the CKIs p21, p27, and p57 in HSCs (Yu et al., 2006), expectedly resulting in their inhibition of cyclins, thus arresting the cell cycle.

Cell Cycle Regulation in Hibernators

Cell Cycle Arrest in Torpor

The majority of the pathways involved in stem cell quiescence have also been implicated in hibernators, as torpor phases feature the molecular signature of cell cycle arrest and a reduction of energy-consuming processes such as transcription and translation (Biggar and Storey, 2009; Ruf et al., 2012; Wu and Storey, 2012a; Schwartz et al., 2013; Blanco and Zehr, 2015; Al-attar and Storey, 2020). Modulation of key players in cell cycle arrest due to low nutrient levels is mainly effectuated through the reduction in cellular ATP-consuming processes. A low [ATP]:[AMP] ratio activates the energy-sensing AMP-activated protein kinase (AMPK), initiating a signaling cascade that minimizes energy expenditure. Many genes involved in the cell cycle arrest are upregulated by AMPK dependent phosphorylation, including the transcription factors Hes1, JunB, and FOXO3a. In turn, they induce transcription of CIP/KIP CKIs that strongly inhibit cyclin D and E, which in proliferating cells halts the cell cycle and initiates G_0 cell arrest (Coller et al., 2006; Li and Bhatia, 2011; Valcourt et al., 2012). In line with these molecular changes, the long term torpor molecular profile matches suppression of cell cycle progression in the liver of thirteen-lined ground squirrel (*Ictidomys tridecemlineatus*) reflected in upregulation of CKIs ($p15^{INK4b}$ and $p21^{CIP1}$) and downregulation of cyclins (D and E) and CDKs2/4/6 (Andrews, 2007). Moreover, the highly proliferative intestinal epithelial cells of thirteen-lined ground squirrel and *Caenorhabditis elegans* embryos (Nystul et al., 2003) halt their mitotic activity during deep torpor because of arrest in the G_2 phase of the cell cycle (Matthews and Fisher, 1968; Kruman et al., 1988; Kruman, 1992). Yet, similar changes have been observed in terminally differentiated skeletal muscle cells of Brand's bat (*Myotis brandtii*) (Wu and Storey, 2016) and brown adipose tissue of arctic ground squirrel (*Urocitellus parryii*) (Zhu et al., 2005; Yan et al., 2008). Furthermore, cellular stress such as low temperature, UV radiation and hypoxia, upregulates the expression of the cold-inducible RNA-binding protein (CIRP), which induces the translation of the CKI, $p27^{KIP1}$. High activity of CIRP has been reported both in HSCs and during torpor in brain, which suggests that this protein plays a crucial role in inducing cell cycle arrest and in inhibiting proliferation of HSCs at low temperatures (Zhu et al., 2016; Roilo et al., 2018).

Reversing Cell Cycle Arrest in Arousal

Changes observed in torpor are basically reversed during interbout arousals. While HES1 constitutes an essential factor to leave cell quiescence in HSC, there is currently limited information about HES1 activity in hibernators, warranting further studies to understand its role in hibernation-induced cellular dormancy.

METABOLIC CHARACTERISTICS

With their survival depending on an inherent mechanism to maintain adequate metabolic function even during unfavorable environmental conditions, quiescent cells and torpid hibernators undergo a series of interconnected adjustments in metabolism. Key changes in relevant metabolic processes are depicted in **Figure 2**.

Metabolic Characteristics of Quiescence

Metabolic Switch in Quiescence

One of the remarkable adjustments is the phenotypic switch from glucose fueled mitochondrial OXPHOS to FAO, which involves the differential expression of genes and changes in metabolic processes in response to both intrinsic and extrinsic signals (Lee, 2009; Yao, 2014). Under normal physiological conditions, cellular proliferation requires high levels of energy in the form of ATP, fueled mainly by glucose through mitochondrial OXPHOS of the end product of glycolysis, pyruvate (Yang and Sheridan, 2014). Also, mitochondrial activity, especially

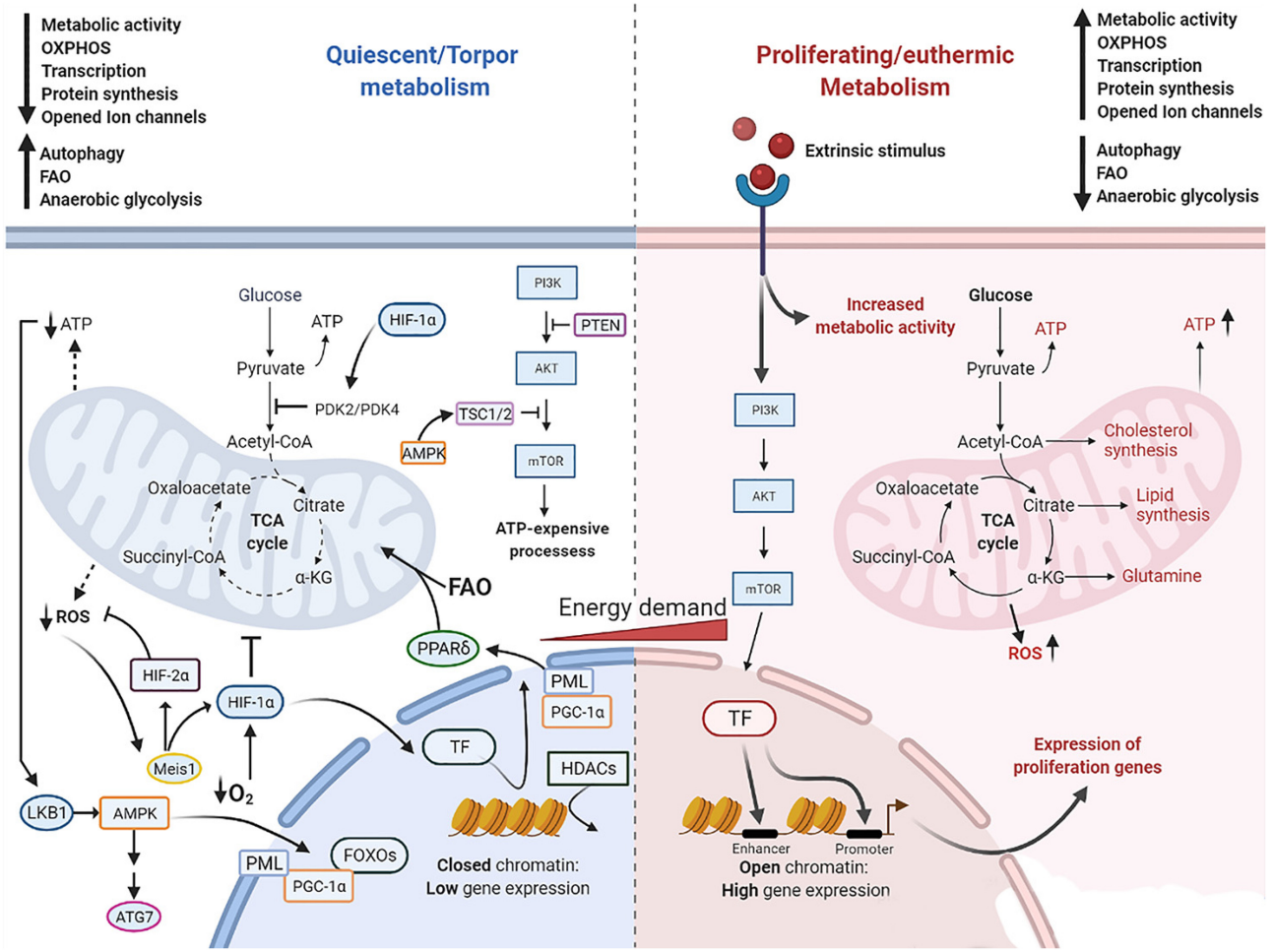

FIGURE 2 | Molecular mechanism governing cell quiescence and torpidity in contrast with cell proliferation and euthermia. Quiescent and torpid cells feature a metabolic shift from glucose fueled OXPHOS to FAO. Low nutrient supply leads to depletion of ATP which is detected by LKB1 that in turn activates AMPK, eliciting a downstream cascade including the activation of TSC1/2 that suppresses PI3K/Akt pathway and downstream ATP-expensive processes. AMPK further shuts down gene expression via activation of HDACs which tightly pack histone-DNA complexes into heterochromatin. Also, AMPK promotes autophagy by activating ULK1/ATG7, lipolysis and fatty acid oxidation via activation of OXPHOS regulator FOXOs proteins and PGC-1α. In addition, PGC-1α, a transcriptional coregulator of PPAR target genes, promotes the upregulation of PPARδ. The PML-PPARδ-FAO further promotes β-oxidation of lipids and the metabolic shift toward FAO. HIF-1α promotes FAO via upregulation of PDK4 and inhibition of the first step in the TCA cycle, and promotes resistance to hypoxia stress and ROS damage. HIF-1α can be activated by its upstream regulator the Meis1 protein, which is activated by the elevation of intracellular ROS, and by low levels of O_2. Dotted lines represent a restricted generation of molecules pointed at. Solid lines represent activated pathways. T lines indicate the suppression of the pathway. AMPK, AMP-activated protein kinase; ATG7, autophagy related 7; FOXOs, forkhead proteins; HDACs, histone deacetylases; HIF-1α, hypoxia-inducible factor 1α; HIF-2α, hypoxia-inducible factor 2α; LKB1, liver kinase B1; OXPHOS, oxidative phosphorylation; PDK4, pyruvate dehydrogenase kinases 4; PGC-1a, peroxisome proliferator-activated receptor-coactivator 1α; PML, promyelocyte leukemia protein; PML, promyelocyte leukemia protein; PPARs, peroxisome proliferator-activated receptors; PTEN, phosphatase and tensin homolog; TCA, tricarboxylic acid cycle; TF, transcription factors; TSC1/2, tuberous sclerosis proteins 1 and 2.

oxidative phosphorylation, is the main cellular ROS generator, which can damage macromolecules and organelles, including DNA, proteins and mitochondria (Ito and Ito, 2016). Quiescent cells thus switch from glucose to FAO (β-oxidation), anaerobic glycolysis and autophagy, to secure a minimal energy supply, thereby protecting them from metabolic dysregulation and DNA-damaging ROS production (Valcourt et al., 2012; Ito and Suda, 2014; Yao, 2014). Hypoxia-inducible factor 1α (HIF-1α) is critically involved in this metabolic switch. HIF-1α is a transcription factor expressed in mammalian cells residing under hypoxic conditions, which activates transcription factors and confers post-translational modifications that lower oxygen consumption. HIF-1α promotes anaerobic glycolysis by upregulating glycolytic genes and repressing glucose fueled OXPHOS through transcription of pyruvate dehydrogenase kinases PDK2 and PDK4 (Takubo et al., 2010, 2013). In turn, these kinases inhibit pyruvate dehydrogenase (PDH) (Zhang et al., 2014), which is an essential enzyme to convert glucose derived pyruvate to acetyl-CoA. Inhibition of PDH lowers carbohydrate use by limiting the flow of glycolysis products toward the citric acid cycle and promoting β-oxidation of ketones and fatty acids. At the same time, the lipolytic

protein triacylglycerol lipase (PTL), which stimulates lipolysis by breaking down adiposomes (fat droplets), liberates fatty acids for FAO. As HSCs reside in a hypoxic niche in the bone marrow, HIF-1α actively maintains the quiescent state relying on glycolysis and β-oxidation to support low levels of ATP generation. Consequently, inhibition of HIF-1α led to the depletion of mice HSCs, while HIF-1α overexpression induced their quiescence (Takubo et al., 2010). Simsek et al. (2010) showed that HIF-1α expression in HSCs is controlled by the DNA-binding transcription factor myeloid ecotropic viral integration site 1 homolog (Meis1). Further, HSCs upregulate PTL to secure the supply of fatty acids (Liu et al., 2018).

In concert with the metabolic rewiring, adaptations also constitute mechanisms that repress energy-consuming processes by inhibiting gene expression related to cell proliferation, anabolic processes and oxidative phosphorylation through the action of HDACs (Sang et al., 2010). Quiescent cells rapidly reduce their energy expenditure by downregulating ATP-demanding processes, such as DNA replication, macromolecular synthesis, macromolecular turnover and ion pumping activities (Cheung and Rando, 2013; Yao, 2014), which is a requirement for HSC quiescence. Signer et al. showed that chemical induction of protein synthesis leads to the loss of quiescence and promotion of proliferation of mice HCSs (Signer et al., 2014). The switch in energy metabolism back from FAO to glucose fueled OXPHOS is essential to meet the energy demand for differentiation. Indeed, inhibition of mitochondrial respiration blocks differentiation of HSCs (Yu et al., 2013), while inhibition of FAO led to cell proliferation (Ito et al., 2012).

Hypoxia also induces expression of the RNA binding motif protein 3 (RBM3), a critical translation facilitator (Wellmann et al., 2010; Zhu et al., 2019). Loss of RBM3 results in increased damage, mitotic dysfunction and apoptosis (Sureban et al., 2008), reduced neuronal structural plasticity (Peretti et al., 2015) and has been postulated to increase the translational efficacy in HSCs under hypoxic conditions. Other genes that are upregulated in quiescent cells may enhance resistance to apoptosis (NFKB2, MET) (Lin and Karin, 2003; Huh et al., 2004), suppress proliferation (MXI1, TP53, FAT) (Schreiber-Agus et al., 1998; Coller et al., 2006) and protect against accumulating oxidative damage (FOXO, HIF-1α, LKB1, SOD3, PRDX4, EPHX1) (Kops et al., 2002; Shen and Nathan, 2002; Serra et al., 2003; Shackelford and Shaw, 2009; Gurumurthy et al., 2010; Takubo et al., 2010).

mTOR in Cell Quiescence

The mammalian target of rapamycin (mTOR) pathway regulates growth and metabolism and embodies a crucial switch from high-expensive energy state (anabolic) to hypometabolism (catabolic). Upstream of mTOR is the highly conserved phosphatidylinositol-3 kinase/protein kinase B (PI3K/Akt) signaling pathway, which is activated by various signals from activated tyrosine kinase receptors. When activated, mTOR drives cell proliferation, growth and survival by activating cyclin-D-CDK4/6 complexes. The Akt/mTOR pathway is regulated by the tumor suppressors phosphatase and tensin homolog (PTEN) and tuberous sclerosis complex (TSC1/2). PTEN and TSC1/2 regulate reversible protein phosphorylation (RPP) of the mTOR pathway determining the "on" or "off" state of many energy-expensive processes. PTEN is considered a major regulator of metabolic reprogramming and has been shown to regulate PDK1, a critical activator of the insulin pathway. Normally, when carbohydrates and glucose are plentiful, insulin signaling activates the PI3K/Akt pathway, which induces glucose uptake and breakdown via glycolysis mechanisms (Rigano et al., 2017; Jansen et al., 2019). In the absence of nutrients, Akt/mTOR is inactivated by the action of PTEN (Yilmaz et al., 2006) and TSC 1/2 (Chen et al., 2008), reducing the energy-intensive processes and inducing catabolism. In a low nutrient environment, levels of glucose are reduced as well as insulin signaling (Martin, 2008; McCain et al., 2013), which reduces PI3K/Akt signaling, activating the forkhead protein (FOXO) family that lowers ROS production to protect from oxidative damage. Quiescent HSCs show the typical changes related to mTOR suppression, including the upregulation of PTEN (Zhang et al., 2006; Kalaitzidis et al., 2012; Porter et al., 2016). In HSCs, activation of the PI3K/Akt/mTOR pathway, reversing the upregulation of PTEN, occurs when cells migrate toward a more oxygen-rich microenvironment, which induces a switch from FAO to glucose fueled OXPHOS and promotes cellular respiration, in turn increasing the levels of ROS and cell cycle progression.

Mitochondria in Cell Quiescence

Mitochondrial respiration and production of ROS are strictly regulated by the activity of FOXOs and HIF-1α. Following their activation by growth-repressive signals in the PI3/Akt/mTOR pathway, FOXO proteins repress a large number of mitochondrial genes, inhibiting not only mitochondrial activity, but also biogenesis. Consistent with HSCs' low dependency on mitochondrial respiration as a source of energy, HSCs are characterized by a low number of mitochondria, which are immature and display underdeveloped cristae with globular morphology (Piccoli et al., 2005). Because of their low metabolic activity, quiescent stem cells produce low levels of ROS (Eckers et al., 2014), yet deploy unique mechanisms protecting them against DNA-damaging ROS (Wanet et al., 2015). The role of Meis1 in counteracting oxidative stress is well established (Kocabas et al., 2012; Unnisa et al., 2012; Papa et al., 2019), by serving as an upstream regulator in response to high ROS levels through activation of HIF-1α and HIF-2α (Simsek et al., 2010; Kocabas et al., 2012; Simonetti et al., 2016). In addition to Meis1, FOXO proteins are essential regulators of oxidative stress and deemed essential to maintain quiescence in long term HSCs. FOXOs inhibit mitochondrial respiratory chain protein expression and transcriptionally activate antioxidant enzymes such as catalases, sestrins, and superoxide dismutase 2 (SOD2). FOXO proteins, notably FOXO3a but also FOXO1, FOXO4, and FOXO6, inhibit mitochondrial gene expression (Tothova et al., 2007; Rimmelé et al., 2015). FOXO3a is highly expressed in HSCs and is also a main transcriptional regulator of antioxidants enzymes (Yalcin et al., 2010; Liang et al., 2016). Conditional deletion of FOXO 1/2/3/4, especially FOXO3a, results in a reduction of the HSC pool (Tothova et al., 2007; Liang et al., 2016; Bigarella et al., 2017). Apart from regulating mitochondrial ROS production and biogenesis, FOXOs also

induce the expression of CKIs of the CIP/KIP family (Kops et al., 2002; Camperio et al., 2012), thereby inducing HSC cell cycle arrest. FOXOs are activated by the tumor suppressor liver kinase B1 kinase (LKB1), which also activates AMPK (Shackelford and Shaw, 2009). LKB1 regulates AMPK activity and downstream promotion of ATP production. A relatively high AMP level is indicative of an energy-depleted state and leads to the activation of LKB1, a master kinase that in turn activates the downstream AMPK and 12 other related kinases (Lizcano et al., 2004; Shackelford and Shaw, 2009). Conditional deletion of LKB1 led to loss of quiescence and increased the number of hematopoietic progenitor cells, while depleting HSCs in mice (Gan et al., 2010; Nakada et al., 2010). In addition, LKB1 is an upstream regulator of the peroxisome proliferator-activated receptor-coactivator 1α (PGC-1α), a central regulator of mitochondrial biogenesis and oxidative metabolism, and the deletion of LKB1 in HSCs led to a downregulation of PGC-1α resulting in mitochondrial dysfunction (Gan et al., 2010). On the other hand, the knockout of PGC-1α in early subsets of HSCs showed that hematopoiesis is minimally affected in these cells. Nevertheless, knockout of PGC-1α lead to susceptibility to oxidative stress and modulation of long-term HSC re-population (Basu et al., 2013).

When HSCs commit to proliferation by moving to the high oxygen osteoblastic niche, there is a rapid increase in mitochondrial biogenesis and activity (Jang and Sharkis, 2007; Chen et al., 2008; Valcourt et al., 2012; Nakamura-Ishizu et al., 2014). Proliferating HSCs face high ROS levels and upregulate p38 mitogen-activated protein kinase (MAPK) and mTOR, compatible with the proliferative and differentiation phenotype (Kopp et al., 2005; Parmar et al., 2007). Recent investigation suggests that FOXO3a regulates mitochondrial biogenesis gene transcription, and loss of FOXO3a leads to a dysfunctional metabolic shift and impaired OXPHOS (Rimmelé et al., 2015; Menon and Ghaffari, 2018). However, the mechanism of this regulation remains unknown.

Fatty Acid Oxidation in Cell Quiescence

Inhibition of mTOR increases PPARs signaling in HSCs, which has the function of nutrient sensing and transcriptional control of metabolic pathways (Desvergne and Wahli, 1999), especially fatty acid transport and FAO (Braissant et al., 1996; Takahashi et al., 2007). HSC fate and self-renewal decisions are critically dependent on the PML-PPARδ pathway. Promyelocyte leukemia protein (PML) nuclear bodies maintain quiescence in HSC by activating peroxisome proliferator-activated receptors (PPARs), which in turn reprogram cellular metabolism by suppressing the Akt/mTOR pathway. The deletion of PML led to the loss of HSCs quiescence and subsequent exhaustion. Further investigation showed that PPAR signaling and FAO were significantly reduced during HSCs differentiation, while induction of PPARδ by a PML-targeting compound induced quiescence (Ito et al., 2012). The depletion of PML and inhibition of mitochondrial FAO in HSC resulted in symmetric division (two committed HSC daughter cells, i.e., cells with a progressive differentiation toward a particular type of red or white blood cell) both *in vitro* and *in vivo*. Conversely, pharmacological activation of PPARδ increased asymmetric division (one daughter committed, the other for self-renewal) (Ito et al., 2012; Ito and Ito, 2013). Hence, PML and PPARδ activation play an essential role in maintaining the stem cell pool (Lallemand-Breitenbach and de Thé, 2010; Ito and Suda, 2014).

Autophagy in Cell Quiescence

Autophagy is a conserved mechanism by which cytoplasmic proteins and organelles are engulfed within autophagosomes and degraded in lysosomes, providing ATP and metabolites. Autophagy is governed by the activation of AMPK in response to nutritional deprivation, leading to phosphorylation of TSC1/2, which in turn inhibits mTORC1 (Yang and Klionsky, 2010). Low levels of mTORC1 activate Unc-51 like autophagy activating kinase, ULK1 (Kim et al., 2008; Mizushima, 2010), which recruits additional proteins to form a complex that promotes autophagosome formation and autophagy. Autophagy related 7 (Atg7) is consistently upregulated in quiescent cells, and deletion of Atg7 in mice decreased the number of HSCs and progenitors cells of various lineages and increased the number of abnormal mitochondria and ROS levels (Mortensen et al., 2011). Furthermore, a mutation in the autophagy gene Atg12 increased levels of ROS, protein synthesis and glucose fueled OXPHOS in mouse HSCs (Vessoni et al., 2012; Revuelta and Matheu, 2017). These results suggest that disruption of autophagy induces a loss of quiescence and a switch back to the proliferating phenotype in HSCs, consistent with the idea that autophagy influences cell fate decisions through metabolic reprogramming of HSC.

Metabolic Characteristics of Hibernation

Metabolic Switch in Hibernation

Hibernators have implemented metabolic adaptations very similar to those found in quiescence. Mammalian hibernators also switch from carbohydrate fueled OXPHOS to lipid-based metabolism (FAO) during torpor (Vermillion et al., 2015). This is reflected in the respiratory quotient (RQ: the quotient of CO_2 production over O_2 use), which reflects carbohydrate (RQ $\sim$ 1.0) *versus* lipid oxidation (RQ $\sim$ 0.7). During torpor, European hedgehog (*Erinaceus europaeus*) and Arctic ground squirrel show RQ values of 0.7 indicating an exclusive use of FAO. However, during arousals, RQ rises to values $>$ 0.85 suggesting a partial return to glucose fueled OXPHOS metabolism (Tähti, 1978; Buck and Barnes, 2000). Hibernator cells also readily suppress most ATP-consuming processes, including transcription and translation responsible for an estimated 20–30% of cellular energy consumption (Frerichs et al., 1998; Wieser and Krumschnabel, 2001; Armitage et al., 2003). This is thought to be only one of the mechanisms contributing to the metabolic reduction in hibernation, since the metabolic rate reduction during hibernation is much larger ($\sim$83%) (Armitage et al., 2003; Storey and Storey, 2004). Although global transcription inhibition during hibernation is still debated (Carey and Martin, 1996; Hittel D. and Storey, 2002), there is increasing evidence that transcription modulation is tissue-dependent during torpor (Soukri et al., 1996; Van Breukelen and Martin, 2002). For example, thirteen-lined ground squirrels suppress DNA transcription and replication by a twofold decrease in transcriptional initiation, reducing elongation during

torpor (Storey, 2003; Tsiouris, 2005; Tessier and Storey, 2014). To avoid energy expenditure by transcription of genes unnecessary in torpor, histone deacetylases (HDACs) silence genes through chromatin remodeling. Protein levels of HDAC1 and HDAC4 are significantly upregulated, and RNA polymerase II activity is downregulated by 57% in thirteen-lined ground squirrels during torpor (Morin and Storey, 2006), suggesting a tight regulation of energy-consuming gene transcription by chromatin remodeling and protein synthesis due to low temperature and low levels of mRNA turnover in hibernation. Given that protein synthesis is even more energetically expensive than transcription, expectedly, most of protein synthesis is actively repressed during torpor. Global mRNA translation is inhibited in torpid golden-mantled ground squirrels (Zhegunov et al., 1988) and Syrian hamsters (Osborne et al., 2004), even though some proteins are tissue-specifically synthesized at low rate during torpor. Conversely, very high rates of protein synthesis and cell proliferation are observed shortly after interbout arousal compared to squirrels that had been active for 1–2 days after hibernation, suggesting an initial compensatory mechanism to replenish proteins lost during torpor (Zhegunov et al., 1988).

Although the mechanistic control of the switch from glucose to fat combustion during hibernation has not been fully elucidated, it seems to be similar to mechanisms observed in starvation (Pilegaard et al., 2003), diabetes (Wu et al., 1999; Kim et al., 2006), and caloric restriction (Lee C. K. et al., 2002). Animals tested in these conditions show upregulation of the transcriptional targets of HIF-1α, including PDK4, PTL, and repression of PDH. However, HIF-1α was not investigated in these studies. Similarly, hibernating ground squirrels showed upregulation of PDK4 and PTL in heart, skeletal muscle and white adipose tissue (Andrews et al., 1998; Buck et al., 2002; Brauch et al., 2005). PTL shows high lipolytic activity at low ambient temperatures as an intrinsic feature of the protein across all mammal lineages. Yet, during torpor, PTL is further upregulated, which is an unique feature observed only in hibernators (Squire et al., 2004). While regulation of PDK4 and PTL only suggests involvement of HIF-1α, direct evidence for its upregulation in torpor comes from two studies. Maistrovski et al. (2012) found increased HIF-1α protein levels in skeletal muscle of 13-lined squirrels and little brown bat (*Myotis lucifugus*), and in liver of little brown bat during hibernation. Previously, HIF-1α protein levels were shown to increase by 60–70% in brown adipose tissue in 13-lined squirrels (Morin and Storey, 2005). Moreover, a recent study using fasting-induced daily torpor in B6N and B6J mice showed that the promoters of the HIF-1α signaling pathway are highly activated during torpidity (Sunagawa et al., 2018). On the other hand, some species such as Arctic ground squirrels (AGS) show significantly higher levels of HIF-1α during late-arousal and euthermic conditions compared to torpor (Ma et al., 2005). These contrasting findings could be due to species differences and/or differences in timing of sample collection. For example, normalization of oxygen consumption rate (OCR) in the brain upon arousal differs greatly among species, taking ∼60 min in Horseshoe bats (*Rhinolophus ferrumequinum*) (Lee M. et al., 2002), while taking ∼4 h in AGS (Zhu et al., 2005). Since the expression and activity of HIF-1α is also regulated by oxygen-independent mechanisms such as ROS levels, mechanical stress, and growth factors (Chun et al., 2002), HIF-1α expression during hibernation might be tissue-specific with differential expression associated with species differences.

In addition to HIF-1α, the hypoxia related RBM3 provides cytoprotection in hibernators by maintaining protein homeostasis under low metabolic conditions (Fedorov et al., 2009). Moreover, several of the genes offering protection in quiescent cell are reported upregulated in hibernating 13-lined ground squirrels, including FOXOs, HIF-1α, SOD3, p21, and p27, as discussed above.

mTOR in Hibernation

Hibernation also features changes in expression of the negative regulators of mTOR, i.e., PTEN and TSC1/2. PTEN levels are significantly elevated (1.4 fold) in late torpor in skeletal muscle of thirteen-lined squirrels compared to summer euthermic controls (Wu et al., 2013a, 2015). Activation and inhibition of the Akt/mTOR pathway are paramount for cell cycle arrest during torpor and proliferation during arousal (Huang and Manning, 2008; Wu and Storey, 2012b). Moreover, hibernators re-activate the mTOR pathway upon arousal by supporting the switch from FAO to glucose fueled OXPHOS, increasing oxygen consumption and mitochondrial biogenesis (Wilson et al., 2008; Foudi et al., 2009).

Mitochondria in Hibernation

Hibernating thirteen-lined squirrels reduce their O_2 consumption by 98% from basal levels and increase it by 300% during arousals (Boyer and Barnes, 1999). In addition, an increase in mitochondrial ROS production also activates HIF-1α via the oxidative stress-sensitive transcription factor nuclear factor erythroid 2-related factor 2 (NRF2) (Hawkins et al., 2016; Lacher et al., 2018), which inhibits mitochondrial respiration and sequentially activates LKB1/AMPK (Simsek et al., 2010). However, the underlying mechanism of these molecular processes are not fully understood (Hwang et al., 2014; Li et al., 2015). Recent reports showed a significant upregulation of HIF-1α in the heart and skeletal muscle tissue of thirteen-lined squirrels during hibernation, suggesting that it confers protection against mitochondrial hyperpolarization as a possible mechanism against cellular stress (Maistrovski et al., 2012; Wu et al., 2013b). Mitochondrial hyperpolarization results from the disruption of their electrochemical gradient by the blockade of ATP-synthase, which may ultimately lead to Fas-induced apoptosis (Gergely et al., 2002; Perl et al., 2004). Recently, Ou et al. (2018) reported that exposure of human induced pluripotent stem cell-derived neurons (iPSC-neurons) to low temperature (4°C) produced mitochondrial hyperpolarization and accumulation of ROS, while mitochondrial from iPSC-neurons from thirteen-lined squirrels were depolarized and produced significant less ROS (Ou et al., 2018). High levels of ROS also induced accumulation of HIF-1α in brown adipose tissue (BAT), while HIF-1α knockdown in mice BAT led to reduced levels of glucose consumption, lactate export and glycolytic capacity (Choudhry and Harris, 2018). This suggests that glycolysis is dependent on HIF-1α regulation under hypoxic conditions, which maximizes metabolism in BAT.

Mitochondrial numbers and activity are differentially regulated between torpor and interbout arousal (Martin et al., 1999; Staples, 2014). Mitochondrial activity during hibernation of the 13-lined ground squirrel is tissue-specifically regulated and significantly increases in BAT and brain cortex (Ballinger et al., 2016), while mitochondria number was reported unchanged in ground squirrel liver (Brown et al., 2012), skeletal muscle (Hittel D. S. and Storey, 2002), and heart muscle (Staples and Brown, 2008) during hibernation. Yet, mitochondrial respiration exhibited no apparent suppression in heart muscle, moderate suppression in skeletal muscle and significant suppression in liver. Suppression of the uptake, transport or synthesis of specific substrates of OXPHOS may be a possible mechanism conferring suppression of mitochondrial respiration in liver cells (Brown et al., 2012). This possibility is in line with the decreased succinate dehydrogenase levels during hibernation reported previously (Gehnrich and Aprille, 1988; Cho, 2018).

While LKB1 is considered a master regulator of cellular metabolism in quiescent cells by inhibiting mitochondrial function and biogenesis through activation of FOXO and PGC-1α proteins, its relevance in torpor is still unknown. Nevertheless, in thirteen-lined ground squirrels, AMPK levels in white adipose tissue (WAT) were three times higher than those of summer animals (Horman et al., 2005). The activity of AMPK and LKB1 might be regulated by sex hormones, as dihydrotestosterone (DHT) inhibits AMPK activation, while androgens and estrogens inhibit LKB1 activation (McInnes et al., 2012) and declines in steroid hormone production seem to be a precondition for males to enter hibernation. As such, high levels of testosterone inhibit entrance into torpor in hamster (Hall and Goldman, 1980), hedgehog (Webb and Ellison, 1998), and Belding's ground squirrel (Lee et al., 1990; Boonstra et al., 2001). Also, transcription of mtDNA and mitochondrial proteins such as PGC-1α, uncoupling proteins (UCP1, UCP3) and AMPK is 4-fold higher in BAT than in other tissues during hibernation (Boyer et al., 1998; Xu et al., 2013; Ballinger et al., 2016). PGC-1α is a central regulator of mitochondrial biogenesis and respiration and it induces the transcription of nuclear respiratory factors (NRF1 and NRF2) that activate the replication of mtDNA.

Fatty Acid Oxidation in Hibernation

The crucial role of PML in HSCs quiescence (Ishida, 2009; Ito et al., 2012) would suggest that a similar mechanism is present during mammalian torpor (Lee et al., 2007). However, to the best of our knowledge, there are no reports about the specific role of PML during hibernation, although increasing evidence suggests downstream PPARs to constitute the master transcriptional regulators of changes in lipid metabolism. For example, both protein and mRNA of PPARα were upregulated in WAT, heart, kidney and liver of six species of hibernating bats (Han et al., 2015), jerboa (*Jaculus orientalis*) (Kabine et al., 2004) and 13-lined squirrels (Eddy et al., 2005). PPARα not only induces the activation of genes involved in lipid metabolism, but also induces the expression of uncoupling proteins (UCPs), which pump protons back into the mitochondrial matrix generating heat without synthesizing ATP. The high uncoupled thermogenesis activity of mitochondrial respiration in BAT plays an essential role in thermoregulation and contributes significantly to the rewarming of the organism during arousal from hibernation. Further, PML was also reported to be highly active in thirteen-lined ground squirrels brain during torpor and is associated with massive SUMOylation and increased tolerance to brain ischemia (Lee et al., 2007; Lee and Hallenbeck, 2013).

Autophagy in Hibernation

Autophagy is poorly examined in hibernators. In the heart of hibernating Syrian hamster, autophagy seems already initiated during (late) torpor and executed during early arousal, reflected by the gradual increase in active autophagosomes during torpor followed by a peak at early arousal, returning to normal late in arousal (Wiersma et al., 2018). This might be due to the build-up of damaged or misfolded proteins being gradually formed during torpor, since there is an accumulation of cells in the G_2 phase during torpor (Matthews and Fisher, 1968; Kruman et al., 1988). While autophagy is an essential mechanism to sustain quiescence in HSC, its role in maintaining cell dormancy in hibernators is poorly understood. More research into autophagy in hibernators may unclose relevant knowledge on the preservation of life under stress conditions.

RADIATION RESISTANCE

Under normal physiological conditions, the body has stem cells in all phases of the cell cycle (Lyle and Moore, 2011). Radiation generates high levels of ROS, which increases cellular stress and causes irreversible cellular damage leading to senescence and apoptosis. Particular stem cells are resistant to radiation: cancer stem cells (CSC). Not surprisingly, HIF-1α is significantly upregulated in cancerous cells due to the hypoxic environment created by the rapidly proliferating cells (Majmundar et al., 2010). HIF-1α regulates the switch from glucose to fatty acid combustion, a characteristic of quiescent cells, indicating that HIF-1α might play an important role in conferring radiation resistance in dormant cells. Other mechanisms, including the reduction in histone acetylation because of increased activity of HDACs, lead to a tighter packing of DNA into heterochromatin, which plays a significant role in the radiation resistance of quiescent cells (Diehn and Clarke, 2006). Quiescent cells, especially human stem cells, significantly upregulate antioxidant gene expression, creating an environment where the cells can resist ROS production by radiation (Oberley et al., 1995). In cancer cells, this appears under the control of a particular gene from the FOXO family, FOXM1. FOXM1 downregulation in quiescent cells elevated expression of antioxidant genes such as manganese superoxide dismutase (MnSOD), catalase (CAT), and peroxiredoxin (PRDX3) (Eckers et al., 2014). Radiotherapy is usually administered when treating cancer cells, but quiescent CSCs are resistant to this therapy designed to eliminate proliferating cells (Luk et al., 1986). Knockdown of FOXM1 increases sensitivity to radiation therapy in quiescent and cancer stem cells. The amount of therapeutic radiation is still restricted by its toxicity to normal tissue. For example, multiple metastases cannot be treated without exceeding the tolerance of the healthy

organ nearby. By putting specific tissues or organs of patients into dormancy, cells may potentially tolerate higher doses of radiation (Cerri et al., 2016).

Studies conducted in hibernators have shown that torpor limits radiation-induced DNA damage in squirrels, hamsters, and mice (Ghosh et al., 2017; Tinganelli et al., 2019), which has awakened the interest of its utility in cancer therapies and long-haul space missions. The mechanisms that mediate radioprotection during torpor are not known. Likely, they parallel those found in quiescent cells, as torpid animals upregulate antioxidant genes and activate HDACs. Recent studies indicate that radiation resistance in torpor may also relate to the hypothermia, as cell cooling limits DNA damage and leads to a different dynamics in DNA damage repair (Baird et al., 2011).

SHARED MOLECULAR MECHANISMS OF CELLULAR QUIESCENCE AND ANIMAL DORMANCY

Main Mechanisms Involved

Quiescent (hematopoietic stem) cells and torpor share many similarities (**Table 1**). First, these include activation of molecular mechanisms that stall the cell cycle of proliferating cells including a major overlap in regulation of essential cell cycle genes and proteins associated with the maintenance of quiescence in HSCs and torpidity during hibernation. In both cases, the entry into dormancy is associated with differential gene expression of proteins that includes cyclins, CDKs and CKIs. Yet the molecular mechanism conferring cellular quiescence in stem cells are described in great detail, whereas this is not the case for hibernators. Moreover, it is evident that induction of HES1 during stem cell quiescence is a prerequisite to enable reversal from cell arrest. However, there is a marked paucity of data on Hes1 activity in hibernators, warranting further studies to understand its role in torpor. HSC may provide a blueprint to disclose mechanisms used by hibernators that govern activation of the molecular machinery of cell cycle arrest in response to environmental changes, even though hibernator cells largely represent terminally differentiated cells.

Secondly, cell quiescence and torpor share a similar metabolic rewiring. Both in quiescent and torpid cells, energy conservation is brought about by the reduction in metabolic rate and the switch from glucose fueled OXPHOS to FAO as the primary mechanism to supply ATP, supported by the radical suppression of anabolic processes, such as DNA replication, transcription and protein synthesis. HIF-1α coordinates the cellular adaptation to restore the balance between oxygen supply and metabolic demand, leading to a reduction in the consumption of oxygen. Under ATP-deprived conditions resulting from nutrient deprivation or hypoxia, activation of the energy-sensing liver kinase B1 (LKB1) and the downstream AMP-activated protein kinase (AMPK) precede the upregulation of HIF-1α (Hudson et al., 2002; Lee et al., 2003). Moreover, the activation of LKB1 and AMPK stimulates autophagy through phosphorylation of ULK1 and inhibits the mTOR pathway (Hudson et al., 2002; Li et al., 2015; Mohammad et al., 2019). The Akt/mTOR pathway regulates many energy-expensive processes and is inhibited in quiescence and hibernation by the action of PTEN and TSC1/2 coupled with downstream RPP signaling. High levels of PTEN and TSCs both in HSCs and during hibernation suggest that these proteins are essential to maintain quiescence and torpor. Several of these pathways need further study in hibernators to define their contribution to metabolic suppression, including HIF-1α

TABLE 1 | Comparison of key events driving quiescence in cells to those found in torpid cells.

Mechanisms in quiescent cells	Main effects	Torpid cells
Upregulation of CKIs	■ Cell cycle block	√
Downregulation of cyclins and CDKs	■ Cell cycle block	√
Upregulation of CIRP	■ Upregulates CKIs	√
Upregulation of HES1	■ Reversibility of quiescence	?
Upregulation of HIF-1α	■ Lowers mitochondrial activity ■ Shift from glucose to fatty acid combustion ■ Activates FOXOs ■ Activates LKB1/AMPK ■ Upregulates PDK4 ■ Activates HDACs	√
Repression of Akt/mTOR	■ Inhibits transcription and translation ■ Limits mitochondrial activity and biogenesis through PGC-1α ■ Activates FOXOs	√
Activation of LKB1/AMPK	■ Inhibits Akt/mTOR ■ Activates FOXOs ■ Activates autophagy	?/√
Upregulation of HDACs	■ Inhibits transcription ■ Radioprotection	√
Upregulation of PDK4	■ Inhibits pyruvate dehydrogenase (PDH)	√
Inhibition of PDH	■ Inhibits OXPHOS by limiting use of glycolysis end products	√
Upregulation of FOXOs	■ Inhibits mitochondrial activity Induces antioxidant gene expression	√
Upregulation of PTL	■ Liberates fatty acids	√
Upregulation of PTEN and TSC1/2	■ Inhibits of Akt/mTOR	√
Upregulation of PML-PPARδ	■ Inhibit Akt/mTOR	√
Downregulation of FOXM1	■ Transcription of antioxidant genes	√
Upregulation of ATG7	■ Activates autophagy	?

√ indicates that the mechanism has been observed in hibernating animals. ? indicates that there is paucity of data in hibernating animals. ?/√ indicates that the mechanism has been observed incompletely and/or only in one tissue of 1 species. AMPK, AMP-activated protein kinase; ATG7, autophagy related 7; CDKs, cyclin-dependent kinases; CIRP, cold-inducible RNA-binding protein; CKIs, cyclin-dependent kinase inhibitors; FOXM1, Forkhead Box M1; FOXOs, forkhead proteins; HDACs, histone deacetylases; HES1, helix-loop-helix protein 1; HIF-1α, hypoxia-inducible factor 1α; LKB1, liver kinase B1; OXPHOS, oxidative phosphorylation; PDH, pyruvate dehydrogenase; PDK4, pyruvate dehydrogenase kinases 4; PGC-1a, peroxisome proliferator-activated receptor-coactivator 1α; PML, promyelocyte leukemia protein; PPARs, peroxisome proliferator-activated receptors; PTEN, phosphatase and tensin homolog; PTL, lipolytic protein triacylglycerol lipase; TSC1/2, tuberous sclerosis proteins 1 and 2.

and autophagy. Further, the PML-PPARδ-FAO pathway appears to play a vital role in the maintenance of HSC quiescence and plays a critical role in its cell fate and self-renewal decisions. However, very little is known about the function and activity of PML during hibernation. Also, quiescent cells and hibernators share the upregulation of cell protective, anti-apoptotic pathways, suggesting that a similar mechanisms is activated during quiescence and mammalian torpor (Heldmaier et al., 2000; Hefler et al., 2015; Zhang et al., 2016).

Thirdly, both quiescent cells and hibernators share radiation resistance, which seems conferred by the combination of upregulation of antioxidant defense and heterochromatin formation. In addition to the antioxidant environment, HIF-1α recruits HDACs to tightly pack the DNA into heterochromatin resulting in resistance to radiation. FOXM1 appears to be a master regulator of antioxidants, and its downregulation resulted in lower radiation sensitivity of cancer stem cells. While strict control over oxidation is crucial for hibernators to survive torpor/arousal switches, there is no literature of the activity and function of FOXM1 in hibernators available. Consequently, mechanisms of radiation resistance in both stem cells and torpor are still ill-defined. At present, it is unclear whether radiation resistance merely exists as a bystander effect of metabolic suppression and antioxidant defense, including a tighter packaging of DNA, or whether it is conferred by specific mechanisms; a question not so easily addressed.

As outlined, the three phenomena discussed above show substantial crosstalk, with the one activating or promoting the other. Although processes are quite similar in HSC and torpor, there may be a clear distinction in their order. For instance, in HSC the regulation of cell cycle and metabolism seems tightly integrated, as interventions in both drive cells out of quiescence. Whether this is true for hibernators is unclear. Possibly, the inhibition of the cell cycle of the differentiated cells in hibernators is merely a consequence of strong metabolic suppression, including the inhibition of DNA synthesis and transcription. To explore differences in orchestration, an accurate delineation of the critical factors and their sequence of events during entry into torpor is warranted.

Reversible Protein Phosphorylation

Reversible protein phosphorylation (RPP) is a crucial post-translational modifier of proteins and regulator of cell homeostasis. In HSCs and hibernators, RPP is especially important to support the exit from and re-entering of the cell cycle without spending much energy on anabolic processes. While the LKB1-AMPK route plays a crucial role in inactivating many anabolic processes such as protein synthesis, RPP signaling seems of crucial importance to inactivate ion channels. The preponderance of cellular processes that expend energy is directly or indirectly affiliated with membranes preserving concentration gradients. Thus, suppression of membrane-associated (ion channels) proteins by RPP has a profound impact on metabolic reduction and ATP turnover reduction. For example, phosphorylation of sodium-potassium pump (Na^+/K^+-ATPase) led to a decrease in activity by up to 60% in golden-mantled squirrels (Storey and Storey, 2004). Therefore, RPP could be responsible for not only maintaining lipid-based metabolism but also to initiate the metabolic repression in hibernation preparation through AMPK signaling.

Future Directions

The large overlap between quiescent (hematopoietic stem) cells and hibernator adaptations may have some future implications. First, studies on (stem) cell quiescence have identified a number of crucial genes/pathways, of which the relevance in hibernation has been insufficiently explored, in particular LKB1, HES1, HIF-1α, and PML. One study explored the effects of LKB1 knockout in *Caenorhabditis elegans* (Narbonne and Roy, 2009). Interestingly, the LKB1 knockout worms entered Dauer state, a survival mechanism that arrests feeding while retaining activity, motility and acquiring stress-resistance, but rapidly consumed their stored energy leading to failure of vital organs and death. Although *C. elegans* is not a true hibernator nor a mammal, the phenotype is similar to LKB1 knockout in HSC. LKB1 might thus also be an essential protein in hibernators under energetically unfavorable conditions to maintain energy and oxidative stress homeostasis. PML-PPARδ regulation of FAO is essential to maintain HSC quiescence and acts as a negative regulator of Akt/mTOR, a crucial element in the metabolic shift. In hibernators, there is only a single study reporting increased PML-PPARδ activity in thirteen-lined squirrel. Given its critical role in FAO and metabolic reprogramming, PML is an interesting target to address in hibernation. Given the activation of the machinery governing cell cycle block during torpidity, it is of great importance to study HES-1, the factor that retains the option for stem cells to re-enter cell cycle, in particular in relation to arousals. Finally, although upregulation of HIF-1α has been documented in hibernators, details of its regulation and effects need a deeper understanding.

Nevertheless, exploring the relevance of these and other proteins in hibernation is not a trivial task. The main limitation to infer causality in factors contributing to hibernation, is the absence of (conditional) knock-out models in true hibernators. Generation of such models would require genetic modification of hibernator blastocyst stem cells to introduce LoxP sites into genes of interest and generation of Cre expressing lines, preferable harboring inducible promotors, like the tamoxifen-induced CRE-ERT2 system. Such developments may be accelerated by the recent advancements of CRISPR/Cas9 technology, but will still require considerable effort and funding, and specialized knowledge. An alternative approach may be to use inducible knockouts of genes in the house mouse (*Mus musculus*), a species long known to be capable of serial daily torpor (Hudson and Scott, 1979). Conditional knockout mouse lines of a number of factors discussed are readily available. Moreover, the present variety of Cre mouse lines and the superior toolbox to introduce LoxP sites, signify that making the appropriate knockout in mouse is far easier compared to true hibernators.

However, it is unclear to date to what extent the molecular mechanisms of mouse daily torpor resemble those of torpor found in true hibernators. The first step should therefore consist of exploring the molecular footprint of cell cycle arrest and metabolic rewiring in mouse torpor. A third option to explore specific genes might be the use of induced pluripotent stem cells (iPSCs) from hibernators (Takahashi and Yamanaka, 2006). These iPSCs can be differentiated into any cell type to study molecular biology *in vitro*. Also, if the selected cell type does not depend on a heterotypic, complex environment, but represents an autonomous cell, it can be further maturated into engineered 3D tissue or organoids to mimic physiological behavior. A recent study showed that iPSC-derived neurons from thirteen-lined squirrel behaved differently than human neurons with higher resistance to cold (Ou et al., 2018). Knocking out genes in iPSC-derived hibernator cells may at least explore the important question whether some of the mechanism present in HSC quiescence may be induced in a cell autonomous way by starvation or hypoxia.

Most cells in a mammal, whether or not a hibernator, are capable of quiescence. The similarity between molecular mechanisms conferring quiescence in HSC and hibernation may signify that there is a unifying (epi)genetic-metabolic program governing the both states. If true, it may mean that all non-hibernator species could be capable of hibernation, provided that cellular quiescence is induced in high energy consuming organs.

AUTHOR CONTRIBUTIONS

All authors listed have made a substantial, direct and intellectual contribution to the work, and approved it for publication.

FUNDING

This study was supported by a grant from the European Space Agency to RH (Research agreement collaboration 4000123556).

REFERENCES

Al-attar, R., and Storey, K. B. (2020). Suspended in time: Molecular responses to hibernation also promote longevity. *Exp. Gerontol.* 134:110889. doi: 10.1016/j.exger.2020.110889

Andrews, M. T. (2007). Advances in molecular biology of hibernation in mammals. *BioEssays* 29, 431–440. doi: 10.1002/bies.20560

Andrews, M. T., Squire, T. L., Bowen, C. M., and Rollins, M. B. (1998). Low-temperature carbon utilization is regulated by novel gene activity in the heart of a hibernating mammal. *Proc. Natl. Acad. Sci. U. S. A.* 95, 8392–8397. doi: 10.1073/pnas.95.14.8392

Armitage, K. B., Blumstein, D. T., and Woods, B. C. (2003). Energetics of hibernating yellow-bellied marmots (*Marmota flaviventris*). *Comp. Biochem. Physiol. A Mol. Integr. Physiol.* 134, 101–114. doi: 10.1016/S1095-6433(02)00219-2

Asai, T., Liu, Y., Di Giandomenico, S., Bae, N., Ndiaye-Lobry, D., Deblasio, A., et al. (2012). Necdin, a p53 target gene, regulates the quiescence and response to genotoxic stress of hematopoietic stem/progenitor cells. *Blood* 120, 1601–1612. doi: 10.1182/blood-2011-11-393983

Baek, J. H., Hatakeyama, J., Sakamoto, S., Ohtsuka, T., and Kageyama, R. (2006). Persistent and high levels of Hes1 expression regulate boundary formation in the developing central nervous system. *Development* 133, 2467–2476. doi: 10.1242/dev.02403

Baird, B. J., Dickey, J. S., Nakamura, A. J., Redon, C. E., Parekh, P., Griko, Y. V., et al. (2011). Hypothermia postpones DNA damage repair in irradiated cells and protects against cell killing. *Mutat. Res. Fundam. Mol. Mech. Mutagen.* 711, 142–149. doi: 10.1016/j.mrfmmm.2010.12.006

Ballinger, M. A., Hess, C., Napolitano, M. W., Bjork, J. A., and Andrews, M. T. (2016). Seasonal changes in brown adipose tissue mitochondria in a mammalian hibernator: From gene expression to function. *Am. J. Physiol. Regul. Integr. Comp. Physiol.* 311, R325–R336. doi: 10.1152/ajpregu.00463.2015

Basu, S., Broxmeyer, H. E., and Hangoc, G. (2013). Peroxisome proliferator-activated-γ coactivator-1α-mediated mitochondrial biogenesis is important for hematopoietic recovery in response to stress. *Stem Cells Dev.* 22, 1678–1692. doi: 10.1089/scd.2012.0466

Beauséjour, C. M., Krtolica, A., Galimi, F., Narita, M., Lowe, S. W., Yaswen, P., et al. (2003). Reversal of human cellular senescence: Roles of the p53 and p16 pathways. *EMBO J.* 22, 4212–4222. doi: 10.1093/emboj/cdg417

Berasain, C., and Avila, M. A. (2015). Regulation of hepatocyte identity and quiescence. *Cell. Mol. Life Sci.* 72, 3831–3851. doi: 10.1007/s00018-015-1970-7

Bigarella, C. L., Li, J., Rimmelé, P., Liang, R., Sobol, R. W., and Ghaffari, S. (2017). FOXO3 transcription factor is essential for protecting hematopoietic stem and progenitor cells from oxidative DNA damage. *J. Biol. Chem.* 292, 3005–3015. doi: 10.1074/jbc.M116.769455

Biggar, K., and Storey, K. (2009). Perspectives in Cell Cycle Regulation: Lessons from an Anoxic Vertebrate. *Curr. Genomics* 10, 573–584. doi: 10.2174/138920209789503905

Blanco, M. B., and Zehr, S. M. (2015). Striking longevity in a hibernating lemur. *J. Zool.* 296, 177–188. doi: 10.1111/jzo.12230

Blomen, V. A., and Boonstra, J. (2007). Cell fate determination during G1 phase progression. *Cell. Mol. Life Sci.* 64, 3084–3104. doi: 10.1007/s00018-007-7271-z

Boonstra, R., Hubbs, A. H., Lacey, E. A., and McColl, C. J. (2001). Seasonal changes in glucocorticoid and testosterone concentrations in free-living arctic ground squirrels from the boreal forest of the Yukon. *Can. J. Zool.* 79, 49–58. doi: 10.1139/z00-175

Boyer, B. B., and Barnes, B. M. (1999). Molecular and metabolic aspects of mammalian hibernation. *Bioscience* 49, 713–724. doi: 10.2307/1313595

Boyer, B. B., Barnes, B. M., Lowell, B. B., and Grujic, D. (1998). Differential regulation of uncoupling protein gene homologues in multiple tissues of hibernating ground squirrels. *Am. J. Physiol. Regul. Integr. Comp. Physiol.* 275, R1232. doi: 10.1152/ajpregu.1998.275.4.r1232

Bracken, A. P., Ciro, M., Cocito, A., and Helin, K. (2004). E2F target genes: Unraveling the biology. *Trends Biochem. Sci.* 29, 409–417. doi: 10.1016/j.tibs.2004.06.006

Braissant, O., Foufelle, F., Scotto, C., Dauça, M., and Wahli, W. (1996). Differential expression of peroxisome proliferator-activated receptors (PPARs): Tissue distribution of PPAR-α, -β, and -γ in the adult rat. *Endocrinology* 137, 354–366. doi: 10.1210/endo.137.1.8536636

Brauch, K. M., Dhruv, N. D., Hanse, E. A., and Andrews, M. T. (2005). Digital transcriptome analysis indicates adaptive mechanisms in the heart of a hibernating mammal. *Physiol. Genomics* 2005, 00076. doi: 10.1152/physiolgenomics.00076.2005

Brown, J. C. L., Chung, D. J., Belgrave, K. R., and Staples, J. F. (2012). Mitochondrial metabolic suppression and reactive oxygen species production in liver and skeletal muscle of hibernating thirteen-lined ground squirrels. *Am. J. Physiol. Regul. Integr. Comp. Physiol.* 2012, 00230. doi: 10.1152/ajpregu.00230.2011

Buck, C. L., and Barnes, B. M. (2000). Effects of ambient temperature on metabolic rate, respiratory quotient, and torpor in an arctic hibernator. *Am. J. Physiol. Regul. Integr. Comp. Physiol.* 279, r255. doi: 10.1152/ajpregu.2000.279.1.r255

Buck, M. J., Squire, T. L., and Andrews, M. T. (2002). Coordinate expression of the PDK4 gene: A means of regulating fuel selection in a hibernating mammal. *Physiol. Genomics* 2002, 5–13. doi: 10.1152/physiolgenomics.00076.2001

Camins, A., Pizarro, J. G., and Folch, J. (2013). Cyclin-Dependent Kinases. *Brenner's Encyclop. Genet.* 2013, 260–266. doi: 10.1016/B978-0-12-374984-0.00370-3

Camperio, C., Caristi, S., Fanelli, G., Soligo, M., De Porto, P., and Piccolella, E. (2012). Forkhead Transcription Factor FOXP3 Upregulates CD25 Expression through Cooperation with RelA/NF-κB. *PLoS One* 7:0048303. doi: 10.1371/journal.pone.0048303

Carey, H. V., and Martin, S. L. (1996). Preservation of intestinal gene expression during hibernation. *Am. J. Physiol. Gastrointest. Liver Physiol.* 271, g805. doi: 10.1152/ajpgi.1996.271.5.g805

Carey, H. V., Andrews, M. T., and Martin, S. L. (2003). Mammalian hibernation: Cellular and molecular responses to depressed metabolism and low temperature. *Physiol. Rev.* 83, 1153–1181. doi: 10.1152/physrev.00008.2003

Cerri, M., Tinganelli, W., Negrini, M., Helm, A., Scifoni, E., Tommasino, F., et al. (2016). Hibernation for space travel: Impact on radioprotection. *Life Sci. Sp. Res.* 11, 1–9. doi: 10.1016/j.lssr.2016.09.001

Chakkalakal, J. V., Jones, K. M., Basson, M. A., and Brack, A. S. (2012). The aged niche disrupts muscle stem cell quiescence. *Nature* 490, 355–360. doi: 10.1038/nature11438

Chen, C., Liu, Y., Liu, R., Ikenoue, T., Guan, K. L., Liu, Y., et al. (2008). TSC-mTOR maintains quiescence and function of hematopoietic stem cells by repressing mitochondrial biogenesis and reactive oxygen species. *J. Exp. Med.* 205, 2397–2408. doi: 10.1084/jem.20081297

Cheng, T., Rodrigues, N., Shen, H., Yang, Y. G., Dombkowski, D., Sykes, M., et al. (2000). Hematopoietic stem cell quiescence maintained by p21(cip1/waf1). *Science* 287, 1804–1809. doi: 10.1126/science.287.5459.1804

Cheung, T. H., and Rando, T. A. (2013). Molecular regulation of stem cell quiescence. *Nat. Rev. Mol. Cell Biol.* 14, 329–340. doi: 10.1038/nrm3591

Cho, E. H. (2018). Succinate as a regulator of hepatic stellate cells in liver fibrosis. *Front. Endocrinol.* 9:00455. doi: 10.3389/fendo.2018.00455

Choi, Y. J., and Anders, L. (2014). Signaling through cyclin D-dependent kinases. *Oncogene* 33, 1890–1903. doi: 10.1038/onc.2013.137

Choudhry, H., and Harris, A. L. (2018). Advances in Hypoxia-Inducible Factor Biology. *Cell Metab.* 27, 281–298. doi: 10.1016/j.cmet.2017.10.005

Chun, Y. S., Kim, M. S., and Park, J. W. (2002). Oxygen-dependent and -independent regulation of HIF-1alpha. *J. Korean Med. Sci.* 2002, 581. doi: 10.3346/jkms.2002.17.5.581

Clevers, H., and Watt, F. M. (2018). Defining Adult Stem Cells by Function, not by Phenotype. *Annu. Rev. Biochem.* 87, 1015–1027. doi: 10.1146/annurev-biochem-062917-012341

Coats, S., Flanagan, W. M., Nourse, J., and Roberts, J. M. (1996). Requirement of p27Kip1 for restriction point control of the fibroblast cell cycle. *Science* 272, 877–880. doi: 10.1126/science.272.5263.877

Coller, H. A., Sang, L., and Roberts, J. M. (2006). A new description of cellular quiescence. *PLoS Biol.* 4:0329–0349. doi: 10.1371/journal.pbio.0040083

Coloff, J. L., Murphy, J. P., Braun, C. R., Harris, I. S., Shelton, L. M., Kami, K., et al. (2016). Differential Glutamate Metabolism in Proliferating and Quiescent Mammary Epithelial Cells. *Cell Metab.* 23, 867–880. doi: 10.1016/j.cmet.2016.03.016

Dai, Y., and Grant, S. (2003). Cyclin-dependent kinase inhibitors. *Curr. Opin. Pharmacol.* 3, 362–370. doi: 10.1016/S1471-4892(03)00079-1

Dannenberg, J. H., Van Rossum, A., Schuijff, L., and Te Riele, H. (2000). Ablation of the retinoblastoma gene family deregulates G1 control causing immortalization and increased cell turnover under growth-restricting conditions. *Genes Dev.* 14, 3051–3064. doi: 10.1101/gad.847700

Dannenmann, B., Lehle, S., Hildebrand, D. G., Kübler, A., Grondona, P., Schmid, V., et al. (2015). High glutathione and glutathione peroxidase-2 levels mediate cell-type-specific DNA damage protection in human induced pluripotent stem cells. *Stem Cell Reports* 4, 886–898. doi: 10.1016/j.stemcr.2015.04.004

Dausmann, K. H., Glos, J., Ganzhorn, J. U., and Heldmaier, G. (2004). Physiology: Hibernation in a tropical primate. *Nature* 429, 825–826. doi: 10.1038/429825a

Denlinger, D. L. (2002). Regulation of diapause. *Annu. Rev. Entomol.* 47, 93–122. doi: 10.1146/annurev.ento.47.091201.145137

Desvergne, B., and Wahli, W. (1999). Peroxisome proliferator-activated receptors: Nuclear control of metabolism. *Endocr. Rev.* 20, 649–688. doi: 10.1210/er.20.5.649

Diehn, M., and Clarke, M. F. (2006). Cancer stem cells and radiotherapy: New insights into tumor radioresistance. *J. Natl. Cancer Inst.* 98, 1755–1757. doi: 10.1093/jnci/djj505

Dong, J. J., Peng, J., Zhang, H., Mondesire, W. H., Jian, W., Mills, G. B., et al. (2005). Role of glycogen synthase kinase 3β in rapamycin-mediated cell cycle regulation and chemosensitivity. *Cancer Res.* 65, 1961–1972. doi: 10.1158/0008-5472.CAN-04-2501

Dyson, N. (1998). The regulation of E2F by pRB-family proteins. *Genes Dev.* 12, 2245–2262. doi: 10.1101/gad.12.15.2245

Eckers, J. C., Kalen, A. L., Sarsour, E. H., Tompkins, V. S., Janz, S., Son, J. M., et al. (2014). Forkhead Box M1 Regulates Quiescence-Associated Radioresistance of Human Head and Neck Squamous Carcinoma Cells. *Radiat. Res.* 182, 420–429. doi: 10.1667/RR13726.1

Eddy, S. F., Morin, P., and Storey, K. B. (2005). Cloning and expression of PPARγ and PGC-1α from the hibernating ground squirrel, *Spermophilus tridecemlineatus*. *Mol. Cell. Biochem.* 269, 175–182. doi: 10.1007/s11010-005-3459-4

Eilers, M., Schirm, S., and Bishop, J. M. (1991). The MYC protein activates transcription of the α-prothymosin gene. *EMBO J.* 10, 133–141. doi: 10.1002/j.1460-2075.1991.tb07929.x

Ezoe, S., Matsumura, I., Tanaka, H., Satoh, Y., Yokota, T., Oritani, K., et al. (2008). SIRT1 Deficiency Suppresses the Maintenance of Hematopoietic Stem Cell Pool. *Blood* 112, 1394–1394. doi: 10.1182/blood.v112.11.1394.1394

Fedorov, V. B., Goropashnaya, A. V., Tøien, O., Stewart, N. C., Gracey, A. Y., Chang, C., et al. (2009). Elevated expression of protein biosynthesis genes in liver and muscle of hibernating black bears (*Ursus americanus*). *Physiol. Genomics* 37, 108–118. doi: 10.1152/physiolgenomics.90398.2008

Figel, S., and Fenstermaker, R. A. (2018). "Cell-Cycle Regulation," in *Handbook of Brain Tumor Chemotherapy, Molecular Therapeutics, and Immunotherap*. H B. Newton (Elsevier: Amsterdam) 257–269. doi: 10.1016/B978-0-12-812100-9.00018-8

Fisher, R. P. (1997). CDKs and cyclins in transition(s). *Curr. Opin. Genet. Dev.* 7, 32–38. doi: 10.1016/S0959-437X(97)80106-2

Foudi, A., Hochedlinger, K., Van Buren, D., Schindler, J. W., Jaenisch, R., Carey, V., et al. (2009). Analysis of histone 2B-GFP retention reveals slowly cycling hematopoietic stem cells. *Nat. Biotechnol.* 27, 84–90. doi: 10.1038/nbt.1517

Fox, P. M., Vought, V. E., Hanazawa, M., Lee, M. H., Maine, E. M., and Sched, T. (2011). Cyclin e and CDK-2 regulate proliferative cell fate and cell cycle progression in the C. elegans germline. *Development* 138, 2223–2234. doi: 10.1242/dev.059535

Frerichs, K. U., Smith, C. B., Brenner, M., Degracia, D. J., Krause, G. S., Marrone, L., et al. (1998). Suppression of protein synthesis in brain during hibernation involves inhibition of protein initiation and elongation. *Proc. Natl. Acad. Sci. U. S. A.* 95, 14511–14516. doi: 10.1073/pnas.95.24.14511

Gan, B., Hu, J., Jiang, S., Liu, Y., Sahin, E., Zhuang, L., et al. (2010). Lkb1 regulates quiescence and metabolic homeostasis of haematopoietic stem cells. *Nature* 468, 701–704. doi: 10.1038/nature09595

Garcia, K., and Su, T. T. (2008). Cell cycle regulation. *Fly* 2, 133–137. doi: 10.4161/fly.6333

Gehnrich, S. C., and Aprille, J. R. (1988). Hepatic gluconeogenesis and mitochondrial function during hibernation. *Comp. Biochem. Physiol. Part B Biochem.* 91, 11–16. doi: 10.1016/0305-0491(88)90107-1

Gergely, P., Grossman, C., Niland, B., Puskas, F., Neupane, H., Allam, F., et al. (2002). Mitochondrial hyperpolarization and ATP depletion in patients with systemic lupus erythematosus. *Arthritis Rheum* 46, 175–190. doi: 10.1002/1529-0131(200201)46:1<175::AID-ART10015<3.0.CO;2-H

Ghosh, S., Indracanti, N., Joshi, J., Ray, J., and Indraganti, P. K. (2017). Pharmacologically induced reversible hypometabolic state mitigates radiation induced lethality in mice. *Sci. Rep.* 7, 15002–15007. doi: 10.1038/s41598-017-15002-7

Gurumurthy, S., Xie, S. Z., Alagesan, B., Kim, J., Yusuf, R. Z., Saez, B., et al. (2010). The Lkb1 metabolic sensor maintains haematopoietic stem cell survival. *Nature* 468, 659–663. doi: 10.1038/nature09572

Hall, V., and Goldman, B. (1980). Effects of gonadal steroid hormones on hibernation in the Turkish hamster (Mesocricetus brandti). *J. Comp. Physiol. B* 135, 107–114. doi: 10.1007/BF00691200

Han, Y., Zheng, G., Yang, T., Zhang, S., Dong, D., and Pan, Y. H. (2015). Adaptation of peroxisome proliferator-activated receptor alpha to hibernation in bats Genome evolution and evolutionary systems biology. *BMC Evol. Biol.* 15:373–376. doi: 10.1186/s12862-015-0373-6

Hao, S., Chen, C., and Cheng, T. (2016). Cell cycle regulation of hematopoietic stem or progenitor cells. *Int. J. Hematol.* 103, 487–497. doi: 10.1007/s12185-016-1984-4

Harbour, J. W., and Dean, D. C. (2000). The Rb/E2F pathway: Expanding roles and emerging paradigms. *Genes Dev.* 14, 2393–2409. doi: 10.1101/gad.813200

Hartman, J., Müller, P., Foster, J. S., Wimalasena, J., Gustafsson, J. Å, and Ström, A. (2004). HES-1 inhibits 17β-estradiol and heregulin-β1-mediated upregulation of E2F-1. *Oncogene* 23, 8826–8833. doi: 10.1038/sj.onc.1208139

Hawkins, K. E., Joy, S., Delhove, J. M. K. M., Kotiadis, V. N., Fernandez, E., Fitzpatrick, L. M., et al. (2016). NRF2 Orchestrates the Metabolic Shift during Induced Pluripotent Stem Cell Reprogramming. *Cell Rep.* 14, 1883–1891. doi: 10.1016/j.celrep.2016.02.003

Hefler, J., Wu, C. W., and Storey, K. B. (2015). Transcriptional activation of p53 during cold induced torpor in the 13-lined ground squirrel Ictidomys tridecemlineatus. *Biochem. Res. Int.* 2015, 731595. doi: 10.1155/2015/731595

Heldmaier, G., Klingenspor, M. F., and Klaus, S. (2000). *Life in the Cold: Eleventh International Hibernation Symposium*. New York,NY: Springer

Hittel, D. S., and Storey, K. B. (2002). Differential expression of mitochondria-encoded genes in a hibernating mammal. *J. Exp. Biol.* 205, 1625–1631.

Hittel, D., and Storey, K. B. (2002). The translation state of differentially expressed mRNAs in the hibernating 13-lined ground squirrel (*Spermophilus tridecemlineatus*). *Arch. Biochem. Biophys.* 401, 244–254. doi: 10.1016/S0003-9861(02)00048-6

Horman, S., Hussain, N., Dilworth, S. M., Storey, K. B., and Rider, M. H. (2005). Evaluation of the role of AMP-activated protein kinase and its downstream targets in mammalian hibernation. *Comp. Biochem. Physiol. B Biochem. Mol. Biol.* 142, 374–382. doi: 10.1016/j.cbpb.2005.08.010

Hosokawa, K., Arai, F., Yoshihara, H., Takubo, K., Ito, K., Matsuoka, S., et al. (2006). Reactive Oxygen Species Control Hematopoietic Stem Cell-Niche Interaction through the Regulation of N-Cadherin. *Blood* 108, 86–86. doi: 10.1182/blood.v108.11.86.86

Huang, J., and Manning, B. D. (2008). The TSC1-TSC2 complex: A molecular switchboard controlling cell growth. *Biochem. J.* 412, 179–190. doi: 10.1042/BJ20080281

Hudson, C. C., Liu, M., Chiang, G. G., Otterness, D. M., Loomis, D. C., Kaper, F., et al. (2002). Regulation of Hypoxia-Inducible Factor 1α Expression and Function by the Mammalian Target of Rapamycin. *Mol. Cell. Biol.* 22, 7004–7014. doi: 10.1128/mcb.22.20.7004-7014.2002

Hudson, J. W., and Scott, I. M. (1979). Daily Torpor in the Laboratory Mouse, Mus musculus Var. *Albino. Physiol. Zool.* 1979, 30152564. doi: 10.1086/physzool.52.2.30152564

Huh, C. G., Factor, V. M., Sánchez, A., Uchida, K., Conner, E. A., and Thorgeirsson, S. S. (2004). Hepatocyte growth factor/c-met signaling pathway is required for efficient liver regeneration and repair. *Proc. Natl. Acad. Sci. U. S. A.* 101, 4477–4482. doi: 10.1073/pnas.0306068101

Hwang, A. B., Ryu, E. A., Artan, M., Chang, H. W., Kabir, M. H., Nam, H. J., et al. (2014). Feedback regulation via AMPK and HIF-1 mediates ROS-dependent longevity in Caenorhabditis elegans. *Proc. Natl. Acad. Sci. U. S. A.* 111, E4458–E4467. doi: 10.1073/pnas.1411199111

Infante, A., Laresgoiti, U., Fernández-Rueda, J., Fullaondo, A., Galán, J., Díaz-Uriarte, R., et al. (2008). E2F2 represses cell cycle regulators to maintain quiescence. *Cell Cycle* 7, 3915–3927. doi: 10.4161/cc.7.24.7379

Ishida, N. (2009). Role of PPAR in the control of torpor through FGF21-NPY pathway: From circadian clock to seasonal change in mammals. *PPAR Res.* 2009:412949. doi: 10.1155/2009/412949

Ito, K., and Ito, K. (2013). Newly identified roles of PML in stem cell biology. *Front. Oncol.* 3:00050. doi: 10.3389/fonc.2013.00050

Ito, K., and Ito, K. (2016). Metabolism and the Control of Cell Fate Decisions and Stem Cell Renewal. *Annu. Rev. Cell Dev. Biol.* 32, 399–409. doi: 10.1146/annurev-cellbio-111315-125134

Ito, K., and Suda, T. (2014). Metabolic requirements for the maintenance of self-renewing stem cells. *Nat. Rev. Mol. Cell Biol.* 15, 243–256. doi: 10.1038/nrm3772

Ito, K., Carracedo, A., Weiss, D., Arai, F., Ala, U., Avigan, D. E., et al. (2012). A PML-PPAR-δ pathway for fatty acid oxidation regulates hematopoietic stem cell maintenance. *Nat. Med.* 18, 1350–1358. doi: 10.1038/nm.2882

Jang, Y. Y., and Sharkis, S. J. (2007). A low level of reactive oxygen species selects for primitive hematopoietic stem cells that may reside in the low-oxygenic niche. *Blood* 110, 3056–3063. doi: 10.1182/blood-2007-05-087759

Jansen, H. T., Trojahn, S., Saxton, M. W., Quackenbush, C. R., Evans Hutzenbiler, B. D., Nelson, O. L., et al. (2019). Hibernation induces widespread transcriptional remodeling in metabolic tissues of the grizzly bear. *Commun. Biol.* 2, 574–574. doi: 10.1038/s42003-019-0574-4

Johnson, D. G., Schwarz, J. K., Cress, W. D., and Nevins, J. R. (1993). Expression of transcription factor E2F1 induces quiescent cells to enter S phase. *Nature* 365, 349–352. doi: 10.1038/365349a0

Kabine, M., El Kebbaj, Z., Oaxaca-Castillo, D., Clémencet, M. C., El Kebbaj, M. S., Latruffe, N., et al. (2004). Peroxisome proliferator-activated receptors as regulators of lipid metabolism; Tissue differential expression in adipose tissues during cold acclimatization and hibernation of jerboa (Jaculus orientalis). *Biochimie* 86, 763–770. doi: 10.1016/j.biochi.2004.10.003

Kalaitzidis, D., Sykes, S. M., Wang, Z., Punt, N., Tang, Y., Ragu, C., et al. (2012). MTOR complex 1 plays critical roles in hematopoiesis and pten-loss-evoked leukemogenesis. *Cell Stem Cell* 11, 429–439. doi: 10.1016/j.stem.2012.06.009

Kalamakis, G., Brüne, D., Ravichandran, S., Bolz, J., Fan, W., Ziebell, F., et al. (2019). Quiescence Modulates Stem Cell Maintenance and Regenerative Capacity in the Aging Brain. *Cell* 176, 1407.e–1419.e. doi: 10.1016/j.cell.2019.01.040

Kent, L. N., and Leone, G. (2019). The broken cycle: E2F dysfunction in cancer. *Nat. Rev. Cancer* 19, 326–338. doi: 10.1038/s41568-019-0143-7

Kim, E., Goraksha-Hicks, P., Li, L., Neufeld, T. P., and Guan, K. L. (2008). Regulation of TORC1 by Rag GTPases in nutrient response. *Nat. Cell Biol.* 10, 935–945. doi: 10.1038/ncb1753

Kim, Y. I., Lee, F. N., Choi, W. S., Lee, S., and Youn, J. H. (2006). Insulin regulation of skeletal muscle PDK4 mRNA expression is impaired in acute insulin-resistant states. *Diabetes* 55, 2311–2317. doi: 10.2337/db05-1606

Kippin, T. E., Martens, D. J., and Van Der Kooy, D. (2005). P21 Loss Compromises the Relative Quiescence of Forebrain Stem Cell Proliferation Leading To Exhaustion of Their Proliferation Capacity. *Genes Dev.* 19, 756–767. doi: 10.1101/gad.1272305

Kocabas, F., Zheng, J., Thet, S., Copeland, N. G., Jenkins, N. A., DeBerardinis, R. J., et al. (2012). Meis1 regulates the metabolic phenotype and oxidant defense of hematopoietic stem cells. *Blood* 120, 4963–4972. doi: 10.1182/blood-2012-05-432260

Kopp, H. G., Avecilla, S. T., Hooper, A. T., and Rafii, S. (2005). The bone marrow vascular niche: Home of HSC differentiation and mobilization. *Physiology* 20, 349–356. doi: 10.1152/physiol.00025.2005

Kops, G. J. P. L., Dansen, T. B., Polderman, P. E., Saarloos, I., Wirtz, K. W. A., Coffer, P. J., et al. (2002). Forkhead transcription factor FOXO3a protects quiescent cells from oxidative stress. *Nature* 419, 316–321. doi: 10.1038/nature01036

Kowalik, T. F., DeGregori, J., Schwarz, J. K., and Nevins, J. R. (1995). E2F1 overexpression in quiescent fibroblasts leads to induction of cellular DNA synthesis and apoptosis. *J. Virol.* 69, 2491–2500. doi: 10.1128/jvi.69.4.2491-2500.1995

Kretzner, L., Blackwood, E. M., and Eisenman, R. N. (1992). Myc and Max proteins possess distinct transcriptional activities. *Nature* 359, 426–429. doi: 10.1038/359426a0

Kruman, I. I. (1992). Comparative analysis of cell replacement in hibernators. *Comp. Biochem. Physiol. Part A Physiol.* 1992, 90620–90626. doi: 10.1016/0300-9629(92)90620-6

Kruman, I. I., Ilyasova, E. N., Rudchenko, S. A., and Khurkhulu, Z. S. (1988). The intestinal epithelial cells of ground squirrel (Citellus undulatus) accumulate at G2 phase of the cell cycle throughout a bout of hibernation. *Comp. Biochem. Physiol. Part A Physiol.* 90, 233–236. doi: 10.1016/0300-9629(88)91109-7

Lacher, S. E., Levings, D. C., Freeman, S., and Slattery, M. (2018). Identification of a functional antioxidant response element at the HIF1A locus. *Redox Biol.* 19, 401–411. doi: 10.1016/j.redox.2018.08.014

Lacorazza, H. D., Yamada, T., Liu, Y., Miyata, Y., Sivina, M., Nunes, J., et al. (2006). The transcription factor MEF/ELF4 regulates the quiescence of primitive hematopoietic cells. *Cancer Cell* 9, 175–187. doi: 10.1016/j.ccr.2006.02.017

Lallemand-Breitenbach, V., and de Thé, H. (2010). PML nuclear bodies. *Cold Spring Harb. Perspect. Biol.* 2:a000661. doi: 10.1101/cshperspect.a000661

Lee, C. K., Allison, D. B., Brand, J., Weindruch, R., and Prolla, T. A. (2002). Transcriptional profiles associated with aging and middle age-onset caloric restriction in mouse hearts. *Proc. Natl. Acad. Sci. U. S. A.* 99, 14988–14993. doi: 10.1073/pnas.232308999

Lee, M., Choi, I., and Park, K. (2002). Activation of stress signaling molecules in bat brain during arousal from hibernation. *J. Neurochem* 2002:01022.x. doi: 10.1046/j.1471-4159.2002.01022.x

Lee, M., Hwang, J. T., Lee, H. J., Jung, S. N., Kang, I., Chi, S. G., et al. (2003). AMP-activated protein kinase activity is critical for hypoxia-inducible factor-1 transcriptional activity and its target gene expression under hypoxic conditions in DU145 cells. *J. Biol. Chem.* 278, 39653–39661. doi: 10.1074/jbc.M306104200

Lee, R. E. (2009). "Hibernation," in *Encyclopedia of Insects*. V H. Resh and R T. Cardé (Cambridge, MA: Academic Press)449–449. doi: 10.1016/B978-0-12-374144-8.00127-2

Lee, T. M., Pelz, K., Licht, P., and Zucker, I. (1990). Testosterone influences hibernation in golden-mantled ground squirrels. *Am. J. Physiol. Regul. Integr. Comp. Physiol.* 259:r760. doi: 10.1152/ajpregu.1990.259.4.r760

Lee, Y. J., and Hallenbeck, J. M. (2013). SUMO and ischemic tolerance. *NeuroMolecular Med.* 15, 771–781. doi: 10.1007/s12017-013-8239-9

Lee, Y. J., Miyake, S. I., Wakita, H., McMullen, D. C., Azuma, Y., Auh, S., et al. (2007). Protein SUMOylation is massively increased in hibernation torpor and is critical for the cytoprotection provided by ischemic preconditioning and hypothermia in SHSY5Y cells. *J. Cereb. Blood Flow Metab.* 27, 950–962. doi: 10.1038/sj.jcbfm.9600395

Li, H., Satriano, J., Thomas, J. L., Miyamoto, S., Sharma, K., Pastor-Soler, N. M., et al. (2015). Interactions between HIF-1α and AMPK in the regulation of cellular hypoxia adaptation in chronic kidney disease. *Am. J. Physiol. Ren. Physiol.* 309, F414–F428. doi: 10.1152/ajprenal.00463.2014

Li, L., and Bhatia, R. (2011). Stem cell quiescence. *Clin. Cancer Res.* 17, 4936–4941. doi: 10.1158/1078-0432.CCR-10-1499

Liang, R., Rimmelé, P., Bigarella, C. L., Yalcin, S., and Ghaffari, S. (2016). Evidence for AKT-independent regulation of FOXO1 and FOXO3 in haematopoietic stem and progenitor cells. *Cell Cycle* 15, 861–867. doi: 10.1080/15384101.2015.1123355

Lim, S., and Kaldis, P. (2013). Cdks, cyclins and CKIs: Roles beyond cell cycle regulation. *Dev.* 140, 3079–3093. doi: 10.1242/dev.091744

Lin, A., and Karin, M. (2003). NF-κB in cancer: A marked target. *Semin. Cancer Biol.* 13, 107–114. doi: 10.1016/S1044-579X(02)00128-1

Liu, C., Han, T., Stachura, D. L., Wang, H., Vaisman, B. L., Kim, J., et al. (2018). Lipoprotein lipase regulates hematopoietic stem progenitor cell maintenance through DHA supply. *Nat. Commun.* 9, 03775–y. doi: 10.1038/s41467-018-03775-y

Liu, Y., Elf, S. E., Miyata, Y., Sashida, G., Liu, Y., Huang, G., et al. (2009). p53 Regulates Hematopoietic Stem Cell Quiescence. *Cell Stem Cell* 4, 37–48. doi: 10.1016/j.stem.2008.11.006

Lizcano, J. M., Göransson, O., Toth, R., Deak, M., Morrice, N. A., Boudeau, J., et al. (2004). LKB1 is a master kinase that activates 13 kinases of the AMPK subfamily, including MARK/PAR-1. *EMBO J.* 23, 833–843. doi: 10.1038/sj.emboj.7600110

Luk, C. K., Keng, P. C., and Sutherland, R. M. (1986). Radiation response of proliferating and quiescent subpopulations isolated from multicellular spheroids. *Br. J. Cancer* 54, 25–32. doi: 10.1038/bjc.1986.148

Lyle, S., and Moore, N. (2011). Quiescent, slow-cycling stem cell populations in cancer: A review of the evidence and discussion of significance. *J. Oncol.* 2011:396076. doi: 10.1155/2011/396076

Ma, Y. L., Zhu, X., Rivera, P. M., Tøien, Ø, Barnes, B. M., LaManna, J. C., et al. (2005). Absence of cellular stress in brain after hypoxia induced by arousal from hibernation in Arctic ground squirrels. *Am. J. Physiol. Regul. Integr. Comp. Physiol.* 2005:00260. doi: 10.1152/ajpregu.00260.2005

Maistrovski, Y., Biggar, K. K., and Storey, K. B. (2012). HIF-1α regulation in mammalian hibernators: Role of non-coding RNA in HIF-1α control during torpor in ground squirrels and bats. *J. Comp. Physiol. B Biochem. Syst. Environ. Physiol.* 182, 849–859. doi: 10.1007/s00360-012-0662-y

Majmundar, A. J., Wong, W. J., and Simon, M. C. (2010). Hypoxia-Inducible Factors and the Response to Hypoxic Stress. *Mol. Cell* 40, 294–309. doi: 10.1016/j.molcel.2010.09.022

Malumbres, M., and Barbacid, M. (2005). Mammalian cyclin-dependent kinases. *Trends Biochem. Sci.* 30, 630–641. doi: 10.1016/j.tibs.2005.09.005

Malumbres, M., and Barbacid, M. (2009). Cell cycle, CDKs and cancer: A changing paradigm. *Nat. Rev. Cancer* 9, 153–166. doi: 10.1038/nrc2602

Martin, S. L. (2008). Mammalian hibernation: A naturally reversible model for insulin resistance in man? *Diabetes Vasc. Dis. Res.* 5, 76–81. doi: 10.3132/dvdr.2008.013

Martin, S. L., Maniero, G. D., Carey, C., and Hand, S. C. (1999). Reversible depression of oxygen consumption in isolated liver mitochondria during hibernation. *Physiol. Biochem. Zool.* 72, 255–264. doi: 10.1086/316667

Masaki, S. (2009). Aestivation. *Encyclop. Insects* 2009, 2–4. doi: 10.1016/B978-0-12-374144-8.00002-3

Matsui, K., Ezoe, S., Oritani, K., Shibata, M., Tokunaga, M., Fujita, N., et al. (2012). NAD-dependent histone deacetylase, SIRT1, plays essential roles in the maintenance of hematopoietic stem cells. *Biochem. Biophys. Res. Commun.* 418, 811–817. doi: 10.1016/j.bbrc.2012.01.109

Matthews, L. H., and Fisher, K. C. (1968). Mammalian Hibernation III. *J. Anim. Ecol.* 37:724. doi: 10.2307/3087

Maynard, S., Swistowska, A. M., Lee, J. W., Liu, Y., Liu, S.-T., Da Cruz, A. B., et al. (2008). Human Embryonic Stem Cells Have Enhanced Repair of Multiple Forms of DNA Damage. *Stem Cells* 26, 2266–2274. doi: 10.1634/stemcells.2007-1041

McCain, S., Ramsay, E., and Kirk, C. (2013). The effects of hibernation and captivity on glucose metabolism and thyroid hormones in American black bear (*Ursus Americanus*). *J. Zoo Wildl. Med.* 44, 324–332. doi: 10.1638/2012-0146R1.1

McEachern, M. A., Yackel Adams, A. A., Klug, P. E., Fitzgerald, L. A., and Reed, R. N. (2015). Brumation of Introduced Black and White Tegus, Tupinambis merianae (Squamata: Teiidae), in Southern Florida. *Southeast. Nat.* 14, 319–328. doi: 10.1656/058.014.0207

McInnes, K. J., Brown, K. A., Hunger, N. I., and Simpson, E. R. (2012). Regulation of LKB1 expression by sex hormones in adipocytes. *Int. J. Obes.* 36, 982–985. doi: 10.1038/ijo.2011.172

Menon, V., and Ghaffari, S. (2018). Transcription factors FOXO in the regulation of homeostatic hematopoiesis. *Curr. Opin. Hematol.* 25, 290–298. doi: 10.1097/MOH.0000000000000441

Miyamoto, K., Miyamoto, T., Kato, R., Yoshimura, A., Motoyama, N., and Suda, T. (2008). FoxO3a regulates hematopoietic homeostasis through a negative feedback pathway in conditions of stress or aging. *Blood* 112, 4485–4493. doi: 10.1182/blood-2008-05-159848

Mizushima, N. (2010). The role of the Atg1/ULK1 complex in autophagy regulation. *Curr. Opin. Cell Biol.* 22, 132–139. doi: 10.1016/j.ceb.2009.12.004

Mohammad, K., Dakik, P., Medkour, Y., Mitrofanova, D., and Titorenko, V. I. (2019). Quiescence entry, maintenance, and exit in adult stem cells. *Int. J. Mol. Sci.* 20:20092158. doi: 10.3390/ijms20092158

Mohrin, M., Bourke, E., Alexander, D., Warr, M. R., Barry-Holson, K., Le Beau, M. M., et al. (2010). Hematopoietic stem cell quiescence promotes error-prone DNA repair and mutagenesis. *Cell Stem Cell* 7, 174–185. doi: 10.1016/j.stem.2010.06.014

Morin, P., and Storey, K. B. (2005). Cloning and expression of hypoxia-inducible factor 1α from the hibernating ground squirrel, *Spermophilus tridecemlineatus*. *Biochim. Biophys. Acta Gene Struct. Expr.* 2005:009. doi: 10.1016/j.bbaexp.2005.02.009

Morin, P., and Storey, K. B. (2006). Evidence for a reduced transcriptional state during hibernation in ground squirrels. *Cryobiology* 53, 310–318. doi: 10.1016/j.cryobiol.2006.08.002

Mortensen, M., Soilleux, E. J., Djordjevic, G., Tripp, R., Lutteropp, M., Sadighi-Akha, E., et al. (2011). The autophagy protein Atg7 is essential for hematopoietic stem cell maintenance. *J. Exp. Med.* 208, 455–467. doi: 10.1084/jem.20101145

Murata, K., Hattori, M., Hirai, N., Shinozuka, Y., Hirata, H., Kageyama, R., et al. (2005). Hes1 Directly Controls Cell Proliferation through the Transcriptional Repression of p27Kip1. *Mol. Cell. Biol.* 25, 4262–4271. doi: 10.1128/mcb.25.10.4262-4271.2005

Murray, A. W. (2004). Recycling the Cell Cycle: Cyclins Revisited. *Cell* 116, 221–234. doi: 10.1016/S0092-8674(03)01080-8

Nakada, D., Saunders, T. L., and Morrison, S. J. (2010). Lkb1 regulates cell cycle and energy metabolism in haematopoietic stem cells. *Nature* 468, 653–658. doi: 10.1038/nature09571

Nakamura-Ishizu, A., Takizawa, H., and Suda, T. (2014). The analysis, roles and regulation of quiescence in hematopoietic stem cells. *Dev.* 141, 4656–4666. doi: 10.1242/dev.106575

Narbonne, P., and Roy, R. (2009). Caenorhabditis elegans dauers need LKB1/AMPK to ration lipid reserves and ensure long-term survival. *Nature* 457, 210–214. doi: 10.1038/nature07536

Nystul, T. G., Goldmark, J. P., Padilla, P. A., and Roth, M. B. (2003). Suspended Animation in C. elegans Requires the Spindle Checkpoint. *Science* 302, 1038–1041. doi: 10.1126/science.1089705

Oberley, T. D., Schultz, J. L., Li, N., and Oberley, L. W. (1995). Antioxidant enzyme levels as a function of growth state in cell culture. *Free Radic. Biol. Med.* 19, 53–65. doi: 10.1016/0891-5849(95)00012-M

Orford, K. W., and Scadden, D. T. (2008). Deconstructing stem cell self-renewal: Genetic insights into cell-cycle regulation. *Nat. Rev. Genet.* 9, 115–128. doi: 10.1038/nrg2269

Osborne, P. G., Gao, B., and Hashimoto, M. (2004). Determination in vivo of newly synthesized gene expression in hamsters during phases of the hibernation cycle. *Jpn. J. Physiol.* 54, 295–305. doi: 10.2170/jjphysiol.54.295

Ou, J., Ball, J. M., Luan, Y., Zhao, T., Miyagishima, K. J., Xu, Y., et al. (2018). iPSCs from a Hibernator Provide a Platform for Studying Cold Adaptation and Its Potential Medical Applications. *Cell* 173, 851.e–863.e. doi: 10.1016/j.cell.2018.03.010

Papa, L., Djedaini, M., and Hoffman, R. (2019). Mitochondrial role in stemness and differentiation of hematopoietic stem cells. *Stem Cells Int.* 2019:4067162. doi: 10.1155/2019/4067162

Parmar, K., Mauch, P., Vergilio, J. A., Sackstein, R., and Down, J. D. (2007). Distribution of hematopoietic stem cells in the bone marrow according to regional hypoxia. *Proc. Natl. Acad. Sci. U. S. A.* 104, 5431–5436. doi: 10.1073/pnas.0701152104

Peng, H., Park, J. K., Katsnelson, J., Kaplan, N., Yang, W., Getsios, S., et al. (2015). MicroRNA-103/107 family regulates multiple epithelial stem cell characteristics. *Stem Cells* 33, 1642–1656. doi: 10.1002/stem.1962

Peretti, D., Bastide, A., Radford, H., Verity, N., Molloy, C., Martin, M. G., et al. (2015). RBM3 mediates structural plasticity and protective effects of cooling in neurodegeneration. *Nature* 518, 236–239. doi: 10.1038/nature14142

Perl, A., Gergely, P., Nagy, G., Koncz, A., and Banki, K. (2004). Mitochondrial hyperpolarization: A checkpoint of T-cell life, death and autoimmunity. *Trends Immunol.* 25, 360–367. doi: 10.1016/j.it.2004.05.001

Piccoli, C., Ria, R., Scrima, R., Cela, O., D'Aprile, A., Boffoli, D., et al. (2005). Characterization of mitochondrial and extra-mitochondrial oxygen consuming reactions in human hematopoietic stem cells: Novel evidence of the occurrence of NAD(P)H oxidase activity. *J. Biol. Chem.* 280, 26467–26476. doi: 10.1074/jbc.M500047200

Pietras, E. M., Warr, M. R., and Passegué, E. (2011). Cell cycle regulation in hematopoietic stem cells. *J. Cell Biol.* 195, 709–720. doi: 10.1083/jcb.201102131

Pilegaard, H., Saltin, B., and Neufer, P. D. (2003). Effect of short-term fasting and refeeding on transcriptional regulation of metabolic genes in human skeletal muscle. *Diabetes* 52, 657–662. doi: 10.2337/diabetes.52.3.657

Pimienta, G., and Pascual, J. (2007). Canonical and alternative MAPK signaling. *Cell Cycle* 6, 2628–2632. doi: 10.4161/cc.6.21.4930

Porter, S. N., Cluster, A. S., Signer, R. A. J., Voigtmann, J., Monlish, D. A., Schuettpelz, L. G., et al. (2016). Pten cell autonomously modulates the hematopoietic stem cell response to inflammatory cytokines. *Stem Cell Reports* 6, 806–814. doi: 10.1016/j.stemcr.2016.04.008

Rahl, P. B., Lin, C. Y., Seila, A. C., Flynn, R. A., McCuine, S., Burge, C. B., et al. (2010). C-Myc regulates transcriptional pause release. *Cell* 141, 432–445. doi: 10.1016/j.cell.2010.03.030

Renfree, M. B., and Shaw, G. (2000). Diapause. *Annu. Rev. Physiol.* 62, 353–375. doi: 10.1146/annurev.physiol.62.1.353

Revuelta, M., and Matheu, A. (2017). Autophagy in stem cell aging. *Aging Cell* 16, 912–915. doi: 10.1111/acel.12655

Richmond, C. A., Shah, M. S., Carlone, D. L., and Breault, D. T. (2016). An enduring role for quiescent stem cells. *Dev. Dyn.* 245, 718–726. doi: 10.1002/dvdy.24416

Riether, C., Schürch, C. M., and Ochsenbein, A. F. (2015). Regulation of hematopoietic and leukemic stem cells by the immune system. *Cell Death Differ.* 22, 187–198. doi: 10.1038/cdd.2014.89

Rigano, K. S., Gehring, J. L., Evans Hutzenbiler, B. D., Chen, A. V., Nelson, O. L., Vella, C. A., et al. (2017). Life in the fat lane: seasonal regulation of insulin sensitivity, food intake, and adipose biology in brown bears. *J. Comp. Physiol. B Biochem. Syst. Environ. Physiol.* 187, 649–676. doi: 10.1007/s00360-016-1050-9

Rimmelé, P., Liang, R., Bigarella, C. L., Kocabas, F., Xie, J., Serasinghe, M. N., et al. (2015). Mitochondrial metabolism in hematopoietic stem cells requires functional FOXO 3. *EMBO Rep.* 16, 1164–1176. doi: 10.15252/embr.201439704

Risal, S., Adhikari, D., and Liu, K. (2016). Animal models for studying the in vivo functions of cell cycle CDKs. *Methods Mol. Biol.* 1336, 155–166. doi: 10.1007/978-1-4939-2926-9_13

Rivard, N., L'Allemain, G., Bartek, J., and Pouysségur, J. (1996). Abrogation of p27(Kip1) by cDNA antisense suppresses quiescence (G0 state) in fibroblasts. *J. Biol. Chem.* 271, 18337–18341. doi: 10.1074/jbc.271.31.18337

Rocheteau, P., Vinet, M., and Chretien, F. (2014). Dormancy and quiescence of skeletal muscle stem cells. *Results Probl. Cell Differ.* 56, 215–235. doi: 10.1007/978-3-662-44608-9_10

Roilo, M., Kullmann, M. K., and Hengst, L. (2018). Cold-inducible RNA-binding protein (CIRP) induces translation of the cell-cycle inhibitor p27Kip1. *Nucleic Acids Res.* 46, 3198–3210. doi: 10.1093/nar/gkx1317

Ruf, T., and Geiser, F. (2015). Daily torpor and hibernation in birds and mammals. *Biol. Rev.* 90, 891–926. doi: 10.1111/brv.12137

Ruf, T., Bieber, C., and Turbill, C. (2012). "Survival, Aging, and Life-History Tactics in Mammalian Hibernators," in *Living in a Seasonal World*. T. RufClaudia, B. Arnold, E. Millesi (New York, NY:Springer). doi: 10.1007/978-3-642-28678-0_11

Sabbatinelli, J., Prattichizzo, F., Olivieri, F., Procopio, A. D., Rippo, M. R., and Giuliani, A. (2019). Where Metabolism Meets Senescence: Focus on Endothelial Cells. *Front. Physiol.* 10:1523. doi: 10.3389/fphys.2019.01523

Sage, J., Miller, A. L., Pérez-Mancera, P. A., Wysocki, J. M., and Jacks, T. (2003). Acute mutation of retinoblastoma gene function is sufficient for cell cycle re-entry. *Nature* 424, 223–228. doi: 10.1038/nature01764

Sánchez-Martínez, C., Gelbert, L. M., Lallena, M. J., and De Dios, A. (2015). Cyclin dependent kinase (CDK) inhibitors as anticancer drugs. *Bioorganic Med. Chem. Lett.* 25, 3420–3435. doi: 10.1016/j.bmcl.2015.05.100

Sang, L., and Coller, H. A. (2009). Fear of commitment: Hes1 protects quiescent fibroblasts from irreversible cellular fates. *Cell Cycle* 8, 2161–2167. doi: 10.4161/cc.8.14.9104

Sang, L., Coller, H. A., and Roberts, J. M. (2008). Control of the reversibility of cellular quiescence by the transcriptional repressor HES1. *Science* 321, 1095–1100. doi: 10.1126/science.1155998

Sang, L., Roberts, J. M., and Coller, H. A. (2010). Hijacking HES1: how tumors co-opt the anti-differentiation strategies of quiescent cells. *Trends Mol. Med.* 16, 17–26. doi: 10.1016/j.molmed.2009.11.001

Schreiber-Agus, N., Meng, Y., Hoang, T., Hou, H., Ghen, K., Greenberg, R., et al. (1998). Role of Mxi1 in ageing organ systems and the regulation of normal and neoplastic growth. *Nature* 393, 483–487. doi: 10.1038/31008

Schwartz, C., Hampton, M., and Andrews, M. T. (2013). Seasonal and Regional Differences in Gene Expression in the Brain of a Hibernating Mammal. *PLoS One* 8:0058427. doi: 10.1371/journal.pone.0058427

Seger, R., and Krebs, E. G. (1995). The MAPK signaling cascade. *FASEB J.* 9, 726–735. doi: 10.1096/fasebj.9.9.7601337

Seger, R., and Wexler, S. (2016). "The MAPK Signaling Cascades," in *Encyclopedia of Cell Biology*. R. A. Bradshaw and P. D. Stahl (Amsterdam: Elsevier) doi: 10.1016/B978-0-12-394447-4.30014-1

Serra, V., Von Zglinicki, T., Lorenz, M., and Saretzki, G. (2003). Extracellular superoxide dismutase is a major antioxidant in human fibroblasts and slows telomere shortening. *J. Biol. Chem.* 278, 6824–6830. doi: 10.1074/jbc.M207939200

Shackelford, D. B., and Shaw, R. J. (2009). The LKB1-AMPK pathway: Metabolism and growth control in tumour suppression. *Nat. Rev. Cancer* 9, 563–575. doi: 10.1038/nrc2676

Shen, C., and Nathan, C. (2002). Nonredundant antioxidant defense by multiple two-cysteine peroxiredoxins in human prostate cancer cells. *Mol. Med.* 8, 95–102. doi: 10.1007/bf03402079

Signer, R. A. J., Magee, J. A., Salic, A., and Morrison, S. J. (2014). Haematopoietic stem cells require a highly regulated protein synthesis rate. *Nature* 508, 49–54. doi: 10.1038/nature13035

Simonetti, G., Padella, A., Manfrini, M., do Valle, I. F., Papayannidis, C., Fontana, M. C., et al. (2016). Aggressive Aneuploid Acute Myeloid Leukemia Is Dependent on Alterations of P53, Gain of APC and PLK1 and Loss of RAD50. *Blood* 128, 1702–1702. doi: 10.1182/blood.v128.22.1702.1702

Simsek, T., Kocabas, F., Zheng, J., Deberardinis, R. J., Mahmoud, A. I., Olson, E. N., et al. (2010). The distinct metabolic profile of hematopoietic stem cells reflects their location in a hypoxic niche. *Cell Stem Cell* 7, 380–390. doi: 10.1016/j.stem.2010.07.011

Soukri, A., Valverde, F., Hafid, N., Elkebbaj, M. S., and Serrano, A. (1996). Occurrence of a differential expression of the glyceraldehyde-3-phosphate dehydrogenase gene in muscle and liver from euthermic and induced hibernating jerboa (Jaculus orientalis). *Gene* 181, 139–145. doi: 10.1016/S0378-1119(96)00494-5

Squire, T. L., Lowe, M. E., Bauer, V. W., and Andrews, M. T. (2004). Pancreatic triacylglycerol lipase in a hibernating mammal. II. Cold-adapted function and differential expression. *Physiol. Genomics* 16, 131–140. doi: 10.1152/physiolgenomics.00168.2002

Staples, J. F. (2014). Metabolic suppression in mammalian hibernation: The role of mitochondria. *J. Exp. Biol.* 217, 2032–2036. doi: 10.1242/jeb.092973

Staples, J. F., and Brown, J. C. L. (2008). Mitochondrial metabolism in hibernation and daily torpor: A review. *J. Comp. Physiol. B Biochem. Syst. Environ. Physiol.* 178, 811–827. doi: 10.1007/s00360-008-0282-8

Storey, K. B. (2003). Mammalian hibernation: Transcriptional and translational controls. *Advances in Experimental Medicine and Biology* 2003, 21–38. doi: 10.1007/978-1-4419-8997-0_3

Storey, K. B., and Storey, J. M. (2004). Metabolic rate depression in animals: Transcriptional and translational controls. *Biol. Rev. Camb. Philos. Soc.* 79, 207–233. doi: 10.1017/S1464793103006195

Storey, K. B., and Storey, J. M. (2012). Aestivation: Signaling and hypometabolism. *J. Exp. Biol.* 215, 1425–1433. doi: 10.1242/jeb.054403

Storey, K. B., Heldmaier, G., and Rider, M. H. (2010). Mammalian hibernation: Physiology, cell signaling, and gene controls on metabolic rate depression. *Top. Curr. Genet.* 21, 227–252. doi: 10.1007/978-3-642-12422-8_13

Sunagawa, G. A., Deviatiiarov, R., Ishikawa, K., Gazizova, G., Gusev, O., and Takahashi, M. (2018). Integrative Transcription Start Site Analysis and Physiological Phenotyping Reveal Torpor-specific Expressions in Mouse Skeletal Muscle. *bioRxiv* 2018:374975. doi: 10.1101/374975

Sureban, S. M., Ramalingam, S., Natarajan, G., May, R., Subramaniam, D., Bishnupuri, K. S., et al. (2008). Translation regulatory factor RBM3 is a proto-oncogene that prevents mitotic catastrophe. *Oncogene* 27, 4544–4556. doi: 10.1038/onc.2008.97

Tähti, H. (1978). Seasonal differences in O2 consumption and respiratory quotient in a hibernator (Erinaceus europaeus L.). *Ann. Zool. Fenn.* 15, 69–75.

Takahashi, K., and Yamanaka, S. (2006). Induction of Pluripotent Stem Cells from Mouse Embryonic and Adult Fibroblast Cultures by Defined Factors. *Cell* 126, 663–676. doi: 10.1016/j.cell.2006.07.024

Takahashi, S., Tanaka, T., and Sakai, J. (2007). New therapeutic target for metabolic syndrome: PPARδ. *Endocr. J.* 54, 347–357. doi: 10.1507/endocrj.KR-99

Takubo, K., Goda, N., Yamada, W., Iriuchishima, H., Ikeda, E., Kubota, Y., et al. (2010). Regulation of the HIF-1α level is essential for hematopoietic stem cells. *Cell Stem Cell* 7, 391–402. doi: 10.1016/j.stem.2010.06.020

Takubo, K., Nagamatsu, G., Kobayashi, C. I., Nakamura-Ishizu, A., Kobayashi, H., Ikeda, E., et al. (2013). Regulation of glycolysis by Pdk functions as a metabolic checkpoint for cell cycle quiescence in hematopoietic stem cells. *Cell Stem Cell* 12, 49–61. doi: 10.1016/j.stem.2012.10.011

Tessier, S. N., and Storey, K. B. (2014). To be or not to be: The regulation of mRNA fate as a survival strategy during mammalian hibernation. *Cell Stress Chaperones* 19:9. doi: 10.1007/s12192-014-0512-9

Tessier, S. N., Wu, C. W., and Storey, K. B. (2019). Molecular control of protein synthesis, glucose metabolism, and apoptosis in the brain of hibernating thirteen-lined ground squirrels. *Biochem. Cell Biol.* 97, 536–544. doi: 10.1139/bcb-2018-0256

Theeuwes, W. F., Gosker, H. R., Langen, R. C. J., Verhees, K. J. P., Pansters, N. A. M., Schols, A. M. W. J., et al. (2017). Inactivation of glycogen synthase kinase-3β (GSK-3β) enhances skeletal muscle oxidative metabolism. *Biochim. Biophys. Acta Mol. Basis Dis.* 1863, 3075–3086. doi: 10.1016/j.bbadis.2017.09.018

Tinganelli, W., Hitrec, T., Romani, F., Simoniello, P., Squarcio, F., Stanzani, A., et al. (2019). Hibernation and radioprotection: Gene expression in the liver and testicle of rats irradiated under synthetic torpor. *Int. J. Mol. Sci.* 20:20020352. doi: 10.3390/ijms20020352

Tothova, Z., Kollipara, R., Huntly, B. J., Lee, B. H., Castrillon, D. H., Cullen, D. E., et al. (2007). FoxOs Are Critical Mediators of Hematopoietic Stem Cell Resistance to Physiologic Oxidative Stress. *Cell* 128, 325–339. doi: 10.1016/j.cell.2007.01.003

Trimarchi, J. M., and Lees, J. A. (2002). Sibling rivalry in the E2F family. *Nat. Rev. Mol. Cell Biol.* 3, 11–20. doi: 10.1038/nrm714

Tsiouris, J. A. (2005). Metabolic depression in hibernation and major depression: An explanatory theory and an animal model of depression. *Med. Hypotheses* 65, 829–840. doi: 10.1016/j.mehy.2005.05.044

Turbill, C., Bieber, C., and Ruf, T. (2011). Hibernation is associated with increased survival and the evolution of slow life histories among mammals. *Proceedings.Biological Sci. R. Soc.* 278, 3355–3363. doi: 10.1098/rspb.2011.0190

Unnisa, Z., Clark, J. P., Roychoudhury, J., Thomas, E., Tessarollo, L., Copeland, N. G., et al. (2012). Meis1 preserves hematopoietic stem cells in mice by limiting oxidative stress. *Blood* 120, 4973–4981. doi: 10.1182/blood-2012-06-435800

Valcourt, J. R., Lemons, J. M. S., Haley, E. M., Kojima, M., Demuren, O. O., and Coller, H. A. (2012). Staying alive: Metabolic adaptations to quiescence. *Cell Cycle* 11, 1680–1696. doi: 10.4161/cc.19879

Van Breukelen, F., and Martin, S. L. (2002). Reversible depression of transcription during hibernation. *J. Comp. Physiol. B Biochem. Syst. Environ. Physiol.* 172, 355–361. doi: 10.1007/s00360-002-0256-1

Vermillion, K. L., Anderson, K. J., Marshall, H., and Andrews, M. T. (2015). Gene expression changes controlling distinct adaptations in the heart and skeletal muscle of a hibernating mammal. *Physiol. Genomics* 47, 58–74. doi: 10.1152/physiolgenomics.00108.2014

Vessoni, A. T., Muotri, A. R., and Okamoto, O. K. (2012). Autophagy in stem cell maintenance and differentiation. *Stem Cells Dev.* 21, 513–520. doi: 10.1089/scd.2011.0526

Viatour, P., Somervaille, T. C., Venkatasubrahmanyam, S., Kogan, S., McLaughlin, M. E., Weissman, I. L., et al. (2008). Hematopoietic Stem Cell Quiescence Is Maintained by Compound Contributions of the Retinoblastoma Gene Family. *Cell Stem Cell* 3, 416–428. doi: 10.1016/j.stem.2008.07.009

Wanet, A., Arnould, T., Najimi, M., and Renard, P. (2015). Connecting Mitochondria, Metabolism, and Stem Cell Fate. *Stem Cells Dev.* 24, 1957–1971. doi: 10.1089/scd.2015.0117

Wang, L., Siegenthaler, J. A., Dowell, R. D., and Yi, R. (2016). Stem cells: Foxc1 reinforces quiescence in self-renewing hair follicle stem cells. *Science* 351, 613–617. doi: 10.1126/science.aad5440

Webb, P. I., and Ellison, J. (1998). Normothermy, torpor, and arousal in hedgehogs (erinaceus europaeus) from Dunedin. *N. Zeal. J. Zool.* 25, 85–90. doi: 10.1080/03014223.1998.9518139

Wellmann, S., Truss, M., Bruder, E., Tornillo, L., Zelmer, A., Seeger, K., et al. (2010). The RNA-binding protein RBM3 is required for cell proliferation and protects against serum deprivation-induced cell death. *Pediatr. Res.* 67, 35–41. doi: 10.1203/PDR.0b013e3181c13326

Wiersma, M., Beuren, T. M. A., de Vrij, E. L., Reitsema, V. A., Bruintjes, J. J., Bouma, H. R., et al. (2018). Torpor-arousal cycles in Syrian hamster heart are associated with transient activation of the protein quality control system. *Comp. Biochem. Physiol. Part - B Biochem. Mol. Biol.* 223, 23–28. doi: 10.1016/j.cbpb.2018.06.001

Wieser, W., and Krumschnabel, G. (2001). Hierarchies of ATP-consuming processes: Direct compared with indirect measurements, and comparative aspects. *Biochem. J.* 355, 389–395. doi: 10.1042/0264-6021:3550389

Wilson, A., Laurenti, E., Oser, G., van der Wath, R. C., Blanco-Bose, W., Jaworski, M., et al. (2008). Hematopoietic Stem Cells Reversibly Switch from Dormancy to Self-Renewal during Homeostasis and Repair. *Cell* 135, 1118–1129. doi: 10.1016/j.cell.2008.10.048

Wilz, M., and Heldmaier, G. (2000). Comparison of hibernation, estivation and daily torpor in the edible dormouse, Glis glis. *J. Comp. Physiol. Biochem. Syst. Environ. Physiol.* 170, 511–521.

Wu, C. W., and Storey, K. B. (2012a). Pattern of cellular quiescence over the hibernation cycle in liver of thirteen-lined ground squirrels. *Cell Cycle* 11, 1714–1726. doi: 10.4161/cc.19799

Wu, C. W., and Storey, K. B. (2012b). Regulation of the mTOR signaling network in hibernating thirteen-lined ground squirrels. *J. Exp. Biol.* 215, 1720–1727. doi: 10.1242/jeb.066225

Wu, C. W., and Storey, K. B. (2016). Life in the cold: Links between mammalian hibernation and longevity. *Biomol. Concepts* 7, 41–52. doi: 10.1515/bmc-2015-0032

Wu, C. W., Bell, R. A., and Storey, K. B. (2015). Post-translational regulation of PTEN catalytic function and protein stability in the hibernating 13-lined ground squirrel. *Biochim. Biophys. Acta Gen. Subj.* 1850, 2196–2202. doi: 10.1016/j.bbagen.2015.07.004

Wu, C.-W., Bell, R., and Storey, K. B. (2013a). 49. Regulation of PTEN function and structural stability in hibernating thirteen-lined ground squirrels. *Cryobiology* 66, 355–356. doi: 10.1016/j.cryobiol.2013.02.055

Wu, J., Chen, P., Li, Y., Ardell, C., Der, T., Shohet, R., et al. (2013b). HIF-1α in heart: Protective mechanisms. *Am. J. Physiol. Hear. Circ. Physiol.* 305, H821–H828. doi: 10.1152/ajpheart.00140.2013

Wu, P., Inskeep, K., Bowker-Kinley, M. M., Popov, K. M., and Harris, R. A. (1999). Mechanism responsible for inactivation of skeletal muscle pyruvate dehydrogenase complex in starvation and diabetes. *Diabetes* 48, 1593–1599. doi: 10.2337/diabetes.48.8.1593

Xu, R., Andres-Mateos, E., Mejias, R., MacDonald, E. M., Leinwand, L. A., Merriman, D. K., et al. (2013). Hibernating squirrel muscle activates the endurance exercise pathway despite prolonged immobilization. *Exp. Neurol.* 247, 392–401. doi: 10.1016/j.expneurol.2013.01.005

Yalcin, S., Marinkovic, D., Mungamuri, S. K., Zhang, X., Tong, W., Sellers, R., et al. (2010). ROS-mediated amplification of AKT/mTOR signalling pathway leads to myeloproliferative syndrome in Foxo3 -/- mice. *EMBO J.* 29, 4118–4131. doi: 10.1038/emboj.2010.292

Yan, J., Barnes, B. M., Kohl, F., and Marr, T. G. (2008). Modulation of gene expression in hibernating arctic ground squirrels. *Physiol. Genomics* 32, 170–181. doi: 10.1152/physiolgenomics.00075.2007

Yang, N., and Sheridan, A. M. (2014). "Cell Cycle," in *Encyclopedia of Toxicology*.P. Wexler (Amsterdam:Elsevier) 753–758. doi: 10.1016/B978-0-12-386454-3.00273-6

Yang, Z., and Klionsky, D. J. (2010). Eaten alive: A history of macroautophagy. *Nat. Cell Biol.* 12, 814–822. doi: 10.1038/ncb0910-814

Yao, G. (2014). Modelling mammalian cellular quiescence. *Interface Focus* 4:0074. doi: 10.1098/rsfs.2013.0074

Yilmaz, ÖH., Valdez, R., Theisen, B. K., Guo, W., Ferguson, D. O., Wu, H., et al. (2006). Pten dependence distinguishes haematopoietic stem cells from leukaemia-initiating cells. *Nature* 441, 475–482. doi: 10.1038/nature04703

Yu, W. M., Liu, X., Shen, J., Jovanovic, O., Pohl, E. E., Gerson, S. L., et al. (2013). Metabolic regulation by the mitochondrial phosphatase PTPMT1 is required for hematopoietic stem cell differentiation. *Cell Stem Cell* 12, 62–74. doi: 10.1016/j.stem.2012.11.022

Yu, X., Alder, J. K., Chun, J. H., Friedman, A. D., Heimfeld, S., Cheng, L., et al. (2006). HES1 Inhibits Cycling of Hematopoietic Progenitor Cells via DNA Binding. *Stem Cells* 24, 876–888. doi: 10.1634/stemcells.2005-0598

Zhang, J., Grindley, J. C., Yin, T., Jayasinghe, S., He, X. C., Ross, J. T., et al. (2006). PTEN maintains haematopoietic stem cells and acts in lineage choice and leukaemia prevention. *Nature* 441, 518–522. doi: 10.1038/nature04747

Zhang, S., Hulver, M. W., McMillan, R. P., Cline, M. A., and Gilbert, E. R. (2014). The pivotal role of pyruvate dehydrogenase kinases in metabolic flexibility. *Nutr. Metab.* 11:10. doi: 10.1186/1743-7075-11-10

Zhang, Y., Aguilar, O. A., and Storey, K. B. (2016). Transcriptional activation of muscle atrophy promotes cardiac muscle remodeling during mammalian hibernation. *PeerJ* 2016:2317. doi: 10.7717/peerj.2317

Zhegunov, G., Kudokotseva, E., and Mikulinsky, Y. (1988). Hyperactivation of protein synthesis in tissues of hibernating animals on arousal. *Cryo-Left* 9, 236–245.

Zhu, X., Bührer, C., and Wellmann, S. (2016). Cold-inducible proteins CIRP and RBM3, a unique couple with activities far beyond the cold. *Cell. Mol. Life Sci.* 73, 3839–3859. doi: 10.1007/s00018-016-2253-7

Zhu, X., Smith, M. A., Perry, G., Wang, Y., Ross, A. P., Zhao, H. W., et al. (2005). MAPKs are differentially modulated in arctic ground squirrels during hibernation. *J. Neurosci. Res.* 80, 862–868. doi: 10.1002/jnr.20526

Zhu, X., Yan, J., Bregere, C., Zelmer, A., Goerne, T., Kapfhammer, J. P., et al. (2019). RBM3 promotes neurogenesis in a niche-dependent manner via IMP2-IGF2 signaling pathway after hypoxic-ischemic brain injury. *Nat. Commun.* 10:11870–x. doi: 10.1038/s41467-019-11870-x

Zimmermann, A. (2004). Regulation of liver regeneration. *Nephrol. Dial. Transplant.* 19, iv6–iv10. doi: 10.1093/ndt/gfh1034

Conflict of Interest: The authors declare that the research was conducted in the absence of any commercial or financial relationships that could be construed as a potential conflict of interest.

frontiers in Physiology

ORIGINAL RESEARCH
published: 07 July 2021
doi: 10.3389/fphys.2021.626779

Body Temperature and Activity Adaptation of Short Photoperiod-Exposed Djungarian Hamsters (*Phodopus sungorus*): Timing, Traits, and Torpor

Elena Haugg, Annika Herwig and Victoria Diedrich*

Institute of Neurobiology, Ulm University, Ulm, Germany

To survive the Siberian winter, Djungarian hamsters (*Phodopus sungorus*) adjust their behavior, morphology, and physiology to maintain energy balance. The reduction of body mass and the improvement of fur insulation are followed by the expression of spontaneous daily torpor, a state of reduced metabolism during the resting phase to save additional energy. Since these complex changes require time, the upcoming winter is anticipated *via* decreasing photoperiod. Yet, the extent of adaptation and torpor use is highly individual. In this study, adaptation was triggered by an artificially changed light regime under laboratory conditions with 20°C ambient temperature and food and water *ad libitum*. Two approaches analyzed data on weekly measured body mass and fur index as well as continuously recorded core body temperature and activity during: (1) the torpor period of 60 hamsters and (2) the entire adaptation period of 11 hamsters, aiming to identify parameters allowing (1) a better prediction of torpor expression in individuals during the torpor period as well as (2) an early estimation of the adaptation extent and torpor proneness. In approach 1, 46 torpor-expressing hamsters had a median torpor incidence of 0.3, covering the spectrum from no torpor to torpor every day within one representative week. Torpor use reduced the body temperature during both photo- and scotophase. Torpor was never expressed by 14 hamsters. They could be identified by a high, constant body temperature during the torpor period and a low body mass loss during adaptation to a short photoperiod. Already in the first week of short photoperiod, approach 2 revealed that the hamsters extended their activity over the prolonged scotophase, yet with reduced scotophase activity and body temperature. Over the entire adaptation period, scotophase activity and body temperature of the scoto- and photophases were further reduced, later accompanied by a body mass decline and winter fur development. Torpor was expressed by those hamsters with the most pronounced adaptations. These results provide insights into the preconditions and proximate stimuli of torpor expression. This knowledge will improve experimental planning and sampling for neuroendocrine and molecular research on torpor regulation and has the potential to facilitate acute torpor forecasting to eventually unravel torpor regulation processes.

Keywords: circadian rhythms, metabolism, phenotypes, radiotelemetry, Siberian hamster, spontaneous daily torpor

OPEN ACCESS

Edited by:
Alessandro Silvani, University of Bologna, Italy

Reviewed by:
David A. Bechtold, The University of Manchester, United Kingdom
Rebecca Oelkrug, University of Lübeck, Germany

****Correspondence:***
Elena Haugg
elena.haugg@uni-ulm.de

Specialty section:
This article was submitted to Integrative Physiology, a section of the journal Frontiers in Physiology

Received: *06 November 2020*
Accepted: *24 May 2021*
Published: *07 July 2021*

Citation:
Haugg E, Herwig A and Diedrich V (2021) Body Temperature and Activity Adaptation of Short Photoperiod-Exposed Djungarian Hamsters (Phodopus sungorus): Timing, Traits, and Torpor. Front. Physiol. 12:626779. doi: 10.3389/fphys.2021.626779

INTRODUCTION

The investigation of seasonal winter adaptation, including metabolic downstates like hibernation and daily torpor, in mammals has a long history (Jastroch et al., 2016), with promising implications for human life sciences, medicine, and manned spaceflight (Dave et al., 2012; Choukèr et al., 2019). Diverse species (bears, lemurs, marmots, bats, birds, squirrels, and dormice) in various environmental contexts (season, photophase, temperature, social context, food, and sleep) have been characterized *via* measurements of many different parameters at the whole animal level (behavior, morphology, and physiology) (Geiser, 2008). Over the years, the underlying regulatory mechanisms on the (neuro)endocrine and molecular genetic levels have become of increasing interest, and new analytical methods have opened. These methods either enable the measurement of classical *in vivo* parameters like activity, metabolic rate, body temperature, and body composition with higher resolution or the *in vitro* detection of new parameters like structure or transport proteins, enzymes, and RNA/DNA on the cellular and molecular levels. This rich repertoire offers countless possibilities to characterize the mechanisms of seasonal adaptation with a high degree of precision and standardization, improving comparability and reproducibility. However, the study of torpor regulatory mechanisms has remained complicated since torpor is a sensitive and difficult to anticipate physiological state. Hence, research would benefit from a method that better predicts adaptive strategies, including torpor.

Seasonal adaptations have been thoroughly investigated in the small rodent *Phodopus sungorus* (Pallas 1773). In long photoperiods, Djungarian hamsters are reproductively active and have a high body mass and a light brown summer fur. As soon as photophase length falls below 13 h per day (Hoffmann, 1982), the hamsters start to prepare for the harsh Siberian winter by reducing body mass as well as reproductive organs and by growing a well-insulating, white winter fur, to name only a few adaptation parameters (Scherbarth and Steinlechner, 2010; Cubuk et al., 2016). Approximately 3 months later, the morphological and physiological adaptations are largely completed, and the animals start to express spontaneous daily torpor. They use this metabolic downstate to save additional energy during their resting phase (photophase), while they are normothermic and active during the scotophase (Heldmaier and Steinlechner, 1981b; Diedrich et al., 2020). This complex temporal organization requires sensitivity to photoperiod length, based on daily light information as *zeitgeber*.

Most laboratory Djungarian hamsters are kept indoors in artificial light and subjected to abrupt changes of photoperiod. Independently of the time of year, they are bred in long photoperiod and transferred to short photoperiod to study the adaptation processes and spontaneous daily torpor. Although performed countless times since the beginnings of research in the 1970s, it has not been reported how the hamsters' physiology reacts to this abrupt photoperiod change in the short and long terms.

Timing and the extent of seasonal adaptation in Djungarian hamsters can be highly individual within a hamster population. The morphology and physiology of respective adaptation phenotypes have been thoroughly characterized and categorized as responders, late responders, partial responders, or non-responders (Ruf et al., 1991, 1993; Przybylska et al., 2019), whereby responsiveness refers to the reaction to the change in photoperiod length. Non-responders retain a constant body mass and a brown summer fur and therefore do not express torpor. Responders show the already described morphological and physiological adaptations, yet with a high variability in timing and extent of single adaptive parameters. Even in responders, torpor expression is not obligatory under laboratory conditions. Although parameters like activity or food intake could be related to the incidence of torpor bouts (Ruf et al., 1991), it is still not possible to reliably extrapolate from certain adaptation parameters to later torpor expression.

In most institutes that contributed to the multiple studies on Djungarian hamsters during the last 40 years, torpor research comprises the *in vivo* characterization of responding hamsters and their torpor expression as well as a postmortem organ sampling for *in vitro* molecular analyses. The metabolic state of each hamster can be estimated from body temperature. Spontaneous daily torpor in Djungarian hamsters has been defined as a hypothermic core body temperature (T_b) below 32°C (Ruf and Heldmaier, 1992; Ruf et al., 1993) for more than 30 min (Paul et al., 2005; Diedrich et al., 2015; Cubuk et al., 2017a,b). Single torpor bouts and the expression patterns can be further characterized using parameters like torpor incidence, torpor onset, minimal temperature during a torpor bout, torpor offset, as well as torpor duration (Kirsch et al., 1991; Ruf et al., 1993; Paul et al., 2004).

With continuous radiotelemetry measurements (Scribner and Wynne-Edwards, 1994; Schöttner et al., 2011; Jones et al., 2014), hypothermic hamsters with a body temperature below 32°C (HT, torpor) can be differentiated from normothermic hamsters (NT, no torpor) on the day of sampling (Bank et al., 2015). Usually, the sampling paradigm also comprises a temporal component allowing to differentiate circadian factors (Herwig et al., 2007; Bank et al., 2017; Cubuk et al., 2017a,b). This high degree of sampling standardization is of great value for the *in vitro* characterization of the molecular mechanisms underlying the different stages of torpor expression.

However, the sampling paradigm is based on each hamster's acute torpor expression. The high interindividual variability in torpor incidence as well as the torpor onset or torpor bout duration might affect the desired equal distribution across sampling groups.

To define parameters in order to better predict torpor expression in individuals during the torpor period, the present study examined the existing body temperature and activity datasets of responders, which had been dedicated to molecular organ analyses on torpor regulation. In an additional approach,

Abbreviations: HT, hypothermic—body temperature below 32°C for more than 30 min, spontaneous daily torpor (on day of sampling); NT, normothermic—no spontaneous daily torpor (on day of sampling); LP, long photoperiod—16 h light and 8 h darkness per day; SP, short photoperiod—8 h light and 16 h darkness per day; Std. Dev., standard deviation of the mean; T_b, core body temperature; ZT, *zeitgeber* time, with ZT0 as the beginning of photophase.

data were analyzed over the entire adaptation process to a short photoperiod, aiming at the early estimation of the adaptation extent and torpor proneness. Additionally, winter fur development and body mass reduction were determined over the course of adaptation in all animals. The phenotyping toward torpor incidence may help improve the *a priori* planning of experimental groups for a refined sampling with high standardization. Furthermore, the identification of potential predictors on general torpor capability would enable a preselection of torpor-prone hamsters early during adaptation in favor of animal reduction in future experiments.

MATERIALS AND METHODS

Breeding and Housing

Djungarian hamsters (*P. sungorus*) were bred, raised, and kept at the Institute of Neurobiology, Ulm University, at 20 ± 1°C ambient temperature. Artificial light (150 lx) was provided 16 h per day in long photoperiod (LP) and 8 h per day in short photoperiod (SP). Additional constant red light (<5 lx) enabled animal handling during the scotophase. The hamsters were housed in Makrolon type III cages (26.5 cm × 42.5 cm × 18.0 cm) with wooden bedding and tissue as the nesting material. Tap water and food (Altromin hamster breeding diet 7014, Lage, Germany) were provided *ad libitum*. Additionally, cucumber, oak flakes, and sunflower seeds were fed once a week. The hamsters were bred in artificial long photoperiod by an outbred crossing scheme in accordance with the local ethics committee (35/9185.46-3) at Ulm University, Germany. During breeding, hamster pairs were provided with additional nesting material and a red transparent plastic house. Litters were weaned at an age of 3 weeks and housed in same-gender sibling groups. The hamsters were single housed since the age of 6 weeks. They were transferred to the short photoperiod earliest at 12 weeks of age. The expression of spontaneous daily torpor was expected during the torpor period after adaptation to the short photoperiod was largely completed.

The Experiment

Between 2018 and 2020, 80 adult hamsters were adapted to SP with an average age of 4 months and sampled approximately 4 months later during the torpor period for molecular torpor research. The change of light regime from long to short photoperiod delayed the zeitgeber time 0 (ZT0) by 1 h and advanced the beginning of the scotophase by 7 h to favor the later realization of the described temporal sampling paradigm. The hamsters were approached daily by the caretaker between ZT07 and ZT08 for a visual check. Once a week, the animals were handled just before ZT08 by the experimenter to assess the progress of short photoperiod adaptation. Therefore, the relative body mass change (in percent) with respect to the absolute body mass of the last week in LP was monitored. In addition, the hamsters' fur index was scored from 1 for a light brown summer fur to 6 for a dense white winter fur (Figala et al., 1973). During handling, wooden bedding and nesting material were refreshed every other week.

To measure body temperature and activity, a radiofrequency transmitter [Data Sciences International (DSI), Harvard Bioscience Inc., St. Paul, MN, United States] was implanted intraperitoneally under isoflurane anesthesia (2.5% and 1 ml/min for induction, 0.75–2.0% and 0.4 ml/min for maintenance) and carprofen analgesia (5 mg/kg, i.p.; Rimadyl, Zoetis Deutschland GmbH, Berlin, Germany). Recovery from surgery was supported by additional oat flakes, sunflower seeds, cucumber, and nesting material. Body mass, coat care, posture, and behavior were monitored daily for about 7 days. Experimental and surgical procedures were approved by the Regierungspräsidium Tübingen, Germany (1411).

Twenty hamsters, implanted during the torpor period, expressed spontaneous daily torpor within 2 weeks after implantation and were directly sacrificed. Data of the remaining 60 hamsters were used for this study, which required radiotelemetry data of 1 week after at least 1 week of recovery from surgery.

Approach 1: Torpor Behavior (*n* = 60)

The torpor behavior of 60 hamsters (41 males and 19 females) was analyzed using radiotelemetry data recorded during the torpor period after SP exposure for 15 ± 2 weeks. For animals that expressed torpor, the last week before sacrifice was chosen as the representative week of analysis. To favor a comparable adaptation state, the first possible week after 1 week of recovery from surgery was chosen as the week of analysis for hamsters that never expressed torpor during their individual total observation interval. Detailed background information on each hamster's age when transferred to SP and the weeks spent in SP at implantation, observation, and sacrifice is listed in the **Supplementary Table 1**.

Torpor incidence was calculated as the number of torpor bouts divided by the number of observation days, i.e., 7 days of the analysis week (**Figure 1A**). Furthermore, a decrease of body temperature to at least 33°C which did not result in a torpor bout per definition is referred to as a torpor bout attempt. The minimal body temperature is the lowest value during a torpor bout. Temporal values are given in hours and minutes after the beginning of the photophase at ZT0. Torpor onset was defined by the time point or ZT when a hamster reached a body temperature of 32°C first and consequently entered a torpor. Torpor offset was defined by the time point or ZT when the body temperature exceeded the threshold of 32°C first during the hamsters' arousal from a torpor bout. Torpor duration was defined as the time between torpor onset and torpor offset (Ruf et al., 1993; Paul et al., 2005).

Approach 2: Change of Light Regime and Adaptation to Short Photoperiod (*n* = 11)

Eleven of the 60 hamsters analyzed in approach 1 (five females and six males, bred in 2020) had already been implanted in long photoperiod for long-term radiotelemetry measurements until sacrifice for molecular torpor research in SP14. Data acquisition started after one and a half weeks of surgical recovery and comprised 1 week in long photoperiod (referred to as LP baseline or SP00) and 13 weeks in short photoperiod (from SP01 to SP13). The development of body mass, fur index, body temperature,

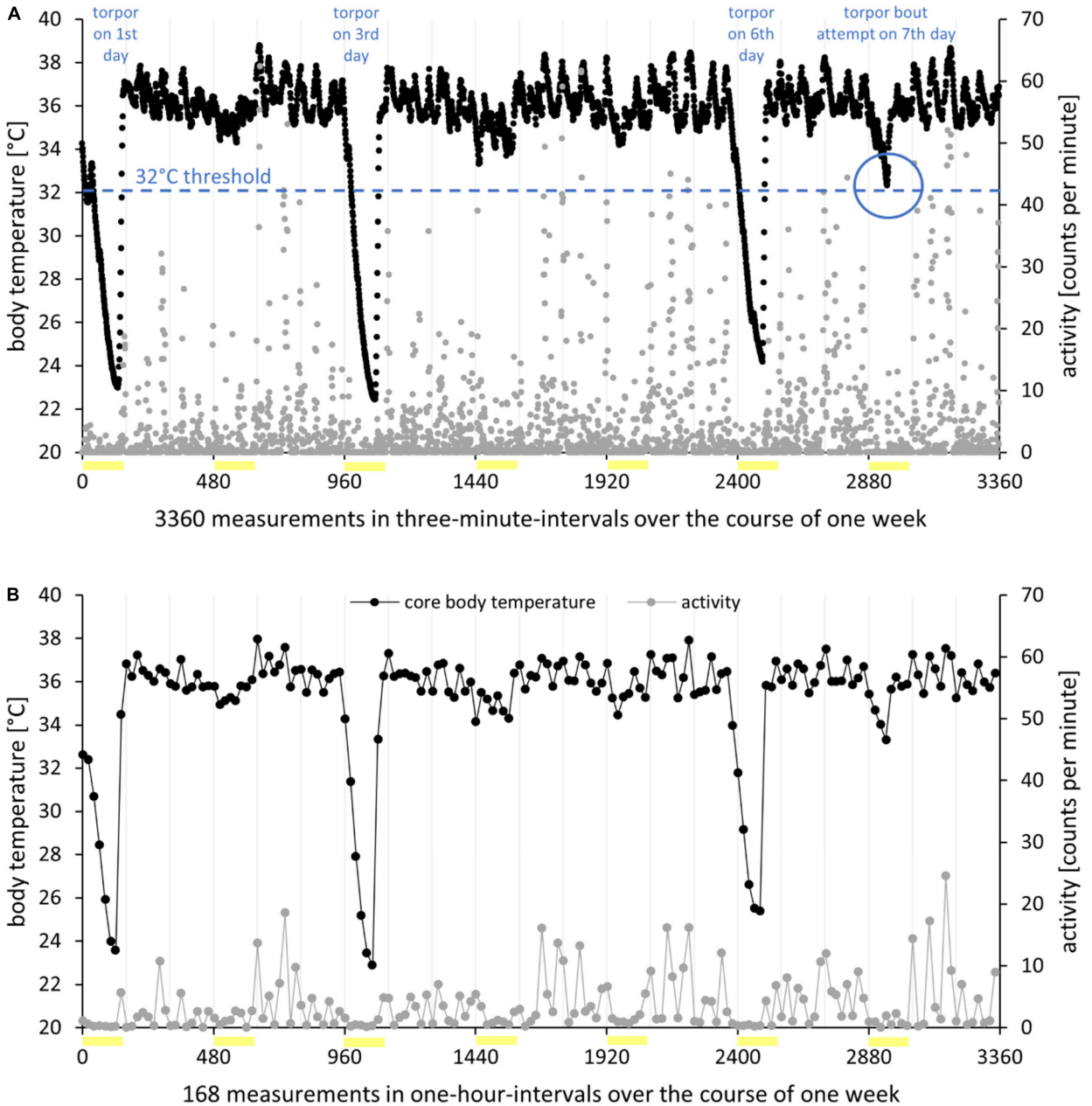

FIGURE 1 | Processing of radiotelemetry data I. Body temperature (in degree Celsius, *black*) and activity (in counts per minute, *gray*) of hamster EH02-27 over the course of 1 week in the short photoperiod (L/D 8:16 h). Photophases are indicated as *yellow bars*. **(A)** High resolution. Real-time raw data recorded in 3-min intervals. Within the 7 days, the hamster expressed three torpor bouts per definition with body temperature below 32°C for at least 30 min, resulting in a torpor incidence of 0.43. On the last day of the analysis week, the hamster showed a torpor bout attempt. While the body temperature hardly changed from one measurement to the next, the activity data were highly variable. **(B)** Low resolution. Processing of raw data to mean values per hour resulted in a smoothing of the body temperature measurements; however, the activity data became more accessible.

and locomotor activity over the course of SP adaptation was shown for individuals and the cohort to provide a visualization of variance within the cohort and statistical analyses of trends.

Data on relative body mass reduction and relative torpor incidence of 10 hamsters (2018 breed) have already been published in another research context (Piscitiello et al., 2021), while studies on molecular analyses of the hamsters' tissues are in progress. Therefore, the radiotelemetry data of this study are not yet published for free use, but can be provided on request.

Radiotelemetry

The radiotelemetry system (Dataquest ART^{TM} Bronze System, DSI, Harvard Bioscience Inc., St. Paul, MN, United States) comprised a pre-calibrated and silicone-coated TA11TA-F10

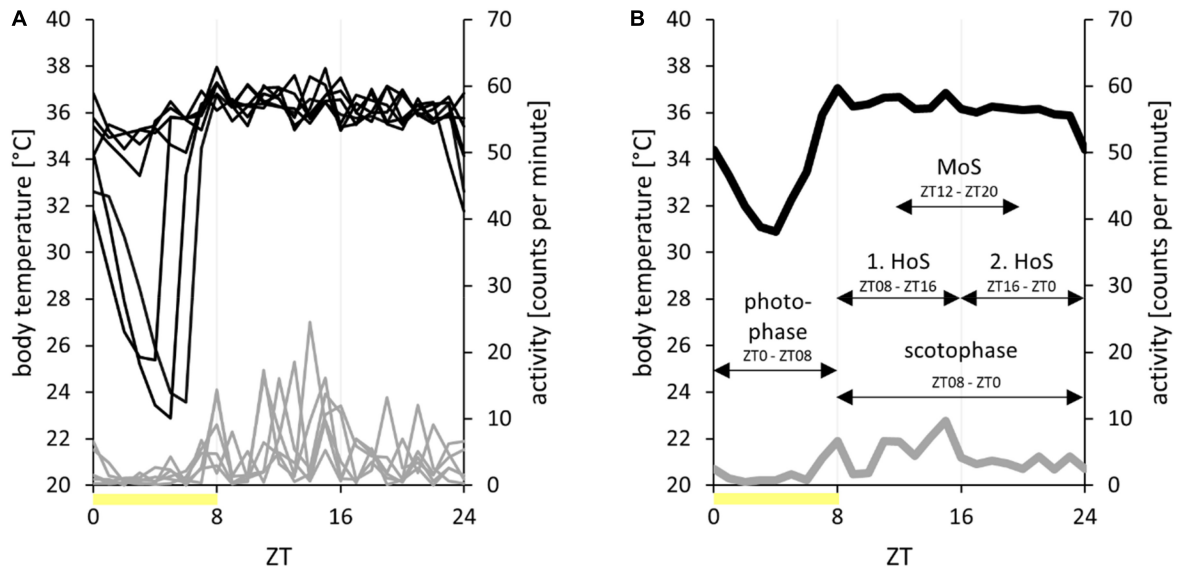

FIGURE 2 | Processing of radiotelemetry data II. Data of body temperature (in degree Celsius, *black*) and activity (in counts per minute, *gray*) of hamster EH02-27 over the course of 1 week in the short photoperiod (L/D, 8:16 h) with the photophases indicated as *yellow bars*. **(A)** Overlay. The data of each of the 7 days of the analysis week are overlaid for visualization on an *x*-axis from zeitgeber time 0 (ZT0) to ZT24. **(B)** Time frames. The data were averaged per ZT and week to visualize the body temperature and activity patterns of hamster EH02-27 over 1 week. In this study, the data were averaged per time frame and week (*arrows*). The time frames photophase, scotophase, first half of scotophase (*1. HoS*), second half of scotophase (*2. HoS*), and middle of scotophase (*MoS*) were used. Please note that the mean values per time frame and their standard deviations have been directly calculated from the raw dataset, on which the analysis of torpor parameters was also based.

radiofrequency transmitter (PhysioTel^{TM}, DSI, 1.1 cc volume, 1.6 g weight, 0.15°C measurement accuracy) implanted in the hamster's peritoneal cavity, a receiver plate (RPC-1, DSI) underneath the hamsters' home cage, a 20-channel Data Exchange Matrix (DEM, DSI), and a personal computer (Windows 7, 64-bit) outside the animal room. The raw data of core body temperature (in degree Celsius) and activity (counts per minute, cpm) were recorded in intervals of 3 min by the software "DataquestARTbronze" (2013). Body temperature was measured at the end of every 3-min interval. Activity was derived from the change of signal strength induced by the hamster, and therefore transmitter movement, relative to the receiver plate. This change was measured every 10 s and transformed by the system to cpm. At the end of every 3-min interval, an average activity value with the time-dependent unit cpm was recorded. An absolute activity could not be provided by the system.

Data Processing

Raw data processing and graphical representation were performed with Microsoft Excel (Microsoft Office 365, 2016), unless otherwise stated. While the activity dataset remained raw, the body temperature dataset was corrected for measurement errors by deleting physiologically impossible temperatures below ambient temperature or above 42°C as well as values with unphysiological fluctuations of more than 0.5°C per 3-min interval (Heldmaier and Ruf, 1992; **Figure 1A**). On these corrected data, the analyses of torpor parameters and the standard deviation of the mean body temperature were based. For analyses on a larger scale, data were averaged per hour (**Figure 1B**), week (**Figure 2A**), and time frame (**Figure 2B**). This allowed for comparisons between time frames within 1 week of analysis (approach 1) and the development of body temperature and activity in steps of 1 week over the course of adaptation to the short photoperiod (approach 2).

Time Frames

The total time frame accounted for the entire dataset of each analysis week. In SP, the photophase expands from ZT0 (including) to ZT08 (excluding), as shown in **Figures 1–3**. Accordingly, the scotophase expands from ZT08 to ZT0. For comparative analysis, the scotophase was split in the first half of scotophase from ZT08 to ZT16 and in the second half of scotophase from ZT16 to ZT0. Furthermore, the time frame middle of scotophase from ZT12 to ZT20 was used to exclude the potential interference of early torpor onsets and late torpor arousals (**Figure 2B**). In LP, the photophase expands from ZT0 to ZT16. Accordingly, the scotophase expands from ZT16 to ZT0. The time frames enabled a general description of the absolute locomotor activity extent during the hamsters' active and resting phases and, furthermore, the calculation of the activity ratios to compare the circadian patterns independent of the individual activity extent. For the photophase-to-scotophase activity ratio, values below 1 indicate a higher activity during scotophase and, therefore, nocturnality. The second-to-first half of scotophase activity ratio was calculated to further characterize the different activity phenotypes, whereby values below 1 indicate a higher activity during the first half of scotophase.

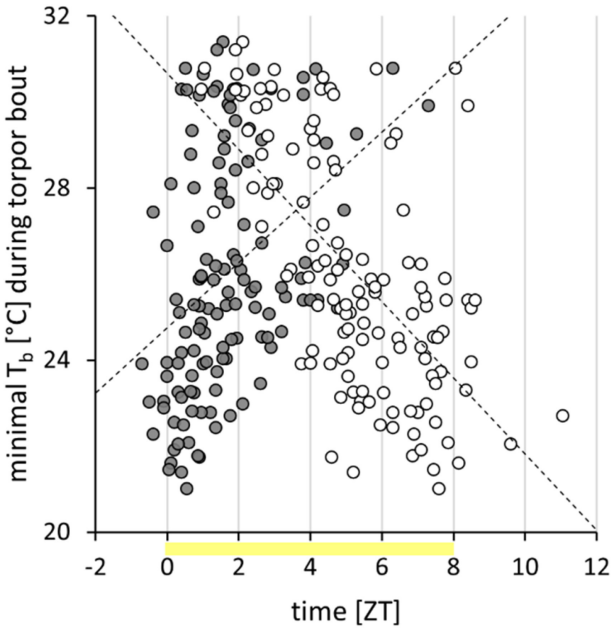

FIGURE 3 | Torpor characteristics of approach 1. Within the torpor analysis week, 127 torpor bouts, performed by 42 Djungarian hamsters, were examined. Of each bout, the torpor onset (*gray circles*) and the torpor offset (*white circles*) are shown. The minimal body temperature (T_b) during each torpor bout is positively correlated with its onset (r = 0.385, $p < 0.05$) and negatively correlated with its offset (r = -0.628, $p < 0.05$). Most bouts were performed within the photophase (*yellow*).

Statistics and Plotting

Data are given as the mean ± standard deviation of the mean, unless otherwise stated. Statistical tests were performed with SigmaPlot version 11 (Systat Software, San Jose, CA, United States). Data were tested for normality with the Shapiro–Wilk test. One-way repeated measures ANOVA with Holm–Sidak *post hoc* test was used for dependent, normally distributed data; Friedman repeated measures ANOVA with Tukey's *post hoc* test was used for dependent, non-normally distributed data. A two-tailed *t*-test was used for the comparison of two groups with independent, normally distributed data. Comparisons of more than two groups were done by one-way ANOVA with Holm–Sidak *post hoc* test for independent, normally distributed data and Kruskal–Wallis one-way ANOVA with Dunn's *post hoc* test for independent, non-normally distributed data. Two dependent datasets per animal were analyzed with the paired *t*-test for normally distributed data and with the Wilcoxon signed-rank test for non-normally distributed data.

Correlation of two parameters is shown in scatterplots. Pearson's product moment correlation was used to interpret normally distributed parameter correlations, with $p < 0.05$ as statistically significant. Statistically significant correlations are indicated by the *p*-value, the *r*, and the coefficient of determination R^2. Data distribution is shown in boxplots. The middle line represents the median, while the cross stands for the mean value. Each box extends from the 25th percentile to the 75th percentile. The whiskers depict the minimum and maximum values.

In the actograms, consecutive activities per hour were double plotted using the ActogramJ plugin for ImageJ (U.S. National Institutes of Health, Bethesda, MD, United States[1], 1997–2018). Labeling was done with Inkscape (1.0, ©2020, Inkscape Developers[2]) and Adobe® Photoshop CS2 (9.0, 1990–2005, Adobe Systems Incorporated, San Jose, CA, United States). Activities above the upper limit of 10 cpm are shown as 10 cpm. Since ZT0 was 1 h later in SP, an empty hour was inserted to align SP to LP for the actograms. The day of photoperiod change from LP to SP was excluded as photophase began according to the LP regime and ended according to the SP regime, resulting in an intermediate photophase length of 9 h.

RESULTS

Approach 1—Spontaneous Daily Torpor

For this approach, one representative SP week, SP15 ± 2 weeks, was chosen to analyze the adaptation and radiotelemetry parameters of 60 responders in relation to their individual torpor behavior. At least once during their individual data acquisition interval, 46 of the 60 animals expressed torpor, yet not necessarily during the week of analysis, while the remaining 14 animals were never observed in torpor.

In torpor-expressing hamsters (n = 46), the torpor incidence during the week of analysis had a median of 0.3 and ranged from 0.0 (no torpor, n = 3) to 1.0 (torpor every day, n = 1). Below 30°C reached 84 ± 33% of torpor bouts. Additionally, up to four torpor bout attempts were made per individual, with a median incidence of 0.1 for this cohort. The 46 animals showed either a torpor bout attempt or a torpor bout per definition on 55 ± 28% of the analyzed days.

Torpor Parameters

Within the week of analysis, the cohort expressed 127 torpor bouts, which were analyzed in detail. Torpor onset was at ZT1.6 ± 1.4 h and torpor offset at ZT5.3 ± 2.0 h (**Figure 3**). The torpor bouts had a duration of 218 ± 122 min. The minimal body temperature per bout was 26.0 ± 2.8°C. With an earlier torpor onset, a lower minimal body temperature (r = 0.385, $p < 0.05$; **Figure 3**) and a longer torpor bout duration (r = -0.384, $p < 0.05$) were reached, despite an earlier torpor offset (r = 0.323, $p < 0.05$). Nevertheless, a later torpor offset was generally associated with a longer duration (r = 0.750, $p < 0.05$) and a lower minimal body temperature (r = -0.628, $p < 0.05$; **Figure 3**).

To use the torpor parameters for phenotyping, the values were averaged for each of the 42 animals. Consequently, the cohort's torpor behavior was characterized by a torpor onset at 1.9 ± 1.4 h, a torpor offset at 5.4 ± 1.7 h, a torpor duration of 208 ± 101 min, and a minimal body temperature of 26.3 ± 2.4°C. Hamsters with an earlier mean torpor onset showed a lower standard deviation of their mean torpor onset (hamsters with at least two bouts,

[1]http://imagej.nih.gov/ij/

[2]http://inkscape.org/*developer/

$n = 35$, $r = 0.528$, $p < 0.05$) and a higher torpor incidence ($n = 42$, $r = -0.361$, $p < 0.05$).

The majority of torpor bouts had their on- and offsets within the photophase from ZT0 to ZT08 (**Figure 3**), but six torpor bouts started before ZT0 and ten ended after ZT08. Although some early torpor bouts already started during the second half of the preceding scotophase, and some very long or late torpor bouts reached into the first half of the following scotophase, torpor did not expand into the middle of the scotophase. The lowest body temperatures per hour and hamster recorded during the analysis week were 21.2°C during photophase, 22.9°C during the first half, and 30.7°C during the second half of scotophase, but 35.5°C during middle of scotophase.

Torpor Incidence Groups

After analysis of the torpor parameters, all 60 hamsters were assigned to four torpor incidence groups (**Figure 4**) to relate torpor behavior, adaptation, body temperature, and activity parameters. Hamsters of the group "never torpor" ($n = 14$) did not express torpor during their entire individual observation interval. Hamsters of the group "rarely torpor" ($n = 12$) were capable of torpor expression, but expressed no or one torpor bout during the week of analysis. Hamsters of the group "sometimes torpor" ($n = 22$) had a torpor incidence between 0.3 and 0.5, while those of the group "often torpor" ($n = 12$) had a torpor incidence of 0.5 or higher. Consequently, the median torpor incidence values were 0.1 in the group "rarely torpor", 0.3 in the group "sometimes torpor", and 0.7 in the group "often torpor" (**Table 1**). The torpor incidence groups differed in torpor onset, with ZT2.6 in hamsters of the group "rarely torpor", ZT2.0 in hamsters of the group "sometimes torpor", and ZT1.0 in hamsters of the group "often torpor".

The adaptation phenotype (**Table 2**) indicated that the "never torpor" group could be discriminated from the "often torpor" group by absolute body mass in SP12 and from all other torpor incidence groups by the relative body mass change in SP07 and SP12. Regarding no torpor and torpor expression only, "never torpor" hamsters showed a lower relative body mass change than did torpor-expressing hamsters after SP03 (**Figure 5A**).

Activity phenotyping per time frame showed that the "rarely torpor" group was more active than the "often torpor" group during scotophase, first half of scotophase, and middle of scotophase. Body temperature phenotyping per time frame revealed differences between the torpor incidence groups in all time frames (**Table 3**). Firstly, the "sometimes torpor" and "often torpor" groups had lower body temperatures than the "never torpor" and "rarely torpor" groups, even during the middle of scotophase. Secondly, the "sometimes torpor" and "often torpor" groups could be discriminated by the scotophase body temperature as well as by the standard deviation of the mean body temperature during the middle of scotophase. Thirdly, the groups "never torpor" and "rarely torpor" could be discriminated by the standard deviation of the mean body temperature during the middle of scotophase. The "never torpor" hamsters had higher mean body temperatures within all time frames than all "torpor" hamsters, also during the middle of scotophase [two-tailed t-test: $t_{(58)} = -4.026$, $p < 0.001$; "torpor": 36.0 ± 0.0°C SEM; "never torpor": 36.4 ± 0.1°C SEM)]. The lower the mean body temperature during the middle of scotophase, the smaller was its standard deviation in "torpor" hamsters, while this correlation was not given for the "never torpor" hamsters (**Figure 5B**).

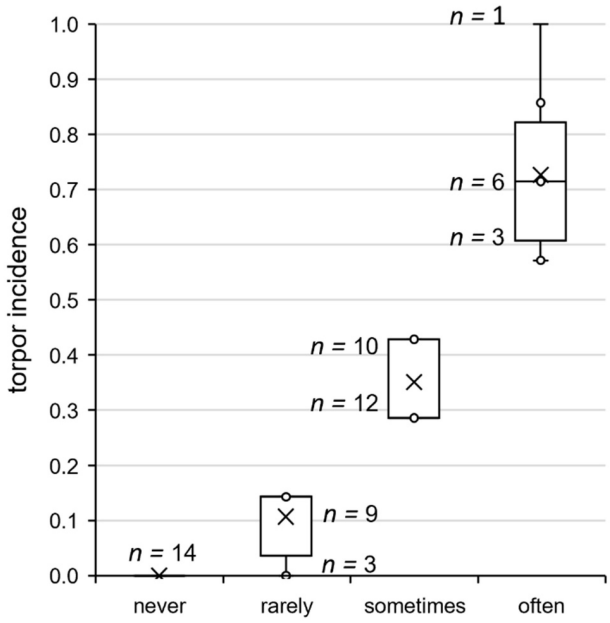

FIGURE 4 | Torpor incidence groups of approach 1. Grouping of all hamsters according to their individual torpor incidence shown in the week of analysis. From the distribution of the torpor incidence values of the hamsters expressing torpor, yet not necessarily during the week of analysis, three groups were derived for phenotyping. Taking the 25th percentile (torpor incidence of 0.2) and the 75th percentile (torpor incidence of 0.5) as thresholds, the animals were assigned to the groups "rarely torpor" (<25%, $n = 12$), "sometimes torpor" (25–75%, $n = 22$), and "often torpor" (>75%, $n = 12$). The torpor incidence varied between hamsters of the same group, as indicated with the sample sizes per torpor incidence value *next to the boxplots*. Responders that never expressed torpor during their individual implantation time accounted for the fourth group "never torpor" ($n = 14$).

Approach 2—Initial and Long-Term Effects of Short Photoperiod

Twenty-three percent of the hamsters which adapted to SP between 2018 and 2020 never expressed torpor. In approach 1, they could be discriminated from the torpor-expressing hamsters by the weaker body mass reduction and, thus, already during SP adaptation. Since 11 of the 60 hamsters had already been implanted before the beginning of SP, their body temperature and activity profiles were analyzed during the change from LP to SP and the following SP adaptation to identify potential additional predictors of torpor proneness early during adaptation. Due to the low sample size, comparisons of "torpor" hamsters ($n = 8$) and "never torpor" hamsters ($n = 3$) were statistically invalid. The values per parameter, time frame, experimental week, and individual are given in the supplementary tables (**Supplementary Tables 4–8**).

TABLE 1 | Phenotyping of the torpor incidence groups according to the torpor parameters of approach 1.

Torpor characteristics	Given values	Torpor incidence group				ANOVA		*Post hoc* test with $p < 0.050$
		Never torpor ($n = 14$)	Rarely torpor ($n = 12$)	Sometimes torpor ($n = 22$)	Often torpor ($n = 12$)	Test statistics	*p*-value	Comparison
Torpor per definition incidence	Median	–	**0.1**	**0.3**	**0.7**	$H_{(2)} = 40.0$	<0.001	Rarely *vs*. sometimes Rarely *vs*. often Sometimes *vs*. often
Torpor attempt incidence	Median	–	**0.0**	**0.2**	**0.1**	$H_{(2)} = 3.1$	0.215	–
Torpor onset (ZT)	Median	–	**2.6**	**2.0**	**1.0**	$H_{(2)} = 8.4$	0.015	Rarely *vs.* often Sometimes *vs.* often
Torpor offset (ZT)	Mean	–	**5.5**	**5.5**	**5.1**	$F_{(41,2)} = 0.2$	0.823	–
Torpor duration (min)	Mean	–	**174**	**200**	**246**	$F_{(41,2)} = 1.4$	0.259	–
Minimal torpor T_b (°C)	Mean	–	**27.2**	**26.5**	**25.4**	$F_{(41,2)} = 1.6$	0.219	–

*One week was analyzed. The grouping is based on the torpor per definition incidence (**Figure 4**). Each hamster's mean value per torpor parameter (onset, offset, duration, and minimal torpor body temperature) was included in the comparison. More details on the statistical tests are listed in **Supplementary Table 2**.*

TABLE 2 | Phenotyping of the torpor incidence groups according to the adaptation parameters of approach 1.

Adaptation parameters	Given values	Torpor incidence group				ANOVA		*Post hoc* test with $p = 0.050$
		Never torpor ($n = 14$)	Rarely torpor ($n = 12$)	Sometimes torpor ($n = 22$)	Often torpor ($n = 12$)	Test statistics	*p*-value	Comparison
Fur index in SP07	Median	**1.8**	**1.5**	**2.0**	**1.3**	$H_{(3)} = 3.6$	0.310	–
Fur index in SP12	Median	**3.3**	**3.0**	**3.3**	**3.3**	$H_{(3)} = 0.0$	0.998	–
Body mass in SP00 (g)	Mean	**35.0**	**35.9**	**37.2**	**35.3**	$F_{(56,3)} = 0.6$	0.615	–
Body mass in SP07 (g)	Mean	**30.5**	**28.9**	**30.4**	**28.4**	$F_{(56,3)} = 0.8$	0.475	–
Body mass in SP12 (g)	Mean	**29.9**	**27.3**	**28.2**	**25.5**	$F_{(56,3)} = 3.1$	0.035	Never *vs*. often
Body mass change in SP07 (%)	Mean	**–8.7**	**–19.3**	**–17.4**	**–19.2**	$F_{(56,3)} = 5.0$	0.004	Never *vs*. rarely Never *vs*. sometimes Never *vs*. often
Body mass change in SP12 (%)	Mean	**–10.7**	**–23.5**	**–23.3**	**–27.4**	$F_{(56,3)} = 12.5$	< 0.001	Never vs. rarely Never *vs.* sometimes Never *vs.* often

*Fur index, scored from 1 for a light brown summer fur to 6 for a dense white winter fur (Figala et al., 1973), and absolute body mass were assessed weekly over the course of adaptation to the short photoperiod. The relative body mass change was calculated in relation to SP00. Three weeks of interest were chosen, namely, SP00: start of adaptation; SP07: before torpor expression; and SP12: after first torpor bouts had been observed. More details on the statistical tests are listed in **Supplementary Table 2**.*

Body Temperature

To assess the initial effects of SP exposure, the cohort's body temperature measurements of the last week in LP and the first week in SP were compared (**Figure 6A**). In both LP and SP01, body temperature was significantly lower during the photophase than during the scotophase, while the reduction from LP to SP01 was only significant during the scotophase. The body temperature of the cohort further decreased over the course of SP adaptation (**Figure 6B**). The individual development of body temperature during the scoto- and photophases was diverse (**Figures 6C,D**). Hamster #06 was excluded from this and most other cohort models, as indicated in the figure legends. It expressed a torpor bout on the second day of SP, which is atypical or usually not noticed. It further developed a stereotypic jumping during photophase from SP04 to SP11.

First torpor bouts were expressed in SP07 (first torpor of hamster #03), SP08 (hamster #11), SP09 (hamsters #06 and #08), SP10 (hamsters #05 and #07), and SP11 (hamsters #09 and #10),

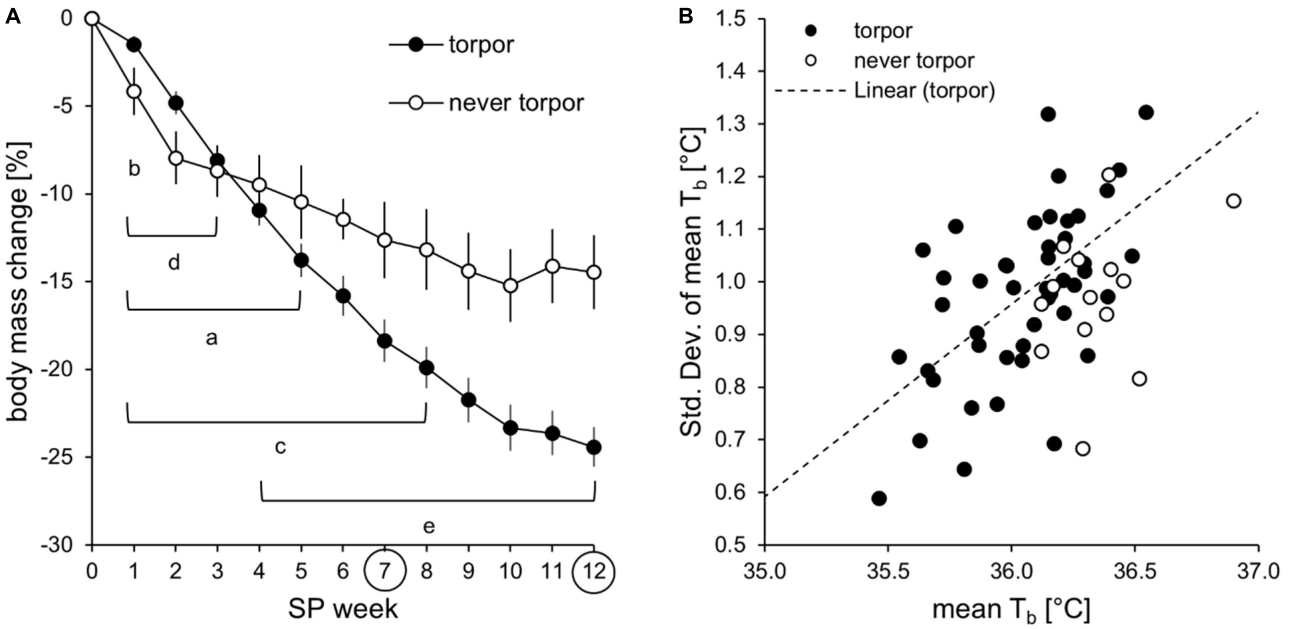

FIGURE 5 | Comparison of hamsters with and without torpor expression of approach 1. **(A)** Mean (±standard error) relative body mass change during adaptation to the short photoperiod [n_{torpor} = 46, $n_{never\ torpor}$ = 14]. Significant differences to SP07 of "torpor" (*a*) and "never torpor" (*b*) hamsters. Significant differences to SP12 of "torpor" (*c*) and "never torpor" (*d*) hamsters. Significant differences between "torpor" and "never torpor" hamsters (*e*) [two-way repeated measures ANOVA: $F_{(11,638)}$ = 10.124, $p < 0.001$, with Holm–Sidak $p < 0.001$]. **(B)** Correlation of the mean body temperature and its standard deviation during the middle of scotophase. The higher the mean body temperature, the lower is its standard deviation in "torpor" hamsters (n = 46, with R^2 = 0.3489, r = 0.591, $p < 0.050$). This correlation could not be confirmed in "never torpor" hamsters.

with a median of 67 days of SP adaptation. The eight hamsters expressed between one and 12 torpor bouts until SP13, with a median of four. The absolute number of torpor bouts from SP08 to SP13 was positively correlated with the torpor incidence of SP13 (n = 8, r = 0.948, $p < 0.05$), the week of torpor analysis in approach 1. Three hamsters (#01, #02, and #12) did not express torpor until termination in SP14.

In this study, the delta body temperature was used as an indicator of the body temperature spectrum covered by the hamsters. It was calculated by subtracting the minimal body temperature per hour from the maximal body temperature per hour individually detected within a time frame per week. The cohort's scotophase delta was significantly lower in SP00 until SP05 when compared to SP12. Furthermore, it increased linearly in all 11 hamsters over the course of SP adaptation (**Figure 7A**). In contrast, the photophase delta was highly individual, especially when including torpor expression after SP07. Until SP13, the photophase delta rose to maximal 14.4°C, reflecting the difference between the coldest and the warmest hour of an animal within photophase and week (**Figure 7B**).

Activity

To assess the initial effects of SP exposure, the cohort's activity measurements of the last week in LP and the first week in SP were compared (**Figure 8A**). In the first week of SP, the cohort reduced its activity during scotophase, while its activity during the photophase remained constant. In both photoperiods, the hamsters were nocturnal, with a higher activity during scotophase.

According to observations and the radiotelemetry data, the activity levels strongly differed due to the hamsters' broad behavioral spectrum from calm to active. The highest activity per hour determined in each hamster's LP scotophase varied from 11 cpm in the calmest to 158 cpm in the most active hamster, while the variations during the LP photophase ranged from 6 to 60 cpm. In contrast, the highest activity per hour in SP01 varied from 12 to 101 cpm during the scotophase and from 5 to 26 cpm during the photophase.

Over the course of 13 weeks in SP, the scotophase activity was further reduced in general, while the photophase activity slightly increased (**Figure 8B**). However, the scoto- and photophase activities were differently modulated by the 11 hamsters (**Figures 8C,D**). Activity onset occurred sharply at the beginning of the scotophase, while activity faded over the course of the scotophase so that the offset was difficult to define (**Figure 9**). The hamsters adapted to the immediate change from LP to SP by expanding their activity gradually into the prolonged scotophase and shifted their activity peak to the new beginning of the scotophase. According to eye fitting using actograms, seven animals adapted their activity within the first SP week and two others during the second SP week, while adaptation occurred after 4 weeks in hamster #09 and after 8 weeks in the "never torpor" hamster #01.

The hamsters' nocturnality was additionally confirmed by a photophase-to-scotophase activity ratio calculated per

TABLE 3 | Phenotyping of the torpor incidence groups of approach 1 according to the activity and body temperature per time frame.

Parameters		Given values	Torpor incidence group				ANOVA		*Post hoc* test with $p = 0.050$
			Never torpor ($n = 14$)	Rarely torpor ($n = 12$)	Sometimes torpor ($n = 22$)	Often torpor ($n = 12$)	Test statistics	*p*-value	Comparison
Activity	Total (cpm)	Median	**4.0**	**4.8**	**4.4**	**2.9**	$H_{(3)} = 7.4$	0.060	–
	Photophase (cpm)	Median	**2.1**	**2.0**	**2.0**	**1.5**	$H_{(3)} = 3.4$	0.334	–
	Scotophase (cpm)	Median	**5.1**	**6.0**	**5.5**	**3.6**	$H_{(3)} = 9.2$	0.026	Rarely *vs*. often
	First half of scotophase (cpm)	Median	**5.8**	**8.0**	**6.9**	**3.9**	$H_{(3)} = 10.2$	0.017	Rarely *vs*. often
	Second. half of scotophase (cpm)	Median	**4.4**	**4.3**	**4.0**	**3.4**	$H_{(3)} = 4.1$	0.248	–
	Middle of scotophase (cpm)	Median	**4.9**	**6.0**	**5.5**	**3.7**	$H_{(3)} = 8.4$	0.039	Rarely *vs*. often
	Std. Dev. of middle of scotophase (cpm)	Median	**10.3**	**13.0**	**11.7**	**9.5**	$H_{(3)} = 4.8$	0.189	–
	Photophase-to-scotophase ratio	Median	**0.4**	**0.4**	**0.4**	**0.5**	$H_{(3)} = 0.3$	0.951	–
	Second-to-first half of scotophase ratio	Median	**0.7**	**0.5**	**0.7**	**0.8**	$H_{(3)} = 6.8$	0.078	–
Body temperature	Total (°C)	Median	**36.1**	**35.8**	**35.4**	**34.6**	$H_{(3)} = 47.8$	<0.001	Never *vs*. sometimes
									Never *vs*. often
									Rarely *vs*. sometimes
									Rarely *vs*. often
	Photophase (°C)	Median	**35.7**	**35.1**	**34.3**	**32.1**	$H_{(3)} = 47.0$	< 0.001	Never *vs*. sometimes
									Never *vs*. often
									Rarely *vs*. sometimes
									Rarely *vs*. often
	Scotophase (°C)	Mean	**36.4**	**36.2**	**36.0**	**35.8**	$F_{(56,3)} = 18.5$	<0.001	Never *vs*. sometimes
									Never *vs*. often
									Rarely *vs*. sometimes
									Rarely *vs*. often
									Sometimes *vs*. often
	First half of scotophase (°C)	Median	**36.5**	**36.4**	**36.3**	**35.9**	$H_{(3)} = 27.7$	<0.001	Never *vs*. sometimes
									Never *vs*. often
									Rarely *vs*. often
	Second half of scotophase (°C)	Median	**36.2**	**36.0**	**35.9**	**35.6**	$H_{(3)} = 27.5$	<0.001	Never *vs*. sometimes
									Never *vs*. often
	Middle of scotophase (°C)	Mean	**36.3**	**36.3**	**36.0**	**35.9**	$F_{(56,3)} = 13.4$	<0.001	Never *vs*. sometimes
									Never *vs*. often
									Rarely *vs*. sometimes
									Rarely *vs*. often
	Standard deviation of middle of scotophase (°C)	Mean	**0.97**	**1.1**	**0.98**	**0.84**	$F_{(56,3)} = 7.8$	<0.001	Never *vs*. rarely
									Never *vs*. often
									Rarely *vs*. often
									Sometimes *vs*. often

Data of one analysis week were used. More details on the statistical test results are listed in ***Supplementary Table 3****. The lower the photophase-to-scotophase activity ratio, the higher the degree of nocturnality. The lower the second-to-first half of scotophase activity ratio, the higher the activity during the first half of scotophase.*

hamster and week (**Figure 10**). Ratios below 1 indicate a higher activity during scotophase and, therefore, nocturnality. Nocturnality of the cohort was most pronounced in LP and became weaker until SP05 (the ratio increased from about 0.2 to 0.5). From SP05, the ratio remained at about 0.5, indicating that the photophase activity was half that of the scotophase activity. The hyperactivity hamster #06 expressed during photophase after SP04 was reflected by ratios higher than 1, indicating diurnality (**Figure 10**, insert).

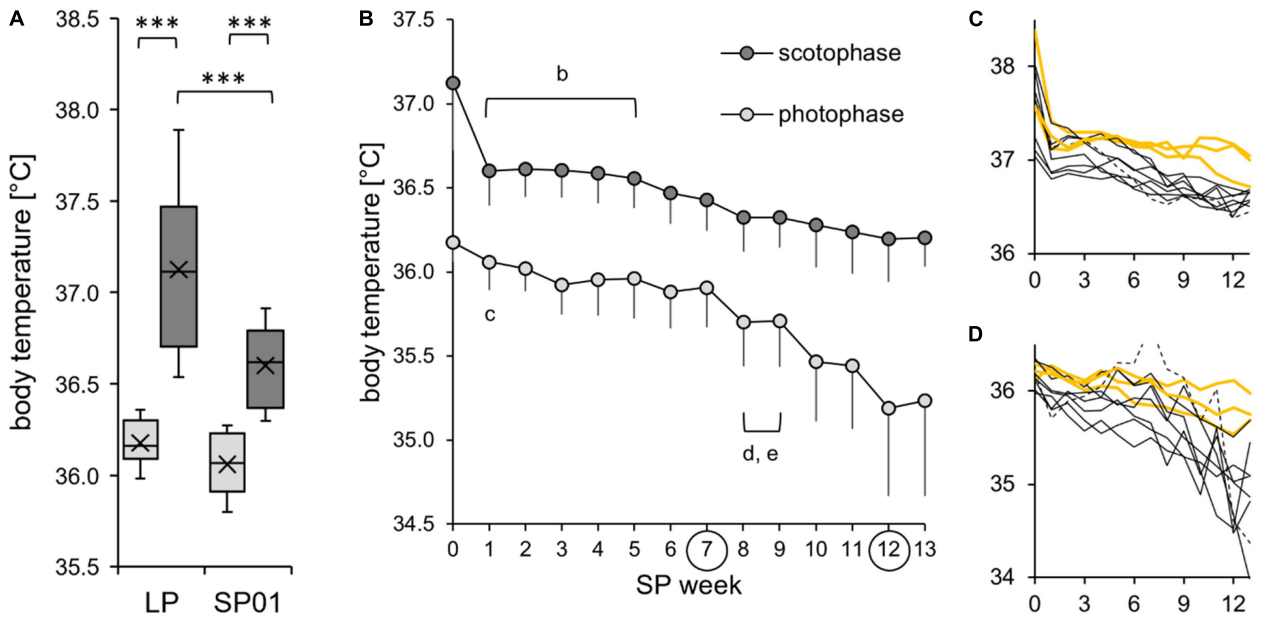

FIGURE 6 | Body temperature during the short photoperiod adaptation of approach 2. The exact values per hamster can be found in **Supplementary Table 4**. **(A)** The cohort's initial reduction of body temperature after the change of the light regime (n = 10). Comparison of body temperature during photophase (*light gray*) and scotophase (*dark gray*) of the last week of the long photoperiod (*LP*) and the first week of the short photoperiod (*SP01*). According to a two-way repeated measures ANOVA, body temperature was affected by both time frame [$F_{(1,9)} = 62.256$, $p < 0.001$, power = 1.0] and light regime [$F_{(1,9)} = 83.125$, $p < 0.001$, power = 1.0]. In addition, there was an interaction between the effects of time frame and light regime [$F_{(1,9)} = 15.373$, $p = 0.004$, power = 0.9). *Post hoc* Holm–Sidak tests confirmed that body temperature was significantly higher during the scotophase in both LP and SP01 (***$p < 0.001$). Furthermore, body temperature during the scotophase (***$p < 0.001$) was significantly higher in LP than that in SP01. Hamster #06 was excluded because it performed a torpor bout on the second day of SP, which is atypical or usually not noticed. **(B)** The cohort's further reduction of body temperature (n = 10). With focus on the weeks from SP01 to SP07 without torpor expression, body temperature was reduced over the course of SP adaptation. Significant differences to the SP07 of scotophase (*b*) [one-way repeated measures ANOVA: $F_{(6,54)} = 7.599$, $p < 0.001$] as well as of photophase (*c*) [one-way repeated measures ANOVA: $F_{(6,54)} = 4.851$, $p < 0.001$], both confirmed with Holm–Sidak $p < 0.001$. With focus on the weeks from SP08 to SP12 including torpor bouts, body temperature was further decreased. Significant differences to the SP12 for scotophase (*d*) [one-way repeated measures ANOVA: $F_{(5,45)} = 4.978$, $p = 0.001$, with Holm–Sidak $p = 0.002$] as well as for photophase (*e*) [Friedman repeated measures ANOVA: $\chi^2_{(5)} = 30.114$, $p < 0.001$, with Tukey's test $p < 0.05$]. Hyperactive hamster #06 was excluded since a stereotypic jumping during photophase was also reflected in the body temperature. **(C,D)** Individual reduction of body temperature during scotophase **(C)** and photophase **(D)** for each of the 11 hamsters. Body temperature (in degree Celsius) is shown on the *y*-axis, the SP week on the *x*-axis, with hamster #06 as *dotted line*, the three "never torpor" hamsters as *yellow lines*, and all others as *thin black lines*.

The cohort maintained a higher activity in the first than in the second half of scotophase, with an average second-to-first half of scotophase activity ratio smaller than 1, namely, 0.7 ± 0.3 in SP01 and 0.6 ± 0.2 in later weeks. Exceptions were a ratio of 1.7 in hamster #09 during SP01 and a ratio of 1.3 in hamster #07 during SP09, as they were more active in the second half of the scotophase. The extremely slow activity adaptation of hamster #01 was reflected by a ratio decline from 8.3 in SP01 to 0.7 in SP13, with ratios smaller than 1 after SP08.

Body Mass and Fur

All hamsters reduced their body mass during SP adaptation (**Figure 11A**). The cohort had an initial body mass of 32.7 ± 5.2 g, which was reduced by -19 ± 8% to 26.5 ± 4.3 g in SP07. "Never torpor" hamsters seem to have a less drastic reduction of body mass, as already shown in approach 1 (**Figure 5A**). All hamsters changed their light brown summer fur to a dense white winter fur over the course of SP adaptation (**Figure 11B**). The first changes became visible in SP04 in three of 11 animals. Hamster #08 started to change its fur in SP10, when most other animals already finished their fur change.

DISCUSSION

In the present study, the high variability of the adaptation parameters and torpor use in Djungarian hamsters was confirmed for all the observed parameters; however, the two analytic approaches for a large and detailed sample set also revealed new aspects. Overall, the hamster colony at Ulm University resembles the animals in early reports after domestication (Figala et al., 1973; Ross, 1998), yet with a weaker adaptation response. This likely results from the high ambient temperature of 20°C, corresponding to the lower limit of the hamsters' thermoneutral zone when SP-adapted (Heldmaier and Steinlechner, 1981a). Although the present animals have a domestication history of 50 years, outbreeding could preserve their circadian and seasonal phenotype, i.e., nocturnality as well as a body mass reduction

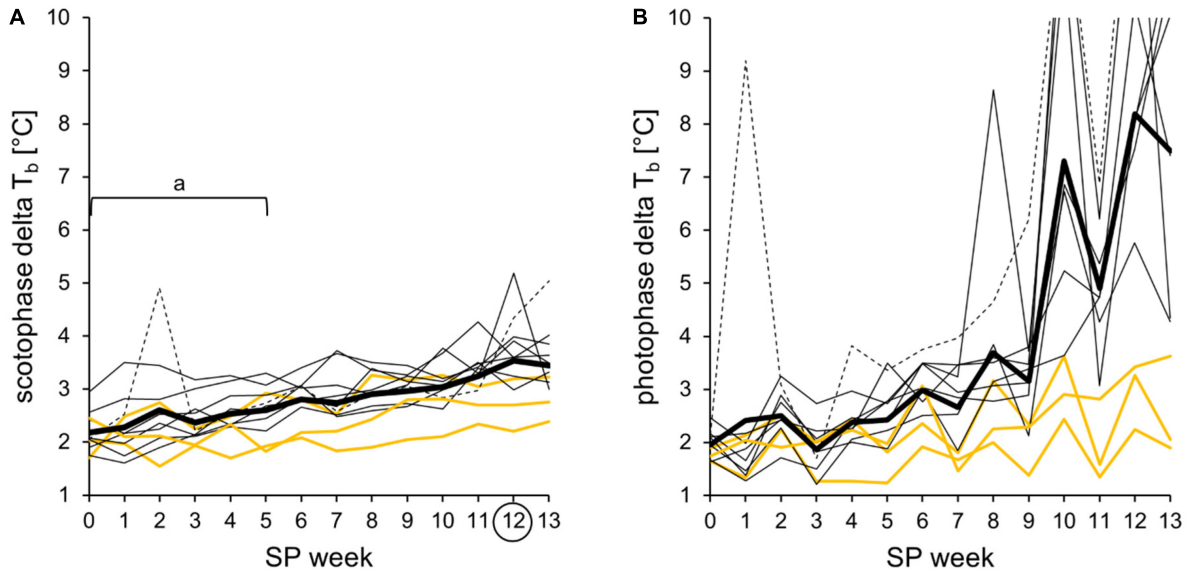

FIGURE 7 | Delta body temperature during the short photoperiod adaptation of approach 2. The difference between the highest value per hour and the lowest value per hour, detected within a time frame, is shown for each animal and week. Hamster #06 is represented as *dotted line*, the three "never torpor" hamsters as *yellow lines*, all others as *thin black lines*, and the cohort's mean delta body temperature as *thick black line*. The exact values per hamster can be found in **Supplementary Table 5**. **(A)** Delta body temperature of scotophase. The values per individual were averaged as delta of the cohort (n = 11, *thick line*), which showed a linear development (from SP00 to SP13: R^2 = 0.936, r = 0.967, $p < 0.05$). For the cohort, significant differences to SP12 are indicated with "*a*" [Friedman repeated measures ANOVA: $\chi^2_{(13)}$ = 93.566, $p < 0.001$, with Tukey's test $p < 0.05$]. **(B)** Delta body temperature of photophase. Spontaneous daily torpor, irregularly expressed by hamster #06 in SP01 and regularly expressed by eight of the 11 hamsters after SP07, caused high delta body temperatures during photophase.

of 20%, a fur index between 3 and 5, and torpor expression in most animals.

Torpor

The expression of spontaneous daily torpor in Djungarian hamsters has been shown to be under strict circadian control (Ruf et al., 1989; Ruby and Zucker, 1992). The analyses of the present study, however, indicate a rather flexible timing of torpor during photophase (**Figure 3** and **Table 1**). The 127 torpor bouts analyzed had their onset at ZT1.6 ± 1.4 h. It is important to notice that the reduction of the metabolic rate below the resting metabolic rate during torpor entrance precedes the reduction of body temperature below 32°C by almost an hour (Ruf and Heldmaier, 2000; Heldmaier et al., 2004). Consequently, all torpor onsets determined by body temperature measurements before ZT01 already occurred before the end of the scotophase and thus without light as a proximate induction stimulus.

The 46 torpor-expressing hamsters analyzed in approach 1 had shown at least one torpor bout within their individual observation interval. For reasons of comparability, the approach analyzed one representative SP week during the torpor period, resulting in a median torpor incidence of 0.3 with some hamsters that did not show torpor in this specific week. The respective torpor parameters were analyzed for single torpor bouts irrespective of animal (n = 127) and means per animal (n = 42). Both analyses revealed useful correlations for future interpretations of individual torpor behavior. Increasing the torpor incidence resulted in a higher probability of early and therefore deeper and longer bouts with an early torpor offset, and *vice versa*. Interestingly, torpor onset and its standard deviation correlated positively in the cohort, indicating a lower variability of early torpor bouts and an increasing degree of synchronization to ZT0 with increasing torpor incidence.

Torpor bouts that start early may favor energy saving because they resulted in lower minimal body temperatures per bout and longer torpor bouts in the present study (see also Ruf and Heldmaier, 1992). The hypothermic body temperature and the reduced activity at the beginning of the scotophase additionally indicate post-torpor effects on the hamsters' scotophase behavior (**Table 3**). Earlier studies have shown that the hamsters' circadian rhythm diminishes in SP, whereby torpor might impair sleep during the resting phase (Deboer et al., 2000; Deboer and Tobler, 2003; Scherbarth and Steinlechner, 2008). Time might get lost for feeding, and this energy deficit might directly demand for the next even deeper and longer torpor bouts. This is supported by the observations of a low scotophase activity coinciding with a low scotophase body temperature (**Table 3**), consequently a smaller standard deviation of body temperature (**Figure 5B**), and a higher torpor incidence with early, deep, and long torpor bouts (**Table 1** and **Figure 3**).

Furthermore, the present study revealed a remarkable incidence of torpor bout attempts in torpor-expressing hamsters (**Table 1**) never reported in the literature. They started at the same time and in the same shape as torpor bouts, but were interrupted at about 33°C (**Figure 1**). It is unclear whether torpor bouts were interrupted by yet undefined external disturbances or due to internal physiological factors. So far, the energy-saving potential of torpor bout attempts remains unknown, but should

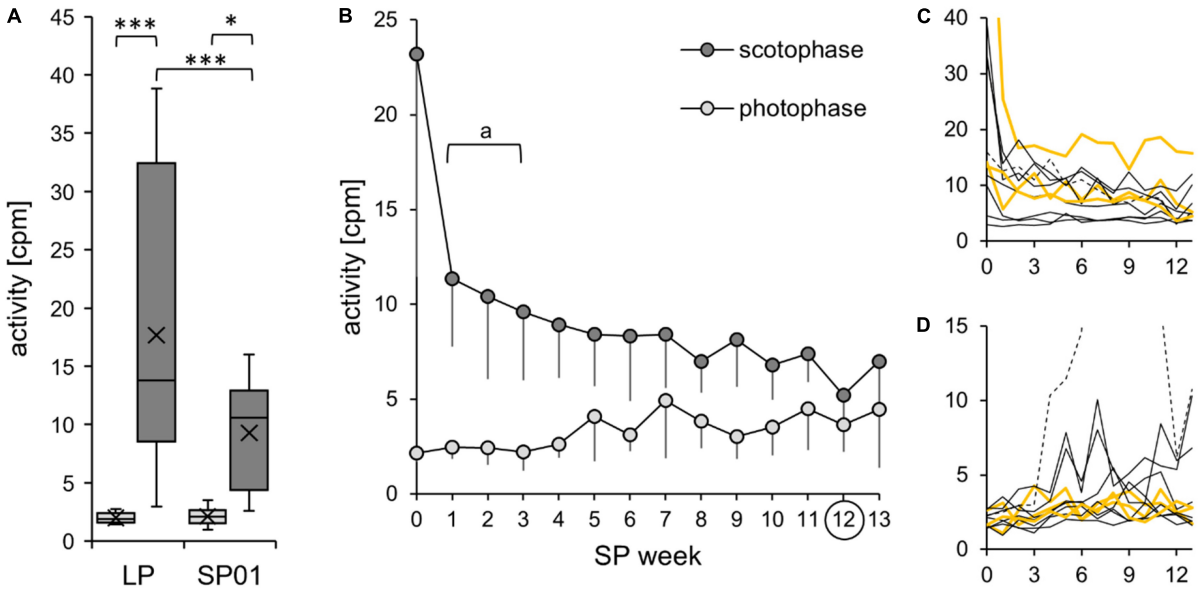

FIGURE 8 | Activity during the short photoperiod adaptation of approach 2. The exact values per hamster can be found in **Supplementary Table 6**. **(A)** The cohort's initial adaptation of activity after the change of the light regime (n = 10). Comparison of activity during photophase (*light gray*) and scotophase (*dark gray*) of the last week of the long photoperiod (*LP*) and the first week of the short photoperiod (*SP01*). According to the two-way repeated measures ANOVA, the activity was affected by both time frame [$F_{(1,9)}$ = 21.155, p = 0.001, power = 0.984] and light regime [$F_{(1,9)}$ = 7.689, p = 0.022, power = 0.637]. In addition, there was an interaction between the effects of time frame and light regime [$F_{(1,9)}$ = 7.815, p = 0.021, power = 0.645]. *Post hoc* Holm–Sidak tests confirmed that the activity was significantly higher in LP scotophase (***$p < 0.001$) and in SP01 (*$p < 0.026$) compared to that in photophase. Furthermore, scotophase activity was higher in LP than that in SP01 (***$p < 0.001$), yet with a low power. Hamster #02 was excluded from the cohort's model since it had an outlying scotophase activity level in LP (beyond the three times interquartile distance threshold of the cohort), with a drastic initial decrease from 79 cpm during LP scotophase to 25 cpm during SP01 scotophase. **(B)** Further activity development of the cohort (n = 6). When comparing the adaptation period from SP01 to SP12, the scotophase activity was reduced. Significant differences to SP12 are indicated with "*a*" [one-way repeated measures ANOVA: $F_{(12,60)}$ = 4.750, $p < 0.001$, with Holm–Sidak $p < 0.001$]. The photophase activity slightly rose, yet with a significant difference from SP04 to SP08 only [Friedman repeated measures ANOVA: $\chi^2_{(13)}$ = 36.229, $p < 0.001$, with Tukey's test $p < 0.05$]. Excluded were hamster #01, with high LP activity and an extremely slow activity adaptation to SP; hamster #02, with outlying LP activity; hamster #06, with stereotypic jumping behavior in the cage corners during photophase from SP04 to SP11; and the hamsters #10 and #11, which were extremely calm and did not modulate initial activity. **(C,D)** Individual reduction of body temperature during scotophase **(C)** and photophase **(D)** for each of the 11 hamsters. Activity (in counts per minute) is displayed on the y-axis, the SP week on the x-axis with hamster #06 as *dotted line*, the three "never torpor" hamsters as *yellow lines*, and all others as *thin black lines*.

be examined *via* metabolic rate measurements in conditions carefully controlled for external disturbance factors as they might also reveal new insights into the other functions of torpor (Geiser and Brigham, 2012).

Rare reports of torpor expression without SP adaptation or food restriction exist (Steinlechner et al., 1986). Hamster #06 expressed an irregular torpor bout on the second SP day with an onset at ZT23, which accounts for the ZT0 of LP. Like the other hamsters of the cohort, hamster #06 started to express torpor bouts regularly in SP09 and had a torpor incidence of 0.7 ("often torpor") in SP13.

The torpor analysis of this study is not free of bias. Data analysis started and ended at ZT0 (beginning of photophase). While individual torpor incidence included all recorded torpor bouts per hamster, torpor bouts starting before ZT0 on the first day of the analysis week could not be analyzed in detail. An alternative data analysis starting and ending at ZT08 (beginning of scotophase) would have resulted in a much higher number of incomplete torpor bouts, as torpor offset after ZT08 was more common than torpor onset before ZT0. Furthermore, the present results show that torpor affected the second half of scotophase prior to torpor as well as the first half of scotophase after torpor. Consequently, the choice of the start and end of an observation interval must be considered thoroughly regarding aims of future studies.

Sampling Paradigm

The phenotyping of the torpor incidence groups was also used to reassess previous organ sampling schemes (Herwig et al., 2007; Bank et al., 2017; Cubuk et al., 2017a,b). In these sampling paradigms, hypothermic (HT) hamsters were sampled at torpor onset (ZT01), deep torpor (ZT04), torpor offset (ZT07), and after torpor (ZT16), along with time-matched normothermic (NT) hamsters. As there are high inter-individual variabilities of the torpor incidence, onset, depth, and duration within a cohort, not every hamster can be sampled for each group, which impedes a random assignment beforehand. Assuming that the individual torpor timing and torpor incidence are an integrative part of the hamster's long-term adaptational response, which is determined by a set of hitherto unknown genetic and environmental factors, the data might reflect not only acute effects but also prerequisites of torpor behavior. Consequently, the individual torpor behavior

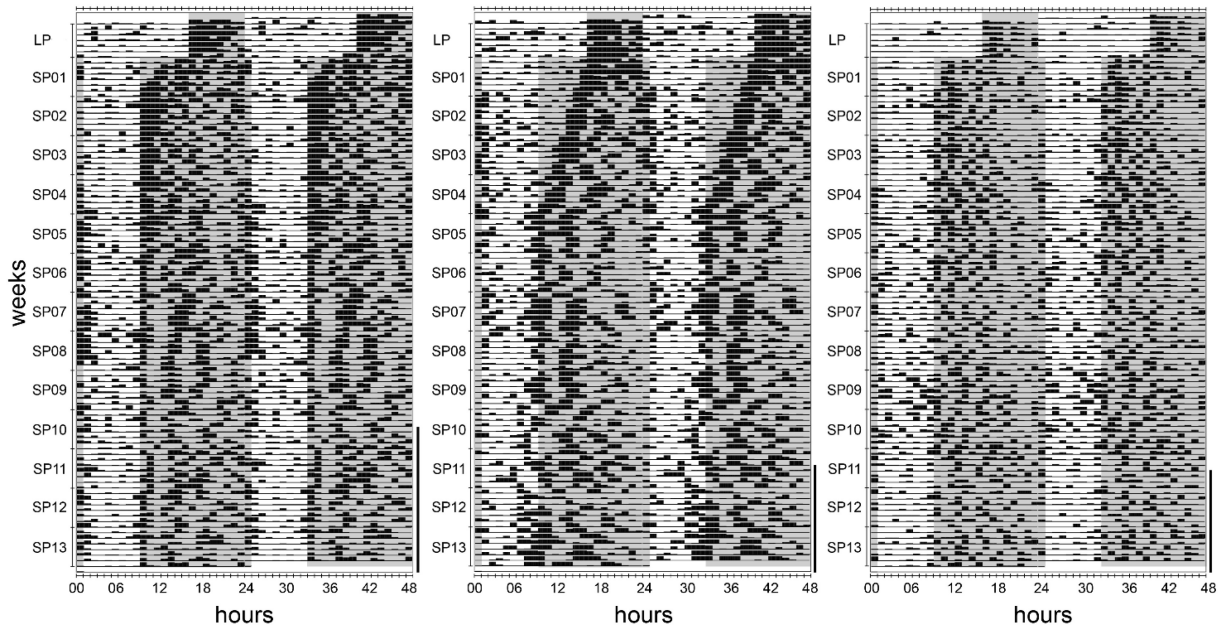

FIGURE 9 | Actograms of three individuals of approach 2 during 1 week in the long photoperiod and adaptation to the short photoperiod. *Black bars* indicate the activity performed within an hour, while values from 0 to 10 cpm are displayed. The long photoperiod (LP) and short photoperiod (SP) scotophases are indicated with *gray areas*. The days following the first torpor bout are marked with a *vertical line on the right side* of each actogram. All 11 hamsters adapted gradually to the immediate change from LP to SP, however at different paces. The *left actogram* (hamster #07) serves as an example for the majority of hamsters that showed a fast adaptation within days. The *middle actogram* (hamster #09) represents one of two hamsters with a gradual adaptation within weeks. The *right actogram* represents one of two hamsters showing a fast adaptation, but a very low activity level that impeded the analysis of temporal activity organization (hamster #10).

must be determined beforehand to achieve an equal distribution among sampling groups.

The majority of torpor-expressing hamsters (22 out of 46, 48%) showed torpor sometimes (incidence between 0.3 and 0.5; **Figure 4**) and fit best for all the sampling groups and time points (**Table 1**). However, torpor attempt incidence is highest in these hamsters (**Table 2**). A torpor bout attempt would not allow sampling for the particular day since the hamster was neither in torpor per definition nor constantly normothermic (**Figure 1A**). Hamsters never or rarely expressing torpor are indeed likely to be sampled as normothermic controls. Yet, given their flexible torpor timing, they are also adequate for sampling in hypothermia at ZT01 and ZT07. Hamsters with a high torpor incidence are more likely to be sampled for the hypothermic sampling group, but are not always adequate for sampling at ZT01 and ZT07 since they tended to be almost in deep torpor at ZT01 and finished the torpor bout before ZT07 (**Figure 3**). Thus, it cannot be assumed that hamsters often expressing torpor are all sampled for the HT group and those that express torpor rarely are all sampled in the NT group.

In future studies, the torpor behavior should be assessed in detail during 1 week of radiotelemetry tracking before sampling. Respective conclusions can be drawn to plan the assignment of each hamster to a certain sampling group in the following week since a stable torpor behavior from one to the next week was assumed due to the positive correlation between the absolute number of torpor bouts until SP12 and the torpor incidence in SP13 of approach 2.

However, this study also indicates restrictions of the rigid yet adequate sampling paradigm. The described flexibility in torpor incidence, timing of torpor, and course of body temperature during a torpor bout is respected in the paradigm as well as possible. An expansion of the sampling time points, from, e.g., ZT01 to ZT0–ZT02, would be eligible for studies on hypo- and normothermia alone, but inconvenient for studies on the circadian rhythm of hypo- and normothermic hamsters. Adapting the 32°C torpor definition threshold is impeded by both torpor bout attempts, which might be misinterpreted as torpor bouts, and the high minimal body temperatures of hamsters rarely expressing torpor. In relation to this, it should be mentioned that the torpor definition threshold of the present and many earlier studies (32°C for at least 30 min) is under constant debate (Boyles et al., 2011; Brigham et al., 2011) and might be refined by including metabolic rate measurements (Diedrich et al., 2015).

Never Torpor

The present study enables a better identification of responders without torpor expression. In approach 1, 14 "never torpor" hamsters out of a cohort with 60 individuals responded more weakly to SP in terms of body mass reduction (**Figure 5A** and **Table 2**). A high mean body temperature with a low standard deviation during the middle of scotophase allows discriminating "never torpor" hamsters not only from "torpor" hamsters but also from "rarely torpor" hamsters, with no to one torpor bout within the analysis week (**Figure 5B** and **Table 3**). Yet, due to the

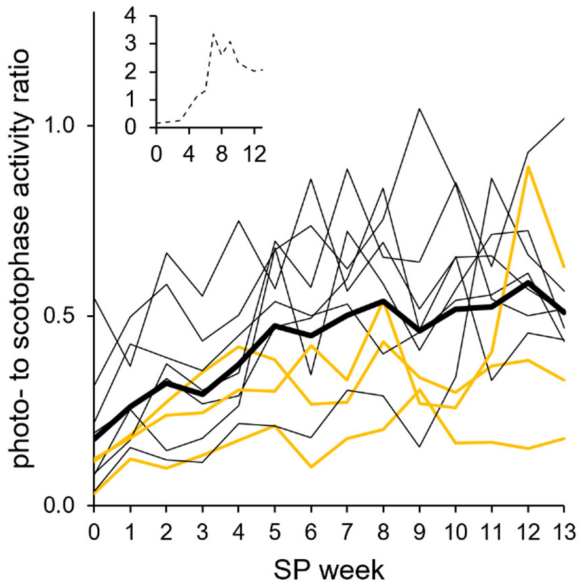

FIGURE 10 | Photophase-to-scotophase activity ratio during the short photoperiod adaptation of approach 2. For each animal and week, the photophase-to-scotophase activity ratio was calculated to identify nocturnality (ratio < 1) and diurnality (ratio > 1). Individual ratios (the three "never torpor" hamsters as *yellow lines* and all others as *thin black lines*; *inset*: graph of hyperactive hamster #06) were averaged for the cohort's ratio (*thick line*). The cohort's ratio (n = 10, without hamster #06) showed a positive linear correlation with progressing adaptation to the short photoperiod (SP) (R^2 = 0.8144, r = 0.902, $p < 0.05$). Significant differences to SP07 before torpor expression were found in SP00 and SP01, while differences to SP12 occurred in SP00, SP01, and SP03 [Friedman repeated measures ANOVA: $\chi^2_{(13)}$ = 68.811, $p < 0.001$, with Tukey's test $p < 0.05$]. The exact values per hamster can be found in **Supplementary Table 7**.

small sample size of the early implanted hamsters of approach 2 with three "never torpor" hamsters out of 11, this study cannot reveal at which time point of adaptation these differences became significant. However, an identification of the "never torpor" hamsters 2 weeks after implantation is not sufficient to reduce the number of animals in an experiment or the number of invasive transmitter implantations.

In approach 2, "never torpor" hamsters appeared to respond more weakly in all the observed parameters, suggesting a different metabolic programming of hamsters never expressing torpor at given circumstances (Cubuk et al., 2016; Diedrich et al., 2020). The most promising indicators of "never torpor" hamsters might be a higher body temperature during scotophase over the entire course of SP adaptation (**Figure 6C**) and a smaller delta body temperature and, therefore, variation during both scoto- and photophases (**Figure 7**). Indirect calorimetry could be used as a non-invasive alternative to extrapolate from individual fluctuations of metabolic rate to those of body temperature and, thus, torpor or no torpor expression. Body temperature and the metabolic rate correlate (Heldmaier and Ruf, 1992), and our own preliminary measurements in SP-adapted hamsters regarding the middle of scotophase also revealed a positive correlation between the standard deviation of the mean body temperature and the standard deviation of the mean metabolic rate (n = 7, R^2 = 0.74, r = 0.86, p = 0.006). Furthermore, non-invasive infrared cameras with tracking software would enable more attention on the peculiarities regarding the activity levels and activity patterns of "never torpor" hamsters, e.g., a high scotophase activity in LP (hamster #02), a very slow activity adaptation to SP (hamster #01), as well as a photophase-to-scotophase activity ratio below the cohort's mean, suggesting a more pronounced nocturnality in "never torpor" hamsters (**Figure 10**).

Next Torpor

Besides the early identification of torpor-expressing responders, the acute prediction of the next torpor bout in individual hamsters would be of interest to improve planning of sampling. While a study on marsupial sugar gliders has suggested reductions of activity and body temperature as acute predictors of torpor (Christian and Geiser, 2007), efforts to use radiotelemetry data have been hitherto without success. A relation between the activity pattern and the torpor behavior was not found (**Figures 1**, **2**, 9), but the activity ratios on, e.g., a daily instead of a weekly basis, a refined correlation analysis between activity and body temperature, and the standard deviations of the mean values seem to be promising (**Figures 5**, **10**, 11). The most reliable parameter for acute torpor prediction has been and still is the previous torpor incidence, which seems to be rather stable within an individual.

Adaptation to Short Photoperiod

Djungarian hamsters should be more active in LP than in SP since they expect mating and the intense care for their litters. The resulting high energy demand requires a high foraging activity, which can be reduced during the early stages of SP adaptation as a function of decreasing food intake, body mass, and reproductive activity (Ruf and Heldmaier, 2000). Indeed, a high activity and body temperature in LP and lower values when SP-adapted have been reported (Hamann, 1987; Prendergast et al., 2013) and were confirmed in this study. While body temperature was lower in SP during all time frames (**Figure 6**), activity was similar in both LP and SP photophase and differed only in scotophase (**Figure 8**).

The transition of the activity and body temperature patterns from LP to SP has not yet been described for hamsters kept in artificial photoperiods. In this study, the hamsters were subjected to an abrupt light shift from LP to SP, whereby the photophase began 1 h later and ended 7 h earlier. This manner of transition has been used for several hamster cohorts and experiments at Ulm University to allow for the described sampling paradigm when SP-adapted. Consequently, the responses shown in this study may have reflected this specific circadian phase entrainment to the photic *zeitgeber*. Regardless of the transition pattern, the potential influence of a certain shift on the hamster's individual adaptation and torpor capability must be considered. A fast activity adaptation was previously shown for diverse complex light regime changes, yet with high variations within the cohort including individuals with a low or no adaptation performance (Gorman and Elliott, 2004). Most hamsters were able to re-entrain to a ZT0 shift by 5 h (16:8 h) within 14 days, while some showed a free-running activity pattern

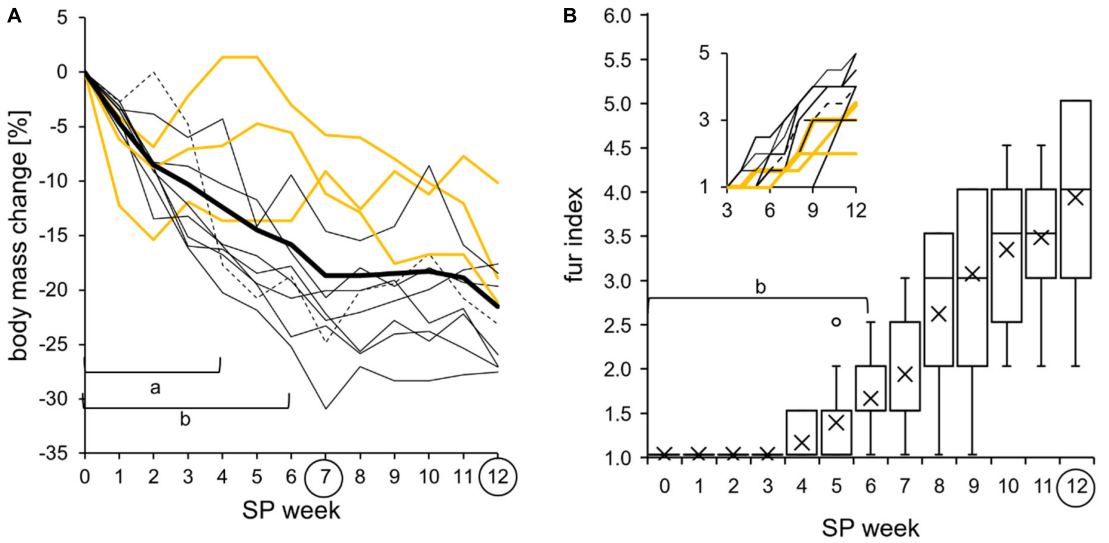

FIGURE 11 | Body mass change and molt into a white winter fur during the short photoperiod adaptation of approach 2 (n = 11). The exact values per hamster can be found in **Supplementary Table 8**. **(A)** Relative body mass change with the long photoperiod (LP) as baseline. The cohort's significant differences of the relative body mass change (*thick line*) to SP07 are indicated with "*a*" e.g., to SP12 with "*b*" [one-way repeated measures ANOVA: $F_{(12,120)} = 28.777$, $p < 0.001$, with Holm–Sidak $p < 0.001$]. All hamsters changed their body mass during the short photoperiod (SP) adaptation (hamster #06 as *dotted line*, the three "never torpor" hamsters as *yellow lines*, and all others as *thin black lines*). **(B)** Fur index from 1 for summer fur to 6 for winter fur. The cohort's significant differences of fur index (*boxplots*) to SP12 are indicated with "*b*" [Friedman repeated measures ANOVA: $\chi^2_{(12)} = 122.375$, $p < 0.001$, with Tukey's test $p < 0.05$]. All hamsters increased their fur index. *Inset*: graph with color code of graph **(A)**.

or even arrhythmia (Barakat et al., 2004, 2005). In the present study, the majority of hamsters showed a fast response to the new light regime by an immediate synchronization as well as reductions of activity and body temperature during the first SP week (**Figures 6A**, 8A). In contrast, the body mass and fur index, two parameters strongly influencing thermoregulation, remained initially unchanged (**Figure 11**).

Activity requires an increase in the metabolic rate, which produces heat and increases body temperature. Thus, the immediate reduction of the scotophase body temperature after the change from LP to SP was largely attributable to the immediate decrease in scotophase activity, although the velocity of this change was rather impressive. As activity recordings have been shown to largely reflect feeding bouts (Ruf and Heldmaier, 1993), the activity decrease observed in this study might have resulted from a decreased drive to feed in order to initiate body mass reduction during SP adaptation (Knopper and Boily, 2000). Earlier studies have already measured lower scoto- and photophase body temperatures in SP- than in LP-adapted Djungarian hamsters (Heldmaier and Steinlechner, 1981a; Korhonen et al., 2008). The present study, however, showed for the first time that this decrease in body temperature already occurs at the very beginning of the SP adaptation and further proceeds during the adaptation process (**Figure 6**). The hamsters appeared to tolerate the rather acute body temperature reduction and additionally showed an increasing difference between the maximum and minimum body temperatures prior to the beginning of torpor expression, surprisingly not only during photophase but also during scotophase (**Figure 7**). This observation might be a first indication for an SP-induced early change in body temperature set point, which is gradually adjusted and integrated in the complex morphological and physiological adaptation processes until the beginning of the torpor period. Although this study cannot provide sufficient information on the mechanisms behind the body temperature adjustments, it can be assumed that they contribute to the overall energy-saving purpose of the Djungarian hamster's adaptative syndrome (Heldmaier and Lynch, 1986).

The high variability in adaptation is considered to be natural and not indicative of the negative effects of domestication and genetic bottlenecks (Figala et al., 1973), as a hamster population should benefit from a certain degree of individual flexibility and variation to cope with acute and unpredictable changes in environmental conditions (Ruf et al., 1991, 1993). Nevertheless, since the Siberian winter is usually long and harsh, nature should have selected for hamsters with a fast and strong adaptation in response to the decreasing photoperiod length, followed by flexible torpor use as anticipation of acute energetic challenges, which are not given in laboratory conditions (Diedrich et al., 2015, 2020).

Nocturnality

According to the developer, the DSI activity data indicate no, low, or high activity per 3-min recording interval. The method developed for this study made the activity data accessible in more detail by using larger data bins, namely, time frames per week, which leveled natural and technical outliers, while a sufficient time increment was maintained for both long- and short-term observations (**Figures 1**, **2**). Nevertheless, the absolute activity

data, recorded and analyzed in cpm, are based on the signal strength changes, which might slightly vary with position and speed the transmitter moving over its receiver. The activity mean values of several animals must be interpreted with caution (**Table 3** and **Figure 8**), while the introduced activity ratios are a promising tool to characterize activity in relative terms with each animal as its own control (**Table 3** and **Figure 10**).

For the present study, using both absolute and relative activity data complemented and verified each other. A higher activity during scotophase than during photophase has been described for rodents in general and has incidentally been shown for Djungarian hamsters (Wynne-Edwards et al., 1999; Refinetti, 2006; Weinert et al., 2009), which could be confirmed in the present study (**Figures 8–10**, **Table 3**, and **Supplementary Table 6**). Previously, different circadian phenotypes have been described, ranging from wild type over delayed onset and arrhythmic to non-responder (Margraf et al., 1991; Gorman and Zucker, 1997; Schöttner et al., 2011). In the present study, all hamsters were nocturnal, with higher absolute activity values during the scotophase and a photophase-to-scotophase activity ratio below 1, while hamster #06's hyperactivity during the photophase was reflected by photophase-to-scotophase activity ratios higher than 1, proving diurnality. Unlike the other hamsters of the cohort, the calm sibling hamsters #10 and #11, did not decrease their activity over the course of SP adaptation, probably because they could not fall below the basal activity level. Their nocturnality was difficult to detect due to the irregular and shallow activity bouts, but was proven with the photophase-to-scotophase activity ratio.

The activity ratios for the smaller time frames enable a more subtle discrimination of the circadian phenotypes, e.g., the second-to-first half of scotophase activity ratio. In most hamsters, activity started and peaked at the beginning of the scotophase, declined over the course of the scotophase, and had already faded at the beginning of the photophase without clear-cut ending, which could be proven by second-to-first half of scotophase activity ratios smaller 1. SP caused a shift of the hamsters' activity phase and its peak toward the new beginning of scotophase, which was visualized by actograms and reflected by both activity ratios. This pace enabled defining one slow (hamster #09) and one very slow (hamster #01, "never torpor") activity responder. During progressing SP adaptation, the actograms of this study suggest increasing flexibility of the daily activity–rest rhythm. This was supported by a decreasing degree of nocturnality, indicated by an increasing photophase-to-scotophase activity ratio. The activity ratios used in this study had no significant influence on and were not influenced by the torpor incidence.

CONCLUSION

The incidence, timing, and traits of spontaneous daily torpor show low intra- but high inter-individual variabilities over the torpor period in Djungarian hamsters. Therefore, a detailed body temperature analysis of one representative SP week after complete adaptation might contribute to a refinement of the organ sampling schemes realized in the following week. Hamsters with different torpor incidences, and therefore phenotypes, could then be assigned more equally to different sampling groups regarding metabolic state (hypothermic *vs*. normothermic) at a defined time (torpor entry, deep torpor, and arousal). This standardization will further improve the outcomes of molecular analyses of the torpor regulatory pathways.

Hamsters that never expressed torpor had a low body mass reduction and could be discriminated from torpor-expressing hamsters by high mean body temperatures with low fluctuations in the middle of the scotophase. Moreover, weak or slow SP adaptations of body temperature, activity body mass, and fur index were found. However, an early estimation of the subsequent torpor behavior, and therefore a reduction of animals subjected to implantation, remains difficult because of the high variability of the SP adaptation pace and extent within a hamster cohort. Non-invasive alternative methods like infrared cameras with tracking software to assess activity or indirect calorimetry for metabolic rate measurements should be considered to analyze hamsters' adaptation and torpor phenotypes before transmitter implantation.

As an immediate response to an abrupt change from LP to SP, scotophase activity and the body temperature decreased in the hamsters, indicating profound physiological changes at the very beginning of adaptation. This underpins the importance of a careful control of the experimental photoperiod regimes and suggests focusing more on the initial metabolic profiles of SP adaptation.

The adaptation parameters gradually changed, even weeks before the anticipated beginning of the energy-demanding winter. This preparatory period allows a fine-tuning of parameters since they start and develop with high variability. The individually fine-tuned set point of body temperature might have a central meaning for torpor integration into the overall energy balance of SP-adapted hamsters.

DATA AVAILABILITY STATEMENT

The raw data supporting the conclusions of this article will be made available by the authors, without undue reservation.

ETHICS STATEMENT

The animal study was reviewed and approved by Regierungspräsidium Tübingen, Germany (1411).

AUTHOR CONTRIBUTIONS

All the authors conceived the project, interpreted the data, and agreed to be accountable for the content of the work. EH and VD performed the experiments and analyzed the data. EH wrote the manuscript, which was carefully revised by all authors.

FUNDING

EH was funded by a grant from the German Research Foundation to AH (HE 6383/2).

ACKNOWLEDGMENTS

We thank Sabine Schmidt and Elisabeth Picca for animal breeding and care as well as Insa Krey and Alexandra Hentrich for their contribution to the method development. We also thank the reviewers for their valuable comments.

SUPPLEMENTARY MATERIAL

The Supplementary Material for this article can be found online at: https://www.frontiersin.org/articles/10.3389/fphys.2021.626779/full#supplementary-material

Supplementary Table 1 | Background information about the hamsters of this study. The hamsters' ID comprises the cohorts' name and a running number. Besides males (m) and females (f), the torpor incidence group is indicated by a raster, from "often torpor" in the first block over "sometimes torpor" and "rarely torpor" to "never torpor" in the last block. The transmitter runtime is given in weeks. The 11 animals of cohort EH04 were implanted already in LP and used in both approaches, while those of the cohorts EH02 and EH03 were implanted when adapted to SP and used in approach 1 only.

Supplementary Table 2 | Additional statistics of analysis of approach 1 regarding torpor characteristics and adaptation parameters of the analysis week per torpor incidence group (**Tables 1**, **2**).

Supplementary Table 3 | Additional statistics of the radiotelemetry analysis of approach 1 regarding pattern of activity and body temperature of one experimental week per torpor incidence group (**Table 3**).

Supplementary Table 4 | Body temperature values per time frame, week in long photoperiod (LP) and short photoperiod (SP) as well as individual of approach 2. Yellow marked hamsters did not express spontaneous daily torpor. Sparklines in the last column indicate the individual change, with the hamster's highest value as 100% and its lowest as 0%.

Supplementary Table 5 | Delta body temperature values per time frame, week in long photoperiod (LP) and short photoperiod (SP) as well as individual of approach 2. Yellow marked hamsters did not express spontaneous daily torpor. Sparklines in the last column indicate the individual change, with the hamster's highest value as 100% and its lowest as 0%.

Supplementary Table 6 | Activity values per time frame, week in long photoperiod (LP) and short photoperiod (SP) as well as individual of approach 2. Yellow marked hamsters did not express spontaneous daily torpor. Sparklines in the last column indicate the individual change, with the hamster's highest value as 100% and its lowest as 0%.

Supplementary Table 7 | Activity ratio values per time frame, week in long photoperiod (LP) and short photoperiod (SP) as well as individual of approach 2. Yellow marked hamsters did not express spontaneous daily torpor. Red color marks ratios above 1.0 indicating diurnal activity patterns (upper part) or higher activity during the second half of the scotophase (lower part). Sparklines in the last column indicate the individual change, with the hamster's highest value as 100% and its lowest as 0%. Second to first half of scotophase ratio was not raised for LP with a scotophase of eight hours.

Supplementary Table 8 | Adaptation parameter values per week in long photoperiod (LP) and short photoperiod (SP) as well as individual of approach 2. Yellow marked hamsters did not express spontaneous daily torpor. Sparklines in the last column indicate the individual change, with the hamster's highest value as 100% and its lowest as 0%.

REFERENCES

Bank, J. H. H., Cubuk, C., Wilson, D., Rijntjes, E., Kemmling, J., Markowsky, H., et al. (2017). Gene expression analysis and microdialysis suggest hypothalamic triiodothyronine (T3) gates daily torpor in Djungarian hamsters (*Phodopus sungorus*). *J. Comp. Physiol. B Biochem. Syst. Environ. Physiol.* 187, 857–868. doi: 10.1007/s00360-017-1086-1085

Bank, J. H. H., Kemmling, J., Rijntjes, E., Wirth, E. K., and Herwig, A. (2015). Thyroid hormone status affects expression of daily torpor and gene transcription in Djungarian hamsters (*Phodopus sungorus*). *Horm. Behav.* 75, 120–129. doi: 10.1016/j.yhbeh.2015.09.006

Barakat, M. T., O'Hara, B. F., Cao, V. H., Heller, H. C., and Ruby, N. F. (2005). Light induces c- fos and per1 expression in the suprachiasmatic nucleus of arrhythmic hamsters. *Am. J. Physiol. Integr. Comp. Physiol.* 289, R1381–R1386. doi: 10.1152/ajpregu.00695.2004

Barakat, M. T., O'Hara, B. F., Cao, V. H., Larkin, J. E., Heller, H. C., and Ruby, N. F. (2004). Light pulses do not induce c-fos or per1 in the SCN of hamsters that fail to reentrain to the photocycle. *J. Biol. Rhythms* 19, 287–297. doi: 10.1177/0748730404266771

Boyles, J. G., Smit, B., and McKechnie, A. E. (2011). Does use of the torpor cut-off method to analyze variation in body temperature cause more problems than it solves? *J. Therm. Biol.* 36, 373–375. doi: 10.1016/j.jtherbio.2011.07.007

Brigham, R. M., Willis, C. K. R., Geiser, F., and Mzilikazi, N. (2011). Baby in the bathwater: should we abandon the use of body temperature thresholds to quantify expression of torpor? *J. Therm. Biol.* 36, 376–379. doi: 10.1016/j.jtherbio.2011.08.001

Choukèr, A., Bereiter-Hahn, J., Singer, D., and Heldmaier, G. (2019). Hibernating astronauts — science or fiction? *Eur. J. Physiol.* 471, 819–828. doi: 10.1007/s00424-018-2244-2247

Christian, N., and Geiser, F. (2007). To use or not to use torpor? activity and body temperature as predictors. *Naturwissenschaften* 94, 483–487. doi: 10.1007/s00114-007-0215-215

Cubuk, C., Bank, J. H. H., and Herwig, A. (2016). The chemistry of cold: mechanisms of torpor regulation in the siberian hamster. *Physiology* 31, 51–59. doi: 10.1152/physiol.00028.2015

Cubuk, C., Kemmling, J., Fabrizius, A., and Herwig, A. (2017a). Transcriptome analysis of hypothalamic gene expression during daily torpor in Djungarian hamsters (*Phodopus sungorus*). *Front. Neurosci.* 11:122. doi: 10.3389/fnins.2017.00122

Cubuk, C., Markowsky, H., and Herwig, A. (2017b). Hypothalamic control systems show differential gene expression during spontaneous daily torpor and fasting-induced torpor in the Djungarian hamster (*Phodopus sungorus*). *PLoS One* 12:e0186299. doi: 10.1371/journal.pone.0186299

Dave, K. R., Christian, S. L., Perez-Pinzon, M. A., and Drew, K. L. (2012). Neuroprotection: lessons from hibernators. *Comp. Biochem. Physiol. - B Biochem. Mol. Biol.* 162, 1–9. doi: 10.1016/j.cbpb.2012.01.008

Deboer, T., and Tobler, I. (2003). Sleep regulation in the Djungarian hamster: comparison of the dynamics leading to the slow-wave activity increase after sleep deprivation and daily torpor. *Sleep* 26, 567–572. doi: 10.1093/sleep/26.5.567

Deboer, T., Vyazovskiy, V. V., and Tobler, I. (2000). Long photoperiod restores the 24-h rhythm of sleep and EEG slow-wave activity in the Djungarian hamster (*Phodopus sungorus*). *J. Biol. Rhythms* 15, 429–436. doi: 10.1177/074873040001500508

Diedrich, V., Haugg, E., Dreier, C., and Herwig, A. (2020). What can seasonal models teach us about energy balance? *J. Endocrinol.* 244, R17–R32.

Diedrich, V., Kumstel, S., and Steinlechner, S. (2015). Spontaneous daily torpor and fasting-induced torpor in Djungarian hamsters are characterized by distinct patterns of metabolic rate. *J. Comp. Physiol. B Biochem. Syst. Environ. Physiol.* 185, 355–366. doi: 10.1007/s00360-014-0882-884

Figala, J., Hoffmann, K., and Goldau, G. (1973). Zur jahresperiodik beim dsungarischen zwerghamster *Phodopus sungorus* pallas. *Oecologia* 12, 89–118. doi: 10.1007/BF00345511

Geiser, F. (2008). Ontogeny and phylogeny of endothermy and torpor in mammals and birds. *Comp. Biochem. Physiol. - A Mol. Integr. Physiol.* 150, 176–180. doi: 10.1016/j.cbpa.2007.02.041

Geiser, F., and Brigham, R. M. (2012). "The other functions of torpor," in *Living in a Seasonal World*, eds T. Ruf, C. Bieber, W. Arnold, and E. Millesi (Berlin: Springer).

Gorman, M. R., and Elliott, J. A. (2004). Dim nocturnal illumination alters coupling of circadian pacemakers in *Siberian hamsters*, *Phodopus sungorus*. *J. Comp. Physiol.* 190, 631–639. doi: 10.1007/s00359-004-0522-527

Gorman, M. R., and Zucker, I. (1997). Environmental induction of photononresponsiveness in the *Siberian hamster*, *Phodopus sungorus*. *Am. J. Physiol. - Regul. Integr. Comp. Physiol.* 272, 887–895. doi: 10.1152/ajpregu.1997.272.3.r887

Hamann, U. (1987). Zu Aktivität und verhalten von drei Taxa der zwerghamster der gattung phodopus miller, 1910. *Mamm. Biol.* 52, 65–76.

Heldmaier, G., and Lynch, G. R. (1986). Pineal involvement in thermoregulation and acclimatization. *Pineal Res. Rev.* 4, 97–139.

Heldmaier, G., Ortmann, S., and Elvert, R. (2004). Natural hypometabolism during hibernation and daily torpor in mammals. *Respir. Physiol. Neurobiol.* 141, 317–329. doi: 10.1016/j.resp.2004.03.014

Heldmaier, G., and Ruf, T. (1992). Body temperature and metabolic rate during natural hypothermia in endotherms. *J. Comp. Physiol. B* 162, 696–706. doi: 10.1007/BF00301619

Heldmaier, G., and Steinlechner, S. (1981a). Seasonal control of energy requirements for thermoregulation in the Djungarian hamster (*Phodopus sungorus*), living in natural photoperiod. *J. Comp. Physiol. B Biochem. Syst. Environ. Physiol.* 142, 429–437. doi: 10.1007/BF00688972

Heldmaier, G., and Steinlechner, S. (1981b). Seasonal pattern and energetics of short daily torpor in the Djungarian hamster, *Phodopus sungorus*. *Oecologia* 48, 265–270. doi: 10.1007/BF00347975

Herwig, A., Ivanova, E. A., Lydon, H., Barrett, P., Steinlechner, S., and Loudon, A. S. I. (2007). Histamine H3 receptor and orexin a expression during daily torpor in the Djungarian hamster (*Phodopus sungorus*). *J. Neuroendocrinol.* 19, 1001–1007. doi: 10.1111/j.1365-2826.2007.01620.x

Hoffmann, K. (1982). "The critical photoperiod in the djungarian hamster *Phodopus sungorus*," in *Vertebrate Circadian Systems. Proceedings in Life Sciences*, eds J. Aschoff, S. Daan, and G. A. Groos (Berlin: Springer).

Jastroch, M., Giroud, S., Barrett, P., Geiser, F., Heldmaier, G., and Herwig, A. (2016). Seasonal control of mammalian energy balance: recent advances in the understanding of daily torpor and hibernation. *J. Neuroendocrinol.* 28, 1–10. doi: 10.1111/jne.12437

Jones, J. S., Fileccia, E. L., Murphy, M., Fowler, M. J., King, M. V., Shortall, S. E., et al. (2014). Cathinone increases body temperature, enhances locomotor activity, and induces striatal c-fos expression in the *Siberian hamster*. *Neurosci. Lett.* 559, 34–38. doi: 10.1016/j.neulet.2013.11.032

Kirsch, R., Ouarour, A., and Pévet, P. (1991). Daily torpor in the Djungarian hamster (*Phodopus sungorus*): photoperiodic regulation, characteristics and circadian organization. *J. Comp. Physiol. A* 168, 121–128. doi: 10.1007/BF00217110

Knopper, L. D., and Boily, P. (2000). The energy budget of captive siberian hamsters, *Phodopus sungorus*, exposed to photoperiod changes: mass loss is caused by a voluntary decrease in food intake. *Physiol. Biochem. Zool.* 73, 517–522. doi: 10.1086/317730

Korhonen, T., Mustonen, A.-M., Nieminen, P., and Saarela, S. (2008). Effects of cold exposure, exogenous melatonin and short-day treatment on the weight-regulation and body temperature of the *Siberian Hamster* (*Phodopus sungorus*). *Regul. Pept.* 149, 60–66. doi: 10.1016/j.regpep.2007.09.033

Margraf, R. R., Zlomanczuk, P., Liskin, L. A., and Lynch, G. R. (1991). Circadian differences in neuronal activity of the suprachiasmatic nucleus in brain slices prepared from photo-responsive and photo-non-responsive *Djungarian hamsters*. *Brain Res.* 544, 42–48. doi: 10.1016/0006-8993(91)90883-W

Paul, M. J., Freeman, D. A., Jin, H. P., and Dark, J. (2005). Neuropeptide Y induces torpor-like hypothermia in *Siberian hamsters*. *Brain Res.* 1055, 83–92. doi: 10.1016/j.brainres.2005.06.090

Paul, M. J., Kauffman, A. S., and Zucker, I. (2004). Feeding schedule controls circadian timing of daily torpor in SCN-ablated *Siberian hamsters*. *J. Biol. Rhythms* 19, 226–237. doi: 10.1177/0748730404264337

Piscitiello, E., Herwig, A., Haugg, E., Schröder, B., Breves, G., Steinlechner, S., et al. (2021). Acclimation of intestinal morphology and function in Djungarian hamsters (*Phodopus sungorus*) related to seasonal and acute energy balance. *J. Exp. Biol.* 224:jeb232876. doi: 10.1242/jeb.232876

Prendergast, B. J., Cable, E. J., Cisse, Y. M., Stevenson, T. J., and Zucker, I. (2013). Pineal and gonadal influences on ultradian locomotor rhythms of male *Siberian hamsters*. *Horm. Behav.* 63, 54–64. doi: 10.1016/j.yhbeh.2012.11.001

Przybylska, A. S., Wojciechowski, M. S., and Jefimow, M. (2019). Photoresponsiveness affects life history traits but not oxidative status in a seasonal rodent. *Front. Zool.* 16:11. doi: 10.1186/s12983-019-0311-3

Refinetti, R. (2006). Variability of diurnality in laboratory rodents. *J. Comp. Physiol. A Neuroethol. Sensory Neural Behav. Physiol.* 192, 701–714. doi: 10.1007/s00359-006-0093-x

Ross, P. D. (1998). Phodopus sungorus. *Mamm. Species* 595, 1–9. doi: 10.2307/3504390

Ruby, N. F., and Zucker, I. (1992). Daily torpor in the absence of the suprachiasmatic nucleus in *Siberian hamsters*. *Am. J. Physiol.* 263, R353–R362. doi: 10.1152/ajpregu.1992.263.2.R353

Ruf, T., and Heldmaier, G. (1992). The impact of daily torpor on energy requirements in the *Djungarian hamster*. *Phodopus sungorus*. *Physiol. Zool.* 65, 994–1010. doi: 10.2307/30158554

Ruf, T., and Heldmaier, G. (1993). "Individual energetic strategies in winter-adapted *Djungarian hamsters*: the relation between daily torpor, locomotion, and food consumption," in *Life in the Cold*, ed. C. Carey (Boca Raton, FL: CRC Press), 99–107.

Ruf, T., and Heldmaier, G. (2000). "*Djungarian hamsters* — Small graminivores with daily torpor," in *Activity Patterns in Small Mammals. Ecological Studies (Analysis and Synthesis)*, 141, eds S. Halle and N. C. Stenseth (Berlin: Springer), 217–234. doi: 10.1007/978-3-642-18264-8_14

Ruf, T., Klingenspor, M., Preis, H., and Heldmaier, G. (1991). Daily torpor in the Djungarian hamster (*Phodopus sungorus*): interactions with food intake, activity, and social behaviour. *J. Comp. Physiol. B* 160, 609–615.

Ruf, T., Steinlechner, S., and Heldmaier, G. (1989). "Rhythmicity of body temperature and torpor in the *Djungarian hamster*, *Phodopus sungorus*," in *Proceedings of the Living in the Cold: 2nd International Symposium*, eds A. Malan and B. Canguilhem (Le Hohwald: Colloques INSERM/John Libbey Eurotext Ldt), 53–61.

Ruf, T., Stieglitz, A., Steinlechner, S., Blank, J. L., and Heldmaier, G. (1993). Cold exposure and food restriction facilitate physiological responses to short photoperiod in Djungarian hamsters (*Phodopus sungorus*). *J. Exp. Zool.* 267, 104–112. doi: 10.1002/jez.1402670203

Scherbarth, F., and Steinlechner, S. (2008). The annual activity pattern of Djungarian hamsters (*Phodopus sungorus*) is affected by wheel-running activity. *Chronobiol. Int.* 25, 905–922. doi: 10.1080/07420520802544514

Scherbarth, F., and Steinlechner, S. (2010). Endocrine mechanisms of seasonal adaptation in small mammals: from early results to present understanding. *J. Comp. Physiol. B Biochem. Syst. Environ. Physiol.* 180, 935–952. doi: 10.1007/s00360-010-0498-492

Schöttner, K., Waterhouse, J., and Weinert, D. (2011). The circadian body temperature rhythm of Djungarian Hamsters (*Phodopus sungorus*) revealing different circadian phenotypes. *Physiol. Behav.* 103, 352–358. doi: 10.1016/j.physbeh.2011.02.019

Scribner, S. J., and Wynne-Edwards, K. E. (1994). Disruption of body temperature and behavior rhythms during reproduction in dwarf hamsters (*Phodopus*). *Physiol. Behav.* 55, 361–369. doi: 10.1016/0031-9384(94)90147-90143

Steinlechner, S., Heldmaier, G., Weber, C., and Ruf, T. (1986). "Role of photoperiod: pineal gland interaction in torpor control," in *Living in the Cold: Physiological and Biochemical Adaptions*, eds H. C. Heller, L. C. H. Wang, and X. Musacchia (New York, NY: Elsevier Science Publishing Co., Inc.), 301–307.

Weinert, D., Schöttner, K., Surov, A. V., Fritzsche, P., Feoktistova, N. Y., Ushakova, M. V., et al. (2009). Circadian activity rhythms of dwarf hamsters (*Phodopus spp.*) under laboratory and semi-natural conditions. *Russ. J. Theriol.* 8, 47–58. doi: 10.15298/rusjtheriol.08.1.05

Wynne-Edwards, K. E., Surov, A. V., and Telitzina, A. Y. (1999). Differences in endogenous activity within the genus *Phodopus*. *J. Mammal.* 80, 855–865. doi: 10.2307/1383254

Conflict of Interest: The authors declare that the research was conducted in the absence of any commercial or financial relationships that could be construed as a potential conflict of interest.

Advantages of publishing in Frontiers

OPEN ACCESS
Articles are free to read for greatest visibility and readership

FAST PUBLICATION
Around 90 days from submission to decision

HIGH QUALITY PEER-REVIEW
Rigorous, collaborative, and constructive peer-review

TRANSPARENT PEER-REVIEW
Editors and reviewers acknowledged by name on published articles

Frontiers
Avenue du Tribunal-Fédéral 34
1005 Lausanne | Switzerland

Visit us: www.frontiersin.org
Contact us: frontiersin.org/about/contact

REPRODUCIBILITY OF RESEARCH
Support open data and methods to enhance research reproducibility

DIGITAL PUBLISHING
Articles designed for optimal readership across devices

FOLLOW US
@frontiersin

IMPACT METRICS
Advanced article metrics track visibility across digital media

EXTENSIVE PROMOTION
Marketing and promotion of impactful research

LOOP RESEARCH NETWORK
Our network increases your article's readership